The Mechanism of Trichloroethylene Neurotoxicity and its Relation to Parkinsonism

Paul Keane
BSc. (Hons)

Thesis submitted in accordance with the requirements
of the regulations for the degree of

Doctor of Philosophy

Newcastle University
Faculty of Medical Sciences
Institute of Neuroscience
Medical Toxicology Research Centre

September 2013

Abstract

Parkinson's Disease (PD) is a progressive, neurodegenerative condition characterised by deterioration of the dopaminergic (DA) neurons of the substantia nigra pars compacta (SNpc). The exact mechanism by which SNpc cell death in PD occurs is poorly understood but several lines of evidence implicate both environmental and genetic factors. Trichloroethylene (TCE) is an industrial solvent used as a degreasing agent and in dry cleaning. TCE is a major environmental contaminant in the air, the water system and soil and is therefore exposed at low levels to various groups in the population. There have been links between chronic exposure to TCE and Parkinson-like symptoms reported and in vivo experiments support this link. It has also been discovered that TCE can be converted, via chloral, to a potentially DA neurotoxin TaClo in man. This project investigated this link between TCE and PD and to elucidate any causative mechanisms.

Cellular exposure paradigms were used to show neurotoxicity of TCE, chloral and TaClo in DA neurons. The mechanism of this cell death in TaClo was found to be necroptotic - and not apoptotic - in nature and involve induction of autophagy, DNA damage and an increase in reactive oxygen species (ROS) in exposed cells. A possible source of this ROS was suggested with the findings that TaClo significantly inhibits Complex I of the mitochondrial oxidative phosphorylation chain - an effect known to produce superoxide - and an increase in mitochondrial ROS seen in cells following TaClo treatment. The cell death induced by chloral was found to follow a different path, with neither apoptotic or necroptotic characteristics observed in exposed cells, and Complex I only inhibited at high doses. However, chloral was found to block the reduction of cytochrome c at lower doses, a property that may be involved in the neurotoxicity seen with chloral.

Animal models of TCE, chloral and TaClo exposure found no significant motor or cognitive abnormalities in behavioural testing of either wild-type mice or rats or human A30P mutated α-synuclein overexpressing mice. However, TCE and TaClo exposed wild-type and A30P mice did show a significant decrease in DA neuronal number and density in the SNpc, suggesting both compounds are neurotoxic to DA neurons *in vivo*. An LC-MS/MS assay was developed to assess neurotransmitter levels in the brains of toxin exposed animals, however the method was not found to be consistently accurate and showed extreme variability in results.

In conclusion, the main results of this thesis suggest that TCE does lead to DA neurodegeneration in the SNpc of exposed individuals, probably through metabolism to the

neurotoxic compound TaClo. The neurotoxic properties of TaClo are DA specific and relatively potent. The mechanism of neurotoxicity is hypothesised to be through inhibition of mitochondrial Complex I, inducing increased ROS production and damage of intracellular organelles, DNA and proteins, which in turn leads to the activation of autophagy and PARP activation. This intracellular stress instigates RIP1 mediated necroptosis and death of the cells.

Table of Contents

List of Figures

List of Tables

Abbreviations

10% GM	Growth Medium
5-HIAA	5-Hydroxyindoleacetic acid
5-HT	Serotonin
6-OHDA	6-Hydroxydopamine
AA	Amino Acid
AAT	Amino Acid Transporter
ACD	Autophagic Cell Death
AIF	Apoptosis Inducing Factor
AMPA	α-amino-3-hydroxy-5-methyl-4-isoxazolepropionic Acid
ANOVA	Analysis of Variance
ATG	Autophagy Related Gene
ATP	Adenosine Triphosphate
ATP13A2	Lysosomal Type 5 P-type ATPase
BBB	Blood Brain Barrier
BDNF	Brain Derived Neurotrophic Factor
BSA	Bovine Serum Albumin
CI/II/III/IV	Complex I/II/III/IV
cAMP	Cyclic Adenosine Monophosphate
Cav1.3	Calcium Channel Voltage Dependent L-type α-10 Subunit
CBD	Corticobasal Degeneration
CE	Coefficient of Error
CMA	Chaperone Mediated Autophagy
CNS	Central Nervous System
COMT	Catechol-O-Methyl Transferase
CSF	Cerebrospinal Fluid
CYP2E1	Cytochrome P450 2E1
DA	Dopamine
DAPI	4',6-Diamidino-2-Phenylindole
DAT	Dopamine Active Transporter
DCA	Dichloroacetic Acid
DCFDA	2',7' –dichlorofluorescein diacetate
DCPIP	2,6-dichlorophenol-indo-phenol
ddH_20	Double distilled Water
DDM	n-dodrecyl-β-D-maltoside

DISC	Death Inducing Signalling Complex
DLB	Dementia with Lewy Bodies
DMSO	Dimethylsulfoxide
DNA	Deoxyribonucleic Acid
DOPAC	3,4-Dihydroxyphenylacetic Acid
Drp1	Dynamin-related protein
DTNB	5-5'-dithiobis(2-nitrobenzoic acid)
EDTA	Ethylenediaminetetraacetic Acid
ESI	Electrospray Ionization Source
FBXO7	F-box Only Protein-7
FGF_8	Fibroblast Growth Factor 8
FKPB12	Immunophilin 12-kDa FK506-binding Protein
FSC-A	Forward Scatter
GABA	Gamma-Aminobutyric Acid
GAL	Galactose Growth Media
GAPDH	Glyceraldehyde-3-phosphate Dehydrogenase
GC-ECD	Gas Chromatography with Electrochemical Detection
GDNF	Glial Cell Line Derived Neurotrophic Factor
GFP	Green Fluorescent Protein
GSH	Glutathione
GIGYF2	Grb10-Interacting GYF Protein 2
H_2O_2	Hydrogen Peroxide
HCl	Hydrochloric Acid
HVA	Homovanillic Acid
IC_{50}	Half Maximal Inhibitory Concentration
IDO	Indoleamine 2,3-dioxygenase
ILBD	Incidental Lewy Body Disease
i.p.	Intra-peritoneal
KCN	Potassium Cyanide
LB	Lewy Body
LBS	L-buthionine Sulfoxamine
LC3-B	Microtubule-associated protein1 light chain 3
LC-MS/MS	Liquid Chromatography Tandem Mass Spectrometry
LD_{50}	Median Lethal Dose
L-DOPA	L-3,4-dihydroxyphenylalanine
LOAEL	Lowest Observed Adverse Effect Level

LPS	Lipopolysaccharide
LRRK2	Leucine-Rich Repeat Kinase 2
MAGICK	Stem cell growth medium
MAO	Monoamine Oxidase
MDMA	3,4-methylenedioxy-N-methylamphetamine
MEF	Mouse embryonic fibroblast
Min	Minutes
MLKL	Mixed lineage kinase domain-like protein
MnSOD/SOD2	Manganese Superoxide Dismutase
MSA	Multiple System Atrophy
mTOR	Mammalian Target of Rapamycin
MPP+	1-methyl-4phenyl-2,3-dihydropyridium ion
MPTP	1-methyl-4-phenyl-1,2,3,6-tetrahydropyridine
mtDNA	Mitochondrial DNA
MTP	Mitochondrial Transmembrane Pore
NA	Noradrenaline
NAC	N-acetylcysteine
NADH	Nicotinamide Adenine Dinucleotide
NADPH	Nicotinamide Adenine Dinucleotide Phosphate
Nec-1	Necrostatin-1
NMDA	N-methyl-D-aspartate
NO	Nitric Oxide
NOS	Nitric Oxide Synthase
$\cdot O_2^-$	Superoxide Anion
·OH	Peroxide Radical
OXPHOS	Oxidative Phosphorylation
PLA_2	Phospholipase A 2
PARP	Poly (ADP-ribose) Polymerase 1
PAT	Polyamine Transporter
PBS	Phosphate Buffered Saline
PCR	Polymerase Chain Reaction
PD	Parkinson’s Disease
PGAM5	Mitochondrial Phosphoglyceratemutase 5
pH2AX	Phospho-histone H2A.X Ser139
PHM	Pig Heart Mitochondria
PI	Propidium Iodide

PINK1	PTEN induced putative kinase 1
PLAG6	Calcium-independent Phospholipase A2
p.o.	Oral
POLG1	Mitochondrial DNA Polymerase γ1
PSP	Progressive Supranuclear Palsy
REM	Rapid Eye Movement
RIP	Receptor Interacting Protein
RNA	Ribonucleic Acid
RNAi	Inhibitory RNA
RNA	Reactive Nitrogen Species
ROS	Reactive Oxygen Species
s.c.	Subcutaneous
SHH	Sonic Hedgehog Homolog
shRNA	Short Hairpin Ribonucleic Acid
SNpc	Substantia Nigra pars compacta
SOD	Superoxide Dismutase
SPE	Solid Phase Extraction
SSA	Sulfosalicylic Acid
SSC-A	Side Scatter
TaClo	1-Trichloromethyl-1,2,3,4-tetrahydro-β-carboline
TBS	Tris-buffered Saline
TBST	TBS-Tween
TCE	Trichloroethylene
t.d.	Transdermal
TFAM	Transcription Factor A
TGF	Transforming Growth Factor
TH	Tyrosine Hydroxylase
TLR	Toll-like Receptor
TNF	Tumour Necrosis Factor
TU/ml	Viral Titre
UCH-L1	Ubiquitin C-terminal hydrolase-L1
UI	Units of Insulin
UPS	Ubiquitin-Proteasomal System
vDC	Ventral diencephalon
wt	Wild-Type
zVAD.fmk	Carbobenzoxy-valyl-alanyl-aspartyl-[O-methyl]- fluoromethylketone

Publications

Mitochondrial Dysfunction in Parkinson's Disease. **P. C. Keane**, M. Kurzawa, P. G. Blain, C. M. Morris (Parkinson's Dis. 2011; 2011: 716871)

Real-time monitoring of superoxide generation and cytotoxicity in neuroblastoma mitochondria induced by 1-trichloromethyl-1,2,3,4-tetrahydro-beta-carboline. S.J. Boulton, **P. C. Keane**, C. M. Morris, C. J. McNeil, P. Manning *(*Redox Report, 2012, 17(3))

Courses/Conferences Attended

June 2010	**Introduction to live Cell Imaging,** University of East Anglia.
September 2010	**Integrative Mammalian Biology Neuroscience Summer School,** University of Glasgow/University of Strathclyde.
September 2010	**North East Postgraduate Conference**, Newcastle *Poster presentation entitled 'The Mechanism of Trichloroethylene Neurotoxicity and its Relation to Parkinsonism*
March 2011	**British Toxciologocal Society/Dutch Society of Toxicology Annual Congress**, Durham *Oral presentation entitled 'The Mechanism of Tricholoroethylene Neurotoxicity and its Relation to Parkinsonism'*
October 2011	**North East Postgraduate Conference**, Newcastle *Oral presentation entitled 'The Involvement of Oxidative Stress in the Neurotoxic Mechanism of the Potentially Parkinsonian Toxin TaClo in SH-SY5Y'*
March 2012	**Society of Toxicology 51st Annual Meeting**, San Francisco *Poster presentation entitled 'An Investigation into the Mechanism of Trichloroethylene Neurotoxicity in Relation to Parkinsonism'*

Acknowledgements

I would like to thank the many people that have kindly helped me during my PhD studies.

Firstly, I would like to thank my supervisors Dr. Chris Morris, Dr. Sarah Judge and Prof. Peter Blain for making this project possible. In particular, the supervision of Dr. Morris during the project and his open door and willingness to advise on any matter no matter how large or small has been invaluable. I am also very grateful to Prof. Robert Taylor and Dr. Langping He from the NHS Mitochondrial Diagnostic Service for allowing me to use their facilities to measure the activity of mitochondrial respiratory chain complexes, Dr. Ahmad Khundakar for his help with the immunohistochemical staining and stereology, Dr. Michael Dunn, Margaret Knight and Clair Roper for the use of their equipment, expertise and assistance with the mass spectrometric analysis of neurotransmitters, Dr. Alex Laude of the Bio-Imaging Unit for his assistance with confocal microscopy, Dr. David McDonald of the Flow Cytometry Core Facility for his advice and guidance with flow cytometry studies and all in the Newcastle University Comparative Biology Centre for all their help with all *in vivo* work.

Special thanks to all of those in the Medical Toxicology Centre who helped me with innumerable things day to day, especially Dr. Peter Hanson and Dr. Marzena Kurzawa-Akanbi who provided generous help with cell culture and Western blotting and were always more than willing to help when things mysteriously went wrong! Also, thank you to my friends and fellow students Claire Savy, Ann Fitchett, Preeti Singh and Joanne Wallace amongst many others for keeping me sane in one way or another throughout the process and generally making my PhD more fun.

Finally, I would like to thank my family and friends for their unconditional support throughout my education, particularly my dad and Anna for the unenviable task of proof reading my thesis.

Declaration

This thesis is submitted for the degree of Doctor of Philosophy to Newcastle University. The research described within was performed at the Medical Toxicology Centre within the Institute of Neuroscience and is my own work unless otherwise stated. The research was carried out under the supervision of Dr Christopher M Morris, Dr Sarah J Judge and Prof Peter G Blain between September 2009 and September 2013.

I declare that the work presented in this thesis has not been submitted for any other award and that it is all my own work.

Chapter 1
Introduction

Parkinson's Disease (PD) is a progressive, neurodegenerative condition characterised by deterioration of the dopaminergic (DA) neurons of the substantia nigra pars compacta (SNpc) (Bernheimer, Birkmayer et al. 1973; Dickson, Braak et al. 2009; Lees, Hardy et al. 2009). The exact mechanism by which SNpc cell death in PD occurs is poorly understood but several lines of evidence implicate both environmental and genetic factors.

Trichloroethylene (TCE) is an industrial solvent used as a degreasing agent and in dry cleaning. TCE is a major environmental contaminant in the air, the water system and soil and is therefore exposed at low levels to various groups in the population.

There have been links between chronic exposure to TCE and Parkinson-like symptoms reported (Guehl, Bezard et al. 1999; Reif, Burch et al. 2003; Gash, Rutland et al. 2008) and *in vivo* experiments support this link (Liu, Choi et al. 2010). It has also been discovered that TCE can be converted, via chloral, to a potentially DA neurotoxin 1-Trichloromethyl-1,2,3,4-tetrahydro-β-carboline (TaClo) in man (Bringmann, God et al. 1999).

This project intends to investigate this link between TCE and PD and to elucidate any causative mechanisms.

1.1 Parkinson's Disease

PD is a progressive, neurodegenerative condition characterised by deterioration of the DA neurons of the SNpc (Bernheimer, Birkmayer et al. 1973; Dickson, Braak et al. 2009; Lees, Hardy et al. 2009) (Fig 1.1) leading to disruption of the nigrostriatal pathway and control of movement.

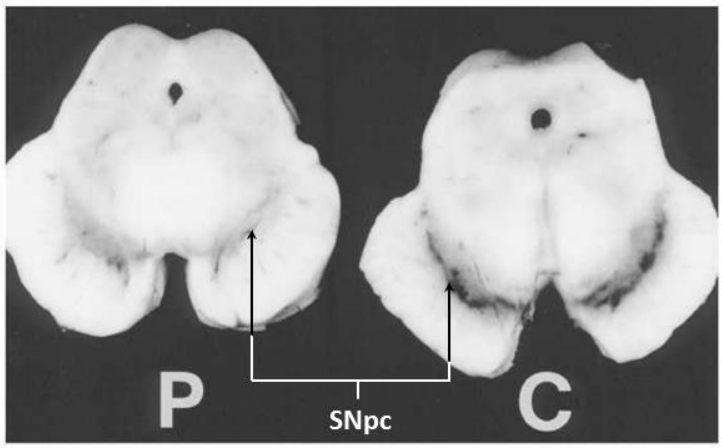

Fig. 1.1 Degeneration of SNpc DA neurons in PD PD is characterised by the loss of DA neurons in the area of the midbrain known as the SNpc. These neurons are a dark brown colour due to a high content of neuromelanin and their deterioration can be seen in the loss of pigmentation in horizontal sections of the midbrains of a PD patient (P) compared to a healthy control (C) (adapted from (Mackenzie 2001)).

The condition was first characterised in 1817 in James Parkinson's 'Essay on the Shaking Palsy', and involvement of the DA system was confirmed in 1967 with the discovery that oral administration of L-DOPA (L-3,4-dihydroxyphenylalanine), a DA precursor molecule, was successful at inducing remission of PD symptoms (Cotzias, Van Woert et al. 1967). Forms of the disease can be either familial or idiopathic, with idiopathic cases making up approximately two-thirds of those diagnosed. PD is the second most common neurodegenerative condition after Alzheimer's disease and affects approximately 0.25% of people in industrial countries. The disease is age-related with the majority of patients aged over 50 (Schrag, Ben-Shlomo et al. 2000) and prevalence rising exponentially to 1% of the population over 60 and 4% by 80 years and over. PD appears to have a higher incidence in men than women with a reported prevalence ratio of 155 males per 100 females in the USA (Wright Willis, Evanoff et al. 2010).

1.1.1 Pathogenesis & Clinical Development of Parkinson's Disease

1.1.1.1 Diagnosis & Clinical Signs

Idiopathic PD is most commonly diagnosed according to the UK Parkinson's Disease Society Brain Bank clinical diagnostic criteria, which state that the patient must suffer from bradykinesia, as well as at least one of muscular rigidity, 4-6 Hz resting tremor or postural instability not caused by primary visual, vestibular, cerebellar or proprioceptive dysfunction. If these primary symptoms are present, the patient must, in addition, not show evidence of any of the following exclusion criteria:

- history of repeated strokes with stepwise progression of Parkinsonian features
- history of repeated head injury
- history of definite encephalitis
- oculogyric crises
- neuroleptic treatment at onset of symptoms
- more than one affected relative
- sustained remission
- strictly unilateral features after three years
- supranuclear gaze palsy
- cerebellar signs
- early severe autonomic involvement
- early severe dementia with disturbances of memory, language and praxis
- Babinski sign
- presence of a cerebral tumour or communicating hydrocephalus on CT scan.
- negative response to large doses of levodopa (if malabsorption excluded)
- MPTP exposure

Finally three or more of the following supportive prospective positive criteria are required for diagnosis of definite PD:

- unilateral onset
- rest tremor present
- progressive disorder
- persistent asymmetry affecting the side of onset most
- excellent response (70-100%) to levodopa
- severe levodopa-induced chorea
- levodopa response for 5 years or more
- clinical course of 10 years or more

(criteria taken from (Gibb and Lees 1988)).

Clinically, PD manifests as the triad of classic symptoms mentioned above: bradykinesia, rigidity and resting tremor which become apparent when 50-70% of the DA neurons of the SNpc have been lost (Hirsch, Graybiel et al. 1988; Fearnley and Lees 1991). This motor disruption is due to the lack of DA projection to the striatum brought about by the degeneration of DA neurons in the SNpc leading to a loss of input to the nucleus of the basal ganglia which consists of a complex network that integrates cortical areas, basal ganglia nuclei and thalamus and controls movement (Alexander, Delong et al. 1986). A model has been proposed to explain how DA depletion in the striatum leads to motor dysfunction (Albin, Young et al. 1989; DeLong 1990) through a lack of DA input from the striatum to the GABAergic medium spiny neurons of both the direct (induces movement) and indirect (supresses movement) pathways of motor behaviour control in the basal ganglia. This deletion affects the balance of these pathways and results in motor alterations (deficits in movement initiation and execution) deriving from the lack of DA neurotransmission in the striatum. Figure 1.2 summarises the pathways of the basal-ganglia in health and PD.

In addition to these core indications, patients may display disturbances in balance and posture as well as non-motor signs including neuropsychiatric symptoms, sleep disorders, autonomic symptoms, gastrointestinal symptoms, sensory dysfunctions and more (PD non-motor symptoms are detailed in Table 1.1) (Chaudhuri, Healy et al. 2006) and are due to disruption of noradrenergic, serotonergic and cholinergic systems; PD is therefore now considered a multi-system disorder.

Neuropsychiatric symptoms
Depression, apathy, anxiety
Anhedonia
Attention deficit
Hallucinations, illusion, delusions
Dementia
Obsessional behaviour (usually drug induced), repetitive behaviour
Confusion
Delirium (could be drug induced)
Panic attacks
Sleep disorders
Restless legs and periodic limb movements
Rapid eye movement (REM) sleep behaviour disorder and REM loss of atonia
Non-REM-sleep related movement disorders
Excessive daytime somnolence
Vivid dreaming
Insomnia
Sleep disordered breathing
Autonomic symptoms
Bladder disturbances
Sweating
Orthostatic hypotension
Sexual dysfunction
Dry eyes (xerostomia)
Gastrointestinal symptoms (overlaps with autonomic symptoms)
Dribbling of saliva
Ageusia
Dysphagia and choking
Reflux, vomiting
Nausea
Constipation
Unsatisfactory voiding of bowel
Faecal incontinence
Sensory symptoms
Pain
Paraesthesia
Olfactory disturbance
Other symptoms
Fatigue
Diplopia
Blurred vision
Seborrhoea
Weight loss
Weight gain (possibly drug induced)

Table 1.1 Summary non-motor symptoms of PD (adapted from (Chaudhuri, Healy et al. 2006))

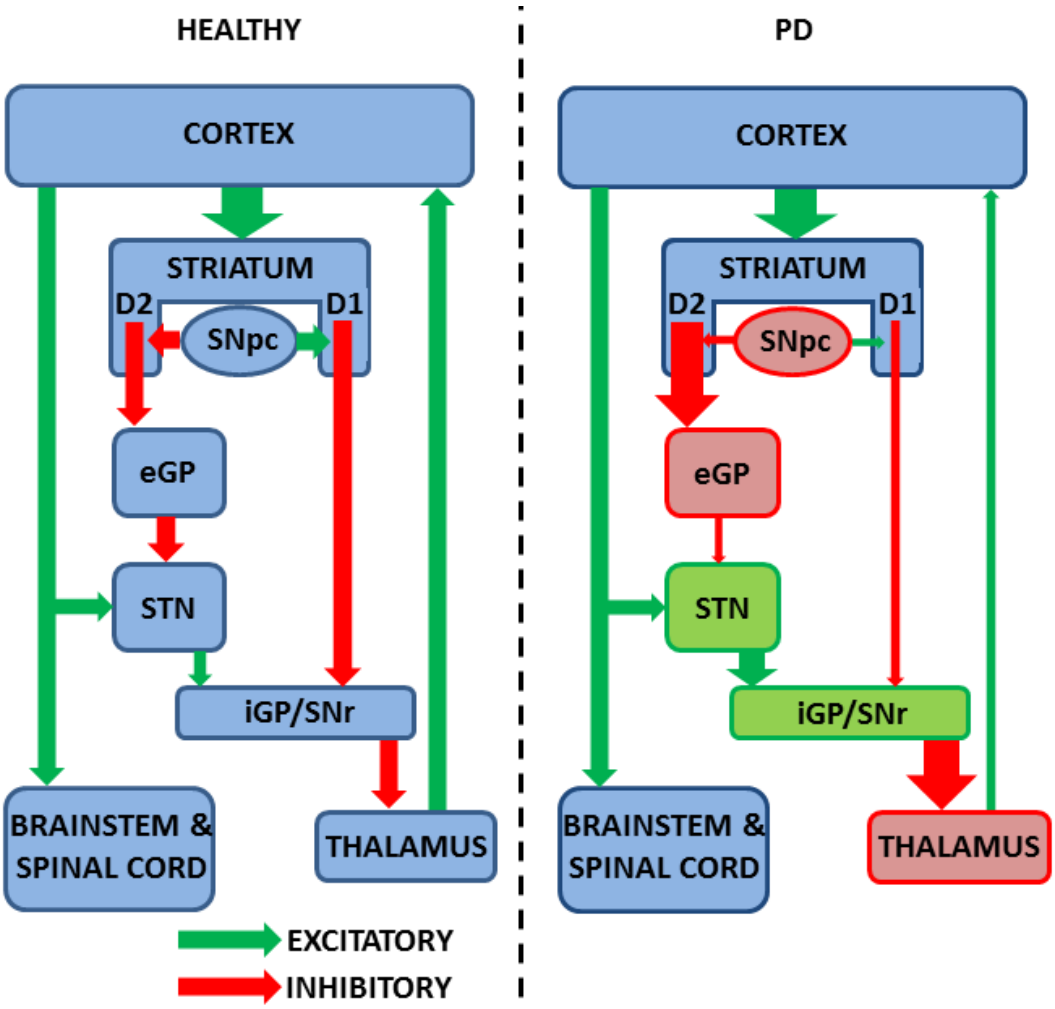

Fig. 1.2 Proposed major pathophysiological changes in the basal ganglia in PD Schematic diagram of basal ganglia in a healthy and in PD individual. The relative size of the arrows indicates the increases or decreases in neuronal activity in the various pathways, and the green (increase) and red (decrease) boxes represents the increase or decrease in neuronal activity within each of the nuclei. Abbreviations: D1/D2 = dopamine receptors; e/iGP = external/internal segment of globus pallidus; STN = subthalamic nucleus; SNpc = substantia nigra pars compacta; SNr = substantia nigra pars reticulata; . Green and red lines indicate excitatory and inhibitory connections, respectively.

Dementia is a very common non-motor symptom of PD, with reports suggesting 40-50% of PD patients also suffer from dementia (Cummings 1988; Hely, Morris et al. 2005). Indications of dementia in PD may be seen with the presence of Lewy bodies (pathological hall marks of PD, described in more detail in section 1.1.1.2 below) in cortical brain regions with the number of Lewy bodies in several cortical areas significantly correlating with cognitive impairment (Mattila, Rinne et al. 2000). The basis for dementia in PD has been suggested to be due to the presence of co-morbid Alzheimer's disease, with a number of studies reporting Alzheimer's pathology in the cerebral cortex of most PD patients with dementia (Boller, Mizutani et al. 1980; Mann and Jones 1990; Jellinger 1997; Jellinger, Seppi et al. 2002). Dementia in PD has

been correlated with atrophy of nucleus basalis Meynert, resulting in a cholinergic deficit, a feature that is shared with Alzheimer's patients, giving a pathological basis for the condition (Candy, Perry et al. 1983; Whitehouse, Hedreen et al. 1983). For a more detailed review of dementia in PD see (Emre 2003).

Olfactory and gastrointestinal disturbances have been reported to be amongst the earliest clinical symptoms of PD (Abbott, Petrovitch et al. 2001; Ponsen, Stoffers et al. 2004; Ross, Petrovitch et al. 2008) and suggested as possible preclinical markers to aid earlier diagnosis of the disease. The early manifestation of olfactory impairment in PD concurs with the developmental staging of the disease proposed by Braak *et al.* (discussed in detail in section 1.1.1.3 below) which suggests early degeneration of extranigral neurons in the olfactory bulb and anterior olfactory nucleus in the presymptomatic early stages of the disease (Braak, Ghebremedhin et al. 2004). The early presentation of gastrointestinal dysfunction can also be related to early Braak staging with the degeneration of the dorsal nucleus of the vagus nerve seen in Braak stage 1. However, loss of DA neurons in the enteric nervous system is also seen in PD (Singaram, Gaumnitz et al. 1995), but gastrointestinal symptoms do not respond to DA treatment suggesting a possible non-DA pathogenic mechanism is involved (Byrne, Pfeiffer et al. 1994).

1.1.1.2 Pathological Features

The primary pathological characteristic of PD is the death of DA neurons in the SNpc. The severity of the DA neuronal degeneration is not homogeneous in PD, with the cell loss preferentially occurring in the ventrolateral region of the SNpc (Fig 1.3), followed by the mediolateral and then dorsal tiers respectively, directly opposite to the cell loss pattern seen across the SNpc of aging controls (Fearnley and Lees 1991). The ventrolateral region of the SNpc contains the majority of the projections to the striatum (i.e. the nigrostraital DA neurons), leading directly to the depletion in striatal dopamine seen in the PD.

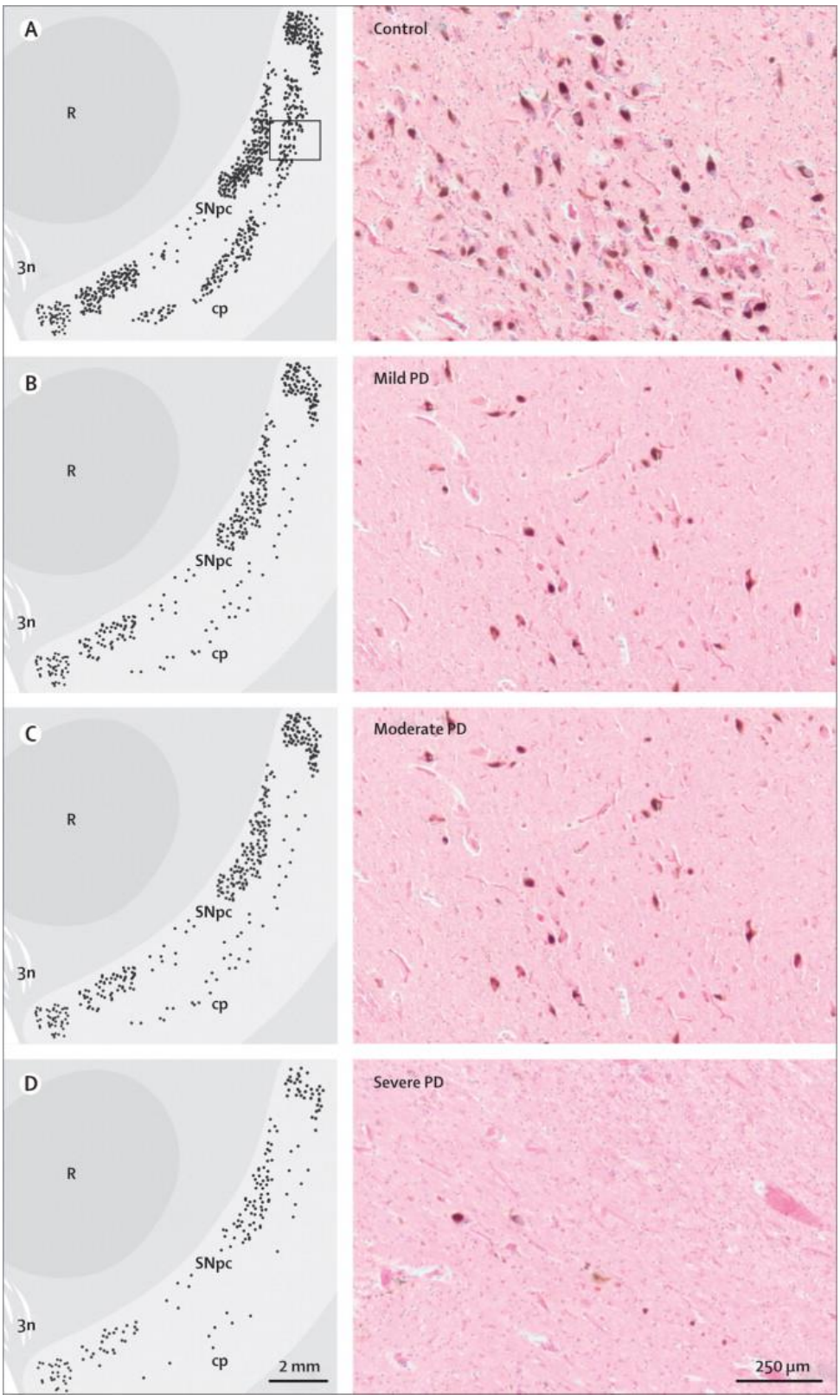

Fig. 1.3 DA neuron distribution & number in PD SNpc The severity of the DA neuronal loss in PD is not homogeneous and is more pronounced in the ventral and lateral regions of the SNpc. Left images show templates of the distribution of pigmented neurons and right show examples of SNpc DA neuron density (x40 magnification, haematoxylin & eosin stained sections) in (A) healthy controls and in patients with (B) mild, (C) moderate, or (D) severe PD. 3n=exiting 3rd nerve fibres. cp=cerebral peduncle. R=red nucleus. (Taken from (Dickson, Braak et al. 2009))

The second major pathological hallmark of PD is the presence of proteinaceous intraneuronal inclusions termed Lewy bodies (LBs) along with the presence of Lewy neurites within neuronal dendrites and axons of surviving cells of the SNpc as well as other brain regions (Spillantini, Crowther et al. 1998; Wakabayashi, Tanji et al. 2007) (Fig. 1.4). LBs are typically found in brainstem nuclei and in limbic and neocortical regions in PD, and additionally can be identified in autonomic ganglia in the periphery (McKeith, Galasko et al. 1996). There are two morphological types of LBs: brainstem (classic) and cortical Lewy bodies. Classic Lewy bodies are intracytoplasmic eosinophylic inclusions that consist of a dense core surrounded by a pale halo (Spillantini, Crowther et al. 1998). They are spherical in shape; however a recent report of Kanazawa et al. also showed convoluted LBs and their continuity with Lewy neurites, which may suggest LBs evolve from Lewy neurites (Kanazawa, Uchihara et al. 2008). Typically, classic LBs are seen in dopaminergic neurons of the substantia nigra and noradrenergic neurons of the locus coeruleus, although they were originally described in neurons of the basal forebrain (Burkhardt, Filley et al. 1988). Cortical LBs are less well-defined structures compared to classic LBs, lacking the halo and located predominantly in limbic areas of the brain, such as the amygdala, entorhinal, insular and cingulate cortices (McKeith, Galasko et al. 1996). Ultrastructurally, both classic and cortical LBs are composed of filamentous material that is insoluble in SDS and resembles neurofilament (Galloway, Mulvihill et al. 1992).

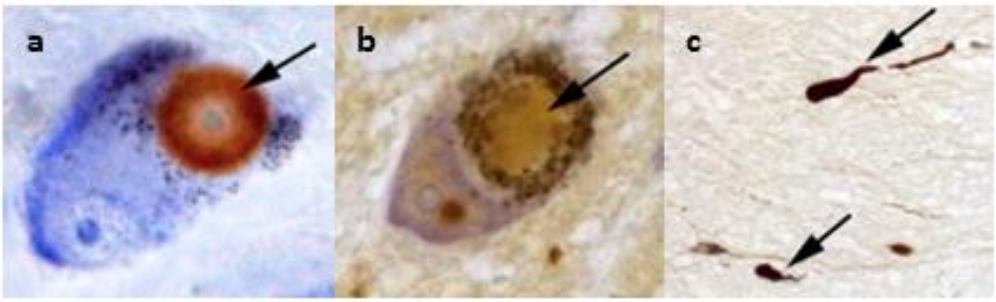

Fig. 1.4 Lewy bodies & neurites Immunohistological staining of Lewy bodies & neurites in the SNpc of a PD patient brain. (a) Lewy body stained for α-synuclein, (b) Lewy body stained for ubiquitin, (c) Lewy neurite stained for α-synuclein. (Adapted from (Licker, Kövari et al. 2009))

Electron-microscope examination of Lewy bodies demonstrates that the core contains dense granular material, whereas the outer halo is composed of radiating filaments of 7-20 nm in diameter (Spillantini, Crowther et al. 1998). Immunohistochemical staining and proteomic analyses have deciphered the complexities of the molecular composition of Lewy bodies and Lewy neurites. α-synuclein (Spillantini, Schmidt et al. 1997; Spillantini, Crowther et al. 1998), ubiquitin (Kuzuhara, Mori et al. 1988) and neurofilaments (Schmidt, Murray et al. 1991) appear to be the major components (Fig. 1.4 a & b), with α-synuclein representing the most

prominent and consistent marker of LBs. More recently triple immunolabeling for these epitopes has revealed a three-layered internal structure of LBs and neurites (Kanazawa, Uchihara et al. 2008). These primary molecular constituents are stratified into concentric layers with ubiquitin staining in the centre, surrounded by α-synuclein and neurofilament on the periphery, which is consistent with previous observations (McNaught, Shashidharan et al. 2002). This accumulation of abnormal aggregated α-synuclein in the brains of PD patients classifies the disease as a synuclienopathy.

Dysfunction of protein metabolism appears to be an important factor in LB formation and the neurodegeneration associated with their presence (for review see(Ciechanover and Brundin 2003)), but the significance of these aggregates is still a subject of debate. It is unclear if LBs are pathogenic and mechanistically cause neuronal death (Trojanowski, Goedert et al. 1998) or rather the actual function of LBs is neuroprotective by sequestering unwanted, potentially toxic proteins such as mutated α-synuclein (Lashuel, Hartley et al. 2002; Lashuel, Petre et al. 2002; Olanow, Perl et al. 2004). The latter hypothesis is supported clinically by evidence, particularly from autosomal recessive juvenile Parkinson's disease due to Parkin mutation, demonstrating that neurodegeneration can occur without the presence of LBs in both apparently sporadic and familial forms of PD (Mori, Kondo et al. 1998; Wakabayashi, Toyoshima et al. 1999). LBs are also reported in cognitively intact individuals over 65 years (Braak, Del Tredici et al. 2003) although this may indicate an early phase of PD prior to cell loss and clinical presentation.

1.1.1.3 Development

The progression of PD has been assessed post mortem leading to the development of a neuropathological staging scheme based on the distribution of α-synuclein/Lewy bodies throughout the brain by Braak *et al.* (Braak, Ghebremedhin et al. 2004). The stages are characterised by sequential involvement of brain regions, defined by the presence of LBs, starting with the dorsal nucleus of the vagus nerve and anterior olfactory nucleus and spreading through the rest of the brainstem, mid and forebrain and finally throughout the cortex with symptoms increasing in severity and scope as more brain regions develop pathology (See Fig. 1.5 for further details). Patients are typically described as presymptomatic in stages 1-3 until a threshold is passed with sufficient pathology and DA cell death in the SNpc accumulating at stage 3 or 4 to manifest as motor dysfunction through loss of dopamine neurotransmission in the striatum. Further neurodegeneration proceeds to first order sensory

and premotor and high-order sensory association areas, prefrontal neocortex, and finally into primary sensory and motor areas. This degeneration induces several late stage PD symptoms including hallucinatory episodes, dementia and states of confusion.

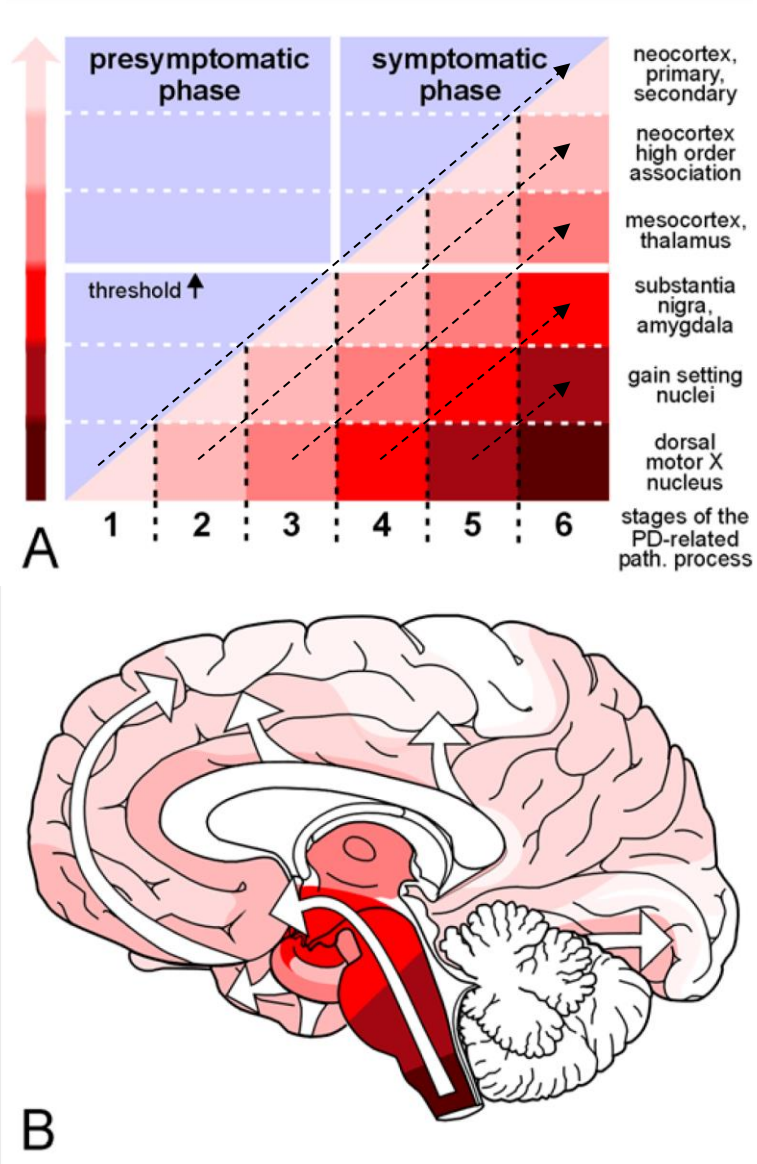

Fig. 1.5 Progression of PD-related intraneuronal pathology (A)The pathological process targets specific subcortical and cortical induction sites. Lesions initially occur in the dorsal IX/X motor nucleus and frequently in the anterior olfactory nucleus as well. Thereafter, less susceptible brain structures gradually become involved (see white arrows). The pathology in the anterior olfactory nucleus expands less readily into related areas than that evolving in the brain stem. The brain stem pathology takes an upward course (see white arrows). Cortical involvement follows, commencing with the anteromedial temporal mesocortex. From there, the neocortex succumbs, beginning with high order sensory association and prefrontal areas. First order sensory association/premotor areas and, thereafter, primary sensory and motor fields follow suit. The gradual decrease in shading intensity is intended to represent the topographical expansion of the lesions during the course of the disease.
(B) Simplified diagram showing the topographic expansion of the lesions (from bottom to top: dorsal motor X nucleus to neocortex, primary, secondary) and, simultaneously, the growing severity on the part of the overall pathology (from left to right: stages 1–6). With the addition of further predilection sites, the pathology in the previously involved regions increases. (Adapted from (Braak, Del Tredici et al. 2003; Braak, Ghebremedhin et al. 2004))

1.1.1.4 Management

Although there are currently no cures for PD available, there are a number of ways that the disease can be managed. Pharmacologically, PD can be treated by modulating DA levels at the synapse of remaining DA neurons, using a variety of strategies; DA production can be increased, breakdown of DA inhibited, or the actions of DA mimicked (Fig 1.6).

The major and most successful treatment strategy is to increase DA levels by administering the DA precursor molecule L-DOPA, known by the trade name Levodopa. *In vivo*, DA is formed from L-DOPA by the enzyme dopa decarboxylase; therefore increasing levels of L-DOPA in the brain will lead to an increase in DA levels in the striatum and a reduction in the motor dysfunction seen in PD. DA cannot be used directly to treat PD as it does not cross the blood brain barrier; however Levodopa can be actively transported into the brain by the L-type amino acid transporter (Oldendorf and Szabo 1976). The major problems with Levodopa are that chronic treatment can lead to dyskinesia, tolerance and diminished effects, and rapid fluctuations in clinical state where hypokinesia and rigidity suddenly worsen for a period of time, known as an 'on-off effect'. Despite this, Levodopa is currently the most commonly used and effective PD treatment.

Mimicking the effect of DA by the use of DA receptor agonists is another strategy used in the management of PD. Current therapeutic agents in use include the D_2, D_3 and D_4 specific agonists Pramipexole (Shannon, Bennett Jr et al. 1997) and Ropinirole (Adler, Sethi et al. 1997), and the non-specific DA agonist Apomorphine (Merims, Galili-Mosberg et al. 2000). Although these DA agonists do show some effect in reducing motor dysfunction and do not show the tolerance and dyskinesia seen with Levodopa, they have been shown to be less effective than Levodopa (Holloway, Shoulson et al. 2000) and can cause hallucinations, oedema, excessive diurnal somnolence, and impulse control disorder (Gottwald, Bainbridge et al. 1997). Further compounds are in development with varying DA receptor specificity and solubility to try and improve efficacy and reduce adverse effects.

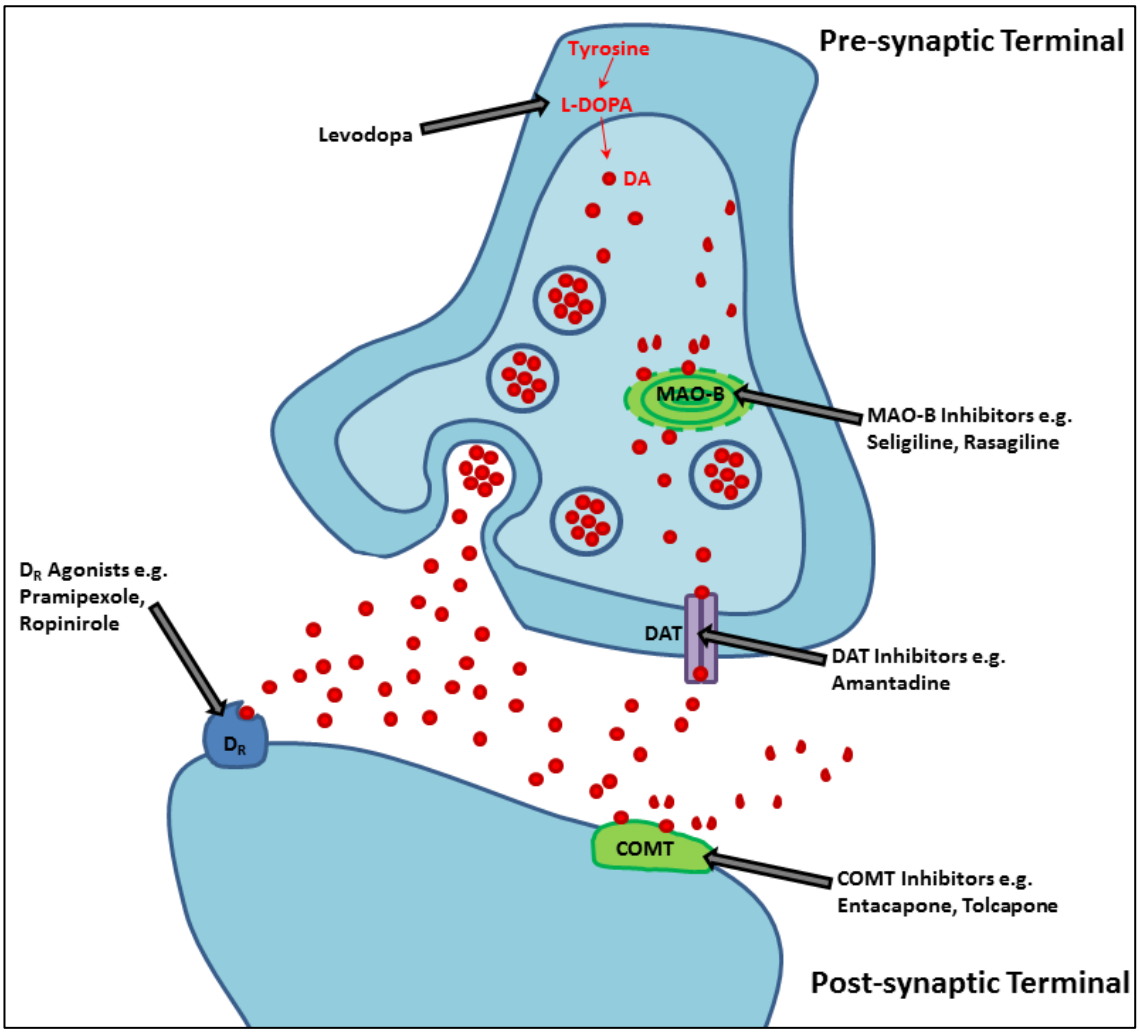

Fig. 1.6 Pharmacological strategies for PD management Schematic representation of a DA neuronal synapse showing the molecular targets of various pharmacological agents used to manage the disease. Key: COMT – Catechol-O-Methyl Transferase, D_R- DA receptor 1/2, MAO-B – monoamine-oxidase-B.

To increase striatal DA, compounds that inhibit the enzymes that breakdown DA can be used. Monoamine-oxidase-B (MAO-B), an enzyme located in the outer mitochondrial membrane, and Catechol-O-methyl-transferase (COMT), an enzyme located in the synaptic cleft, sequentially catalyse the breakdown of DA to its major metabolite homovanillic acid (HVA) in neurons and glia. Inhibition of MAO-B by Selegiline and Rasagiline has been shown to increase free levels of DA and so reduce motor dysfunction in the striatum of PD patients particularly when used in combination with Levodopa (Przuntek, Conrad et al. 1999; Rabey, Sagi et al. 2000). COMT is also responsible for the breakdown of L-DOPA, so the COMT inhibitors Entacapone and Tolcapone are often given in combination with Levodopa to improve efficacy and have been shown to reduce the 'on-off effect' seen with Levadopa treatment alone (Dupont, Burgunder et al. 1997; Smith, Jackson et al. 2005).

Preventing DA reuptake using the DAT (dopamine active transporter) inhibitor Amantadine is used to treat motor dysfunction and Levodopa induced dyskinesia in PD patients by increasing the amount of DA in the synaptic cleft. However, reviews on Amantadine use have found inadequate evidence to support its use for either the motor disruption or Levodopa induced dyskinesia in PD (Crosby, Deane et al. 2003; Crosby, Deane et al. 2003).

As well as the pharmacological management of PD mentioned above, surgical and rehabilitation techniques can be used to alleviate symptoms. There are two main surgical approaches used to manage PD - generally in cases where drug therapy is no longer effective - deep brain stimulation and lesioning of overactive cortical regions. Deep brain stimulation involves the bilateral implantation of a device in the brain which sends electrical impulses to the subthalamic nucleus or globus pallidus of the brain to activate them. Although it has been shown to be more effective than pharmacological therapy, it is far more invasive and associated with an increased risk of serious adverse events so not widely used (Weaver, Follett et al. 2009). Although destruction of specific brain regions has been shown to alleviate PD symptoms, leisioning is most widely and successfully used to treat the dyskinesia suffered following long term Levodopa treatment by destroying cells in the globus palladius by pallidotomy (Laitinen, Bergenheim et al. 1992; Lozano, Lang et al. 1995). Surgery is not a routine occurrence and generally reserved for patients in the advanced stages of the disease. In addition to the more invasive management strategies described, it has been shown that regular exercise regimes can have a positive effect on motor function in PD patients (Goodwin, Richards et al. 2008), an effect that is more pronounced when combined with a supervised physiotherapy programme (Dereli and Yaliman 2010).

In summary, while the motor symptoms of PD can be reduced, the treatment methods currently available are inadequate, transient and associated with significant adverse effects meaning the prognosis for - and quality of life of - patients is unsatisfactory. Consequently, the disease is still a great unmet medical need with greater knowledge of the pathogenesis and elucidation of the mechanisms underlying PD needed to improve the current situation.

1.1.2 Molecular Mechanisms of Parkinson's Disease

The exact mechanism by which SNpc cell death in PD occurs is poorly understood but several lines of evidence implicate mitochondrial dysfunction, oxidative stress, ubiquitin system impairment and excitotoxicity, all of which may be interlinked (Bedford, Hay et al. 2008; Meredith, Totterdell et al. 2009; Navarro, Boveris et al. 2009).

1.1.2.1 Mitochondrial Dysfunction

Mitochondrial dysfunction with Complex I deficiency and impaired electron transfer in the substantia nigra in PD have been reported (Schapira, Cooper et al. 1990; Keeney, Xie et al. 2006). Moreover, mutations in several mitochondrial proteins have been associated with familial forms of PD (Kitada, Asakawa et al. 1998; Bonifati, Rizzu et al. 2003; Valente, Abou-Sleiman et al. 2004), as well as the presence of deletions in mitochondrial DNA identified in aging controls and PD substantia nigra (Bender, Krishnan et al. 2006). For a detailed review of the involvement of mitochondrial dysfunction in PD see (Keane, Kurzawa et al. 2011).

Mitochondria are found in virtually all eukaryotic cells and function to generate cellular energy in the form of adenosine triphosphate (ATP) by oxidative phosphorylation and are also involved in regulation of cell death via apoptosis, calcium homeostasis, haem biosynthesis, the formation and export of iron-sulphur (Fe-S) clusters (reviewed in detail elsewhere (Jiang and Wang 2004; Lill, Dutkiewicz et al. 2006; Szabadkai and Duchen 2008)), and function in the control of cell division and growth. The mitochondrial electron transport chain is composed of four complexes and an ATP-synthase located in the inner mitochondrial membrane. The function of the chain is to generate cellular energy in the form of ATP. This is accomplished by the transport of electrons between Complexes causing proton (H^+ ions) movement from the matrix to the inter-membrane space generating a proton concentration gradient used by ATP-synthase to produce ATP (for details of individual complex functions see Fig. 1.7 & Table 1.2).

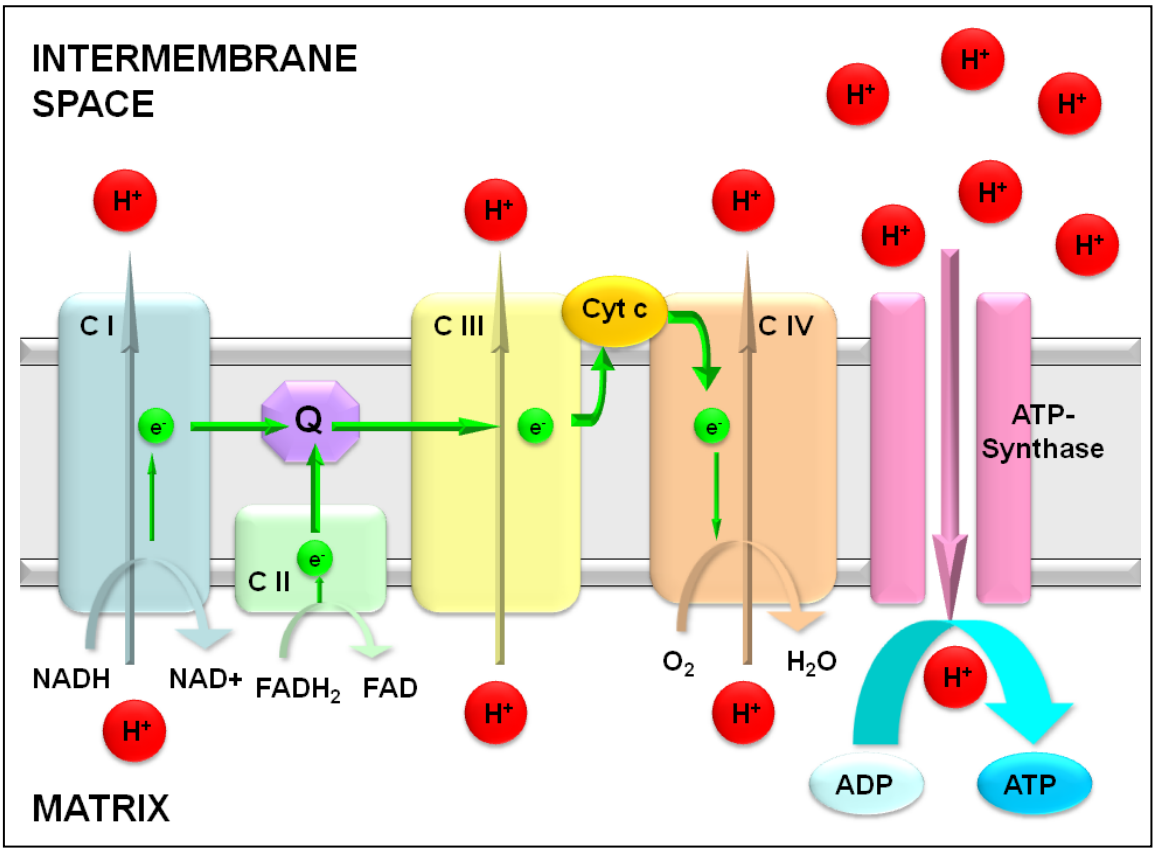

Fig. 1.7 Mitochondrial electron transport chain Schematic representation of the mitochondrial electron transport chain involved in oxidative phosphorylation. CI & II (Complexes I & II) transport electrons (e^-s) generated by the conversion of NADH to NAD+ (CI) or $FADH_2$ to FAD (CII) through Q (ubiquinone), CIII, Cyt c (cytochrome c) and finally CIV, which uses an e^- to convert O_2 to H_2O. During electron transfer, CI, II & IV pump protons (H^+s) from the mitochondrial matrix into the intermembrane space generating an H^+ concentration gradient that drives the formation of ATP from ADP by ATP-synthase (Complex V).

Whilst electron transport is a highly efficient process in mitochondria (Chan 2006), during the process of oxidative phosphorylation, electrons can leak from the chain, specifically from CI (Takeshige and Minakami 1979) and CIII (Beyer 1992), and react with oxygen to form superoxide ($\cdot O_2^-$). Under normal physiological conditions this $\cdot O_2^-$ production occurs at relatively low levels, with approximately 1% of the mitochondrial electron flow forming $\cdot O_2^-$ (Lass, Agarwal et al. 1997), and is removed by mitochondrial antioxidants such as manganese superoxide dismutase (MnSOD) which converts $\cdot O_2^-$ to H_2O_2 which is then converted to H_2O by glutathione (GSH). Given the high activity of the respiratory chain under even normal circumstances, the small leakage of electrons in mitochondria is still a major source of $\cdot O_2^-$ within many eukaryotic cells (Cadenas and Davies 2000). It is thought that dysfunction in this process leading to an increase in $\cdot O_2^-$ production could be one of the main drivers of cell death in the SNpc in PD (Sian, Dexter et al. 1994; Jha, Jurma et al. 2000).

As neurons have a considerable energy need and are also highly equipped with mitochondria they are extremely sensitive to mitochondrial dysfunction. Several neurological disorders are associated with mitochondrial dysfunction and demonstrate enhanced production of free radical species (Finsterer 2006; Lin and Beal 2006). The first line of evidence for a link between mitochondrial dysfunction and PD came from the description of Complex I (CI) deficiency in the post-mortem SNpc of PD patients and has been suggested to be one of the fundamental causes of the disease (Mizuno, Ohta et al. 1989; Schapira, Cooper et al. 1990). This CI deficiency was also seen in the frontal cortex in PD (Parker Jr., Parks et al. 2008), and in peripheral tissues such as platelets (Haas, Nasirian et al. 1995) and skeletal muscle (Bindoff, Birch-Machin et al. 1991) suggesting that there is a global reduction in mitochondrial CI activity in PD. This defect may be due to oxidative damage to CI and its mis-assembly since this is a feature of isolated PD brain mitochondria (Keeney, Xie et al. 2006). Incidental Lewy body disease (ILBD) which is considered by some to be a preclinical indicator of PD, has been shown to have an intermediate level of CI activity in the SNpc between healthy and PD patients (Schapira, Mann et al. 1990) which further supports the theory of mitochondrial dysfunction. This inhibition of CI can lead to the degeneration of affected neurons by a number of mechanisms such as increased oxidative stress and excitotoxicity (Sherer, Betarbet et al. 2002) which will be described below.

A decrease in the function of Complex III (CIII) has also been reported in the lymphocytes and platelets of PD patients (Haas, Nasirian et al. 1995; Shinde and Pasupathy 2006). A link between impairment of mitochondrial CIII assembly, an increase in free radical production and PD has also been identified (Rana, De Coo et al. 2000). This increase in free radical release may be due to the increased leakage of electrons from CIII (as explained below). Alternatively the inhibition of CIII assembly, causes a severe reduction in the levels of functional CI in mitochondria (Acín-Pérez, Bayona-Bafaluy et al. 2004) which could lead to an increase in free radical production through CI deficiency. In addition, the CI and II electron acceptor ubiquinone has also shown to be reduced in the mitochondria of PD patients (Shults, Haas et al. 1997) and loss of DA neurons in aged mice treated with the Parkinsonian neurotoxin 1-methyl-4-phenyl-1,2,3,6-tetrahydropyridine (MPTP) was attenuated by ubiquinone (Beal, Matthews et al. 1998), providing more evidence for the involvement of mitochondrial dysfunction in PD.

There is less evidence for the involvement of Complexes II, IV and ATP-synthase in PD. This being said, a link between Complex IV (CIV) inhibition and PD pathogenesis has been proposed; it has been shown that knockdown of Pink-1, mutations of which have been linked with PD,

leads to inhibition of CIV (Gegg, Cooper et al. 2009) suggesting possible CIV inhibition in the disease. No significant evidence of Complex II (CII) dysfunction has been reported, as any possible inhibition of CII by known PD-linked toxins is small enough to be insignificant in relevance when compared to the extent of CI inhibition mediated by these compounds (Krueger, Tan et al. 1993). Finally, while there has been a report of reduced ATP-synthase levels in the SN of PD patients (Ferrer, Perez et al. 2007), there is no evidence as to whether this is a pathological effect or a consequence of the mitochondrial dysfunction and damage seen in the disease.

Complex	Name	Evidence of involvement in PD
I	NADH dehydrogenase	• Reduced function widely reported in tissue of PD patients. • Range of PD-linked toxins shown to inhibit CI. • Inhibition shown to increase ROS and induce DA neuronal death.
II	Succinate dehydrogenase	• Possible inhibition by toxins but at significantly lower levels to the CI inhibition observed.
III	Cytochrome c reductase	• Reduced function in tissue of PD patients.
IV	Cytochrome c oxidase	• Inhibited when Pink-1 knocked out.
-	ATP-synthase	• Levels reduced in PD patient SN.

Table 1.2 OXPHOS pathway Complexes and involvement in PD Summary of the names of the various OXPHOS Complex enzymes and evidence of their involvement in PD.

Mitochondria have also been shown to be linked to LBs, with large numbers of mitochondria observed in early-stage LBs (Gai, Yuan et al. 2000; Bedford, Hay et al. 2008). Mitochondrial accumulation has also been found in nigral Lewy and pale bodies (possibly precursors of LBs (Dale, Probst et al. 1992)), and cortical LBs, but not in classical LBs in PD patients or a mouse 26S proteasomal knockout model (Bedford, Hay et al. 2008). This may suggest direct involvement of mitochondria in early stages of LB formation. According to the aggresome-related model of LB formation, mitochondria may be sequestered to the inclusion bodies in order to facilitate the removal of unwanted proteins (see (Olanow, Perl et al. 2004) for extensive review).

1.1.2.2 Oxidative Stress

Inhibition of Complex I or III of the mitochondrial electron transport chain described above causes an increase in the release of electrons from the transport chain into the mitochondrial matrix which then react with oxygen to form reactive oxygen species (ROS) such as $\cdot O_2^-$, hydroxyl radicals (·OH) and nitric oxide (NO·). This increase in the normal electron leakage occurs by blockage of electron movement along the chain to the next acceptor molecule. An example of this is the finding that blockade of the electron accepting capability of the ubiquinone binding site of Complex I leads to an increased production of electron radicals in rat skeletal muscle mitochondria (Lambert and Brand 2004). The ROS formed, can act as signalling molecules by causing lipid peroxidation or can promote excitotoxicity, both of which lead to modification of proteins and eventual cell death. The main areas in which ROS cause damage in the cell include oxidative DNA damage, lipid peroxidation, and protein oxidation and nitration. The ·OH radical has been shown to react with the double bond of DNA bases leading to damaging DNA lesions (Cooke, Evans et al. 2003), and an impairment of normal cellular function. There is evidence linking this mechanism of cell death to PD in the finding of increased levels of 8-hydroxyguanosine, produced by oxidative damage to DNA, in the SNpc of PD patients (Alam, Jenner et al. 1997; Zhang, Perry et al. 1999). Peroxynitrite (formation discussed below) also increases DNA single strand breaks (Szabo, Zingarelli et al. 1996) which causes activation of poly(ADP-ribose) polymerase (PARP) which, in turn, disrupts the mitochondrial respiratory chain and ATP production via depletion of intracellular NAD+ stores, so exacerbating the original mitochondrial dysfunction (Przedborski and Vila 2001).

Amongst the most common mechanisms of protein damage caused by ROS are oxidation to form carbonyl groups on proteins and nitration by peroxynitrite. Reactive ROS can readily oxidise amino acids on various cellular proteins to form carbonyl groups which can disrupt the physiological function of the affected protein and lead to cytotoxic protein aggregates, activation of cell death pathways and impairment of neuroprotective pathways (Esrefoglu 2009). An increase in these carbonyl groups has been reported in the SNpc and in the basal ganglia and prefrontal cortex of PD patients (Floor and Wetzel 1998) suggesting a role in the disease which is widespread throughout the brain. Peroxynitrite is formed by the reaction of ROS with nitric oxide and can nitrate tyrosine residues on proteins (Reiter, Teng et al. 2000), damaging them and leading to cell death. These nitrotyrosine residues are present in LBs in PD neurons signifying the possibility that protein nitration may contribute to the pathology of PD (Good, Hsu et al. 1998). Peroxynitrite (Radi, Beckman et al. 1991) and other ROS (Armstrong and Buchanan 1978) can also oxidise sulphydryl groups on glutathione, leading to depletion of anti-oxidant defences, and other thiol containing co-factors, disrupting various cellular

processes and structures. The final link between PD and mitochondrially generated ROS through protein damage comes with the discovery of nitrated and oxidatively damaged misfolded proteins that have strong genetic links with the disease such as α-synuclein, DJ-1, Parkin and PINK-1 (Polymeropoulos, Lavedan et al. 1997; Kitada, Asakawa et al. 1998; Kruger, Kuhn et al. 1998; Bonifati, Rizzu et al. 2003; Valente, Abou-Sleiman et al. 2004; Zarranz, Alegre et al. 2004) suggesting that these disease associated proteins are major targets of free radical damage in sporadic forms of PD.

Lipid peroxidation is another of the main types of cellular damage caused by ROS occurring when ROS react with hydrogen in the lipid leading to the formation of a lipid radical. This radical can then form a further lipid radical via an intermediary by reacting with a hydrogen atom leading to a chain reaction and breakdown of the lipid. In the cell membrane phospholipids are particularly susceptible to this damage due to their polyunsaturated nature, leading to damage of both cell and organelle membranes and severe cellular dysfunction. There have been strong links between increased lipid peroxidation and PD with increased levels shown to be present and cause cell death in the nigral cells of PD patients (Dexter, Carter et al. 1986; Dexter, Carter et al. 1989) suggesting a role for it in the mechanisms of neuronal death.

All of these mechanisms of oxidative stress can feed back to the mitochondria via a series of signalling pathways and cause further exacerbation and mitochondrial dysfunction by damaging mitochondrial DNA (mtDNA). In this way ROS driven mitochondrial dysfunction acts to propagate itself via a feedback loop leading to accelerated cellular damage and death and contributing to PD.

This oxidative damage could be exacerbated in PD by the discovery of reduced antioxidant defences in patients with the disease. The main line of evidence relates to reduced GSH, which has been found to be selectively decreased in the SNpc of patients with PD (Jenner, Dexter et al. 1992), leading to a decline in cellular capability to inactivate H_2O_2 and peroxynitrite. This is thought to be an early event in PD pathology since lower levels of reduced GSH in incidental LB disease are of the same magnitude as those found in PD (Jenner 1993). There have not been consistent reports of changes in the levels of most of the other major antioxidant systems; however cases of an increase in mitochondrially located MnSOD in PD patients have been described (Saggu, Cooksey et al. 1989; Yoritaka, Hattori et al. 1997). This supports a link between mitochondrial dysfunction generated superoxide and PD since MnSOD is the main $\cdot O_2^-$ scavenging system in mitochondria.

Since there are elevated markers of oxidative damage in the brains of PD patients, including lipid peroxidation (Dexter, Carter et al. 1989) protein damage (Floor and Wetzel 1998; Good, Hsu et al. 1998) and oxidative DNA damage (Alam, Jenner et al. 1997; Zhang, Perry et al. 1999) oxidative stress is an established event in PD. This evidence combined with the PD-like effects of known Complex I inhibitors and ROS inducers such as MPTP (Przedborski, Tieu et al. 2004) and rotenone (Betarbet, Sherer et al. 2000) and an increase in the activity of neutralising Superoxide Dismutase (SOD), particularly the mitochondrially localised MnSOD, being found in neurodegenerative disease patients (Yoshida, Mokuno et al. 1994) points to a strong link between ROS and PD.

Iron has also been suggested to be involved in the production and propagation of oxidative stress in DA neurons in PD. Iron is intrinsically linked with mitochondrial function and particularly the brain, since iron is an integral component of all respiratory chain complexes and the uptake of iron by the brain is linked with mitochondrial energy demands (Mash, Pablo et al. 1990). Increased iron levels in the brain have long been associated with PD (Lhermitte J 1924; Sofic, Riederer et al. 1988; Gerlach, Ben-Shachar et al. 1994; Gerlach, Double et al. 1997) although this increase may be an effect of the normal pathological clearance of iron during cell death that occurs in PD. More recently a specific increase in intracellular iron has been observed in SNpc neurones in PD patients (Oakley, Collingwood et al. 2007) suggesting an increase in the cellular accumulation of iron in the disease. Cellular iron normally enters into neurones via the transferrin receptor system and evidence suggests that there is a reduction of this system in PD (Morris, Candy et al. 1994; Mastroberardino, Hoffman et al. 2009), although this may relate more to the loss of SNpc neurones in PD (Faucheux, Hauw et al. 1997). This iron may also be taken up into the mitochondria in the SNpc via the transferrin receptor 2 and increased levels of ferritin have been reported in the mitochondria of SNpc DA neurons of PD patients and rats treated with rotenone (Mastroberardino, Hoffman et al. 2009). ROS with a low oxidative potential, like $\cdot O_2^-$ generated via dysfunction of oxidative phosphorylation, can increase the release of reactive ferrous iron from this ferritin so leading to the creation of more ROS via the Fenton reaction (Double, Maywald et al. 1998) and increasing oxidative stress and cell damage. The evidence that abnormal iron homeostasis is present in PD is clear; however the role of iron in PD as either an initiator or a consequence of pathology remains to be elucidated.

1.1.2.3 Impaired Protein Degradation

The build-up of abnormal protein aggregates is one of the pathological hallmarks of PD, and as such, impairments in the systems involved in protein degradation have been implicated in the disease.

The ubiquitin–proteasome system (UPS) is one of the major mechanisms of protein degradation in the cell whereby proteins for degradation are tagged by multiple ubiquitin molecules and recognised and degraded by the 26/20S proteasome. Impairment of the UPS has been shown to lead to DA neuron degeneration and the formation of LB-like α-synuclein inclusions in surviving neurons (McNaught, Mytilineou et al. 2002). The UPS has also been shown to be involved in the degradation of wild-type α-synuclein in healthy cells (Webb, Ravikumar et al. 2003), suggesting dysfunction in the system may contribute to α-synuclein pathology and DA degeneration in PD. This is supported by the finding that LBs contain components of the ubiquitin-proteasome system, although unlike functional aggresomes in healthy cells, they fail to degrade abnormal proteins, but are thought to sequester them to delay their ability to damage, and lead to the death of, DA neurons (McNaught, Shashidharan et al. 2002). This build-up of ubiquitinated protein aggregates may be explained by reports that 26/20S proteasome structure and function is disrupted in the SNpc of PD patients (McNaught and Jenner 2001; McNaught, Belizaire et al. 2002; McNaught, Belizaire et al. 2003), meaning that while toxic protein aggregates are tagged, they are not able to be degraded. However, care is needed in the interpretation of this, as it is not clear whether the inhibition of the proteasome actually results in a reduced capacity of the UPS to degrade protein *in vivo* and, if so, whether the reduction is large enough to inflict sufficient damage to the cells to lead to the neurodegeneration seen in PD.

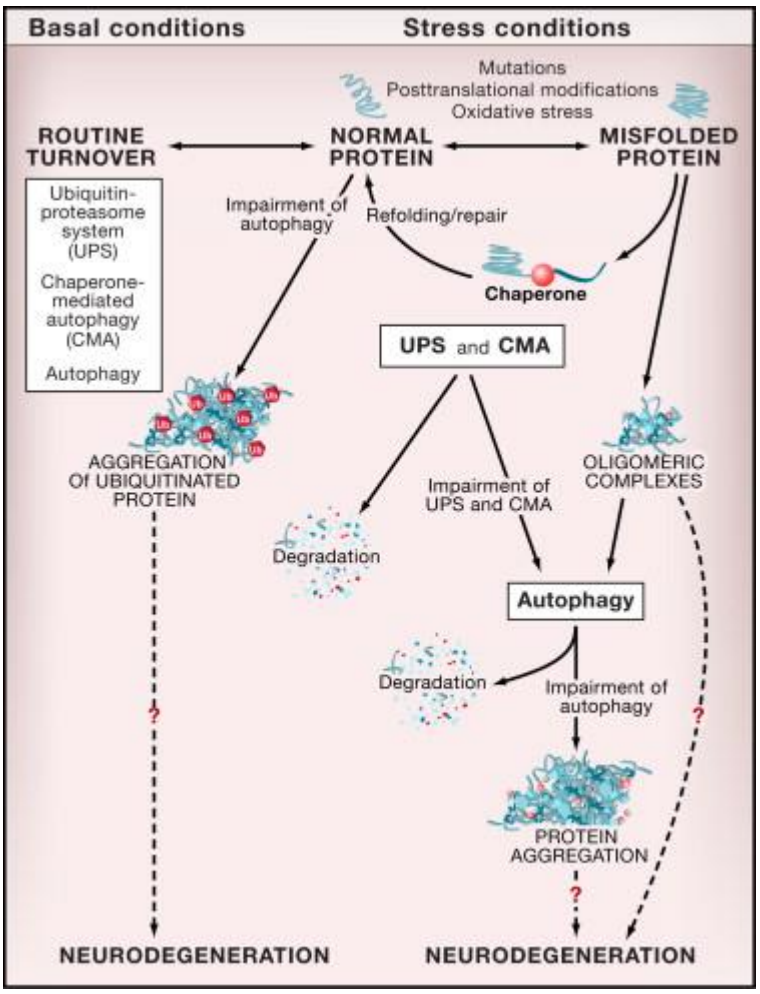

Fig. 1.8 UPS, autophagy, protein quality control, and neurodegeneration in PD Normal proteins are routinely turned over by different protein degradation systems, including the ubiquitin-proteasome system (UPS), chaperone-mediated autophagy (CMA), and macroautophagy (referred to herein as "autophagy"). In autophagy-deficient neurons, there is an accumulation of ubiquitinated protein aggregates which is associated with neurodegeneration. Proteins altered by mutations, posttranslational modifications, or stress (such as oxidative stress, UV irradiation, toxins) undergo a conformational change, are recognized by molecular chaperones, and are either refolded and repaired or delivered to protein degradation systems (usually UPS or CMA). If these protein degradation systems are impaired or if the altered proteins form oligomeric complexes that cannot be recognized by the UPS or CMA, autophagy may be the primary route for the removal of these abnormal and potentially toxic proteins. Impaired autophagy is associated with the formation of protein aggregates and increased neurodegeneration. (Taken from (Levine and Kroemer 2008))

The second major group of pathways by which proteins are degraded are the autophagic pathways whereby cellular contents are engulfed in autophagasomes and fuse with lysosomes for degradation (discussed in more detail in section 1.3.3). Autophagy has been linked with PD as an increase in autophagic vacuoles and autophagasomes has been reported in PD patients (Anglade 1997) and exposure of mice to the PD-linked neurotoxin MPTP is reported to increase autophagy in DA-neurons (Öztaş and Topal 2003). Autophagy has been reported to be integrally involved in the degradation of wild-type α-synuclein in healthy cells (Webb,

Ravikumar et al. 2003) and the presence of pathogenic A30P & A53T mutated α-synuclein has been shown to impair autophagy, preventing degradation of not only toxic mutant α-synuclein but also other autophagy substrates (Cuervo, Stafanis et al. 2004) providing a hypothesis that impaired autophagic clearance of α-synuclein and other proteins may be an important mechanism in DA neuronal degeneration in PD. Further support for the involvement of autophagy in PD comes when combining the age-related nature of the disease with reports that autophagic activity has been shown to be reduced with age (Terman 1995; Cuervo and Dice 2000). However, these findings suggest that autophagic dysfunction is commonly a secondary contributor to the pathology of PD, driven by the build-up of damaged or mutated proteins. Mutations in proteins involved in protein clearance mechanisms which may be a more primary cause of PD, are discussed in section 1.1.3.

The final major cellular content clearance mechanism linked with PD is mitophagy, the process whereby damaged mitochondria are removed from the cell. As damage to mitochondria and the electron transport chain have been heavily linked to PD, and malfunctioning mitochondria can exacerbate this damage, mitophagy may be extremely important in PD. The involvement of mitophagy in PD will be discussed in relation to mutations in PINK1 and Parkin in section 1.1.3.2 below.

1.1.2.4 Ca^{2+}/Excitotoxicity

Excitotoxicity is the mechanism by which nerve cells are damaged by over activity and excessive depolarisation due to overstimulation of N-methyl-D-aspartate (NMDA) and AMPA receptors by neurotransmitter substances such as glutamate. Although, in itself, excitotoxicity is not thought to be a driving mechanism behind PD, glutamate mediated changes to the SNpc may contribute to the induction of the disease and excitotoxicity may well play a secondary role in the DA cell death seen in PD. Several mechanisms for excitotoxicity in neurodegenerative conditions have been proposed (Albin and Greenamyre 1992; Greene and Greenamyre 1996). Excitotoxicity occurs when depolarisation of the neuronal cell membrane from -90mV to between -60 and -30mV leads to a decrease in the magnesium blockade of NMDA receptors. This, in turn, leads to NMDA receptor activation by latent levels of glutamate and causes an intracellular Ca^{2+} accumulation. This increase in Ca^{2+} is then thought to cause neurotoxicity by two main mechanisms. Firstly, Ca^{2+} causes an increase in intracellular NO via activation of nitric oxide synthase (NOS). The excess of NO in the cell can react with $\cdot O_2^-$ to form peroxynitrite (Dawson and Dawson 1996), which can cause cell death by mechanisms similar to those caused by ROS and mentioned above. As well as the

peroxynitrite, NO itself can lead to cell damage via nitrosylation of various proteins. A second mechanism driven by intracellular Ca^{2+} increase causes toxicity in DA neurons by acting on mitochondria; the Ca^{2+} influx seen in excitotoxicity is extensively accumulated in the mitochondria and leads to effects on mitochondrial membrane potential and ATP synthesis as well as generation of ROS (Nicholls and Budd 1998). This contributes to the oxidative damage discussed above and feeds back causing further malfunction of the cell's Ca^{2+} homeostasis and additional cellular damage.

Mitochondrial dysfunction can lead to excitotoxicity and cause a reduction in cellular ATP levels, an increase in cellular Ca^{2+} or a combination of both (Sherer, Betarbet et al. 2002). Inhibition of Complex I, and consequently ATP generation, lowers intracellular ATP, leading to partial neuronal depolarisation, due to a reduction in the activity of Na^+/K^+-ATPase. The Na^+/K^+-ATPase acts to maintain the resting membrane potential of the cell. A reduction in ATP levels will compromise this function leading to depolarisation and therefore excitotoxicity via over activation of NMDA receptors. Intracellular Ca^{2+} can be increased by two methods: either directly by mitochondrial impairment or by over activity of NMDA receptors. Mitochondria can take up Ca^{2+} from the cytosol via an uniporter transporter or a transient "rapid mode", both of which rely on the mitochondrial membrane potential, reviewed by Gunter *et al*. (Gunter, Buntinas et al. 2000). The ROS generated by mitochondrial respiratory chain dysfunction can damage the mitochondrial membranes and disrupt this mechanism of Ca^{2+} uptake and storage thereby raising intracellular Ca^{2+} levels and exacerbating the excitotoxicity. Sherer et al showed that this could be a viable mechanism for cell death in PD by inhibiting Complex I in SH-SY5Y cells and showing a disruption in the mitochondrial membrane potential leading to an increased susceptibility to calcium overload (Sherer, Trimmer et al. 2001). It has also been shown that there is an increase in glutamate activity linked to excitotoxicity in the SNpc of mice treated with the Parkinsonian toxin MPTP, which may be linked to apoptosis and autophagy (Meredith, Totterdell et al. 2009).

Ca^{2+} has been implicated in other mechanisms of cell death in PD that may involve a compromise in the role of mitochondria as one of the major intracellular Ca^{2+} stores. It has been reported that mitochondria from PD patients showed lower sequestration of calcium than age matched controls implicating Ca^{2+} homeostasis dysfunction in PD (Sheehan, Swerdlow et al. 1997). This would lead to higher intracellular Ca^{2+} levels, which has been shown to amplify free radical production (Dykens 1994) and therefore increase ROS. An increase in cytosolic Ca^{2+} due to mitochondrial dysfunction has also been suggested to activate calpains and so raise levels of toxic α-synuclein proposing another link with PD (Esteves, Arduíno et al.

2010), a discovery supported by the protective effect of calpain inhibition in an MPTP model of PD (Crocker, Smith et al. 2003).

A particular role for Ca^{2+} and mitochondria has been suggested in a mechanism of increased susceptibility to cell death specific to SNpc DA neurons and therefore relevant for PD. SNpc DA neurons are atypical in the brain in that they have self-generated pacemaker activity (Grace and Bunney 1983) mediated by Cav1.3, a rare L-type Ca^{2+} channel (Striessnig, Koschak et al. 2006). This activity means that that the Cav1.3 channels are open for a higher proportion of time than Ca^{2+} channels in other neurons leading to an increased ATP usage in the cells to pump Ca^{2+} across the membrane up steep concentration gradients (Surmeier, Guzman et al. 2010). This elevated need for ATP would lead to an increase in the activity of the electron transport chain, therefore increasing ROS production, exacerbating any mitochondrial dysfunction and making SNpc DA neurons more prone to cell death.

1.1.2.5 Dopamine Metabolism

Oxidative stress generated during DA metabolism has long been implicated in PD (Olanow 1993). Dopamine is normally metabolised to DOPAC (3,4-Dihydroxyphenylacetic acid) by MAO, but can also be oxidised to form a reactive quinone, either by autoxidation, a process that is accelerated in the presence of ROS, metal ions or other catecholamines (Donaldson, McGregor et al. 1982; Nappi, Vass et al. 1995), or by the enzymes tyrosinase (Korner and Pawelek 1982) and prostaglandin H synthase (Hastings 1995) (Fig 1.9).

The major mechanisms by which DA metabolism is thought to contribute to PD pathology are through the formation of ROS (for details on ROS mediated damage in PD see section 1.1.2.2 above) and DA-quinones (Zahid, Saeed et al. 2011) (Fig. 1.9). DA-quinones have been shown to stabilise toxic α-synuclein aggregates in the cell, (Conway, Rochet et al. 2001), to form potentially damaging DNA adducts (Zahid, Saeed et al. 2011), to inactivate oxidative defence molecules (Belluzzi, Bisaglia et al. 2012) and inactivation and to cause conversion of tyrosine hydroxylase into a ROS producing redox quinoprotein (Kuhn, Arthur Jr et al. 1999), suggesting further mechanisms for the involvement of DA metabolism in PD pathology.

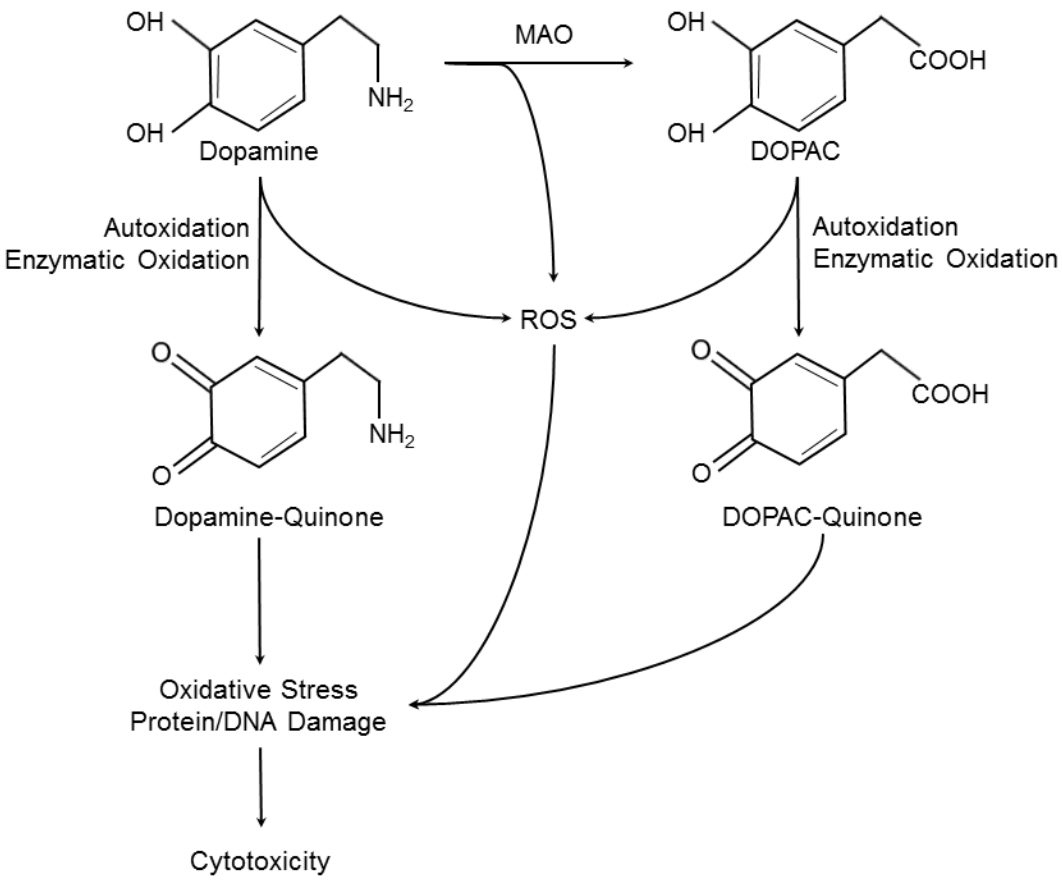

Fig. 1.9 Metabolic pathways of DA Several different pathways of DA metabolism exist in DA neurons. DA can be catabolized by the actions of MAO to DOPAC and DA & DOPAC can both be oxidized through various mechanisms to reactive quinones. ROS are generated during these reactions and it is they and the quinones which lead to cellular damage and death.

It has also been suggested that ROS or DA-quinones, may have an inhibitory effect on the proteins of the mitochondrial respiration chain (Cohen, Farooqui et al. 1997; Berman and Hastings 1999; Gluck and Zeevalk 2004). Hossain-Khan et al. showed that DA inhibits Complexes I and IV, most probably through the actions of the DA-quinones rather than through ROS (Hossain Khan, Sen et al. 2005). MAO-A is bound to the outer mitochondrial membrane and can oxidise dopamine to form the metabolite DOPAC, which can itself, or through oxidation to quinones, locally inhibit Complexes I and IV (Gluck and Zeevalk 2004; Hossain Khan, Sen et al. 2005), although a contradictory report suggests DA but not DOPAC inhibits the electron transport chain (Jana, Maiti et al. 2007). A recent study has shown that DA itself, rather than any oxidation products can directly inhibit Complex I (Brenner-Lavie, Klein et al. 2009); however, more work would need to be carried out to confirm this as there is no corroborating evidence. These links between mitochondrial dysfunction and dopamine are supported by reports that the PD neurotoxins and Complex I inhibitors MPTP and rotenone increase DA oxidation and turnover (Lotharius and O'Malley 2000; Thiffault, Langston et al.

2000), although whether this is indirectly due to the ROS generating effects of the toxins is not clear.

These hypotheses based around DA metabolism could offer explanations as to why DA neurons are more susceptible than others to toxin or mutation mediated mitochondrial dysfunction PD, as they are already under a higher level of oxidative stress due to dopamine metabolism.

1.1.2.6 Neuroinflammation

Neuroinflammation has been proposed as a mechanism involved in PD pathogenesis with reports that increased numbers of glia and astrocytes were found in post mortem brains (Damier, Hirsch et al. 1993; Braak, Sastre et al. 2007) and levels of the pro-inflammatory cytokines tumour necrosis factor-α (TNF-α), interleukins and transforming growth factors (TGFs) are increased in the cerebrospinal fluid and brains of PD patients (Mogi, Harada et al. 1994; Mogi, Harada et al. 1994; Mogi, Harada et al. 1996). One possible mechanism of neuroinflammation in PD could be due to the formation of DA-quinones (see section 1.1.2.5), with reports showing that DA-quinones can lead to activation of microglia and hence cause neurotoxicity (Kuhn, Francescutti-Verbeem et al. 2006). It has also been proposed that neuroinflammatory activation in PD may be due to an effect of aggregates of the PD-linked protein α-synuclein (see section 1.1.3.1 below for more details), as these aggregates have been shown to activate glial cells and initiate production of ROS in the glia by activating NADPH oxidase (Zhang, Wang et al. 2005). The proposed mechanisms of immunological activation contributing to DA neurodegeneration are summarised in Fig. 1.10.

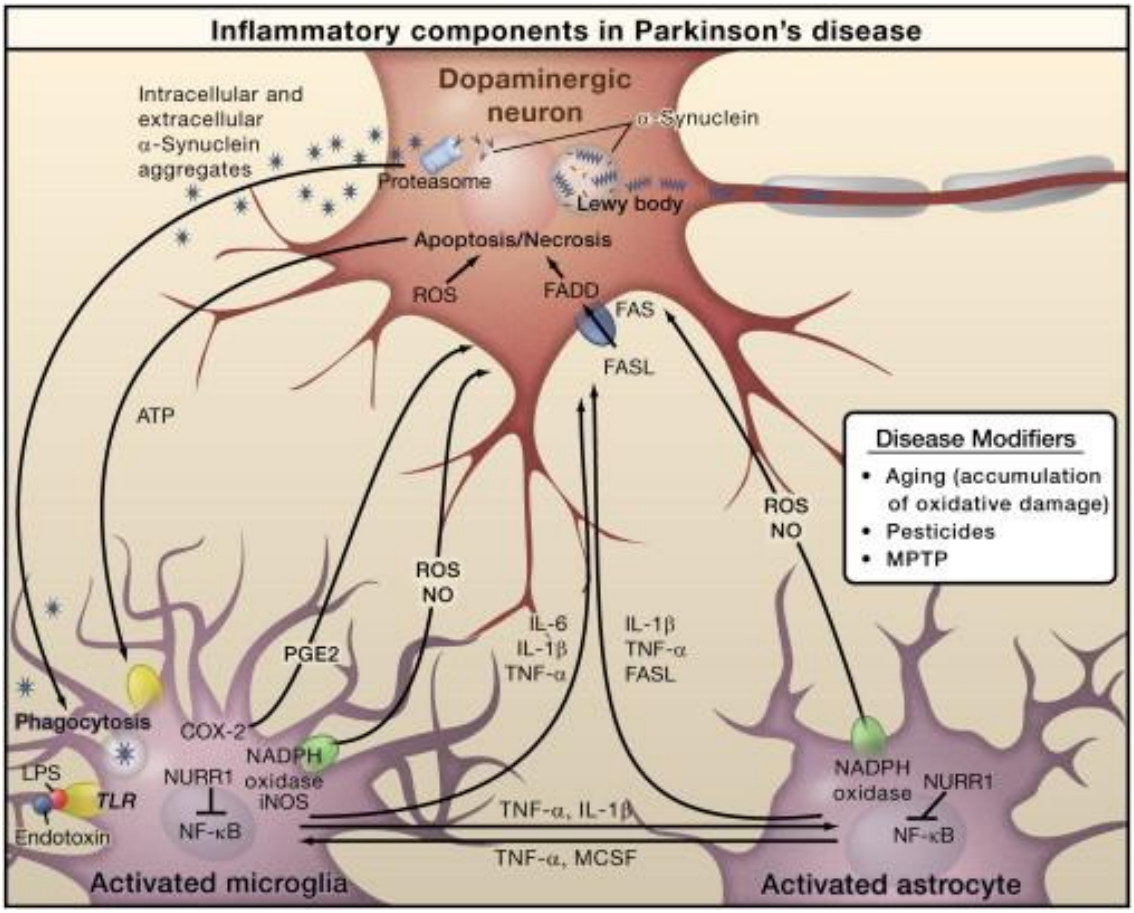

Fig. 1.10 Inflammation in PD Aggregates of α-synuclein form intermediate-state oligomers that when released from neurons activate microglia through Toll-like receptor (TLR)-independent mechanisms. This leads to activation of NF-κB and production of ROS and pro-inflammatory mediators. These factors act directly on DA neurons of the SNpc. These factors also activate microglia, which amplify the inflammatory response in a positive feedback loop, leading to further activation of microglia. Products derived from microglia and astrocytes act in a combinatorial manner to promote neurotoxicity. Bacterial lipopolysaccharide (LPS), acting primarily through TLR4 expressed by microglia, is sufficient to induce an inflammatory response in the SNpc that results in loss of DA neurons. The transcription factor NURR1 acts to suppress inflammatory responses in microglia and astrocytes by inhibiting NF-κB target genes. (Taken from (Glass, Saijo et al. 2010))

1.1.2.7 Interaction of the Molecular Mechanisms of Parkinson's Disease

Although the primary pathology underlying the disease has yet to be elucidated, there is strong evidence for the involvement of all of the mechanisms described in the progression of DA neurodegeneration in PD. In addition, many of the mechanisms are involved in a positive feedback loop that exacerbates cellular damage and enhances the neurodegeneration of DA neurons, aiding disease progression (Fig. 1.11)

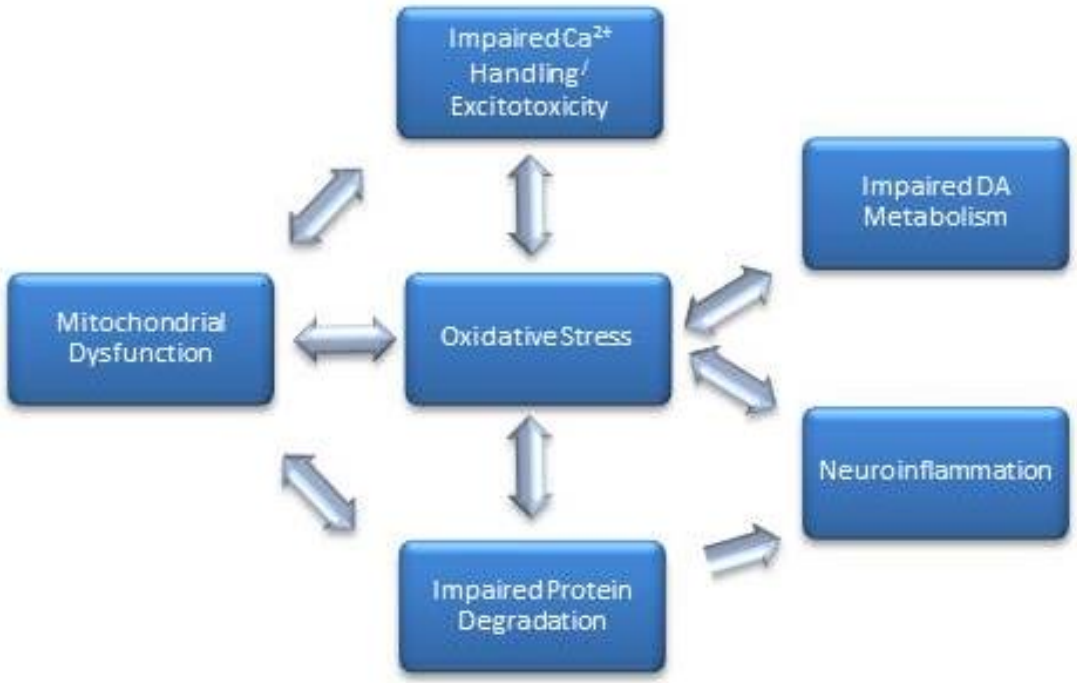

Fig. 1.11 Interaction of molecular mechanisms of PD The major pathological mechanisms linked with PD have been shown to initiate and exacerbate each other during progression of the disease. Oxidative stress appears integral to this feedback loop, with ROS being generated during and contributing to all of the other major mechanisms involved in DA cell death in the SNpc during PD. Mitochondrial dysfunction can lead to altered Ca^{2+} handling and excitotoxicity, as it is a major intracellular Ca^{2+} store, and impaired protein degradation as reduced ATP production will limit the ability of energy dependent processes such as autophagy and UPS. Build-up of toxic protein aggregates due to impaired degradation can trigger neuroinflammation by activating glia and aggravate mitochondrial dysfunction by impaired mitophagy. In conclusion, once triggered, the harmful processes involved in DA neuronal death can feedback to each other, enhancing their damaging effects on the cells and accelerating pathology.

1.1.3 Genetic Mutations linked with Parkinson's disease

Various inherited forms of PD have been discovered with the disease linked to mutations in a number of genes. Genome-wide linkage analysis implicated 16 genetic loci, termed "PARK" loci, linked with monogenetic forms of PD. These loci and the mutations they correspond to are summarised in Table 1.3, and discussed, along with other mutations linked to PD, in more detail below.

1.1.3.1 α-Synuclein

The *α-synuclein* gene encodes a small protein of the synuclein family which is known to be localised to nerve terminals; however the exact physiological functions of α-synuclein remain unclear. The first link between α-synuclein and PD came with the discovery of mutations in the α-synuclein gene in PD patients (Polymeropoulos, Lavedan et al. 1997; Kruger, Kuhn et al. 1998; Zarranz, Alegre et al. 2004). This evidence was supported by the discovery that aggregates of α-synuclein are the major components of LBs (Spillantini, Crowther et al. 1998). The structure of α-synuclein, along with main functional regions and the location of common mutations, is shown in Fig. 1.12.

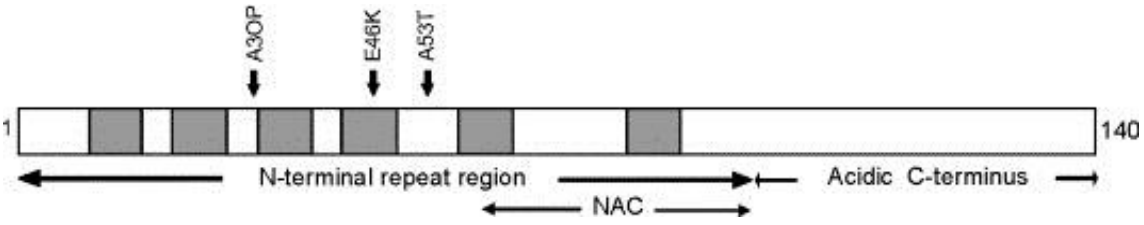

Fig. 1.12 α-synuclein structure The α-synuclein protein is divided into three overlapping regions, namely an N-terminal repeat region (aa. 1–95), a central hydrophobic NAC region (aa. 60–95) and an acidic C-terminus (aa. 96–140). The repeat region contains six conserved repeat motifs (grey boxes) and is believed to be involved in α-synucleins interactions with lipids; the NAC domain is essential for the aggregation of α-synuclein, whereas the C-terminus is critical for binding of various ions and proteins. The locations of 3 major mutations (A30P, E46K & A53T) are shown; all are present in the N-terminal repeat region, without the NAC domain essential for aggregation. (Taken from (Lundvig, Lindersson et al. 2005)).

There are many theories on the mechanism by which α-synuclein is linked to neuronal cell death in PD, including toxic aggregate build-up, neuroinflammation, disrupted ion homeostasis, impaired DA neurotransmission and mitochondrial dysfunction. Mutant α-synuclein has been shown to form fibrils and oligomers in cells (Conway, Harper et al. 1998; Conway, Lee et al. 2000), reportedly through exposure to ROS (Hashimoto, Hsu et al. 1999), and these protein aggregates have been shown to be toxic to the cell (El-Agnaf, Jakes et al. 1998). The mechanism of this toxicity and involvement in PD pathology has not been completely elucidated but may include a combination of various properties of the aggregates. Primarily, α-synuclein has been widely reported to disrupt the UPS, with fibrils and oligomers

shown to inhibit the activity of the 20 & 26S proteasome (Snyder, Mensah et al. 2003; Lindersson, Beedholm et al. 2004). Overexpression of mutant human α-synuclein in mice has been shown to lead to a decrease in proteasome function proportional to levels of SNpc DA neurodegeneration (Chen, Thiruchelvam et al. 2006). α-synuclein aggregates have also been shown to bind to and inhibit the transcriptional regulator HMGB-1 suggesting an effect on gene expression (Lindersson, Højrup et al. 2004), and oligomers have been shown to form pores in vesicle membranes altering Ca^{2+} permeability and therefore exerting an effect on ionic homeostasis in the cell (Volles, Lee et al. 2001; Volles and Lansbury Jr 2002). Finally, extracellular α-synuclein aggregates released from damaged nigral neurons have been reported to activate microglia, suggesting a role in the neuroinflammation associated with PD (Zhang, Wang et al. 2005).

In addition to the effects of aggregated α-synuclein described, wild-type α-synuclein has been shown to be involved in DA neurotransmission, with α-synuclein null mice shown to have altered DA release (Abeliovich, Schmitz et al. 2000), possibly due to impaired vesicle mobilisation at nerve terminals (Cabin, Shimazu et al. 2002) or an effect on DA biosynthesis (Perez, Waymire et al. 2002). It is reasonable to surmise, therefore, that mutations which affect the function of α-synuclein could cause problems in DA neurotransmission in PD. Wild-type α-synuclein may also have a protective effect in neurons that is lost in PD, as wild-type, but not A53T α-synuclein, has been shown to protect against apoptosis inducing agents in a neuronal cell line (Da Costa, Ancolio et al. 2000).

It has also recently been reported that there is an association between α-synuclein and mitochondrial dysfunction (Devi, Raghavendran et al. 2008; Nakamura, Nemani et al. 2008). Overexpression of α-synuclein has been reported to alter mitochondria resulting in increased oxidative stress in a neuronal cell line (Hsu, Sagara et al. 2000), and mutant α-synuclein has been shown to be targeted to, and accumulate in, the inner mitochondrial membrane and cause Complex I impairment and an increase in ROS, possibly leading to cell death (Devi, Raghavendran et al. 2008). Finally, wild-type α-synuclein has been shown to be protective against excitotoxic injury in neurons (Leng and Chuang 2006), and may have an antioxidant effect that is lost in mutant forms of the protein (Orth, Tabrizi et al. 2004; Zhu, Qin et al. 2006). A lack of these protective abilities in PD due to mutant or aggregated α-synuclein may contribute towards disease pathology by increasing the risk of excitotoxcity and oxidative damage.

The relative involvement of these findings in the progression and pathology of PD have not been fully explored; however - with evidence of the involvement of α-synuclein in a wide range of the pathogenic molecular mechanisms of the disease - it is strongly suggestive that a combination of the toxic effects of mutated and aggregated α-synuclein and a loss of protective characteristics of wild-type α-synuclein play a major role in the mechanism of DA degeneration in the SNpc of PD patients.

1.1.3.2 Parkin/PINK1/DJ-1

The Parkin gene encodes an E3 ubiquitin ligase involved in the ubiquitin-proteasomal system (Shimura, Hattori et al. 2000), marking proteins for degradation by the proteasome. Mutations in Parkin have been linked to a form of autosomal recessive juvenile parkinsonism (Kitada, Asakawa et al. 1998). This mutation leads to a form of PD without Lewy bodies, probably related to the loss of the ability of Parkin to ubiquinate synphilin-1, a protein that interacts with α-synuclein in the formation of LBs (Chung, Zhang et al. 2001). Parkin has been shown to be localised to LBs (Schlossmacher, Frosch et al. 2002) and has been shown to interact with and promote degradation of α-synuclein, possibly through sequestration into LBs (Shimura, Schlossmacher et al. 2001; Kim, Sung et al. 2003); therefore a loss of function Parkin mutation could contribute to the build-up of toxic α-synuclein and subsequently cause the cell death present in PD. Pael-R, a substrate of Parkin, has also recently been shown to be a component of LBs (Murakami, Shoji et al. 2004), providing more links between Parkin and LB pathology in PD. It has been suggested that Parkin may also be involved in mitochondrial function and protection from mitochondrially generated ROS. Recent work in Parkin null mice has shown a reduction in subunits of Complex I & IV and reduced function in the mitochondrial respiratory chain along with increased oxidative stress in brain tissue (Palacino, Sagi et al. 2004). This is supported by reduced mitochondrial Complex I activity in Parkinsonian patients with Parkin mutations (Muftuoglu, Elibol et al. 2004) and the increased age-dependent or rotenone (a Complex I inhibitory toxin) induced DA neuronal degeneration and mitochondrial abnormalities in Parkin mutant drosophila (Wang, Lu et al. 2007). Moreover, a recently generated zebrafish model of Parkin deficiency showed increased sensitivity of Parkin mutants to proteotoxic stress with no manifestation of dopaminergic neuron loss or affected mitochondrial morphology or function (Fett, Pilsl et al. 2010).

PTEN induced putative kinase 1 (PINK1) is a serine/threonine kinase located in the inner mitochondrial membrane (Silvestri, Caputo et al. 2005) which functions to protect neurons against various types of cell stress. Mutations in PINK-1 are found to be associated with a autosomal recessive form of PD (Valente, Abou-Sleiman et al. 2004). This pathogenesis may be

associated with the loss of kinase activity as PINK-1 is known to protect against cell death only if the kinase function is intact (Petit, Kawarai et al. 2005). Several independent groups reported a role for PINK1 in mitochondrial integrity by regulating the mitochondrial fission machinery (Hoppins, Lackner et al. 2007), which might have an impact on dopaminergic synapses and contribute to DA neuron degeneration (Yang, Ouyang et al. 2008; Dagda, Cherra et al. 2009; Gispert, Ricciardi et al. 2009). Knockdown of PINK1 has been shown to induce mitochondrial oxidative stress, mitochondrial fragmentation, autophagy, dysregulated calcium homeostasis, α-synuclein aggregation and disrupt the UPS in cell models (Dagda, Cherra et al. 2009; Gandhi, Wood-Kaczmar et al. 2009; Liu, Vives-Bauza et al. 2009), suggesting links between PINK1 and a wide range of PD-linked pathologies.

Moreover, there is evidence of interplay between PINK1 and Parkin since Parkin can reduce mitochondrial dysfunction caused by down-regulation of PINK1 (Exner, Treske et al. 2007). Furthermore, it has been shown recently that both PINK1 and Parkin are involved in removal of damaged mitochondria. The proposed model suggests that in response to mitochondrial depolarization PINK1 accumulates on the mitochondrial membrane and recruits Parkin to promote mitophagy (Geisler, Holmstrom et al. 2010; Narendra, Jin et al. 2010). Therefore, the pathology of mutant PINK1 and/or Parkin in parkinsonism may arise from the inability to remove dysfunctional mitochondria (Chu 2010).

The DJ-1 gene encodes a widely expressed protein found in neurons and glia in all central nervous system (CNS) regions (Bader, Zhu et al. 2005). Bonifati *et al*. first identified an association between DJ-1 and autosomal recessive early-onset PD (Bonifati, Rizzu et al. 2003), with numerous further familial mutations in DJ-1 being identified (Van Duijn, Dekker et al. 2001). One of these mutations is a large scale deletion in the gene, which effectively knocks out the protein, while the other is a L166P point mutation which has been shown to lead to increased degradation of DJ-1 (Miller, Ahmad et al. 2003). Proteomic analysis of mitochondrial protein composition of the substantia nigra of mice treated with MPTP compared to controls showed significant changes in expression of numerous proteins. Of these proteins, DJ-1 protein levels were significantly increased in the toxin-treated mice and also colocalised with α-synuclein in LB-like inclusions in the remaining nigral neurons. Moreover, DJ-1 was present in the halo of classical LBs in nigral tissue of PD patients (Jin, Meredith et al. 2005).

Reports have shown that DJ-1 is present in mitochondria and protects against oxidative neuronal death (Canet-Aviles, Wilson et al. 2004), DJ-1 deficient mice are more susceptible to MPTP (Kim, Smith et al. 2005) and DJ-1 knockdown in a neuroblastoma cell line renders the

cells vulnerable to oxidative stress (Taira, Saito et al. 2004). Finally, a critical role for DJ-1 in mitochondrial function is shown by a rescue effect of DJ-1 on neuronal cell death caused by PINK-1 but not Parkin deletion (Hao, Giasson et al. 2010), suggesting a possible interplay with PINK1 in maintaining mitochondrial populations and function. Moreover, loss of DJ-1 leads to mitochondrial fragmentation, impaired dynamics, induced oxidative stress and autophagy (Irrcher, Aleyasin et al. 2010; Krebiehl, Ruckerbauer et al. 2010). In conclusion, DJ-1 protein has been observed to have pleiotropic functions (see (Cookson 2010) for further review), with an anti-oxidative role being the most consistent finding. This may provide a link to PD whereby a loss of function mutation of DJ-1 causes an increase in mitochondrial dysfunction and oxidative damage leading to nigral neuron cell death.

Despite all the evidence implicating Parkin, PINK1 and DJ-1 loss of function mutations in PD, studies have shown that knocking out these proteins individually or in combination does not lead to PD pathology in mice (Kitada, Tong et al. 2009), suggesting that other contributing factors are needed in combination with loss of Parkin, PINK1 and DJ-1 for development of the disease or that it is the presence of the mutated forms of the proteins that is more important in their toxic mechanisms.

1.1.3.3 LRRK2

Leucine-rich repeat kinase 2 (LRRK2) is a large (280kDa) protein with kinase activities. Mutations in LRRK2 were first linked with autosomal dominant PD by Zimprich et al. in 2004 (Zimprich, Biskup et al. 2004) and represent the most significant cause of autosomal dominant PD. The precise mechanisms by which LRRK2 functions are as yet unclear, however, the kinase activity of the protein has been shown to be integral to the toxic properties of mutant forms of LRRK2 (Greggio, Jain et al. 2006; Smith, Pei et al. 2006; Lee, Shin et al. 2010). LRRK2 has been shown to be involved in the autophagic clearance of damaged proteins in the cell with LRRK2 knockout cells and mice shown to have impaired clearance of autophagic structure suggesting an impaired process (Alegre-Abarrategui, Christian et al. 2009; Tong, Giaime et al. 2012), although these findings were only in the kidney and similar results were not seen in these studies in the brain. However, overexpression of mutant LRRK2 in mice resulted in loss of DA neurons and autophagic abnormalities (Ramonet, Daher et al. 2011) and a similar study in SH-SY5Y, a DA model cell line, found abnormal accumulation of autophagic vacuoles in the brain (Plowey, Cherra Iii et al. 2008). A study has also reported a high level of LRRK2 in dopamine innervated areas of the brain (Gaiter, Westerlund et al. 2006), supporting the involvement of LRRK2 mutation and autophagic disruption in PD.

LRRK2 has been shown to be localised to the outer mitochondrial membrane (West, Moore et al. 2005; Biskup, Moore et al. 2006) and Drosophila with LRRK2 mutations showed increased DA neurodegeneration and increased susceptibility to the Complex I inhibitor rotenone, effects that could be reversed by expression of mitochondrially protective protein Parkin in Drosophila (Ng, Mok et al. 2009) providing associations between mutations in this protein in PD and mitochondrial dysfunction in PD.

1.1.3.4 UCH-L1

Ubiquitin C-terminal hydrolase-L1 (UCH-L1) is a neuron-specific enzyme involved in various ubiquitin modulating activities (Wilkinson, Lee et al. 1989; Liu, Fallon et al. 2002; Osaka, Wang et al. 2003), that was first linked to PD by an autosomal dominant point mutation (I93M) that was identified in two siblings with a strong family history of PD (Leroy, Boyer et al. 1998). Furthermore, UCH-L1 levels have also been shown to be down regulated and oxidatively damaged in idiopathic PD brains (Choi, Levey et al. 2004), suggesting an integral role for this protein in the pathogenesis of the disease. As previously mentioned in section 1.1.2.3, disruption in the UPS has been strongly implicated in PD, and, due to the role of UCH-L1 in ubiquitin homeostasis, this is the most likely mechanism by which it contributes to the disease. Indeed, mutant forms of UCH-L1 linked with the disease have been shown to increase α-synuclein levels in a cellular model (Liu, Fallon et al. 2002). Interestingly, however, a polymorphism of *UCH-L1* (S18Y) in a Japanese population has been shown to have a weakly protective effect against PD (Zhang, Hattori et al. 2000), possibly due to an increased hydrolase and decreased ligase activity in comparison to the harmful 193M mutation (Liu, Fallon et al. 2002; Nishikawa, Li et al. 2003). These findings suggest a complex involvement of this protein and a sensitive balance of the UPS which may be disrupted in PD.

1.1.3.5 Other nuclear mutations

Omi/Htra2 is a mitochondrially located stress protective serine protease which has been linked to neurodegeneration (Jones, Datta et al. 2003; Martins, Morrison et al. 2004) with loss of function mutations being seen in some PD patients (Strauss, Martins et al. 2005). Although certain studies report no clear genetic association between the *Omi/HtrA2* gene sequence variations and PD (Kruger, Sharma et al. 2009), there is evidence of mitochondrial pathology caused by loss of the Omi/HtrA2 protein function (Jones, Datta et al. 2003). Omi/Htra2 has also been shown to have links with PINK1 in protecting against oxidative stress (Plun-Favreau, Klupsch et al. 2007) and interacting in a pro-survival pathway (Whitworth, Lee et al. 2008; Tain,

Chowdhury et al. 2009). Omi/Htra2 has also been shown to co-localise with LBs in the brain of PD patients (Kawamoto, Kobayashi et al. 2008), suggesting a role in LB pathology or UPS protein trafficking. Therefore, mutations in this mitochondrially targeted gene may predispose cells to damage via oxidative stress generated from mitochondrial dysfunction.

A loss of function mutation in the brain and stomach located lysosomal type 5 P-type ATPase, ATP13A2, has been shown to have links with a hereditary form of autosomal recessive early onset PD with dementia (Ramirez, Heimbach et al. 2006) and missense mutations of the gene have been linked with juvenile/early onset PD (Di Fonzo, Chien et al. 2007). It has been reported that functional ATP13A2 can protect against α-synuclein over expression induced toxicity and that knockdown of ATP13A2 enhances α-synuclein misfolding in neuronal models of PD (Gitler, Chesi et al. 2009), probably due to the role ATP13A2 plays in the degradation of abnormal proteins with ATP13A2 mutant patient derived cell lines showing disrupted UPS activity and increased endoplasmic reticulum stress (Park, Mehta et al. 2011). In addition to its effects on protein handling, *ATP13A2* mutations have also been linked with abnormal iron and manganese handling and their resultant accumulation in the brain (Schneider, Paisan-Ruiz et al. 2010; Tan, Zhang et al. 2011), which have been shown to contribute to excess ROS production and oxidative damage.

PLA2G6 is a calcium independent Phospholipase A2 linked to infantile neuroaxonal dystrophy (Khateeb, Flusser et al. 2006) and neurodegeneration with brain iron accumulation (Morgan, Westaway et al. 2006) that has recently been implicated in PD (Tan, Ho et al. 2010; Yoshino, Tomiyama et al. 2010). PLA2G6 has been shown to locate to (Seleznev, Zhao et al. 2006), and have a protective role against oxidative stress in (Zhao, Zhang et al. 2010), pancreatic β-cell mitochondria providing a possible link between loss of function mutations in this protein and mitochondrial dysfunction in PD. How, for example, PLA2G6 regulates iron, a major mitochondrial cofactor is not clear.

F-box only protein 7 (FBXO7) is a substrate recognition component of a set of E3 ubiquitin ligases and so involved in protein degradation by the UPS. Mutations in the gene encoding FBXO7 have been linked with a recessive, early onset, progressive form of PD (Fonzo, Dekker et al. 2009). FBXO7 function is relatively poorly characterised but has been reported to be involved in control of proteasome activity, the cell cycle and apoptosis (Laman, Funes et al. 2005; Chang, Cheng et al. 2006; Kirk, Laman et al. 2008; Bader, Benjamin et al. 2011); a loss of any or a combination of these functions could be involved in PD pathology seen in patients with mutations in FBXO7.

There have been reports that mutations in Grb10-Interacting GYF Protein-2 (GIGYF2) had been proposed as having a genetic association with familial PD (Lautier, Goldwurm et al. 2008; Guo, Jankovic et al. 2009). However, since these reports, a number of further studies have been unable to find consistent evidence of the link between GIGFY2 mutations and PD and suggest that a mutation in another un-investigated gene in the patients in the primary investigations could be the cause of the disease in this group (Bras, Simán-Sánchez et al. 2009; Di Fonzo, Fabrizio et al. 2009; Nichols, Kissell et al. 2009; Vilariño-Güell, Ross et al. 2009; Zimprich, Schulte et al. 2009). This lack of effect of a GIGYF2 mutation is supported in a study in mice which found no differences between cells expressing wild-type or PD-linked mutant GIGYF2, and low levels of GIGYF2 in the SN and striatum relative to other brain regions and organ systems (Higashi, Iseki et al. 2010). A further study found that a GIGYF2 deficient zebrafish model did not show any DA neuronal degeneration (Guella, Pistocchi et al. 2011). Taken together, this evidence suggests that the primary reports of PD due to GIGFY2 mutation are more likely due to a separate, undetected, mutation.

MnSOD is an enzyme found in the mitochondria (Weisiger and Fridovich 1973) that protects against superoxide induced oxidative damage by catalysing the dismutation of superoxide into oxygen and hydrogen peroxide (McCord, Keele Jr et al. 1971). There have been suggestions that a polymorphism in the mitochondrial targeting sequence of the MnSOD gene may have a link with PD in Japanese patients with an allelic frequency of 19.3% in PD patients compared to 12.2% in controls (Shimoda-Matsubayashi, Matsumine et al. 1996). However, a further study on a German population did not support a link between this mutation, or a separate mutation affecting the stability of MnSOD, and PD (Grasbon-Frodl, Kösel et al. 1999). As MnSOD is involved in defence against oxidative stress at the mitochondria, and this has been widely implicated in PD pathology, it makes an interesting candidate for a PD-linked mutation; however, the evidence to date is inconclusive.

1.1.3.6 mtDNA mutations

As well as nuclear DNA mutations there have been links between mtDNA mutations and PD, with a number of studies reporting high levels of mtDNA deletions in neurons in the SNpc of PD patients (Bender, Krishnan et al. 2006; Kraytsberg, Kudryavtseva et al. 2006). It has been hypothesised that these pathologic DNA rearrangements are not primary drivers of the disease but may be caused by oxidative stress generated during mitochondrial dysfunction and this may further exacerbate cellular damage (Kirches 2009). The mitochondrial transcriptional factor A (TFAM) regulates transcription of mtDNA and was linked to PD by the finding that

TFAM knockout mice (MitoPark mice) had reduced mtDNA expression and a respiratory chain deficiency in SNpc DA neurons, which lead to a parkinsonian phenotype (Ekstrand, Terzioglu et al. 2007). Although some studies showed that TFAM mutations do not significantly increase the risk of PD (Belin, Björk et al. 2007; Alvarez, Corao et al. 2008), an investigation into the influence of TFAM variants on PD depending on mtDNA haplogroup found certain variants increased the chances of developing PD (Gaweda-Walerych, Safranow et al. 2010) suggesting a possible role for mtDNA, in some instances, and respiratory chain dysfunction in PD. Mitochondrial DNA polymerase γ 1 (POLG1) is an enzyme involved in the synthesis and regulation of mtDNA and has been shown to have links with PD, including reduced activity of mitochondrial respiratory chain complexes (Luoma, Melberg et al. 2004; Davidzon, Greene et al. 2006). The involvement of mutations of this protein in PD suggests a role for dysregulation of mtDNA in mitochondrial dysfunction in the disease. However, whether or not there is a common hereditary role for POLG1 in PD needs further study, since a large scale study does not support this hypothesis (Tiangyou, Hudson et al. 2006).

PARK locus (Chromosomal position)	Gene	Inheritance	Proposed Pathological Involvement in PD					
			Mitochondrial dysfunction	Oxidative stress	Impaired protein degradation	Ca2+/ excitotoxicity	Dopamine metabolism	Neuro-inflammation
PARK1 (4q21-q23)	*α-synuclein**	Dominant	✓	✓	✓	✓	✓	✓
PARK2 (6q25.2-q27)	*Parkin*	Recessive	✓	✓	✓			
PARK3 (2p13)	*Unknown*	Dominant						
PARK4 (4p14-16.3)	*α-synuclein**	Dominant	✓	✓	✓	✓	✓	✓
PARK5 (4p14)	*UCH-L1*	Dominant			✓			
PARK6 (1p35-p36)	*PINK1*	Recessive	✓	✓	✓	✓		
PARK7 (1p36.33 - p36.12)	*DJ-1*	Recessive	✓	✓	✓			
PARK8 (12p11.23-q13.11)	*LRRK2*	Dominant			✓			
PARK9 (1p36)	*ATP13A2*	Recessive		✓	✓			
PARK10 (1p32)	*Unknown*	Dominant						
PARK11 (2q36-q37)	*GIGYF2***	Dominant						
PARK12 (Xq21-q25)	*Unknown*	X-linked						
PARK13 (2p12)	*Omi/Htra2*	Dominant	✓	✓	✓			
PARK14 (18q11)	*PLA2G6*	Recessive		✓				
PARK15 (22q12-q13)	*FBXO7*	Recessive			✓			
PARK16 (1q32)	*Unknown*	Risk Gene						

* PARK1 and PARK4 were initially assigned to different regions on chromosome 4, but were later ascribed to the same underlying locus.

** Link to PD not confirmed

Table 1.3 Summary of PD mutations Summary of the major PARK PD-linked mutations and their proposed involvement in disease pathology

1.1.4 Environmental toxins linked with Parkinson's Disease

There is extensive evidence that PD can be caused by neurotoxins, specifically MPTP (Davis, Williams et al. 1979), rotenone (Greenamyre, MacKenzie et al. 1999), paraquat (Liou, Tsai et al. 1997), diquat (Sechi, Agnetti et al. 1992) and TaClo (Bringmann, God et al. 1995; Bringmann, God et al. 1995).

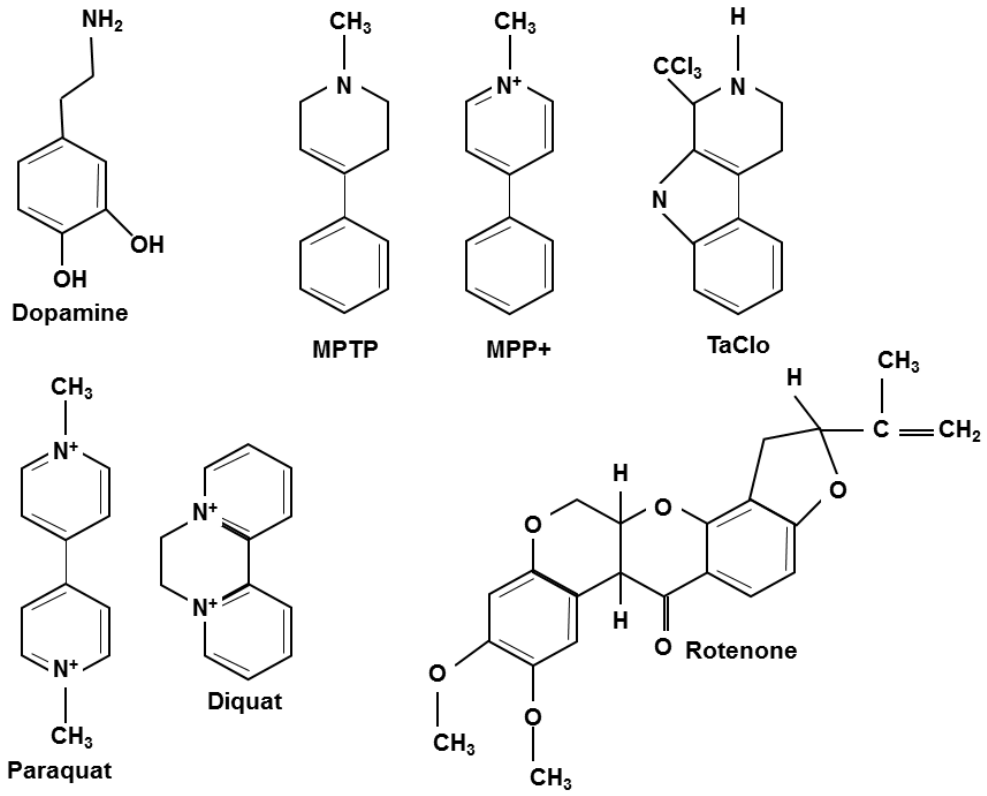

Fig. 1.13 Parkinson's Disease linked toxins Structures of the PD linked neurotoxins MPTP/MPP+, Rotenone, Paraquat, Diquat and TaClo and similarity to DA

1.1.4.1 MPTP

MPTP (Fig 1.13) is produced as a by-product of the synthesis of a meperidine analogue with heroin-like properties (Ziering, Berger et al. 1947). Langston et al described in 1983 that users of meperidine reported striking Parkinsonian symptoms and related this to the presence of MPTP (Langston, Ballard et al. 1983). It has since been shown to closely reproduce the DA degeneration and symptoms of PD in various animal experimental models (Burns, Chiueh et al. 1983; Seniuk, Tatton et al. 1990; Hantraye, Varastet et al. 1993) and has been the most widely used toxin in animal models of PD (Beal 2001). MPTP readily crosses the blood brain barrier and is converted to the toxic 1-methyl-4-phenyl-2,3-dihydropyridium ion (MPP+) (Fig. 1.13) by MAO-B in astrocytes (Nicklas, Vyas et al. 1985) following uptake by various transporters (Brooks, Jarvis et al. 1989; Marini, Lipsky et al. 1992). MPP+ is taken up into DA neurons by

DAT, seen as a reduction in MPTP toxicity in DAT deficient mice (Bezard, Gross et al. 1999), and then taken up into mitochondria via passive transport due to the large mitochondrial transmembrane gradient (Hoppel, Greenblatt et al. 1987). MPP+ inhibits mitochondrial Complex I (Nicklas, Vyas et al. 1985; Nicklas, Youngster et al. 1987) leading to cell death via energy deficits (Przedborski, Jackson-Lewis et al. 2000), free radical and ROS generation (Cleeter, Cooper et al. 1992) and possibly excitotoxicity (Bezard, Gerlach et al. 2006) (Fig. 1.16). Although there is extensive evidence for this theory of MPTP toxicity, there has been a contradictory report that MPTP exposure in marmosets that displayed PD behavioural symptoms, reduced DA levels and DA neurodegeneration in the SNpc, showed no mitochondrial dysfunction or increased oxidative damage markers when assessed *ex vivo* a week following end of MPTP administration (Gerlach, Gotz et al. 1996). In an MPTP mouse model of PD, α-synuclein is nitrated disrupting its normal properties (Przedborski, Chen et al. 2001) providing another link between MPTP and PD. Despite all of the evidence of links between MPTP and PD in humans and animal models, there are differences between MPTP derived PD and idiopathic forms of the disease with MPTP PD showing an acute onset, variations in progression, and a lack of typical LB formation (Forno, DeLanney et al. 1993).

1.1.4.2 6-OHDA

6-hydroxydopamine (6-OHDA) is DA analogue (Fig. 1.14) and experimental tool that has been shown to be specifically neurotoxic to central monoamine neurons (Ungerstedt 1968). As it is not able to cross the blood brain barrier, and is not thought to be produced *in vivo*, the effects of 6-OHDA have been studied via direct injection into the SNpc.

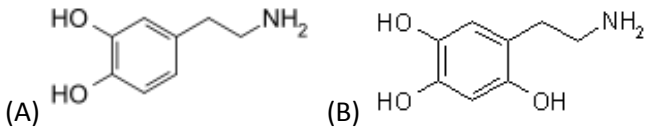

Fig. 1.14 DA and 6-OHDA Structural similarity of DA (A) and the analogue 6-OHDA (B)

Unilateral injection of 6-OHDA into the SNpc has been shown to cause a drastic reduction in the number of DA neurons of the SNpc and lead to motor dysfunction in rodent models (Javoy, Sotelo et al. 1976; Iancu, Mohapel et al. 2005) (Fig. 1.15). Due to this potent degeneration, the reproducibility of this and the ease of assessment of motor function with unilateral degeneration, this animal model of PD has been widely used to investigate the disease (Beal 2001).

The mechanism by which 6-OHDA causes neurodegeneration is thought to be via inhibition of mitochondrial Complex I and generation of ROS leading to oxidative stress and cell death (Betarbet, Sherer et al. 2002) (Fig. 1.16). In addition to this, an up regulation in genes that would lead to a strong inflammatory response has recently been reported suggesting a role for inflammation in the neurotoxicity of 6-OHDA (Na, DiLella et al. 2010).

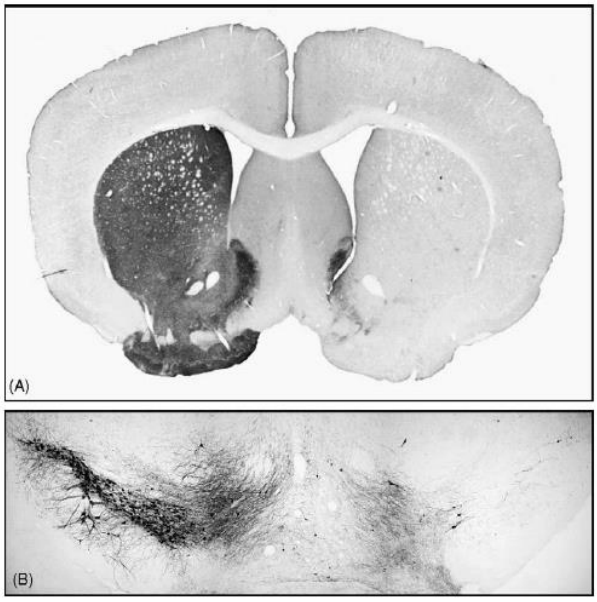

Fig.1.15 6-OHDA lesion Representative microphotographs of a mouse (A) striatum and (B) SNpc stained for TH (representing DA neurons) following unilateral treatment with 6-OHDA (right hemisphere as seen). Approximately 97% degeneration of TH positive DA neurons seen. (Taken from (Iancu, Mohapel et al. 2005))

Whilst being a good model for PD, 6-OHDA does lack some of the main pathological and clinical traits of the disease. 6-OHDA does cause motor dysfunction; however it does not regularly produce tremor in animal models, a primary trait of PD. It also does not produce LB or LB-like inclusions in the brains of affected animals. So, while 6-OHDA is a reasonable model of the degeneration of DA neurons, it is not a completely reliable model of the pathology and symptoms of PD.

1.1.4.3 Rotenone

Rotenone (Fig. 1.13) is a widely used pesticide and naturally occurring neurotoxin that has been found to have links to PD (Greenamyre, MacKenzie et al. 1999). Rotenone is highly lipophilic and able to easily cross the blood brain barrier and enter neuronal cells and intracellular organelles, such as mitochondria, without the aid of transporters. Rotenone specifically blocks the ubiquinone binding site of Complex I, preventing the transport of electrons from Complex I to ubiquinone leading to the release of free radicals into the mitochondrial matrix and ROS formation (Lambert and Brand 2004) (Fig. 1.16). This evidence

that rotenone is a specific inhibitor of Complex I which in turn leads to ROS production and oxidative stress can also cause PD-like behavioural symptoms such as akinesia and rigidity in rats (Bashkatova, Alam et al. 2004). Rotenone administration has been shown to oxidatively modify DJ-1 and cause α-synuclein aggregation, effects linked to PD and localised to the DA neurons of the SNpc (Betarbet, Canet-Aviles et al. 2006) and LB-like ubiquitin and α-synuclein containing cytoplasmic inclusions have been reported in the brains of rotenone treated rats (Betarbet, Sherer et al. 2000). *In vitro*, chronic low dose exposure of SH-SY5Y neuroblastoma to rotenone (5nM for 4 weeks) has been shown to induce accumulation and aggregation of α-synuclein and ubiquitin, oxidative damage, and cell death (Sherer, Betarbet et al. 2002). This evidence, taken together, presents a strong link between rotenone exposure and PD via mitochondrial dysfunction. However there is also evidence to suggest rotenone causes damage to neurons in the striatum but not the SNpc (Ferrante, Schulz et al. 1997) suggesting that it may not be DA specific and therefore not an entirely accurate model of PD.

1.1.4.4 Paraquat/diquat

Paraquat and diquat are widely used herbicides shown to have links with PD (Sechi, Agnetti et al. 1992; Liou, Tsai et al. 1997). They are hydrophilic compounds and therefore do not readily cross the blood brain barrier and the mechanism by which they enter the brain is unclear, although uptake by a neutral amino acid (McCormack and Di Monte 2003) or polyamine (Karl and Friedman 1983) transporter has been suggested. Paraquat can then be taken up into DA or other neurons via DAT or the organic cation transporter-3 respectively (Rappold, Cui et al. 2011). As paraquat and diquat have very similar structures to MPTP and MPP+ (Fig. 1.13), it was thought that they would act via a similar toxic mechanism. However, unlike rotenone and MPP+, paraquat does not inhibit Complex I and is not taken up by DAT, suggesting an alternative mechanism of cell death (Richardson, Quan et al. 2005). A likely toxic mechanism is described where paraquat is reduced to the paraquat radical. There are a number of proposed mechanisms for the formation of this radical: firstly reduction of paraquat by Complex I leading to accelerated lipid peroxidation (Fukushima, Tawara et al. 1995; Cochemé and Murphy 2008); and secondly whereby paraquat is reduced to the paraquat radical by Complex II has also been reported (Castello, Drechsel et al. 2007). A final hypothesis for the formation of the paraquat radical is that paraquat is reduced by NADPH-cytochrome p450 reductase (Clejan and Cederbaum 1989) or NADPH-cytochrome c reductase (Fernandez, Subirade et al. 1995) in the cell. Whichever complex or enzyme is involved, the paraquat radical can react with oxygen to form $\cdot O_2^-$ leading to oxidative stress and generation of further ROS by mitochondrial dysfunction (Cochemé and Murphy 2008) (Fig. 1.16). This mechanism of cell death may target

the DA neurons specifically because of their constant state of oxidative stress leaving them more vulnerable than other cells. A large scale mouse study into the pharmacokinetics and SNpc and striatal toxicity of paraquat found that systemically administered paraquat can reach the brain, did reduce DA neurons in the SNpc of exposed animals in some studies but not in others when assessed by stereology, but did not affect DA levels or find evidence of cell death markers (Breckenridge, Sturgess et al. 2013). This study does not show conclusive evidence of paraquat toxicity in mouse brain but shows some contradictory evidence that it may, and suggests that more work needs to be carried out to confirm or deny the hypothesis. It has also been shown that paraquat can lead to an increase in both α-synuclein levels and aggregation (Manning-Bog, McCormack et al. 2002). Although the exact mechanism has yet to be elucidated, mitochondrially derived paraquat radical, combined with its effects on α-synuclein, indicate paraquat toxicity as a possible causative agent in PD, although this needs confirming. The structurally similar compound diquat also generates oxygen radicals in rat brain microsomes (Yumino, Kawakami et al. 2002), a discovery that, when coupled with its similarity in structure and properties with paraquat, suggests a possible similar role for diquat in radical generation and PD.

The TCE derived β-carboline TaClo has also been implicated in PD; this will be discussed in more detail in Section 1.2.2.3.

However, this evidence of mitochondrial Complex I inhibition leading to neuronal cell death in PD following toxin exposure requires further investigation following the findings of Choi et al. that midbrain neurons in mice without Complex I activity were still susceptible to cell death following rotenone, MPTP or paraquat treatment and were, in the case of rotenone, more susceptible (Choi, Kruse et al. 2008). This suggests that mitochondrial dysfunction could either be occurring parallel to another non-mitochondrial cell death mechanism or as a secondary effect driven by some other cellular stress or damage such as toxic protein accumulation due to ubiquitin-proteasome system impairment (McNaught, Olanow et al. 2003), inflammation (Bartels and Leenders 2007) or DNA damage (Kao 2009). However, these results have not been confirmed and do not seem to be compatible with the literature, and in particular, a study carried out by Marella *et al.*. They found that expression of NDI1 - a yeast NADH-quinone oxidoreductase that can act as an alternative to Complex I - in a rat model significantly protected against rotenone toxicity (Marella, Seo et al. 2008) suggesting the results seen by Choi *et al*. are unlikely to be relevant, possibly due to incomplete knockdown of Complex I.

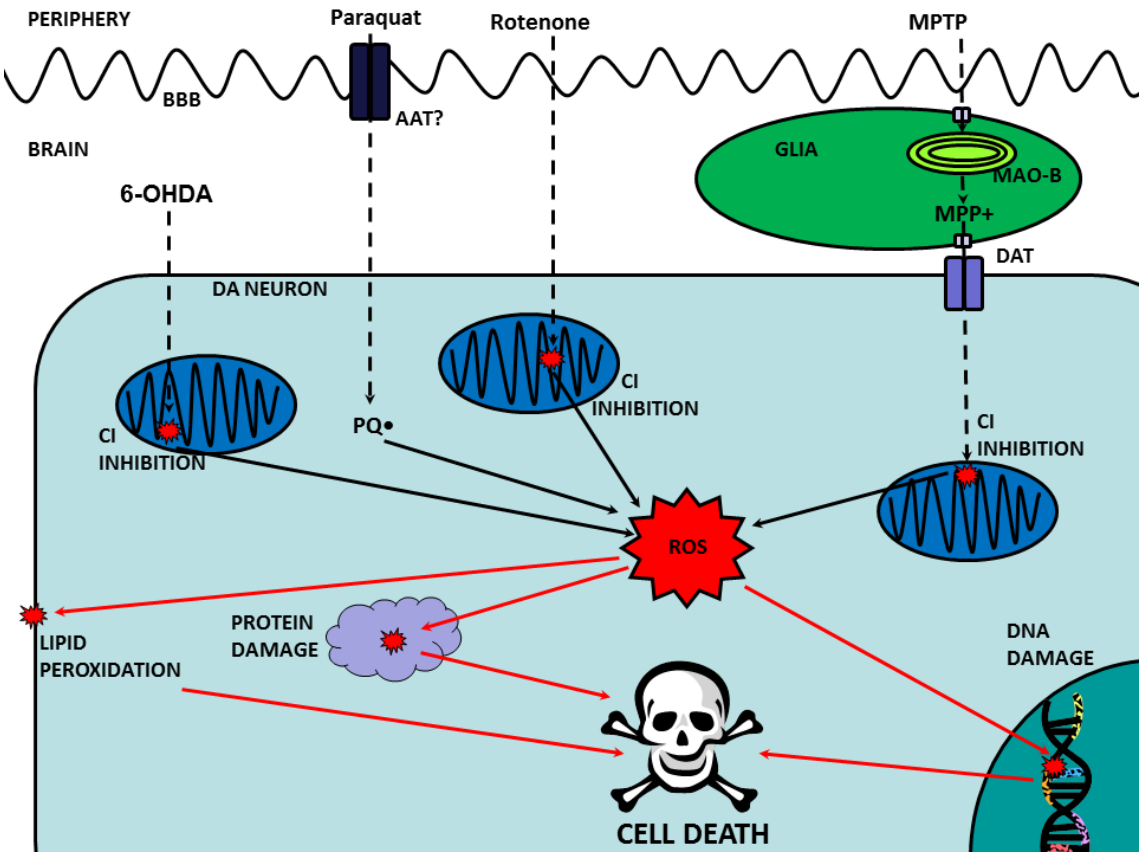

Fig. 1.16 Mechanisms of DA cell death mediated by common PD neurotoxins Paraquat crosses the blood brain barrier (BBB) by an as yet unclear mechanism, possibly via an amino acid transporter (AAT) /polyamine transporter (PAT), where it enters the cell and is spontaneously reduced to the paraquat radical (PQ·) and can then form ROS. 6-OHDA can be injected directly into the brain and rotenone can cross from the periphery, from where they enter neurons and can cause CI inhibition which leads to the production of ROS. MPTP enters the brain where it is taken up and converted to MPP+ in glial cells by MAO-B. This MPP+ is then transported out of the glia and taken up into neurons by the DAT. Once in the cell MPP+ also causes CI inhibition and generation of ROS. ROS formed by these environmental toxins can then lead to lipid peroxidation, protein damage, DNA damage and, ultimately, cell death

1.1.5 Animal Models of Parkinson's Disease

1.1.5.1 Toxin induced Models of PD

A number of PD models have been generated using exposure to compounds shown to replicate elements of the disease. The major toxin induced models of PD that have been studied are 6-OHDA, MPTP, rotenone and paraquat and have all been mentioned in detail in section 1.1.4 above. 6-OHDA was the first major animal model of the disease but has since been replaced by MPTP due to easier delivery methods and a more accurate replication of the disease pathology. Rotenone and paraquat are more recently developed models that are not as fully characterised but do seem to relatively accurately reproduce the symptoms of the disease.

One less commonly used toxin that may induce PD like symptoms and pathology in animal models is methamphetamine. Extremely high methamphetamine exposure in rats has been shown to produce selective reduction in tyrosine hydroxylase, a common marker of DA neurons, in the nigro-striatum (Trulson, Cannon et al. 1985), possibly inducing cell death through increased DA release and turnover leading to higher levels of oxidative stress. While it may show promise, this model is not very reliable nor is it as accurate in replicating PD as the other models mentioned. Another PD model not widely used is systemic Reserpine administration. This leads to a depletion of DA in the striatum and mimics the motor dysfunction seen in the disease (Fernandes, Santos et al. 2012); however, the Reserpine model does not recreate the underlying pathology of PD so is of limited use. Recently, an animal model has been developed to test the effects of oxidative stress on PD pathology by administration of 3-nitrotyrosine, a compound formed by the reaction of peroxynitrite with protein molecules possibly involved in protein aggregation. Injection of free 3-nitrotyrosine induced a correlated reduction in motor function and striatal DA neurons (Mihm, Schanbacher et al. 2001), suggesting this may be a useful model in the study of PD. However, 3-nitrotyrosine does not seem to mimic the progressive nature of PD and needs to be characterised more fully to elucidate its use in studying the disease.

1.1.5.2 Genetic Models of PD

In addition to the toxin induced models of PD, a number of transgenic animal lines have been generated that have attempted to replicate the pathology of the disease.

A number of models have been developed using α-synuclein, with mutated (mainly A30P & A53T mutations) or wild-type forms of the protein expressed under the control of various promoters. Early α-synuclein transgenic mice used a tyrosine hydroxylase promoter to try and target the mutations to DA neurons, however, these models expressing wild-type or mutant α-synuclein only produced minor motor dysfunction and little to no PD pathology (Masliah, Rockenstein et al. 2000; Matsuoka, Vila et al. 2001). A strain of mouse expressing human A30P mutant α-synuclein under the pan-neuronal Thy1 promoter develops a condition that mimics the development of PD with abnormal age dependent α-synuclein accumulation in the brainstem and an overexpression of tau phosphorylation (Kahle, Neumann et al. 2000; Frasier, Walzer et al. 2005) as well as decreased motor function occurring with age (Freichel, Neumann et al. 2007). However, as with other models, there are no reports of decreased DA levels or decreased DA neuron number in this model. As PD pathology has been suggested to occur at an early stage in the olfactory bulb, a model expressing A30P mutant α-synuclein under a promoter specific for olfactory neuron reported a significant decrease in DA in this region and a decrease in DA neuron number, that was not quite significant (P=0.08) (Nuber, Petrasch-Parwez et al. 2011), showing promise as a good model of the disease. A recent study expressed wild-type, A30P and A53T mutant forms of α-synuclein in mice under the mouse prion protein promoter and found LB-like α-synuclein inclusions, mitochondrial defects and cell death in neocortical, brainstem and motor neurons in A53T mutants, with similar but less severe pathology in A30P mutants and little to no pathology in wild-type mutant animals (Martin, Pan et al. 2006).

LRRK2 is another mutation that has been used to try and recreated the features of PD in a mouse model. G2019S mutant LRRK2 has been expressed in mice under a bacterial artificial chromosome promoter, and showed altered DA transmission in the striatum but no DA cell loss or motor dysfunction by 12 months (Li, Patel et al. 2010);this may be a good model of early pathology in PD, but does not fully replicate the disease progression. A more recent model expressing wild-type and two mutant forms of LRRK2 under a CMV enhanced human platelet derived growth factor β promoter showed more promise in replicating PD pathology. G2019S mutant LRRK2 overexpressing animals showed an age-dependent reduction in DA neurons and dysfunctional autophagic and mitochondrial activities in the nigrostriatal

pathway, but no motor dysfunction, and R1441C mutant mice showed reduced motor function, but no striatal pathology, due to a lack of expression (Ramonet, Daher et al. 2011).

Due to the probable involvement of the UPS and the presence of misfolded proteins in PD pathology, a model has been developed whereby the 26S proteasome is inactivated in the SN and forebrain of a strain of mice. These mice have been shown to develop intraneuronal inclusions similar to LBs and extensive neurodegeneration in the nigrostriatal pathway and forebrain (Bedford, Hay et al. 2008). In addition to this model, mice expressing a mutated version of the ubiquitin modulating enzyme UCH-L1, were reported to show a loss of DA neurons of the SN and decrease in striatal DA content (Setsuie, Wang et al. 2007).

DA D_2 receptors are found in the SN on DA nerve terminals where they act to inhibit the neuron following DA release. A D_2-knockout mouse has been generated which shows PD-like motor impairments, evidence of increased oxidative stress and LB inclusions in neurons of the SN, but although there is evidence of DA neuron axonal degeneration, no progressive cell loss is seen in the SNpc (Baik, Picetti et al. 1995; Tinsley, Bye et al. 2009).

The 'MitoPark' mouse is a model of mitochondrial dysfunction generated by conditionally knocking out TFAM in DA neurons. TFAM is essential for mitochondrial gene expression and maintenance so knocking it out leads to mitochondrial dysfunction in the DA neurons. These mice have been shown to replicate the slow progressive motor deficit seen in PD, which can be reversed by L-DOPA treatment, and is preceded by the formation of intraneural inclusions, reduced DA levels in the striatum and DA cell loss in the SNpc (Ekstrand, Terzioglu et al. 2007; Galter, Pernold et al. 2010; Good, Hoffman et al. 2011). MitoPark mice seem to be a promising model of PD pathology and clinical features; however, in contrast to the disease, the inclusions seen in the model have not been shown to contain α-synuclein.

Current transgenic models have been shown to replicate some features of the disease and are useful in investigating the mechanisms that lead to the SNpc DA cell loss seen but none, so far, are accurate replications of the complex pathology and clinical signs of PD.

1.1.5.3 Non-mammalian Animal Models of PD

Although mammal models of PD are the most useful in replicating disease pathology and progression, non-mammal models can often be used to mimic facets of the disease to better understand the mechanisms underlying the condition.

Human gene	*C. elegans* ortholog	*Drosophila* ortholog	Zebrafish ortholog
α-synuclein	*UNK*	*UNK*	*UNK*
PINK1	*pdr-1*	*Parkin*	*Parkin*
Parkin	*pink-1*	*Pink-1*	*Pink-1*
DJ-1	*djr1.1, djr1.2*	*DJ-1α, DJ-1β*	*Dj-1*
LRRK2	*lrk-1*	*Lrrk*	*Lrrk2*

Table 1.4 Summary of human PD genes and non-mammalian orthologs

Caenorhabditis elegans (*C. elegans*) is nematode worm that is well characterised and a commonly used experimental organism. The neurobiology of *C. elegans* has been widely studied and been shown to be highly conserved with that of mammals (Bargmann 1998), and all the major PD-linked genes, apart from *α-synuclein*, have been shown to have analogues in *C. elegans* (Table 1.4), which when combined with its ease of care and maintenance in a laboratory have led to its widespread use in investigating PD. *C. elegans* have been generated with GFP tagged DA neurons, making them easy to visualise, and these worms have been shown to have selective DA neurodegeneration when exposed to 6-OHDA (Nass, Hall et al. 2002). Although *C. elegans* has not been shown to express α-synuclein, worms transgenically manipulated to overexpress wild-type or mutated human α-synuclein have been shown to suffer DA degeneration, abnormal motor function and the formation of LB-like inclusions (Lakso, Vartiainen et al. 2003; Kuwahara, Koyama et al. 2006; Van Ham, Thijssen et al. 2008). In addition, *C. elegans* expressing α-synuclein, or undergoing deletion of *pdr-1* (*parkin* ortholog) or *djr1.1* & *djr1.2* (*DJ-1* orthologs) showed increased vulnerability to rotenone (Ved, Saha et al. 2005).

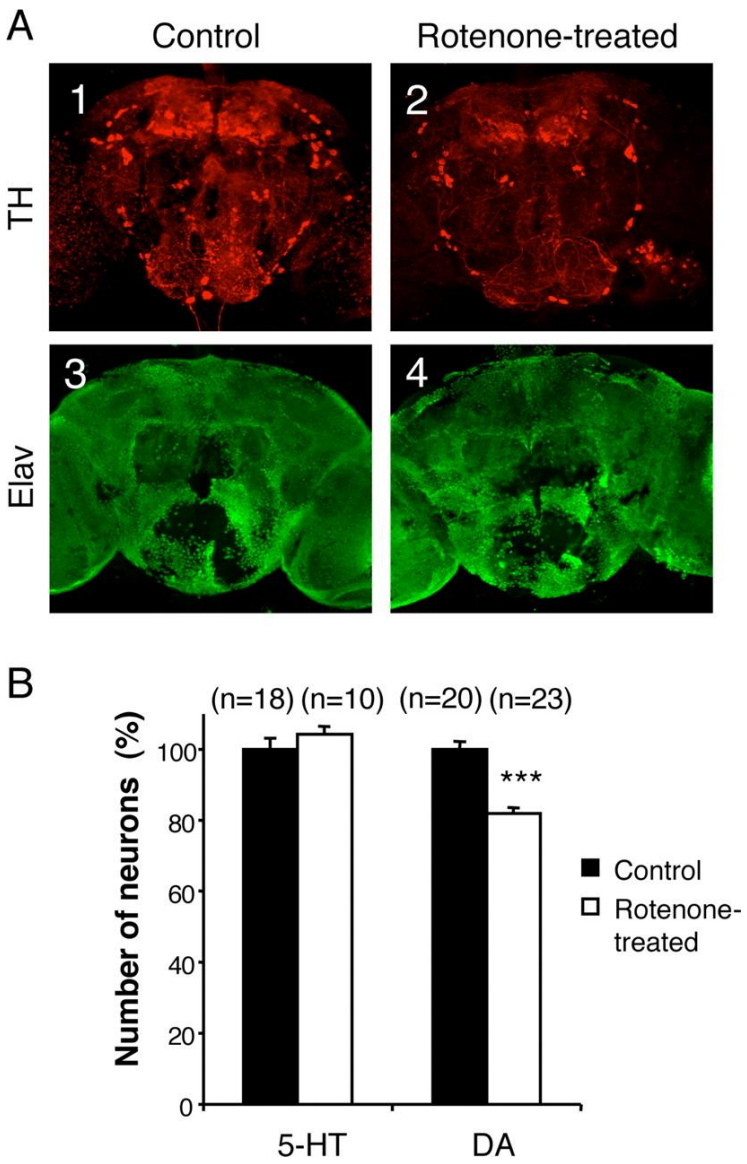

Fig. 1.17 Selectivity of the neuronal degeneration induced by rotenone in *drosophila* (A) Co-immunolabeling of adult brains with anti-tyrosine hydroxylase (TH) (A1, A2) and anti-Elav (A3, A4) antibodies after 7 d of exposure to 125 µm rotenone. The pesticide induced obvious dopaminergic neuron loss, whereas the general pattern of the pan-neuronal Elav marker was not modified.
(B) Total number of serotoninergic (5-HT) and dopaminergic (DA) neurons in fly brains exposed for 7 d to 125 µm rotenone (white bars) compared with control brains (black bars), expressed as a percentage of the mean value of the control. n indicates the number of brain hemispheres examined in each condition. ***P<0.001 (Taken from (Coulom and Birman 2004))

Drosophila melanogaster (*drosophila*) is a fruit fly that is widely used in biological research due to its well characterised genome and cost and ease of culturing. Its nervous system is more complex than *C. elegans* but still far more simple than its mammalian counterpart, and *drosophila* has been shown to have orthologs of the major PD-linked genes apart from *α-synuclein* (Table 1.4). *Drosophila* has been shown to be a good model for sporadic PD with chronic rotenone exposure leading to a loss of DA neurons (Fig 1.17) and motor dysfunction assessed by climbing activity that can be reversed by L-DOPA administration (Coulom and Birman 2004). *Drosophila* expressing human wild-type or mutant α-synuclein were found to have DA neurodegeneration, loss of climbing ability and developed intraneuronal a-synuclein-positive inclusions that resemble LBs (Feany and Bender 2000). Finally, flies which have been modified to knockout *parkin*, *pink1*, *dj-1α* and *lrrk2* have all shown DA neuronal cell loss and

behavioural abnormalities relating to PD (Yang, Gehrke et al. 2005; Park, Lee et al. 2006; Wang, Lu et al. 2007; Liu, Wang et al. 2008), providing a variety of *drosophila* models of the disease.

The zebrafish, *Danio rerio*, is widely used as a biological model system due to its relative closeness to humans in comparison to invertebrate models and the fact that it is more easily visualised and manipulated than other common vertebrate model species. The zebrafish genome has been sequenced and is well characterised and it has orthologs of the major human genes linked with PD (Table 1.4); however, although orthologs of various synuclein proteins have been found in the zebrafish, an *α-synuclein* ortholog has not, as yet, been established (Sun and Gitler 2008). In zebrafish DA neuron clusters in the ventral diencephalon (vDC) have been shown to be analogous to the ascending midbrain DA of the nigrostriatal pathway in mammals (Rink and Wullimann 2002). Zebrafish exposed to 6-OHDA and MPTP have been reported to show behavioural deficits and reduced DA levels (Anichtchik, Kaslin et al. 2004), and further studies have shown a decrease in DA neurons in specific areas of the vDC of zebrafish exposed to MPTP (Wen, Wei et al. 2008). Knockout of zebrafish Parkin, PINK1 and DJ-1 othologs have not been reported to show any DA degeneration; however, in all three cases, knockout of these genes has increased susceptibility of DA neurons to environmental stress and subsequent cell death (Bretaud, Allen et al. 2007; Fett, Pilsl et al. 2010; Sallinen, Kolehmainen et al. 2010), similar to mouse models.

1.1.5.4 Problems with Animal Models of PD

Animal models have been key in reaching the levels of understanding of PD we are at today; however, there are problems with, and limitations to, these models. Primarily, the difference in physiological make-up between model species and humans leads to difficulties in accurately replicating the disease; this can be seen in the varying results seen between species with different species showing markedly differing sensitivities to certain genetic manipulations and toxin exposures. Although some models have come close to replicating the features of the disease, none have as yet managed to produce a model that accurately reproduces PD meaning results seen cannot be entirely extrapolated to fully represent the disease. In addition to this, slight differences in the techniques used to generate and measure PD pathology and clinical signs in different laboratories seem to give widely varying results in similar experiments, with this especially apparent in mammalian behavioural studies, casting doubt on some findings. While animal models are extremely useful in PD research, more representative and robust models are needed to advance understanding more fully.

1.1.6 Other Parkinsonian Syndromes

There are a number of other syndromes that share the clinical hallmarks of PD but have been shown to have differing pathologies, including multiple system atrophy, progressive supranuclear palsy and corticobasal degeneration. A summary of clinical and pathological differences can be seen in Table 1.5.

	PD	MSA	PSP	CBD
Clinical discriminators of parkinsonian syndromes				
Tremor	Asymmetrical; post 4–8 Hz, rest 3–5 Hz; arms and legs, jaw, eyelids; latency to onset	Asymmetrical; post 4–8 Hz, rest 3–5 Hz; arms or legs; latency	Uncommon	Asymmetrical; postural, with stimulus sensitive myoclonus
Rigidity	Asymmetrical; limb	Asymmetrical; limb	Symmetrical; axial >limb	Asymmetrical; limb
Finger Movements	Progressive slowing with decreasing amplitude	Progressive slowing with decreasing amplitude	Spared early	Early apraxia—hand can become useless
Facies	Early loss of expression and blinking. Late blepharoclonus	Early loss of expression; facial dyskinesias	Lid retraction; staring; eye opening apraxia	Early loss of expression; orobuccal apraxia
Dysautonomia	Early impotence, late OH, bladder, constipation	Early OH, bladder, impotence, constipation	Early impotence, bladder, OH rare	Early impotence, bladder, OH rare
Ulbar	Late dysarthria; hypophonia	Early dysarthria, dysphagia; night stridor	Early dysarthria, dysphagia	Early dysarthria, dysphagia
Gait and posture	Late falls; retropulsion; festination, flexed posture	Early falls, flexed posture; antecollis ++	Early falls, retrocollis	Early falls
Eye movements	Hypometric	Nystagmus, hypometric	Eye deviation to OKN, SGP	Occasional SGP
Ataxia	None	Frequent	Rare	Rare
Apraxia	None	None	End stage limb; eye opening	Limb, alien phenomena
Pathological discriminators of parkinsonian syndromes				
Neurodegeneration	SNpc	Olivopontocerebellar & striatonigral	Brain stem, basal ganglia and occular motor nucleii	Cerebral cortex and subcortical nuclei
Pathological hallmarks	LB (α-synuclein)	GCI (α-synuclein)	Neurofibrillary tangles (tau)	Astrocytic plaques& neurofibrillary tangles (tau)

Table 1.5 Summary of clinical and pathological differences in parkisonian syndromes Abbreviations: OH, orthostatic hypotension; OKN, opticokinetic nystagmus; SGP, supranuclear gaze palsy (adapted from (Brooks 2002)).

1.1.6.1 Multiple System Atrophy

Multiple system atrophy (MSA) is a neurodegenerative condition which combines a variety of parkinsonian clinical signs with dysautonomia and cerebellar symptoms. It has a prevalence of 4-5 cases per 100,000 (Tison, Yekhlef et al. 2000) and develops more rapidly than PD with a life expectancy of less than 9 years following diagnosis (Schrag, Wenning et al. 2008) and no current treatments. MSA was first characterised by Papp *et al.* who found a common pathological feature of glial cytoplasmic inclusions in the brains of patients diagnosed with what was then thought to be three separate conditions: olivopontocerebellar atrophy, striatonigral degeneration and Shy-Drager syndrome (Papp, Kahn et al. 1989). The presence of these glial cytoplasmic inclusions (GCI) is now a hallmark of the disease and, when combined with olivopontocerebellar and striatonigral neurodegeneration, used for neuropathological diagnosis of MSA. A pathological link with PD was discovered when it was reported that GCIs, along with similar inclusions in neurons of the nigra, pontine and inferior olivary nuclei, and dentate fascia, in MSA patients were shown to contain α-synuclein (Wakabayashi, Yoshimoto et al. 1998). Clinically, MSA is subcategorised into a parkinsonian (MSA-P) or a cerebellar (MSA-C) form dependent on the predominance of a parkinsonian or cerebellar symptoms, with dysautonomia present in both subtypes and including urinary incontinence, respiratory failure, dysarthria, dysphagia and orthostatic hypotension (Gilman, Low et al. 1999; Gilman, Wenning et al. 2008), but clinical symptoms can substantially differ between patients. *In vitro* findings that mutated α-synuclein can lead to activation of glia and increased inflammatory modulators suggest a possible role for neuroinflammation in the disease mechanism (Klegeris, Pelech et al. 2008; Su, Federoff et al. 2009).

There have been reports of inherited familial forms of MSA in Germany and Japan (Soma, Yabe et al. 2006; Hara, Momose et al. 2007; Filosto, Tonin et al. 2009); however, due to the limited numbers of individuals affected, a causative gene has not yet been identified. Due to the presence of α-synuclein in GCIs in MSA, mutations in this gene may be involved in the disease, with genetic variants of the α-synuclein gene shown to lead to an increased risk of MSA (Al-Chalabi, Dürr et al. 2009; Scholz, Houlden et al. 2009; Ross, Vilariño-Güell et al. 2010). Another candidate gene for mutation in MSA is microtubule associated protein tau, with the H1-haplotype having been shown to be present in a number of MSA cases and shown to confer an increased risk of developing the disease (Vilariño-Güell, Soto-Ortolaza et al. 2011). This is interesting as MSA is primarily thought of as a synucleinopathy and has not been thought to have tau pathology.

Attempts have been made at using toxin induced animal models to try and recreate the symptoms and pathology of MSA-P. The simultaneous injection of PD-linked toxins MPTP or 6-OHDA, with the neuroinflammation-linked excitotoxic compound quinolinic acid or the succinate dehydrogenase inhibitor 3-nitropropionic to create lesions in the striatum and nigra has produced the motor impairment seen in the disease; however these models have not been able to replicate the GCIs characteristic of the disease so are only of limited use (Scherfler, Puschban et al. 2000; Waldner, Puschban et al. 2001; Ghorayeb, Fernagut et al. 2002).

1.1.6.2 Progressive Supranuclear Palsy

Progressive Supranuclear Palsy (PSP) is the second most common parkinsonian syndrome that was first distinguished from PD by Steele *et al.* in 1964 (Steele, Richardson et al. 1964) and has a prevalence of 6.5 per 100,000 people in the UK (Nath, Ben-Shlomo et al. 2001). The disease is characterised by early gait and balance impairment, with postural instability and recurrent falls being primary signs of the disease (Birdi, Rajput et al. 2002), followed by development of the ocular manifestations characteristic of the condition, namely supranuclear ophthalmoparesis (paralysis of down gaze) (Litvan, Campbell et al. 1997) and saccades (rapid eye movement between two stimuli) (Bhidayasiri, Riley et al. 2001) as well as general eye complaints such as blurred vision, diplopia, eye irritation or discomfort, eyelid abnormalities and photophobia (Friedman, Jankovic et al. 1992). PSP patients may also present with dementia, dysarthria, dysphagia and dystonia (Kluin, Foster et al. 1993; Pillon, Deweer et al. 1994; Barclay and Lang 1997; Nath, Ben-Shlomo et al. 2003). Pathologically, PSP manifests as neurofibrillary tangles composed of intracellular aggregates of the microtubule-associated protein tau in neurons and glia (Pollock, Mirra et al. 1986) and degeneration of neurons and a proliferation of glia in the globus pallidus, subthalamic nucleus, red nucleus, substantia nigra, periaqueductal grey matter, pontine tegmentum and dentate nucleus (Armstrong, Lantos et al. 2007).

A report of an autosomal dominant inherited form of PSP with incomplete penetrance has been published (Rojo, Pernaute et al. 1999) and mutations in *MAPT* have been linked with the disease development (Conrad, Andreadis et al. 1997; Baker, Litvan et al. 1999) suggesting a possible familial form of the disease related to mutations in tau. It has also been suggested that PSP may be due to mutations in mtDNA, leading to mitochondrial electron transport chain misassembley, Complex I dysfunction and increased oxidative stress (Swerdlow, Golbe et al. 2000). The involvement of environmental toxins in the pathology of PSP has been proposed but there have been no significant reports of this so far.

1.1.6.3 Corticobasal Degeneration

Corticobasal Degeneration (CBD) is a neurodegenerative condition similar to PSP that was first described as a distinct condition by Gibb *et al.* in a review of 3 patients (Gibb, Luthert et al. 1989). It combines asymmetric parkinsonian symptoms with a phenomenon known as 'Alien Hand Syndrome', apraxia, aphasia and, occasionally, dementia (Rinne, Lee et al. 1994). CBD is characterised pathologically by the presence of astrocytic plaques and 'ballooned' neurons (Takahashi, Amano et al. 1996) as well as asymmetrical atrophy of the cerebral cortex and subcortical nuclei, especially the substantia nigra (Ikeda 1997).

CBD is generally considered a sporadic disease; however there have been reports that the condition shares a common tau haplotype with PSP (Di Maria, Tabaton et al. 2000; Houlden, Baker et al. 2001), suggesting a possible genetic component in CBD development through MAPT. Although environmental factors may be involved in the pathology of CBD, no wide scale studies into this have been carried out as yet.

1.2 Trichloroethylene

TCE (Fig. 1.18) is a volatile industrial solvent that is used as a metal degreasing agent, paint stripper and as an ingredient in paints and varnishes (Wu and Schaum 2000), as well as being used in the past in industrial scale dry cleaning and as an inhalational anaesthetic (Lock and Reed 2006). TCE is also found in the food chain and water system to due to environmental contamination (Wu and Schaum 2000; Lock and Reed 2006), which, combined with the occupational contact, leads to a proportion of the population exposed to chronic low levels of the chemical.

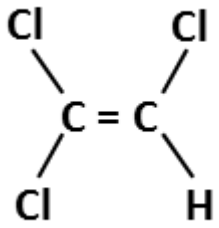

Fig. 1.18 TCE Chemical structure of TCE

1.2.1 Trichloroethylene Exposure

TCE is released in to the environment during its manufacture, use and disposal. Most TCE is released into the atmosphere, although it is also present, due to disposal, in water and landfill sites. Due to its volatile nature most environmental TCE is present in the atmosphere but also at lower levels in the groundwater as a result of its moderate water solubility (Wu and Schaum 2000). Once in the air, TCE has a relatively short half-life of seven days, due to degradation by reacting with hydroxyl radicals, meaning that is not a persistent atmospheric contaminant. However, owing to the constant release of TCE, it is continually present in areas of production (Williams-Johnson, Eisenmann et al. 1997).

Workers in industrial areas, especially the degreasing trade, have the highest exposure to TCE, mainly through inhalation, with levels ranging from 1-100 ppm (Williams-Johnson, Eisenmann et al. 1997). The general public can also be exposed to lower levels of TCE through drinking water with the U.S. state surveys reporting between 9% and 34% of drinking water sources contaminated with TCE (Williams-Johnson, Eisenmann et al. 1997), and a separate study found that subjects from a community adjacent to a known TCE contaminated water supply were exposed to TCE at levels up to 19.1 ppb (Reif, Burch et al. 2003). The U.S. Department for Health and Human Services document on the toxicological profile for TCE estimated average daily intakes of TCE of 11-33mg/day from air and 2-20mg/day from drinking water in America. This data shows that the populace can be exposed to chronic low levels of TCE both

occupationally and through proximity to environmental contamination. A study of an individual exposed to TCE occupationally for twenty years reported TCE present in exhaled air up to six years following final exposure, with 128ng/l present three years post exposure which had reduced to 3ng/l by six years (Kochen, Kohlmüller et al. 2003). Re-exposure was absolutely excluded in this individual suggesting that TCE is persistent in the body for a relatively long period following exposure.

1.2.2 General Trichloroethylene Toxicity

In 1976, the U.S. Department of Health, Education and Welfare published a paper on the links between TCE and carcinogenicity in animals (U.S. Department of Health 1976). Since then studies have shown links between TCE and its metabolites and renal, respiratory, reproductive and hepatic carcinogenicity in animal models although there is some dispute whether this will translate into risk in humans (Davidson and Beliles 1991; Committee on Human Health Risks of Trichloroethylene 2006). Lock & Reed reviewed renal carcinogenicity data of adenoma and carcinoma formation in animal studies following TCE exposure, and propose a weak association between high level TCE and renal carcinoma. They suggest a mechanism for this carcinogenicity that involves conjugation with GSH leading to formation of a reactive electrophile (Lock and Reed 2006).

There have also been reported links between TCE and pulmonary carcinogenicity in mouse models (Davidson and Beliles 1991) but it has been suggested that this is due to the high activity of p450 in the mouse lung, approximately 600-fold that in humans, and therefore will not translate to humans (Green 2000). Further to the possible pulmonary carcinogenicity, TCE has also been linked to toxicity in the lungs, specifically the Clara cells of the bronchiolar epithelium in mice after acute dosing (Forkert and Birch 1989). Comparable to the lung cancer causing effects of TCE, hepatic tumours have been found, mainly in mouse models, and are thought to be associated with peroxisome proliferation and increased cell division. These are also thought not to translate well to humans due to metabolic differences between the species (Green 1997).

TCE has also been reported to cause severe damage to kidney, intestine, liver and brain, as well as altered carbohydrate metabolism in rats, with suppressed antioxidant defence system suggested as a possible mechanism for this (Khan, Priyamvada et al. 2009). This suspected reduction in antioxidant defence was given further credence by previous reports that the

activity of molecules involved in endogenous antioxidant defence, superoxide dismutase and glutathione peroxidase were decreased in dogs (Aslan, Tütüncü et al. 2000).

1.2.3 Trichloroethylene Neurotoxicity & Metabolism

There have been widespread reports of neurotoxicological effects of TCE. In humans, acute TCE exposure has been shown to lead to headache, fatigue, drowsiness, inability to concentrate, dizziness, loss of facial sensation and unconsciousness (Williams-Johnson, Eisenmann et al. 1997; Committee on Human Health Risks of Trichloroethylene 2006), and chronic low exposure, has been linked to general neurobehavioral deficits (Reif, Burch et al. 2003). TCE has also been shown to depress conductance in squid giant axons, at least partly due to a decrease in resting potassium permeability, leading to a potential for general anaesthetic properties in mammals (Bhushan Shrivastav, Narahashi et al. 1976). In animal models, inhibition of long term potentiation and plasticity in mouse hippocampus has been reported in TCE exposed mice (Ohta, Saito et al. 2001; Altmann, Welge et al. 2002), suggesting a possible role of TCE in memory impairment. In studies into early life exposure of TCE, altered social behaviours and increased aggression associated with markers of oxidative stress in the brain were seen. The mechanism of these pre-natal effects of TCE on the brain which may involve modulation of the immune system by a redox-associated differentiation of T-cells in the thymus and an associated increase in pro-inflammatory cytokines from CD4+ T-cells affecting the developing brain (Blossom, Doss et al. 2008). TCE exposure in juvenile MRL +/+ mice, has been shown to lead to an increased oxidative state and decreased expression of neurotrophic factors in the hippocampus (Blossom, Melnyk et al. 2012) , suggesting a possible cellular mechanism for the neurotoxic effects of TCE discussed.

TCE exposure has been suggested to have links with idiopathic PD, with small scale case report studies showing high levels of occupational TCE exposure in PD patients and a higher than expected occurrence of motor deficits in similarly exposed co-workers (Guehl, Bezard et al. 1999; Kochen, Kohlmüller et al. 2003; Gash, Rutland et al. 2008). More recently, an investigation into ninety-nine pairs of twins discordant for PD found that occupational exposure to TCE increased the odds ratio of developing PD by over six times (Goldman, Quinlan et al. 2012), supporting the case reports in a population based study. Trichloroethylene has been identified in at least 861 of the 1,428 hazardous waste sites that have been proposed for inclusion on the EPA National Priorities List in the USA (Williams-Johnson, Eisenmann et al. 1997) and a geographical comparison of these sites with PD prevalence among Medicare beneficiaries (Wright Willis, Evanoff et al. 2010) reinforced the

link between TCE and PD with areas showing high PD prevalence (orange and red areas in Fig. 1.19 B), such as the northeast and south central regions of the country, generally correlating well with the areas shown to have >10 TCE waste sites (dark grey and large dotted areas in Fig. 1.19 A). These links between TCE exposure and PD have recently been supported by a report that rats orally dosed with TCE over six weeks showed a reduction in DA neurons in the SNpc, reduced levels of DA metabolism, motor deficits and reduced mitochondrial Complex I activity (Liu, Choi et al. 2010). A study in rats reportS a reduction in mitochondrial function in the striatum of TCE exposed rats and reduced motor performance and SNpc TH positive neuron number in animals that suffered traumatic brain injury in addition to this TCE exposure (Sauerbeck, Hunter et al. 2012). This study further indicates a link between TCE and PD but suggests concurrent insults may be needed for neuronal damage and functional development of the disease. As well as potential links with PD, a number of patients with the severe Parkinsonian syndrome MSA have been found to have had high exposure levels to TCE (Blain, personal communication), providing more evidence of the link between the chemical and DA neurodegeneration.

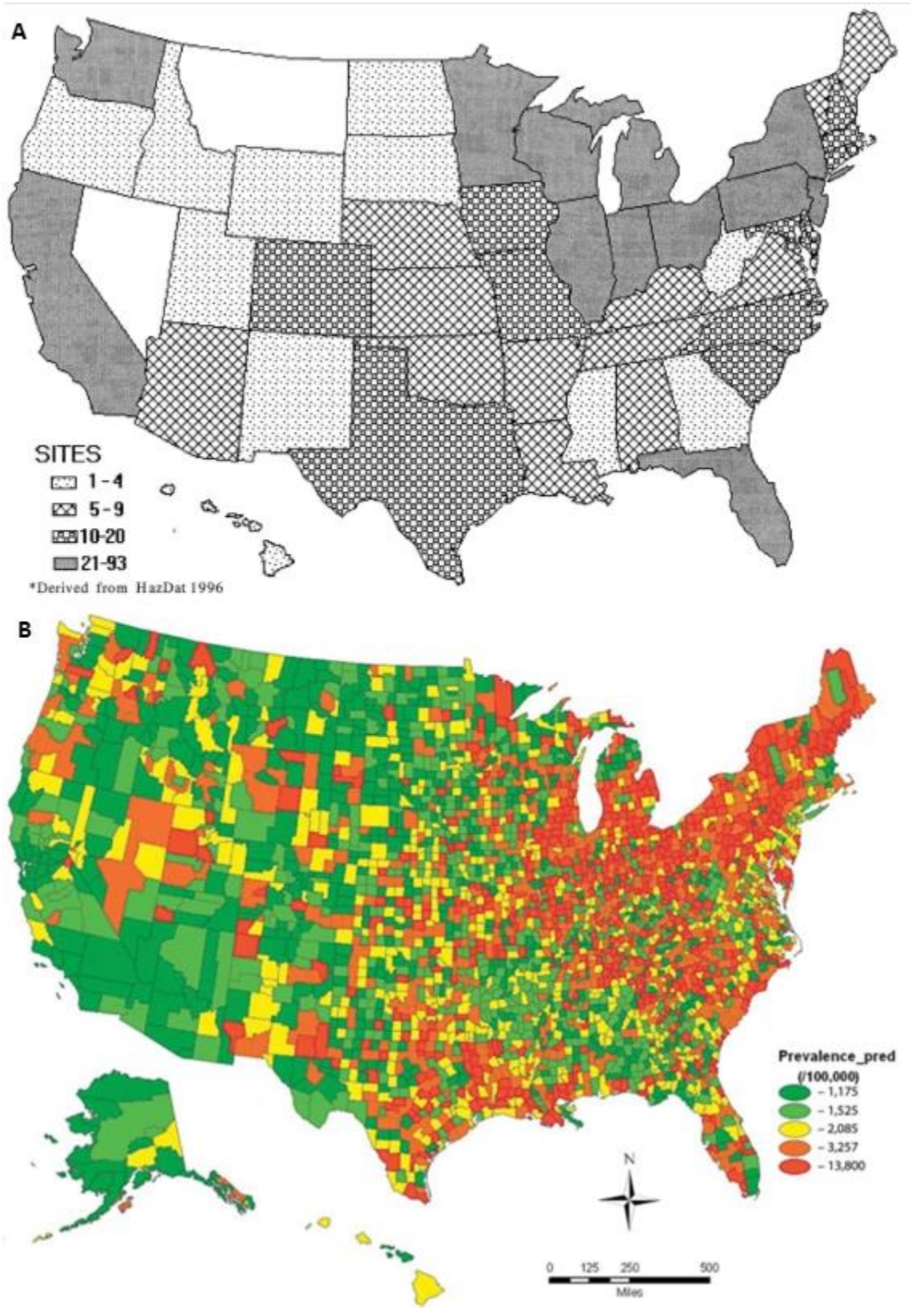

Fig. 1.19 Comparison of TCE waste sites and PD prevalence in the USA (A) Frequency of EPA National Priorities List hazardous waste sites with TCE contamination. Taken from (Williams-Johnson, Eisenmann et al. 1997)(B) County level age- and race-standardized prevalence (per 100,000) of Parkinson disease among Medicare beneficiaries in the United States (year = 2003). Taken from (Wright Willis, Evanoff et al. 2010)

1.2.3.1 TCE Metabolism

It has been hypothesised that some of these neurotoxicological effects of TCE may be mediated by products of TCE metabolism. TCE is metabolised predominantly by two major routes, either by the cytochrome p450 oxidative pathway (Fig. 1.20) or the GSH conjugation pathway, with the oxidative pathway predominating and being the pathway that generates the major toxic metabolites of TCE (Maull and Lash 1998) and will be discussed in more detail.

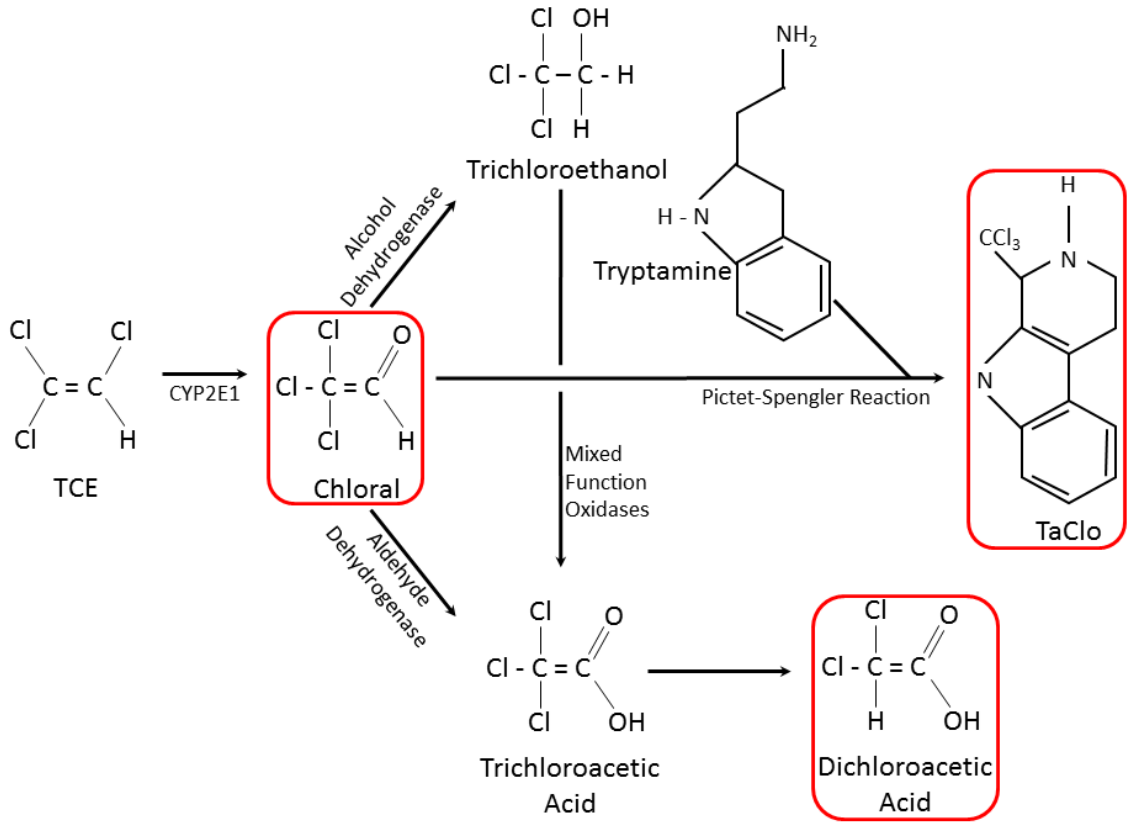

Fig. 1.20 TCE metabolic pathway Schematic of the oxidative pathway of TCE metabolism leading to formation of potentially toxic metabolites; chloral, TaClo and dichloroacetic acid (highlighted red)

In the oxidative pathway (Fig. 1.20), TCE is metabolised to the aldehyde chloral by a cytochrome p450 enzyme, most likely CYP2E1 (Jiang, Mutch et al. 2007). Chloral can spontaneously react with endogenous tryptamine by a Pictet-Spengler type condensation to form TaClo (Bringmann, Feineis et al. 2000). Chloral can also be oxidised by aldehyde dehydrogenase to trichloroacetic acid or reduced by alcohol dehydrogenase to form trichloroethanol. Trichloroethanol can be further metabolised by mixed function oxidases to form more trichloroacetic acid which can undergo final additional metabolism to become dichloroacetic acid (DCA) (Maull and Lash 1998). The metabolites that have been most strongly linked with neurological effects are chloral, TaClo and DCA and are discussed in more detail below.

1.2.3.2 Chloral Neurotoxicity

Chloral has been widely used as an anaesthetic agent in its hydrate form, particularly in infants. The main neurotoxic effects of chloral are thought to be mediated by its metabolites such as TaClo and DCA (described later in more detail), but there have been some reports of neurotoxicity caused by the compound itself. Primarily, a study found that chloral induced neuroapoptosis (cell death in the brain) in the infant mouse brain, particularly the cerebral cortex and caudate-putamen, at doses as low as 100mg/kg i.p. (Cattano D., Straiko M.M.W. et al. 2008). Chloral has also been shown to antagonise the neurotoxic effects of the recreational drug 3,4-methylenedioxymethamphetamine (MDMA), an effect thought to be due to a blockade of DA release (Schmidt, Black et al. 1990). While this has not been confirmed, if it is true, interference with DA transmission could have relevance in the suspected PD effects seen with TCE exposure. While these are single studies that have not been supported, there is at least an indication that chloral itself may possibly be neurotoxic at some level.

1.2.3.3 TaClo Neurotoxicity

As β-carbolines such as TaClo (Fig. 1.13 & 1.20) have structures similar to that of MPTP, they could be neurotoxic for DA neurons in the SNpc and lead to a PD-like syndrome supported by the finding that the β-carboline norharmon leads to reduced motor function and cell death in the DA neuron model cell line PC12 (Östergren, Fredriksson et al. 2006). TaClo can cross the blood brain barrier following intraperitoneal injection in the rat (Riederer, Foley et al. 2002), suggesting peripherally exposed TCE or TaClo can enter brain neuron, although these results should be viewed with caution as they use doses higher than those required to elicit behavioural changes.

Reports have shown that micromolar concentrations of TaClo caused up to 50% cell death in primary C57/B16 mouse mesencephalon cultures of DA neurons and astrocytes (Rausch, Abdel-Mohsen et al. 1995), and in the human neuroblastoma cell line SK-N-SH, possibly by an apoptotic mechanism (Akundi, Hüll et al. 2003; Akundi, Macho et al. 2004). This was supported by *in vivo* studies showing intranigral TaClo exposure led to a reduction in DA metabolism (Grote, Clement et al. 1995), with further studies showing a progressive reduction in locomotion and increase in apomorphine induced rotations in behavioural tests (Sontag, Heim et al. 1995; Heim and Sontag 1997; Sontag, Lange et al. 2009) and the discovery of a strong inhibition of mitochondrial Complex I *in vitro* (Janetzky, God et al. 1995). This Complex I inhibition is supported by work that shows a real time increase in superoxide released from isolated mitochondria exposed to TaClo which is similar in magnitude and response time to

known Complex I inhibitor rotenone (Boulton, Keane et al. 2012). A possible explanation for the DA specificity of TaClo may come with the finding that β-carbolines have high binding affinity to neuromelanin, a pigment found particularly in DA neurons, and to have high retention times (>30days) in neuromelanin containing tissues (Östergren, Annas et al. 2004). Taken together these data presented a strong case for the neurotoxic properties of TaClo against DA neurons. Interestingly, further work showed that N-methyl-TaClo is a more potent inhibitor of mitochondrial Complex I and more neurotoxic than TaClo itself (Janetzky, Gille et al. 1999). This is thought to be due to the fact that N-methylation would enhance the lipophilicity of the compound, enhancing its ability to cross membranes. When combined with the fact that tetrahydro-β-carbolines have been shown to undergo N-methylation in the brain (Matsubara, Collins et al. 1993), this gives further evidence of TCE generated TaClo neurotoxicity.

A study of the effects of TaClo on motor behaviour in rats found that motor deficits do not occur immediately following treatment, with no effects on motor function seen four to nine days after a chronic dosing period, but decreased motor function observed twelve weeks later (Sontag, Heim et al. 1995). This indicates that TaClo may be acting as a persistent neurotoxin - possibly due to retention in the neuromelanin previously mentioned - in this model producing slowly progressive lesions of the SN rather than immediate effects seen with other PD-linked toxins such as MPTP, and possibly providing a model system that better represents the condition in humans.

It has also been reported that TaClo can cause single strand DNA breaks in cell-free plasmids, possibly caused due to the formation of a reactive species by a Cu(II)/Cu(I) mediated redox cycle (Bringmann, Münchbach et al. 2001). However, further work is required before accepting this finding as a factor in TaClo mediated cell death.

A significant increase in extracellular serotonin (5-HT) and a non-significant increase in DA release immediately after dosing rats with TaClo, followed by an increase in the production of hydroxyl radicals, has been shown (Gerlach, Xiao et al. 1998) and in work carried out in 5-HTergic JAR cells, TaClo has been shown to be cytotoxic and to cause a release of 5-HT (Bringmann, Bruckner et al. 2000). This finding led to suggestions that TaClo may be more specific to 5-HT than DA neurons (Bringmann, Bruckner et al. 2000) and not selectively toxic to DA as previously proposed. This lack of specificity of TaClo is supported by the reports that show, *in vitro*, TaClo shows no selective toxicity for DA neurons or cells expressing DAT (Storch,

Hwang et al. 2006). These recent findings on the neurotoxicity of TaClo to 5-HT neurons *in vitro* need more investigation but provide an interesting novel scheme of TaClo neurotoxicity.

While more work needs to be carried out to elucidate the effects by which TaClo leads to cell death in the neurotransmitter pathways in the central nervous system, and whether or not it is involved in the neurotoxicity of TCE, there is compelling evidence that this compound is neurotoxic at some level.

1.2.3.4 DCA Neurotoxicity

DCA (Fig. 1.20) is another metabolite that it is thought to contribute to the neurotoxicity of TCE. Toxicology studies on dogs and rats have shown DCA to cause myelin vacuolation and gliosis in the white matter of the forebrain, cerebrum, cerebellum, brainstem and spinal cord, accompanied at high doses by partial hind leg paralysis (Yount, Felten et al. 1981; Bhat, Kanz et al. 1991; Cicmanec, Condie et al. 1991). A therapeutic trial in 1995 found a polyneuropathy with areflexia with reduced nerve conduction in the peroneal nerve in children treated with DCA for Complex I deficiency (Kurlemann, Paetzke et al. 1995), with a further trial of DCA being discontinued due to peripheral neuropathies in seventeen of nineteen patients (Kaufmann, Engelstad et al. 2006). This evidence led to a study into the neurobehavioural effects of DCA in the rat which found that DCA produced a reversible peripheral neurotoxicity that consisted of limb weakness, deficits in gait and righting reflex and mild tremors (Moser, Phillips et al. 1999). There were distinct age and strain differences in this effect, which should be taken in to account in any further research. Exposure of cultured dorsal root ganglia neurons and Schwann cells to DCA over twelve days shows a reversible decrease in myelination and a moderate decrease in cell viability (Felitsyn, Stacpoole et al. 2007) that could explain the effects described in the rat study above. This evidence suggests a possible peripheral effect of DCA in the neurotoxicity of TCE, although there have been no studies into any direct link between TCE and peripheral neuropathies.

1.3 Cell Death Pathways

Programmed cell death is a regulated process of death that can occur in cells for a number of reasons, including during development or when cells are no longer needed. The death of cells in this manner is generally an advantageous process; however, programmed cell death pathways can be activated when cells undergo stress and damage and may lead to the death of cells that are otherwise needed, for example DA neurons in PD. There are three major methods of cell death, apoptosis, programmed necrosis and autophagy mediated death, which are described in more detail below.

1.3.1 Apoptosis

Apoptosis was the first major programme of cell death described in 1972 (Kerr, Wyllie et al. 1972) and has since been extensively studied and characterised. Apoptosis is a mode of programmed cell death linked with cell shrinkage, membrane blebbing, nuclear fragmentation and chromatin condensation. There are two main families of proteins involved in apoptosis, a group of proteases known as caspases (for in depth review see (Fuentes-Prior and Salvesen 2004)) and the Bcl-2 family of proteins (for in depth review see (Youle and Strasser 2008)). The Bcl-2 proteins are involved in modulating mitochondrial integrity during apoptosis, and can be pro- or anti-apoptotic in nature. The caspases are proteases that mediate cleavage of specific cellular substrates causing cell death; they can be split into initiator caspases (2, 8, 9 & 10), which activate other proteins involved in the apoptotic cascade, and executor caspases (3, 6 & 7), which carry out the breakdown of cellular components and lead to cell death.

Apoptosis can be initiated by two main methods, extrinsic - mediated by stimulation of death receptors - or intrinsic, mediated by cellular stress. During the intrinsic pathway of apoptosis intracellular stress induces or activates the BH3-only class of proteins (Puthalakath, O'Reilly et al. 2007; Steckley, Karajgikar et al. 2007). These BH3-only proteins then inhibit the Bcl-2 family of proteins, leading to disinhibition of the pro-apoptotic factors Bax and Bak (Willis, Fletcher et al. 2007). Bax and Bak dimerise and form pores in the mitochondrial membrane leading to release of pro-apoptotic proteins (Korsmeyer, Wei et al. 2000). One of these proteins is cytochrome-c which associates with Apaf-1 forming the apoptosome and activating the initiator caspase-9, which, in turn, activates the downstream executioner caspases which carry out the breakdown and destruction of the cell (Li, Nijhawan et al. 1997). Also released from the mitochondria by Bax/Bak are pro-apoptotic molecules such as Smac/Diablo, which are thought to contribute to the apoptosis pathway via inhibition of pro-survival molecules, such

as cIAP1 & 2 (described in more detail below), so facilitating activation of the caspase cascade (Du, Fang et al. 2000).

The extrinsic pathway is induced by activation of the TNFR family of death receptors such as TNF, Fas and TRAIL-R and bypasses the mitochondrial involvement of the intrinsic pathway by the formation of intracellular death inducing signalling complexes (DISCs) containing FADD which directly activates the initiator caspases (8,10) (Micheau and Tschopp 2003; Duprez, Wirawan et al. 2009). These initiator caspases then activate the executor caspases (3,6,7) (Stennicke, Jürgensmeier et al. 1998), which execute cell death by cleaving intracellular substrates, activating DNases and causing destruction of cellular contents (Cohen 1997; Enari, Sakahira et al. 1998). Initiator caspase-8 can also cleave the BH3-only protein Bid which amplifies the death process by activating the intrinsic mitochondrial pathway of apoptosis by BCl-2 inhibition, and possibly direct activation of Bax/Bak (Li, Zhu et al. 1998; Luo, Budihardjo et al. 1998).

Activation of TNFR does not always lead to apoptosis. When activated, TNFR1 recruits receptor interacting protein 1 (RIP1), TRADD and TRAF2 and forms a pre-DISC complex I (Hsu, Xiong et al. 1995; Hsu, Huang et al. 1996; Shu, Takeuchi et al. 1996). If present, cIAP1 & 2 can interact with TRAF2 thereby associating with complex I and ubiquitinating RIP1. This contributes to activation and relocation of NF-κB to the nucleus where it up regulates expression of anti-apoptotic genes, promoting cell survival (Mahoney, Cheung et al. 2008). Fig 1.21 shows a schematic representation of the various apoptotic pathways discussed.

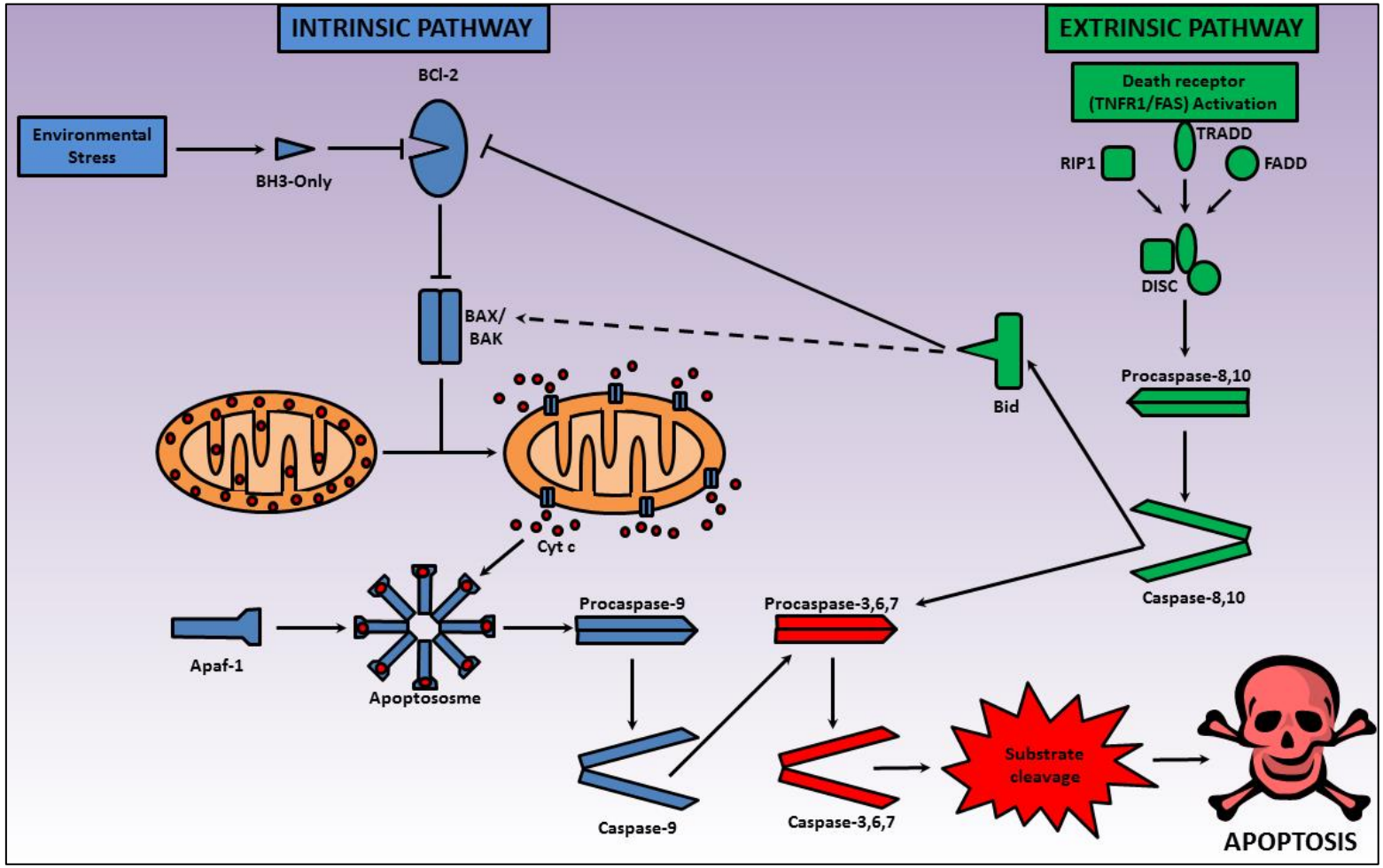

Fig. 1.21 Intrinsic and extrinsic pathways of apoptosis Apoptosis can be induced by cell surface receptors (TNFR1/FAS) (extrinsic pathway, green), or by various environmental stresses (intrinsic pathway, blue). The intrinsic pathway starts with BH3-only protein induction or activation, which results in the inactivation of some BCL-2 family members. This relieves inhibition of BAX and BAK activation, which in turn promotes apoptosis. Some BH3-only proteins, such as Bid, may also be able to activate Bax/Bak via the extrinsic pathway (as shown by the dotted line). Once activated, Bax and Bak promote cytochrome c (cyt c) release, which leads to the assembly of APAF1 into an apoptosome and activates caspase-9 to initiate executor caspases (3/ 6/7). Executor caspases in turn cleave a series of substrates, activate DNases and orchestrate the demolition of the cell (red). The extrinsic pathway can bypass the mitochondrial step and activate caspase-8/10 by the formation of DISC, which leads to caspase-3 activation and cell death.

1.3.2 Necroptosis (Programmed Necrosis)

Necrosis had long been thought to be an unregulated form of cell death but more recently a programmed, caspase-independent form of cell death with a necrotic morphology has been described that has been termed 'necroptosis' (Degterev, Huang et al. 2005) and the name was formally defined and recommended for use in 2009 (Kroemer, Galluzzi et al. 2009). It is thought that this death mechanism is induced by activation of the same death receptors that bring about apoptosis. A small molecule that specifically inhibits necroptosis over apoptosis subsequent to death receptor activation has been discovered and named 'necrostatin-1'(Nec-1)(Degterev, Huang et al. 2005). Nec-1 has since been found to act via inhibition of the kinase domain of RIP1 and hence reduce its ability to associate with RIP3 (Degterev, Hitomi et al. 2008), the serine/threonine kinase previously linked to caspase-independent death receptor initiated cell death (Holler, Zaru et al. 2000). RIP3 has also been implicated in control and execution of necroptosis (Cho, Challa et al. 2009; He, Wang et al. 2009; Zhang, Shao et al. 2009). Studies suggest that RIP3 complexes with RIP1 via direct interaction of their RIP homotypic interaction motif domains and that the complex acts as a switch between apoptosis and necroptosis following death receptor activation (Declercq, Vanden Berghe et al. 2009; He, Wang et al. 2009). The formation of this complex requires caspase 8 inhibition, suggesting that caspase 8 cleavage of RIP1 during propagation of apoptosis blocks the progress of necroptosis (He, Wang et al. 2009). The RIP1/RIP3 complex has been named Complex IIb or the necrosome and involves other proteins such as FADD and caspase 8 (He, Wang et al. 2009; Christofferson and Yuan 2010), as well as the mixed lineage kinase domain-like protein (MLKL), a protein which has been found to associate with RIP3 and is essential for necroptosis (Sun, Wang et al. 2012). The mitochondrial phosphoglyceratemutase 5 (PGAM5) has also been reported to be associated with the RIP1/3 complex, through association with RIP3 (Wang, Jiang et al. 2012). The ubiquitination state of RIP1 may be involved in the interaction of Complex IIb and downstream effectors, as evidenced by the finding that the RIP1 acting deubiquitinase CYLD can protect against necroptosis (Hitomi, Christofferson et al. 2008).

The downstream pathways of necroptosis have yet to be clearly characterised; however there is some evidence to indicate involvement of certain cell death mediators. Increased ROS levels have been suggested as a major mediator of cell death in necroptosis. ROS producing enzyme phospholipase A2 (PLA_2) has been suggested as a possible necroptosis mediator; when death receptors are stimulated during apoptosis, PLA_2 is activated but rapidly cleaved and deactivated by activate caspases; however, with caspases inactive during necroptosis, PLA_2 could increase ROS production and contribute to necroptotic cell damage and death (Tait and

Green 2008). RIP3 is known to interact with several metabolic enzymes and increase energy metabolism-associated ROS (Zhang, Shao et al. 2009) Another possible involvement of ROS in necroptosis is suggested with evidence that activation of the NADPH oxidase Nox1 via an interaction with RIP1 leads to an increase in ROS (Kim, Morgan et al. 2007). However, this evidence of the involvement of ROS in executing necroptosis needs to be balanced by other studies suggesting that ROS is not a key mediator with antioxidants having been reported to not inhibit necroptosis in certain cell lines (Degterev, Huang et al. 2005). This conflicting evidence proposes a possible role for ROS in necroptosis execution, but suggests this effect may be cell type specific and requires more investigation.

Mitochondria are known to be involved in many types of cell death and have been implicated in necroptosis. Cyclophillin D and adenine nucleotide translocase have been shown to interact with RIP1 to form the mitochondrial transmembrane pore (MTP) during necroptosis (Temkin, Huang et al. 2006). The mitochondrially related BH3-only protein Bmf has also been linked with necroptosis in a genetic screen (Hitomi, Christofferson et al. 2008) and further studies have shown that knockdown of Bmf can block necroptosis (Nagley, Higgins et al. 2010) implicating it in the execution of necroptotic death. The mitochondrial apoptosis inducing factor (AIF) has been strongly implicated as a mediator of necroptosis (Boujrad, Gubkina et al. 2007). Release of AIF from mitochondria in a similar caspase independent form of cell death designated 'partanthos' has been shown to be induced by PARP1 (Wang, Dawson et al. 2009) which could indicate a possible mechanism for AIF release in necroptosis. Mitochondrial fission has been a reported characteristic of necroptosis, a possible mechanism for this can be hypothesised by the finding that the regulator of mitochondrial fission dynamin-related protein 1 (Drp1) can be dephosphorylated by PGAM5, a component of Complex IIb (Wang, Jiang et al. 2012). This combination of evidence suggests a strong probability that mitochondria are involved in the execution of necroptosis.

Autophagy may also be involved in necroptosis execution; studies have shown that 3-methyladenine and RNAi inhibition of autophagy can inhibit necroptotic cell death, in certain cell types (Tait and Green 2008; Christofferson and Yuan 2010) and an autophagy phenotype has been observed in necroptotic cells (Bonapace, Bornhauser et al. 2010). A link between necroptosis and autophagy has also been demonstrated by showing the presence of the autophagy marker microtubule –associated protein 1 light chain 3 (LC3-B) in necroptotic systems, an effect that can be blocked by Nec-1 administration (Degterev, Huang et al. 2005). While there appear to be links between excess autophagy and necroptosis, this is a relatively unexplored field. Another link between necroptosis and autophagy comes with the finding

that the anti-tumour agent granulysin has been shown to cause release of lysosmal contents into the cytoplasm leading to AIF release from the mitochondria and necroptotic cell death (Zhang, Zhong et al. 2009). However, it is unclear whether excessive autophagy leads to cell death or is cytoprotective in necroptosis. Fig 1.22 shows the proposed mechanisms of necroptotic cell death.

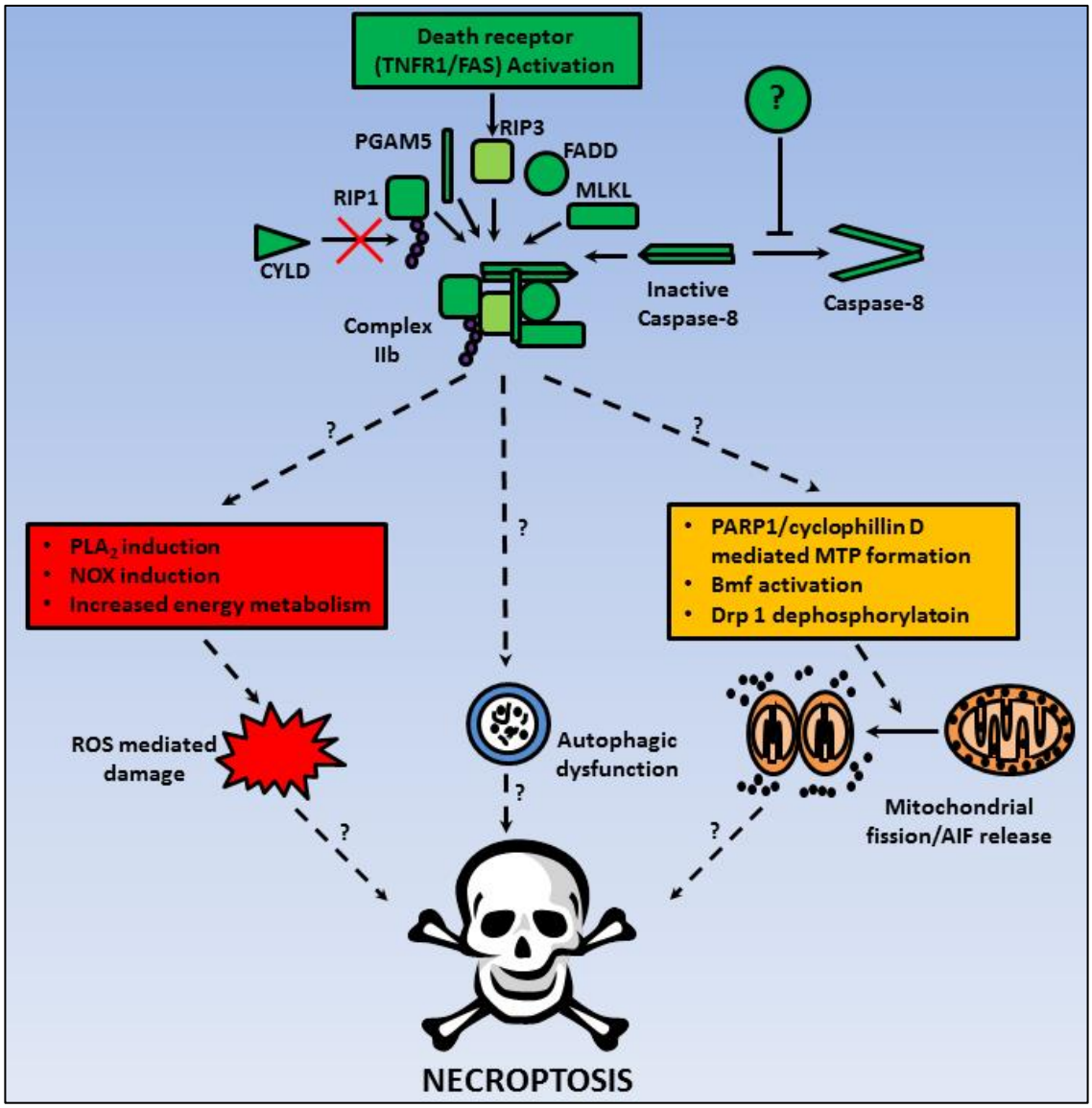

Fig. 1.22 Potential pathways of necroptosis Necroptosis is triggered by the formation of Complex IIb from RIP1 & 3, FADD, MLKL, PGAM5 and inactive caspase-8 following death receptor activation when caspase activation is inhibited. This may leads to a necrotic cell death phenotype by unknown mechanisms thought to include increased ROS production, dysregulated autophagy and mitochondrial fission/AIF release. In the presence of the RIP1 deubiquitinating enzyme CYLD, Complex IIb formation is pro-survival as opposed to inducing necroptosis.

However, thinking of apoptosis and necrosis as 2 completely distinct pathways may not be the correct view as findings such as that of Pang and Geddes that the mitochondrial toxin 3-nitropropionic acid has been shown to cause acute necrosis mediated by NMDA receptor driven excitotoxicity, followed by delayed apoptosis, suggesting both death mechanisms can occur in sequence (Pang and Geddes 1997).

1.3.3 Autophagy

Autophagy is a process by where the cell proteolyses damaged or unwanted cytosolic components by use of the lysosomal machinery and is thought to be activated in times of starvation to regenerate amino acids; however, over activation of autophagy can lead to cell death by excessive degradation of cellular contents. Autophagy can be split into three subtypes: macro-autophagy, micro-autophagy and chaperone mediated autophagy - all of which involve sequestration of cell contents for breakdown by the lysosome. Macro-autophagy delivers cellular components for degradation in a structure known as the autophagosome which then fuses with a lysosome allowing lysis of its contents. In micro-autophagy and chaperone mediated autophagy however, the targets are taken up directly in to the lysosome, with chaperone mediated cargo forming a complex with a chaperone protein which is recognised by the lysosomal-associated membrane protein 2A and translocated across the lysosomal membrane (Saftig, Beertsen et al. 2008)

Macroautophagy, referred to as 'autophagy' from now on, is the most studied and well characterised. The first step in autophagy is the sequestration of the cargo proteins for degradation by elongation and encircling of the phagophore to form the autophagosome. The autophagosome then fuses with the lysosome leading to degradation of the protein cargo by the lysosomal enzymes with the degradation products being exported out of the lysosome back into the cytosol for re-use (Fig. 1.23).

So far, there are approximately thirty autophagy related genes (ATGs) identified in yeast, which are conserved in most phyla, including mammals (Nakatogawa, Suzuki et al. 2009), and are thought to be involved in the control of autophagy. Autophagy is initiated via inhibition of the mammalian target of rapamycin (mTOR) which senses a reduction of nutrients and/or growth factors. Under these conditions various ATGs and phosphatidylinositol 3-kinase catalytic subunit 3 interact to induce phosphatidylinositol 3-phosphate formation, lipidation of LC3 and recruitment of more ATGs which facilitate elongation of the phagophore and engulfment of proteins for destruction in the autophagosome (for a review of the control and

mechanism of autophagosome formation see (Xie and Klionsky 2007)). The autophagosome then binds to the lysosome to form the autolysosome by a mechanism that is yet to be characterised but thought to involve microtubules (Webb, Ravikumar et al. 2004) and lysosomal-associated membrane protein 1 & 2 (Tanaka, Guhde et al. 2000). The aspects and mechanisms of autophagy are summarised in Fig. 1.23.

Autophagy has been proposed as a direct mediator of cell death called autophagic cell death (ACD) characterised by the presence of vacuoles in the cytoplasm due to the presence of autophagosomes (Kroemer, Galluzzi et al. 2009). However, current opinion is tending towards seeing the presence of autophagic vacuolisation in end stage dying cells as a "death with autophagy" as opposed to "death by autophagy", with the autophagy seen as an attempt to protect against cell death or an effect of the death mechanism rather than the causative factor (Kroemer and Levine 2008).

Whether or not it is a mediator of cell death in and of itself, autophagy may have a particularly relevant role in this project as PD is characterised by the accumulation of misfolded proteins; a dysfunction of autophagy may contribute to the build-up of these toxic protein aggregates, alternatively over activation of autophagy due to the presence of so many damaged proteins may contribute to cell death.

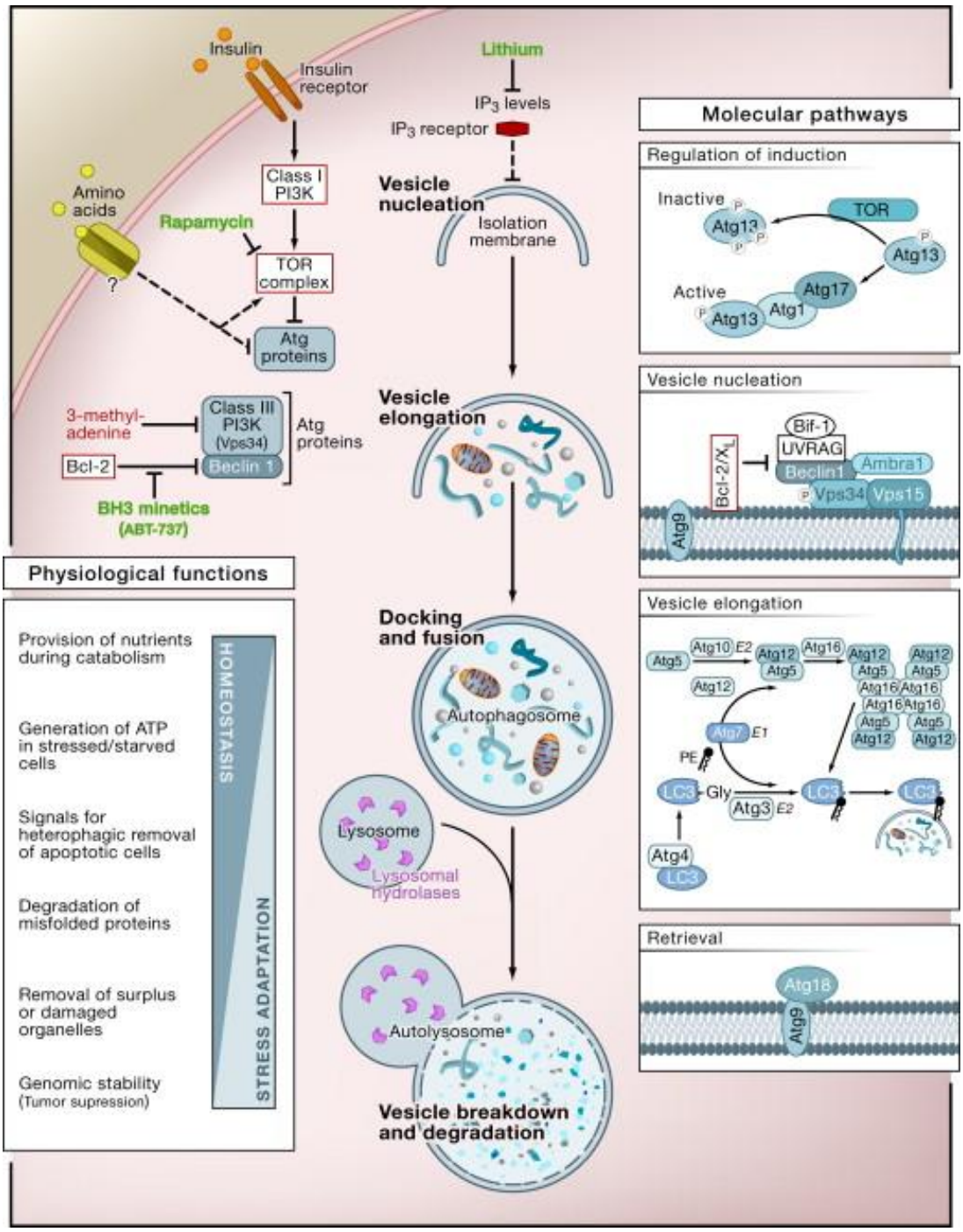

Fig. 1.23 The cellular, molecular, and physiological aspects of autophagy The cellular events during autophagy follow distinct stages: vesicle nucleation (formation of the isolation membrane/phagophore), vesicle elongation and completion (growth and closure), fusion of the double-membraned autophagosome with the lysosome to form an autolysosome, and lysis of the autophagosome inner membrane and breakdown of its contents inside the autolysosome. This process occurs at a basal level and is regulated by numerous different signaling pathways. Shown here are only the regulatory pathways that have been targeted pharmacologically for experimental or clinical purposes. Inhibitors and activators of autophagy are shown in red and green, respectively. At the molecular level, Atg proteins form different complexes that function in distinct stages of autophagy. Shown here are the complexes that have been identified in mammalian cells, with the exception of Atg13 and Atg17 that have only been identified in yeast (Taken from (Levine and Kroemer 2008)).

1.4 Study Aims & Outline

1.4.1 Hypothesis

Parkinson's disease is a major neurodegenerative condition with a complex and unknown pathological mechanism. Environmental exposure to chemical agents, possibly through disruption of mitochondrial function, is regarded as a possible cause of Parkinson's disease. Trichloroethylene, an industrial solvent and environmental contaminant is one agent that has recently been discussed in relation to this. In this thesis we will test the hypotheses that:

A) Trichloroethylene and metabolites cause cell death in both human neuroblastoma and stem cell derived midbrain neuronal cells through programmed cell death
B) The method of cell death is driven by disruption of mitochondrial function
C) Trichloroethylene and metabolites cause degeneration of dopaminergic neurons in the substantia nigra of treated C57BL/6 mice and Wistar rats
D) Trichloroethylene and metabolites cause an acceleration in the development of symptoms and degeneration of dopaminergic neurons in the substantia nigra of human A30P α-synuclein over expressing C57BL/6 mice

1.4.2 Aims

The aim of this project is to elucidate the mechanism of TCE neurotoxicity and to investigate possible links with PD. This will be achieved using a number of techniques. *In vitro* models of TCE, chloral and TaClo exposure will be developed based on a previous exposure paradigm that has been developed. We will utilise both tumour - specifically SH-SY5Y neuroblastoma - and stem cell approaches to understand toxic mechanisms of TCE exposure. Cell viability assays in the presence of specific inhibitors or gene transfection studies along with immunocytochemistry, biochemical assays, FACS and Western blotting will be used to characterise the pathways leading to cell death.

To establish if TCE exposure causes motor impairment in exposed animals, longitudinal assessment of motor function will be undertaken using a variety of measures. Determination of pathology in the SN of exposed animals will be used and will utilise stereological analysis of neurone and glial numbers in paraffin sections of brain as well as LC-MS/MS to determine the levels of various neurotransmitters in specific brain regions.

Chapter 2
Materials & Methods

2.1 Cell Culture

2.1.1 General Cell Culture

2.1.1.1 SH-SY5Y & MEF

SH-SY5Y neuroblastoma cells (European Collection of Cell Cultures (Salisbury, UK)), mouse embryonic fibroblasts (MEF) (GlobalStem (Maryland, USA)) and RIP1 knockout MEFs (sourced from the lab of Liu, Z.G. (NIH National Cancer Institute, Bethesda, US)) were grown and maintained in 75ml vented tissue culture flasks (Scientific Laboratory Services Ltd. (Nottingham, UK) in growth medium (10% GM) containing 90% Dulbecco's Modified Eagle's Media-High Glucose (D6546), 10% Heat-Inactivated Fetal Bovine Serum, 4mM L-Glutamine, 40 units/ml Penicillin, 200µg/ml Streptomycin, 1% MEM Non-Essential Amino Acids (all Sigma Aldrich Chemical Co. (Poole, UK)) and 5µg/ml Fungizone (Amphetericin B) (Invitrogen Ltd. (Paisley, UK)) at 37^{o}C in a humidified atmosphere of 95% air/5% CO_2 and split 1:3 when they reached ~80% confluence.

2.1.1.2 Embryonic stem cell derived midbrain neurons

2.1.1.2.1 Differentiation

M1997 embryonic stem cells (generated in house), were differentiated into a representative midbrain neuronal population by following the method described by Yan et. al. (Yan, Yang et al. 2005) and Yang et. al. (Yang, Zhang et al. 2008).

Cells were initially grown in Dulbecco's Modified Eagle's Media/F12 containing 2mM L-Glutamine, 20 units/ml Penicillin, 1% MEM Non-Essential Amino Acids (all Sigma Aldrich), 5µg/ml Fungizone (Amphotericin B) (Invitrogen), 1:100 Insulin-Transferrin-Selenium x 100, 1:100 N2 Supplement x100, 1:100 B27 Supplement x 100 (all Invitrogen), 400µM Ascorbic Acid, 0.75mg/ml $NaHCO_3$, 675ng/ml D-Glucose, 5µg/ml Heparin (all Sigma Aldrich), 25ng/ml Fibroblast Growth Factor 2, 20ng/ml Epidermal Growth Factor (both R & D Systems, Abingdon, UK) and 5ng/ml Leukaemia Inhibitory Factor (Sigma Aldrich) (MAGICK) at 37^{o}C in a humidified atmosphere of 95% air/5% CO_2 and split 1:3 when they reached ~80% confluence.

Cells were plated into 48-well plates pre-coated with 1:100 GelTrex (Invitrogen) in Dulbecco's Modified Eagle's Media and differentiated into midbrain neurons along an 18 day pathway, summarised in Table 2.1;

Day	Treatment
0	MAGICK
5	75% MAGICK + 25% N2 + 20ng/ml SHH + 100ng/ml FGF_8
7	50% MAGICK + 50% N2 + 20ng/ml SHH + 100ng/ml FGF_8
9	25% MAGICK + 75% N2 + 20ng/ml SHH + 100ng/ml FGF_8 + 20ng/ml BDNF + 200µM AA
11	N2 + 20ng/ml SHH + 100ng/ml FGF_8 + 20ng/ml BDNF + 200µM AA
12	N2 + 20ng/ml BDNF + 20ng/ml GDNF + 1ng/ml $TGF\beta_3$ + 200µM AA + 500µM cAMP
14	N2 + 20ng/ml BDNF + 20ng/ml GDNF + 1ng/ml $TGF\beta_3$ + 200µM AA + 500µM cAMP
16	N2 + 20ng/ml BDNF + 20ng/ml GDNF + 1ng/ml $TGF\beta_3$ + 200µM AA 500µM cAMP
18	N2 + 20ng/ml BDNF + 20ng/ml GDNF + 1ng/ml $TGF\beta_3$ + 200µM AA + 500µM cAMP – Cells differentiated & ready for treatment.

*Key: N2 – N2 supplemented media (*Dulbecco's Modified Eagle's Media/F12, 2mM L-Glutamine, 20 units/ml Penicillin, 1% MEM Non-Essential Amino Acids, 5µg/ml Fungizone (Amphotericin B)), *SHH – sonic hedgehog homolog, FGF_8 – fibroblast growth factor 8,* $TGF\beta_3$ – transforming growth factor 3 (all R & D Systems), *BDNF – brain derived neurotrophic factor, GDNF – glial cell line derived neurotrophic factor (both ProSpec Bio, Ness Ziona, Isreal), AA – ascorbic acid, cAMP – dibutyryl cyclic adenosine monophosphate (both Sigma Aldrich).*

Table 2.1 Differentiation pathway for midbrain neurons from embryonic stem cells

2.1.1.2.2 Maintenance

Differentiated midbrain neurons were maintained in Geltrex coated 48-well plates in growth media (N2, 20ng/ml BDNF, 20ng/ml GDNF, 1ng/ml $TGF\beta_3$, 200µM AA, 500µM cAMP). Media was exchanged for fresh every two days.

2.1.2 Cell Viability Assay

2.1.2.1 Alamar Blue

SH-SY5Y were grown in 48-well plates (Scientific Laboratory Services Ltd.) at a density of ~1 x 10^5 cells per well in 350µl 10% GM and incubated overnight to allow recovery for assay. TaClo (Supplied by Exclusive Chemistry Ltd. (Obninsk, Russia)) and TCE (Sigma-Aldrich Chemical Co. (Poole, UK)) were dissolved in Dimethylsulfoxide (DMSO) (Sigma-Aldrich) while Chloral and DCA (Sigma-Aldrich) were dissolved directly into 10% GM for toxicity assays. Cell death modulators were dissolved in DMSO unless specified and summarised in Table 2.2.

Toxins, modulators or a combination were added to cells (modulator wells pre-treated for 1 hour prior to toxin dosing unless mentioned elsewhere) in 10% GM (final DMSO concentration 0.2%), incubated overnight for 21 hours and cell viability assessed by Alamar Blue assay (Nakayama, Caton et al. 1997). Alamar Blue solution was prepared by dissolving resazurin (Sigma Aldrich) in Phosphate Buffered Saline (Sigma Aldrich) at 100µg/ml and sterile filtered before adding to cell media to give a final concentration of 10µg/ml. Alamar Blue reduction was measured at an excitation wavelength of 530nm and emission wavelength of 590nm following 4 hours incubation with cells.

Name	Supplier	Concentrations	Vehicle
zVAD.fmk	Enzo Life Sciences (Exeter, UK)	10 & 20µM	DMSO
Necrostatin-1	Enzo Life Sciences	50 & 100µM	DMSO
1-methyl-L-tryptophan	Enzo Life Sciences	200µM	DMSO
N-acetylcysteine	Sigma-Aldrich	2.5 & 5mM	DMSO
L-Buthionine Sulfoxamine	Sigma-Aldrich	2.5mM	10% GM
PJ-34	Tocris Biosciences (Abingdon, UK)	20µM	DMSO
Rapamycin	Enzo Life Sciences	2.5 & 5µM	DMSO
Bafilomycin A1	Enzo Life Sciences	500nM & 1µM	DMSO

Table 2.2 Summary of cell death modulator compounds used

2.1.2.2 Crystal Violet

SH-SY5Y treated as for Alamar Blue assay (Section 2.1.2.1), but cell viability assessed as follows;

Following 21 hour toxin incubation, media removed from well and cells fixed with 4% formaldehyde (Sigma Aldrich). Cells then incubated in Crystal Violet stain (0.5% Crystal Violet (Sigma Aldrich), 20% ethanol in ddH_2O) for 10 minutes at room temperature. Crystal Violet stain removed and well washed with ddH_2O to remove excess stain. Dye extracted from live cells with Sorenson's Buffer (0.1% sodium citrate (Sigma Aldrich), 50% ethanol in ddH_2O, pH 4.2) and measured at an absorbance of 540nm and the background fluorescence from the blank wells subtracted from all other readings for analysis.

2.1.3 Confocal Microscopy

2.1.3.1 Immunocytochemistry

Plate wells were treated for required time and fixed in 4% paraformaldehyde (Sigma Aldrich) for 10 minutes and stored at 4^{o}C in 10% Glycerol (Sigma Aldrich) phosphate buffer saline (PBS) containing Sodium Azide (Sigma Aldrich).

Supplier	Antibody	Dilution	Secondary Antibody
Primary Antibody			
Abcam (Cambridge, UK)	Rabbit polyclonal Tyrosine Hydroxylase (Ab112)	1:1000	Goat anti-rabbit Alexa Fluor® 488
Secondary Antibody			
Invitrogen (Paisley, UK)	Goat anti-rabbit Alexa Fluor® 488	1:500	

Table 2.3 ICC primary and secondary antibody details and dilutions used.

For staining, cells were permeabilised with 0.1% Triton-X-100 (Sigma Aldrich) PBS for 10 minutes and then blocked in 1% BSA in PBS for 30 minutes. Cells were incubated overnight with primary antibodies (see Table 2.3 for details) at 4^{o}C and gently agitated, washed with PBS 3 times and treated with Image-iT^{TM} FX signal enhancer (Invitrogen) for 30 minutes at room temperature. Cells were washed with PBS 3 times and incubated with secondary antibodies (see Table 2.3 for details) for 60 minutes protected from light. Counterstaining of total cell nuclei was carried out using DAPI (Invitrogen). Cells were treated with 500nM DAPI in PBS for 5 minutes and then washed in PBS 3 times. Cells were then stored at 4^{o}C in PBS protected from light until viewing.

2.1.3.2 Confocal Microscopy

Images of stained cells were taken using a Nikon A1r point scanning confocal microscope running NIS Elements software (Nikon, v3.2). The microscope was located in the Newcastle University Bio-Imaging Unit using. Cells were observed 40x (air,0.6NA) objective with the following instrument configurations: DAPI, DNA (405 nm laser and 450 nm emission filter); Alexa Fluor® 488, TH positive neurons (488nm laser and 525 nm emission filter). Images were captured at 1024 x 1024 pixel resolution and taken as volume acquisitions with 9 stacks 6.177µm apart. Images were represented and analysed as maximum intensity projections (MIP) where the final images is formed from pixels with the greatest intensity over the z-stack

volume captured. This allowed in each channel, a two dimensional view of the volume captured to be represented and analysed (see below).

2.1.3.2 Image Analysis & Quantification

MIP for each well were analysed for estimated total cell number and total TH-positive neurons using Volocity (version 6.1) image analysis software (PerkinElmer).

Due to the high density of cells and the high level of background fluorescence observed, at the magnification used, in many fields of view it was not possible to distinguish individual nuclei. Therefore an alternative method of cell counting was adopted; this was based upon the average nuclei size. Nuclei size was calculated using fields of view taken from areas of low cell density / background fluorescence. Volocity was used to quantify nuclei intensity and shape; using these measurements, an average DAPI nucleus size was calculated to be 82 μm^2. This figure was used to estimate total cell number by measuring the total area of DAPI staining above a constant threshold and dividing by this the average nuclei size.

Based upon fluorescence intensity (AF488 signal), the number of TH positive neurons was estimated by using Volocity.

2.1.4 Fluorescence Microscopy

SH-SY5Y cells were grown in 4-well chamber slides (BD Biosciences, Oxford, UK) in 1ml 10% GM at a density of 3 x 10^5 cells per chamber and incubated overnight to allow recovery for imaging. Cells were treated with 0.2% DMSO, 100 & 150µM TaClo or 850µM H_20_2 and at 0, 4, 8, 12 & 24 hours in all experiments.

2.1.4.1 Cellular and Mitochondrial Superoxide Imaging

Cells were pre-loaded with the $DCFDA_2$ (10µM) (Invitrogen) to detect superoxide in 1ml 10% GM for 1 hour before treatment when assessing cellular superoxide levels, or cells loaded with 1ml 10% GM containing the mitochondrial superoxide detector MitoSOX Red (5µM) (Invitrogen) for 10 minutes immediately following treatment when assessing mitochondrial superoxide. Following treatment all slides were then fixed with 3.7% formaldehyde (Sigma Aldrich) before mounting and viewed under a Ziess Imager 21 microscope and representative pictures captured.

2.1.4.2 Aggresome Imaging

Following treatment all slides were stained for aggresomes using the ProteoStat® Aggresome Detection Kit (Enzo Life Sciences) as manufacturer's instructions. Briefly, cells were fixed with 3.7% formaldehyde (Sigma Aldrich), permeabilised on ice with 0.5% Triton X-100, 3 mM EDTA, pH 8, and stained with ProteoStat® Aggresome Detection Reagent and Hoechst 33342 Nuclear Stain before mounting and viewed under a Ziess Imager 21 microscope and representative pictures captured.

Aggresomes were quantified manually by counting Hoechst 33342 stained nuclei to ascertain total cell number and red ProteoStat® foci to estimate aggresome number with aggresome number normailised to total cells.

2.1.5 Glutathione Assay

Total glutathione levels were measured using an adaption of the method developed by Shaik and Mehvar (Shaik and Mehvar 2006), briefly described below.

2.1.5.1 Sample Generation

SH-SY5Y cells were grown in 25ml flasks at a density of $1.5x10^6$ in 5ml 10% GM and incubated overnight to allow recovery before assay. Flask were treated with 100µM TaClo and at 0, 4, 8, 12 & 24 hours cells were harvested in quadruplicate by scraping in 100µl ice cold 5% 5-Sulfosalicylic acid dihydrate (SSA) (Sigma Aldrich), before centrifuging at 8000g for 5 minutes. 5µl supernatant was diluted 1:2 with 5% SSA, further diluted to 1:2 with 400mM sodium carbonate, then further diluted 1:8 with Phosphate-EDTA Dilution Buffer (100 mM Na3PO4 – 1 mM EDTA, pH 7.4), total final dilution 1:32. Samples were then stored at -20^{o}C until all samples were taken for assay.

2.1.5.2 GSH Assay

GSH levels were determined by reduction of 5-5'-dithiobis(2-nitrobenzoic acid) (DTNB) to the coloured product 2-nitro-5-thiobenzoic acid (abs 415nm). Samples, standards QC samples and blanks were loaded onto a 96-well plate in duplicate in reaction buffer (1.9 units/ml glutathione reductase, 0.4 mM NADPH in phosphate dilution buffer) and incubated with DTNB for 10 minutes at room temperature before reading at an absorbance of 415nm.

2.2 SH-SY5Y Genetic Manipulation

2.2.1 MnSOD Over Expression

2.2.1.1 Transfection and Selection

SH-SY5Y cells were seeded in a 25ml vented tissue culture flask and left to grow to ~70% confluence. Cells were primed for transfection with 10µg/ml polybrene and then treated with 25µl of at least 1 $x10^8$ TU/ml $MnSOD_2$ Precision LentiORF lentivrus vector (Thermo Fisher Scientific Open Biosystems (St. Leon-Rot, Germany)) (clones PLOHS_100003217 (2.80 $x10^8$ TU/ml) & PLOHS_100063998(4.54 $x10^8$ TU/ml)) and incubated at 37°C in a humidified atmosphere of 95% air/5% CO_2 for 48 hours.

The viral vector co-expresses GFP and confers blasticidin resistance to allow selection. Cells were transferred to a 75ml vented tissue culture flask and transfected cells were selected for by introducing 50µg/ml blasticidin (Invivogen (San Diego, USA)) to the media and growing to confluence. Selection was confirmed by seeding 4-well chamber slides with 3 x 10^5 cells per chamber, growing overnight and then fixing and counterstaining with DAPI. Slides were viewed for GFP and DAPI under a Ziess Imager 21 microscope to assess transfection and representative pictures captured.

MnSOD over expressing cells were maintained in 75ml vented tissue culture flasks in 10% GM containing 50µg/ml blasticidin at 37°C in a humidified atmosphere of 95% air/5% CO_2 and split 1:3 when they reached ~80% confluence.

2.2.1.2 Assessment of MnSOD Level

MnSOD over expressing or control SH-SY5Y cells were assessed for MnSOD levels as method in section 2.3.1 using relevant primary and secondary antibodies detailed in Tables 2.5 and 2.6.

2.2.1.3 Toxicity Assay

MnSOD over expressing or control SH-SY5Y cells were assessed for relative susceptibility to TaClo toxicity by Alamar Blue viability assay as method in section 2.1.2.1 but in 48-well plates with 24 wells containing control and 24 wells containing MnSOD overexpressing cells.

2.2.2 RIP1 Knockdown

2.2.2.1 Transfection

SH-SY5Y cells were seeded in a 25ml vented tissue culture flask and left to grow to ~70% confluence. Cells were primed for transfection with 10µg/ml polybrene and then treated with 25µl of at least $1x10^8$ TU/ml relevant RIP1 or control GIPZ lentiviral shRNAmir (Thermo Fisher Scientific Open Biosystems) (see Table 2.4 for clone numbers and TU/ml) and incubated at 37°C in a humidified atmosphere of 95% air/5% CO_2 for 48 hours.

shRNA	Clone no.	TU/ml
Control	V3LHS_365648	6.22×10^8
RIP1	V2LHS_241668	5.13×10^8
	V3LHS_340513	3.02×10^8

Table 2.4 Clone number and titre of GIPZ lentivral SHRNAmir

The viral vector co-expresses GFP and confers purimycin resistance to allow selection. Cells were transferred to a 75ml vented tissue culture flask and transfected cells were selected for by introducing 1µg/ml puromycin (Sigma Aldrich) to the media and growing to confluence. Selection was confirmed by seeding 4-well chamber slides with 3×10^5 cells per chamber, growing overnight and then fixing and counterstaining with DAPI. Slides were viewed for GFP and DAPI under a Ziess Imager 21 microscope to assess transfection and representative pictures captured.

Knockdown or control cells were maintained in 75ml vented tissue culture flasks in 10% GM containing 1µg/ml puromycin at 37°C in a humidified atmosphere of 95% air/5% CO_2 and split 1:3 when they reached ~80% confluence.

2.2.2.2 Assessment of Knockdown Extent

RIP1 or control SH-SY5Y cells were assessed for relevant protein levels as method in section 2.3.1 using relevant primary and secondary antibodies detailed in Tables 2.5 and 2.6.

2.2.2.3 Toxicity Assay

Clone 668 treated RIP1 or control SH-SY5Y cells were assessed for relative susceptibility to TaClo toxicity by Alamar Blue viability assay as method in section 2.1.2.1 but in 48-well plates with 24 wells containing control and 24 wells containing relevant knock down cells.

2.3 Protein Expression

2.3.1 Sample Generation & Quantification

2.3.1.1 Sample Generation

SH-SY5Y cells following toxin exposure were scraped from flasks into Tris-buffered Saline (Sigma-Aldrich) containing 1% TritonX-100 (Sigma-Aldrich) and EDTA-free protease inhibitor cocktail (Roche, Welwyn, UK) on ice and stored at -20^{o}C.

2.3.1.2 Protein Quantification

Protein in samples was determined using Bradford Reagent (Sigma-Aldrich) against bovine serum albumin (BSA) as a standard.

2.3.2 Western Blotting

2.3.2.1 Blotting

Protein samples concentrations were standardised in buffer and NUPAGE Reducing Agent and LDS Sample Buffer (Invitrogen) were added. Samples were heated to 70^{o}C in a hot block for 10 minutes, loaded into wells of NUPAGE 4-12% Bis-Tris gels (Invitrogen) and electrophoresed in NUPAGE MOPS SDS Running Buffer (Invitrogen) containing antioxidant (Invitrogen) alongside SeeBlue Plus2 Pre-Stained Standard (Invitrogen) and Biotinylated Protein Ladder (New England Biolabs (Hitchin, UK)) markers for band size comparison. Proteins were transferred to 0.2µm nitrocellulose membranes using an iBlot® Gel Transfer Device (Invitrogen), with transfer efficiency assessed by reversibly staining protein with Ponceau S solution (Invitrogen). Membranes were blocked with tris buffered saline with 0.2% Tween 20 (Sigma-Aldrich) (TBST) containing 5% non-fat skimmed milk powder for 30 minutes and then incubated with primary antibody or peroxidise conjugated GAPDH monoclonal rabbit antibody for one hour before being washed in TBST and then incubated with the appropriate secondary antibodies for 30 minutes (for antibody details and dilutions see Table 1). The membranes were exposed to ECL western blotting substrate (Perbio Science Ltd, UK) for 1 minute and developed onto Super RX Medical X-ray Film (FujiFilm, Bedford, UK) in a dark room using Kodak Processing for Audioradiography Films Solution (P7042) and Kodak GBX Fixer and Replenisher (P7167) (both Sigma Aldrich) at various time points to optimise resolution.

2.3.2.2 Primary Antibodies

Primary antibodies used are summarised in Table 2.5.

Supplier	Antibody	Dilution	Secondary Antibody
New England Biolabs	PARP & cPARP (#9542)	1:1000	Rabbit IgG
New England Biolabs	RIP1 & c RIP1 (#3493)	1:1000	Rabbit IgG
New England Biolabs	Cleaved Caspase-3 (#9664)	1:1000	Rabbit IgG
New England Biolabs	LC3- B (#3868)	1:1000	Rabbit IgG
New England Biolabs	Phospho-Histone H2A.X (Ser139) (#2577)	1:1000	Rabbit IgG
GeneTex	Calpain-1 (GTX102240S)	1:1000	Rabbit IgG
Santa Cruz Biotechnology (Heidelberg, Germany)	DJ-1	1:1000	Mouse IgG
Abcam	MnSOD2 (ab16956)	1:4000	Mouse IgG
Santa Cruz Biotechnology	GAPDH (FL-335)	1:1000	Rabbit IgG

Table 2.5 Primary antibody details and dilutions used.

2.3.2.3 Secondary Antibodies

Secondary antibodies used are summarised in Table 2.6.

Supplier	Antibody	Dilution
New England Biolabs	HRP linked Rabbit IgG	1:4000
New England Biolabs	HRP linked Mouse IgG	1:2000

Table 2.6 Secondary antibody details and dilutions used.

2.3.2.4 Quantification

Films were scanned and quantified by measuring band intensity by area using ImageJ (1.44p) software. GAPDH was used to normalise results and protein/GAPDH ratios and fold change from control was calculated for all samples.

2.4 Mitochondrial Function Assays

2.4.1 Mitochondrial Isolation

Mitochondria were isolated from SH-SY5Y cells by differential centrifugation as follows: SH-SY5Y grown to confluence in T150 flasks, were removed from media and re-suspended in 1ml ice cold Medium A (250mM sucrose, 2mM HEPES, 0.1mM EGTA. pH 7.4) before cell membrane disrupted by 20 passes in a dounce homogenizer (Ryobi CCD-1201) with a tight-fitting power-driven Teflon plunger. Homogenate was centrifuged at 600g for 10 minutes at 4^{o}C and the mitochondria rich supernatant collected. Cell debris pellet was re-suspended in 800µl Medium A and centrifuged as before. Supernatants were pooled and centrifuged at 11,000g for 10 minutes at 4^{o}C with four pellets combined, re-suspended in 400µl Medium A, aliquoted and stored at - 80^{o}C until use.

2.4.2 Mitochondrial Activity Assays

All mitochondrial activity assays were carried out as described by Kirby et al.(Kirby, Thorburn et al. 2007) on a Cary WinUV spectrophotometer at 30^{o}C in the presence of various concentrations of TaClo, chloral or vehicle (0.2% DMSO) to investigate the effect of the test compounds on mitochondrial OXPHOS function. Test compounds were added to the buffer immediately prior to the assay. Pig heart mitochondrial (PHM) fraction (supplied by the Mitochondrial Diagnostic Service Laboratory, Newcastle University) was used as an internal control before each experiment to check normal function of assay, according to acceptance criteria described by Kirby et al.(Kirby, Thorburn et al. 2007). All samples were diluted 1:7 in relevant Complex buffer (specific buffer details below) and stored on ice prior to assay. Complex specific assay details are described below.

2.4.3.1 Complex I

Complex I activity was calculated as rotenone-sensitive NADH:ubiquinone oxioreductase activity as determined by following the decrease in absorbance due to the oxidation of Nicotinamide adenine dinucleotide (NADH) at 340nm with 425nm as the reference wavelength using the following method:

Prior to assay, mitochondrial fraction was diluted 1:5 and flash freeze thawed three times in liquid nitrogen to maximise Complex I activity. Assay performed in Complex I buffer (25mM potassium phosphate, 5mM magnesium chloride in distilled water, adjusted to pH 7.2 with potassium hydroxide (prepared in advance and stored at 4^{o}C for up to 3 months), BSA

(2.5mg/ml) and potassium cyanide (KCN) (3mM) added prior to use). NADH (0.13mM), Ubiquinone$_1$ (65µM) and Antimycin A (2µg/ml) added to buffer and activity read as absorbance change at 340nm for 30 sec. 10µl mitochondrial fraction added and activity recorded for 5 minutes. Rotenone (2µg/ml) added and activity recorded for 3-4 minutes.

Complex I activity calculated as nmols of NADH oxidised/min as follows:

$$\frac{\delta \text{ slope}}{6.22} \times \frac{1000 \times \text{dilution factor} \times 1000}{\text{mitochondrial sample volume (µl)}}$$

where 6.22/cm/mM is the extinction coefficient for NADH at 340nm (to account for the contribution of Ubiquinone$_1$ to absorbance at 340nm (Watmough, Birch-Machin et al. 1989)) and δ slope = slope following mitochondrial addition (absorbance/min) - slope following rotenone addition (absorbance/min).

2.4.3.2 Complex II

Complex II activity was measured as succinate:ubiquinone$_1$ oxioreductase activity by following the reduction of the artificial electron acceptor 2,6-dichlorophenol-indo-phenol (DCPIP) at 600nm using the following method:

Prior to assay, mitochondrial fraction was diluted 1:5 and flash freeze thawed three times in liquid nitrogen to maximise Complex II activity. Assay performed in Complex II buffer (25mM potassium phosphate, 5mM magnesium chloride in distilled water, adjusted to pH 7.2 with potassium hydroxide (prepared in advance and stored at 4^{o}C for up to 3 months), 3mM KCN added prior to use). 10 µl mitochondrial fraction was incubated at 30^{o}C in CII buffer containing Sodium Succinate (20mM) for 30 minutes prior to assay to allow activation of the Complex II enzyme. DCPIP (50µM), Antimycin A (2µg/ml), and rotenone (2µg/ml) added to mitochondria containing buffer and baseline activity read as absorbance change at 600nm for 30 sec. Ubiquinone$_1$ added and activity recorded for 5 minutes.

Complex II activity calculated as nmols DCPIP reduced/min as follows:

$$\frac{\delta \text{ slope}}{19.1} \times \frac{1000 \times \text{dilution factor} \times 1000}{\text{mitochondrial sample volume (µl)}}$$

where 19.1/cm/mM is the extinction coefficient for DCPIP at 600nm and δ slope = slope following ubiquinone$_1$ addition (absorbance/min).

2.4.3.3 Complex III

Complex III activity measured by following the oxidation of ubiquinol$_2$ with cytochrome *c* as the electron acceptor and monitoring the increase in absorbance due to the reduction of cytochrome *c* (oxidised) at 550nm with a relative wavelength of 580nm, expressed as an apparent first order rate constant after reduction of the remaining cytochrome *c* with ascorbate. Ubiquinol$_2$ prepared and Complex III activity was measured using the following methods:

2.4.3.3.1 Ubiquinol$_2$ Preparation

Ubiquinol$_2$ prepared in acidified ethanol and quantified prior to the assay and stored at -80^{o}C until use. Ubiquinone$_2$ dissolved in 100% ethanol (acidified to pH 2 with HCl) before being reduced to Ubiquinol$_2$ by addition of a few grains of $NaBH_4$ causing the sample to go colourless. The solution was vortexed in 2:1 diethylether/cyclohexane, with the Ubiquinol$_2$ separating to the solvent phase and was removed and vortexed with 2M NaCl again separating into the solvent phase. The solvent is removed and evaporated to dryness in nitrogen before being dissolved in acidified ethanol. The Ubiquinol$_2$ was quantified by measuring its absorbance at 285nm. Ubiquinol$_2$ concentration (mM) calculated as follows:

$$\frac{\delta \text{ abs}}{3.5} \times \frac{1000}{\text{sample volume (µl)}}$$

where δ abs is the difference in absorbance between the peak and baseline of the trace and 3.5 is the extinction coefficient for Ubiquinol$_2$ at 285nm.

2.4.3.3.2 Complex III Activity Assay

Assay performed in CIII buffer (25mM potassium phosphate, 5mM magnesium chloride in distilled water, adjusted to pH 7.2 with potassium hydroxide, prepared in advance and stored at 4^{o}C for up to 3 months, 3mM KCN and 2.5mg/ml essentially fatty acid free, Fraction V, BSA added prior to use). Rotenone (2µg/ml), Cytochrome *c* (oxidised) (15µM) and n-dodrecyl-β-D-maltoside (DDM) (0.6mM) added to buffer and spectrophotometer 'zeroed' and baseline activity read as absorbance change at 550nm for 30 seconds. Ubiquinol$_2$ (35µM) added and activity measured for 1 minute. 10µl mitochondrial fraction added and activity measured for 5 minutes before addition of a few grains of *L*-ascorbic acid to allow reduction of remaining cytochrome *c*.

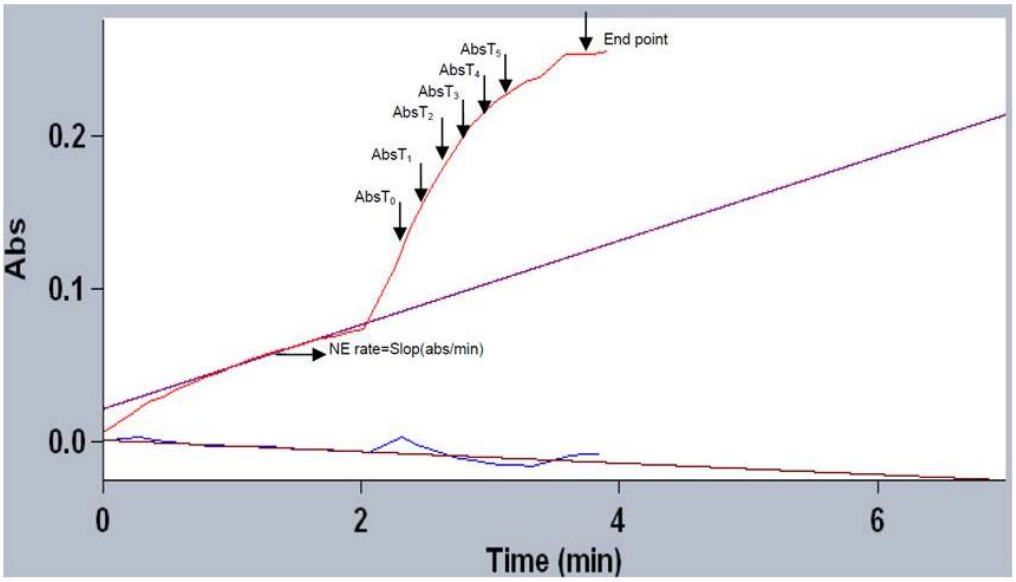

Fig. 2.1 Mitochondrial Complex III activity assay trace Example trace showing end point absorbance (End point), non-enzymatic absorbance rate change (NE rate) and 6 continuous absorbance timepoints ($AbsT_{0-5}$) of mitochondrial Complex III activity assay (taken from Newcastle NHS Foundation Trust Mitochondrial NCG Service SOP 7957).

As the increase in absorbance rapidly becomes non-linear after the addition of the mitochondrial fraction, Complex III activity is expressed as an apparent first-order rate constant after reduction of the remaining cytochrome c with ascorbate. Six continuous time points and corresponding absorbances were picked from the exponential phase of the trace ($AbsT_0$-$AbsT_5$) (see Fig. 2.1) and the difference in absorbance between $AbsT_1$-$AbsT_5$ and the end point calculated (X_1-X_5 respectively). Complex III activity was then calculated as 10^{-3}K.sec^{-1} as follows:

$$\left(\frac{\log A/X_1 - \log A/X_5}{\text{time period} - \text{NE rate}/60}\right) \times \frac{2.303 \times 1000 \times \text{dilution} \times 1000}{\text{mitochondrial sample volume (µl)}}$$

Where A is the change in absorbance between $AbsT_0$ and the end point (see Fig. 2.1), the time period is the time difference between $AbsT_1$ and $AbsT_5$ in seconds, NE rate is the slope between cytochrome *c* addition and ubiquinol$_2$ addition (see Fig. 2.1) and 2.303 is the conversion factor for $\log_{10}$ to natural log.

2.4.3.3.3 Non-enzymatic reduction of Cytochrome c (Oxidised)

To examine the effect of chloral on the non-enzymatic reduction of cytochrome c (oxidised) the Complex II assay protocol was followed in the presence of various concentrations of chloral up to immediately before the addition of the mitochondrial fraction. At this point the recording was stopped and the non-enzymatic reduction of cytochrome *c* (oxidised) measured as the slope of the line following cytochrome *c* (oxidised).

2.4.3.4 Complex IV

Complex IV activity was measured by following the oxidation of cytochrome *c* (II) at 550nm with 580nm as the reference wavelength, expressed as an apparent first-order rate constant after oxidation of the remaining cytochrome *c* by potassium ferricyanide. Cytochrome *c* (II) was prepared and Complex IV activities were measured using the following methods:

2.4.3.4.1 Cytochrome c II Preparation

Cytochrome c II was prepared by reducing cytochrome *c* (III) (oxidised) with ascorbic acid and purified by gel filtration on Sephadex G-25M Column (Pharmacia, Sandwich, UK) equilibrated with CIV buffer (see below). The dark fraction is collected and quantified prior to the assay and stored at -20^{o}C until use. The Cytochrome *c* (II) was quantified by measuring its absorbance at 285nm. Cytochrome c II concentration (mM) calculated as follows:

$$\frac{\delta \text{ abs}}{29} \times \frac{1000}{\text{sample volume } (\mu l)}$$

where δ abs is the difference in absorbance between the peak and baseline of the trace at 550nm and 29 is the extinction coefficient for cytochrome cII at 500nm.

Cytochrome *c* (II) purity was determined by measuring its absorbance at 500nm and 565nm and calculating the ratio of the difference in absorbance between the peak and baseline at 550nm to 565nm. If the ratio was lower than 6 the cytochrome *c* (II) was considered too oxidised to use in the assay.

2.4.3.4.2 Complex IV Activity Assay

Assay performed in CIV buffer (20mM potassium phosphate in distilled water adjusted to pH 7.2 with potassium hydroxide prepared in advance and stored at 4^{o}C for up to 3 months). Cytochrome *c* (II) (15µM) and DDM (0.345mM) added to buffer and spectrophotometer 'zeroed' and baseline activity read as absorbance change at 550nm for 30 sec. 10µl mitochondrial fraction added and activity measured for 2 minutes before addition of a few grains of Potassium Ferricyanide to oxidise of remaining cytochrome *c* (II).

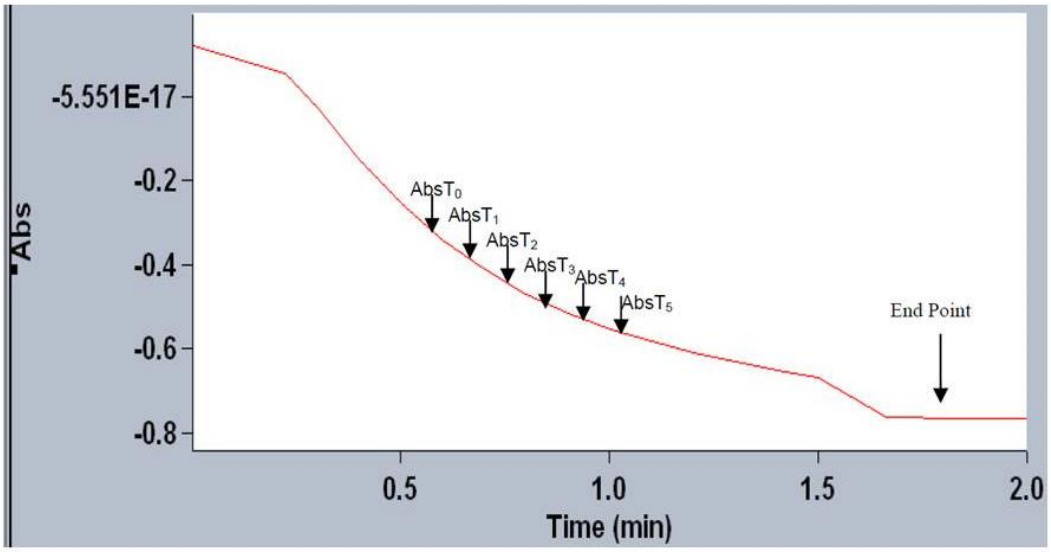

Fig. 2.2 Mitochondrial Complex IV activity assay trace Example trace showing end point absorbance (End point) and 6 continuous absorbance timepoints ($AbsT_{0-5}$) of mitochondrial Complex IV activity assay (taken from Newcastle NHS Foundation Trust Mitochondrial NCG Service SOP 8878).

As the absorbance declines exponentially and becomes nonlinear after the addition of the mitochondrial fraction, Complex IV activity is expressed as an apparent first-order rate constant after oxidation of the remaining cytochrome *c* (II) with Potassium Ferricyanide. Six continuous time points and corresponding absorbances were picked from the exponential phase of the trace ($AbsT_0$-$AbsT_5$) (see Fig. 2.2) and the difference in absorbance between $AbsT_1$-$AbsT_5$ and the end point calculated (X_1-X_5 respectively). Complex IV activity was then calculated as 10^{-3}K.sec^{-1} as follows:

$$\left(\frac{\log A/X_1 - \log A/X_5}{\text{time period}} \right) \times \frac{2.303 \times 1000 \times \text{dilution} \times 1000}{\text{mitochondrial sample volume (µl)}}$$

Where A is the change in absorbance between $AbsT_0$ and the end point (see Fig. 2.1), the time period is the time difference between $AbsT_1$ and $AbsT_5$ in seconds and 2.303 is the conversion factor for $\log_{10}$ to natural log.

2.5 Flow Cytometry

2.5.1 Sample Generation

SH-SY5Y cells were seeded in 25ml vented tissue culture flasks in 5ml 10% GM at a density of 5 x 10^6 per flask for flow cytometric analysis and incubated overnight following seeding to allow recovery before treatment. Cells were treated with 0.2% DMSO, 100 or 150µM TaClo or 500nM staurosporine (Sigma) as a positive control for apoptosis (cell death mechanism assay only) for 0, 4, 8, 12, 16 or 24 hours before being trypsinised and spun down in to pellets at 200g for 10 minutes and then assessed for cell death phenotype, mitochondrial superoxide or lysosome number.

Cells to be assessed for cell death phenotype were probed using the 'Chromatin Condensation / Dead Cell Apoptosis Kit with Hoechst 33342 and PI for Flow Cytometry' kit (Invitrogen) as per manufacturer's instructions. Briefly, cell pellets were re-suspended in 1ml PBS + 0.5% BSA, washed in 1ml PBS + 0.5% BSA and then spun down before being re-suspended in 200µl PBS + 0.5% BSA containing Hoescht 33342 (5µg/ml) and Propidium Iodide (PI) (1µg/ml) for 20-30 min for analysis.

Cells were probed for lysosome levels using Lysotracker Red probe (Invitrogen) or mitochondrial superoxide using MitoSOX™ Red probe (Invitrogen) as per manufacturer's instructions. In short, cell pellets were re-suspended in 1ml PBS + 0.5% BSA containing 5µM MitoSOX™ Red for 10 minutes or 50nM Lysotracker (Invitrogen) for 30 minutes. Cells were washed in 1ml PBS + 0.5% BSA and spun down twice and finally re-suspended in 200µl PBS + 0.5% BSA for analysis.

2.5.2 Flow Cytometry

Samples were acquired on a FACSCanto II flow cytometer (BD Biosciences, Oxford, UK) using FACSDiva (v.6.0) software. At least 10,000 events were analysed and a signal threshold was applied for forward (FSC-A) to exclude debris from which a distinct cell population was gated (Fig. 2.3) and fluorescence measured in this population.

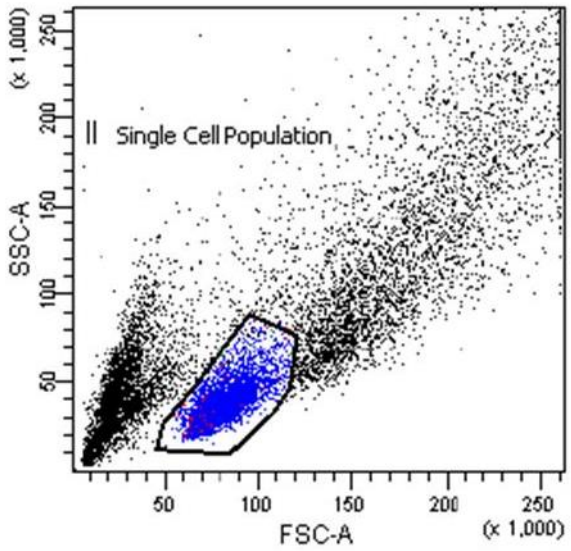

Fig. 2.3 Representative flow cytometry density plot showing selection of whole single cells based on SSC-A and FSC-A

When assessing cell death phenotype, distinct cell population gated events were defined as 'Healthy', 'Apoptotic', 'Necrotic' and 'Late Cell Death' populations based on relative fluorescence of PI and Hoechst33342 (measured by 488/595nm and 405/450nm lasers, respectively), with approximately 90-95% of events defined in the 'Healthy' population of untreated or control samples (Fig. 3.26). Results were analysed using FACSDiva (v.6.0) software.

When assessing lysosome levels, distinct cell population gated events were defined as low or high lysosome populations based on Lysotracker Green fluorescence (measured by 488/585nm laser), with approximately 95% of events defined in the low lysotracker population of untreated or control samples (Fig. 3.32). Quantification of mitochondrial superoxide levels involved defining distinct cell population gated events as low, medium or high mitochondrial superoxide populations based on MitoSOX™ Red fluorescence (measured by 488/585nm laser), with approximately 95% of events defined in the low mitochondrial superoxide population, and medium and high populations defined in relation to the presence of two distinct peaks on histogram display (Fig. 4.14 B). Lysosome and mitochondrial superoxide level assay results were analysed using Cyflogic (v. 1.2.1) software.

2.6 In Vivo Assays

All experiments were carried out in accordance with the UK Animals (Scientific procedures) Act of 1986, with UK Home Office Guidance on the implementation of the Act and with all applicable Codes of Practice for the care and housing of laboratory animals, and the European Community Council Directive of 24 November 1986 (86/609/EEC).

2.6.1 Subjects

2.6.1.1 Sourcing

Wild-type C57BL/6 mice and Wistar rats were sourced from Charles River UK (Margate, UK) and A30P mutant human α-synuclein overexpressing C57BL/6 mice were sourced from Prof. Philipp Kahle, University of Tubingen, Germany (Kahle, Neumann et al. 2000). The animals were examined on arrival and prior to the study; all animals were healthy and considered suitable for experimental use.

2.6.1.2 Husbandry

Animals were housed in clean holding rooms in the Comparative Biology Centre, Newcastle University, for the duration of all studies. Mice were kept in groups of up to six in solid bottomed, saw dust filled, filter top individually ventilated cages within a barrier facility which underwent 20 air changes per hour. Rats were kept in groups of up to four in solid bottomed, saw dust filled, open topped cages in rooms that underwent 15 air changes per hour. Animals were transferred to cages with fresh bedding twice weekly and all cages had environmental enrichment available throughout the study period. The rooms were illuminated by fluorescent lights set to give a twelve- hour light-dark cycle (on 07.00, off 19.00) and the air temperature and relative humidity were controlled and measured. All were within normal ranges for study duration. Animals were fed a diet of expanded RM03 rodent diet pellets (Special Diet Services, Edinburgh, UK) *ad libitum* and had access to mains tap water *ad libitum*.

2.6.1.3 Animals

Pilot study mice were in the age range 14-15 weeks and weight range 26-30g and rats were in the age range 14-15 weeks and the weight range 454-557g while A30P study wild-type and A30P mutant mice were in the age and weight range summarised in Table 2.7. All animals were considered healthy and suitable for experimental use upon study start. Pilot study animals were identified by waterproof tail markings and A30P study animals were identified by ear punch and waterproof tail markings; tail markings were reapplied as necessary throughout study duration.

Wild-Type		
	Age (week)	Weight Range (g)
Male	14-15	28-35
Female	14-15	22-26
A30P Mutant		
	Age (week)	Weight Range (g)
Male	13-16	29-39
Female	13-15	23-28

Table 2.7 Summary of A30P study mouse age and weight upon study start

2.6.3.1 A30P Genotyping

A30P mutant human α-synuclein overexpressing C57BL/6 mice were bred in house from 2 F1 trios and genotyped as follows:

Tissue biopsies were taken from the mice via ear punches and DNA isolated by Qiagen DNeasy Blood and Tissue DNA extraction kit (Qiagen, Crawley, UK) according to manufacturer's instructions.

A30P mutation presence was confirmed by PCR. The primers used for the A30P gene were forward 5'-TGTAGGCTCCAAAACCAAGG-3' and reverse 5'-TGTCAGGATCCACAGGCATA-3' (personal communication, Heinrich Schell, University of Tubingen, Germany) and were synthesised by Eurofins (Eurofins MWG Operon, Ebesberg, Germany) . PCR was performed on DNA samples generated from each animal along with wild type C57BL/6 DNA as a negative control, using Hot StarTaq Master Mix Kit (Qiagen) on a Hybaid PCR Express cycler (Thermo Fisher Scientific). The cycling conditions used were 5 minutes at 94°C, 32× (30 s at 94°C, 30 s at 62°C and 30 s at 72°C) and 5 minutes at 72°C before being held at 12°C. The PCR products obtained were then run on a 1% agarose gel (Agarose in Tris/Borate/EDTA Buffer (both Sigma) + SYBR® Safe DNAGel Stain) for 1 hour at 80 V alongside 2-Log DNA Ladder (0.1–10.0 kb) (New England Biolabs) and visualized under ultraviolet using a Syngene GeneSnap Imaging software (v7.04) on a Synoptics G:Box transilluminator.

2.6.2 Dosing & Welfare Checks

Mice in the pilot study were split into five groups of six by cage and rats into four groups of four by cage assigned to the dosing regimens in Tables 2.8 for the study.

Group	Animals	Dose	Vehicle
1	1-6	10 ml/kg	Olive oil
2	7-12	500 mg/kg TCE	Olive oil
3	13-18	100mg/kg Chloral	0.9% NaCl
4	19-24	1 mg/kg TaClo	0.1% DMSO in 0.9% NaCl
5	25-30	10 mg/kg MPTP	0.9% NaCl

Group	Animals	Dose	Vehicle
1*	1-4	N/A	N/A
2	9-12	500 mg/kg TCE	Olive oil
3	13-16	100mg/kg Chloral	0.9% NaCl
4	17-20	1 mg/kg TaClo	0.1% DMSO in 0.9% NaCl

*It was intended to dose Group 1 with olive oil but due to licensing issues this did not occur and Group 1 were an untreated control

Table 2.8 Pilot study dosing regimen

Mice were split into four groups of five male (group xMx) and four groups of five female (group xFx) for both wild-type (W) and A30P (A) and assigned to the dosing regimens in Table 2.9 for the study. A30P mutant mice were staggered in groups born at the same time.

Wild Type

Group	Animals	Dose	Vehicle
WM1	W1M -W5M	10 ml/kg	Olive oil
WM2	W6M -W10M	1000 mg/kg TCE	Olive oil
WM3	W11M -W15M	2 mg/kg TaClo	0.1% DMSO in 0.9% NaCl
WF1	W1F -W5F	10 ml/kg	Olive oil
WF2	W6F -W10F	1000 mg/kg TCE	Olive oil
WF3	W11F-W15F	2 mg/kg TaClo	0.1% DMSO in 0.9% NaCl

A30P

Group	Animals	Dose	Vehicle
AM1	A1, 5, 9, 13 & 17M	10 ml/kg	Olive oil
AM2	A2, 6, 10, 14 & 18M	1000 mg/kg TCE	Olive oil
AM3	A3, 7, 11, 15 & 19M	2 mg/kg TaClo	0.1% DMSO in 0.9% NaCl
AF1	A1, 5, 9, 13 & 17F	10 ml/kg	Olive oil
AF2	A2, 6, 10, 14 & 18F	1000 mg/kg TCE	Olive oil
AF3	A3, 7, 11, 15 & 19F	2 mg/kg TaClo	0.1% DMSO in 0.9% NaCl

Table 2.9 Wild type & mutant C57BL/6 mouse A30P study dosing regimen

Mice were dosed i.p. with a Microlance 25G X 5/8” and rats with a Microlance 23G X 1” needle (Scientific Laboratory Services) twice weekly for 8 weeks, in alternating sides of the abdomen.

Animals were observed constantly for 1 hour following the first dosing in case of adverse events occurring and for following this were checked every morning and at 1 & 4 hours after every dose. Animal weight was recorded on dosing days

2.6.3 Behaviour

Motor and cognitive function were assessed in all pilot and A30P animals according to the schedule set out in Figure 2.4, using the behavioural battery described below.

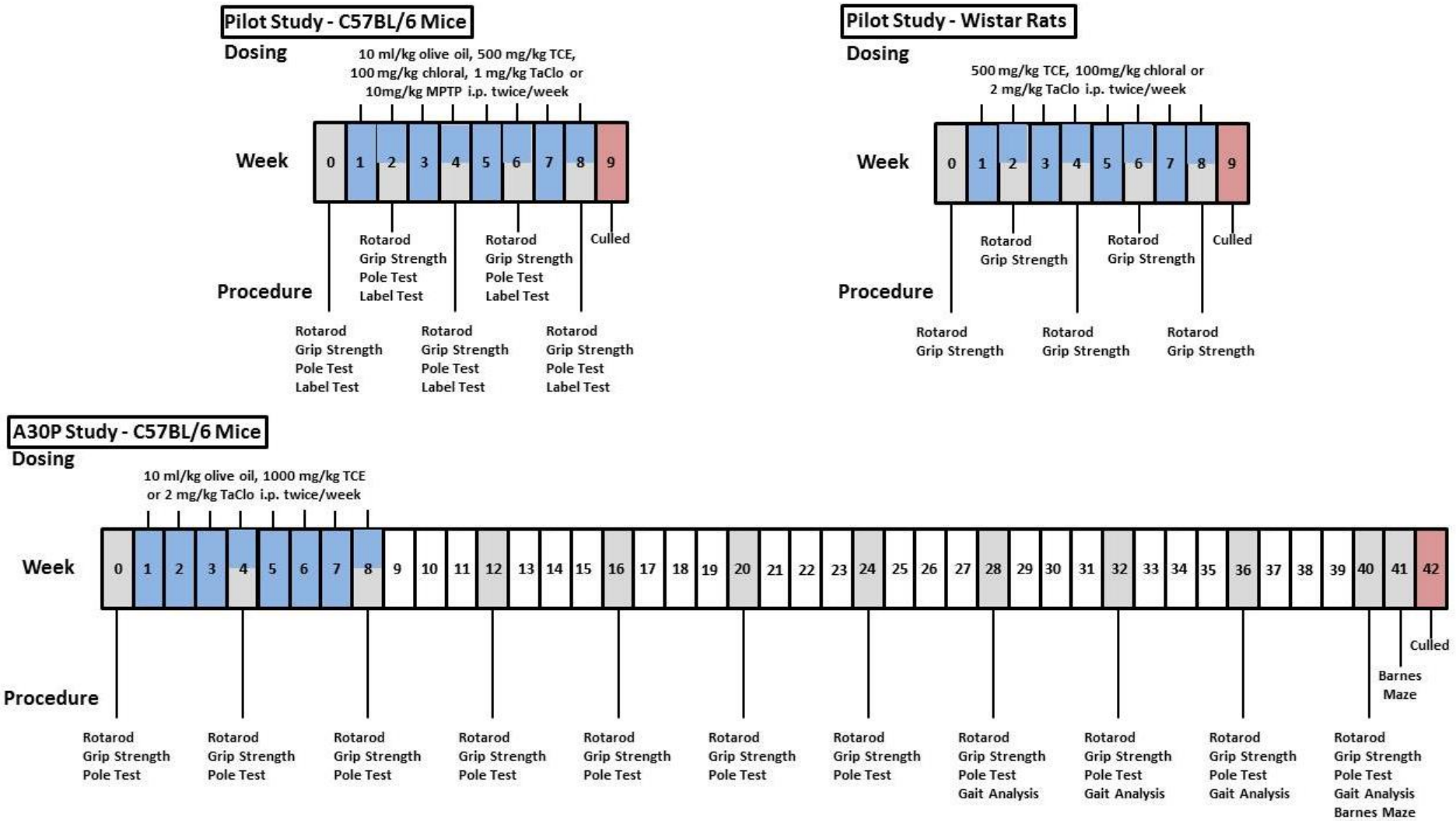

Fig. 2.4 *In vivo* study summary Schematic representation of procedures carried out on all animals on pilot and A30P study.

2.6.3.1 Rotarod (all animals)

Motor function was assessed by an accelerating rotarod protocol (Jones and Roberts 1968) , using the IITC Life Sciences Rotarod treadmill for rats and mice (WPI, Hertfordshire, UK). Animals in the pilot study were trained on the rotarod for three consecutive trials of 1 minute with the rod rotating at a constant speed of 4 rpm prior to testing. On test days, animals were tested in three trials with 15 minutes between trials. For each trial animals were placed on the rod at a rotating speed of 4 rpm. When all the animals were on the rod the rod steadily accelerated to 40 rpm over 300 seconds and the fall latency for each animal was recorded. If they did not fall, a latency of 300 seconds was recorded. Due to low latencies seen in the pilot study, the protocol for mice in the A30P study was slightly modified so that animals were trained at 3 rpm and the rotarod accelerated from 3-30 rpm on trial days.

2.6.3.2 Grip Strength (all animals)

Four-paw grip strength was tested using a modified method of that described by Cabe et al. (Cabe, Tilson et al. 1978) using the Bioseb Grip Strength Tester (Bioseb, Vitrolles, France). Animals were positioned so that they grabbed hold of the transducer mesh and then gently pulled backwards until they released their grip on the mesh. The maximum force attained was recorded over three separate trials with at least one minute between.

2.6.3.3 Pole Test (mice only)

Fine motor function was assessed the pole test (Matsuura, Kabuto et al. 1997). Animals were trained to grip, face up - on to the top of a 8mm diameter, 55cm high polypropylene threaded pole (Shop4fasteners.co.uk, Sheffield, UK) standing in the home cage - and turn and to climb down on three separate occasions prior to testing. On test days, animals were timed in the activity for three trials separated by at least 15 minutes. Time to turn, time to descend, total time and number of falls over three trials were recorded. If the animal did not complete the task or fell, a time of 30 seconds was recorded.

2.6.3.4 Label Test (pilot study mice only)

Fine motor function was assessed the label test (Fleming, Salcedo et al. 2004). A small (10mm diameter) adhesive label was placed on the snout of the animal and time to remove label was recorded up to a maximum of 60 seconds in three trials separated by at least 15 minutes. All testing was performed in the animal's home cage, and cage mates were temporarily removed during testing because they can interfere with stimulus removal. If the animal did not remove the stimulus within 60 seconds, the experimenter removed it, and the trial for the next mouse was initiated.

2.6.3.5 Gait Analysis (A30P mice only)

Fine motor function was assessed by gait analysis by a modified version of the method described by Carter et al. (Carter, Lione et al. 1999) in A30P study animals from week 28 onwards. Animals were trained to run along a paper floored corridor to the home cage. On test days, animals' hind paws were covered with 'Måla' water soluble, non-toxic blue paint (IKEA, Newcastle-Upon-Tyne, UK) before being run along the paper floored corridor to the home cage. The length of three strides was measured in mm and averaged.

2.6.3.6 Barnes Maze (A30P mice only)

Spatial learning and memory were assessed in the A30P study using the Barnes maze (Barnes 1979; Patil, Sunyer et al. 2009) in weeks 40 and 41. The paradigm consists of a 96 cm diameter grey plastic disk maze with twenty equally spaced (7.5 cm between holes) holes (5 cm diameter) 2cm from the maze edge (see Fig. 2.6). One hole, the 'target', has access to a small dark escape chamber located under the maze for the mice to exit, with no visual discrimination between this and other holes. A cardboard barrier surrounded the maze with distinct visual cues (A4 size filled square, circle, triangle and cross) attached at the cardinal points to give the animals spatial reference points while the rest of the room, including the experimenter, was kept in constant configuration throughout the duration of the experimental protocol. All experimental procedures were recorded using Panasonic SDR-S26 video camera for scoring. The test was carried out according to the timeline summarised in Fig. 2.5 as described below.

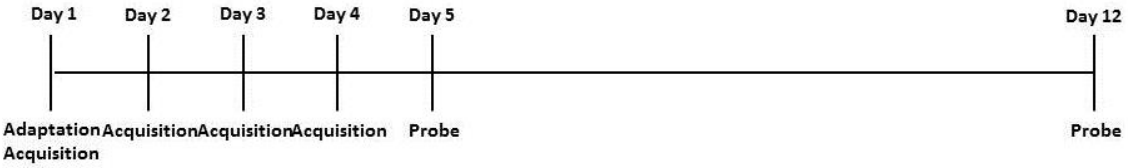

Fig. 2.5 Barnes maze timeline Animals adapted to Barnes maze on Day 1 and learning investigated in the acquisition phase on Days 1-4. Long and short term retention investigated on Days 5 & 12 in the probe phase.

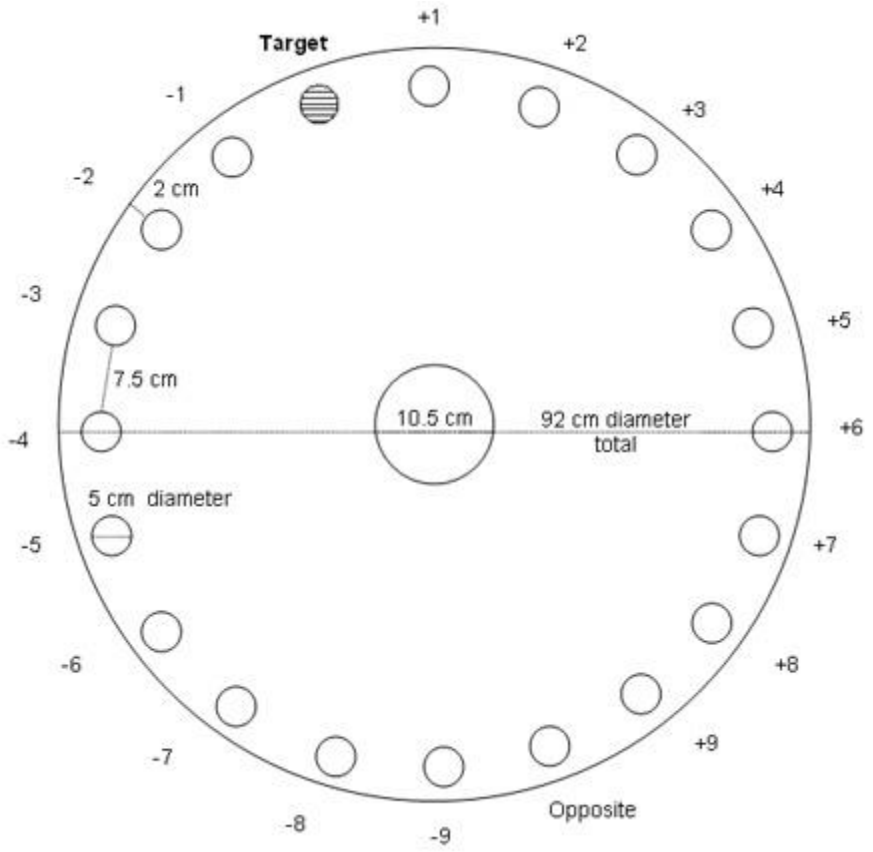

Fig. 2.6 Schematic of Barnes maze Maze is a 92cm grey plastic disc elevated above the floor with 20 identical 5cm diameter holes spread evenly around the circumference, 2 cm from the edge. Holes are numbered -1 to -9 on the right hand side of the target and +1 to +9 on the left. The target hole has an escape chamber underneath attached by magnets. Taken from (Sunyer, Patil et al. 2007) [http://www.nature.com/protocolexchange/protocols/349/uploads/705]

2.6.3.6.1 Adaptation Phase

On Day 1 mice were placed in the 10.5cm diameter chamber in the centre of the maze (start chamber) for 10 seconds before being released. The mouse was then gently guided to the target hole an encouraged to enter the escape chamber. Once in the escape chamber, the entrance was covered and the mouse was left there for 2 minutes then returned to the home cage.

2.6.3.6.2 Spatial Acquisition (Training Days)

Mice were placed in the start chamber for 10 seconds and then released into the maze where they were allowed to explore for 3 minutes. During the exploration period, primary errors (the number of times incorrect holes were explored before finding the target), total number of errors (the number of times incorrect holes were explored before entering the target hole escape chamber), primary latency (the amount of time taken to find target hole) and total latency (the amount of time taken to enter target hole) were recorded. The trial ended when the mouse entered the escape chamber or 3 minutes had elapsed. If the escape chamber was

not entered in the 3 minutes, a total latency of 180 seconds was recorded and the mouse was gently encouraged to enter the chamber. Once in the escape chamber, the entrance was covered and the mouse was left there for 1 minute then before being returned to the home cage.

The test was repeated four times per day on days 1-4 with a 15 min inter-trial interval. Between trials, the maze was cleaned with 50% ethanol and the maze was rotated 90^{o} to try to remove any olfactory cues.

2.6.3.6.3 Reference Memory (Probe Trial)

On Day 5, 24 hours following last training day, and on Day 12, a probe trial was conducted to assess short and long term retention respectively. Mice were placed in the start chamber for 10 seconds and then released into the maze and allowed to explore for 90 seconds. The number of pokes (errors) in each numbered hole, along with primary latency and total latency were all recorded. Error scores were calculated by assigning each error a value according to the distance from the target (i.e. -2 and + 2 = 2, opposite = 10 etc.) and combined to give a final numerical value.

2.6.4 Post Mortem

Animals were anaesthetised in 3% isofluorane (Isoflo® 100% w/w inhalation vapour, liquid isofluorane, Abbott Laboratories Ltd, Maidenhead, UK) in O_2 and terminated by decapitation at 8 weeks post dose for the pilot study and at 42 weeks post dose for A30P study. General post mortem observation carried out on major organs. Brains dissected from animals and 3x2mm (mouse) or 6x2mm (rat) sections taken from anterior and flash frozen before storage at -80^{o}C until neurotransmitter level assay. Posterior fixed in 10% formaldehyde (Sigma).

2.6.4.1 Neurotransmitter Level Assay

2.6.4.1.1 Brain Homogenate Preparation

Caudate Putamen and Forebrain were dissected from both hemispheres of frozen brain slices as Figure 2.7, weighed and homogenised for 20 seconds in 100µl 0.5M formic / 0.1M perchloric acid using a Kontes Pellet Pestle® Motor homogeniser fitted with a blue polypropylene disposable pellet pestle (Sigma). Samples were centrifuged at 13,000g for 15 min at 4^{o}C, supernatants removed and pellets and supernatants stored separately at -20 / 80^{o}C until sample clean up.

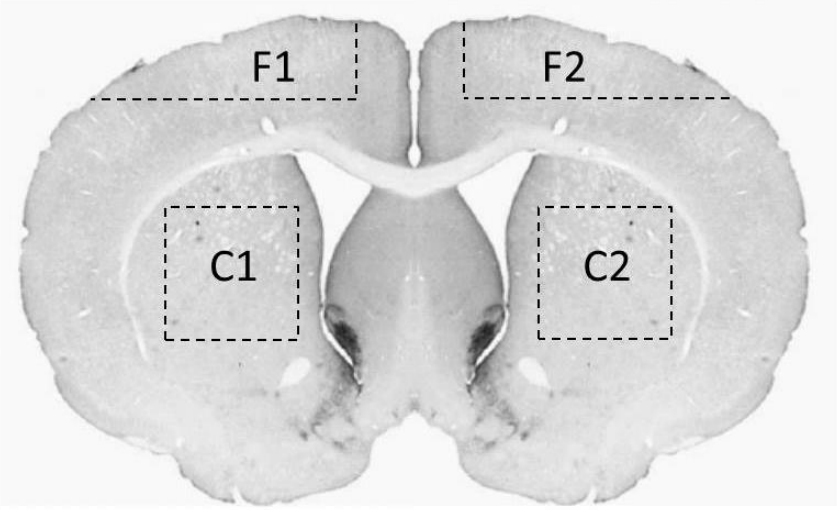

Fig. 2.7 Brain areas dissected for neurotransmitter level assay Areas dissected from frozen brain samples for caudate putamen (C1 & 2) and forebrain (F1 & 2) for neurotransmitter level assay.

2.6.4.1.3 Solid Phase Extraction

30µl of each sample (DA, DOPAC, HVA, 5-HT, 5-HIAA, GABA and glutamate at 20, 10, 5, 2, 1 & 0.5 ng/ml in mobile phase) made up to 150µl with ddH_2O, acidified with 350µl 2% phosphoric acid. Varian Bond Elut Plexa PCX 30 mg 96-well plate conditioned with methanol and H_2O before samples drawn through plate by vacuum pump. Plate washed with 2% (v/v) formic acid (Sigma) before samples eluted. Primary acid elution in 1:1 methanol/acetonitrile and

secondary basic elution in 1:1 methanol/acetonitrile + 5% (v/v) ammonia. Both elutes evaporated to dryness at 40°C and 17psi under nitrogen in a TurboVap®LV evaporation system (Caliper Life Sciences, Cambridge, UK). Acid containing elute reconstituted in 100µl 90:10 H_2O/methanol and basic in 100µl 90:10 H_2O/methanol + 0.1% (v/v) formic acid. Samples were treated with dansyl chloride to add dansyl groups to the neurotransmitters to improve chromatography. Briefly, 100µl dansyl chloride and 100µl of sodium bicarbonate/sodium carbonate buffer (pH 11) and incubated for 30 minutes in a water bath at 35°C protected from light. The reaction was stopped by addition of 5µl 15% formic acid, samples centrifuged an supernatants stored at -80°C until mass spectrometry.

2.6.4.1.4 LC-MS/MS

Chromatographic analyses were performed in a Shimadzu Prominence LC system (Shimadzu, Milton Keynes, UK), using an Accucore column (100mm × 2.1mm × 1.8µM) from Thermo. Mass spectrometric detection was carried out using a QTRAP 550 tandem quadrupole mass spectrometer (AB Sciex, Warrington, UK). The instrument was operated using an electrospray ionization source (ESI) in positive mode. ESI parameters were ion spray voltage 5500 V, source temperature 600 ◦C, cone gas flow 40 L/h and desolvation flow 30 L/h (both gases were nitrogen). Collision induced dissociation was performed using nitrogen as the collision gas at the medium pressure setting in the collision cell. The multiple reaction monitoring transitions as well as the collision energies are shown in Table 2.10. Data acquisition was performed using Analyst v1.52 software (AB Sciex).

Analyte	RTW (min)	Transitions (Ce)	
		Quantification	Confirmation
DA	12.0	853.1 > 170.1 (50)	853.1 > 619.2 (35)
DOPAC	11.1	635.1 > 170.1 (35)	635.1 > 401.1 (30)
HVA	9.8	416.1 > 170.1 (33)	416.1 > 156.1 (35)
5-HT	11.1	643.2 > 170.1 (50)	643.2 > 235.1 (50)
5-HIAA	9.8	425.1 > 170.1 (35)	425.1 > 381.2 (30)
GABA	8.2	337.1 > 170.3 (30)	337.1 > 157.1 (40)
Glutamate	7.5	381.0 > 170.1 (25)	381.0 > 251.9 (25)

Table 2.10 Retention time and MS/MS parameters of neurotransmitters Abbreviations: Ce; Collision energy, RTW; retention time window.

The analytes were separated with a mobile phase consisting of water and 0.1% formic acid (eluent A) and methanol and 0.1% formic acid (eluent B) at a flow rate of 0.3 mL/min. A gradient profile was used, starting at 10 % of eluent B, it was then increased linearly to 95 % in 10 min. This composition was held for a further 5 min, before being returned to the initial conditions in 10 min, followed by a re-equilibration time of 2 min, to give a total run time of 27 min. 5µL was injected into the chromatographic system.

2.6.4.2 Substantia Nigra Stereology

2.6.4.2.1 Sample Processing & Immunohistochemistry

Brain tissue was fixed above (Section 2.7.3.4) for six animals (three male & three female) from each treatment group - of both wild type and A30P mutant mice - was processed in a Leica TP1020 processor for 2 hours under vacuum in each of the following reagents in sequence:

- 70% ethanol
- 80% ethanol
- 95% ethanol
- 100% ethanol (x3)
- Xylene (x2)
- Parrafin wax @ 65^{o}C (x2)

Processed tissue was embedded in paraffin wax with anterior cut face presented.

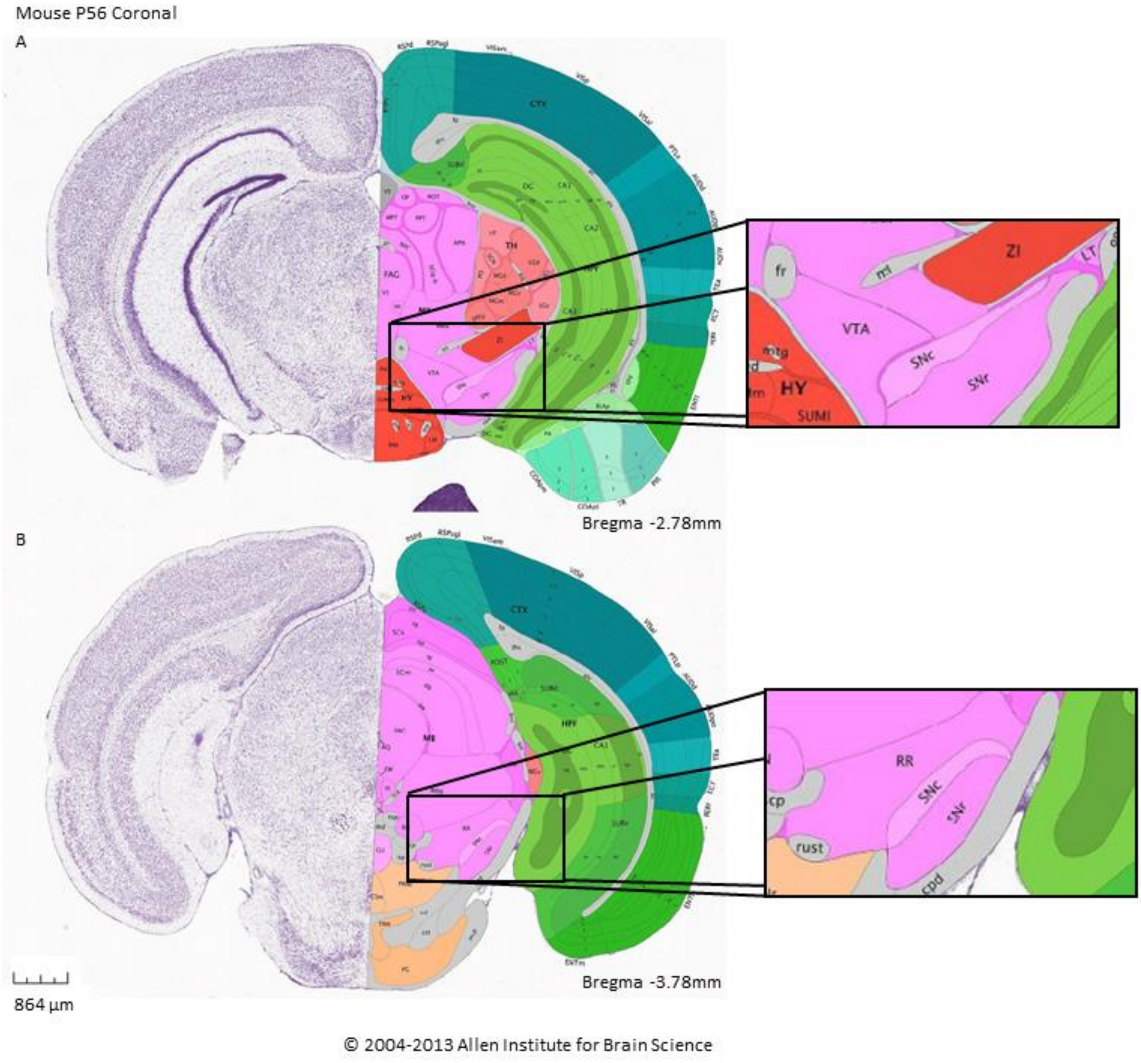

Fig. 2.8 Limits of stereological analysis Representative diagrams of brain slices at the (A) start and (B) end of sampling. Corresponding Bregma coordinates are noted below the diagrams. Adapted from (Lein, Hawrylycz et al. 2007); website: ©2012 Allen Institute for Brain Science. Allen Mouse Brain Atlas [Internet]. Available from: http://mouse.brain-map.org/

Coronal sections of tissue (30µm) were taken rostral to the SNpc at bregma -2.78mm throughout the SNpc until caudal to bregma -3.78mm (Fig. 2.8) and every fifth section was selected for stereological analysis, giving a total of nine sections. They were stained for DA neurons with an anti-tyrosine hydroxylase enzyme using the Vectastain Elite ABC Rabbit IgG kit (Vector, Peterborough, UK) and general nuclei, by Nissl staining, using the following stepped protocol:

- DE-WAXING; 1 x 5 minute and 1 x10 minute wash in xylene (Fisher Scientific)
- REHYDRATION; decreasing ethanol solutions (2 x 100%, 95%, 70% 50% & 0% ethanol in ddH_2O).
- ANTIGEN RETREVAL; boiled in 1.27mM EDTA (Tetrasodium Dihydrate, USB Products, High Wycombe, UK), pH 8 in a microwave at half power for 10 minutes before allowing to cool for 20 minutes and then immediately transferred to ddH_2O.
- QUENCHING; 0.9% H_2O_2 in TBS followed by 3 x 3 minutes TBS wash.
- BLOCKING; goat serum in TBS for 30 minutes.
- PRIMARY ANTIBODY; Rabbit polyclonal antibody to TH (Abcam) 1:500 in TBS containing blocking goat serum at 4^oC overnight.
- SECONDARY ANTIBODY; Vectastain biotinylated anti-rabbit anitody 1:200 in blocking serum in TBS for 30 minutes at room temperature followed by 3 x 3 minutes TBS wash.
- DETECTION; Vectastain ABC reagent (Avidin/Biotinylated Enzyme Complex)) in TBS for 30 minutes at room temperature followed by 3 x 3 minutes TBS wash. 0.25mg/ml 3,3'-Diaminobenzidine in TBS + 0.02% H_2O_2 for exactly 10 min, washed in cold running tap water for 5 minutes.
- NISSL COUNTERSTAIN; 100µg/ml Cresyl Fixed Violet in Acetone Buffer (112.5µM Acetic Acid & 11.75mg/ml sodium acetate in ddH_2O, ph 4.5) for 20 minutes, allowed to air dry.
- COVERSLIP; Dehydrated by 1 x 95% and 2 x 100% ethanol, 2 x xylene washes and coverslips mounted with DPX (Fisher Scientific).

2.6.4.2.2 Stereological Analysis

Tyrosine hydroxylase positive neurones in the SNpc were counted stereologically by a blinded operator using a Zeiss Imager.Z1 microscope attached to an AxiocamMR3c camera with Stereologer^{TM} Ver 2.1 CP-Version (Stereology Resource Centre, Chester, Maryland, US) software. The SNpc was manually outlined at low (x2.5) magnification using TH positive nuclei running alongside the cerebral peduncle as a guide (Fig 2.10 A). Estimated SNpc volumes used for counting all groups are summarised in Fig. 2.9; there was no significant difference between groups (unpaired t-test). Counting frames of 34.5μm^2 were placed throughout the structure at a frame spacing distance of 100 μm^2. A frame height of 12 $\pm$ a guard height of 2µm was used based on an average section thickness following shrinkage during processing of 16.56$\pm$0.31 µm and there was no significant difference between thickness in any treatment group (group thickness data summarised in Table 2.12). Frame heights were measured for each frame by measuring the z-axis positions between the first object coming into focus and the last object leaving focus.

Total number and volume of TH positive neurons with normal morphology were counted at high (x40) magnification using unbiased multi-level (fraction-based) estimates for every fifth section throughout the SNpc. TH- positive neurons were identified as by immunopositively stained neurones containing a clearly defined nucleus. Immunopositive neurons were counted if the nucleus fell inside the counting frame or crossed the inclusion line (green); nuclei that crossed the exclusion line (red) were not counted (Fig. 2.10 B).

Volumes of all TH positive neurons contained in the sampling frame area were estimated using an isotropic uniform randomly (IUR) assigned nucleator probe. This method is based upon the idea that four random one dimensional lines from a point within an object can be used to make an unbiased estimate of its volume (Gundersen, Bagger et al. 1988). The nucleator method developed by Gundersen (Gunderson 1988) employs four randomly oriented rays originating from the nucleolus and measures where they cross the border of the neuronal soma (Fig. 2.10 C). The following formula is then used to calculate the particle volume:

$$\hat{\bar{V}}_N = \frac{4\pi}{3} \bullet \bar{l}_n^3 = \frac{4\pi}{3 \bullet n} \sum_{i=1}^{n} l_{n,i}^3$$

where: l_n= distance from sampling point (nucleolus to edge of object)

The coefficient of error (CE) is a widely used measure of the precision of data acquired by stereological analysis. CE for cell number (num) and volume (vol) estimates were calculated according to the Gundersen-Jensen method (Gundersen and Jensen 1987) (West, Slomianka et al. 1991) using the following formulae:

$$CE_{num} = SD_{num} / mean_{num}$$

$$CE_{vol} = \left(\frac{\sum(I^2)}{(\sum I)^2} + \frac{\sum(Volume^2)}{\sum(Volume)^2} - \frac{2\sum(1 \bullet Volume)}{(\sum I \bullet \sum \ Volume)} \right) \bullet \left(\frac{n}{n-1} \right)$$

where: I = neurons counted

Volume = reference area • (sampling frame density)^2 • section depth

N = number of fields

CE values < 0.10 were considered acceptable and all sampled counts and volumes in this study had acceptable CE values (see Table 2.11 for group CE values).

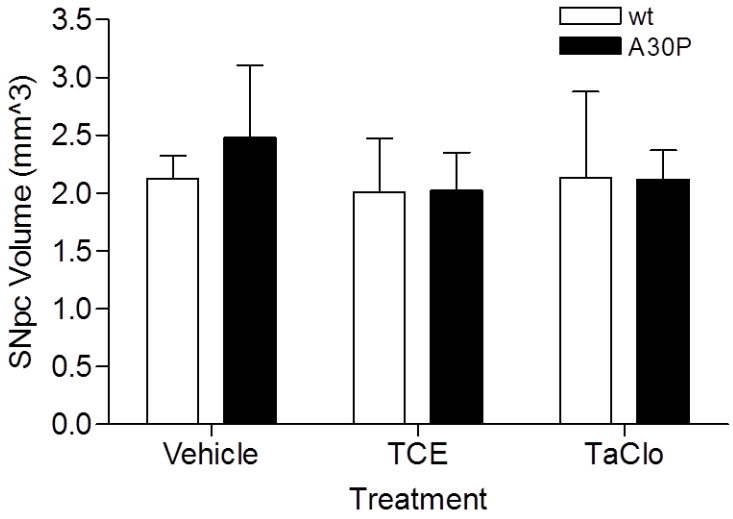

Fig. 2.9 SNpc volume in A30P α-synuclein overexpressing & wt C57BL/6 Mice Total SNpc sampling volume of TCE (1000mg/kg), TaClo (2mg/kg) & vehicle (olive oil) treated wt & A30P overexpressing C57BL/6 mice assessed by stereological analysis. Data presented as mean ± SD (n=5/6). No significant difference between treatment groups or starins, unpaired t-test

Group	Section Thickness (µm)	Cells counted	DA number CE	Cell Volume CE
wt				
Vehicle	16.78±0.31	258±38	0.064	0.017
TCE	16.42±0.24	139±33	0.087	0.018
TaClo	16.62±0.29	144±29	0.086	0.021
A30P				
Vehicle	16.50±0.44	188±43	0.076	0.019
TCE	16.39±0.21	127±15	0.090	0.014
TaClo	16.52±0.24	117±7	0.093	0.016

Table 2.11 Grouped average stereological analysis parameters Section thickness and cells counted presented as mean±SD, CE values presented as mean (n=5/6).

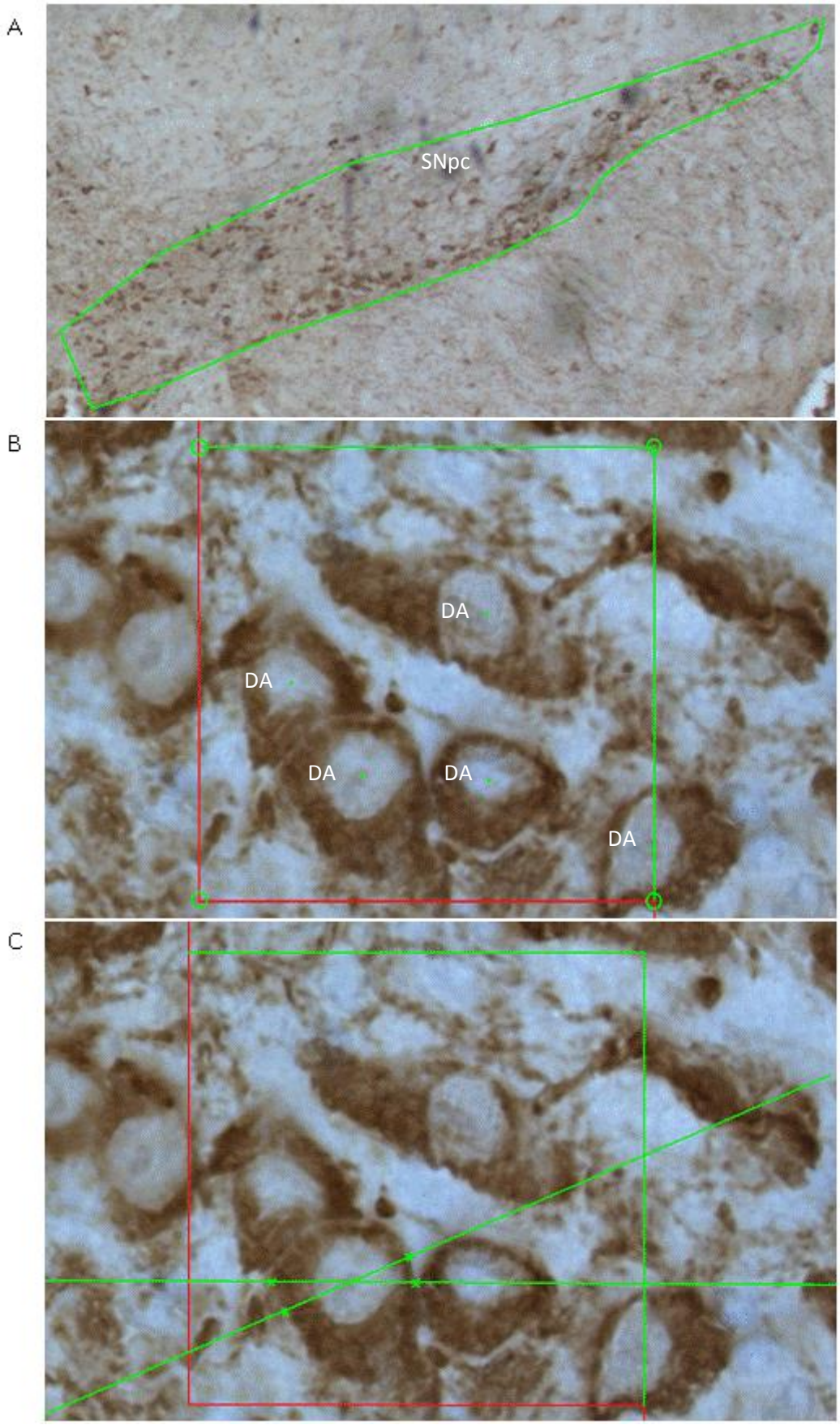

Fig. 2.10 Stereological analysis parameters used to assess DA neuron number in SNpc of C57BL/6 mice brains Example measurement parameters used to measure SNpc DA neuron numbers in fixed C57BL/6 mouse brains(A) outline of SNpc (x2.5) (B) DA neuron (DA) count (x40) (C) DA neuron volume measurement (x40)

2.7 General Statistics

All statistical analysis and graphical representations were carried out using SPSS Statistics 17.0 (2008), GraphPad Prism 4 for Windows (2005) or Microsoft Excel (2007). All graphs represent data as mean ± standard deviation (SD) or ± standard error of the mean (SEM). Statistical significance was considered when *P<0.05, **P<0.01 or ***P<0.001.

2.7.1 General In Vitro Statistics

2.7.1.1 Cell Viability Assays

ANOVA (One-way) was used to analyse differences within groups and Dunnett's t-test to analyse specific difference between groups when investigating the effect of toxins on SH-SY5Y cells and midbrain neurons. ANOVA (Two-way) was used to analyse difference in interaction and bonferroni's t-test was used to investigate specific differences when investigating to effects of cell death manipulators on the toxicity of toxins in SH-SY5Y cells.

2.7.1.2 Western Blot Statistics

ANOVA (One-way) was used to analyse differences within groups and Dunnett's t-test to analyse specific difference between groups when investigating the effect of toxins on protein levels over time.

2.8.1.3 FACS Statistics

ANOVA (Two-way) was used to analyse the effects of TaClo treatment over time on dyes assessed by FACS and bonferroni's t-test was used to investigate specific differences.

2.7.1.4 Mitochondrial Activity Assay Statistics

ANOVA (One-way) was used to analyse differences within groups and Dunnett's Multiple Comparison to analyse specific difference between groups when investigating the effect of toxins on mitochondrial OXPHOS Complex activity.

2.7.2 General In Vivo and Ex Vivo Statistics

2.7.2.1 Weight & Behavioural Assessment Statistics

Repeated measures ANOVA (Two-way) was used to analyse the effect of treatment over time on animal weight and performance in motor function tests and learning in the acquisition phase of the Barnes Maze, with bonferroni's t-test used to investigate specific differences. Kruskal Wallis test was used to assess memory in the probe phase of the Barnes Maze.

2.8.2.2 SNpc DA Neuron Number Assessment Statistics

ANOVA (One-way) was used to analyse differences within groups and Dunnett's t-test to analyse specific difference between groups when investigating the effect of toxins on DA neuronal number in the SNpc of treated animals.

2.8.2.3 Neurotransmitter Level Assessment Statistics

ANOVA (One-way) was used to analyse differences within groups and Dunnett's t-test to analyse specific difference between groups when investigating the effect of toxins on neurotransmitter levels in the brains of treated animals.

For sample outputs of statistical analysis, see Appendix C.

Chapter 3
The Toxicity of TCE & Metabolites

3.1 Introduction

TCE is a commonly used industrial solvent and environmental contaminant. Groups of the population are exposed to this chemical at various levels and it has been shown to have links to motor dysfunction and PD (Guehl, Bezard et al. 1999; Reif, Burch et al. 2003; Gash, Rutland et al. 2008; Goldman, Quinlan et al. 2011). TCE can be extensively metabolised by various pathways into a number of products. As it is, as yet, unknown whether it is TCE itself or one of its metabolites that mediate its neurotoxic effects, this study will examine the neurotoxicity of a number of metabolites in addition to the parent compound. Metabolites to be examined were chosen based on previous evidence of neurotoxicity. The TCE metabolite TaClo, formed via the intermediate compound chloral, has been reported to be neurotoxic and has been linked with PD (Bringmann, God et al. 1995; Bringmann, God et al. 1995); therefore both TaClo and chloral were investigated. An additional metabolite chosen was DCA, exposure to which has been linked with peripheral neuropathies in humans and animal models (Kurlemann, Paetzke et al. 1995; Moser, Phillips et al. 1999; Kaufmann, Engelstad et al. 2006).

SH-SY5Y is a human neuroblastoma cell-line cloned from the SK-N-SH cell-line which was derived from malignant tumours of immature neurons. It is a neuronal-like catecholaminergic cell line that maintains stem-cell characteristics, grows in a monolayer, proliferates rapidly for long periods, possesses tyrosine hydroxylase and dopamine-β-hydroxylase activity (Ross, Spengler et al. 1983), expresses the dopamine transporter and receptors and forms storage vesicles, although dopamine storage in the vesicles is impaired (Colapinto, Mila et al. 2006), and as such is extensively used as a model of DA neurons in studying PD (Xie, Hu et al. 2010). SH-SY5Y is also routinely used in studies of neuronal cell death and a variety of chemicals can induce these cells to differentiate into different phenotypes increasing its usefulness in neurotoxicity studies (Presgraves, Ahmed et al. 2003).

Methods to differentiate embryonic stem cells into representative populations of midbrain neurons have been developed (Yan, Yang et al. 2005; Yang, Zhang et al. 2008). These models allow investigations into the neurotoxic effects of compounds in PD in a more stable model of DA neurons in a mixed cell population closer to that seen *in vivo* than that provided by SH-SY5Y. Due to the stable numbers of cells in the differentiated midbrain line, more chronic studies are also possible.

The actual cell death pathway - apoptosis, necroptosis (programmed necrosis) or another form of death - which occurs in DA neurons during the development of PD, is so far unclear. The driving mechanism behind any cell death is also unknown, although several hypotheses have

been proposed suggesting the involvement of protein misfolding and autophagic/ubiquitin system impairment, mitochondrial dysfunction, oxidative stress, DA metabolism and excitotoxicity/Ca^{2+} dysregulation.

3.1.1 Aims

The aims of this study were to investigate the toxicity of TCE and its metabolites chloral, DCA and TaClo in the DA model cell line SH-SY5Y and midbrain neurons differentiated from embryonic stem cells. The possible involvement of known cell death mechanisms such as apoptosis, necroptosis and autophagy in any toxicity found was also to be investigated.

To achieve these goals, a previously developed exposure paradigm was used and combined with known cell death mediators and gene transfection studies to investigate cell death mechanisms. These methods were supported by Western blotting - to examine any changes in implicated protein levels, flow cytometry - to try and determine death morphology, and bright field and fluorescence microscopy to - visualise toxic effects.

3.2 Methods

For detailed descriptions of all methods see Material and Methods (Section 2), apart from those described below:

3.2.1 TCE Toxicity in a Closed System.

SH-SY5Y were grown in 6-well plates at a density of ~7 x 10^5 cells per well in 350µl 10% GM and incubated overnight to allow recovery for assay. Plates were placed inside 5L airtight containers containing either three vials of 3ml ddH_2O or three vials TCE and incubated overnight for 17 hours. Plates were removed from airtight containers and viability assessed by Alamar Blue assay confirmed by visual inspection as described in section 2.1.2.1. The amount of TCE left in vials was measured to calculate exposure levels.

3.2.2 Statistical Analysis

For information on statistical methods see General Statistics (Sections 2.8, 2.8.1.1, 2.8.1.2 & 2.8.1.3)

3.3 Results

3.3.1 Toxicity of TCE & Metabolites in Model Dopaminergic Cell Lines

3.3.1.1 TCE

SH-SY5Y cells were treated with various concentrations of TCE (1-1000µM) and assessed for toxicity at 21 hours. Midbrain neurons were treated with 250-5000µM TCE with viability assessed at baseline and following 24 hours and 1 & 2 weeks exposure. Viability was assessed by the Alamar Blue assay using the conversion of the non-fluorescent blue dye resazurin to the fluorescent pink dye resorufin by mitochondrial metabolism as an indication of cell survival in both cell lines (Nakayama, Caton et al. 1997). Viability was confirmed by visual inspection. No significant toxicity was observed in either cell line, with all cells appearing morphologically sound when examined under magnification and no decrease in Alamar Blue reduction observed in either SH-SY5Y cells (Fig. 3.1 A) or midbrain neurons at any time point (Fig. 3.1 C)

Midbrain neurons were treated with various concentrations of TCE for 2 weeks and then fixed. Fixed cells were stained for tyrosine hydroxylase (TH) to identify DA neurons and counterstained with DAPI for total cell number. Images were taken and total number of cells and number of DA neurons were estimated using image analysis software. There was no significant difference in DA neurons as quantified by TH staining following 2 weeks treatment with 0.25-5mM TCE (Fig. 3.2).

SH-SY5Y cells were exposed to TCE or ddH_2O in the atmosphere of an enclosed 5L volume airtight container to try and achieve stable TCE levels not attained in previous open systems due to the volatility of TCE. Significant cell death was observed with a dramatic decrease in Alamar Blue fluorescence (Fig. 3.1 B) and near total destruction of cellular integrity when viewed at magnification following 24 hour exposure to TCE in the system when compared to control, suggesting TCE is toxic to SH-SY5Y cells when local levels are maintained. To estimate exposure levels of TCE, TCE volumes were measured pre and post incubation and on all 3 experiments 3ml TCE was observed to have evaporated.

Exposure was calculated based on the assumptions TCE Density = 1.463g/ml, 3ml exposure in 5000ml volume. Therefore:

$$\frac{3 \times 1.463}{5000} \times 100 = 0.08778\%$$

Exposure = 8,778 ppm or 6.7mM

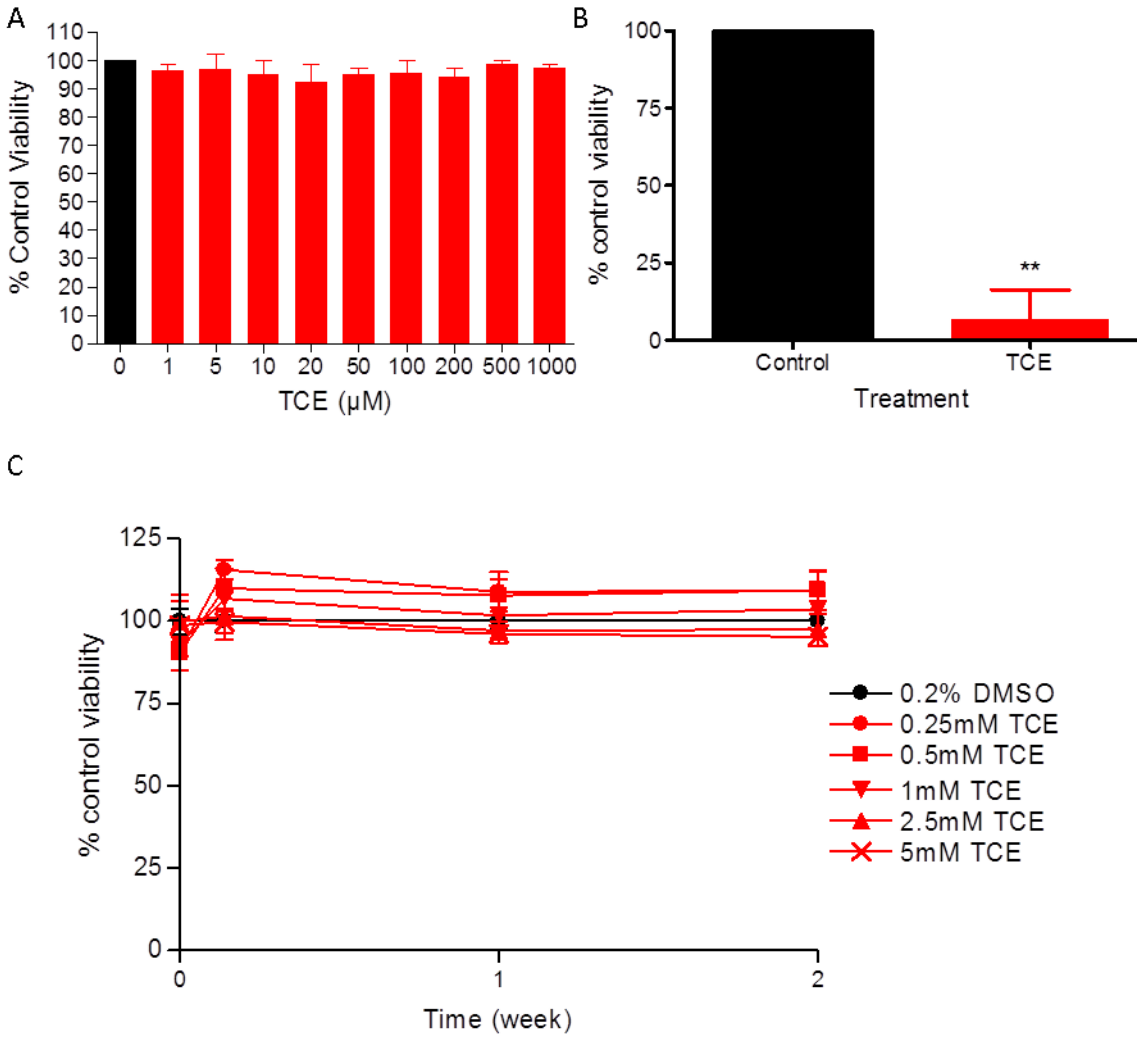

Fig. 3.1 Effect of TCE on cell viability (A)SH-SY5Y cells were treated with various concentrations of TCE for 21 hours and viability measured by reduction of Alamar Blue (resazurin). Data presented as mean % control ± SD from quadruplicate assays (n=3). No significant difference, One-way ANOVA. (B) SH-SY5Y cells were treated with TCE (6,000ppm) or ddH_2O for 24hours and viability measured by reduction of Alamar Blue (resazurin). Data presented as mean % control ± SD from sextuplicate assays (n=3). **P>0.01, paired t-test. (C) Midbrain neurons were treated with various concentrations of chloral and viability measured by reduction of Alamar Blue (resazurin) at baseline, 24 hours, 1 & 2 weeks. Data presented as mean % control + SD from triplicate assays (n=1). No significant effect of TCE treatment over time (P<0.001), Two-way ANOVA.

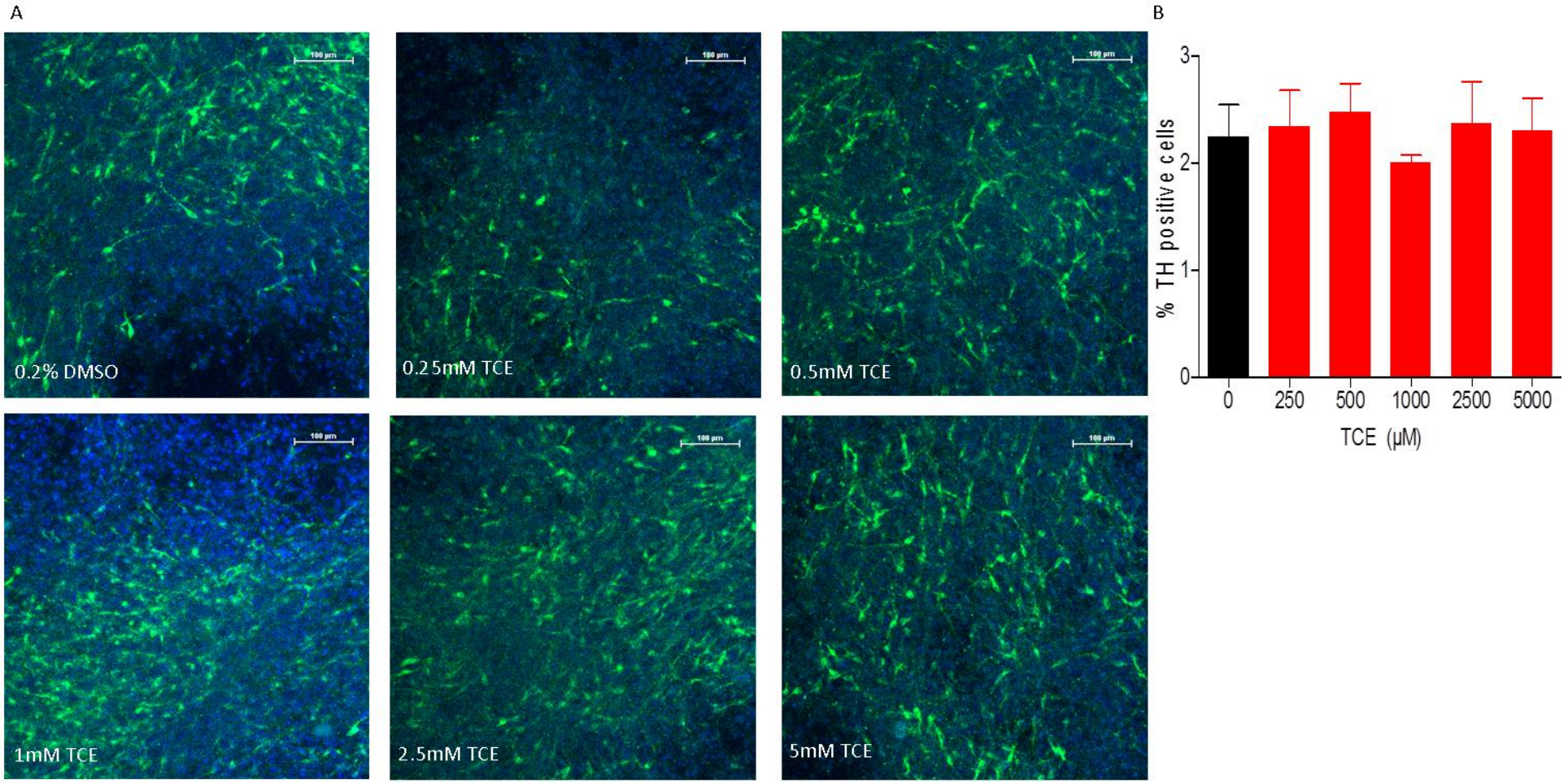

Fig. 3.2 Effect of TCE on DA neurons in a differentiated mixed midbrain culture Midbrain neurons were treated with various concentrations of TCE for 2 weeks and then stained with DAPI for total cell number (blue) and anti-TH for DA neurons (green). (A) Images show cells treated with 0 .2% DMSO, 0.25, 0.5, 1, 2.5 or 5mM Chloral. (B) Graph shows % total cells TH positive. Data presented as mean % control + SD from triplicate assays (n=1). No significant difference, One-way ANOVA

3.3.1.2 Chloral

Chloral is an metabolic intermediate generated *in vivo* following TCE treatment (Jiang, Mutch et al. 2007). SH-SY5Y cells were treated with various concentrations of chloral (5-5000µM) and assessed for toxicity at 21 hours and midbrain neurons with 25-1000µM chloral with viability assessed at baseline and following 24 hours and 1, 2, 3 & 4 weeks. Viability was assessed by the Alamar Blue assay and confirmed by visual inspection. Toxicity was observed in both cell lines, with a significant decrease in Alamar Blue reduction observed in SH-SY5Y cells at chloral concentrations $\geq$ 200µM and 5mM causing near total cell death (Fig. 3.3 A). This finding was supported by visual inspection of the cells under magnification showing a similar percentage of cell losing standard morphology as shown by the Alamar Blue test at the same concentrations.

In the midbrain culture, chloral had a significant toxic effect on viability over time as assessed by Alamar Blue reduction ($P<0.001$, Two-way ANOVA, Fig. 3.6). 100µM chloral treated cultures showed significant cell death following 2 weeks exposure, with 50% cell death seen at week 2 and 75% death by week 3 & 4, 250 & 500 µM reduced viability to less than 50% following 1 week exposures with almost total death occurring by 2 weeks and cells exposed to 1000µM showed almost total death from 1 week ($P<0.001$, Bonferroni post-test, Fig. 3.3 B). All Alamar Blue test results were confirmed by visual inspection of cell number and structural integrity under magnification. These results may show midbrain neurons to be less susceptible to chloral than SH-SY5Y cells, but this phenomenon could be explained by the presence of far higher cell number per well for the midbrain neurons. Although the midbrain cells are differentiated, they were stem cells when plated and, as such, will have been growing for a proportion of the >18 days prior to treatment as opposed to the 24 hours growth seen with the SH-SY5Y cells.

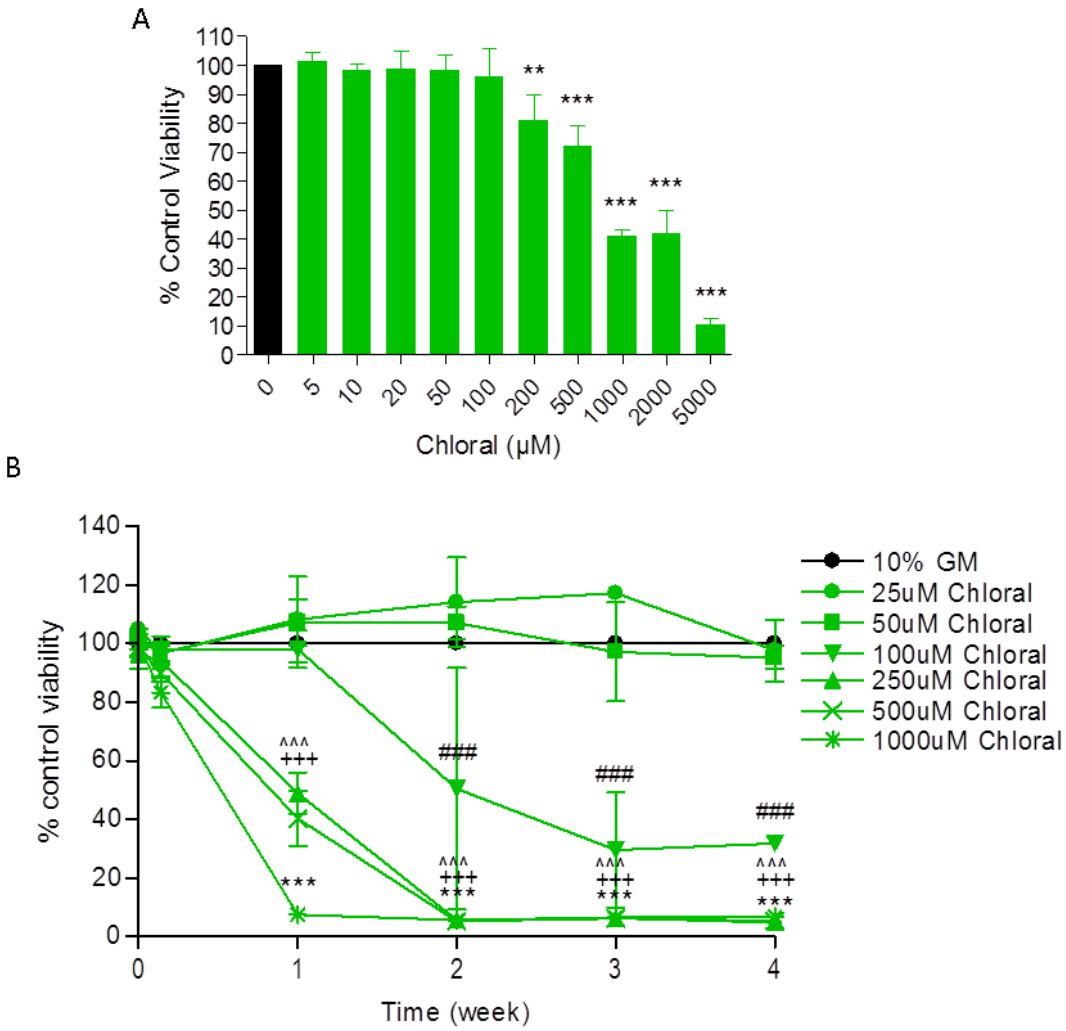

Fig. 3.3 Effect of Chloral on cell viability (A) SH-SY5Y cells were treated with various concentrations of chloral for 21 hours and viability measured by reduction of Alamar Blue (resazurin). Data presented as mean % control ± SD from quadruplicate assays (n=3). *** P<0.001, **P<0.01when compared to 10% GM, One-way ANOVA & Dunnett's post-test. (B) Midbrain neurons were treated with various concentrations of chloral and viability measured by reduction of Alamar Blue (resazurin) at baseline, 24 hours, 1, 2, 3 & 4 weeks. Data presented as mean % control + SD from triplicate assays (n=3). Significant effect of chloral treatment over time (P<0.001), Two-way ANOVA. ***P<0.001 when 1000µM, +++P<0.001 when 500µM, ^^^P<0.001 when 250µM & ###P<0.001 when 100µM chloral compared to 0.2% DMSO, Bonferroni post-test

Midbrain neurons were treated with various concentrations of Chloral for either 2 or 4 weeks and then fixed. Fixed cells were stained for tyrosine hydroxylase to identify DA neurons and counterstained with DAPI for total cell number. Images were taken and total number of cells and number of DA neurons were estimated using image analysis software. A significant reduction in % TH positive cells was seen following 4 week chloral exposure ($P<0.01$, One-way ANOVA); however, there was no significant change in % TH positive cells following 25 & 50µM Chloral treatment and at doses $\geq$100µM Chloral there were no TH positive cells present (Fig. 3.4 A & B). Both of these findings agree with the effects observed in the general population of cells when viability was assessed by Alamar Blue (Fig. 3.6) suggesting that chloral is toxic at similar levels to all DA neurons in comparison to the general cell population in a differentiated mixed midbrain culture.

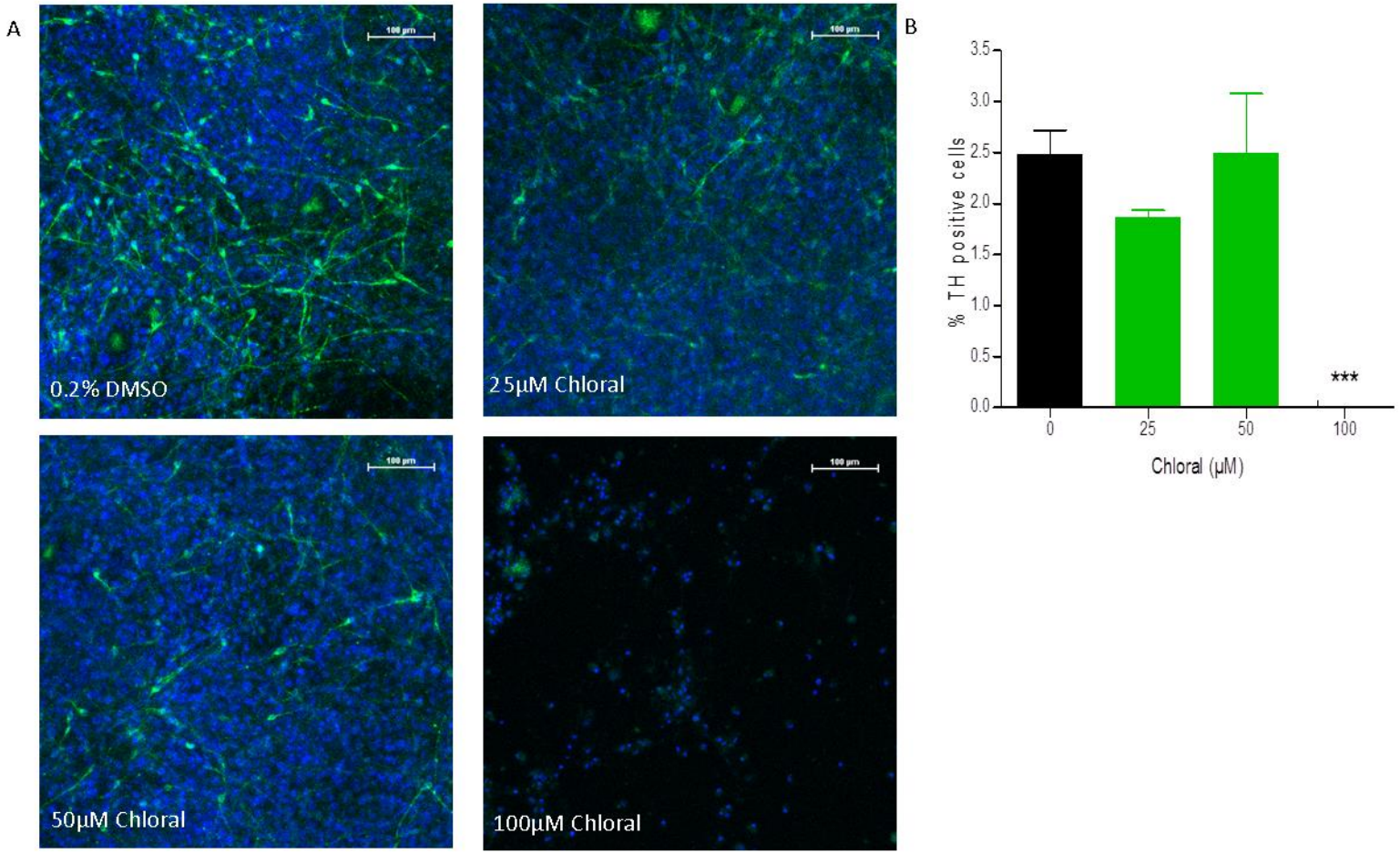

Fig. 3.4 Effect of Chloral on DA neurons in a differentiated mixed midbrain culture Midbrain neurons were treated with various concentrations of Chloral for 4 weeks and then stained with DAPI for total cell number (blue) and anti-TH for DA neurons (green). (A) Images show cells treated with 0 .2% DMSO, 25, 50 & 100µM Chloral. (B) Graph shows % total cells TH positive. Data presented as mean % control + SD from triplicate assays (n=1). *** P<0.001, when compared to 0.2% DMSO, One-way ANOVA & Dunnett's post-test

3.3.1.3 DCA

The TCE metabolite DCA has been to shown to cause both central (Bhat, Kanz et al. 1991; Cicmanec, Condie et al. 1991) and peripheral (Moser, Phillips et al. 1999; Kaufmann, Engelstad et al. 2006) neuronal damage . DA model SH-SY5Y cells were treated with DCA (1-2000µM) for 17 hours and viability assessed by Alamar Blue reduction. No significant toxicity was observed in Alamar Blue reduction (Fig. 3.5) and all cells showed regular morphology when viewed at magnification.

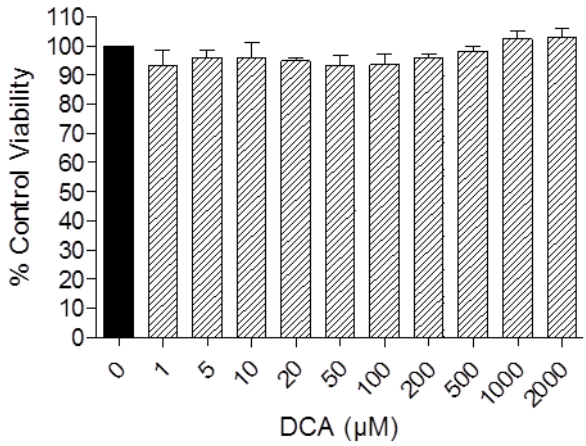

Fig. 3.5 Effect of DCA on SH-SY5Y viability SH-SY5Y cells were treated with various concentrations of DCA for 21 hours and viability measured by reduction of Alamar Blue (resazurin). Data presented as mean % control ± SD from quadruplicate assays (n=3). No significant difference, One-way ANOVA.

3.3.1.4 TaClo

TaClo is a metabolite of TCE formed by the spontaneous reaction of the intermediate compound chloral with endogenous tryptamine (Bringmann, Feineis et al. 2000). SH-SY5Y cells were treated with various concentrations of TaClo (1-1000µM) and assessed for toxicity at 21 hours and midbrain neurons with 5-150µM TaClo with viability assessed at baseline and following 24 hours and 1, 2, 3 & 4 weeks. Viability was assessed by Alamar Blue and confirmed by visual inspection. Toxicity was observed in both cell lines, with a significant decrease in Alamar Blue reduction observed in SH-SY5Y cells at TaClo concentrations $\geq$ 50µM and 200µM causing near total cell death (Fig. 3.6 A). This finding was supported by visual inspection of the cells under magnification showing a similar percentage of cell losing standard morphology as shown by the Alamar Blue test at the same concentrations (Fig. 3.7).

In the midbrain culture, TaClo had a significant toxic effect on viability over time as assessed by Alamar Blue reduction ($P<0.001$, Two-way ANOVA, Fig. 3.13). 100µM TaClo treated cultures showed significant cell death following 2 weeks exposure, with 50% cell death seen at week 2 and almost total death by week 3. 150 µM TaClo reduced viability to less than 25% following 1 week exposure with almost total death occurring by 2 weeks ($P<0.001$, Bonferroni post-test, Fig. 3.6 C). All Alamar Blue test results were confirmed by visual inspection of cell number and structural integrity under magnification. This appears to show a reduction in sensitivity of midbrain cultures to TaClo toxicity; investigations into the selectivity of the toxicity may explain this.

To confirm the accuracy of the Alamar Blue assay, as it measures metabolic activity as an indicator as opposed to actual cell death itself, the toxicity assay was repeated with TaClo concentrations of 5-1000µM and viability assayed by the crystal violet assay. The crystal violet assay works by the stain entering and binding to DNA fixed viable cells; excess dye is removed and the cells are then permeabilised allowing release of the dye trapped in the cells. This dye can then be measured by a spectrophotometer with absorbance corresponding to the number of live cells in the plate. In agreement with Alamar Blue assessed viability, crystal violet assay showed significant TaClo toxicity at doses $\geq$ 50µM, with 200µM leading to the death of nearly all cells (Fig. 3.6 B). This supports the Alamar Blue assay as a reliable method of measuring cell viability in TaClo toxicity assays.

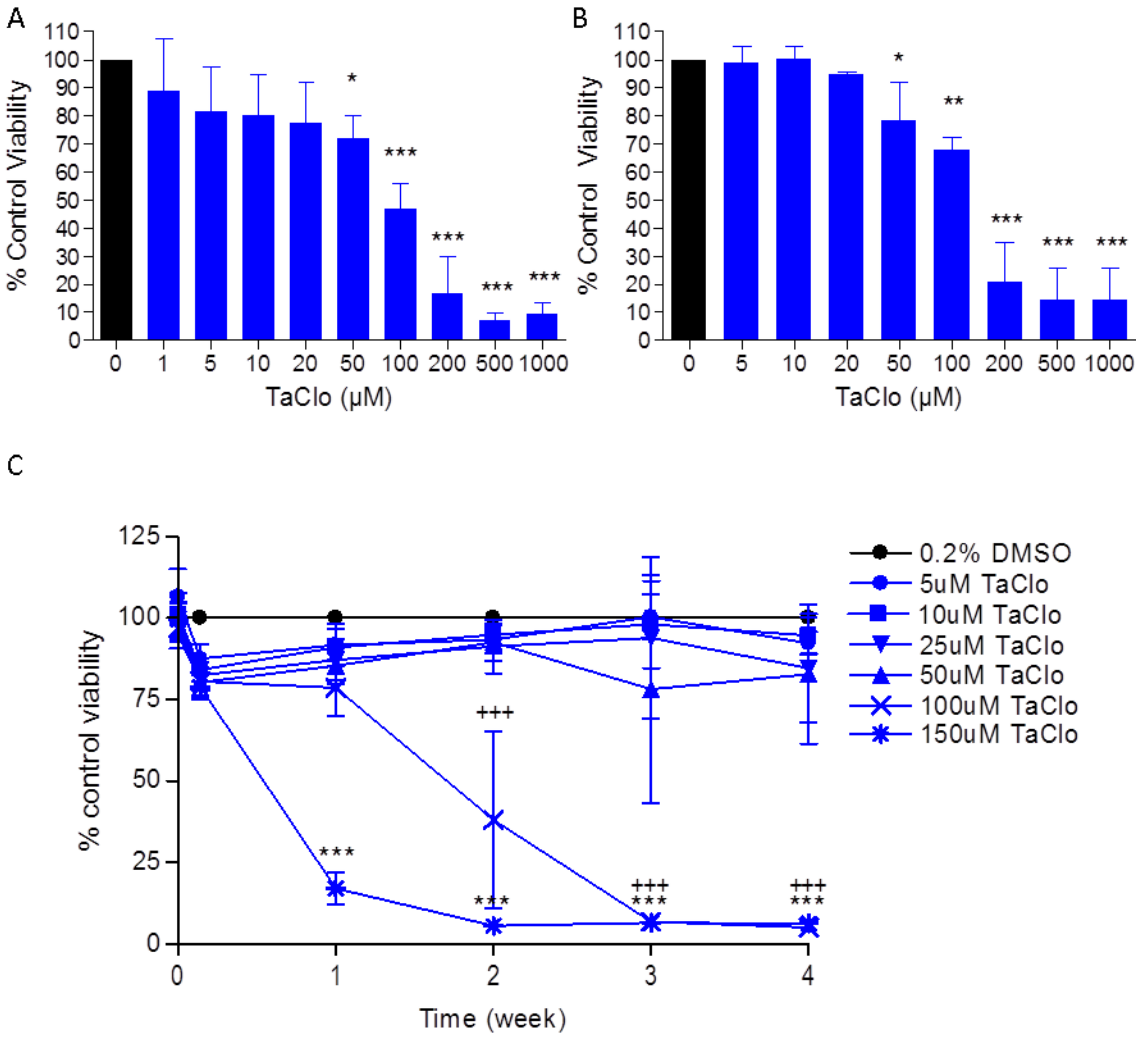

Fig. 3.6 Effect of TaClo on SH-SY5Y viability SH-SY5Y cells were treated with various concentrations of TaClo for 21 hours and viability measured by (A) reduction of Alamar Blue (resazurin) or (B) retention of crystal violet. Data presented as mean % control ± SD from quadruplicate assays (n=3). *** P<0.001, **P<0.01, *P<0.05 when compared to 0.2% DMSO, One-way ANOVA & Dunnett's post-test. (C) Midbrain neurons were treated with various concentrations of TaClo and viability measured by reduction of Alamar Blue (resazurin) at baseline, 24 hours, 1, 2, 3 & 4 weeks. Data presented as mean % control + SD from triplicate assays (n=3). Significant effect of TaClo treatment over time (P<0.001), Two-way ANOVA. ***P<0.001 when 150µM & +++P<0.001 when 100µM TaClo compared to 0.2% DMSO, Bonferroni post-test

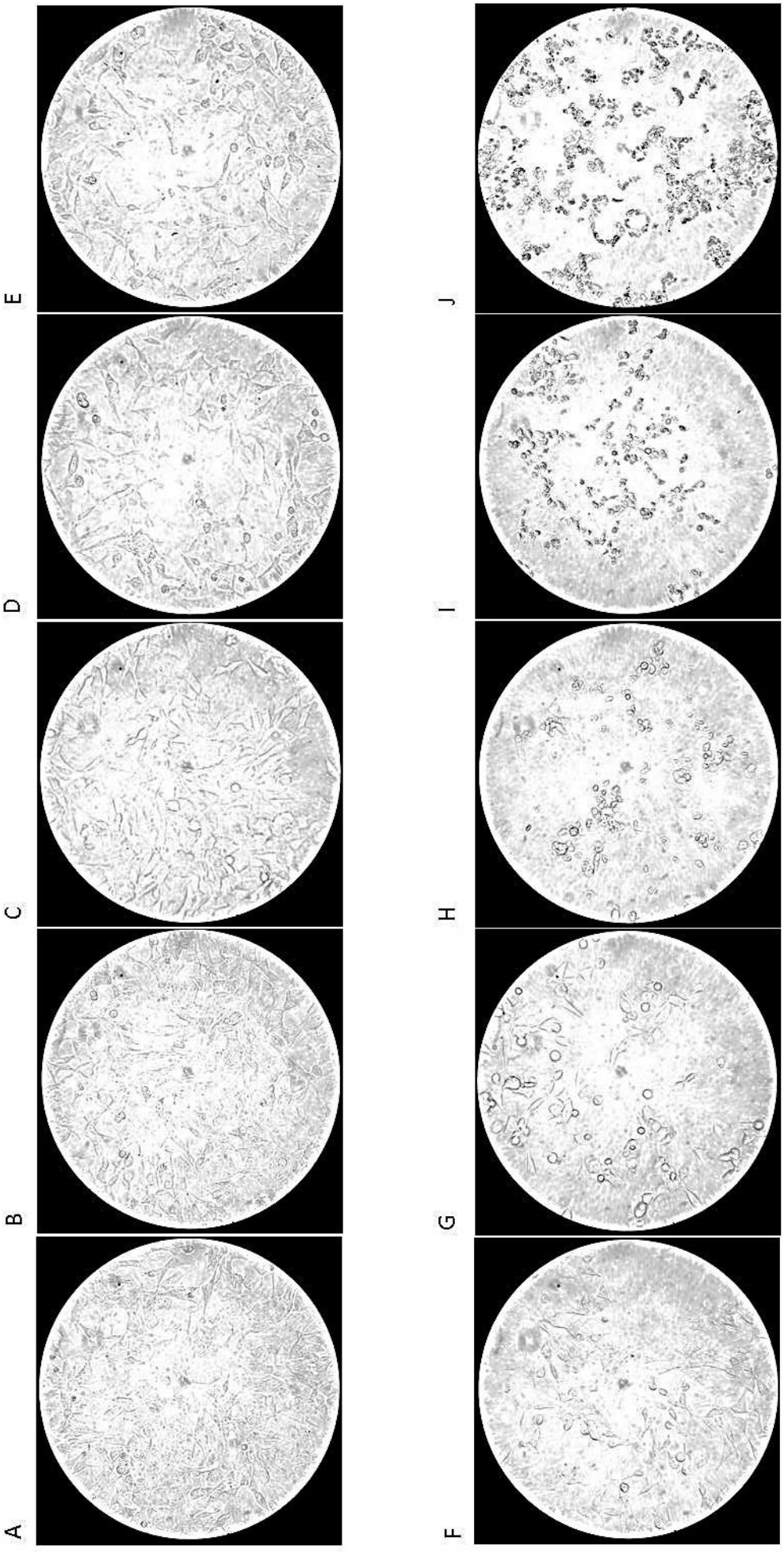

Fig. 3.7 Effect of TaClo on SH-SY5Y morphology SH-SY5Y cells were treated with various concentrations of TaClo for 21 hours. Representative photographs of (A) 0.2% DMSO, (B) 1, (C) 5, (D) 10, (E) 20, (F) 50, (G) 100, (H) 200, (I) 500, (J) 1000µM TaClo at x 40 magnification.

To investigate the time course of TaClo toxicity, SH-SY5Y cells were exposed to 100 or 150µM TaClo for various time points up to 24 hours and viability assessed by Alamar Blue reduction. 100µM TaClo treated cells showed a small but significant level of toxicity at 4 and 8 hours, and a relatively sharp increase in toxicity between 8 and 24 hours with ~50% cell death occurring (Fig. 3.8 A). When treated with 150µM TaClo, significant death was seen ≥8 hours and viability continued to decrease in a linear fashion until 24 hours when nearly all cells were dead (Fig. 3.8 B).

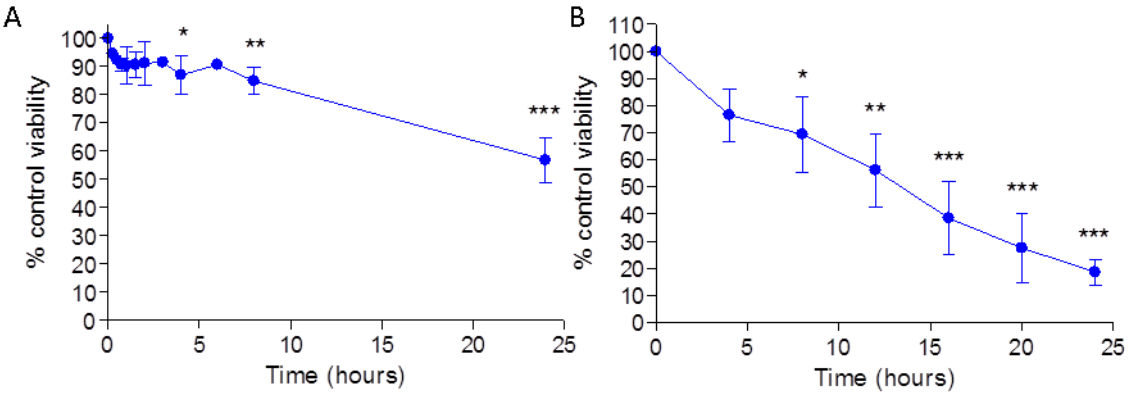

Fig. 3.8 Effect of TaClo on SH-SY5Y viability over time SH-SY5Y cells were treated with (A) 100 & (B) 150µM TaClo and viability assessed by reduction of Alamar Blue (resazurin) at various timepoints. Data presented as mean % control ± SD from quadruplicate assays (n=3). *** P<0.001, **P<0.01, *P<0.05 when compared to 0h treatment, One-way ANOVA & Dunnett's post-test.

Midbrain cultures were fixed following the 4 weeks of TaClo exposure and stained for tyrosine hydroxylase (TH) to identify DA neurons and counterstained with DAPI for total cell number. Images were taken and total number of cells and number of DA neurons were estimated using image analysis software. A significant reduction in per cent TH positive neurons was observed following 4 weeks TaClo treatment (P<0.01, One-way ANOVA). Cultures that were treated with 25 & 50µM TaClo showed a significant reduction in DA neurons (P<0.05, P<0.01 respectively, Dunnett's t-test) with almost total ablation of TH positive cells occurring following 50µM TaClo exposure (Fig. 3.9), despite a lack of significant toxicity apparent in the total population as assessed by Alamar Blue (Fig. 3.13 F). At doses ≥100µM TaClo there were no TH positive cells present (Fig. 3.14 A & B) as there was almost total reduction in the viability of the general population of cells(Fig. 3.13 F). The toxicity of TaClo to DA neurons is slightly higher than that seen in SH-SY5Y; however, this is following far longer exposure time. These findings suggest a specificity of TaClo toxicity to DA neurons when compared to a differentiated mixed midbrain culture and a slightly increased sensitivity to TaClo when compared to SH-SY5Y neuroblastoma.

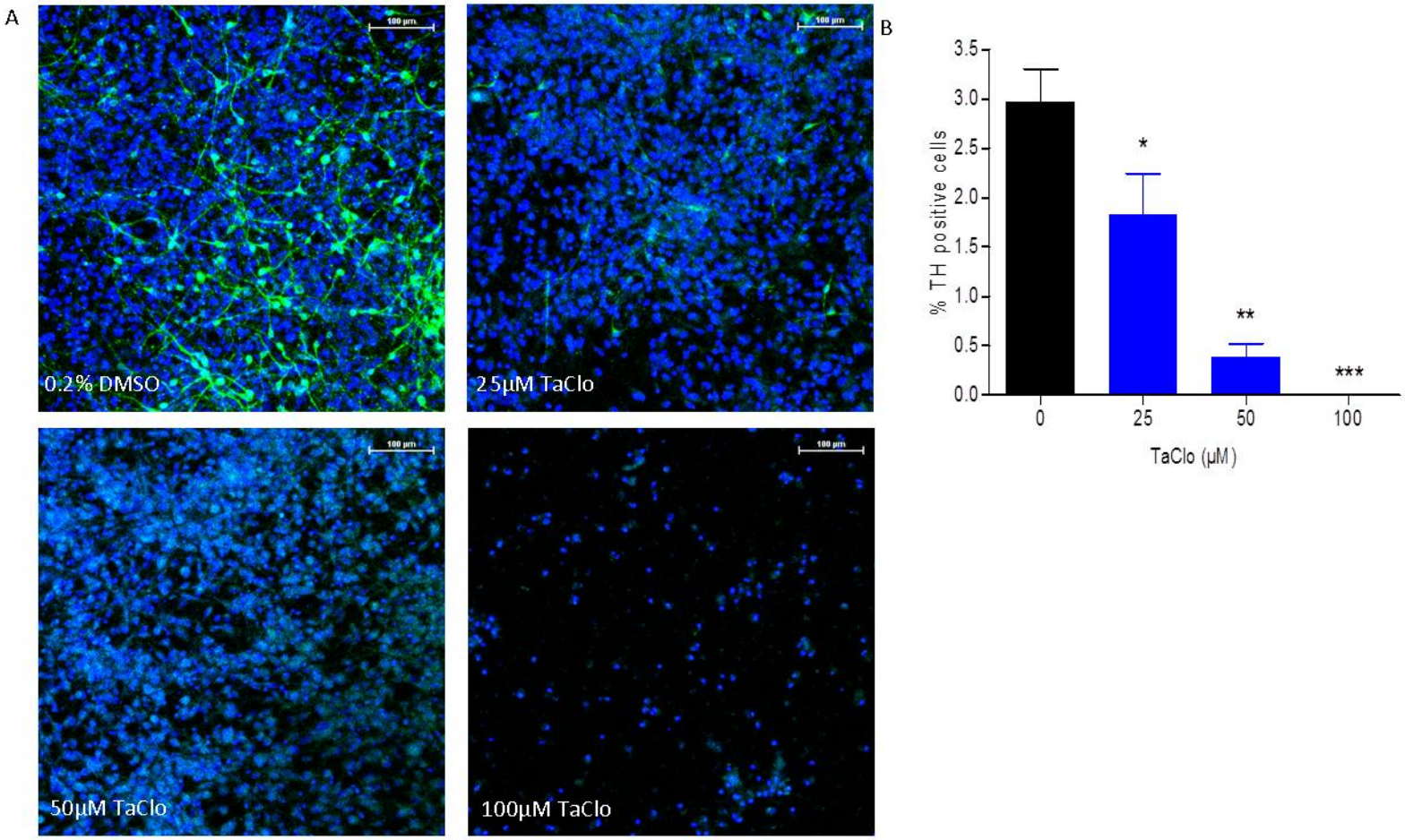

Fig. 3.9 Effect of TaClo on DA neurons in a differentiated mixed midbrain culture Midbrain neurons were treated with various concentrations of TaClo for 4 weeks and then stained with DAPI for total cell number (blue) and anti-TH for DA neurons (green). (A) Images show cells treated with 0.2% DMSO, 25, 50, 100,& 150µM TaClo. (B) Graph shows % total cells TH positive. Data presented as mean % control + SD from triplicate assays (n=2). Significant reduction in %TH-positive cells ($P<0.01$, One-way ANOVA) *** $P<0.001$, **$P<0.01$, *$P<0.05$ when compared to 0.2% DMSO, Dunnett's post-test.

LD_{50} values were estimated for TCE and each of its metabolites studied in SH-SY5Y and midbrain neurons (from exposures previously described) as well as neural stem cells (from data not shown) and summarised in Table 3.1. As observed in the assays, TCE and DCA did not show significant toxicity in SH-SY5Y or midbrain neurons (TCE only). Chloral was most toxic to midbrain neurons (LD_{50} 250µM) followed by SH-SY5Y (LD_{50} 500-1000µM) but showed relatively low toxicity in neural stem cells (LD_{50} 2-5mM). TaClo showed similar levels of toxicity in midbrain neurons and SH-SY5Y (LD_{50} 100µM & 100-150 µM respectively) but was comparatively less toxic in neural stem cells and MEFs (LD_{50} 200-500µM & 200 µM respectively).

Compound	Cell line	LD_{50}
TCE	SH-SY5Y	Not toxic $\leq$1mM
	Midbrain Neurons	Not toxic $\leq$5mM
Chloral	SH-SY5Y	500-1000µM
	Midbrain Neurons	250µM
	Neural Stem Cells	2-5mM
DCA	SH-SY5Y	Not toxic $\leq$2mM
TaClo	SH-SY5Y	100µM
	Midbrain Neurons	100-150µM
	Neural Stem Cells	200-500µM
	MEF	200µM

Table 3.1 TCE & metabolite LD_{50} Estimated LD_{50} of TCE and metabolites in various cell lines following 24 hour treatment in SH-SY5Y and neural stem cells and 1 week in midbrain neurons

3.3.2 Involvement of Apoptosis in TaClo Toxicity

Apoptosis is the main form of programmed cell death in eukaryotes and also the most well characterised and studied. A detailed discussion on the mechanism of apoptosis can be found in section 1.3.1 above.

Caspases are a group of cysteine-aspartic acid protease enzymes (Alnemri, Livingston et al. 1996) known to be integrally involved in the execution of chemically mediated apoptosis (Sun, MacFarlane et al. 1999); therefore inhibition of caspases should protect against apoptotic cell death. The involvement of caspases, and so apoptosis, in the mechanism of TCE mediated cell death through TaClo was investigated by co-treating SH-SY5Y cells with toxic doses of chloral or TaClo and the pan-caspase inhibitor zVAD.fmk (Slee, Zhu et al. 1996). No significant protection from chloral or TaClo induced cell death was conferred on SH-SY5Y cells by caspase blockade (Two-way ANOVA) (Fig.3.10) suggesting the cell death method triggered in SH-SY5Y by either TCE metabolite may not be apoptosis.

Caspase-3 is the primary 'executioner caspase' that plays a key role in the mechanism of apoptosis by cleaving various substrates in what is known as the caspase cascade (Slee, Adrain et al. 2001). Protein was isolated from SH-SY5Y cells treated with TaClo and Western blots were carried out for cleaved caspase 3, with induced Jurkat cell extract used as a positive control and untreated Jurkat cell extract as a negative control. Induced Jurkat cell extract is taken from human macrophage cells induced to undergo apoptosis by the chemotherapeutic agent etoposide (Kaufmann, Desnoyers et al. 1993). No bands were observed for cleaved caspase up to 8 hours after treatment with 100µM TaClo and non-induced Jurkat cell extract but bands were present following 24 hours 100µM TaClo and induced Jurkat cell extract (Fig. 3.11). This suggests that caspase cleavage/activation may occur as a terminal stage event in TaClo mediated toxicity.

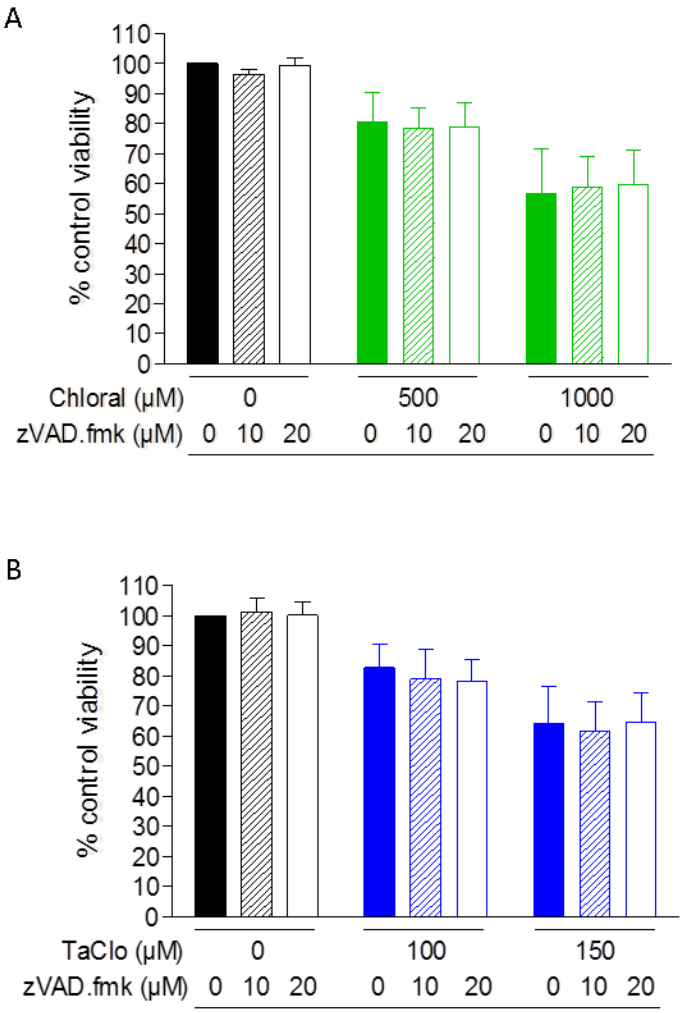

Fig. 3.10 Effect of zVAD.fmk on chloral & TaClo toxicity in SH-SY5Y SH-SY5Y cells were pre-treated with zVAD.fmk (10 & 20μM) for 1 hour and then co-treated with either (A) chloral (500 or 1000μM) or (B) TaClo (50 or 100μM) for 21 hours and viability measured by reduction of Alamar Blue (resazurin). Data presented as mean % control ± SD from quadruplicate assays (n=3). (A & B) No significant effect of zVAD.fmk on chloral or TaClo treatment, Two-way ANOVA.

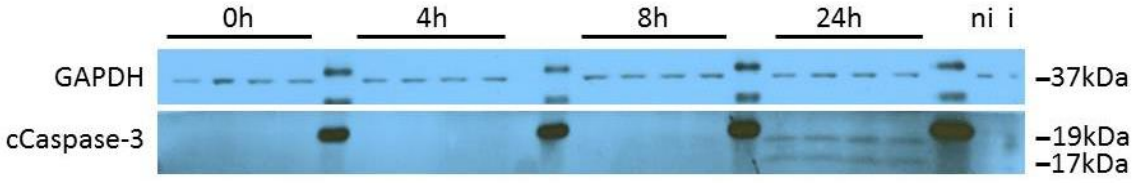

Fig. 3.11 Expression of cleaved Caspase-3 (cCaspase 3) in 0.2% DMSO & 100μM TaClo treated SY-SY5Y SH-SY5Y cells were treated with 0.2% DMSO or 100μM TaClo for 0, 4, 8 & 24 hours and protein harvested. Samples were probed for cCaspase-3 alongside Jurkat cell extract either non-induced (ni) or induced to undergo apoptosis by etoposide treatment (i) as controls. Image is representative blot of cCaspase-3 and GAPDH control.

3.3.3 Involvement of Necroptosis in TaClo Toxicity

It has been shown that when cells are under stress and apoptosis does not occur, the cell can be forced down an alternative necrotic death pathway(Lemaire, Andréau et al. 1998), known as "necroptosis". Necroptosis is a previously uncharacterised, programmed form of cell death that shares morphological features with necrosis but is regulated by the formation of a complex containing RIP1, RIP3 and caspase-8 (He, Wang et al. 2009). The formation of this complex is blocked during apoptosis by cleavage of the component proteins by effector caspases, so it may function as an alternative death mechanism if caspase activation and apoptosis are inhibited (Vercammen, Beyaert et al. 1998). More detail on necroptosis can be found in section 1.3.2 above.

The necroptotic pathway has been shown to be inhibited by the small molecule inhibitor Necrostatin-1(Nec-1) (Degterev, Huang et al. 2005). SH-SY5Y cells were treated with toxic doses of TaClo and Nec-1 to investigate whether this pathway was involved in TaClo mediated SH-SY5Y toxicity. Statistically, there was a significant effect of Nec-1 on both chloral and TaClo induced toxicity ($P<0.05$, Two-way ANOVA). The only significant increase in viability in chloral treated cells was conferred by 100µM Nec-1 on 0.2% DMSO treated cells ($P<0.001$, One-way ANOVA) but not following either dose of chloral treatment (Fig. 3.12 A), suggesting that the effect of Nec-1 observed preferentially occurs in unexposed cells and, therefore, that Nec-1 does not protect against chloral mediated SH-SY5Y death. However, in TaClo treated SH-SY5Y, Nec-1 significantly protected against both 100 & 150µM TaClo mediated toxicity ($P<0.01$, $P<0.001$ respectively, Dunnett's t test) in a dose-dependent manner (Fig. 3.12 B), suggesting that the significant increase in viability mediated by Nec-1 is proportionally higher in TaClo exposed cells when compared to its effect on 0.2% DMSO treated cells - therefore protects against TaClo mediated SH-SY5Y toxicity.

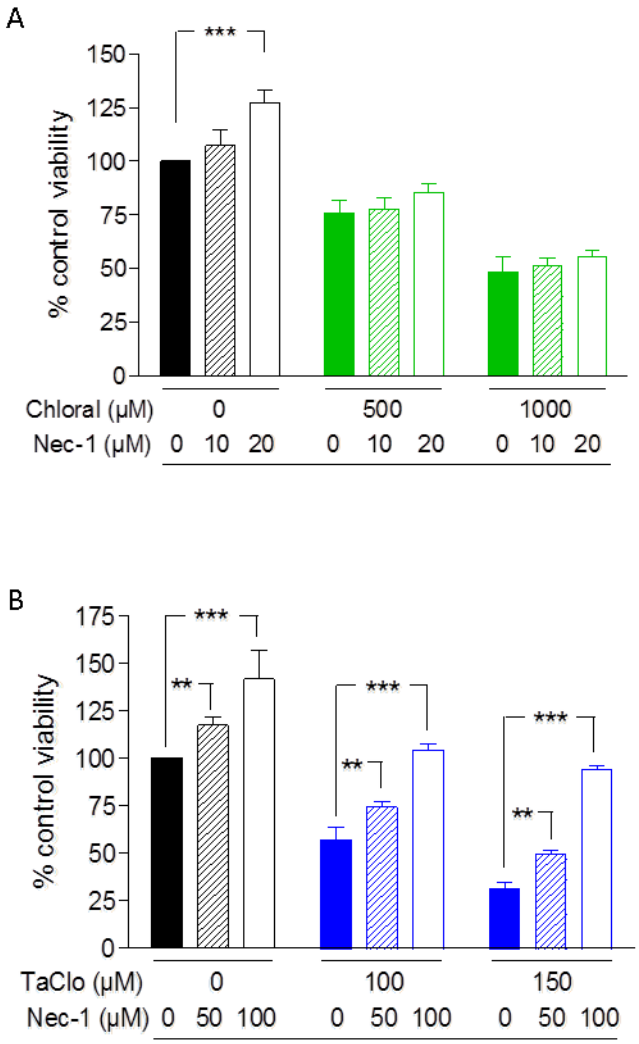

Fig. 3.12 Effect of Necrostatin-1 on chloral & TaClo toxicity in SH-SY5Y SH-SY5Y cells were pre-treated with Nec-1 (50 & 100μM) for 1 hour and then co-treated with either (A) chloral (500 or 1000μM) or (B) TaClo (100 & 150μM) for 21 hours and viability measured by reduction of Alamar Blue (resazurin). Data presented as mean % control ± SD from quadruplicate assays (n=3). (A & B) Significant effect of Nec-1 on chloral & TaClo treatment ($P<0.05$), Two-way ANOVA. ***$P<0.001$, **$P<0.01$ when compared to 0.2% DMSO, Bonferroni post-test

A recent report discovered that Nec-1 has an identical structure as methyl-thiohydantoin-tryptophan, an inhibitor of indoleamine 2,3-dioxygenase (IDO), a rate limiting enzyme of the kynurenine pathway that metabolises tryptophan to NAD+ (Vandenabeele, Grootjans et al. 2013). This lack of specificity of Nec-1, questions whether the protective effects of the compound seen against TaClo toxicity are due to Nec-1 and necroptosis inhibition or IDO inhibition. To further investigate this, SH-SY5Y cells - exposed to toxic doses of TaClo - were co-treated with 1-methyl-L-tryptophan, an IDO inhibitor that does not affect RIP1 (Cady and Sono 1991; Schmidt, Siepmann et al. 2012).

No significant protection from TaClo induced cell death was conferred on SH-SY5Y cells by specific IDO blockade (Two-way ANOVA) (Fig.3.13) suggesting that IDO inhibition is not involved in Nec-1 induced protection against TaClo toxicity. However, Nec-1s also had no significant effect on TaClo toxicity in this assay (Two-way ANOVA) (Fig.3.13), suggesting the possibility that RIP1 inhibition may not be involved in protection against TaClo induced death.

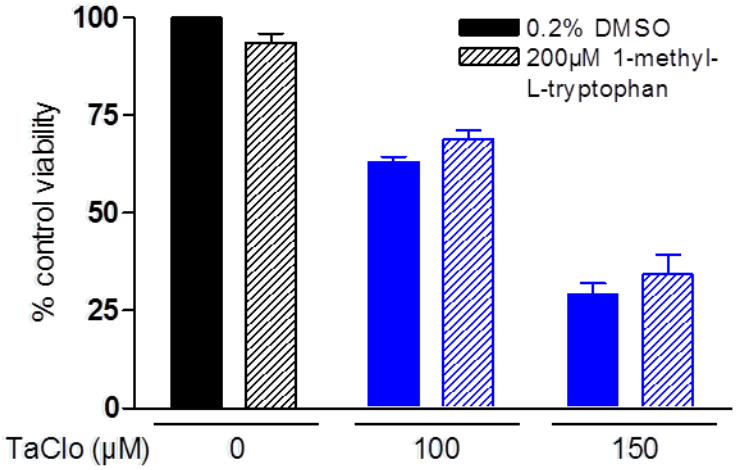

Fig. 3.13 Effect of 1-metyl-L-tryptophan on TaClo toxicity in SH-SY5Y SH-SY5Y cells were pre-treated with 1-methyl-L-tryptophan (200µM) for 1 hour and then co-treated with TaClo (100 & 150µM) for 21 hours and viability measured by reduction of Alamar Blue (resazurin). Data presented as mean % control ± SD from quadruplicate assays (n=3). No significant effect of 1-methyl-L-tryptophan on TaClo toxicity, Two-way ANOVA

Nec-1 acts by inhibiting the kinase activity of the receptor interacting protein 1 (RIP1) (Degterev, Huang et al. 2005), which has been shown to be a critical effector in the switch to necroptosis (Holler, Zaru et al. 2000). Protein isolated from SH-SY5Ys treated with TaClo over various time points was probed for RIP1 levels by Western blot. TaClo treatment significantly reduced the proportion of RIP1 that was present in the cleaved, non-kinase domain-containing form (Fig. 3.14), possibly suggesting a blockage of the caspase-8 or caspase-6 mediated RIP1 cleavage present during apoptosis (Lin, Devin et al. 1999; Van Raam, Ehrnhoefer et al. 2013) and more of a push of the cell towards necroptosis. Full length RIP1 levels were not found to be significantly changed (Fig. 3.14).

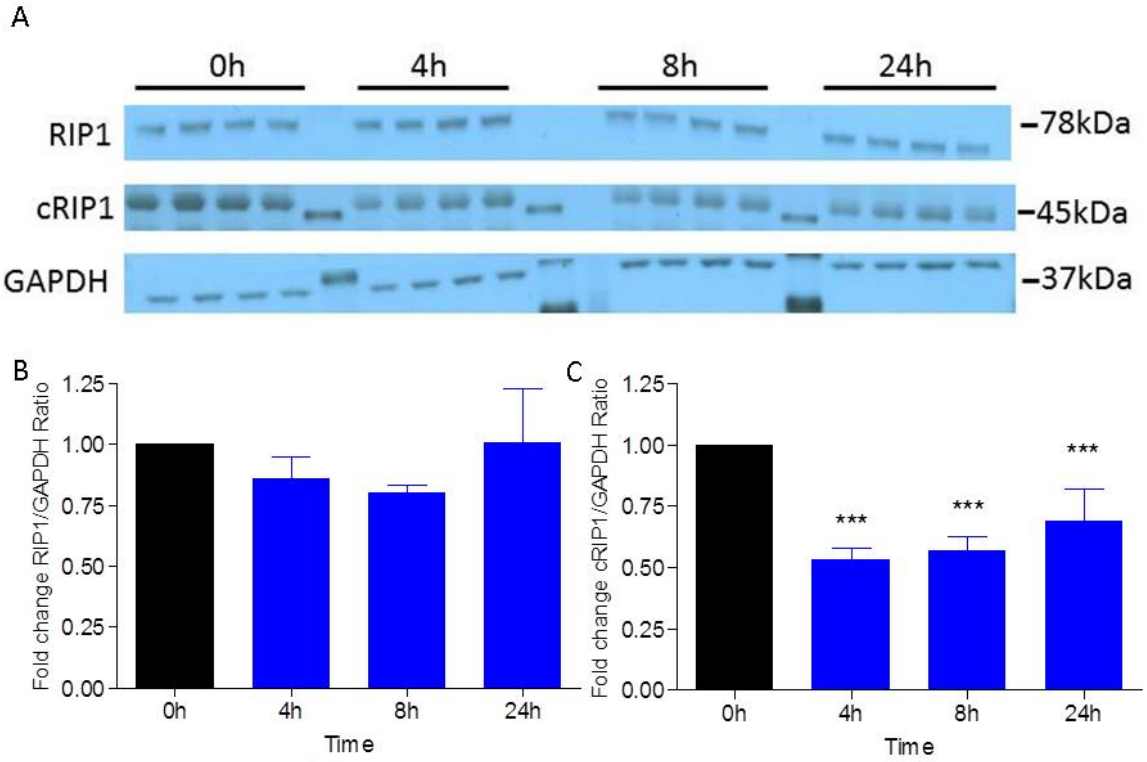

Fig. 3.14 Expression of full length (RIP1) and cleaved (cRIP1) RIP1 in 100µM TaClo treated SY-SY5Y cells SH-SY5Y cells were treated with 100µM TaClo for 0, 4, 8 or 24 hours and protein harvested. Samples were probed for RIP1. (A) Image is representative blot of RIP1, cRIP1 and GAPDH control (B) RIP1 intensity relative to GAPDH. Data presented as fold-untreated + SD from quadruplicate assays (n=3). No significant difference when compared to 0h, One-way ANOVA. (C) cRIP1 intensity relative to GAPDH. Data presented as fold-untreated + SD from quadruplicate assays (n=3). *** P<0.001, when compared to 0h, One-way ANOVA & Dunnett's post-test

SH-SY5Y cells were treated with a shRNA containing lentiviral vector to knockdown RIP1 levels in order to confirm the finding that RIP1 is integrally involved in TaClo mediated SH-SY5Y cell death. Viral take up was good, as seen by the viral conferred GFP expression relative to inherent DAPI staining (Fig. 3.15 A), and probing for RIP1 levels by Western blot showed RIP1 levels knocked down to 60% or 40% of control by viral clones 513 & 668 respectively (Fig. 3.15 B & C). Due to the greater extent of RIP1 knockdown, clone 668 treated cells were used in further studies.

RIP1 knockdown and control lentiviral transfected SH-SY5Y cells were then treated with TaClo (20-150µM) and viability assayed by Alamar Blue fluorescence confirmed by visual inspection. RIP1 knockdown showed a small but significant protection against TaClo toxicity when compared to control cells ($P<0.001$, Two-way ANOVA) (Fig. 3.16 A) with RIP1 knockdown significantly protecting SH-SY5Y at doses of 20, 50, 100 & 150µM TaClo ($P<0.05$, $P<0.001$, $P<0.001$, $P<0.05$, respectively, Dunnett's t-test) supporting the evidence that TaClo treatment leads to SH-SY5Y cell death via necroptosis. To investigate whether the protection mediated by Nec-1 in SH-SY5Y cells seen above was due to inhibition of RIP1 kinase activity, RIP1 knockdown SH-SY5Y cells were treated with toxic doses of TaClo and Nec-1. Nec-1 still had a significant effect on viability in RIP1 knockdown SH-STY5Ys ($P<0.01$, Two-way ANOVA); however, the increase in viability was significantly lower in TaClo treated cells than control (Fig. 3.16 B), suggesting that the protection conferred on SH-SY5Y by Nec-1 seen in wild-type cells may be mediated by RIP1.

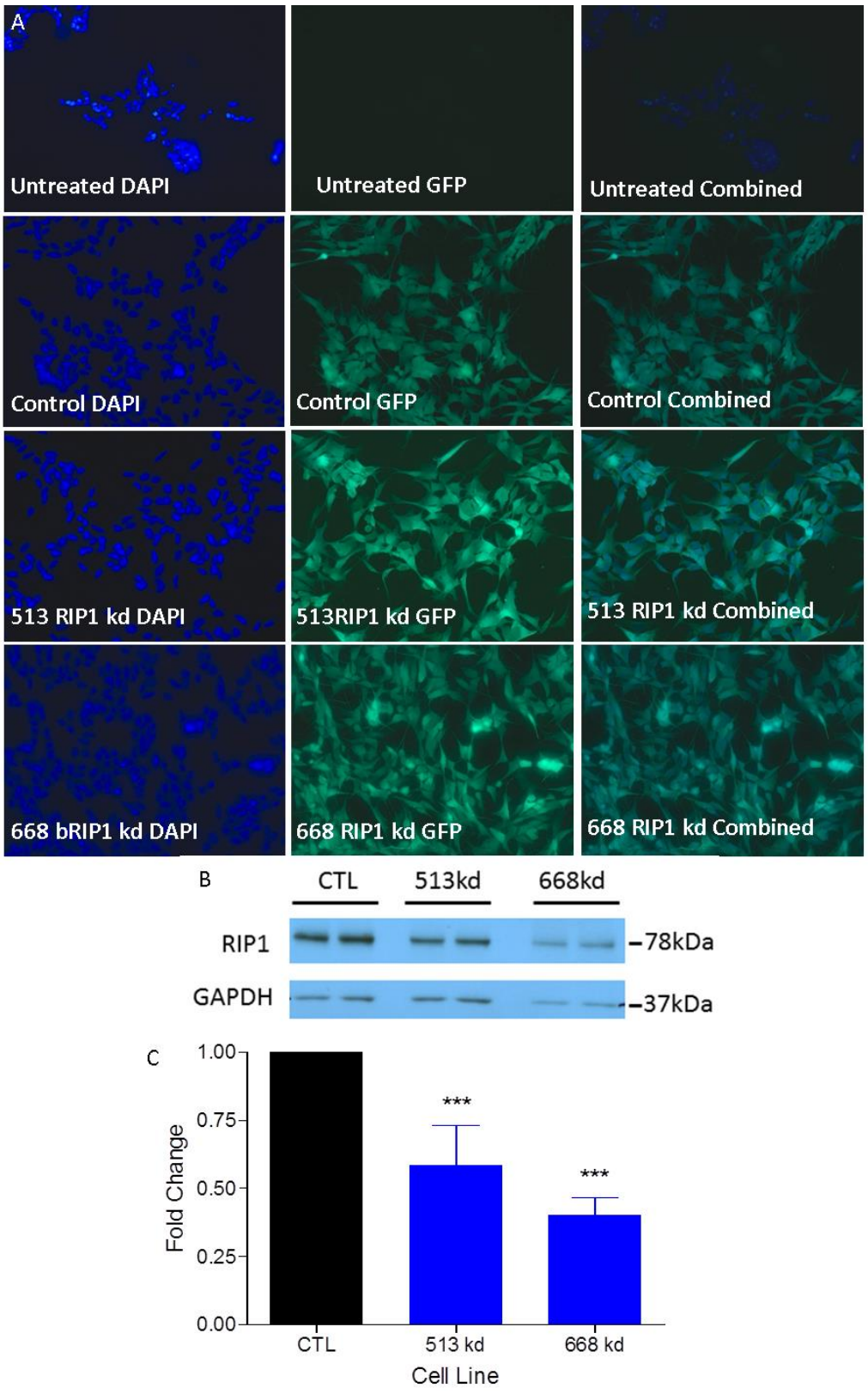

Fig. 3.15 Transfection efficiency and knockdown levels of lentiviral RIP1 knockdown in SH-SY5Y SH-SY5Y cells were untreated or treated with control (CTL) or RIP1 clone 513 or 668 knockdown lentivirus expressing GFP. (A) Images show DAPI stained cell nuclei, GFP expression & DAPI & GFP overlaid (x 40 magnification). (B & C) Protein samples isolated from cells were probed for RIP1. (B) Image is representative blot from CTL and 513 & 668 clone knockdown (kd) cells. (C) Protein intensity in untreated and knockdown cells relative to GAPDH. Data presented as fold-untreated + SD from duplicate assays (n=3). *** P<0.001, when compared to untreated, independent samples t-test

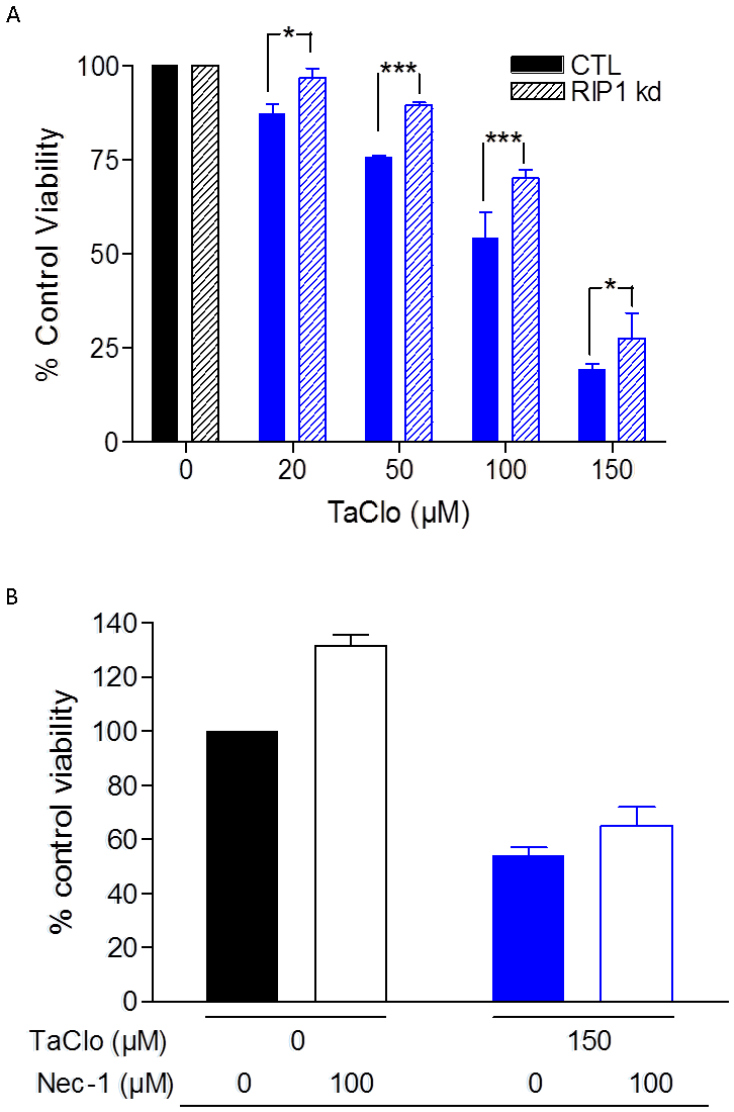

Fig. 3.16 Effect of RIP1 knockdown on TaClo toxicity and Nec-1 efficiency in SH-SY5Y (A) SH-SY5Y cells were transfected with either control (CTL) or RIP1 knockdown lentiviruses and then treated with TaClo (20-150μM) for 21 hours and viability measured by reduction of Alamar Blue (resazurin). Data presented as mean % control + SD from triplicate assays (n=3). Significant effect of RIP1 knockdown on TaClo toxicity ($P<0.001$), ***$P<0.001$, *$P<0.05$ when compared to CTL, Bonferroni post-test. (B) RIP1 knockdown SH-SY5Y cells were pre-treated with Nec-1 (100μM) for 1 hour and then co-treated with TaClo (150μM) for 21 hours and viability measured by reduction of Alamar Blue (resazurin). Data presented as mean % control ± SD from triplicate assays (n=3). Significant effect of Nec-1 on TaClo treatment, $P<0.01$, Two-way ANOVA.

As complete RIP1 knockdown was not achieved in SH-SY5Y by shRNA treatment, RIP1 knockout MEFs were generated from RIP1 $^{-/-}$ C57BL/6 mice in the lab of Liu, Z.G. (NIH National Cancer Institute, Bethesda, US) and obtained to further explore the involvement of RIP1 in TaClo toxicity. RIP1 knockdown in RIP1 $^{-/-}$ MEFs was confirmed by Western blot (Hur, Lewis et al. 2003) (Fig. 3.17 A). Wild-type and RIP1 knockout MEF cells were treated with various concentrations of TaClo (100-500µM) and assessed for toxicity at 21 hours. Viability was assessed by the Alamar Blue and confirmed by visual inspection. RIP1 knockout conferred significant protection against TaClo toxicity when compared to wild-type MEFs ($P<0.001$, Two-way ANOVA) with significant protection of MEFs seen at doses of 200 & 300µM TaClo ($P<0.001$, $P<0.01$, respectively, Bonfferoni post-test) supporting the evidence that TaClo treatment leads to SH-SY5Y cell death via necroptosis (Fig. 3.17 B). These findings were supported by visual inspection of the cells under magnification showing a similar percentage of cells losing standard morphology as shown by the Alamar Blue test at the same concentrations.

To investigate whether the protection mediated by Nec-1 in SH-SY5Y cells seen above was mediated by effects on RIP1, RIP1 $^{-/-}$ MEF cells were treated with toxic doses of TaClo and Nec-1. There was no significant effect of Nec-1 on TaClo toxicity in RIP1 $^{-/-}$ MEFs (Two-way ANOVA) nor any increase in metabolism in the vehicle treated group seen in SH-SY5Y cells (Fig. 3.17 C), suggesting that the protection conferred on TaClo treated SH-SY5Y cells was RIP1 dependent. Rip1 $^{-/-}$ MEF cells were also treated with toxic doses of TaClo and the pan-caspase inhibitor zVAD.fmk, to investigate if the cells were dying by apoptosis. No significant effect of zVAD.fmk was observed in TaClo exposed RIP1 $^{-/-}$ MEFs (Fig. 3.17 C), suggesting that apoptosis was not involved in the toxic mechanism of TaClo. Finally, Rip1 $^{-/-}$ MEF cells were treated with toxic doses of TaClo and the antioxidant NAC, to investigate the effect of oxidative stress on TaClo toxicity. NAC significantly attenuated TaClo toxicity in RIP1 $^{-/-}$ MEFs (Fig. 3.17 C), suggesting that oxidative stress contributes to the toxic mechanism of TaClo.

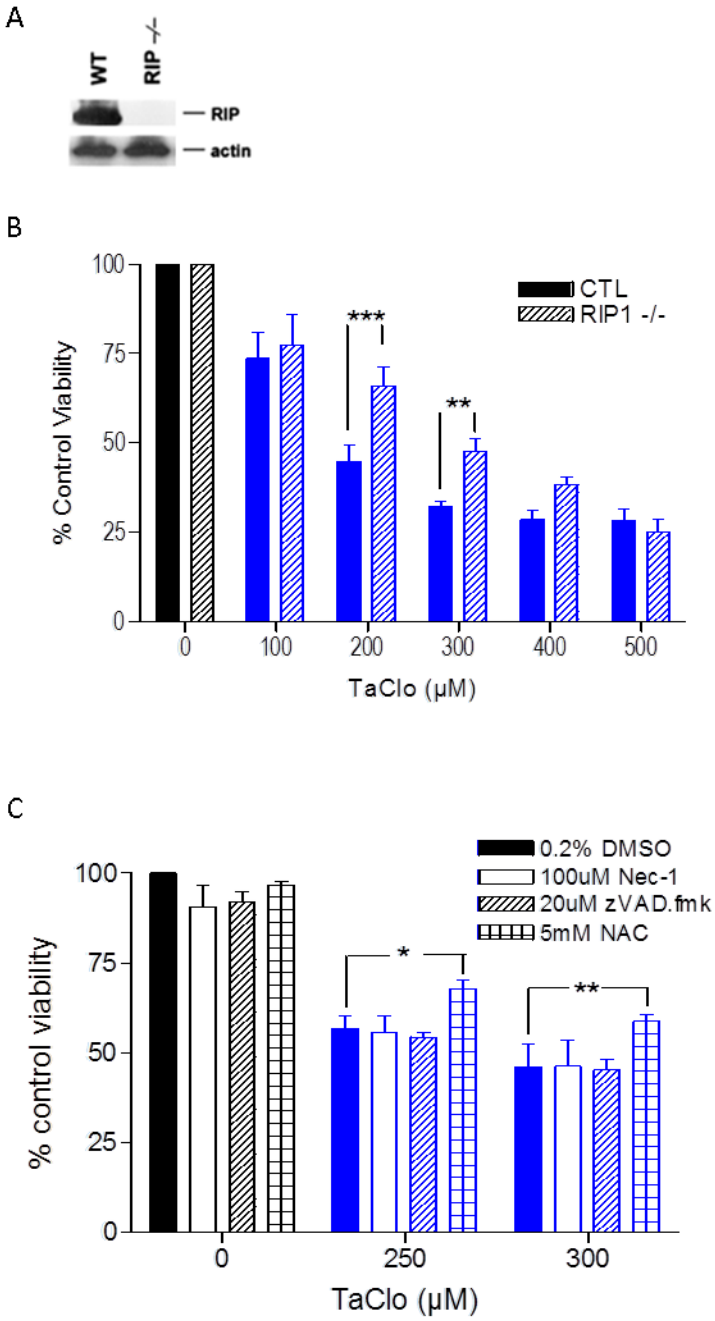

Fig. 3.17 TaClo toxicity in wild-type & RIP1 $^{-/-}$ MEFs and the effect of RIP1 knockout on the effect of Necrostatin-1, zVAD.fmk & NAC on TaClo toxicity (A) RIP1 knockdown levels as assessed by Western blot in wild type (WT) and RIP $^{-/-}$ MEFS. Adapted from (Hur, Lewis et al. 2003). (B) Wild-type & RIP1 $^{-/-}$ MEF cells were treated with various concentrations of TaClo for 21 hours and viability measured by reduction of Alamar Blue (resazurin). Data presented as mean % control ± SD from triplicate assays (n=3). Significant effect of RIP1 knockdown on TaClo toxicity (P<0.001), ***P<0.001, **P<0.01 when compared to CTL, Bonferroni post-test. (C) RIP1 $^{-/-}$ MEF cells were pre-treated with Nec-1 (100µM), zVAD.fmk (20µM) or NAC (5mM) for 1 hour and then co-treated with TaClo (300 & 250µM) for 21 hours and viability measured by reduction of Alamar Blue (resazurin). Data presented as mean % control ± SD from quadruplicate assays (n=3). Significant effect of NAC on TaClo toxicity (P<0.01), no significant effect of Nec-1 or zVAD.fmk on TaClo treatment, Two-way ANOVA. **P<0.01, *P<0.05 when compared to CTL, Bonferroni post-test

3.3.3.1 Analysis of Cell Death Mechanism by Flow Cytometry

Propidium Iodide (PI) is a red fluorescent dye that can be used to assess cell membrane integrity. PI fluorescence increases exponentially when it is bound to nucleic acids compared to when it is not, and binds DNA by intercalating between bases (Tas and Westerneng 1981). The intact membrane of a healthy cell is impermeable to PI but it can enter cells when the membrane is damaged, such as during necrosis. It is then able to come into contact with DNA resulting in an increase in fluorescent signal.

Hoechst 33342(Hoechst) is a blue fluorescent DNA binding dye that fluoresces more brightly when bound to the condensed form of chromatin found in apoptotic cells, but not when bound to chromatin in healthy cells (Ellwart and Dormer 1990).

The properties of these two dyes allow the differentiation of cell death phenotype between necrotic and apoptotic when cells are double stained with PI and Hoechst and sorted by flow cytometry based on the knowledge that necrotic cells have damage cell membranes but no chromatin condensation and early apoptotic cells have chromatin condensation but intact cell membranes (Belloc, Dumain et al. 1994). Staurosprine, a compound known to induce apoptosis in SH-SY5Y (Boix, Llecha et al. 1997), was used as a positive control for apoptosis in the assay.

The population of whole single cells was selected using a plot of forward scatter (FSC-A), which measures cell size, against side scatter (SSC-A), which measures cell shape or granularity, (Fig. 3.18 A) and fluorescence levels for Hoechst 33342 and PI measured in this population. Fig. 3.18 B shows the average number of total events that were included in the whole single cell population. The number of events defined as whole single cells significantly decreases over time ($P<0.001$, Two-way ANOVA). In the 100µM TaClo treated samples, there are significantly fewer whole single cells than in the 0.2% DMSO sample at 16 & 24 hours post treatment ($P<0.05$, $P<0.001$, respectively, Bonferroni post-test). 150µM TaClo treated samples showed significantly reduced levels of whole single cells at 12, 16 & 24 hours post treatment when compared to 0.2% DMSO ($P<0.01$, $P<0.001$, $P<0.001$, respectively, Bonferroni post-test). 500nM Staurosporine treated samples had significantly fewer whole single cells than 0.2& DMSO at 8-24 hours post treatment (all $P<0.001$. Bonferroni post-test). This corresponds with a decrease in viability observed by visual inspection of the samples before processing for flow cytometry.

Gates were defined based on Hoechst and PI fluorescence and defined as healthy (low Hoechst/low PI) apoptotic (high Hoechst/low PI), necrotic (low Hoechst/high PI) and late stage death (high Hoechst/high PI). Healthy gate was set to contain approximately 90-95% of cells for 0.2% DMSO & 0h samples (limits 89.3-96.9%) and quadrants kept consistent within experiments.

Treated cells showed a significant effect of treatment over time in cells defined as healthy, necrotic, late stage death ($P<0.001$, Two-way ANOVA) and apoptotic ($P<0.05$, Two-way ANOVA). In individual populations, the healthy population showed no significant change when treated with 0.2% DMSO, but showed a significant reduction from 12 hours following 100µM TaClo treatment ($P<0.05$) and 8 hours following 150µM TaClo and following 500nM Staurosporine treatment ($P<0.001$, all Bonferroni post-test) (Fig 3.26 A-D & 3.27). The late stage death population also showed no significant change when treated with 0.2% DMSO, but showed a significant increase at 24 hours following 100µM TaClo treatment and from 12 hours following 150µM TaClo ($P<0.05$) and from 8 hours post 500nM Staurosporine treatment ($P<0.001$, all Bonferroni post-test) (Fig 3.19 A-D & 3.20).

When looking at specific death mechanisms, the apoptotic population showed no significant change when treated with 0.2% DMSO, 100 or 150µM TaClo but showed a significant increase at 4-12 hours following 500nM Staurosporine treatment ($P<0.001$, Bonferroni post-test) but no significant change 16 & 24 hours post 500nM Staurosprorine (Fig 3.19 A-D & 3.20). This reduction in apoptotic death following longer Staurosporine treatment is probably due to the almost complete lack of viable cells seen at these times with this treatment.

The necrotic population, however, showed no significant change when treated with 0.2% DMSO or 500nM Staurosporine but showed a significant increase from 12 hours following 100µM TaClo treatment ($P<0.05$) and from 8 hours following 150µM TaClo ($P<0.001$, both Bonferroni post-test) (Fig 3.19 A-D & 3.20).

This evidence suggests that TaClo causes SH-SY5Y cytotoxicity by a death mechanism involving membrane breakdown such as necrosis, unlike Staurosporine, a known apoptotic inducer, which leads to a form of cell death involving chromatin condensation such as apoptosis.

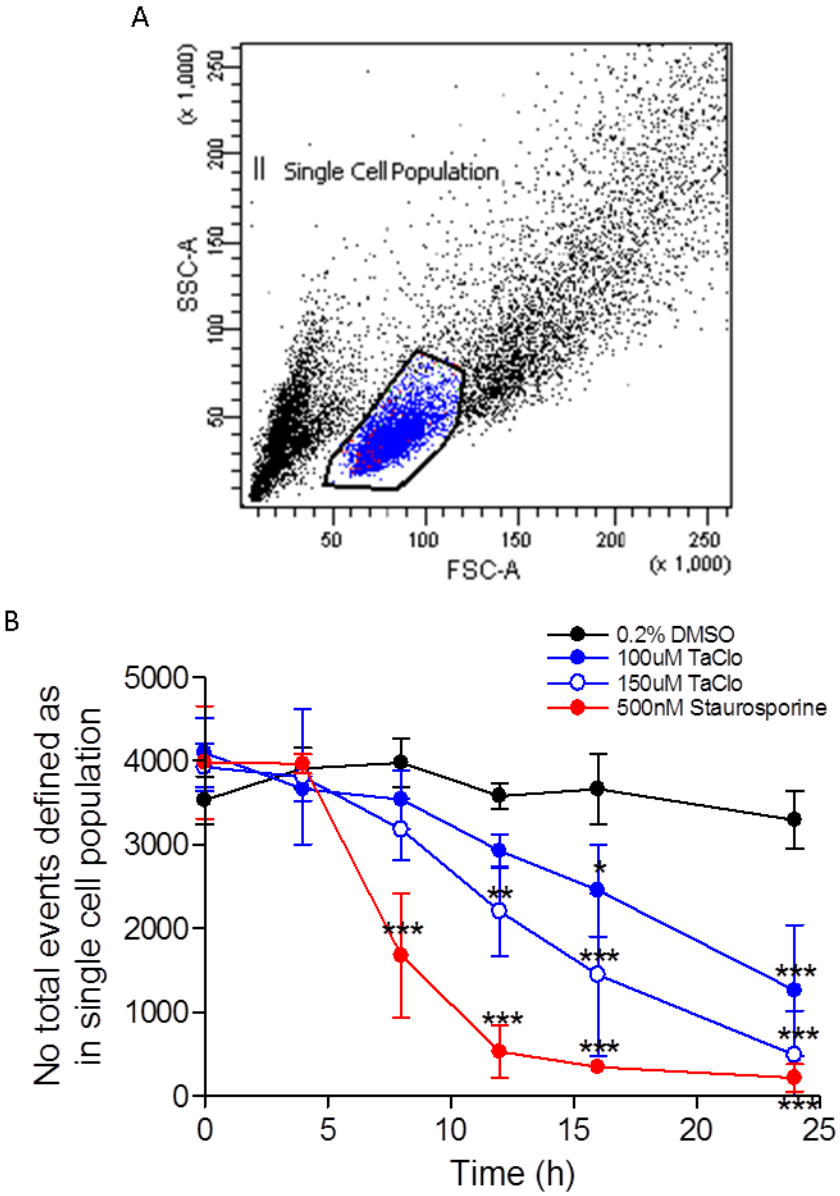

Fig. 3.18 Population definition for flow cytometric analysis of cell death phenotype ¶ SH-SY5Y were treated with 0.2% DMSO, 100µM TaClo, 150µM TaClo or 500nM Staurosporine for 0-24 hours and stained with Hoescht3342 and PI before fluorescence was assessed using flow cytometry (A) Representative density plot showing selection of whole single cells based on SSC-A and FSC-A (B) Average no. total events defined as in single cell population (n=3). Significant effect of TaClo & Staurosporine on single cell population over time (P<0.001, Two-way ANOVA), ***P<0.001, **P<0.01, *P<0.001, Bonferroni post-test.

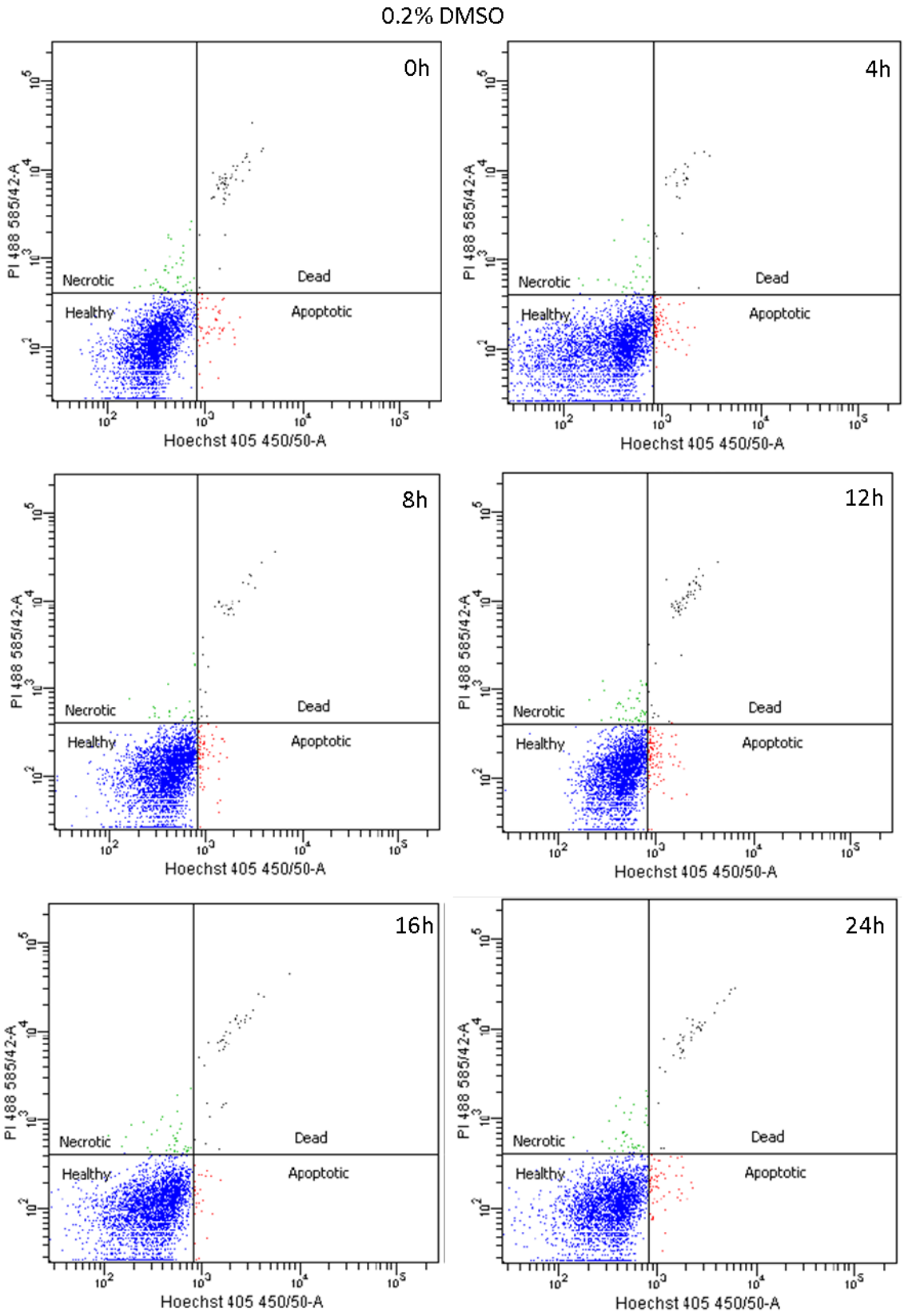

Fig. 3.19 Flow cytometric analysis for cell death phenotype¶ SH-SY5Y cells were treated with 0.2% DMSO, 100µM TaClo, 150µM TaClo or 500nM Staurosporine for 0, 4, 8, 12, 16 or 24 hours and stained with Hoescht3342 and PI before fluorescence was assessed using flow cytometry. Whole Cell populations were defined as healthy (blue), apoptotic (red), necrotic (green) or dead (black) dependent on relative Hoescht3342 or PI staining. Example FACS dot plots shown.

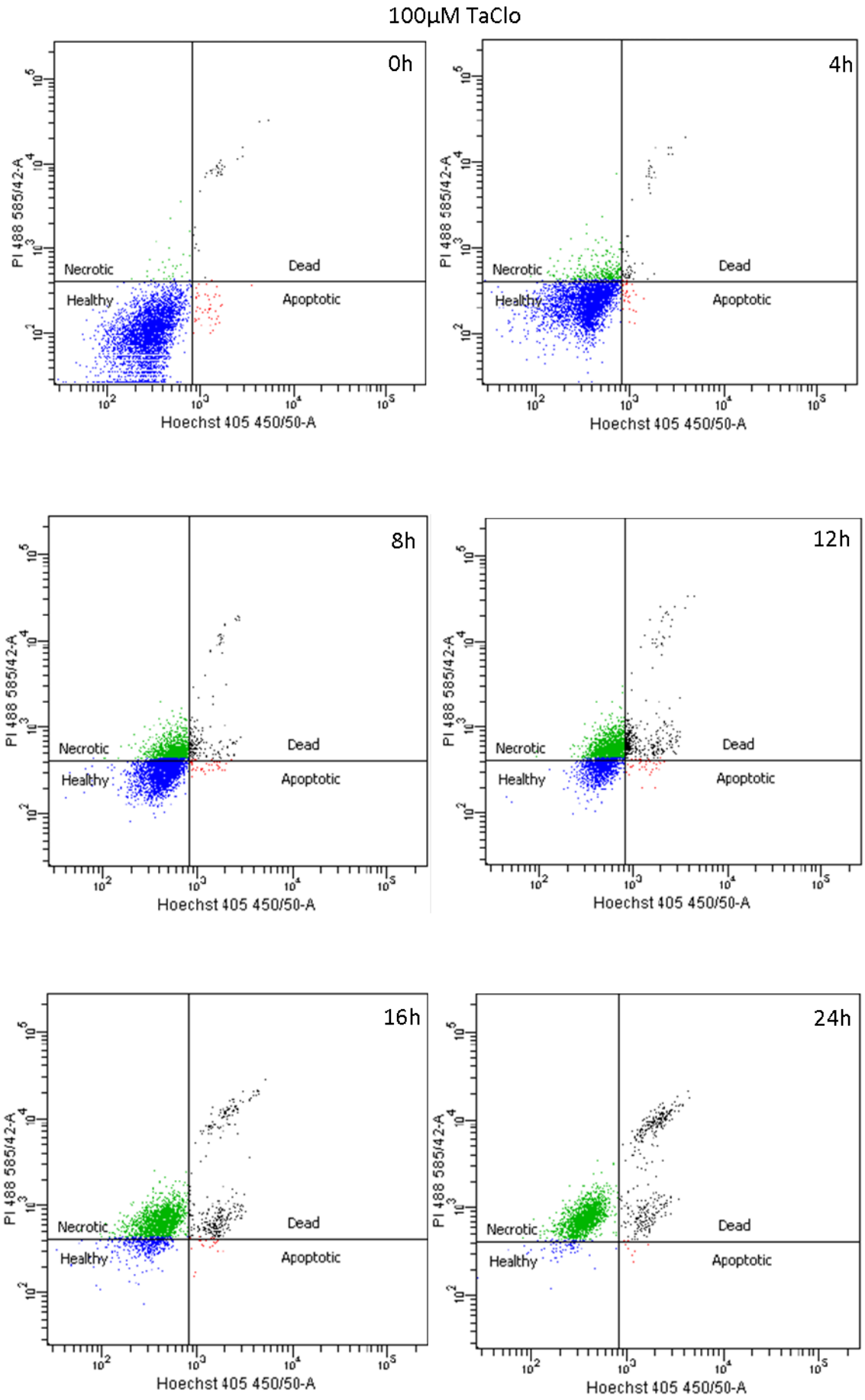

Fig. 3.19 Flow cytometric analysis for cell death phenotype (cont.)

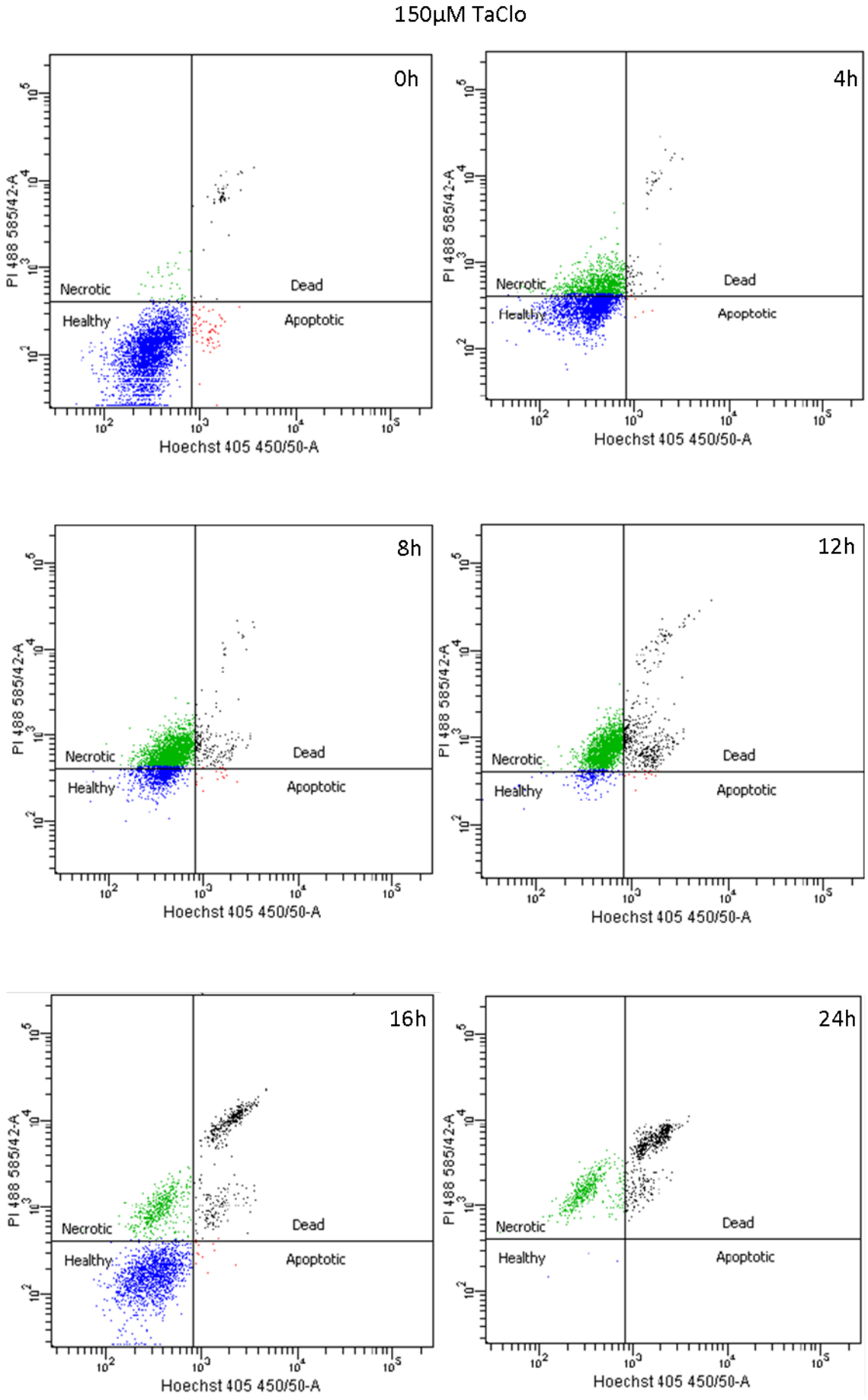

Fig. 3.19 Flow cytometric analysis for cell death phenotype (cont.)

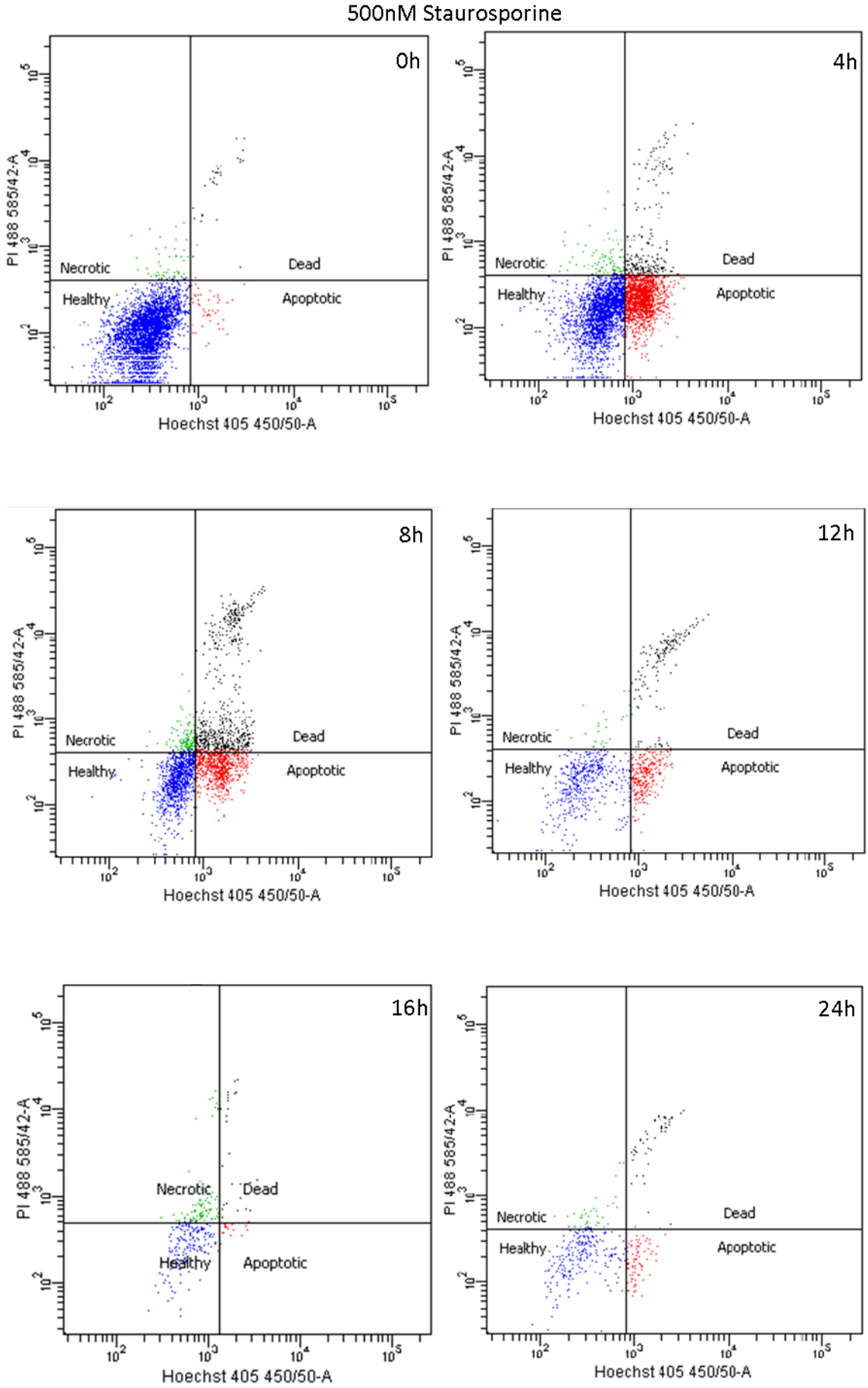

Fig. 3.19 Flow cytometric analysis for cell death phenotype (cont.)

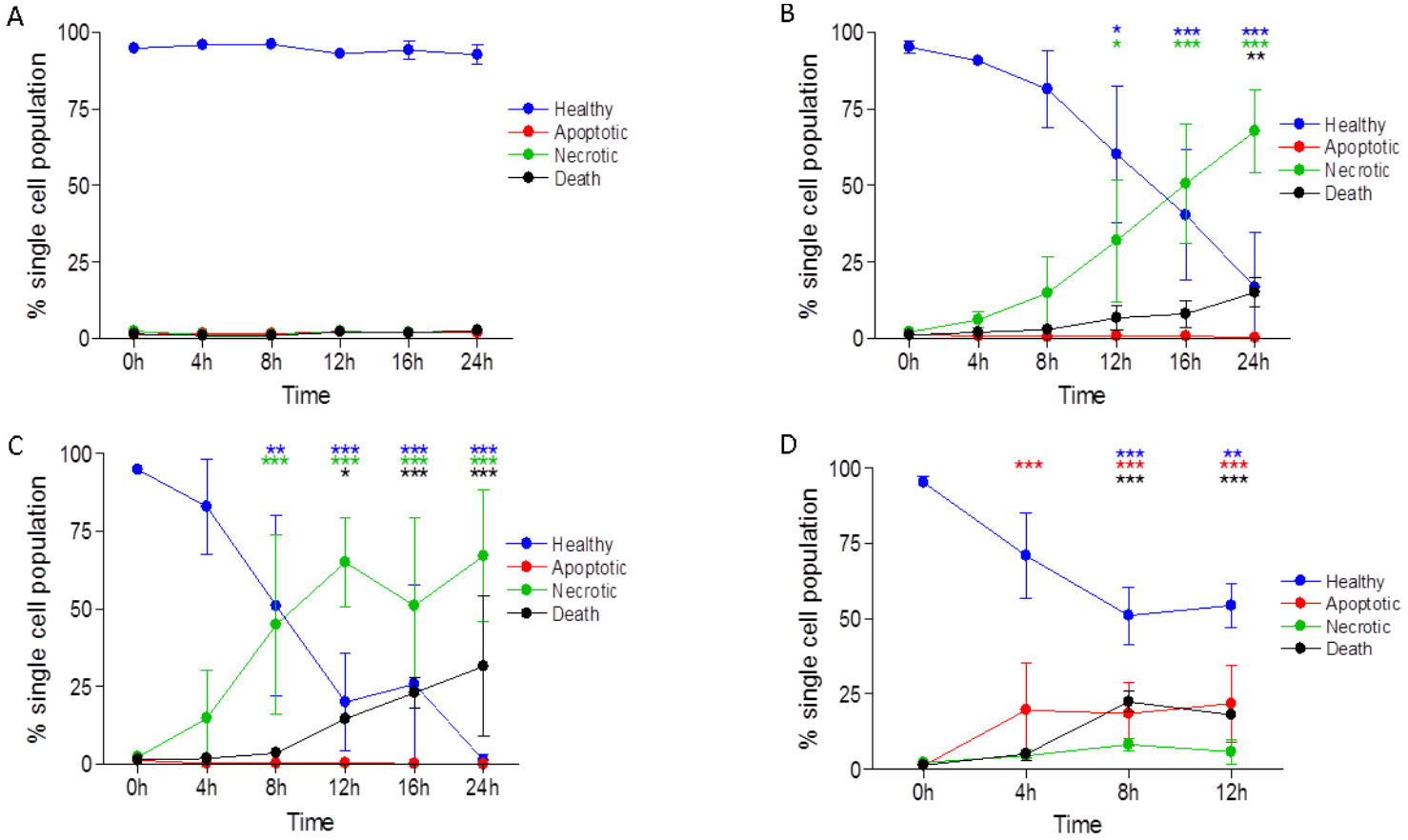

Fig. 3.20 Effect of TaClo treatment on cell phenotype following TaClo & Staurosporine treatment as quantified by flow cytometry SH-SY5Y were treated with (A) 0.2% DMSO, (B) 100µM TaClo, (C) 150µM TaClo or (D) 500nM Staurosporine for 0-24 hours and then loaded with 5µg/ml Hoescht 3342 and 1µg/ml PI before fluorescence was assessed using flow cytometry. % Cells were defined as healthy, apoptotic, necrotic or late cell death dependent on relative Hoescht3342 or PI staining over time following treatment. Data presented as mean + SD (n=3). (A) No significant effect of 0.2 % DMSO on phenotype over time, (B-D) Significant effect of 100 & 150µM TaClo and 500nM Staurosporine treatment on phenotype over time, all P<0.001, Two-way ANOVA. ***P<0.001, **P<0.01, *P<0.05 when compared to 0 hour time point, Bonferroni post-test.

3.3.4 Involvement of Autophagy in TaClo Toxicity

Autophagy is a regulated cellular process that serves to ensure degradation of damaged or un-needed cellular components using the lysosomal machinery and allows for efficient synthesis and recycling of these molecules. However, disruption of normal autophagic function, when un-regulated or overwhelmed, can lead to excessive degradation of cellular contents or insufficient clearance of toxic protein accumulations and eventually cell death. Further detail on autophagy can be found in section 1.3.3 above. The effects of TaClo treatment on autophagy were examined, as dysfunction in this system and misfolded protein build-up have been previously linked with neurodegenerative conditions, in particular PD (Banerjee, Beal et al. 2010).

Rapamycin is a bacterial product that can inhibit mTOR by forming a complex with the intracellular receptor of mTOR immunophilin 12-kDa FK506-binding protein (FKPB12) (Augustine, Bodziak et al. 2007). This inhibition of mTOR induces autophagy in the cells as under normal cellular conditions, mTOR inhibits autophagy (Blommaart, Luiken et al. 1995). SH-SY5Y cells were co-treated with TaClo and Rapamycin to investigate whether this pathway was involved in TaClo mediated SH-SY5Y toxicity. Rapamycin ($P<0.05$, Two-way ANOVA) significantly increased TaClo mediated toxicity in SH-SY5Y cells in a dose dependent manner (Fig. 3.21).

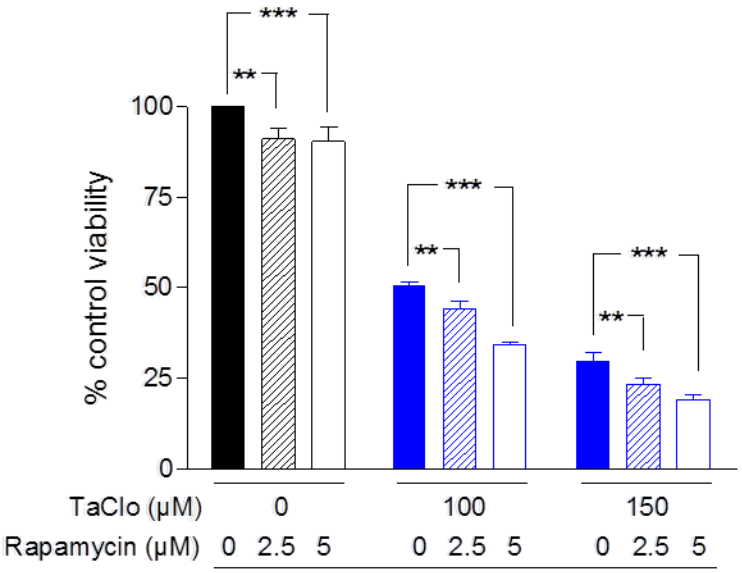

Fig. 3.21 Effect of Rapamycin on TaClo toxicity in SH-SY5Y SH-SY5Y cells were pre-treated with Rapamycin (2.5 & 5µM) for 1 hour and then co-treated with TaClo (100 & 150µM) for 21 hours and viability measured by reduction of Alamar Blue (resazurin). Data presented as mean % control ± SD from quadruplicate assays (n=3). Significant effect of rapamycin on TaClo toxicity ($P<0.05$), Two-way ANOVA. ***$P<0.001$, **$P<0.01$ when compared to 0.2% DMSO, Bonferroni post-test

3.3.4.1 Effect of TaClo Treatment on LC3-B

Microtubule-associated protein1 light chain 3 (LC3) is a homologue of APG8P, which is essential for autophagy in yeast (Liang, Jackson et al. 1999) and present in two forms LC3-A and LC3-B. A fraction of LC3-A is converted to LC3-B which forms an integral part of the autophagosome membranes and, therefore, levels of LC3-B in the cell directly correlate with the extent of autophagosome formation (Kabeya, Mizushima et al. 2000).

Protein isolated from SH-SY5Ys treated with TaClo over various time points was probed for LC3-B levels by Western blot. TaClo treatment significantly increased LC3-B expression in a time dependent manner ($P<0.05$, One-way ANOVA) with expression significantly higher at 8 and 24 hours post treatment when compared to pre-treatment levels ($P<0.05$, Dunnett's t-test) (Fig. 3.22).

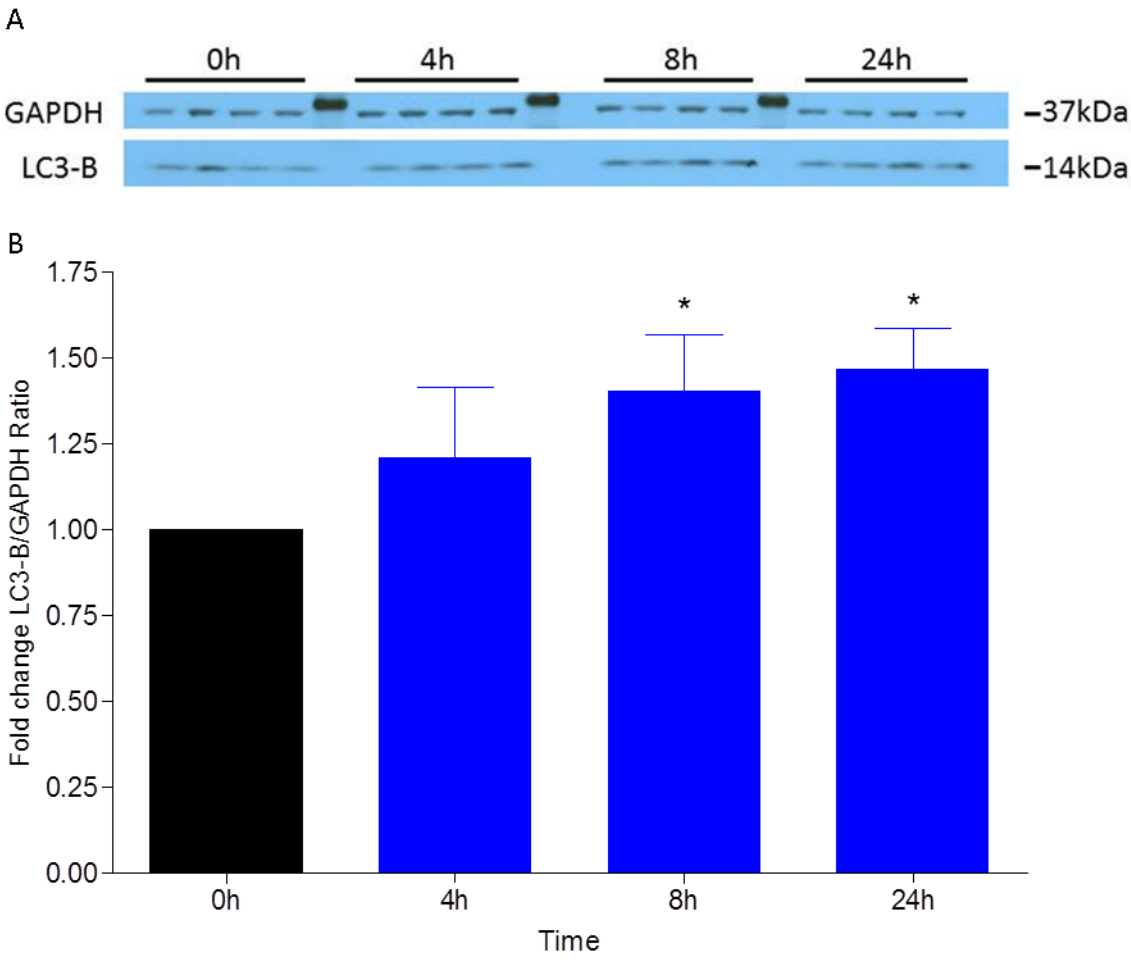

Fig. 3.22 Expression of LC3-B in 100µM TaClo treated SY-SY5Y SH-SY5Y cells were treated with 100µM TaClo for 0, 4, 8 or 24 hours and protein harvested. Samples were probed for LC3-B. (A) Image is representative blot of LC3-B and GAPDH control (B) LC3-B intensity relative to GAPDH. Data presented as fold-untreated ± SD from quadruplicate assays (n=3). * $P<0.05$, when compared to 0h, One-way ANOVA & Dunnett's post-test

3.3.4.2 Involvement of Lysosomes in TaClo Toxicity

Lysosomes are membrane bound organelles containing a range of enzymes capable of degrading cellular contents which are responsible for the degradation of material sequestered during autophagy by fusing with autophagosomes (Klionsky 2007).

Bafilomycin A1 is antibiotic that had been shown to strongly inhibit the vacuolar H(+)-ATPase and so the acidification and protein degradation in lysosomes (Yoshimori, Yamamoto et al. 1991). SH-SY5Y cells were co-treated with Bafilomycin A1 and TaClo and viability assessed by Alamar Blue assay and confirmed by visual inspection. Bafilomycin A1 treatment significantly increased TaClo toxicity ($P<0.05$, Two-way ANOVA) (Fig.3.23), suggesting that functioning lysosomes may provide protection against a TaClo induced toxic insult as part of the autophagic machinery.

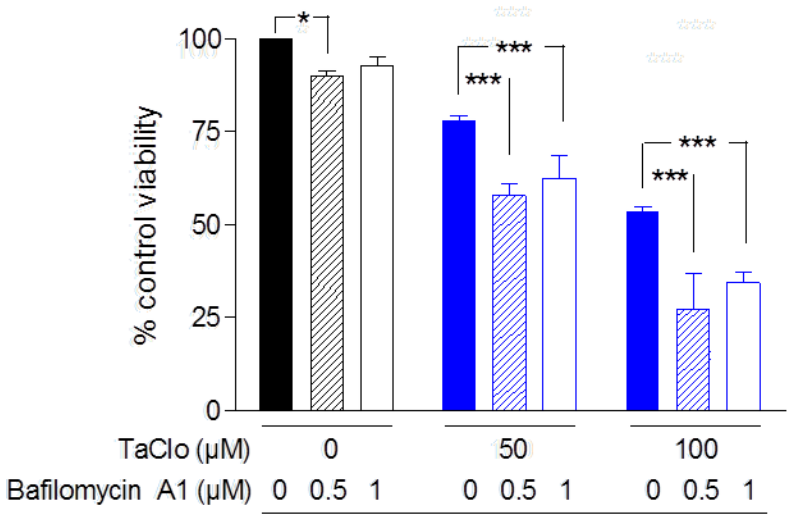

Fig. 3.23 Effect of Bafilomycin A1 on TaClo toxicity in SH-SY5Y SH-SY5Y cells were pre-treated with Bafilomycin A1 (500nM & 1µM) for 1 hour and then co-treated with TaClo (100 & 150µM) for 21 hours and viability measured by reduction of Alamar Blue (resazurin). Data presented as mean % control ± SD from quadruplicate assays (n=3). Significant effect of Bafilomycin A1 on TaClo toxicity ($P<0.05$), Two-way ANOVA. ***$P<0.001$, *$P<0.05$ when compared to 0.2% DMSO, Bonferroni post-test

SH-SY5Y cells were assessed for levels of lysosome formation at various time points following TaClo treatment using Lysotracker™ Red and quantified by flow cytometry. Lysotracker™ Red is an acidotropic probe for labelling and tracking acidic organelles such as lysosomes in live cells (Alberts, Johnson et al. 1994). It consists of a fluorophore linked to a weak base that is only partially protonated at neutral pH; it is freely permeant to cell membranes and typically concentrates in spherical organelles. Its mechanism of retention has not been firmly established but is likely to involve protonation and retention in the membranes of the organelles.

The population of whole single cells was selected using a plot of FSC-A, which measures cell size, against SSC-A, which measures cell shape or granularity, (Fig. 3.24 A) and fluorescence levels measured in this population. Gates were set for high and low fluorescence based upon 95% of control cells being in the low fluorescing population (Fig. 3.24 C). A time and dose-dependent increase in fluorescence was observed in both 100 & 150µM treated SH-SY5Y cells relative to control (Fig. 3.24 B) ($P<0.001$, Two-way ANOVA), with cells seeming to show more lysosome formation after 8 hours and a significant increase in the number of cells (61%) showing high fluorescence in 150µM treated cells at 8 ($P<0.01$) hours post treatment and almost all the cells present in the high fluorescing population by 16 hours ($P<0.001$) (Fig. 3.24 B). In the 100µM treated cells, lysosome formation was slower, with a significant increase also occurring by 16 hours ($P<0.001$) hours in 44% of cells and almost all cells showing high fluorescence by 24 hours ($P<0.001$) (Fig. 3.24 B). These results suggest that lysosome formation is increased as a relatively early event in TaClo mediated SH-SY5Y toxicity.

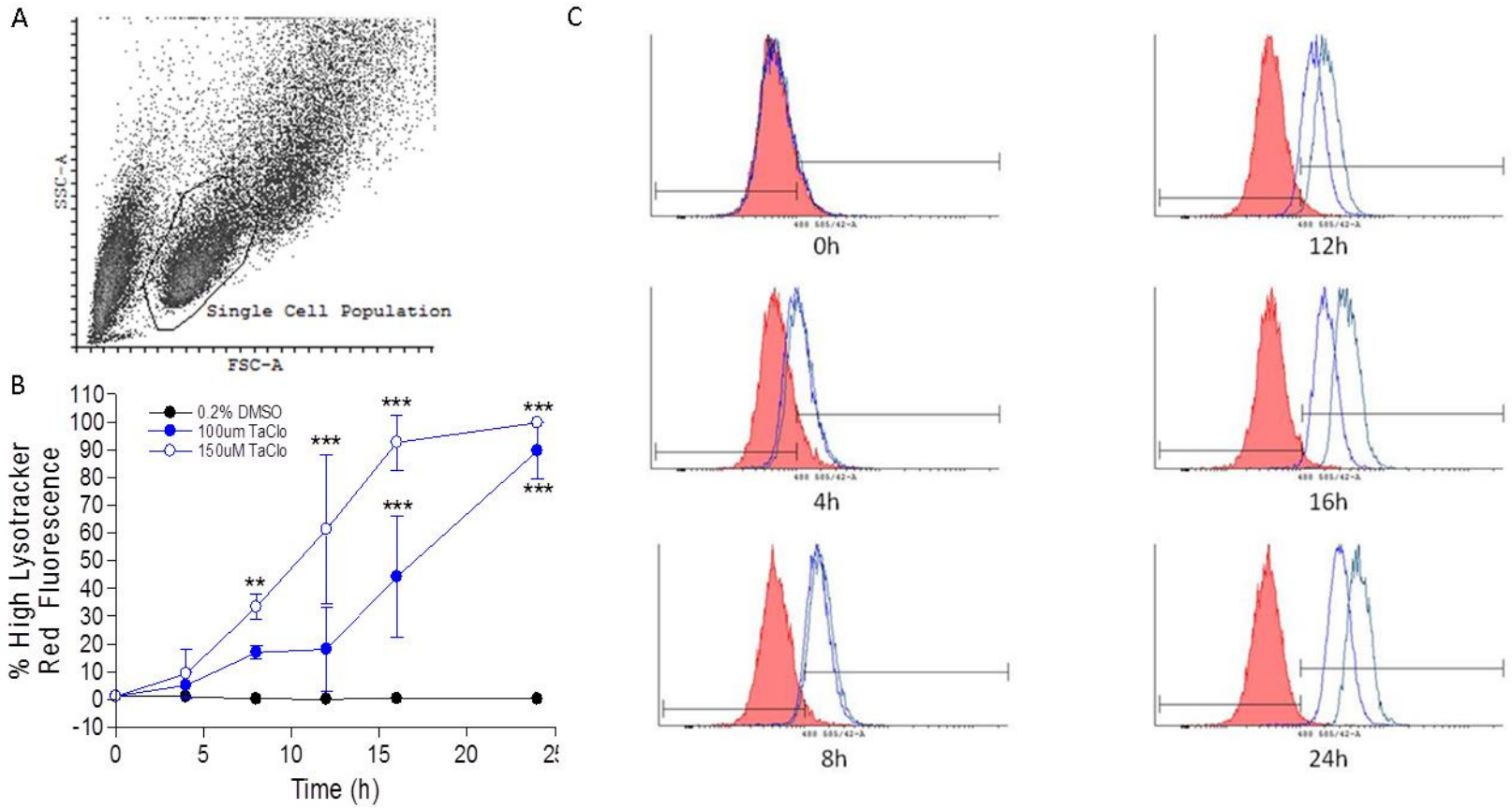

Fig. 3.24 Effect of TaClo treatment on Lysotracker fluorescence in SH-SY5Y as quantified by flow cytometry SH-SY5Y were treated with 0.2% DMSO, 100 or 150µM TaClo for 0-24 hours and then loaded with 50nM lysotracker before fluorescence was assessed using flow cytometry. (A) Representative density plot showing selection of whole single cells based on SSC-A and FSC-A. (B) % Cells defined as having high fluorescence over time following treatment. Data presented as mean + SD (n=3). Significant effect of Taclo treatment on fluorescence over time (P<0.001), Two-way ANOVA. ***P<0.001, **P<0.01 when compared to 0.2% DMOS at same time point, Bonferroni post-test. (C) Representative overlaid histograms of log selected single cell fluorescence at ex/em 488/585 at all timepoints. Bars show defined low and high fluorescing population boundaries.

3.3.4.3 Effect of TaClo Treatment on Aggresome Formation

Aggresomes are inclusion bodies that form when the ubiquitin–proteasome machinery is overwhelmed with aggregation-prone proteins (Amijee, Madine et al. 2009), typically formed in response to cellular stress such as exposure to reactive oxygen species. They appear to have a cytoprotective effect by sequestering toxic misfolded protein into aggregates during oxidative stress, for example LBs that are found in PD brains.

SH-SY5Y were treated with 0.2% DMSO, 100 or 150µM TaClo or H_2O_2 as a positive control for 0-24 hours and then fixed and stained for aggresomes with a red fluorescent molecular rotor dye to specifically detect denatured protein cargo within aggresomes and aggresome-like inclusion bodies in fixed and permeabilised cells.

TaClo treated cells showed an increase in aggresome number and size (examples highlighted by the green arrows in Fig. 3.25) when compared to control in a time and dose dependent manner in 100 & 150µM TaClo, as well as H_2O_2 positive control treated cells (Fig. 3.25). Manual quantification of number of aggresomes per cell confirmed this with a significant increase in number of aggresomes per cell with treatment over time seen ($P<0.001$, Two-way ANOVA) and 100 & 150µM TaClo and H_2O_2 and showing a significant increase when compared to 0.2% DMSO from 24 ($P<0.01$), 12 ($P<0.01$) and 4 ($P<0.01$) hours post treatment respectively (Bonferroni Post test) (Fig. 3.26).

Fig. 3.25 Aggresome formation in TaClo treated SH-SY5Y SH-SY5Y cells were treated with for 0, 4, 8, 12 or 24 hours and then stained with DAPI and an aggresome dye. Images show cells treated with 0.2% DMSO, 100µM TaClo, 150µM TaClo or 850µM H2O2 overlaid Hoechst 33342 and aggresome detector images (x 40 magnification). Aggresomes show as bright red foci (examples highlighted by green arrows).

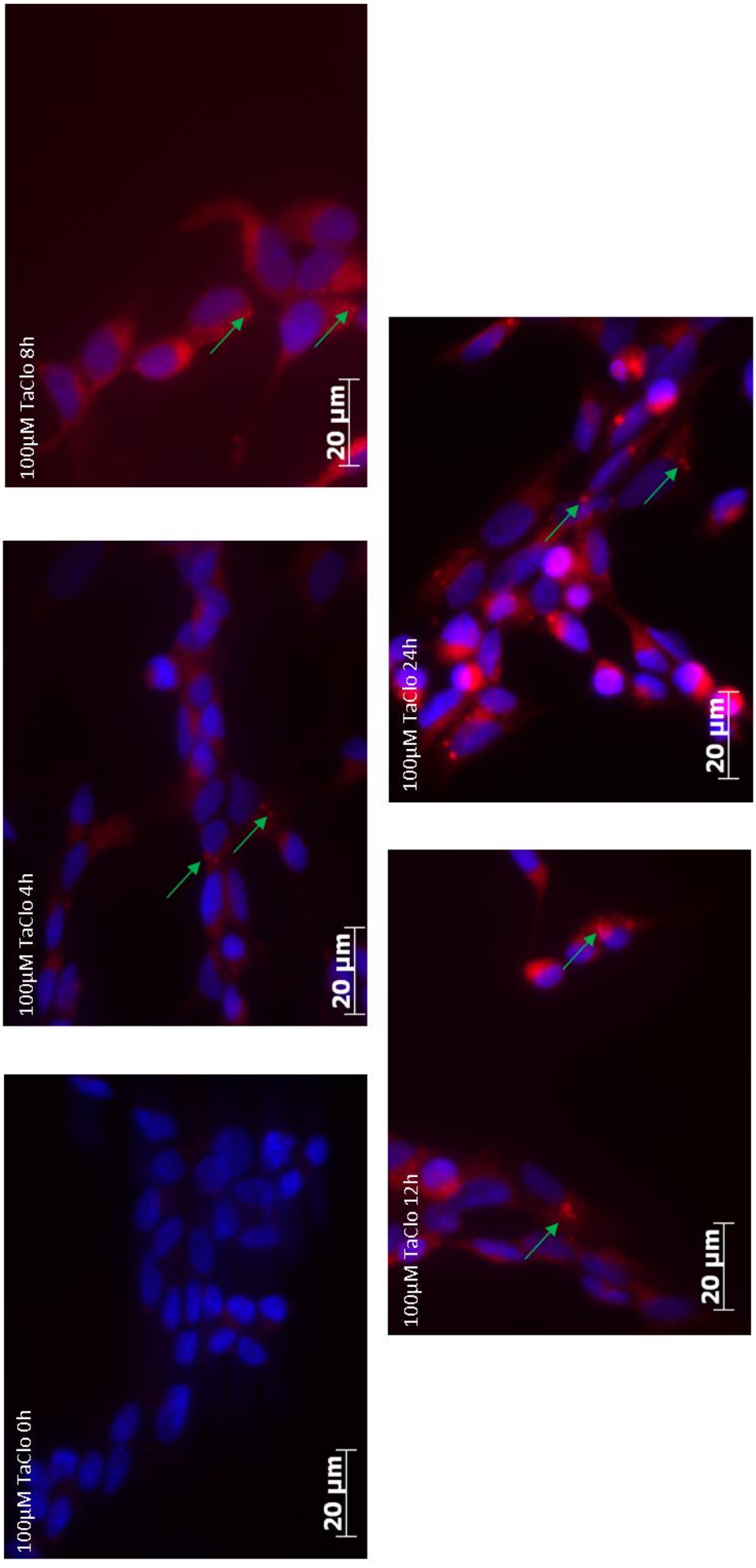

Fig. 3.25 Aggresome formation in TaClo treated SH-SY5Y (cont.)

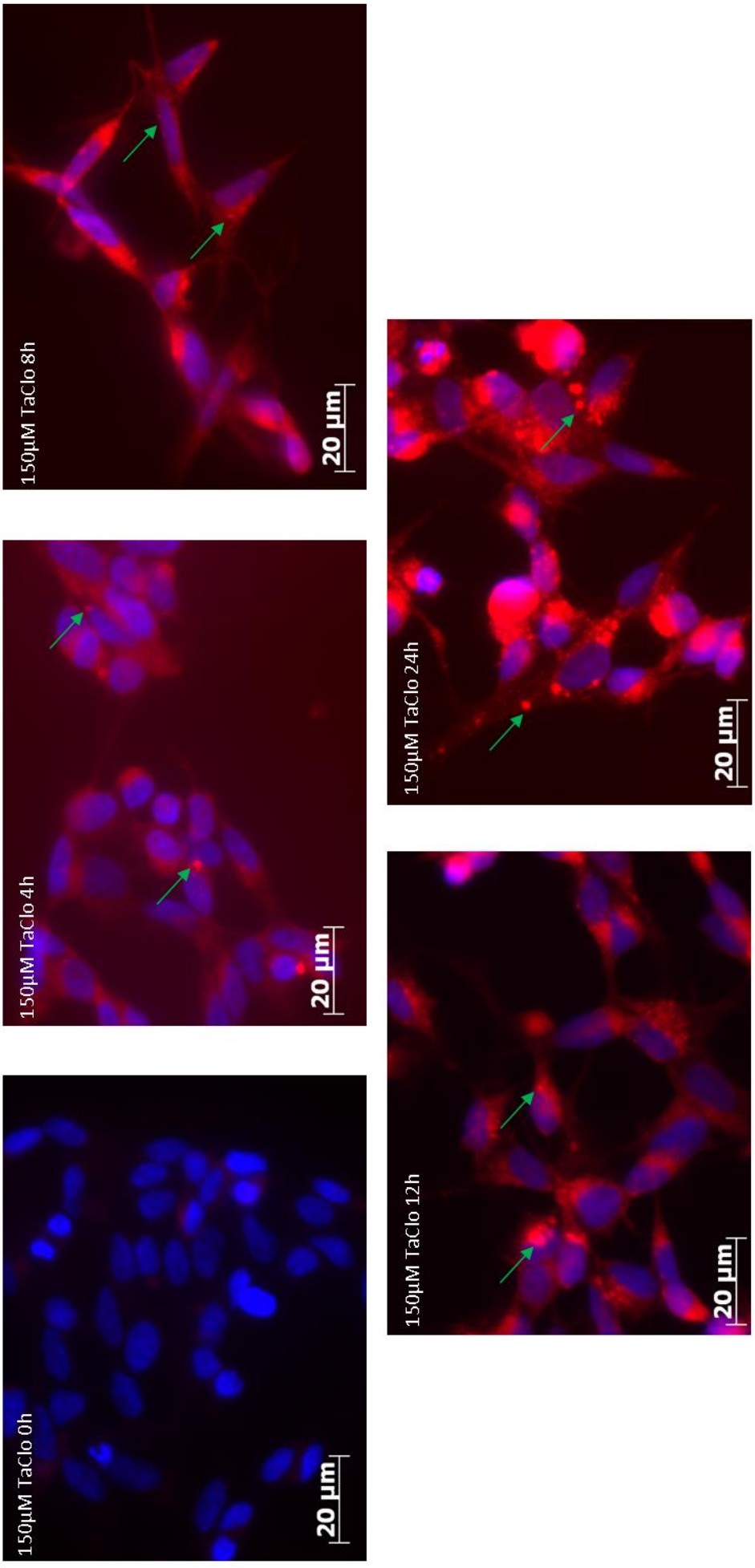

Fig. 3.25 Aggresome formation in TaClo treated SH-SY5Y (cont.)

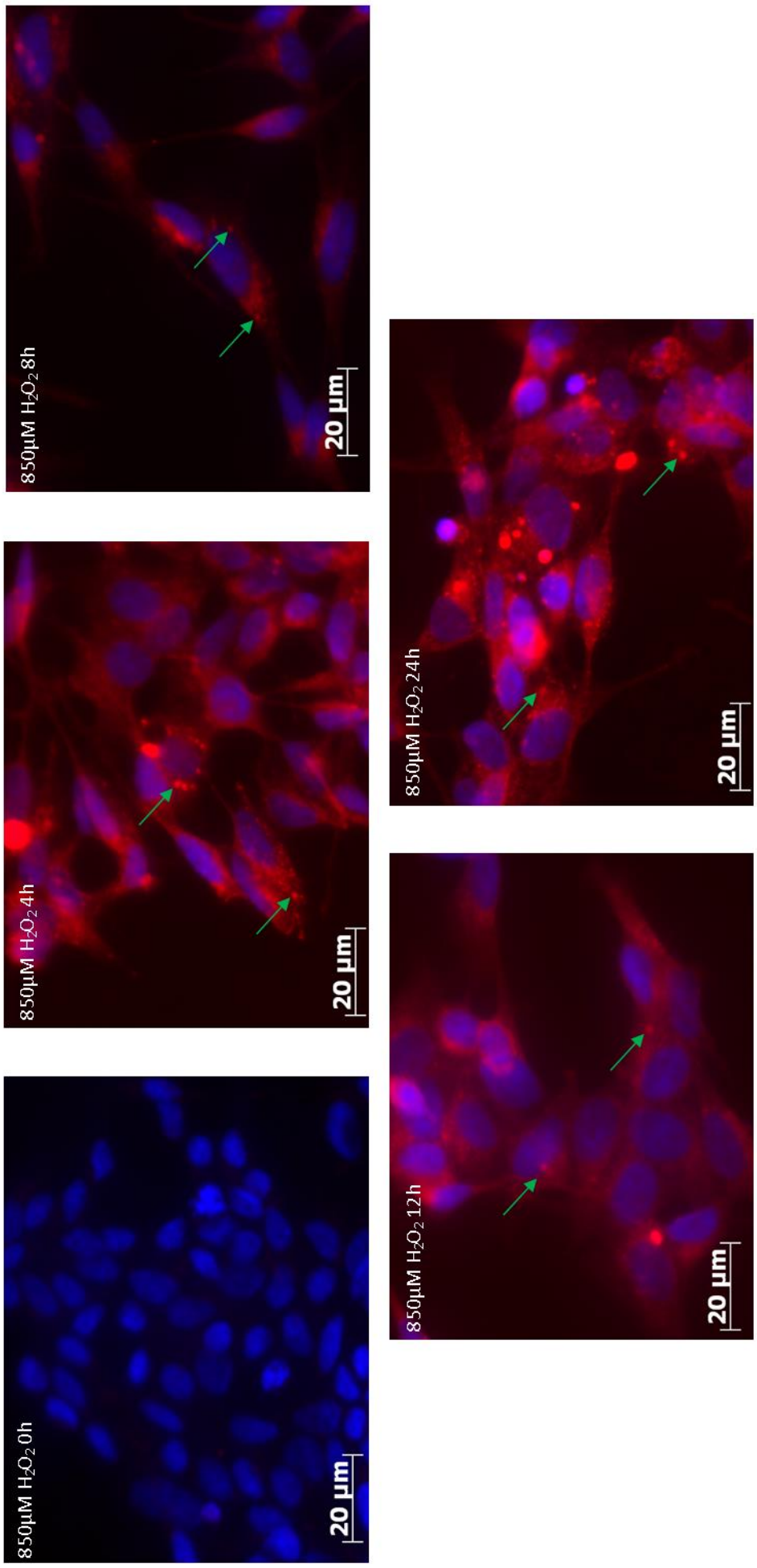

Fig. 3.25 Aggresome formation in TaClo treated SH-SY5Y (cont.)

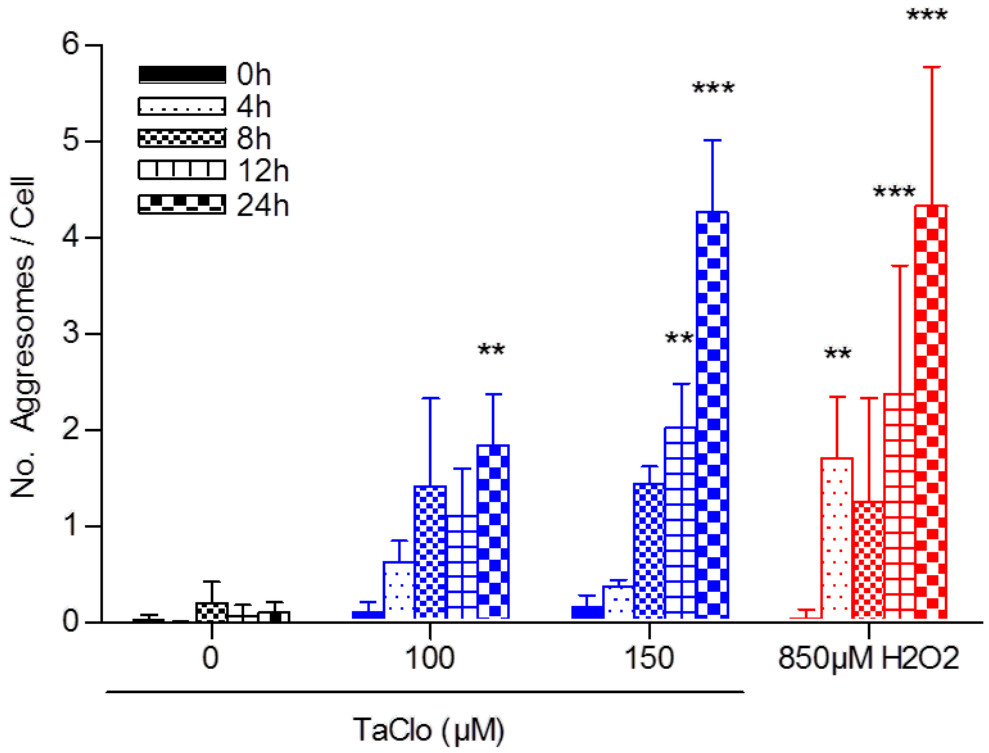

Fig. 3.26 Aggresome quantification in TaClo treated SH-SY5Y SH-SY5Y cells were treated for 0, 4, 8, 12 or 24 hours and then stained with Hoechst 33342 and an aggresome dye. Data shown as mean aggresomes per cell ± SD (n=3). Significant effect of TaClo & H_2O_2 treatment on number of aggresomes/cell over time (P<0.001, Two-Way ANOVA). ***P<0.001, **P<0.01 when compared to 0.2% DMSO at same time point, Bonferroni post-test.

3.3.5 Involvement of DNA Damage in TaClo Toxicity

PARP-1 is a protein involved in DNA repair and cell death. PARP-1 is an integral part of base excision repair of single or double strand breaks in DNA (Dantzer, Schreiber et al. 1999) when in its activated form. Activated PARP, when involved in DNA excision repair, depletes cellular ATP levels, which, in cases of high DNA damage, can ultimately lead to necrosis (Bouchard, Rouleau et al. 2003).

Protein was isolated from SH-SY5Y cells treated with 100µM TaClo and probed for relative full length and cleaved PARP levels by Western blot. Bands for full length PARP were present at all time points (Fig. 3.27 A) and no significant difference was observed in levels for up to 24 hours following 100µM TaClo treatment (One-way ANOVA) (Fig 3.27 B). No bands were visible for cleaved PARP at any time point until 24h (Fig. 3.27 A), suggesting PARP inactivation only occurs late in TaClo mediated cell death.

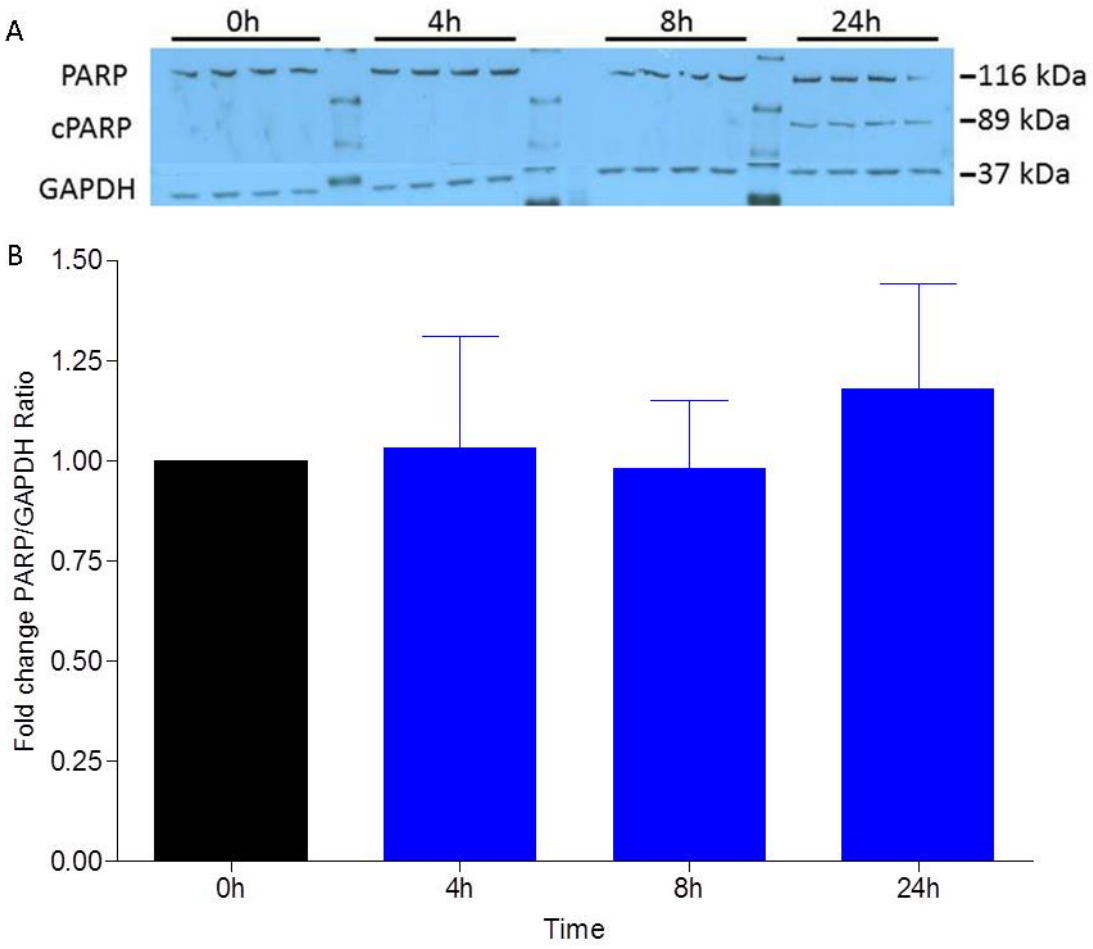

Fig. 3.27 Expression of full length (PARP) and cleaved (cPARP) PARP in 100µM TaClo treated SH-SY5YSH-SY5Y cells were treated with 100µM TaClo for 0, 4, 8 or 24 hours and protein harvested. Samples were probed for PARP. (A) Image is representative blot of PARP, cPARP and GAPDH control (B) PARP intensity relative to GAPDH. Data presented as fold-untreated ± SD from quadruplicate assays (n=3). No significant difference when compared to 0h, One-way ANOVA. (C) cPARP intensity relative to GAPDH. Data presented as fold-untreated ± SD from quadruplicate assays (n=3). No significant difference, One-way ANOVA

SH-SY5Y cells were co-treated with toxic doses of TaClo and the PARP inhibitor PJ-34 (Abdelkarim, Gertz et al. 2001) to investigate the involvement of PARP in TaClo mediated SH-SY5Y toxicity. At low levels of toxicity (<50% cell death) PJ-34 significantly amplified TaClo mediated toxicity in SH-SY5Y cells in a dose dependent manner, whereas at high levels of toxicity (>50% cell death) PJ-34 significantly attenuated TaClo toxicity in a dose dependent manner (Fig. 3.28). This is consistent with results seen with known DNA damaging agents, as under low cellular stress levels, PARP repairs DNA damage, but at high levels of DNA damage, PARP depletes cellular ATP level and leads to necrosis (Bouchard, Rouleau et al. 2003).

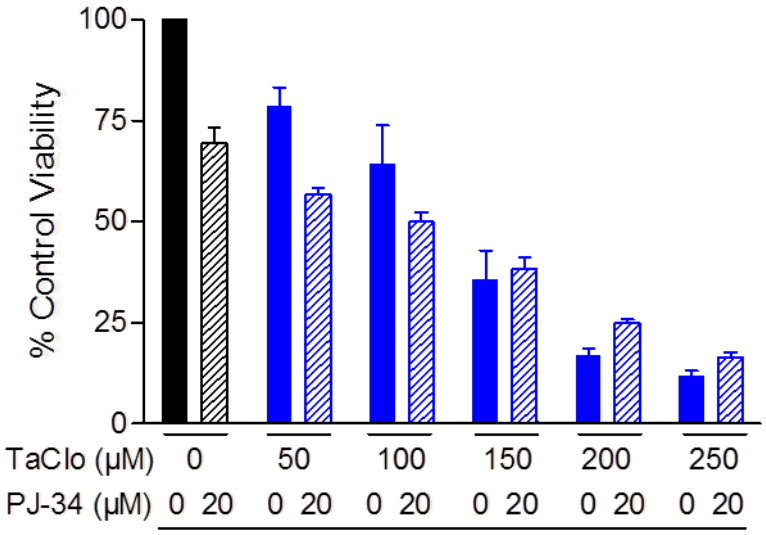

Fig. 3.28 Effect of PJ-34 on TaClo toxicity in SH-SY5Y SH-SY5Y cells were pre-treated with PJ-34 (20μM) for 1 hour and then co-treated with TaClo (50-250μM) for 21 hours and viability measured by reduction of Alamar Blue (resazurin). Data presented as mean % control ± SD from quadruplicate assays (n=3). Significant effect of PJ-34 on TaClo toxicity (P<0.001), Two-way ANOVA.

Histone H2A.X is a histone involved in DNA double strand break repair (Yuan, Adamski et al. 2010) that has been shown to be rapidly phosphorylated at Ser139 following exposure to DNA damaging agents (Rogakou, Pilch et al. 1998). Protein was isolated from SH-SY5Y cells treated with 100µM TaClo and probed for phospho-histone H2A.X Ser139 (pH2AX) levels by Western blot. pH2AX levels were significantly increased following TaClo treatment ($P<0.05$, unpaired t-test) (Fig. 3.29) suggesting TaClo exposure leads to double strand breaks in DNA.

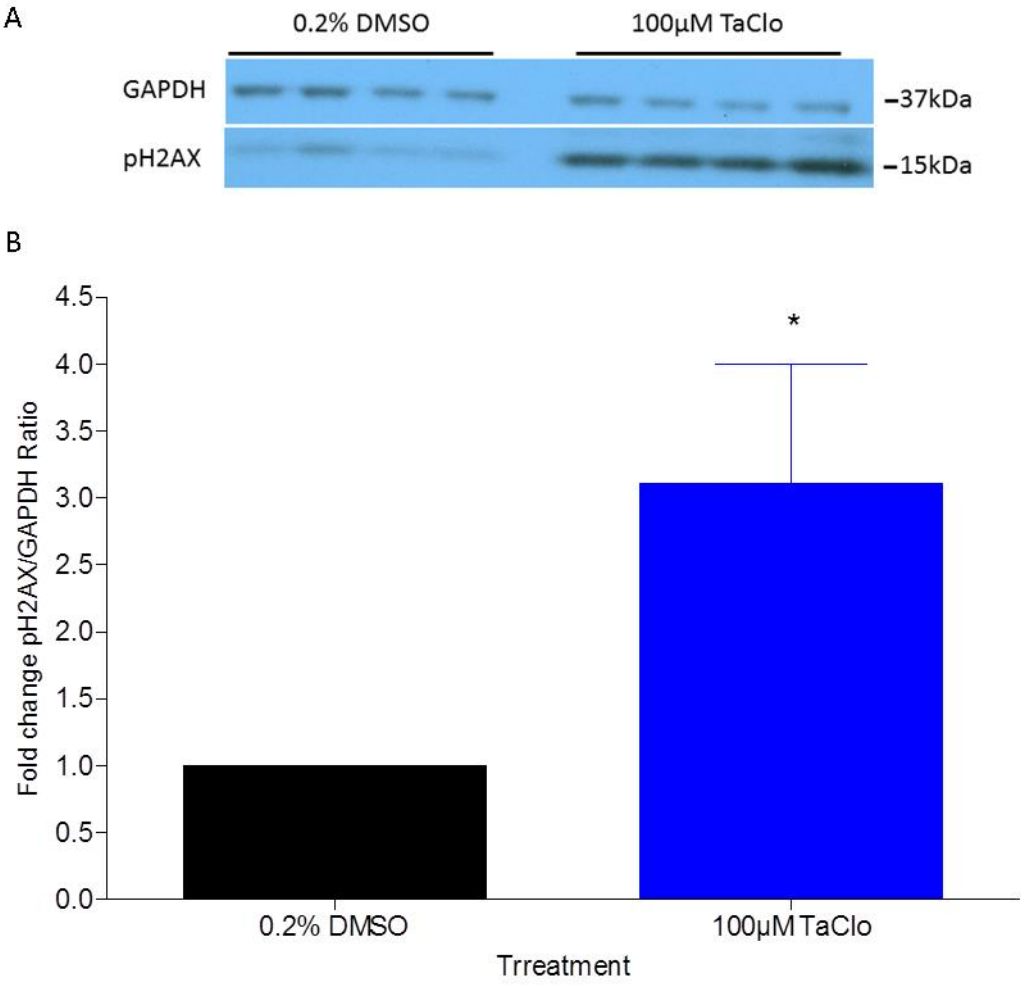

Fig. 3.29 Expression of Phospho-Histone H2A.X (pH2AX) in 100µM TaClo treated SY-SY5Y SH-SY5Y cells were treated with 0.2% DMSO or 100µM TaClo for 24 hours and protein harvested. Samples were probed for pH2AX. (A) Image is representative blot of pH2AX and GAPDH control (B) pH2AX intensity relative to GAPDH. Data presented as fold-untreated ± SD from quadruplicate assays (n=3). *$P<0.05$ when compared to 0.2% DMSO, unpaired t-test

Calpain-1 belongs to a family of calcium-dependent, non-lysosomal cysteine proteases and is expressed in the central nervous system. Calpian-1 is activated by micro-molar concentrations of Ca^{2+} (Glass, Culver et al. 2002) and can cleave a wide range of cellular components (Rami 2003). It has been shown that Calpain-1 is required for necrotic cell death induced by DNA damage and mediated by PARP activation (Moubarak, Yuste et al. 2007).

Protein isolated from SH-SY5Ys treated with TaClo over various time points was probed for Calpain-1 levels by Western blot. TaClo treatment significantly increased Calpain-1 expression in a time dependent manner ($P<0.05$, One-way ANOVA) with expression significantly higher at 24 hours post treatment when compared to pre-treatment levels ($P<0.05$, Dunnett's t-test) (Fig. 3.30).

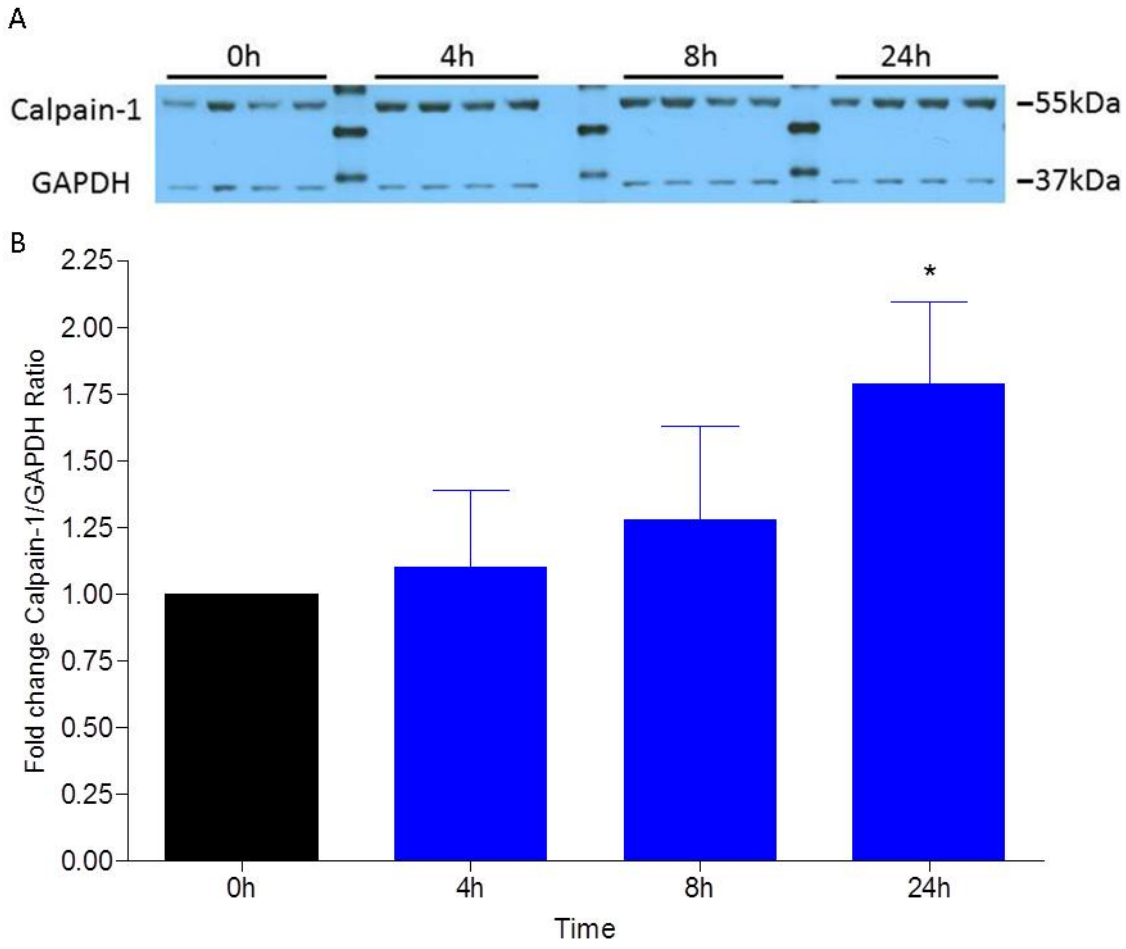

Fig. 3.30 Expression of Calpain-1 in 100µM TaClo treated SY-SY5Y SH-SY5Y cells were treated with 100µM TaClo for 0, 4, 8 or 24 hours and protein harvested. Samples were probed for Calpain-1. (A) Image is representative blot of Calpain-1 and GAPDH control (B) Calpain-1 intensity relative to GAPDH. Data presented as fold-untreated ± SD from quadruplicate assays (n=3). * $P<0.05$, when compared to 0h, One-way ANOVA & Dunnett's post-test

3.3.6 Summary of Effects of Cell Death Pathway Inhibitors on TaClo Toxicity

A summary of other cellular process modulators can be seen in Table 3.2. Modulators have been separated into compounds with possible, but unknown involvement in TaClo toxicity, those that were toxic in the cells and those with no effect.

Modulator	Mechanism	Concentration	Effect on TaClo Toxicity
Possible Involvement			
Resveratrol	Multiple non-specific actions (↑SIRT1, ↑ERK, ↓TNFα, antioxidant, ↓PKC, ↑AMPK)	25 & 50µM	Increased toxicity
Sirtinol	Sirtuin inhibitor	2.5, 5, 25 & 50µM	Increased toxicity
SP600125	JNK Inhibitor	500nM & 1, 2.5, 5 & 20µM	No sig effect up to 20µM which was toxic
Toxic			
Apocynin/Acetylvanillone	NADPH Oxidase inhibitor :. ↓ROS.	500µM & 1mM	Increased toxicity
LY29002	PI3K inhibitor	50 & 100µM	Increased toxicity
PP2	Src tyrosine kinase inhibitor	10 & 20µM	Increased toxicity
PP242	Selective mTOR inhibitor	100 & 500nM	Increased toxicity

Table 3.2 Summary of the effects of cell death pathway modulators on TaClo toxicity in SH-SY5Y

Modulator	Mechanism	Concentration	Effect on TaClo Toxicity
No Effect			
3-Methyladenine	PI3K inhibitor	100µM & 1.5, 3 & 4.5mM	No effect
Bongkrekic Acid	Inhibits MTP formation	10 & 20µM	No effect
Butylatedhydroxyanisole	Mitochondrial-targeting ROS scavenger	25, 50, 100 & 200µM	No effect up to 200µM which increased toxicity
Deprenyl	MAO-B & GAPDH inhibitor	10, 100 & 200µM	No effect
Ebselen	GSH peroxidase mimic	5, 10, 35 & 50µM	No effect
Gö6976	PKC inhibitor	1 & 2.5µM	No effect
GW5074	Raf kinase inhibitor	500nM & 1µM	No effect
Idebenone	analogue of coenzyme Q10 (mitochondrial antioxidant)	500nM & 1, 5 & 10µM	No effect up to 10µM which increased toxicity
K-252a	PKC inhibitor	500nM & 1µM	No effect
MnTBAP	SOD mimetic	25 & 50µM	No effect
MnTmPyP	SOD mimetic	1 & 2.5µM	No effect
Procysteine	Increases GSH levels	1, 5 & 10mM	No effect up to 10mM which increased
Quinazoline	NF-κB & LPS induced TNF inhibitor	500nM & 1µM	No effect
SQ22536	Inhibits adylylcyclase	10, 20, 50 & 100µM	No effect

Table 3.2 Summary of the effects of cell death pathway modulators on TaClo toxicity in SH-SY5Y (cont.)

3.4 Discussion

3.4.1 General Neuronal Toxicity of TCE & Metabolites

TCE did not show any significant toxicity in open system SH-SY5Y, differentiated midbrain neuron or DA neuron models used (Figs. 3.1, 3.2 & 3.3) which may be due to a number of factors:

(i) TCE is not toxic at the doses used in the open system experiments and it requires higher exposure levels or a longer, more chronic, time period of treatment to exert any effect.

(ii) The cell lines used may not express the enzyme (CYP2E1) needed to metabolise TCE into chloral and therefore its suspected toxic metabolites.

(iii) Due to the volatile nature of TCE, the majority of the dose given could have evaporated out of the media and so dramatically reduced exposure.

As SH-SY5Y have been shown to have CYP2E1 present (Posadas, Santos et al. 2012), factor (ii) was discounted and it was concluded that the lack of toxicity was due to (i) or (iii). To try to determine what was happening SH-SY5Y cells were exposed to TCE in an airtight closed system and observed almost total cell death with exposure calculated to be ~6mM or 8500 ppm (Fig. 3.4). These results are in agreement with a previous thesis which exposed SH-SY5Y to TCE using a similar method in a smaller container and measured TCE levels in media and cells GC-ECD. They found that TCE was taken up quickly into the media (at µM levels) and cells (at mM levels) before levels rapidly decreased suggesting either substantial metabolism or ejection of the compound from the cells (Jiang 2008). This suggests that in the open system models the volatility of TCE was likely to have been the main reason we were not seeing any toxicity and to examine TCE toxicity *in vitro* in more detail a more robust system of exposing cells to TCE needs to be developed. The levels used to show toxicity in the closed system were ~100 x higher than those seen in workers in industrial areas of 1-100ppm (Williams-Johnson, Eisenmann et al. 1997), but our model is far more acute, with workers sometimes exposed to low level TCE for decades. A robust, long-term method of exposure in cells is needed to model typical human exposure.

DCA was not found to be toxic at any doses examined in this study (Fig. 3.8), which was expected as we were modelling CNS neuronal populations and DCA mainly shows evidence of causing peripheral neuropathies (Moser, Phillips et al. 1999; Kaufmann, Engelstad et al. 2006; Felitsyn, Stacpoole et al. 2007).

Chloral was found to be toxic to both SH-SY5Y and midbrain neurons in our model in a dose-dependent manner at doses $\geq$ 200µM in SH-SY5Y and in a time and dose dependent manner at doses $\leq$ 100 µM in midbrain neurons (Figs. 3.5 & 3.6). The more potent toxicity observed in the midbrain neurons is likely to be due to the chronic dosing regimen (4 week) as opposed to acute (20 hours) used in the SH-SY5Y. This supports the hypothesis that TCE leads to PD due to the formation of the neurotoxic compound TaClo via chloral (Bringmann, Bruckner et al. 2000; Jiang, Mutch et al. 2007). However, chloral does not appear to show any specific toxicity towards DA neurons (Fig. 3.7) which does not support the theory that TCE exposure leads to DA neurotoxicity and so PD via chloral. The toxic dose level of 100µM corresponds to ~16µg/ml, a far lower exposure level than the dose of 100mg/ml which was shown by Cattano et al. to lead to neuroapoptosis in infant mouse brains (Cattano D., Straiko M.M.W. et al. 2008). The WHO Concise International Chemical Assessment Document 25 on Chloral Hydrate suggests chloral has a very short half-life of approximately 3 minutes and the majority of the dose is converted to trichloroethanol (Benson 2000). It is unclear in our model whether chloral itself or conversion to trichlorethanol is the primary cause of toxicity; it is, therefore, difficult to see how well our toxic dose compares with the dose Cattano found to be neurotoxic *in vivo* and more research is needed into this.

TaClo was acutely toxic in SH-SY5Y at ten times lower levels than chloral with an LD_{50} of ~100µM and almost total cell death at 100µM (Fig. 3.6), supporting our hypothesis, that TCE is converted to the neuroactive TaClo via chloral, in agreement with the law of mass action. This is higher than the toxicity seen by Akundi *et al.* in SK-N-SH neuroblastoma which showed an LD_{50} of ~200µM TaClo (Fig. 3.34) (Akundi, Macho et al. 2004).

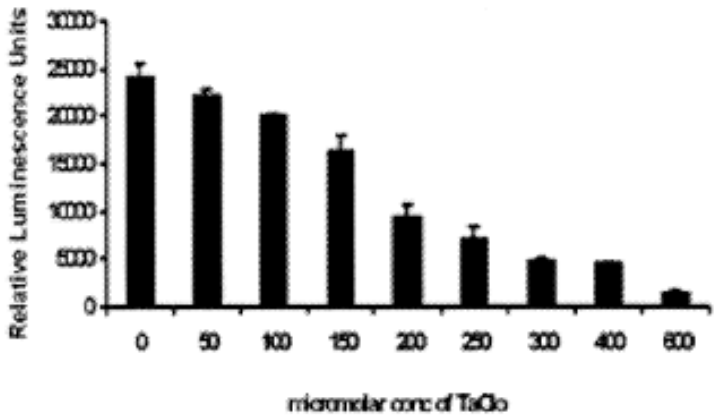

Fig. 3.31 Toxicity of TaClo in SK-N-SH cellsSK-N-SH cells were treated with TaClo for 24 hours and viability assessed by luminescent assay relating to metabolically active cells. Taken from (Akundi, Macho et al. 2004)

In midbrain neurons, TaClo showed a similar toxic profile to chloral, with 4 weeks treatment showing almost total cell death at 100µM and no significant death at 50µM (Figs. 3.6). This may also support the fact that chloral toxicity is due to conversion to TaClo as the longer time period of treatment could allow time for the generation of TaClo from chloral as opposed to the shorter treatment time in SH-SY5Y. In the chronic model, the increased length of exposure does not appear to affect toxicity, with viability following treatment of all doses, apart from 100µM TaClo, consistent from 1 -4 weeks exposure. This suggests there may be some threshold of TaClo concentration that needs to be crossed before toxicity occurs. TaClo produces significant cell death in SH-SY5Y following 20 hour 50µM treatment, but not following 4 week 50µM treatment in midbrain neurons. This could be explained as the hypothesis is that TCE exposure leads to DA cell death and therefore PD, so it would be expected that TaClo would show some specificity for DA neurons. If this is the case, we could expect to see more toxicity in SH-SY5Y when compared to midbrain cultures as SH-SY5Y consist entirely of DA model cells, whereas the midbrain culture contains a mixture of cells, only a proportion of which are DA. To further explore this we stained midbrain cultures treated for 4 weeks for TH, an enzyme involved in DA metabolism widely used as a marker for DA neurons (Margolis, Coker et al. 2010). TaClo showed a significant selectivity for DA neurons in the midbrain cultures, with $\geq$100µM TaClo causing almost total death of all cells but 25 & 50µM TaClo causing no reduction in total cell number but a significant reduction in TH positive neurons (Fig. 3.13 & 3.14). This apparent specificity of TaClo toxicity for DA neurons is supported by the relative LD_{50} values of TaClo in DA model systems SH-SY5Y & midbrain neurons (100-150µM) being lower than those in the more general neural stem cells and MEFs (200-500µM) (Table 3.1). This provides evidence for TCE, through TaClo, being involved in the DA neuron specific cell death and development of PD in exposed individuals. However, as this DA specificity does not occur in chloral treated midbrain cultures (Fig. 3.7), this suggests a scenario where chloral is causing neuronal cell death in different manner to TaClo questioning whether a significant quantity of TaClo is formed from chloral in our models.

When we investigated the time course of acute TaClo toxicity in SH-SY5Y, 150µM TaClo showed a steady decrease in cell number from 0-24 hours; however, 100µM TaClo did not appear lead to significant cell death until 4-8 hours following treatment (Fig. 3.12). This possibly suggests that, at 100µM, a build-up of TaClo in cells is required before any toxic effect is triggered; again proposing some kind of thresholding event may be required for TaClo toxicity. In all experiments discussed so far, the Alamar Blue fluorescence assay has been used to determine viability. This assay uses metabolic activity as a marker for viability, but as metabolic activity may be affected by treatment, we used visual inspection to confirm our

results (Fig. 3.11). To further confirm that the Alamar Blue assay correlates with viability, we compared the results seen with acute TaClo using Alamar Blue to cells treated in the same way but with viability assessed by crystal violet assay. Crystal violet only enters viable cells so correlates directly with cell number. In this experiment, crystal violet results correlated extremely well with Alamar Blue assay results, with both showing toxicity at ≥50µM TaClo and similar levels of viability seen at all doses examined (Fig. 3.10). This supports the Alamar Blue assay as a reliable measure of cell viability in our TaClo toxicity assays. In a study of a patient exposed to TCE for 20 years and diagnosed with PD, TaClo levels of 9ng/ml were recorded in his blood 2 months after last exposure (Kochen, Kohlmüller et al. 2003), an amount far lower than the doses of 7/14 mg/ml (25/50µM) that showed DA neuron toxicity in our models. Moreover, the exposure in this case was for a significantly longer time than our model. Sontag et al. found locomotor deficits in female rats dosed with 0.2 mg/kg/day for 7 weeks (Sontag, Heim et al. 1995), which equates to estimated plasma levels of 5ng/ml/day, based on 3-4 month old female rats weighing ~250g and using the method of Bijsterbosch to estimate plasma volume (Bijsterbosch, Duursma et al. 1981). Over the 7 weeks, this means a total dose of 245ng/ml, a dose more comparable with our shorter model of exposure, suggesting a possible relevance for our data *in vivo*. It has been reported that tetrahydro-β-carbolines, such as TaClo, can undergo N-methylation in the brain (Matsubara, Collins et al. 1993), and N-methyl TaClo was found to be a more potent neurotoxin than TaClo itself (Janetzky, Gille et al. 1999), suggesting that N-methyl TaClo may be the more relevant toxin which needs investigating.

Results in these toxicity assays were used to select doses for further investigation, with doses that showed approximately 50% reduction in viability chosen for future assays; 500µM for chloral and 100µM for TaClo (Table 3.1). In assays where a decrease in toxicity was expected, this dose was combined with a slightly more toxic dose, 1mM for chloral and 150µM for TaClo, to allow observation of an increased viability. In assays where an increase in toxicity was expected, this dose was combined with a slightly less toxic dose, 50µM for TaClo, to allow observation of decreased viability.

3.4.2 What is the Main Mechanism of Neuronal Toxicity Mediated by TCE Metabolites?

Apoptosis is the most studied form of programmed cell death and is characterised by morphological changes such as cellular shrinkage, nuclear condensation, DNA fragmentation and membrane blebbing. It is mediated by the activation endogenous endonucleases, such as caspases, and cleavage of critical cellular substrates. As a number of studies have suggested

that apoptosis is involved in the pathogenesis of some forms of PD (Anglade 1997; Nagatsu 2002; Tatton, Chalmers-Redman et al. 2003) we decided to investigate whether it was involved in the toxicity observed following chloral and TaClo exposure. If chloral or TaClo were causing apoptosis in SH-SY5Y, then blockade of caspase activation by zVAD.fmk, a pan caspase inhibitor, should reduce the decrease in viability seen following treatment with these compounds. Our results showed no significant protection against toxicity conferred by zVAD.fmk in SH-SY5Y treated with either chloral or TaClo (Fig. 3.15). This finding was supported when TaClo treated cell extracts were probed for the presence of the active, cleaved form of caspase-3, one of the main executioner caspases which is essential for apoptosis (Nicholson, Ali et al. 1995). No cleaved caspase-3 was found to be present until 24 hours following TaClo treatment (Fig. 3.16), suggesting that caspase-3 is not a driving factor in TaClo mediated SH-SY5Y toxicity, and only occurs during the final processes of cell death. This correlates well with a study in SK-N-SH cells by Akundi *et al.* which shows an increase in caspase-3 cleavage 24 hours after 150µM TaClo treatment (Akundi, Macho et al. 2004); however, they propose that this indicates TaClo mediates cell death by apoptosis in disagreement with our hypothesis. Finally, PARP has been shown to be cleaved by caspase-3 and so inactivated as an early essential event in the apoptotic cascade to stop activated PARP depleting cellular NAD levels needed for the energy consuming process of apoptosis (Boulares, Yakovlev et al. 1999). TaClo treated SH-SY5Y cell lysates were probed for PARP and PARP cleavage was also only found to occur as a late event, 24 hours following treatment (Fig. 3.35). Taken together these findings suggest that apoptosis is not the main form of cell death initiated by TaClo in SH-SY5Y.

Some of the earliest reports of chemically induced PD cited necrosis as the method of cell death that occurred in these models (Thoenen and Tranzer 1968). Necrosis has previously been thought of as an unregulated form of cell death characterised by a disruption of the cellular membrane and a swelling of the cytoplasm and mitochondria, culminating in the complete disintegration of organelles and total lysis of the cell. However, Degterev detailed a form of programmed, caspase-independent, cell death with a necrotic morphology and termed it 'necroptosis' (Degterev, Huang et al. 2005). As TaClo and chloral do not appear to cause SH-SY5Y death by apoptosis, we investigated whether the toxic mechanism involved was necroptosis by co-treating chloral and TaClo with a small molecule, shown to specifically inhibit necroptosis by inhibiting the kinase activity of RIP1, called Nec-1 (Degterev, Huang et al. 2005). Nec-1 had no significant effect on chloral induced toxicity but significantly protected against TaClo in SH-SY5Y (Fig. 3.17), suggesting that TaClo may cause cell death by necroptosis but chloral may not. This also provides more evidence against our hypothesis that chloral is toxic

via conversion to TaClo and suggests a separate mechanism for chloral induced neurotoxicity in SH-SY5Y. RIP1, and in particular an active kinase domain, has been shown to be a key mediator of necroptosis (Holler, Zaru et al. 2000) and this active domain has been shown to be inactivated due to cleavage by caspase-8 (Lin, Devin et al. 1999) or caspase-6 (Van Raam, Ehrnhoefer et al. 2013) during apoptosis. This is supported by a reported increase in necroptotic cell death in caspase-8 deficient mice (Bohgaki, Mozo et al. 2011) We probed TaClo treated SH-SY5Y cell lysates for full length and cleaved RIP1 and found that while full length RIP1 expression is not affected by TaClo treatment, the amount of cleaved RIP1 present in the cell is significantly reduced to ~50% of control from 4 hours following treatment (Fig. 3.19). This suggests that the cell may be undergoing necroptosis relatively rapidly following TaClo treatment, as there is less of the cleaved, inactive, form present following treatment, due to the involvement of the full length form in necroptosis. This also suggests this effect may be causative as it happens extremely early in the sequence of cell death events, prior to actual cell death being seen. The levels of cleaved RIP are still significantly lower than control by 24 hours post treatment, but appear to be rising. This may be linked with the activation of caspases seem by caspase 3 and PARP cleavage at 24 hours (Figs. 3.16 & 3.35).

When RIP1 levels were knocked down in SH-SY5Y, a small but significant protection against TaClo insult was seen (Fig. 3.22), supporting the involvement of RIP1 in TaClo mediated SH-SY5Y cell death and suggesting necroptosis as a possible mechanism. Although the effect observed is relatively minor (10-20%), RIP1 was only knocked down to 50% of control (Fig. 3.21) despite good viral take-up (Fig. 3.20), and it may be the case that there is still enough RIP1 present to achieve cell death in most cases. To further investigate this, MEF cells with complete RIP1 knockout were sourced and a more significant - although not total - attenuation of TaClo toxicity was seen when compared to wild type MEFs (Fig. 3.24). To support this, the ability of Nec-1 to attenuate TaClo toxicity was examined in RIP1 knockdown SH-SY5Y and RIP1 knockout MEFs. Nec-1 reduced TaClo toxicity in RIP1 knockdown SH-SY5Y (Fig. 3.23), but not to the extent seen in wild-type cells and no protection was seen in RIP1 knockout MEFs (Fig. 3.24), providing more evidence that RIP1 kinase inhibition - and so blockade of necroptosis - is the mechanism by which Nec-1 protects against TaClo mediated toxicity in our models. This suggests that RIP1 is integrally involved in TaClo mediated cell death and that necroptosis is the mechanism of death activated.

Some care needs to be taken, however, with this conclusion with a recent report that Nec-1 has exactly the same structure as methyl-thiohydantoin-tryptophan, an inhibitor of indoleamine 2,3-dioxygenase (IDO), a rate limiting enzyme of the kynurenine pathway that

metabolises tryptophan to NAD+, proposing that Nec-1 is not a specific inhibitor of RIP1 and necroptosis, but also inhibits the kynurenine pathway (Vandenabeele, Grootjans et al. 2013). This is particularly interesting as abnormalities in the kynurenine pathway have been implicated in the pathology of neurological disorders, due to the presence of three neuroactive metabolites in the pathway. One of the diseases kynurenine pathway disruption has been linked with is PD, with abnormalities in metabolites of the pathway found in brains and blood of PD patients (Ogawa, Matson et al. 1992; Hartai, Klivenyi et al. 2005) and altered expression of enzymes in the pathway seen in MPTP treated mice (Knyihár-Csillik, Csillik et al. 2004). For a review of the complex involvement of kynurenine pathway metabolites in neuroprotection and neurotoxicity, and the involvement of the pathway in neurodegenerative disorders see (Sas, Robotka et al. 2007; Tan and Yu 2012). This finding casts some doubt as to whether the protection against TaClo toxicity seen is entirely due to effects on RIP1 and necroptosis, or if inhibition of IDO and disruption of the kynurenine pathway contributes to, or is the major component of, Nec-1 mediated increases in viability following TaClo exposure. To address these concerns, SH-SY5Y were treated with 1-methyl-L-tryptophan, an IDO inhibitor that does not have any effects on RIP1 (Cady and Sono 1991; Schmidt, Siepmann et al. 2012). No significant effect on TaClo toxicity was onserved following 1-methyl-L-tryptophan, supporting the conclusion that the protective effect of Nec-1 on TaClo mediated cell death is due to RIP1 kinase inhibition and blockade of a necroptotic pathway (Fig. 3.18).

As there is still some cell death apparent even in RIP1 knockout cells, the effect of zVAD.fmk and NAC (antioxidant defence inducing agent; see Chapter 4) on TaClo toxicity were investigated in this cell line to see if apoptosis or oxidative stress were involved in this toxicity. No attenuation of TaClo toxicity by zVAD.fmk was seen, suggesting that the cells do not switch to an apoptotic death mechanism when necroptosis is blocked. NAC was protective against TaClo toxicity; however this was to a far lower extent than that seen in wild type SH-SY5Y (Fig. 3.25). This can be explained by the fact that a far higher concentration of TaClo was used in the RIP 1 knockout MEFs than the SH-SY5Y (250 & 300µM compared to 100 & 150µM respectively) due to the relative resistance of these cells to TaClo toxicity so probably inducing higher levels of ROS. This may suggest that TaClo induces cell death by activation of a necroptotic pathway, but if this pathway is blocked, general cellular damage, possibly due to oxidative stress, causes a level of damage to the cell that makes it unable to survive.

Evidence provided so far suggests that the form of cell death mediated by TaClo in SH-SY5Y is likely a form of programmed necrosis and not apoptosis. To further explore this we used a double staining flow cytometry method that discriminates between necrotic and apoptotic cell

death phenotypes based upon known morphological features. Necrotic cell death is known to be characterised by disruption of the cell membrane, a feature not seen in apoptotic cells, and known to cause an increase in PI staining. However, in apoptosis chromatin condensation occurs, and this is not seen in necrotic cells and causes an increase in Hoechst 33342 staining. In SH-SY5Y treated with TaClo for varying time points, stained with both dyes mentioned and sorted by flow cytometry into apoptotic or necrotic categories based on Hoechst 33342/PI staining, we saw a time and dose-dependent increase in necrotic cells and no significant change in those classed as apoptotic (Fig 3.28). We also treated SH-SY5Y with the known apoptosis inducing agent staurosporine as a control for apoptosis, and saw a significant increase in cells classified as apoptotic and no change in necrotic cells (Fig. 3.28), confirming the discriminatory capability of the assay.

Taken together, this evidence suggests that TaClo treatment leads to a necrotic, and probably programmed, form of death in SH-SY5Y.

3.4.3 Is Autophagy Affected During TCE Metabolite Neurotoxicity?

Autophagy has been widely associated with PD, with evidence of both protective and cytotoxic role proposed (Reviewed in (Cheung and Ip 2009)). Autophagy has also been implicated in the pathology of PD due to the importance of clearing toxic protein aggregates linked with the disease, such as mutated α-synuclein (Polymeropoulos, Lavedan et al. 1997; Kruger, Kuhn et al. 1998; Zarranz, Alegre et al. 2004), in disease progression (Pan, Kondo et al. 2008). Also, mutations in Parkin and PINK-1, two proteins liked with autophagy of damaged mitochondria (Narendra, Tanaka et al. 2008; Narendra, Jin et al. 2010), have been shown to lead to PD (Kitada, Asakawa et al. 1998; Valente, Abou-Sleiman et al. 2004).

Rapamycin is a compound that is known to induce autophagy by inhibition of mTOR (Augustine, Bodziak et al. 2007). We found that rapamycin treatment significantly increased TaClo mediated toxicity in SH-SY5Y (Fig. 3.29), suggesting that an increase in autophagy attenuates the mechanism of TaClo induced cell death. This is surprising, as autophagy has been generally thought to have a protective effect in PD by clearing misfolded toxic protein aggregates and rapamycin has been shown to decrease the toxicity of other known PD-linked toxins such as rotenone (Pan, Rawal et al. 2009). Conversely, there are also reports that inhibition of autophagy by melatonin can protect against rotenone induced toxicity in HeLa cells (Zhou, Chen et al. 2012), complicating analysis of this evidence. However, it has been reported that rapamycin can block inhibition of mTOR by RTP801, a protein up regulated

following known PD toxin MPTP and 6-OHDA treatment which inhibits the phosphorylation of the pro-survival protein Akt and leads to cell death (Malagelada, Jin et al. 2010). This suggests that the protective effect of rapamycin may not be due to suppression of autophagy but may be due to other effects it has in the cell. A mechanism by which rapamycin has been shown to attenuate toxicity has also been described in renal tubule cells whereby rapamycin increases the toxicity of cyclosporine A by blocking Akt activation and increasing cell death (Cheng, Chang et al. 2008). These findings do not explain the attenuation of TaClo toxicity seen in SH-SY5Y but suggest a more complex mechanism involving more than autophagy induction may be involved and showing more work is needed before conclusions can be fully drawn from this.

In addition to the effect of autophagy on TaClo induced cell death, we looked at the effect of TaClo on autophagy. We probed TaClo exposed cell lysates for LC3-B, an essential component of autophagic vesicles and a widely used marker for autophagy. We found that LC3-B was significantly increased from 8 hours following TaClo treatment (Fig. 3.30), suggesting that autophagy is induced relatively early after insult and that TaClo may be causing damage to cellular contents.

Lysosomes are acid hydrolase enzyme containing cellular organelles that fuse with autophagic vesicles to break down waste materials and cellular debris. We looked at the expression of lysosomes following TaClo treatment and found increased lysosomes at 12 to 16 hours following TaClo treatment (Fig. 3.32), possibly suggesting an increase in lysosomal size or number needed to degrade debris engulfed in the autophagic vesicles seen with the increase in LC3-B at 8 hours post-treatment. This supports a role for TCE mediated cell death through TaClo as a similar effect was seen in SH-SY5Y treated with the known PD toxin rotenone (Xiong 2012). We also looked at the effect of inhibition of lysosomal function using Bafilomycin A1, a compound which blocks the acidification of lysosomes and so their ability to function and degrade material brought to them by autophagic vesicles. Decreased lysosomal function led to an increase in TaClo mediated toxicity, suggesting that a functioning lysosomal system protects against TaClo mediated cell death. This agrees with evidence reported that the toxicity of PD-linked neurotoxins rotenone and paraquat is attenuated by inhibition of autophagy (González-Polo, Niso-Santano et al. 2007; Xiong 2012). When taken with the increase in lysosomes seen, this evidence suggests TaClo may be damaging cellular contents that - if not cleared efficiently from the cytosol - may contribute to cell death.

Aggresomes are inclusion bodies, such as Lewy Bodies in PD, made up of aggregation prone proteins that form when the autophagic machinery is overwhelmed (Amijee, Madine et al.

2009). They appear to have a cytoprotective effect by sequestering toxic misfolded protein into aggregates during oxidative stress or other forms a cellular damage. SH-SY5Y showed a significant increase in aggresome number and size following TaClo treatment (Fig. 3.33 & 3.34), suggesting that there is a build-up of aggregating, damaged proteins that the autophagic machinery is incapable of clearing. This suggests TaClo treatment may induce neurotoxicity similar to that seen in PD as mutations related to the disease, such as Parkin, have been shown to be involved in aggresome formation (Muqit, Davidson et al. 2004) and protein aggregation has been widely seen in the pathology of the disease (Ross and Poirier 2004) and following exposure to known PD toxins rotenone and MPTP (Forno, Langston et al. 1986; Diaz-Corrales, Asanuma et al. 2005).

Our evidence generally suggests that autophagy is activated following TaClo insult in SH-SY5Y, and that it is most probably functioning as a protective mechanism against damage to cellular contents and toxic protein aggregation. However, our finding that rapamycin treatment increases TaClo toxicity in SH-SY5Y contradicts this hypothesis and suggests that increasing autophagy too much may actually contribute to toxicity. Both findings could be relevant as autophagy is a tightly controlled process and there is evidence that increasing or decreasing autophagic activity can be harmful to cells, suggesting more research is necessary into the role autophagy plays in the toxic mechanism of TaClo.

3.4.4 Does DNA Damage Occur During TCE Metabolite Neurotoxicity?

DNA damage has been shown to be involved in PD with damage reported in the SNpc of PD patients (Zhang, Perry et al. 1999), and seen prior to cell death following exposure to known PD toxin rotenone (Sanders L.H., Mastroberardino P. G. et al. 2010). DNA damage has also been shown to bring about a form of necrotic cell death by over activation of PARP, functioning as a DNA repair mechanism, leading to depletion of NAD and disruption of metabolism and eventually necrotic death (Zong, Ditsworth et al. 2004). It has also been suggested that this mechanism requires the involvement of RIP1 (Xu, Huang et al. 2006), proposing the involvement of DNA damage and PARP over activation in TaClo mediated neurotoxicity.

When PARP was inhibited pharmacologically in SH-SY5Y, an interesting effect was observed. With lower doses of TaClo, and so low toxicity, PARP inhibition increased cell death, but as TaClo doses, and so toxicity and cellular stress, increased, PARP inhibition protected against TaClo mediated toxicity in SH-SY5Y (Fig. 3.36). This supports a hypothesis of TaClo somehow

leading to DNA damage, as at low levels of damage, PARP is repairing strand breaks in the DNA and so blockade of this process is harmful to the cells. However, when DNA damage levels increase, the benefit of the PARP DNA repair mechanism is negated by the consumption of NAD and detrimental effect on cellular metabolism, and as such PARP inhibition protects against this effect. Levels of PARP and cleaved PARP were examined in TaClo treated SH-SY5Y cell lysates following various exposure time points and PARP cleavage was shown to occur only at 24 hours post treatment (Fig. 3.35). PARP cleavage, and so inactivation, occurs as a late event in the cell death process, which may be an attempt by the cell to arrest the depletion of NAD before a critical level is reached. This involvement of PARP and NAD depletion in toxin mediated PD is supported by the findings that PARP inhibition blocks MPTP mediated NAD+ and ATP decreases in mouse brains (Cosi and Marien 1998; Iwashita, Yamazaki et al. 2004; Yokoyama, Kuroiwa et al. 2010), PARP null mice are protected against MPTP neurotoxicity and PARP is activated by MPTP in DA neurons (Mandir, Przedborski et al. 1999).

A substantial increase in histone H2A.X phosphorylation at Ser139 was found in SH-SY5Y exposed to TaClo for 24 hours. H2AX has been shown to be involved in DNA double strand break repair (Yuan, Adamski et al. 2010) and to be rapidly phosphorylated at Ser139 following exposure to DNA damaging agents (Rogakou, Pilch et al. 1998). The increased levels of pH2AX seen in this study provide direct evidence of DNA damage, probably double strand breaks, occurring with TaClo exposure.

The cysteine protease Calpain-1 has been shown to be required for DNA damage driven, PARP mediated, necrotic cell death (Moubarak, Yuste et al. 2007). We found levels of Calpain-1 were significantly increased in SH-SY5Y following TaClo treatment (Fig. 3.37), giving further suggestion that this may be the mechanism of TaClo toxicity. However, Calpains are activated and induced by Ca^{2+} influx into the cell, so as this increase is late in the cell death pathway, it may be incidental in the death mechanism and due to the entry of Ca^{2+} into the cell due to the breakdown in membrane integrity seen in necrosis.

When taken together, this evidence suggests a possible mechanism by which TaClo either directly or indirectly, causes DNA damage, leading to over activation of PARP, depletion of NAD and necrotic cell death. More exploration of this area, however, is needed to confirm this hypothesis.

3.4.5 What Other Pathways are Affected by TCE Metabolite Neurotoxicity?

A variety of other cell death pathway mediators have also been used on the SH-SY5Y TaClo toxicity assay (Summarised Table 3.2). They have been classified as those that have some effect on TaClo mediated SH-SY5Y death and could, therefore, possibly be involved, those that were toxic in the assay, and those that had no effect.

Those that were toxic or had no effect may not necessarily be due to the fact that the targets of these compounds are not involved in the toxicity of TaClo but could be explained by in some cases by the lack of specificity of the compound (resveratrol, quinazoline) or the lack of specificity of the target (K252a, SP600125, SQ22536), with the complexity of cellular control meaning that many are involved in both cell survival and cell death pathways.

Of those that may show involvement, the sirtuin inhibitor, Sirtinol, may be relevant as inhibition of sirtuin 2 has been shown to be protective against neuronal toxicity in models of PD (Outeiro, Kontopoulos et al. 2007). It has also been reported that sirtuin 1 consumes NAD, and when activated may endanger energetically compromised neurons (Liu, Gharavi et al. 2009), an effect that would be expected to attenuate a TaClo toxic mechanism described earlier based on NAD depletion by DNA damage induced PARP overactivation. In contrast to this, we found that sirtinol increased TaClo toxicity (data not shown). However, sirtuin 2 has been shown to be involved in the cells defence against oxidative stress (Wang, Nguyen et al. 2007), and so would have a protective effect. Sirtun 1 has also been shown to have neuroprotective properties (Pfister, Ma et al. 2008), and inhibition of these properties could explain our findings. More research is needed into the specific effects of sirtuins in neurons to allow more conclusive interpretation of these results.

Resveratrol is an antioxidant that has been shown to protect against known PD toxins 6-OHDA and MPTP in animal models (Lu, Ko et al. 2008; Khan, Ahmad et al. 2010) and against DA toxicity in SH-SY5Y (Mi, Soon et al. 2007). In contrast, we found that resveratrol treatment attenuated TaClo toxicity (Data not shown). Although research generally cites the antioxidant properties of resveratrol, it has numerous other effects including up regulation of sirtuin 1, ERK and AMPK and down regulation of TNFα and Protein Kinase C. With this lack of specificity it is difficult to dissect the specific system resveratrol is effecting in our model so we decided to use other cleaner antioxidants to explore the involvement of oxidative stress in the mechanism of TaClo mediated neurotoxicity (see Chapter 4).

The other compound which needs discussion, is the JNK inhibitor SPD600125, which had no effect of TaClo toxicity at normally used doses (Data not shown). As JNK activation had been implicated in a hypothesised necrotic death mechanism driven by DNA damage and involving PARP, and RIP1 (Xu, Huang et al. 2006), this finding suggests that this is not the pathway by which TaClo mediates SH-SY5Y death; however this is an area which requires more research.

3.4.6 Conclusions

We have shown that the TCE metabolite TaClo leads to DA specific neuronal cell death in our model system. This cell death appears to be necroptotic in nature, and not apoptotic, and may involve activation of autophagy and DNA damage. We also found the intermediate compound in TCE metabolism to TaClo, chloral, to be toxic at a 10-fold lower potency than TaClo. This toxicity does not appear to be DA neuron specific and may be mediated by a death mechanism neither apoptotic nor necroptotic in nature. Finally, we did not see any direct toxicity in our open system models of TCE exposure, but did see potent toxicity following a high dose in an airtight closed system. A more robust method of TCE exposure is needed to further investigate this.

Chapter 4
The Involvement of Mitochondria & Oxidative Stress in TCE Mediated Toxicity

4.1 Introduction

The generation of ROS in cells has been shown to cause damage to organelles and cellular structures leading to cytotoxicity and, as such, has been implicated in a wide range of diseases. Studies have shown that this oxidative stress can be a key mediator in necroptosis (Kim, Dayani et al. ; Yu, Wang et al. 2002; Kim, Morgan et al. 2007; Ramana, Patel et al. 2010; Chen, Chiu et al. 2011) and has also been widely linked with PD (Alam, Jenner et al. 1997; Floor and Wetzel 1998) suggesting it could be involved in the cell death mechanism of TaClo.

Under conditions of oxidative stress, the cell has innate defence mechanisms to protect against damage caused by excess ROS. These antioxidant defences are mediated by a series of enzymes that convert superoxide to H_2O_2 which is then further reduced to water. There are two main classes of antioxidant enzyme: superoxide dismutases, that catalyse the breakdown of superoxide to H_2O_2 and oxygen (McCord, Keele Jr et al. 1971); and glutathione, which acts as a reducing agent by donating an electron from its thiol group to free radicals and ROS such as H_2O_2 (Dixon and Quastel 1923). Measuring or altering cellular levels of these enzymes and examining the relationship between this and TaClo toxicity can help provide insight into the involvement of oxidative damage in this toxicity.

Mitochondria are found in virtually all eukaryotic cells and function to generate cellular energy in the form of ATP by OXPHOS. OXPHOS occurs by electron transfer through a chain of four membrane-bound enzyme complexes generating a proton concentration gradient used by ATP-synthase to produce ATP. In healthy functioning mitochondria, a small amount of superoxide is generated by electrons leaking from the chain (Takeshige and Minakami 1979; Beyer 1992), and this is exponentially increased if the OXPHOS complexes are inhibited (Lambert and Brand 2004). OXPHOS dysfunction has been linked with both PD (Mizuno, Ohta et al. 1989; Schapira, Cooper et al. 1990; Schapira, Mann et al. 1990; Rana, De Coo et al. 2000) and necroptosis (Ye, Wang et al. 2012) so is a candidate for involvement in TaClo mediated neurotoxicity.

Loss of function mutations in DJ-1, a mitochondrially linked protein with involvement in antioxidant defence (Yokota, Sugawara et al. 2003), have been linked with PD (Bonifati, Rizzu et al. 2003); therefore the effect of TaClo on expression of this protein could link the toxin with PD and mitochondrial oxidative stress.

4.1.1 Aims

This study aims to investigate the involvement of ROS and oxidative damage in the mechanism of TCE toxicity using the DA model cell line SH-SY5Y and to investigate mitochondria as a possible source of any ROS generated.

To achieve these goals, the exposure paradigm employed in Chapter 3 was combined with investigations into oxidative stress markers and antioxidant defence to examine the involvement of ROS into TaClo toxicity. Any possible effect on mitochondrial respiration was investigated using well-characterised OXPHOS Complex specific biochemical activity assays.

4.2 Methods

For detailed descriptions of all methods see Material and Methods (Section 2), apart from those described below.

4.2.1 Alamar Blue Assay in SH-SY5Y Grown in Galactose Media

SH-SY5Y cells were switched from 10% GM to a growth media with Galactose replacing Glucose as the energy source (GAL). GAL was Dulbecco's Modified Eagle's Media (glucose free)(D5030) made up in ddH_2O, containing 10mM Galactose, 3.7mg/ml $NaCO_3$, 0.11mg/ml Sodium Pyruvate (all Sigma Aldrich), 10% Heat-Inactivated Fetal Bovine Serum, 4mM L-Glutamine, 40 units/ml Penicillin, 200µg/ml Streptomycin, 1% MEM Non-Essential Amino Acids and 5µg/ml Fungizone and grown for 2 weeks to acclimatise to the new media. TaClo toxicity assay was then carried out and viability assessed by Alamar Blue assay as section 2.1.2.1.

4.2.2 Effect of L-buthionine sulfoxamine on TaClo Toxicity in SH-SY5Y

SH-SY5Y were grown in either 10% GM or 10% GM containing 2.5mM L-buthionine sufoxamine for 2 days before being seeded in 24 wells of a 48 well plate each. TaClo toxicity assay was then carried out and viability assessed by Alamar Blue assay as section 2.1.2.1.

4.2.3 Statistical Analysis

For information on statistical methods see General Statistics (Sections 2.8, 2.8.1.1, 2.8.1.2, 2.8.1.3 & 2.8.1.4)

4.3 Results

4.3.1 Effect of TaClo on Cellular Superoxide Production

To investigate whether superoxide was produced in SH-SY5Y following TaClo treatment, the well-characterised superoxide indicator dye 2',7'–dichlorofluorescein diacetate (DCFDA) was used. Following entry into the cell by diffusion, DCFDA is deacetylated by cellular esterases to a non-fluorescent compound, which is later oxidized by ROS into 2', 7' –dichlorofluorescin (DCF) (Bass, Parce et al. 1983). DCF is a highly fluorescent compound which can be detected by fluorescence microscopy.

Superoxide levels in SH-SY5Y cells treated with TaClo were imaged by loading the cells with DCFDA. While there was a small level of fluorescence in untreated cells, an apparent increase in fluorescence intensity in TaClo treated cells when compared to control was observed from approximately 8 hours in both 100 & 150µM, but not 0.2% DMSO, treated SH-SY5Y (Fig. 4.1 A-C) suggesting elevated superoxide levels occurred in cells following TaClo treatment and that oxidative stress may play a role in TaClo mediated SH-SY5Y toxicity. Increased fluorescence is seen in all H_2O_2 treated populations confirming the stain (Fig. 4.1 D). At the later time points, the brightest stained cells appear to have a more spherical morphology than those fluorescing less, suggesting that the cells with the highest level of superoxide are losing structural integrity.

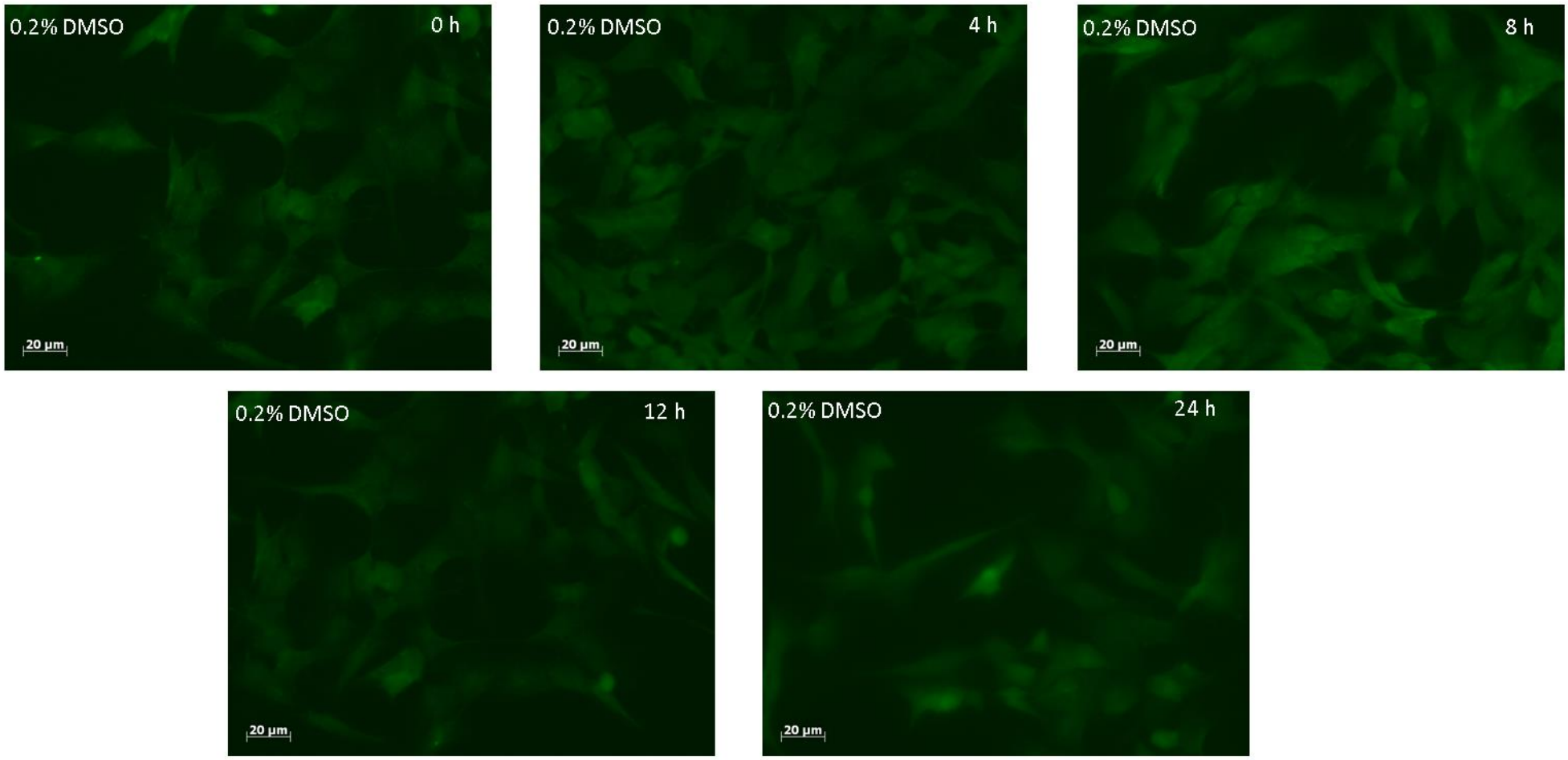

Fig. 4.1 ROS generation in SH-SY5Y cells treated with TaClo SH-SY5Y cells were loaded with DCFDA and then treated with 0.2% DMSO, 100µM TaClo, 150µM TaClo or 850µM H2O2 for 0, 4, 8, 12 or 24 hours. Images show representative fields from 3 replicates (x 40 magnification).

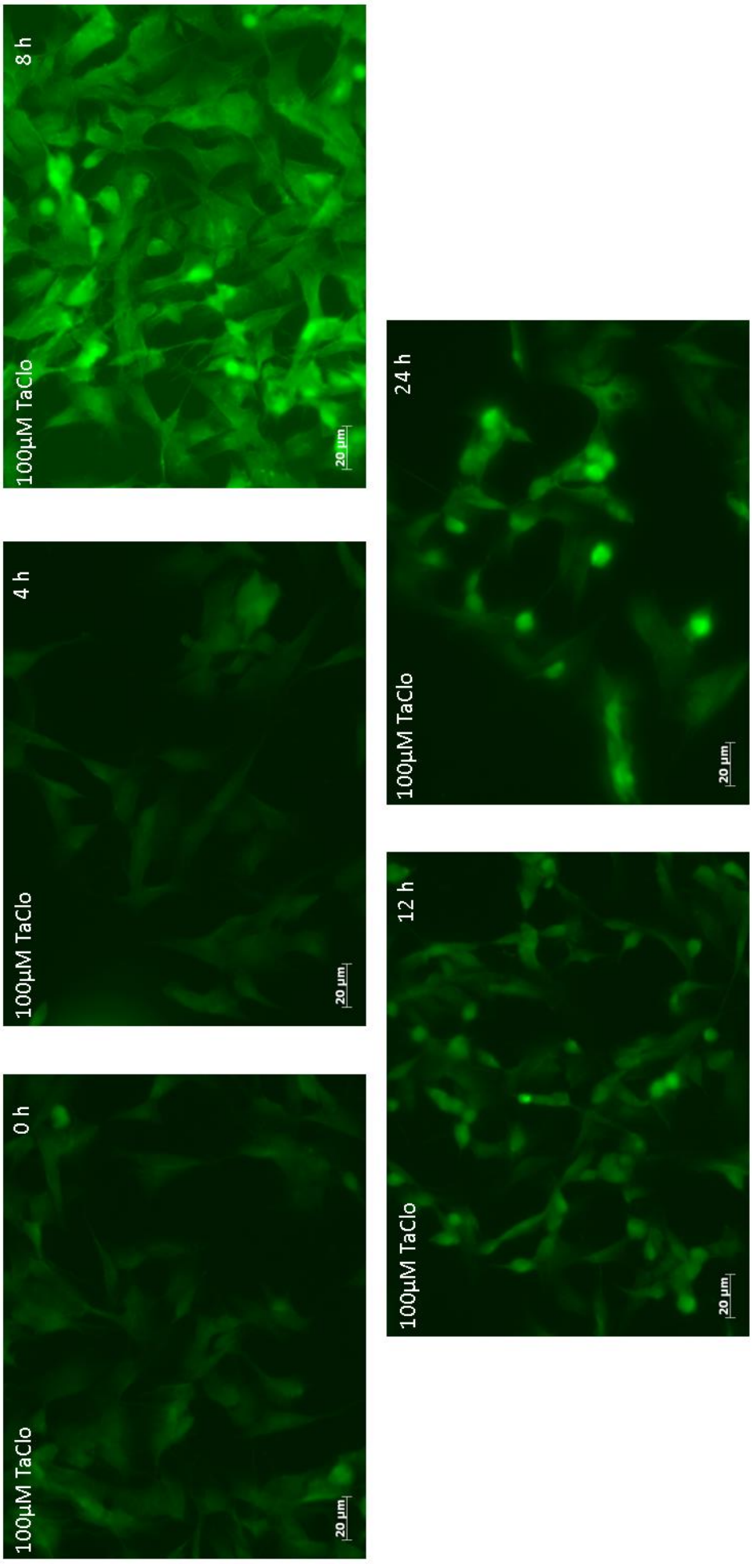

Fig. 4.1 ROS generation in SH-SY5Y cells treated with TaClo (cont.)

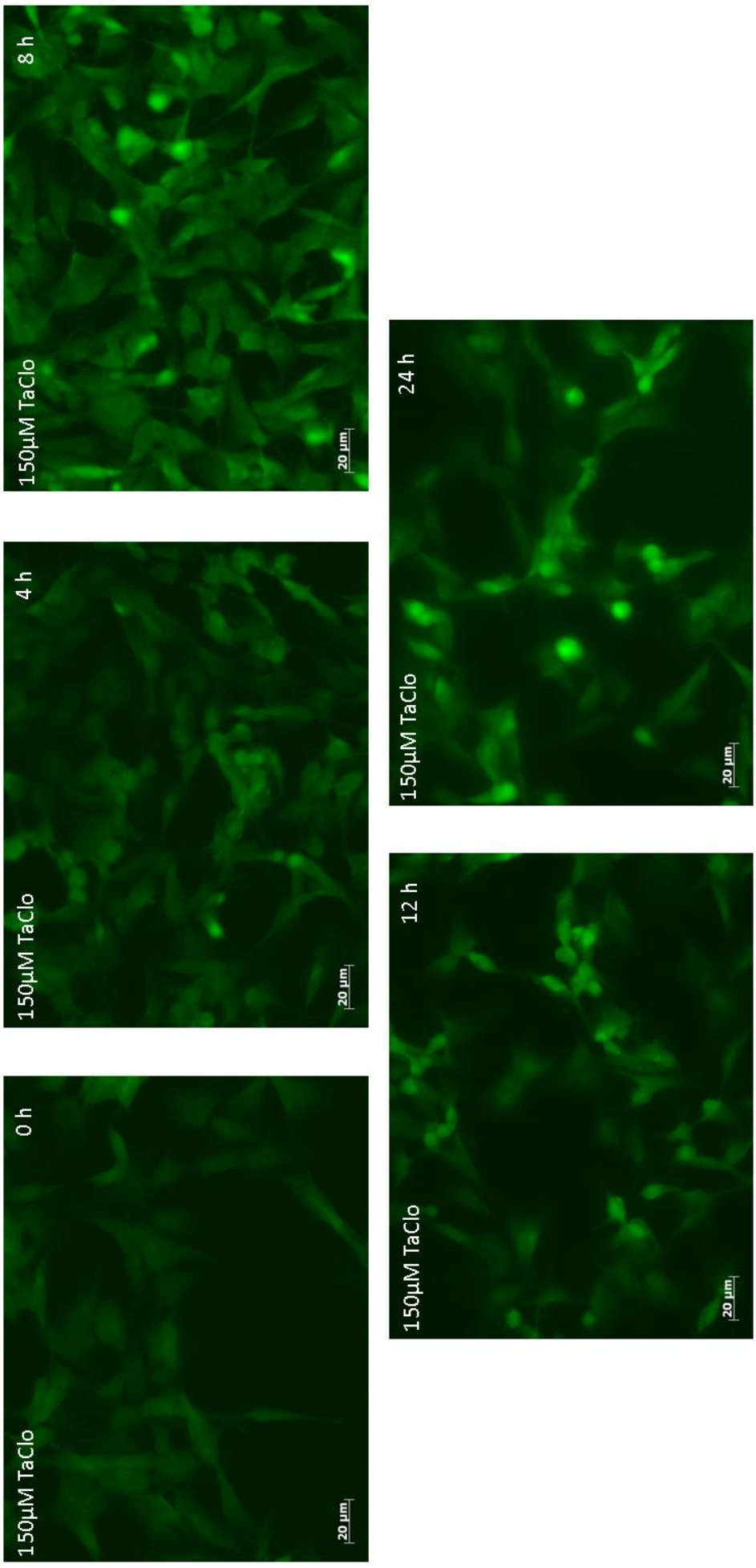

Fig. 4.1 ROS generation in SH-SY5Y cells treated with TaClo (cont.)

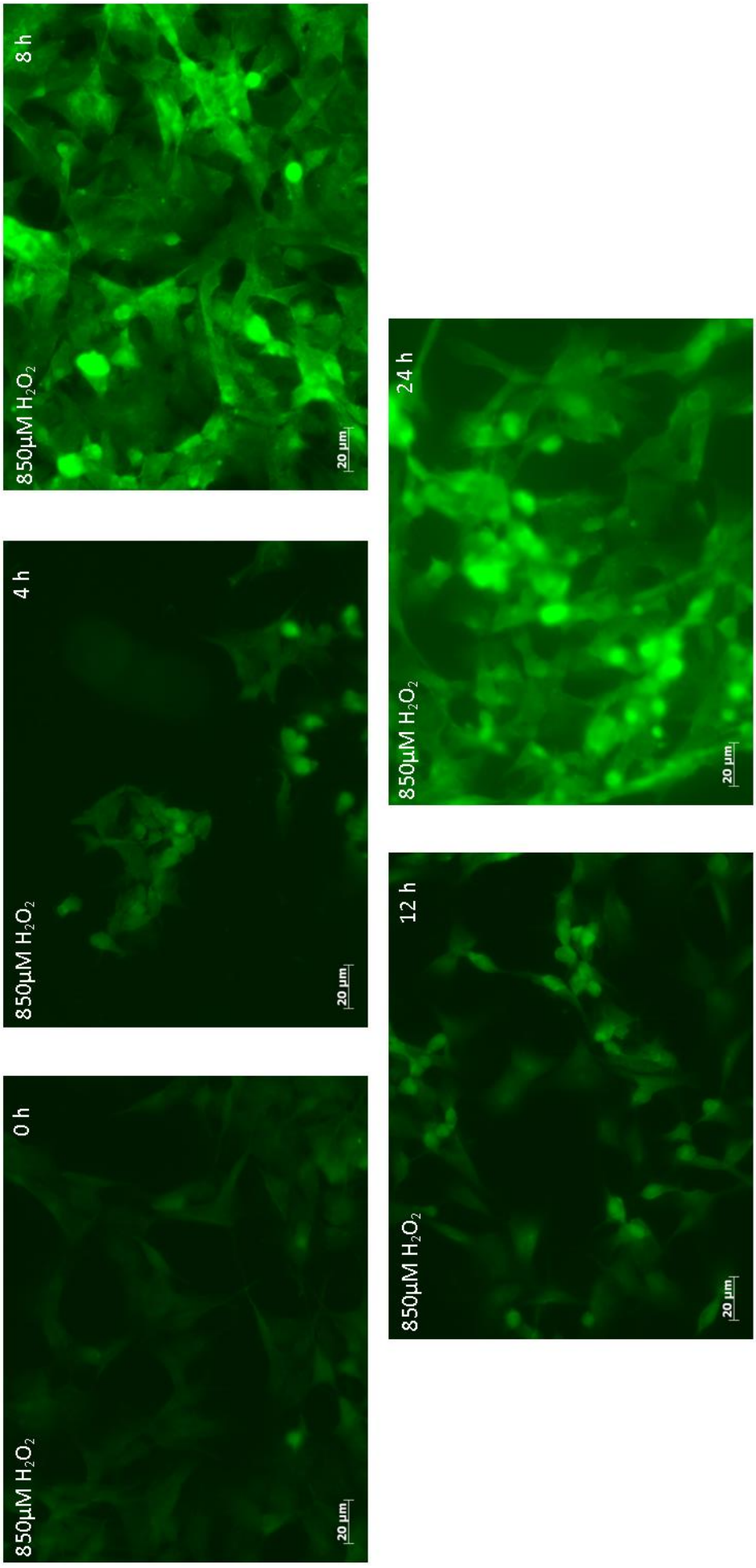

Fig. 4.1 ROS generation in SH-SY5Y cells treated with TaClo (cont.)

4.3.2 GSH and TaClo Toxicity

GSH is an endogenous antioxidant that is up-regulated during oxidative stress (Day, Suzuki et al. 2003). GSH levels in protein isolated from SH-SY5Y cells were assayed at various time points following TaClo treatment by measuring the coloured product 2-nitro-5-thiobenzoic acid formed by the reaction of GSH and DTNB (Shaik and Mehvar 2006). TaClo treatment significantly increased GSH levels in SH-SY5Y ($P<0.001$, One-way ANOVA) in a time-dependent manner with a slight but non-significant increase in GSH levels detected following 8 hours treatment, and an exponential significant increase 12 and 24 hours after treatment ($P<0.05$ and $P<0.001$ respectively, Dunnett's post-test) (Fig. 4.2). This suggests activation of cellular antioxidant defence following TaClo treatment.

L-buthionine sulfoximine (LBS) is known to deplete cellular GSH levels by inhibiting γ-glutamylcysteine synthetase, a rate limiting enzyme in the glutathione biosynthesis pathway (Griffith 1982). SH-SY5Y cells were co-treated with LBS and TaClo and a small but significant increase in TaClo induced toxicity was observed ($P<0.001$, Two-way ANOVA), with LBS significantly reducing viability following 50, 100 and 150µM Taclo treatment ($P<0.05$, $P<0.001$, $P<0.01$ respectively, Bonferroni post-test) (Fig. 4.3). This supports the previous indications that oxidative stress is intrinsically involved in TaClo toxicity as an inhibition of intracellular antioxidant defences leads to an increase in the potency of the toxin.

N-Acetyl Cysteine (NAC) is a precursor molecule for the glutathione, and therefore can promote glutathione production and protect cells from oxidative stress (de Flora, Bennicelli et al. 1985; Issels, Nagele et al. 1988). SH-SY5Y cells were co-treated with toxic doses of chloral or TaClo and NAC (5 & 2.5mM). NAC had no significant effect on chloral toxicity (Fig. 4.4 A), but significantly protected against TaClo induced toxicity in a dose-dependent manner ($P<0.001$, Two-way ANOVA), with 5mM NAC almost totally abrogating toxicity in both 100 & 150µM TaClo treated cells (both $P<0.001$, Bonferroni post-test) bringing viability back up to 85 & 91% of control respectively (Fig. 4.4 B). This suggests a critical involvement of ROS and oxidative stress in the toxic mechanism of TaClo, but not chloral, in SH-SY5Y.

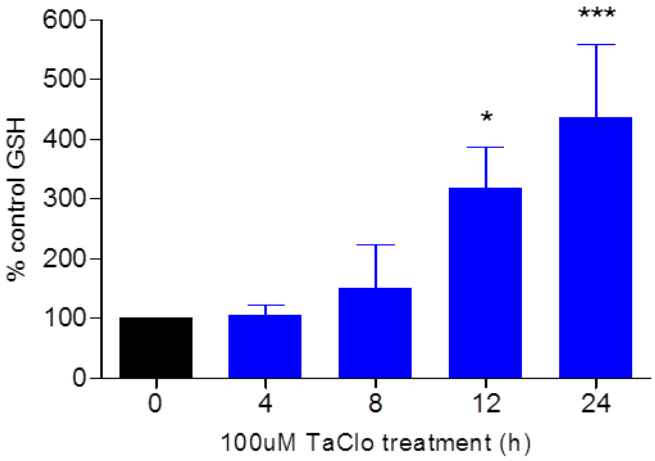

Fig. 4.2 Effect of TaClo on Glutathione levels in SH-SY5Y Protein was isolated from SH-SY5Y neuroblastoma cells treated with 100 µM TaClo for various time points and then assayed for GSH concentration by reduction of DTNB. Data presented as mean % control ± SD from quadruplicate assays (n=3). *** P<0.001, * P<0.05 when compared to 0h, One-way ANOVA & Dunnett's post-test

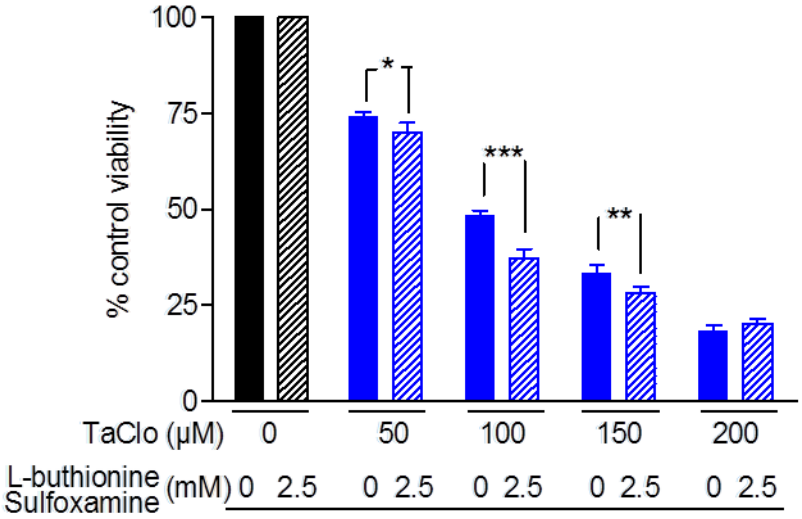

Fig. 4.3 Effect of L-buthionine sulfoxamine on TaClo toxicity in SH-SY5Y SH-SY5Y cells were pre-treated with LBS (2.5mM) for 3 days and then co-treated with TaClo (200, 150, 100 & 50µM) for 21 hours and viability measured by reduction of Alamar Blue (resazurin). Data presented as mean % control ± SD from triplicate assays (n=3). Significant effect of LBS on TaClo toxicity (P<0.001), Two-way ANOVA. ***P<0.001, **P<0.01, *P<0.05 when compared to 0.2% DMSO, Bonferroni post-test

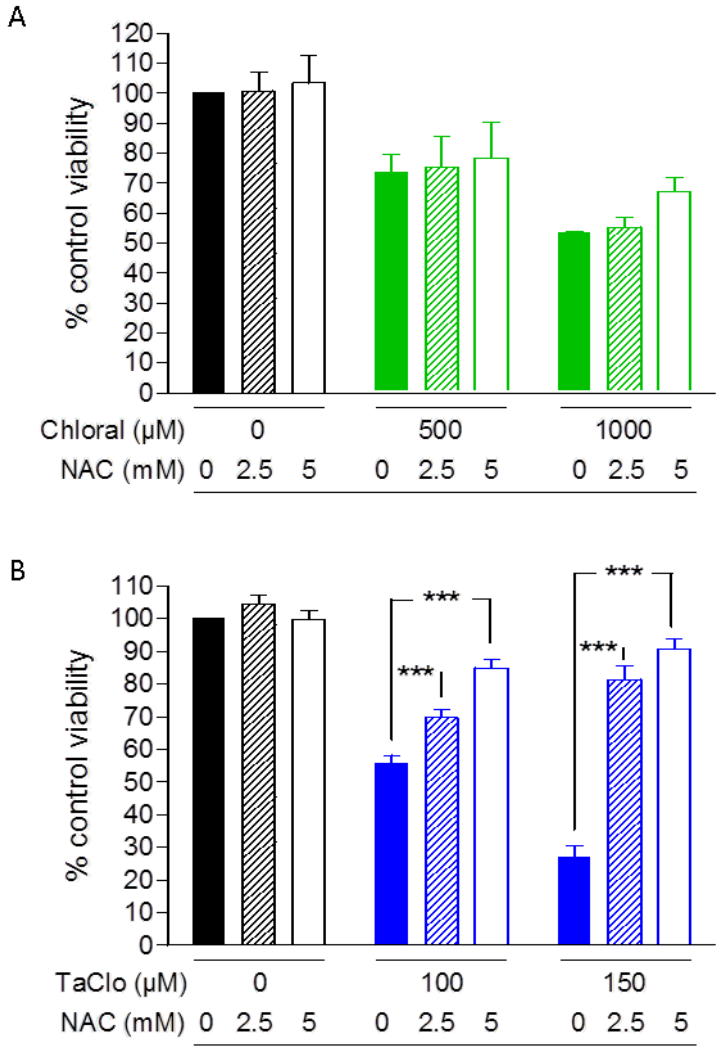

Fig. 4.4 Effect of N-acetylcysteine on chloral & TaClo toxicity in SH-SY5Y SH-SY5Y cells were pre-treated with NAC (2.5 & 5mM) for 1 hour and then co-treated with chloral (2.5 & 5mM) or TaClo (100 & 150μM) for 21 hour and viability measured by reduction of Alamar Blue (resazurin). Data presented as mean % control ± SD from quadruplicate assays (n=3). (A) No significant effect of NAC on chloral treatment (B) Significant effect of NAC on TaClo treatment ($P<0.001$), Two-way ANOVA. ***$P<0.001$ when compared to 0.2% DMSO, Bonferroni post-test

4.3.4 Mitochondrial OXPHOS Activity Assays

Inhibition of Complex I has been widely reported in PD patients and models (Nicklas, Youngster et al. 1987; Mizuno, Ohta et al. 1989; Schapira, Mann et al. 1990; Betarbet, Sherer et al. 2002; Lambert and Brand 2004) as well as disruption of Complexes II & III in PD (Shults, Haas et al. 1997; Rana, De Coo et al. 2000). Therefore, the involvement of TaClo in mitochondrial dysfunction was investigated as a possible site of production of the ROS shown to be involved in toxicity above.

The methods used were based on those of the NHS Mitochondrial Diagnostic Service, Newcastle University, used to diagnose mitochondrial disease in muscle biopsies. In this study Mitochondria were isolated from SH-SY5Y cells and then biochemically assayed for OXPHOS Complex activity in Complex specific assays in the presence of various TaClo concentrations. Pig heart mitochondria were used to confirm assay function on every study day and normal ranges for them and SH-SY5Y mitochondria are listed in Table 4.1.

Complex	PHM* (1:20 dilution)	SH-SY5Y (1:5 dilution)
I	6.93 $\pm$ 1.67	0.79 $\pm$ 0.27
II	10.2 $\pm$ 1.32	0.83 $\pm$ 0.26
I/II	0.68 $\pm$ 0.16	0.94
III	64.00 $\pm$ 14.7	6.72 $\pm$ 3.43
IV	56.78 $\pm$ 9.91	9.92 $\pm$ 1.76

***** Taken from standard operating procedures of Mitochondrial Diagnostic Service, Newcastle University which were generated from a library of results.

Table 4.1 Normal ranges of OXPHOS Complex I, II, III & IV Normal ranges of OXPHOS Complex I (nmols NADH oxidised. min-1 unit citrate synthase^{-1}), II (nmols DCPIP reduce. min-1 unit citrate synthase^{-1}), III (K.sec^{-1}) & IV (x 10^{-3} K.sec^{-1}/unit citrate synthase^{-1}) in untreated pig heart (PHM) and SH-SY5Y mitochondria.

4.3.4.1 TaClo

Complex I activity in SH-SY5Y generated mitochondria was significantly reduced by >10µM TaClo in a dose-dependent manner with an IC_{50} of approximately 50µM (Fig. 4.5). This can also be seen in the example traces (Fig. 4.6) with the slope of the red line (representing the rate of NADH oxidation, corresponding to Complex I activity) prior to rotenone addition at 5 minutes (arrow) decreasing as TaClo concentrations increase. As inhibition of Complex I has been shown to cause generation of superoxide (Lambert and Brand 2004), this suggests mitochondrial dysfunction may be a source of the oxidative damage in the neurotoxic mechanism of TCE mediated by TaClo.

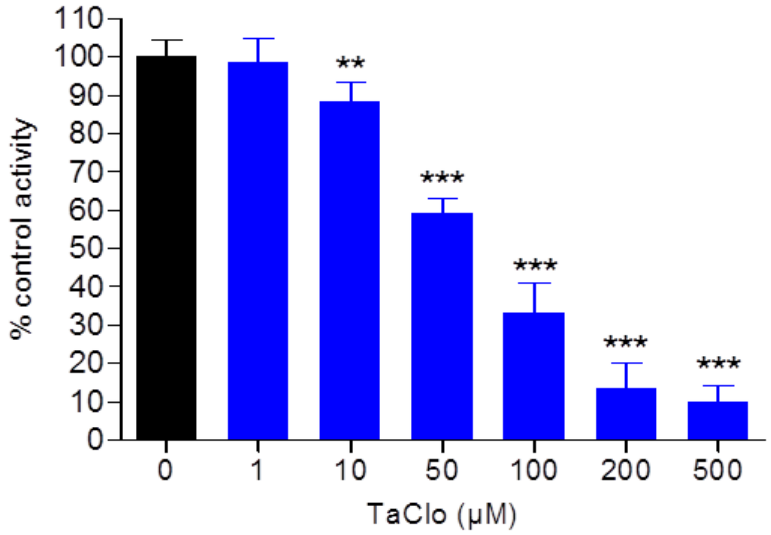

Fig. 4.5 Acute Effect of TaClo on OXPHOS Complex I activity in SH-SY5Y mitochondria OXPHOS Complex I activity in mitochondria isolated from SH-SY5Y cells treated with TaClo (500, 200, 100, 50, 10 & 1µM) or control (0.2% DMSO) as measured as rotenone-sensitive NADH: ubiquinone oxidoreductase activity. Data presented as mean & control ± SD from triplicate assays (n=3). *** P<0.001, ** P<0.01 when compared to 0.2% DMSO, One-way ANOVA & Dunnett's post-test.

Treatment	Mean Complex I activity (µM/min)	Mean Complex II activity (µM/min)	CI/CII
0.2% DMSO	0.79 ± 0.27	0.83 ± 0.26	0.94
100uM TaClo	0.26*** ± 0.10	0.87 ± 0.23	0.30***
500uM TaClo	0.07*** ± 0.02	0.74 ± 0.18	0.09***

Table 4.2 Summary of the effects of TaClo on mitochondrial Complex I & II OXPHOS Complex I & II activity in mitochondria isolated from SH-SY5Y cells treated with TaClo (500 & 100µM) or control (0.2% DMSO) as measured as rotenone-sensitive NADH: ubiquinone oxidoreductase (CI) or succinate: ubiquinone oxioreductase (CII) activity. Data presented as mean ± SD from triplicate assays (n=3). *** P<0.001, when compared to 0.2% DMSO, One-way ANOVA & Dunnett's post-test.

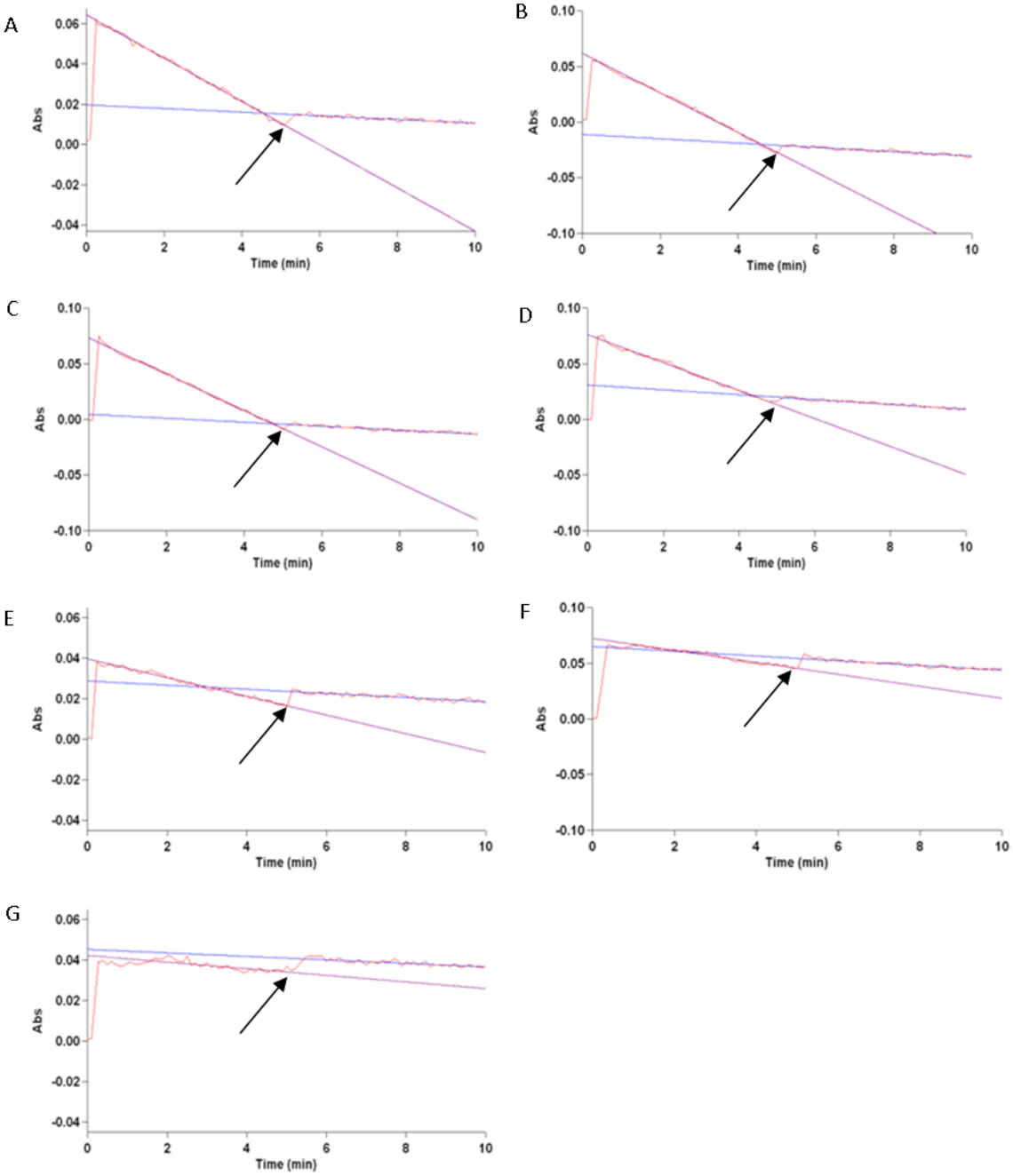

Fig. 4.6 Sample traces for the acute effect of TaClo on OXPHOS Complex I activity in SH-SY5Y mitochondria OXPHOS Complex I activity in mitochondria isolated from SH-SY5Y cells treated with TaClo (500, 200, 100, 50, 10 & 1µM) or control (0.2% DMSO) as µmols NADH oxidised/min (red line). Sample traces from (A) 0.2% DMSO, (B) 1µM TaClo, (C) 10µM TaClo, (D) 50µM TaClo, (E) 100µM TaClo, (F) 200µM TaClo& (G) 500µM TaClo. Blue lines are programme generated gradients pre & post rotenone (5µM) addition (arrow) at ~5 min to account for non-Complex I driven NADH oxidation.

Exposure of Complexes III, and IV to TaClo resulted in a significant decrease in activity in Complexes III & IV at a TaClo dose of 500µM, but no effect was observed following 100 µM exposure (Fig. 4.7). No inhibition of Complex II was seen following exposure to either 100 or 500µM TaClo (Fig. 4.7). This can be seen in the sample traces, with no change in the slope of the line of Complex II, III or IV function apparent following addition of mitochondria in 100µM treated assay but a decrease in the slope following 500µM TaClo treatment in Complex III & IV but not II traces (Fig. 4.8). Complex I:II ratio is a widely used measure of mitochondrial function, and this was significantly reduced in a dose dependent manner following TaClo treatment (Table 4.2).

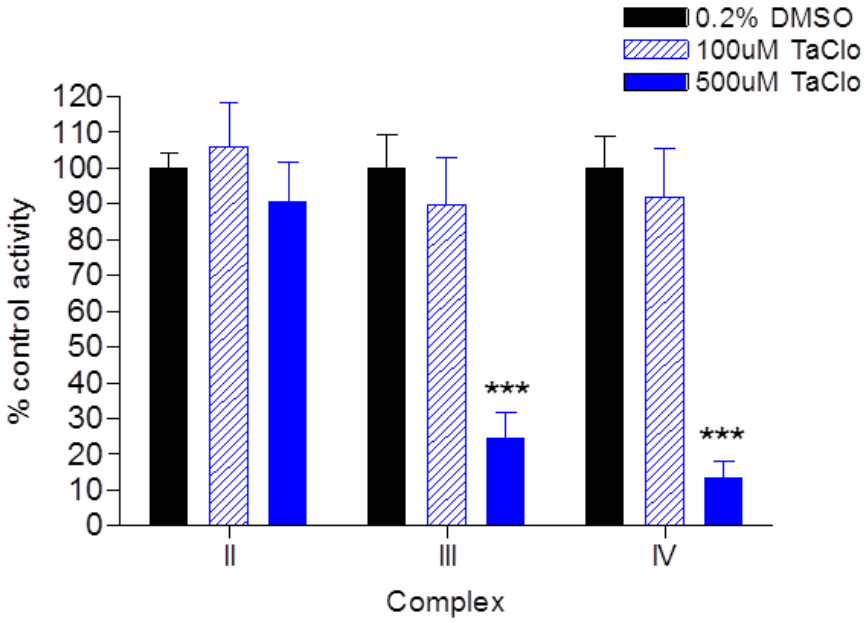

Fig. 4.7 Acute Effect of TaClo on OXPHOS Complex II, III & IV activity in SH-SY5Y mitochondria
OXPHOS Complex II, III & IV activity in mitochondria isolated from SH-SY5Y cells treated with TaClo (500 & 100µM) or control (0.2% DMSO) as measured by succinate: ubiquinone oxioreductase (CII), reduction of oxidised cytochrome c due to the oxidation of ubiquinol-2 (CIII) or oxidation of cytochrome c (II) (CIV) activity respectively. Data presented as mean % control ± SD from triplicate assays (n=3). *** P<0.001 when compared to 0.2% DMSO, One-way ANOVA & Dunnett's post-test.

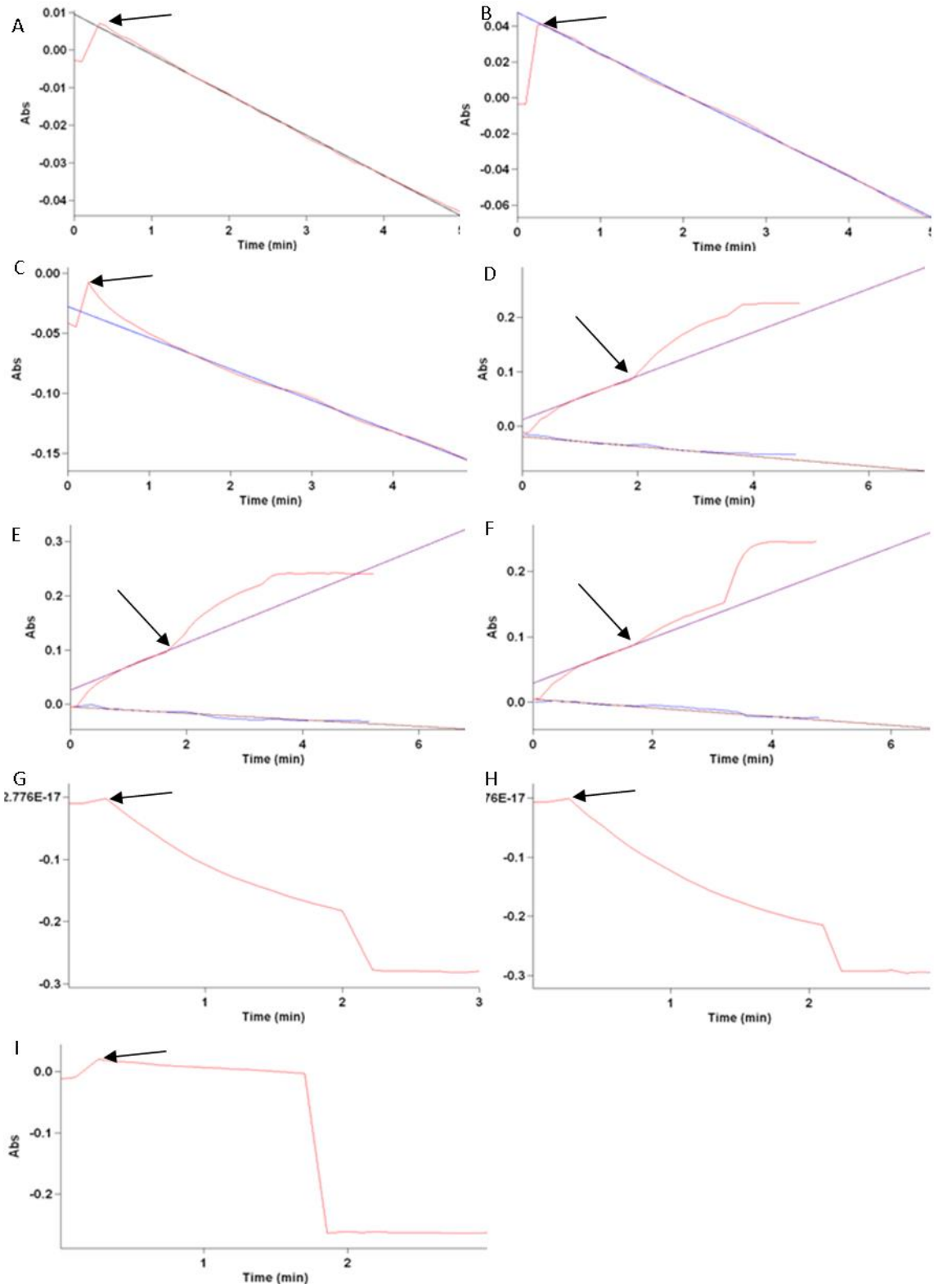

Fig. 4.8 Sample traces for the acute effect of TaClo on OXPHOS Complex II, III & IV activity in SH-SY5Y mitochondria OXPHOS Complex II, III & IV activity in mitochondria isolated from SH-SY5Y cells treated with TaClo (500 & 100µM) or control (0.2% DMSO) as measured as succinate: ubiquinone oxioreductase (CII), reduction of oxidised cytochrome c due to the oxidation of ubiquinol-2 (CIII) or oxidation of cytochrome c (II) (CIV) respectively (red line). Sample traces from Complex II (A) 0.2% DMSO, (B) 100µM TaClo, (C) 500µM TaClo, Complex III (D) 0.2% DMSO, (E) 100µM TaClo, (F) 500µM TaClo, Complex IV (G) 0.2% DMSO, (H) 100µM TaClo, (I) 500µM TaClo. Blue lines are programme generated gradients (non-enzymatic cytochrome c reduction in Complex III graph). Arrows represent mitochondrial addition.

4.3.4.2 Chloral

As chloral has also been shown to be toxic to DA neurons in models above, the activity of OXPHOS Complexes I-IV was also investigated in relation to chloral toxicity. Interestingly, chloral showed a different inhibitory profile of OXPHOS Complexes in comparison to TaClo. 500µM chloral significantly and almost completely inhibited Complexes I and II but only showed a slight, although statistically significant inhibition of Complex IV (Fig. 4.9), concentrations of 100µM and below showed no significant inhibition (data not shown). This is in contrast to TaClo which showed Complex I inhibition at relatively low concentrations and inhibition of Complex III and IV at higher concentrations, but no inhibition of Complex II at all. Although the high chloral concentrations needed for OXPHOS Complex inhibition may not be physiologically relevant, the fact that it shows a different toxicity profile to TaClo questions the hypothesis that chloral toxicity is mediated through conversion to TaClo.

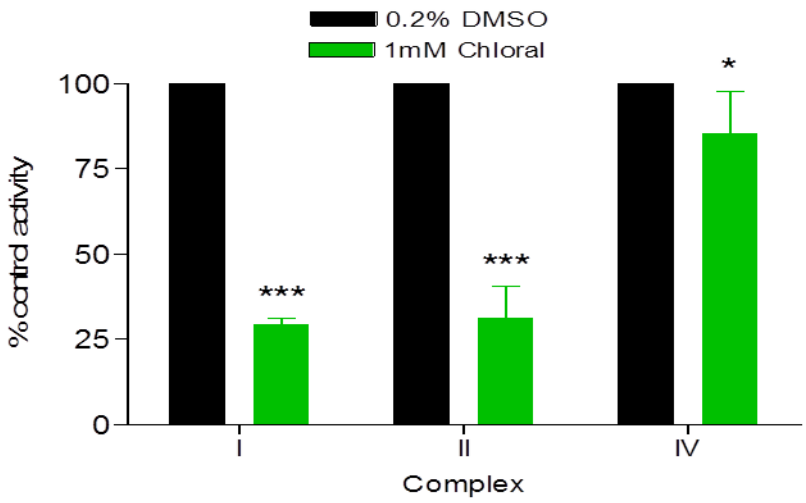

Fig. 4.9 Acute effect of Chloral on OXPHOS Complex I, II &IV activity in SH-SY5Y mitochondria
OXPHOS Complex I, II & IV activity in mitochondria isolated from SH-SY5Y cells treated with Chloral (1mM) or control (0.2% DMSO) as measured by NADH: ubiquinone oxidoreductase activity (CI), succinate: ubiquinone oxioreductase (CII), or oxidation of cytochrome c (II) (CIV) activity respectively. Data presented as mean % control ± SD from triplicate assays (n=3). ***P<0.001, *<P<0.05 when compared to 0.2% DMSO, unpaired t-test.

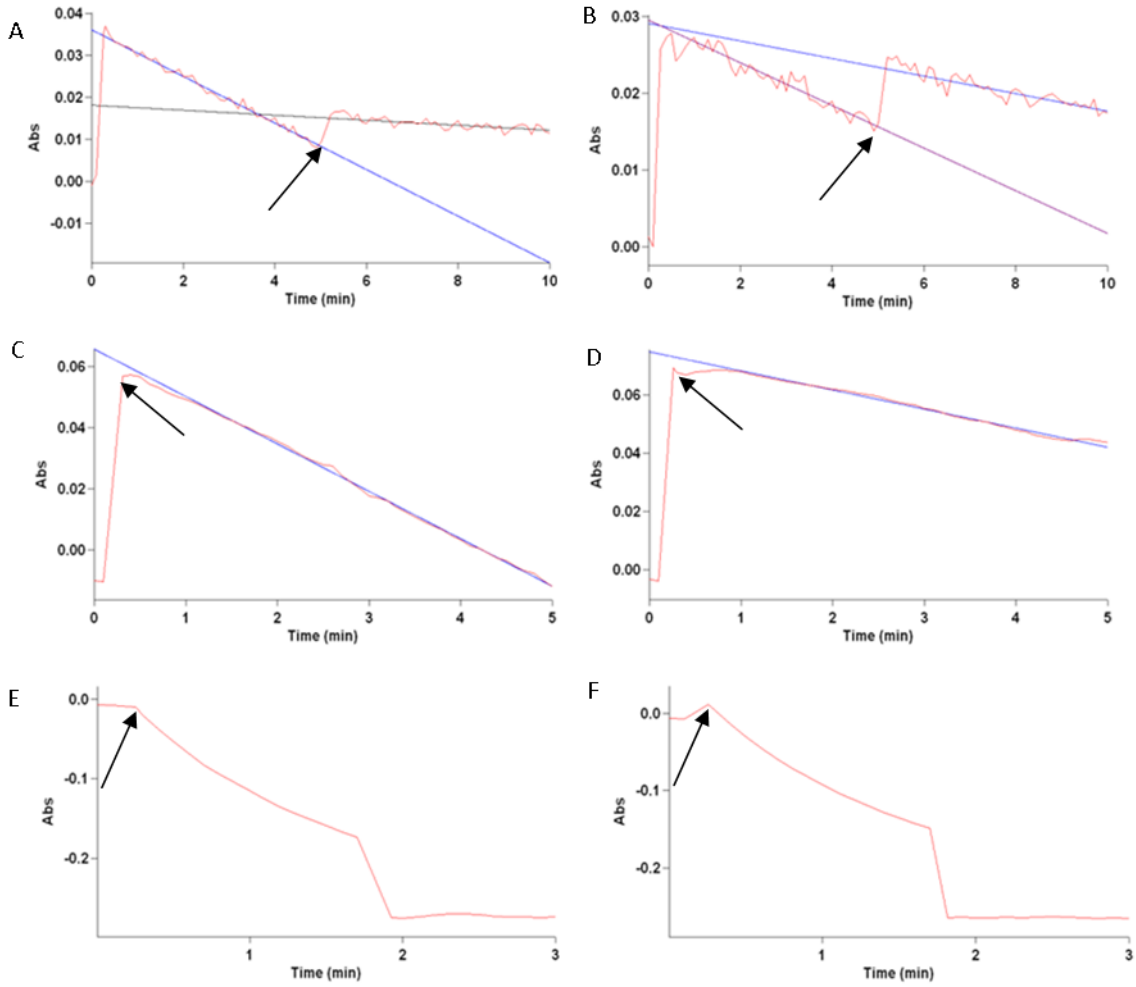

Fig. 4.10 Sample traces for the acute effect of Chloral on OXPHOS Complex I, II & IV activity in SH-SY5Y mitochondria OXPHOS Complex I, II & IV activity in mitochondria isolated from SH-SY5Y cells treated with chloral (1mM) or control (0.2% DMSO) as measured as rotenone-sensitive NADH: ubiquinone oxidoreductase (CI), succinate: ubiquinone oxioreductase (CII) or oxidation of cytochrome c (II) (CIV) respectively (red line). Sample traces from Complex I (A) 0.2% DMSO, (B) 1mM chloral, Complex II (C) 0.2% DMSO, (D) 1mM chloral, Complex IV (E) 0.2% DMSO, (F) 1mM chloral. Blue lines are programme generated gradients (pre & post rotenone (5µM) addition at ~5 min in CI). Arrows represent (A & B) rotenone or (C-D) mitochondrial addition.

When assessing Complex III activity, the oxidation of ubiquinol-2 with cytochrome *c* as the electron acceptor is used as an indicator of function, with the colour change due to cytochrome *c* reduction measured. In this assay there is a background level of cytochrome *c* reduction that occurs sporadically without ubiquinol-2 or mitochondria present which is measured prior to the assay to enable an accurate calculation of the reduction dependent on Complex III. However, when chloral is present in the assay, the sporadic, non-enzymatic, reduction of cytochrome *c* is inhibited in a dose-dependent manner with doses as low as 100µM chloral causing significant inhibition (Fig. 4.11). This can be seen in the sample traces that show a decrease in the slope representing cytochrome *c* activity in a dose dependent manner (Fig. 4.12). This invalidates the assay and does not allow the accurate measurement of the effect of chloral on Complex III activity but suggests chloral may inhibit the electron accepting properties of cytochrome *c*.

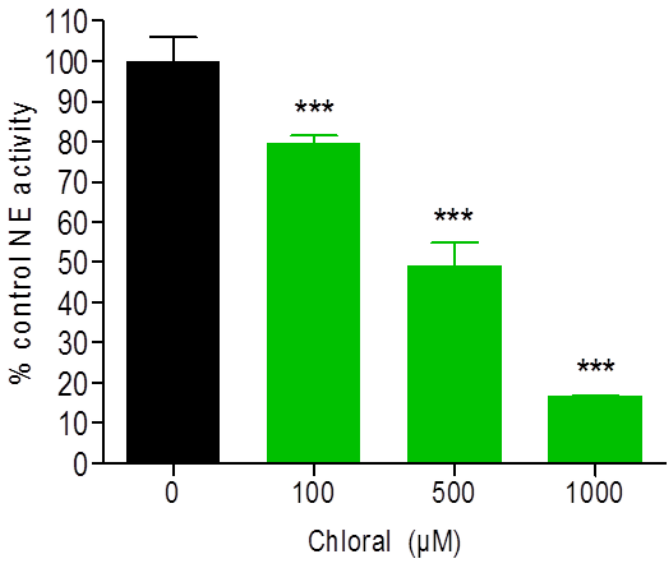

Fig. 4.11 Effect of Chloral on the non-enzymatic reduction of cytochrome *c* (oxidised) Non-enzymatic reduction of cytochrome c by various concentrations of Chloral or control (0.2% DMSO). Data presented as mean % control ± SD from triplicate assays (n=3). *** P<0.001 when compared to 0.2% DMSO, One-way ANOVA & Dunnett's post-test.

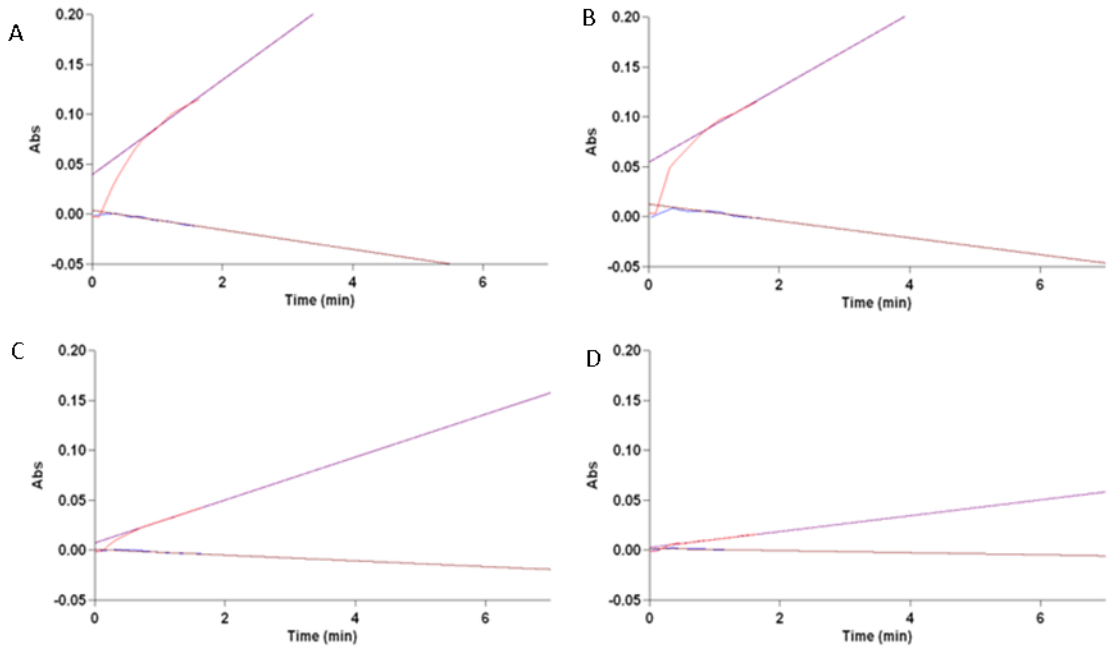

Fig. 4.12 Sample traces for the effect of Chloral on the non-enzymatic reduction of cytochrome c (oxidised) Non-enzymatic reduction of cytochrome c by various concentrations of Chloral or control (0.2% DMSO) (red line). Sample traces from (A) 0.2% DMSO, (B) 100µM chloral, (C) 500µM chloral, (D) 1mM chloral. Blue lines are programme generated gradients.

4.3.5 Mitochondrial Oxidative Stress and TaClo Toxicity

To determine the production of superoxide in the mitochondria following TaClo treatment we used the mitochondrially specific fluorescent superoxide indicator MitoSOX™ Red. MitoSOX™ Red reagent is live-cell permeant and is rapidly and selectively targeted to the mitochondria. Once in the mitochondria, MitoSOX™ Red reagent is oxidized by superoxide, but not other ROS or reactive nitrogen species (RNS), and exhibits red fluorescence. SH-SY5Y were treated with toxic concentrations of TaClo for various amounts of time before loading with MitoSOX™ Red and then imaged or fluorescence measured by flow cytometry.

Representative images of MitoSOX™ Red fluorescence in TaClo treated cells are shown in Fig. 4.13, with an increase in fluorescence apparent from 4 hours in 100 & 150µM TaClo and H_2O_2 treated populations. Flow cytometrically assessed whole single cell populations were selected using a plot of FSC-A, which measures cell size, against SSC-A, the latter measuring cell shape or granularity, (Fig. 4.14 A) and fluorescence levels were measured within this population. There appeared to be 3 distinct populations seen on the fluorescence histograms so gates were set for high, mid and low fluorescence based upon these populations (Fig. 4.14 B).

To examine the basic increase in MitoSOX™ Red fluorescence, mid and high populations were combined and a time and dose-dependent increase in fluorescence was observed in both 100 & 150µM treated SH-SY5Y cells relative to control (Fig. 4.14 C) ($P<0.001$, Two-way ANOVA). 150µM TaClo treated cells seemed to show more mitochondrial superoxide production after 4 hours (Fig. 4. 14 C) with a significant increase in the number of cells (30%) showing high fluorescence at 8 ($P<0.05$) hours post treatment and almost all the cells (98%) present in the high fluorescing population by 16 hours ($P<0.001$) (Fig. 4.14 C). In the 100µM treated cells, mitochondrial superoxide production was slower, with a slight increase in MitoSOX™ Red fluorescence appearing to occur at 4 & 8 hours post dose (Fig. 4.14 B), but a significant increase in cell number not occurring until 16 hours ($P<0.001$) hours in 54% of cells and almost all cells (97%) showing high fluorescence by 24 hours ($P<0.001$) (Fig. 4.14 C). These results suggest that mitochondrial superoxide formation is increased as a relatively early event in TaClo mediated SH-SY5Y toxicity.

When looking at the distribution of cells between the high, mid and low populations, the majority of the 0.2% DMSO treated cells stay in the low fluorescing population (Fig. 4.14 Di), which correlates with imaged cells (Fig. 4.13 A). 100µM treated SH-SY5Y showed a time-dependent increase in mid fluorescing cells from 0 -24 hours post TaClo, but only showed an increase in the high fluorescing population at 16 and 24 hours (Fig. 4.14 Dii). In the 150µM

treated cells, there was also a time-dependent increase in the mid fluorescing population up to 12 hours, where it stabilised and then started to decrease at 24 hours post dose, as well as a time-dependent increase in high fluorescing cells from 12 hours, with the majority of the cells in this population by 24 hours (Fig 4.14 Diii). This is consistent with the imaged cells, with a population of cells that are more fluorescent than those seen in the control groups present for all treated cells, and then a population that is brighter again and seems to be morphologically more spherical that the other populations (Fig. 4.13 A-C). The positive control stained H_2O_2 treated SH-SY5Y showed bright fluorescence in all treated cell populations from 4-24 hours after treatment, confirming the activity of the dye (Fig. 4.13 D). The spread of the populations over time is reasonably similar to the results seen with the flow cytometry, however, in the imaged 100µM treated group, there appears to be an increase in the high fluorescing cells not seen in those analysed by flow cytometry.

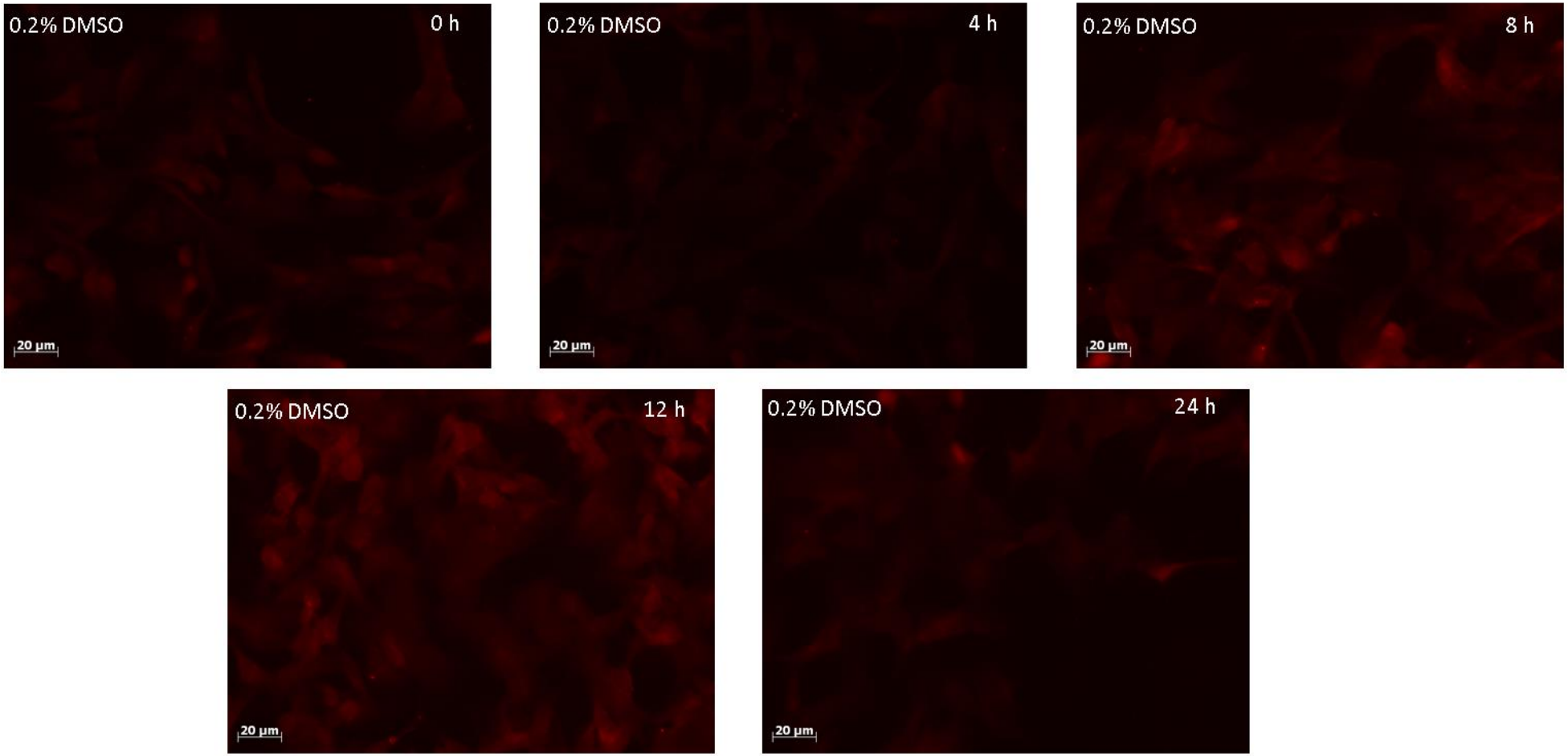

Fig. 4.13 Mitochondrial ROS generation in SH-SY5Y cells treated with TaClo SH-SY5Y cells were loaded with MitoSOX^{TM} Red and then treated with 0.2% DMSO, 100µM TaClo, 150µM TaClo or 850µM H2O2 for 0, 4, 8, 12 or 24 hours. Images show representative fields from 3 replicates (x 40 magnification).

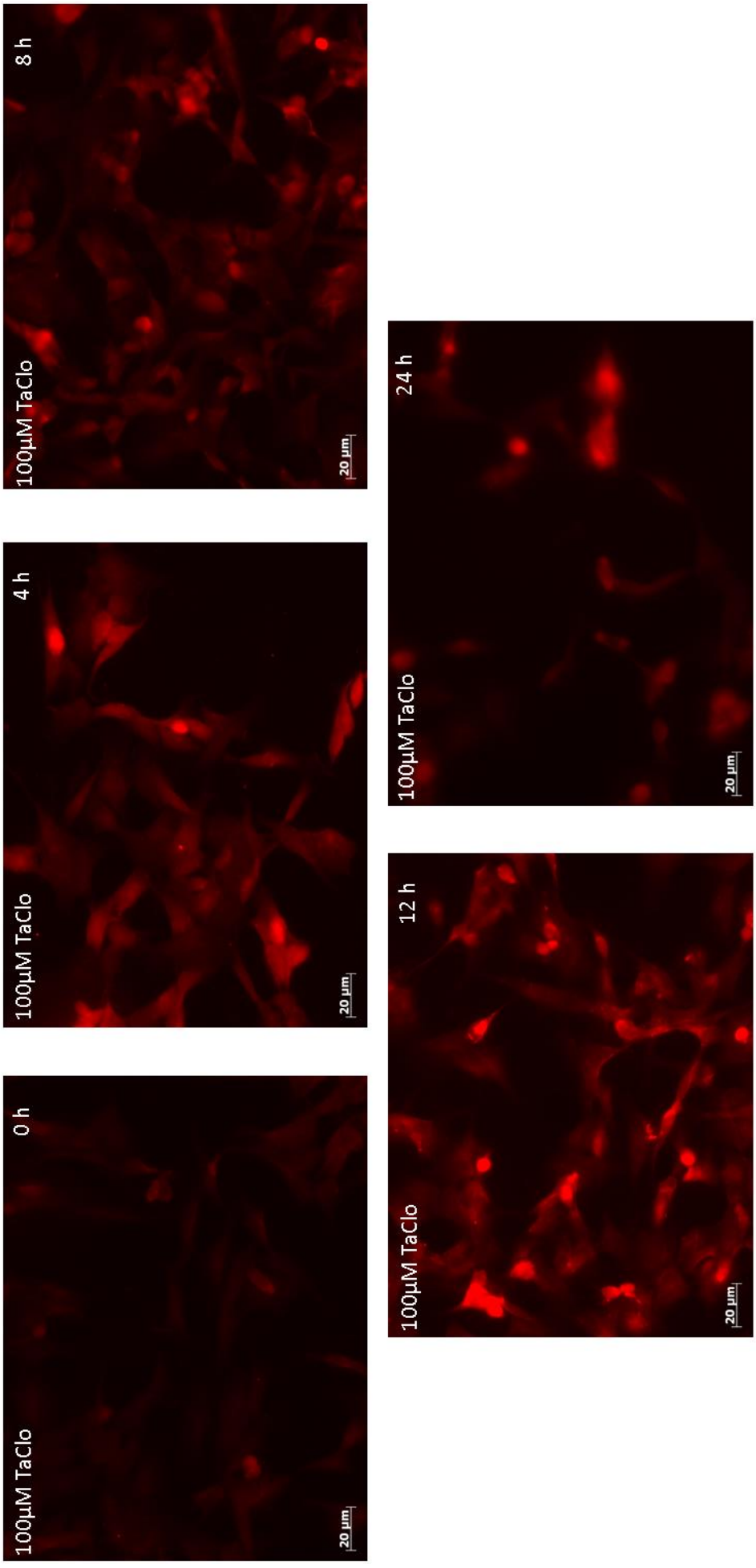

Fig. 4.13 Mitochondrial ROS generation in SH-SY5Y cells treated with TaClo (cont.)

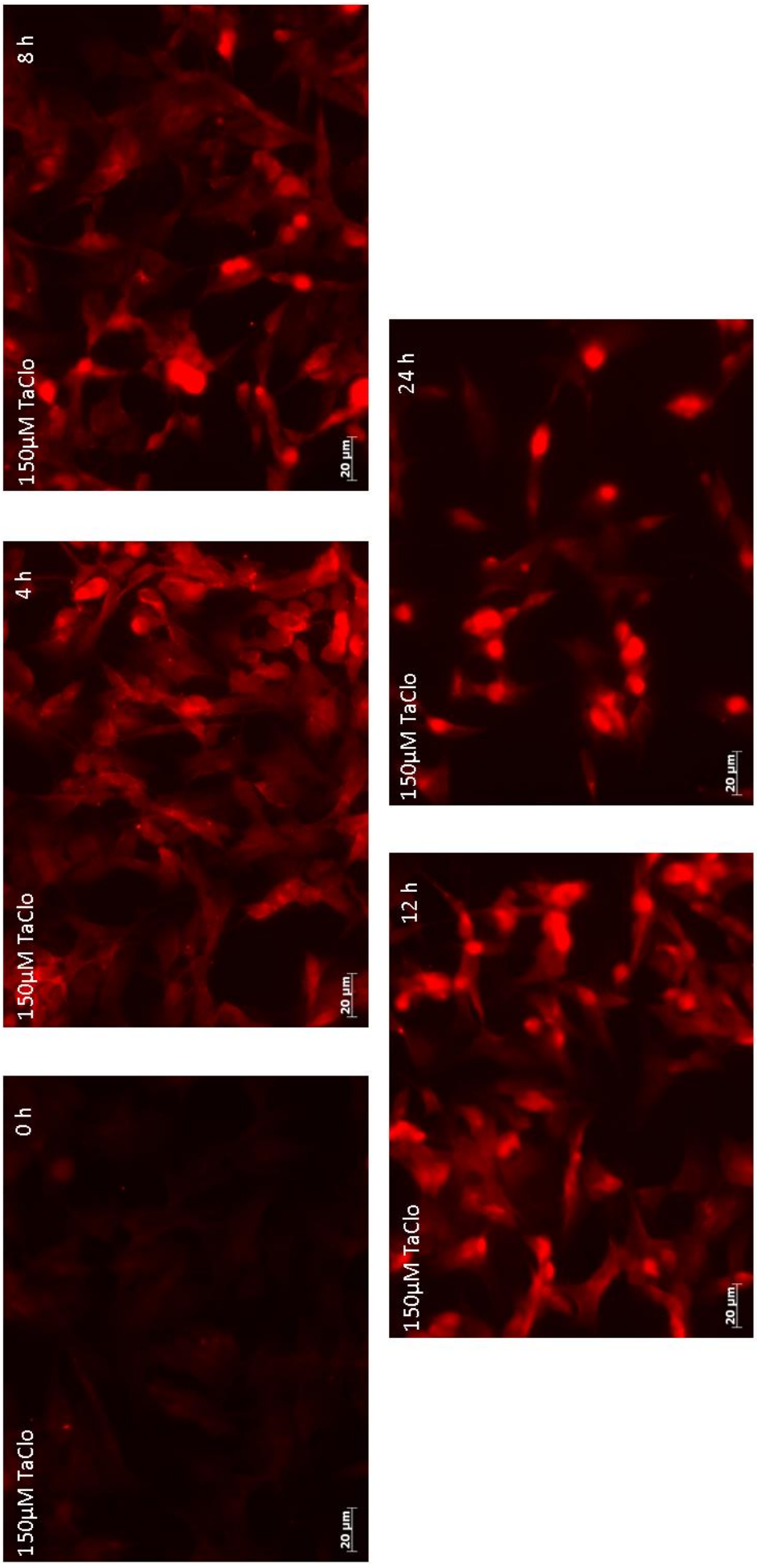

Fig. 4.13 Mitochondrial ROS generation in SH-SY5Y cells treated with TaClo (cont.)

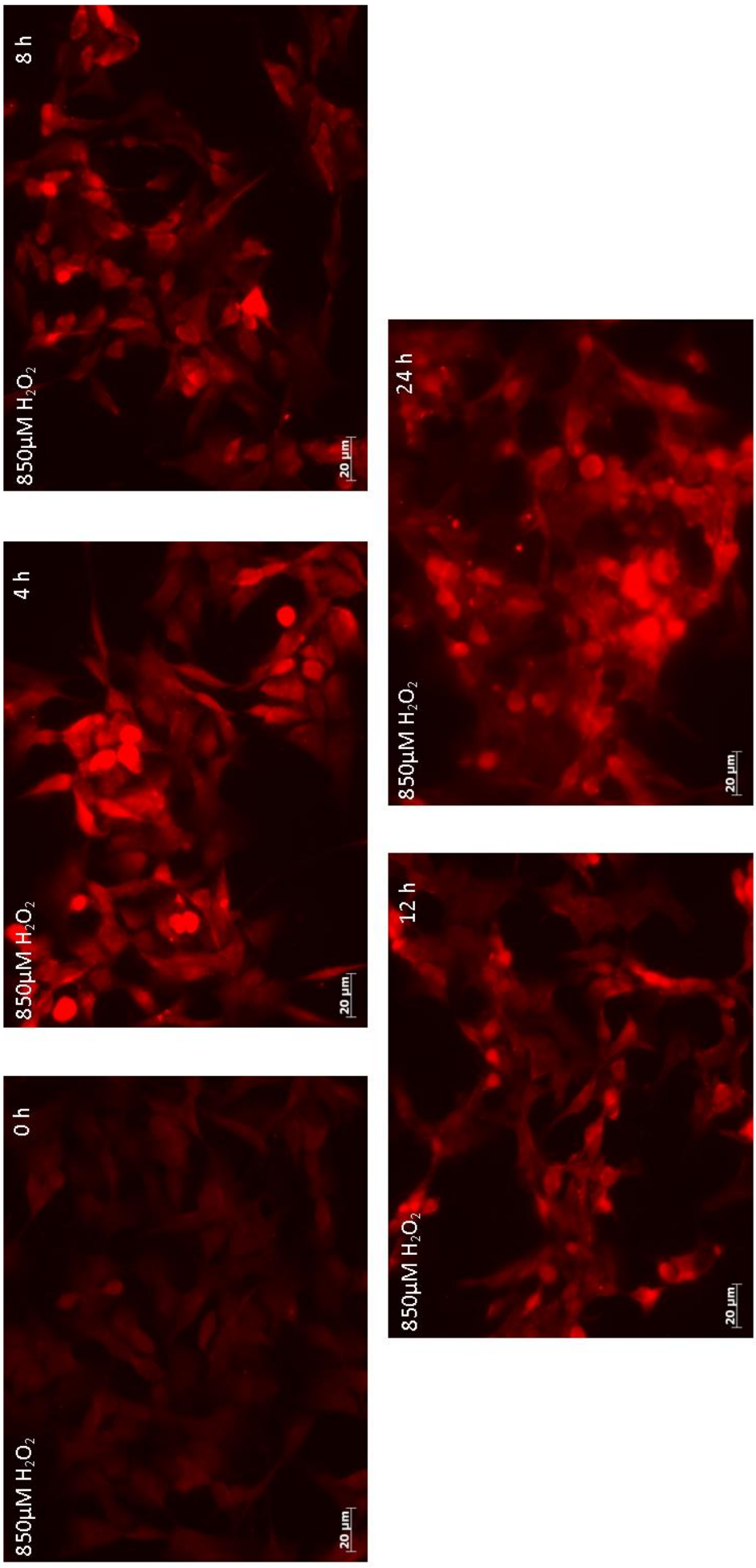

Fig. 4.13 Mitochondrial ROS generation in SH-SY5Y cells treated with TaClo (cont.)

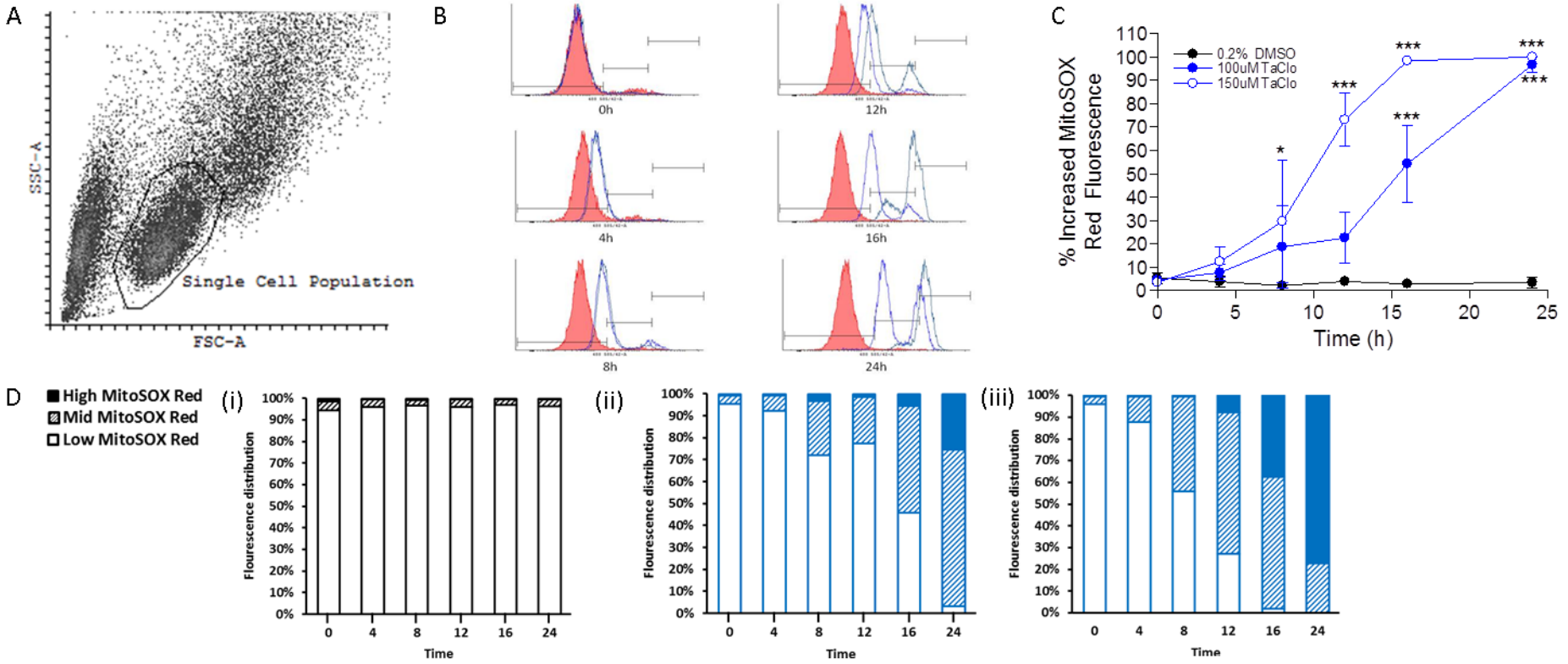

Fig. 4.14 Effect of TaClo treatment on MitoSOX^{TM} Red fluorescence TaClo treatment as quantified by flow cytometry SH-SY5Y were treated with 0.2% DMSO, 100 or 150µM TaClo for 0-24 hours and then loaded with 5µM MitoSOX^{TM} Red before fluorescence was assessed using flow cytometry. (A) Representative density plot showing selection of whole single cells based on SSC-A and FSC-A. (B) Representative overlaid histograms of selected single cell fluorescence at ex/em 488/585 at all time points. Bars show defined low, medium and high fluorescing population boundaries. (C) % Cells defined as having increased (medium or high) fluorescence over time following treatment. Data presented as mean ± SD (n=3). Significant increase in fluorescence over time (P<0.001), Two-way ANOVA. ***P<0.001, *P<0.05 when compared to 0.2% DMOS at same time point, Bonferroni post-test. (D) % cells defined as low, medium or high fluorescence following (i) 0.2% DMSO, (ii) 100 or (iii) 150µM TaClo. Data presented as mean + SD (n=3).

MnSOD is an enzyme found in the mitochondria (Weisiger and Fridovich 1973) that protects against superoxide induced oxidative damage by catalysing the dismutation of superoxide into oxygen and hydrogen peroxide (McCord, Keele Jr et al. 1971).

SH-SY5Y cells were treated with a shRNA containing lentiviral vector to overexpress MnSOD levels in order to investigate the involvement of mitochondrially generated superoxide in TaClo toxicity. Viral take-up was good, as seen by the viral conferred GFP expression relative to inherent DAPI staining (Fig. 4.15 A i-iii), and probing for MnSOD levels by Western blot showed expression increased to ~5-fold that seen in control (Fig. 4.15 B). MnSOD overexpressing control SH-SY5Y cells were then treated with TaClo (20-250µM) and viability assayed by Alamar Blue fluorescence confirmed by visual inspection. MnSOD overexpression showed a small, but significant, protection against TaClo toxicity when compared to control cells ($P<0.05$, Two-way ANOVA) with an increase in viability seen when compared to control in 20, 50 & 100µM TaClo treated cells (Fig. 4.15 C). At doses of >150 µM TaClo, almost total cell death was seen and no protection was seen with MnSOD overexpression at these levels.

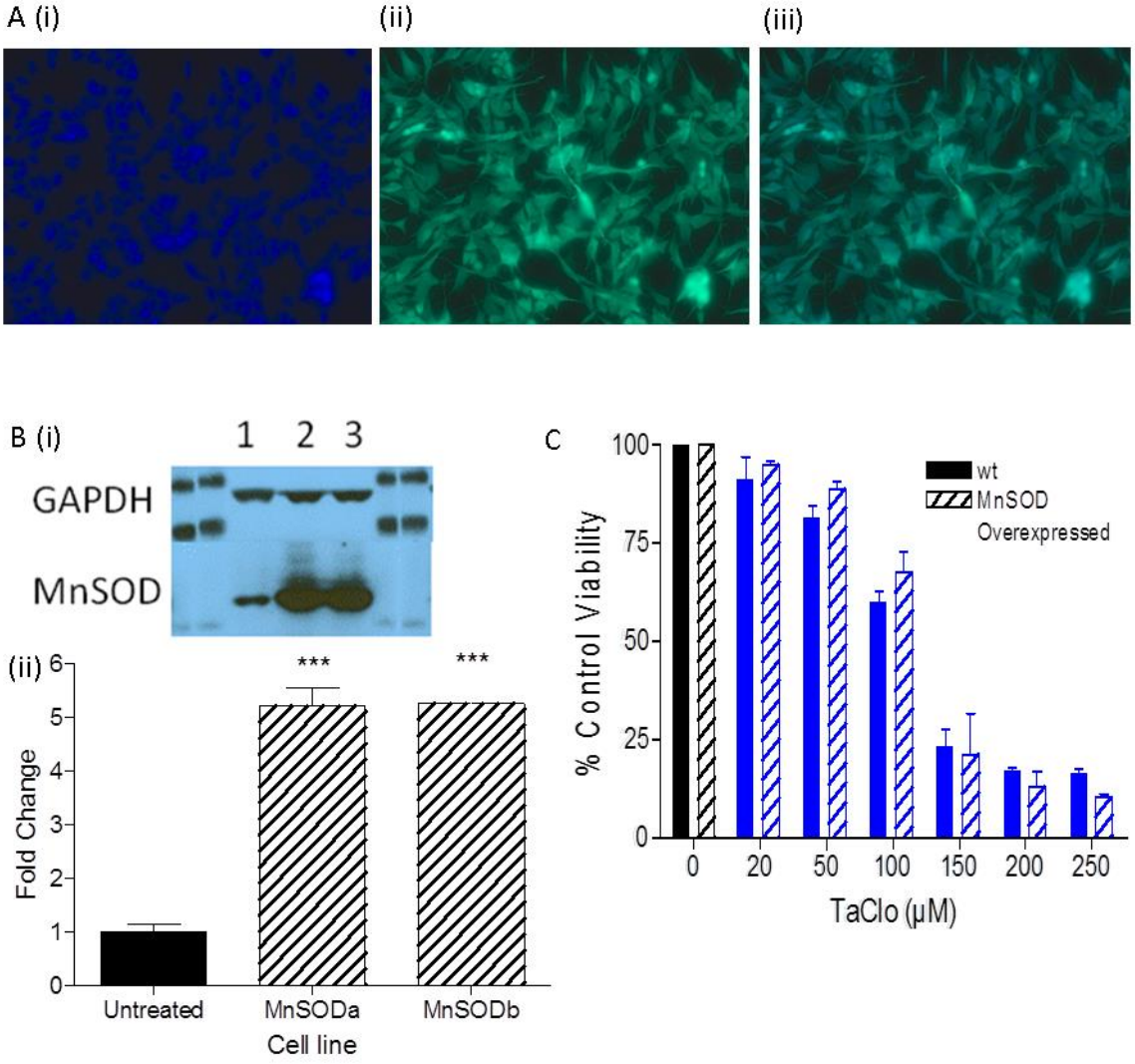

Fig. 4.15 Effect of MnSOD over expression on TaClo toxicity in SH-SY5Y

(A) Transfection efficiency: SH-SY5Y cells were treated with MnSOD overexpressing lentivirus expressing GFP and co-stained with DAPI. Images show (i) DAPI stained cell nuclei, (ii) GFP expression (iii) overlaid (x 40 magnification). (B) MnSOD expression levels: SH-SY5Y cells were treated with MnSOD (duplicate) over expressing lentivirus or untreated. Protein samples isolated from cells were probed for MnSOD. (i)Image is representative blot from (1) untreated, (2 & 3) MnSOD over expressed cells. (ii) Relative MnSOD intensity in untreated and MnSOD over expressed cells a & b relative to GAPDH. Data presented as fold-untreated + SD from triplicate assays (n=3). *** P<0.001, when compared to untreated, unpaired t-test. (C) Wild type and MnSOD over expressed SH-SY5Y cells were treated with TaClo (20-250µM) for 21 hours and viability measured by reduction of resazurin. Data presented as mean % control + SD from triplicate assays (n=3). Significant effect of MnSOD overexpression on TaClo toxicity (P<0.05), Two-way ANOVA.

DJ-1 is a protein found in neurons and axons that appears to have multifaceted functions (Cookson 2003), mutations of which have been shown to have links with PD (Bonifati, Rizzu et al. 2003). As one of the functions of DJ-1 appears to relate to ROS, with the protein functioning as a sensor for ROS (Mitsumoto and Nakagawa 2001) or being protective against oxidative stress (Yokota, Sugawara et al. 2003; Taira, Saito et al. 2004), we decided to look at the effect of TaClo on DJ-1 expression.

Protein isolated from SH-SY5Ys treated with TaClo over various time points was probed for DJ-1 levels by Western blot. TaClo treatment showed a significant increase in DJ-1 expression in a time-dependent manner ($P<0.001$, One-Way ANOVA) with significantly higher levels occurring by 8 hours post treatment ($P<0.001$) which are maintained until 24 hours ($P<0.001$) (Fig. 4.16).

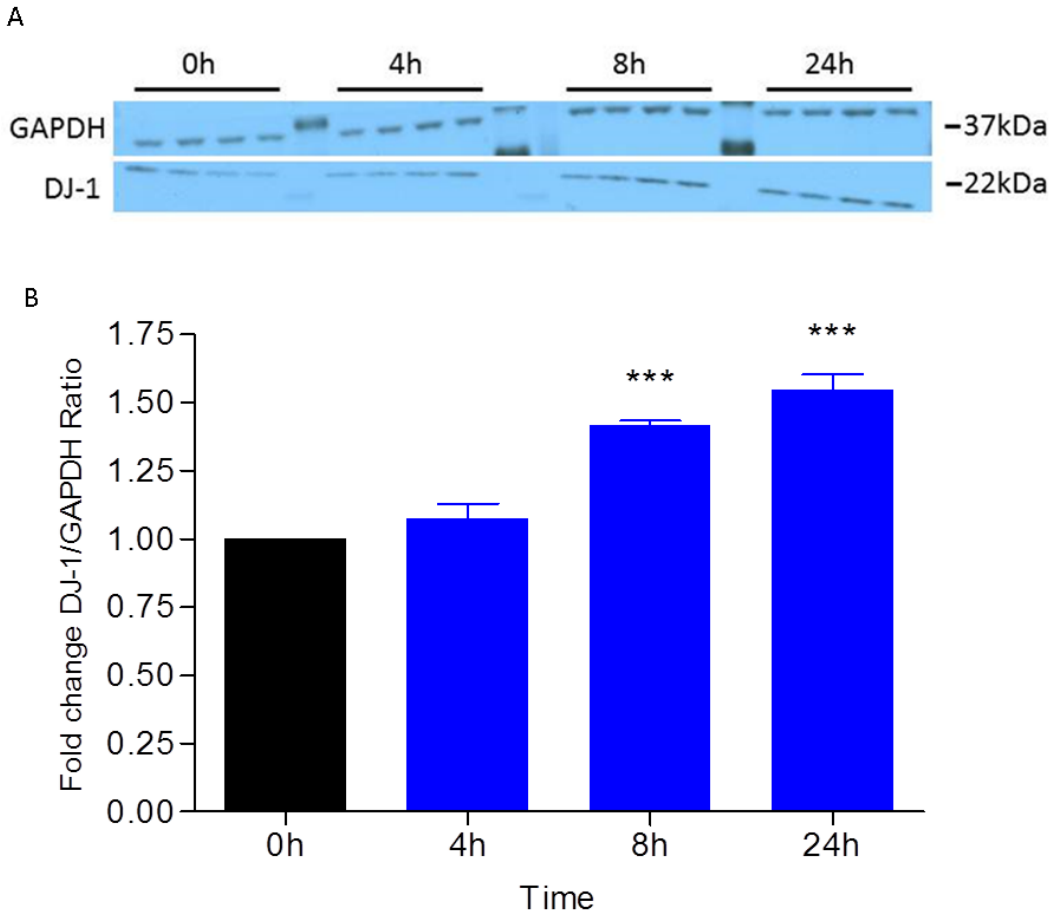

Fig. 4.16 Expression of DJ-1 in 100µM TaClo treated SY-SY5Y SH-SY5Y cells were treated with 100µM TaClo for 0, 4, 8 or 24 hours and protein harvested. Samples were probed for DJ-1. (A) Image is representative blot of DJ-1 and GAPDH control (B) DJ-1 intensity relative to GAPDH. Data presented as fold-untreated ± SD from quadruplicate assays (n=3). Significant difference over time ($P<0.001$) One-way ANOVA. ***$P<0.001$ when compared to 0h, Dunnett's post-test

4.3.6 TaClo Toxicity in SH-SY5Y Under Increased Mitochondrial Respiration

It has been reported that cancer cells, such as SH-SY5Y neuroblastoma, when grown in media using glucose as an energy source, generate most of their energy by glycolysis, but when grown in media using galactose as an energy source, they switch to mainly mitochondrial respiration (Rossignol, Gilkerson et al. 2004). It has also been shown that this switch to mitochondrial metabolism can increase the toxicity of toxins that inhibit mitochondrial OXPHOS Complexes, such as rotenone (Garside, Burnham et al. 2012).

We grew SH-SY5Y in 10mM galactose media for 2 weeks and then exposed them to TaClo and assessed viability using the Alamar Blue assay. We found that TaClo significantly decreased cell viability ($P<0.001$, One-way ANOVA) and that doses $\geq$1µM were significantly toxic when compared to control ($P<0.001$, Dunnett's post-test). SH-SY5Y grown in glucose media did not show significant death until doses $\geq$50µM (Fig. 3.6). However, when the effect of TaClo on galactose versus glucose grown SH-SY5Y was compared, no significant difference in viability was seen (Two-way ANOVA, data not shown).

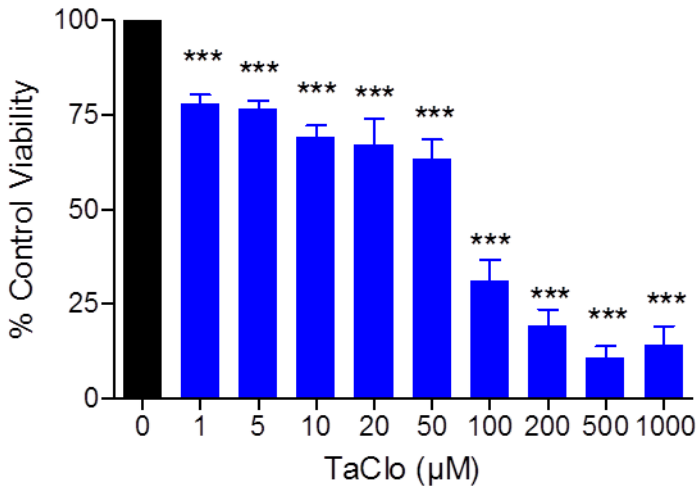

Fig. 4.17 Effect of TaClo on Galactose grown SH-SY5Y viability SH-SY5Y cells were grown in growth media with 10mM galactose replacing glucose as the energy source and treated with various concentrations of TaClo overnight for 21h and viability measured by reduction of Alamar Blue (resazurin). Data presented as mean % control $\pm$ SD from quadruplicate assays (n=3). *** $P<0.001$, when compared to 0.2% DMSO, One-way ANOVA & Dunnett's post-test.

4.4 Discussion

4.4.1 Is Oxidative Stress Increased Following TaClo Treatment?

Oxidative stress has been widely reported to be a factor in the development of PD with markers of oxidative stress, such as lipid peroxidation and oxidative DNA damage in the SNpc of PD patients brains (Dexter, Carter et al. 1989; Alam, Jenner et al. 1997). Exposure to PD-linked neurotoxins rotenone and MPTP has also been shown to lead to oxidative damage in DA model systems (Desole, Miele et al. 1995; Testa, Sherer et al. 2005). In addition to this, ROS have been shown to be integrally involved in programmed necrotic cell death (Morgan, Kim et al. 2008; Chen, Chi et al. 2009), suggesting oxidative stress may be a key mediator in TaClo neurotoxicity. While there appears to be a baseline level of superoxide present in untreated SH-SY5Y, this appears to have increased from ~8 hours following TaClo treatment when assessed by DCFDA fluorescence (fig 4.1 A-C), suggesting TaClo induces superoxide production. At later time points, those cells with the highest levels of fluorescence look as if they have lost structural integrity and become more spherical, suggesting that a high level of superoxide may induce cell death.

4.4.2 How does TaClo Interact with Cellular Antioxidant Defences?

GSH is an endogenous antioxidant that can donate an electron to ROS and so stabilise them and which has been shown to be up regulated during conditions of oxidative stress (Day, Suzuki et al. 2003). Dysfunction in this system has been linked to PD, with GSH levels shown to be reduced in the SNpc of patients with PD (Sofic, Lange et al. 1992; Sian, Dexter et al. 1994) leaving this region susceptible to oxidative damage. We measured expression of GSH and found an exponential increase in levels from 8 -24 hours following TaClo treatment (Fig. 4.2), suggesting activation of antioxidant defences and an increased production of ROS. This appears to support the earlier evidence - and time course - of increased ROS production from 8 hours post TaClo exposure.

LBS, a chemical known to deplete cellular GSH levels (Griffith 1982), was then used in order to investigate whether the removal of GSH would affect TaClo toxicity. We saw a significant decrease in viability following TaClo exposure in those cells co-treated with LBS (Fig. 4.3), suggesting a protective effect of GSH and the involvement of ROS in TaClo neurotoxicity. This finding is consistent with reports that rotenone toxicity in a neuroblastoma cell line is potentiated following GSH depletion with LBS (Sherer, Betarbet et al. 2003), as is MPTP mediated death in DA neurons in an animal model (Wüllner, Löschmann et al. 1996).

NAC has been shown to have antioxidant properties by acting as a precursor for GSH and so increasing GSH levels in the cell (de Flora, Bennicelli et al. 1985; Issels, Nagele et al. 1988) and has been reported to protect against IFN-γ-induced necroptosis in a cell model (Thapa, Basagoudanavar et al. 2011). It has been widely hypothesised that NAC may constitute a valid protective therapy against PD (Martínez, Martínez et al. 1999; Prasad, Cole et al. 1999); it is currently in clinical trials to test this, and it has been shown to protect against DA neuron degeneration in an α-synuclein overexpressing mouse model of the disease (Clark, Clore et al. 2010). NAC has also been reported to show protection against known PD toxins MPTP, rotenone and paraquat (Hoffer, Baum et al. 1996; Li, Ragheb et al. 2003; Molina-Jiménez, Sánchez-Reus et al. 2005; Sharma, Kaur et al. 2007). We found that NAC significantly - and almost totally - abrogated TaClo toxicity in SH-SY5Y (Fig. 4.4 B). This suggests a major role of oxidative damage in the DA neurotoxicity of TCE mediated by TaClo. Interestingly, NAC co-treatment did not have any significant effect of chloral mediated toxicity in our model (Fig. 4.4 A), suggesting ROS may not be involved in chloral toxicity and giving support to previously discussed evidence suggesting separate mechanisms may be responsible for TaClo and chloral mediated cell death. It has been reported that NAC can repair impaired Complex I deficiency in aged mice (Martínez Banaclocha 2000), which may offer an alternative, or summative, protective mechanism to the commonly thought increased oxidative protection mediated through GSH.

4.4.3 Do TCE Metabolites Affect Mitochondrial OXPHOS function?

Mitochondrial dysfunction and generation of ROS have been widely associated with necroptotic cell death (Schulze-Osthoff, Bakker et al. 1992; Goossens, Stangé et al. 1999; Davis, Hawkins et al. 2010). Inhibition of Complex I of the mitochondrial OXPHOS chain has been proposed as the major causative factor in the neurotoxicity of known PD toxins MPTP and rotenone (Nicklas, Vyas et al. 1985; Nicklas, Youngster et al. 1987; Li, Ragheb et al. 2003) and Complex I activity has been shown to be lowered in PD patients (Mizuno, Ohta et al. 1989; Schapira, Cooper et al. 1990). As mitochondrial dysfunction has also been shown to lead to increased ROS production (Lambert and Brand 2004), this evidence suggests OXPHOS inhibition as a possible source of TaClo mediated oxidative stress. In adjusting the parameters of the mitochondrial OXPHOS activity assays from those developed for human muscle biopsies, we found that the normal ranges of activity of all Complexes, I-IV, were significantly lower in our SH-SY5Y generated samples than those generated from pig heart muscle (Table 4.1). This is as a result of the number of mitochondria present in the pig heart muscle being far higher than those from SH-SY5Y due to a far higher number of cells in the original pig heart sample

than the SH-SY5Y, as opposed to any difference in mitochondrial number or activity in the different tissues.

We found that TaClo inhibited Complex I activity in our assay with an IC_{50} of ~50µM and almost total inhibition at 200µM (Fig 4.5 & 4.6). This shows a far more potent inhibition that that found by Janetzky *et al.* who reported an IC_{50} of 250µM and almost total inhibition at 700µM (Janetzky, God et al. 1995). However, Janetzky *et al.* used rat brain homogenates in their assay rather than isolated mitochondria and showed that an increase in incubation time from 5 to 30 minutes increased potency, possibly suggesting that in the homogenate more time is required for exposure of the toxin to the mitochondria than in our isolated mitochondria model. The concentrations of TaClo that brought about Complex I inhibition in SH-SY5Y generated mitochondria correlated well with those that led to SH-SY5Y cell death (Fig 3.9), suggesting Complex I inhibition as a major contributory factor to TaClo neurotoxicity in the system. A recent report stated that although they have been shown to inhibit Complex I, rotenone, MPTP and paraquat are still toxic to DA neurons in a mouse without functioning Complex I, and, in the case of rotenone, toxicity was increased (Choi, Kruse et al. 2008). However, these results have not been confirmed and do not seem to be compatible with the literature, and in particular, a study carried out by Marella *et al.*. They found that expression of NDI1 - a yeast NADH-quinone oxidoreductase that can act as an alternative to Complex I - in a rat model significantly protected against rotenone toxicity (Marella, Seo et al. 2008) suggesting the results seen by Choi *et al*. are unlikely to be relevant, possibly due to incomplete knockdown of Complex I.

We also saw inhibition of Complexes III & IV, but only following exposure to a relatively higher concentration of TaClo (500 µM), and no inhibition of Complex II whatsoever at doses $\leq$500 µM TaClo (Figs. 4.7 & 4.8). Inhibition of Complex III has shown to be present in the brains of PD patients (Haas, Nasirian et al. 1995; Shinde and Pasupathy 2006) and can lead to superoxide formation (Beyer 1992), suggesting possible relevance of this finding in TCE mediated PD. There has also been a link between Complex IV inhibition proposed with the finding that PINK-1 knockdown leads to inhibition of Complex IV (Gegg, Cooper et al. 2009) suggesting possible Complex IV inhibition in the disease. The lack of significant Complex II inhibition concurs with the findings of Krueger *et al.* that inhibition of Complex II by MPP+ and N-methyl β-carbolines in PD, if present, is small enough to be insignificant in relevance when compared to Complex I inhibition (Krueger, Tan et al. 1993). The physiological significance of the inhibition of Complexes III & IV seen in this model is questionable, as prior to the concentrations needed to achieve this building up in the cell, there will have been almost total inhibition of Complex I.

The resultant increase in ROS to which this leads, means the chances of the cell surviving to build up sufficient TaClo to inhibit Complexes III and IV is not likely to physiologically significant.

As yet, there have been no reported studies of the effect of chloral on mitochondrial OXPHOS. We found that 1mM chloral considerably inhibited Complex I & II activity by ~75%, and showed as small, 15% decrease in Complex IV activity (Figs. 4.9 & 4.10). As seen with TaClo, the concentration of chloral needed to inhibit Complexes I & II are similar to those that lead to cell death (Fig 3.5). In this case the inhibition of both Complexes I & II means that the OXPHOS chain will not be able to generate ATP, unlike in the case seen with TaClo exposure where electrons can still travel along the chain and generate the proton gradient needed to produce ATP when Complex I is inhibited as Complex II is fully functioning. In combination with the finding that the antioxidant promoter NAC has no effect of chloral toxicity in SH-SY5Y (Fig. 4.4 A) - suggesting that ROS generation is not a key factor in chloral mediated cell death - this proposes a possible mechanism whereby a lack of ATP may contribute to cytotoxicity.

In the assay we used to measure the activity of Complex III, cytochrome *c* is reduced and this is measured to indicate Complex III activity. However, when attempting to measure baseline cytochrome *c* reduction with chloral present, the rate of cytochrome *c* reduction was reduced, meaning that this assay could not be used to accurately measure Complex III activity. Following further investigation into this property of chloral, we found that it inhibited the reduction of cytochrome *c* in a dose dependent manner, with doses as low as 100µM showing a significant reduction and 1mM almost completely ablating cytochrome *c* reduction (Figs. 4.11 & 4.12). Whilst speculative, this could be explained as chloral has been shown to react with tryptamine by Pictet-Spengler condensation reaction to form TaClo (Bringmann, Feineis et al. 2000); it could do the same with cytochrome *c*. This would propose a hypothesis of chloral reacting with cytochrome *c* and stopping its ability to transfer electrons during OXPHOS, therefore depleting cellular ATP levels causing cell death. More evidence for chloral causing OXHPOS dysfunction can be found in the report that chloral has been shown to dissociate cytochrome *c* oxidase (Complex IV) (Griffin and Landon 1981); however this does not agree with our finding that chloral only has a slight inhibitory effect on Complex IV (Fig. 4.9).

4.4.4 Does TaClo Induce Superoxide in Mitochondria?

MitoSOX™ Red is a mitochondrially targeted superoxide indicator. It has previously been used to show an increase in mitochondrial superoxide production in Pink-1 deficient DA neurons (Wang, Chou et al. 2011) - a mutation that has previously been linked with PD (Valente, Abou-Sleiman et al. 2004) - as well as to show an increase in superoxide not consumed by the cellular antioxidant MnSOD, in HEPG2 cells exposed to known PD toxin rotenone (Dlasková, Hlavatá et al. 2008). We saw an apparent increase in mitochondrial superoxide in a dose dependent manner with150µM TaClo treated cells appearing to show an increase from 4 hours post treatment onwards, which was significantly quantified by flow cytometry at 8 hours (Figs. 4.13 & 4.14). When looking at the images, the increased superoxide appears to begin slightly earlier in the mitochondria than the cell in general, starting at 4 hours in mitochondria compared to 8 hours in the cell as a whole, suggesting that the source of any superoxide may be the mitochondria. However when quantified, the mitochondrial superoxide is only significantly increased by 8 hours, and this cannot be compared with general cellular superoxide as we have been unable to quantify DCFDA fluorescence.

When looking at the increase in fluorescence caused by superoxide production using flow cytometry, two distinct populations of cells can be seen (Fid 4.14 B) and these populations are also visible in the images taken (Fig 4.13). We can find no reports of this in the literature but believe that the separate populations may represent two distinct groups of cells: those that are trying to combat the increased superoxide - the mid fluorescing population; and those that have reached a threshold where the damage incurred by the increased superoxide is excessive enough to cause the cell to become unviable and begin to die - the high fluorescing population. This hypothesis is supported by the observation that in the imaged samples, there are two populations visible and those that have the highest fluorescence appear to have lost regular morphology and have become more spherical. The possibility of a threshold can also be seen when looking at cells with general increased fluorescence when assessed by flow cytometry, and there appears to be a dramatic rise in the number of cells classified as increased in fluorescence between 8 and 12 hours following 150 µM and between 12 and 16 hours following 100µM TaClo (Fig. 4.14 C). This observation of a threshold of superoxide generation, combined with our evidence of a caspase-independent necrotic death phenotype (see Chapter 3), is similar to that seen by Wabnitz *et al.* who reported a threshold effect of H_2O_2 exposure between 12.5 & 50µM led to a caspase-independent mitochondrially linked necrotic death in primary human T-cells (Fig. 4.18) (Wabnitz, Goursot et al. 2010).

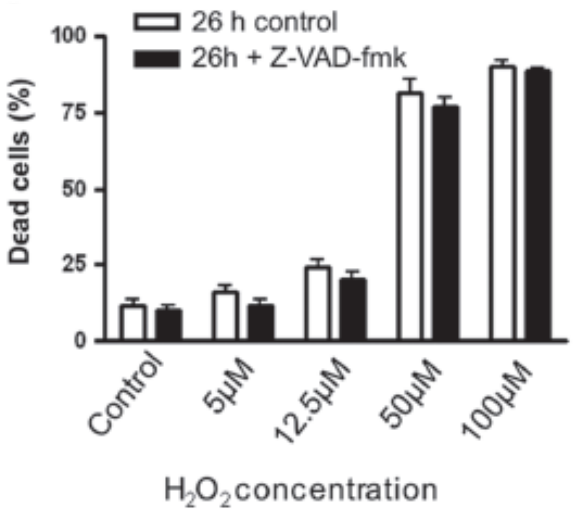

Fig. 4.18 Long-term oxidative stress induces caspase-independent T-cell death in primary human T cells Primary human T cells were treated with the indicated concentrations of H_2O_2 for 26 h in the presence (black columns) or absence (white columns) of the pan-caspase inhibitor Z-VAD-fmk (20 mM). Cell death was analyzed using Annexin V/7-AAD staining. Taken from (Wabnitz, Goursot et al. 2010)

Polymorphisms in the mitochondrially targeted superoxide dismutase, MnSOD, have been linked with PD (Shimoda-Matsubayashi, Matsumine et al. 1996; Wang, Chen et al. 2010) and these polymorphisms have been shown to increase the risk of developing PD when exposed to pesticides (Fong, Wu et al. 2007). MnSOD overexpression in mice also protected against the PD-linked neurotoxin, and mitochondrial Complex I inhibitor, MPTP (Klivenyi, St. Clair et al. 1998) and MnSOD levels in cerebrospinal fluid have been shown to be increased in PD patients (Yoshida, Mokuno et al. 1994). We found that MnSOD overexpressing SH-SY5Y showed a small but significant protection against TaClo cytotoxicity when compared to wild type cells (Fig. 4.15). This evidence implicates mitochondrially generated superoxide is involved in TaClo mediated SH-SY5Y toxicity and provides a link between TaClo, mitochondrial dysfunction and PD.

Mutations in the PARK7 gene, DJ-1, have been linked with PD (Bonifati, Rizzu et al. 2003), and have also been shown to have cytoprotective effects with regard to oxidative stress (Yokota, Sugawara et al. 2003; Taira, Saito et al. 2004). The protective effects of DJ-1in neurons are mediated by translocation to the mitochondria (Junn, Jang et al. 2009), suggesting the mechanism of DJ-1 neuroprotection against ROS involves mitochondria. DJ-1 expression has also been shown to be up-regulated following sub lethal exposure to the PD-linked and ROS generating toxin paraquat (Mitsumoto, Nakagawa et al. 2001), and to protect against rotenone exposure by enhancing clearance of damaged mitochondria via mitophagy (Gao, Yang et al. 2012). We saw a significant increase in DJ-1 expression in SH-SY5Y form 8 hours following treatment (Fig. 4.16). This suggests that TaClo exposure may lead to oxidative damage in the

mitochondria that the cell may be trying to protect against it by increasing production of the antioxidant sensor and defence protein DJ-1 and provides a link between TaClo exposure and PD.

4.4.5 Does the Energy Generation Mechanism Affect TaClo Toxicity in SH-SY5Y?

It has been reported that a switch of energy source from glucose to galactose can make cancer cells switch from mainly glycolytic to a mainly mitochondrial respiration driven method of energy production (Rossignol, Gilkerson et al. 2004) and that this switch can increase the toxicity of compounds that inhibit mitochondrial OXPHOS Complexes, such as the PD-linked toxin rotenone (Garside, Burnham et al. 2012). We found that cells grown in galactose-rich media showed significant cell death when treated with TaClo even at extremely low levels of up to 1µM (Fig. 4.17) whereas glucose grown cells only showed significant death at levels ≥50µM (Fig. 3.9) suggesting a possible lower threshold for toxicity in cells grown in galactose media and the involvement of mitochondrial OXPHOS chain dysfunction in TaClo mediated cell death. However, when TaClo toxicity to SH-SY5Y was compared between cells grown in glucose and galactose media, there was no significant difference observed, suggesting that this previous finding may not be significant and may require more investigation to confirm these preliminary observations. It would also be useful to compare metabolism between the cells grown in the different energy sources to see if a significant shift in energy generation has occurred. A recent report that D-galactose has been shown to cause oxidative stress and necroptosis in SH-SY5Y, although at higher doses than used in this study (>30g/L as opposed to 1.8g/l in this study) question the validity of the work in this cell line (Li, He et al. 2011).

4.4.6 Conclusions

We have shown that oxidative stress is integrally involved in TaClo mediated neurotoxicity with increased levels of ROS and activated antioxidant defences found following TaClo treatment. The observed ROS may be generated by inhibition of the mitochondrial OXPHOS chain with TaClo mainly affecting Complex I and increased superoxide found in mitochondria and PD linked mitochondrial antioxidant defences increased. Finally, we have not seen a similar set of results with chloral, possibly suggesting that chloral may be toxic itself, rather than its toxicity being due to its conversion to TaClo.

Chapter 5
Chronic Tolerance of TCE, Chloral & TaClo in C57BL/6 Mice and Wistar Rats and effect on Motor Function, SNpc Neurons and Neurotransmitter Levels

5.1 Introduction

TCE was classified as a moderately toxic compound by the International Programme on Chemical Safety's Environmental Health Criteria 50 on Trichloroethylene, with oral LD_{50}s of 2400-4920 mg/kg seen, and reported CNS depressant, irritant, and cancer causing effects and toxicity to liver and kidney seen following long term, relatively high dose, exposure in rodents (World Health Organization, United Nations Environment Programme et al. 1985; Williams-Johnson, Eisenmann et al. 1997). Chloral hydrate has been widely used as a sedative and hypnotic in human and veterinary medicine and therefore has similar acute toxic properties to most general anaesthetic, in that overdose can lead to CNS depression, coma and death. The W.H.O. Concise International Chemical Assessment Document on chloral also reports mild hepatotoxicity and possible tumorigenic effects (Benson 2000). There is not a great deal of published data on TaClo toxicity, besides the suspected neurotoxic effect investigated in this study. General tolerance of chronic exposure of the compounds in the strains and species to be studied therefore needs investigation.

Measurement of altered neurotransmitter levels by HPLC or mass spectrometry in PD patients and models has been used as a marker of disease progression (Yang and Beal 2011). Reduced levels of DA and its major metabolites are the main effect studied, due to the degeneration of DA neurons associated with the disease (Bernheimer, Birkmayer et al. 1973). However, there have also been reports of altered levels of serotonin (5-HT), noradrenaline, glutamate and gamma-aminobutyric acid (GABA) in PD (Scatton, Javoy-Agid et al. 1983; de Jong, Lakke et al. 1984; Mayeaux, Stern et al. 1984; Griffith, Okonkwo et al. 2008; Kish, Tong et al. 2008). Exploration of these neurotransmitters would be a useful tool in analysis of PD progression in animal models.

There are a wide range of behavioural tests that have been developed to try and assess motor function in rodents, including the accelerating rotarod (Jones and Roberts 1968), grip strength (Cabe, Tilson et al. 1978), the pole test (Matsuura, Kabuto et al. 1997) and the label test (Fleming, Salcedo et al. 2004). The effectiveness and variability of these tests can lead to problems with reproducibility and a lack of sensitivity so it is preferable to use combinations when assessing motor function in rodent models of PD.

MPTP has been reported to cause SNpc DA neuron degeneration and development of PD by inhibition of mitochondrial OXPHOX Complex I (Langston, Ballard et al. 1983; Seniuk, Tatton et al. 1990; Hantraye, Varastet et al. 1993). Acute MPTP treatment in C57BL/6 mice has been shown to lead to a decrease in SNpc DA neuron numbers and a decrease in motor function

that can be reliably measured using the accelerating rotarod test (Hutter-Saunders, Gendelman et al. 2012). However there are various differing results in behavioural phenotypes seen following different administration and testing regimens (Sedelis, Schwarting et al. 2001). The effect of chronic MPTP treatment on mouse motor function, SNpc neuron number and neurotransmitter level and its possible use as a positive control in PD toxin investigations *in vivo* needs further assessment.

5.1.1 Aims

This study aims to assess to general tolerability of i.p. TCE, chloral, TaClo and MPTP in male C57BL/6 mice and Wistar rats as well as looking at any changes in motor function, neurotransmitter levels or SNpc neuron number in treated animals.

To achieve this, a dosing paradigm will be designed based on previously known toxicological data and longitudinal behavioural testing will be performed. Post mortem, brains will be taken and neurotransmitter levels measured using LC-MS/MS.

5.2 Methods

For detailed methods see Material and Methods (Section 2).

All animals were to be dosed i.p. twice weekly for 8 weeks to model chronic exposure of the chemicals. This route was chosen following discussion with the NACWO and NVS as a reliable and relatively uninvasive method of dosing that would not be expected to lead to high attrition levels over the course of the study. The regimen and length of dosing was selected as the maximum frequency and extent of i.p. dosing in rodents laid out in the licence for this project granted according to the UK Animals (Scientific procedures) Act of 1986.

A dose of 500mg/kg was chosen for TCE exposure based on data from the U.S. Department of Health and Human Services Toxicological Profile for TCE which reported a NOEAL effect on general toxicological events of 1000mg/kg/day in chronic oral dosed studies of over 365 days in rats and mice (Williams-Johnson, Eisenmann et al. 1997) and a lack of overt toxicity reported by Guehl *et al.* in mice dosed 400mg/kg/day TCE for 5 days a week over 4 weeks (Guehl, Bezard et al. 1999).

Chloral was dosed at 100mg/kg based on review of the W.H.O. Concise International Chemical Assessment Document 25 - Chloral Hydrate which reports LOAEL of 144 & 160mg/kg in 14 and 90 day oral exposure studies in mice (Benson 2000).

TaClo has been less widely studied. Sontag *et al.* dosed rats with 0.2mg/kg/day TaClo i.p.and 0.4mg/kg twice daily p.o. for 7 weeks and observed no overt toxicity (Sontag, Heim et al. 1995; Sontag, Lange et al. 2009). As we dosed twice weekly, 1mg/kg TaClo was selected as a dose that was believed not to be toxic.

MPTP is a well-studied PD-linked toxin. Antzoulatos *et al.* reported that a dose of 10mg/kg i.p. was well tolerated in C57BL/6 mice when given daily for 5 days, but higher doses led to mortality (Antzoulatos, Jakowec et al. 2010); therefore a dose of 10mg/kg twice weekly for 8 weeks was used here.

C57BL/6 mice and Wistar rats were used in this study as they are both widely used model species in toxicological and neurotoxicological studies and have a wide range of data published on expected tolerability of neurotoxic compounds and performance in behavioural paradigms. In addition C57BL/6 mice have a range of transgenic PD mutant models which may be useful in further studies.

5.2.1 Statistical Analysis

For information on statistical methods see General Statistics (Sections 2.8 & 2.8.2)

5.3 Results

5.3.1 C57BL/6 Mice

5.3.1.1 General Tolerance

0.9% NaCl, 500mg/kg TCE, 100mg/kg Chloral, 1mg/kg TaClo & 10mg/kg MPTP i.p. at 10ml/kg were well tolerated by all animals dosed throughout the study. No obvious signs of discomfort were displayed following dosing and all animals survived until study termination.

5.3.1.1.1 Clinical Signs

No overt clinical or behavioural abnormalities were observed in any of the treatment groups over the course of the study.

5.3.1.1.2 Weight

Animals in all treatment groups showed similar significant normal increase in weight over time ($P<0.001$, Two-way Repeated Measures ANOVA) with minor fluctuations over the study (Fig 5.1). There was a significant difference in weight between treatment groups ($P<0.05$, Two-way Repeated Measures ANOVA), with chloral and TaClo treated mice showing generally lower weights than vehicle, TCE and MPTP treated groups (Fig 5.1). There was also a significant effect of treatment on weight over time ($P<0.001$, Two-way Repeated Measures ANOVA); however only chloral treated animals showed a periodically significantly lower weight at specific time points when compared to the vehicle group ($P<0.01$ and $P<0.05$, Bonferroni post-test) (Fig. 5.1). This intermittently lower weight was not considered clinically relevant.

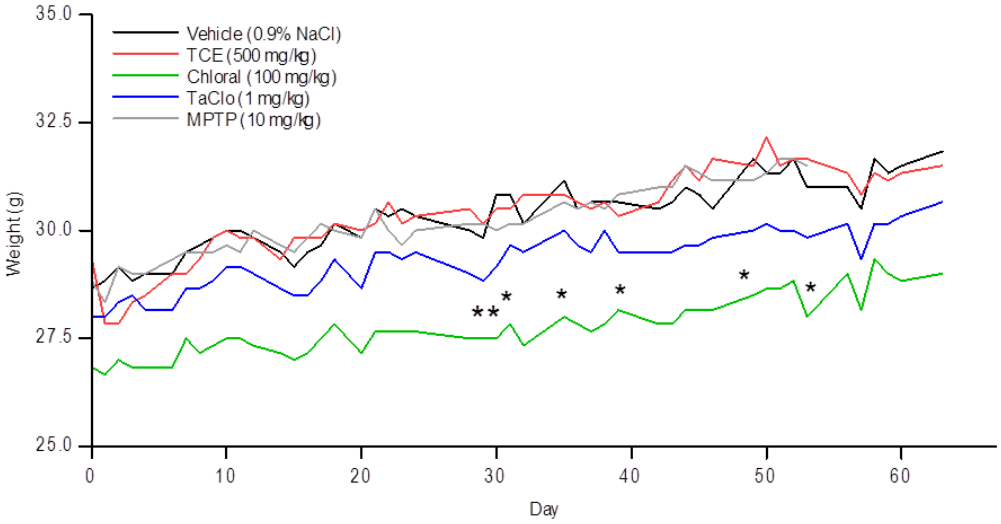

Fig. 5.1 Effect of TCE, Chloral, TaClo & MPTP on C57BL/6 mouse weight Weight (g) of TCE (500mg/kg), Chloral (100mg/kg), TaClo (1mg/kg), MPTP (10mg/kg) or control (10ml/kg Olive Oil) treated C57BL/6 mice. Data presented as mean (n=6). Significant difference over time ($P<0.001$), between treatment groups ($P<0.05$) and of treatment over time ($P<0.001$), Two-way Repeated Measures ANOVA. **$P<0.01$, *$P<0.05$ when compared to vehicle at relevant timepoint, Bonferroni post-test

5.3.1.2 Behavioural Testing

5.3.1.2.1 Rotarod

To assess motor function in this study, the accelerating rotarod, a well characterised behavioural paradigm used in rodent models (Jones and Roberts 1968), was used prior to, and then at 2, 4, 6 & 8 weeks following, the first dose. Animals were placed on a steadily accelerating rotating rod and the time taken to fall off was recorded. No significant differences between treatment groups and no significant effect of treatment over time were found, but there was a significant difference in performance over time across all groups ($P<0.01$, Two-way, Repeated Measures ANOVA) (Fig 5.2). No significant difference was seen at any time point for any treatment when compared to vehicle, apart from a small but significant increase in average fall latency observed in 100mg/kg chloral (131%) and 1mg/kg TaClo (133%) treated animals at 8 weeks ($P<0.001$, Bonferroni post-test) (Fig 5.2). This may suggest slightly improved motor function in animals treated with chloral & TaClo twice weekly for 8 weeks, but no effect following treatment with TCE or MPTP.

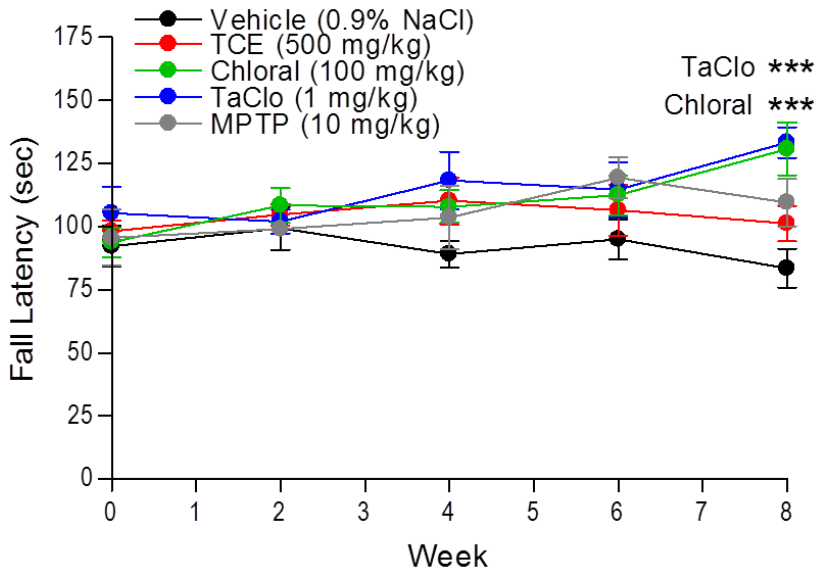

Fig. 5.2 Effect of TCE, Chloral, TaClo & MPTP on C57BL/6 mouse motor function as assessed by the Rotarod test Average fall latency of TCE (500mg/kg), Chloral (100mg/kg), TaClo (1mg/kg), MPTP (10mg/kg) or control (0.9% NaCl) treated C57BL/6 mice over time, triplicate trials. Data presented as mean % control ± SEM (n=6). Significant difference over time ($P<0.01$), No significant difference between treatment groups or of treatment over time, Two-way Repeated Measures ANOVA. ***$P<0.001$ when compared to vehicle at relevant timepoint, Bonferroni post-test

5.3.1.2.2 Pole Test

The pole test; which has been developed to test more fine motor control than the accelerating rotarod in mice (Matsuura, Kabuto et al. 1997), was used in this study to further assess any effects of the treatments on the motor skills of the animals at the same time points as the rotarod test. Animals were placed face up on a pole and total time to complete the trial, time to turn on the pole, time to descend the pole and number of falls per three trials were recorded for all animals.

There were no significant differences observed in total trial time between treatment groups, between the different trials and no significant effect of treatment over time (Two-way, Repeated Measures ANOVA) (Fig 5.3A). Neither were there any significant differences between vehicle and compound treated animals at any time point (Bonferroni post-test), but there did seem to be a possible trend towards an increased time taken to complete the trial in 500mg/kg TCE, 100mg/kg chloral & 10mg/kg MPTP treated mice following 6 weeks dosing. However this increase returns to vehicle levels by 8 weeks treatment (Fig 5.3A).

Similar results were seen when looking at time to turn and time to descend the pole, with no significant differences detected in turn or descent time between treatment groups and no significant effect of treatment over time, but a significant difference in performance was seen over time in both turning and descent latency ($P<0.01$, Two-way, Repeated Measures ANOVA) (Fig 5.3 B & C). Again, there were no significant differences between vehicle and compound treated animals at any time point (Bonferroni post-test), but there did seem to be a possible trend towards an increased time taken to turn on the pole in 100mg/kg chloral treated mice following 6 weeks dosing and in time to descend the pole in 500mg/kg TCE, 100mg/kg chloral & 10mg/kg MPTP dosed animals, again following 6 weeks treatment. However, as with possible differences seen in total trial time, this increase returns to vehicle levels by 8 weeks treatment (Fig 5.3 B & C).

No significant differences in number of falls were seen between treatment groups and no significant effect of treatment over time, but a significant increase in number was observed over time ($P<0.05$, Two-way, Repeated Measures ANOVA) (Fig 5.3 D). A significant increase in the number of falls was detected following 6 weeks 100mg/kg chloral treatment ($P<00.1$, Bonferroni post-test), but this difference was not carried forward following 8 weeks dosing (Fig 5.3 D). Interestingly, no vehicle-treated animal fell throughout the whole study, whereas animals in all other treatment groups did - predominantly from 4 weeks onwards - suggesting a possible loss of fine motor control in TCE, chloral, TaClo & MPTP treated animals (Fig. 5.3 D).

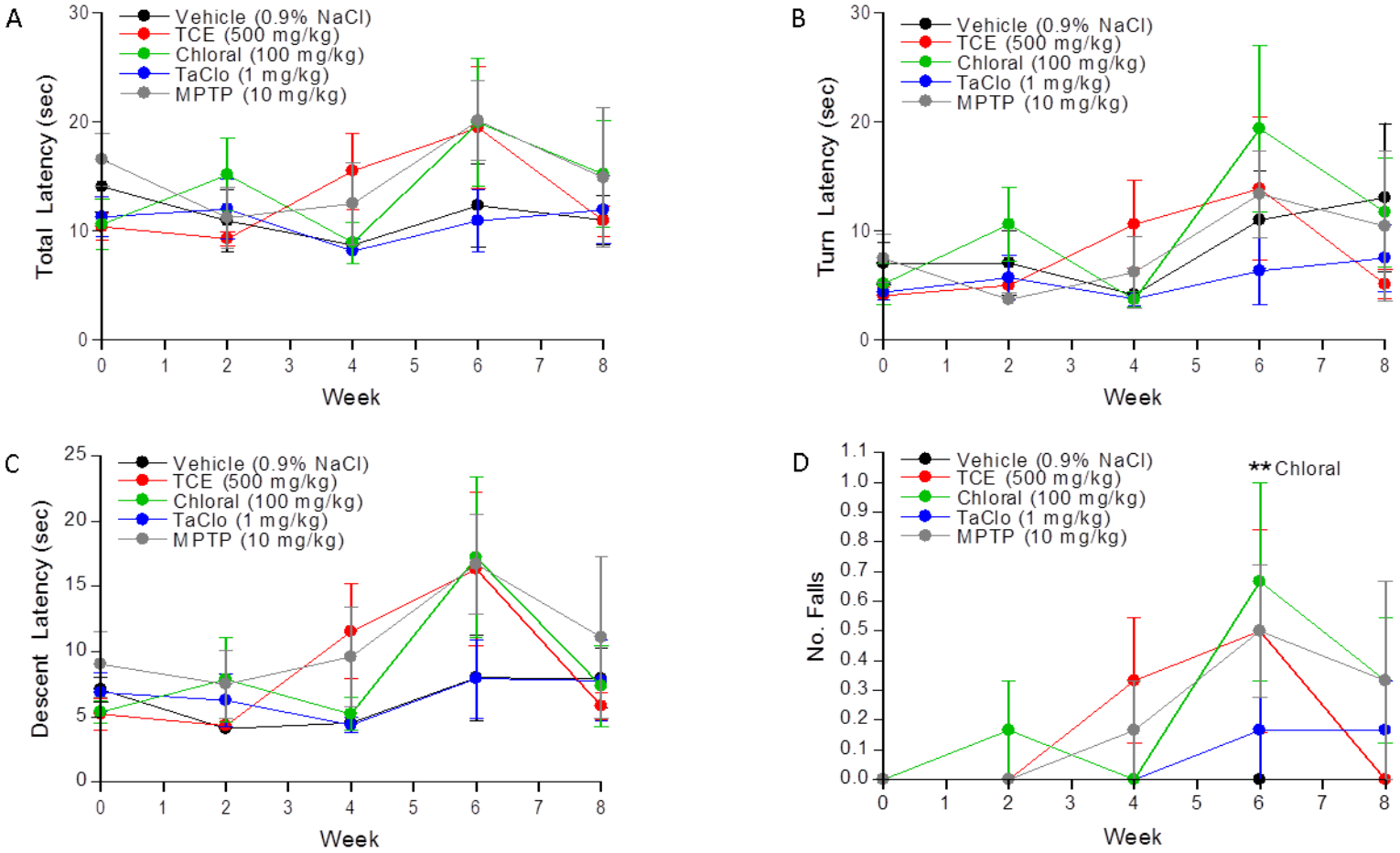

Fig. 5.3 Effect of TCE, Chloral, TaClo & MPTP on C57BL/6 mouse fine motor control as assessed by the Pole test Average (A) Total Time (B) Turn Latency, (C) Descent Latency & (D) Number of Falls of TCE (500mg/kg), Chloral (100mg/kg), TaClo (1mg/kg), MPTP (10mg/kg) or control (0.9% NaCl) treated C57BL/6 mice over time. Data presented as triplicate trial means ± SEM (n=6). Significant difference over time ((B & C, $P<0.01$, D $P<0.05$), No significant difference over time (A), between treatment groups or of treatment over time (A, B, C & D), Two-way Repeated Measures ANOVA. **$P<0.01$ when compared to vehicle at relevant timepoint, Bonferroni post-test

5.3.1.2.3 Label Test

The label test, another test designed to assess motor function - specifically motor response to aversive stimuli (Fleming, Salcedo et al. 2004) - was used in this study. A small sticky label is placed on the snout of the mouse and the time until removal is recorded. No significant differences in label-removal latency were seen between treatment groups and no significant effect of treatment over time, but a significant increase was observed over time ($P<0.001$, Two-way, Repeated Measures ANOVA) (Fig 5.4). No significant differences between vehicle and compound treated animals at any time point were seen (Bonferroni post-test), but there did seem to be a possible trend towards a decreased time taken to remove the label in all compound treated mice when compared to the vehicle group following 4 weeks dosing. It is worth noting that this decrease is not apparent by 6 weeks treatment (Fig 5.4).

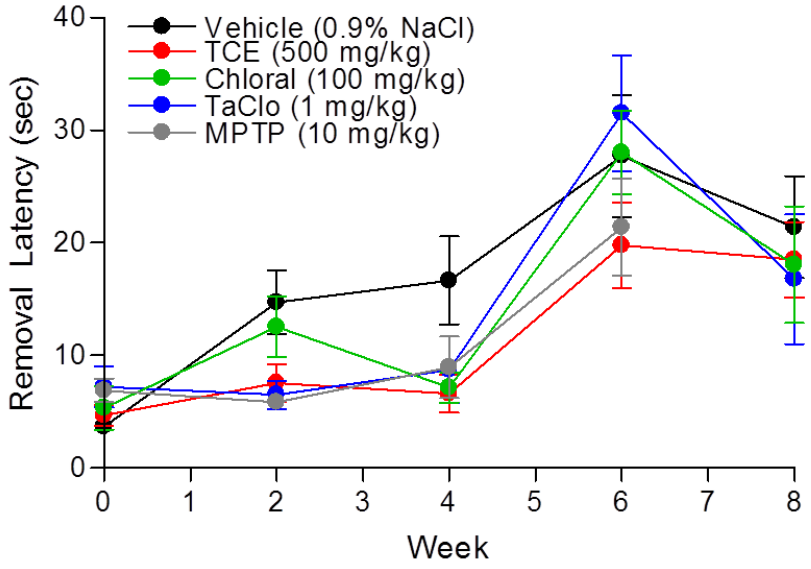

Fig. 5.4 Effect of TCE, Chloral, TaClo & MPTP on C57BL/6 mouse fine motor control as assessed by the Label test Average sticker removal latency of TCE (500mg/kg), Chloral (100mg/kg), TaClo (1mg/kg), MPTP (10mg/kg) or control (0.9% NaCl) treated C57BL/6 mice over time, triplicate trials. Data presented as mean % control ± SEM (n=6). Significant difference over time ($P<0.001$), No significant difference between treatment groups or of treatment over time, Two-way Repeated Measures ANOVA

5.3.1.2.4 Grip Strength

As abnormalities in grip strength have been reported in mouse models of PD (Colotla, Flores et al. 1990), a test of grip strength using a strain gage was used in this study (Cabe, Tilson et al. 1978). There were no significant differences observed in grip strength between treatment groups, between the different trials and no significant effect of treatment over time (Two-way, Repeated Measures ANOVA) (Fig 5.5). Neither were there any significant differences between vehicle and compound treated animals at any time point (Bonferroni post-test), with all treatment groups appearing to stay relatively stable throughout the study (Fig. 5.5). This data suggests that TCE, chloral, TaClo & MPTP have no effect on mouse grip strength at the doses given in this study.

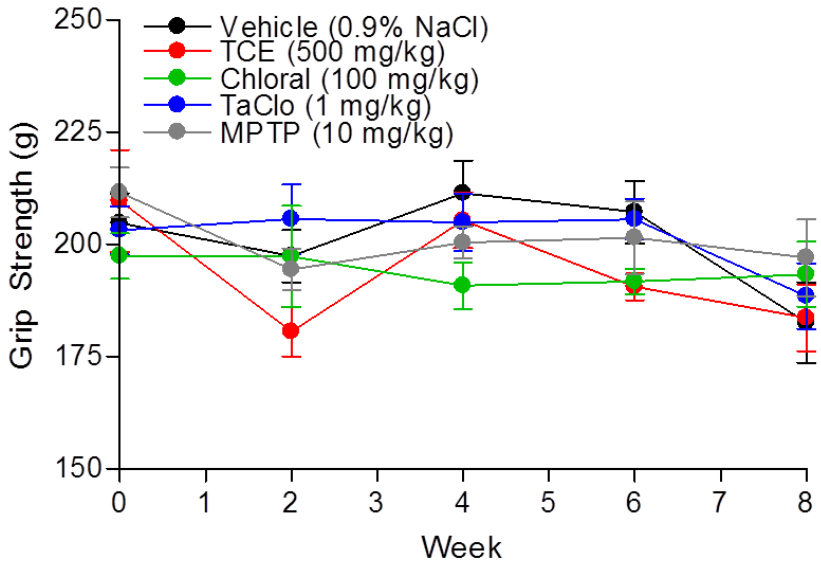

Fig. 5.5 Effect of TCE, Chloral, TaClo & MPTP on C57BL/6 mouse grip strength Average grip strength of TCE (500mg/kg), Chloral (100mg/kg), TaClo (1mg/kg), MPTP (10mg/kg) or control (0.9% NaCl) treated C57BL/6 mice over time, triplicate trials. Data presented as mean % control ± SEM (n=6). Significant difference over time ($P<0.01$), No significant difference between treatment groups or of treatment over time, Two-way Repeated Measures ANOVA

5.3.1.3 Neurotransmitter Levels

Alterations in neurotransmitter levels has been reported in the brains of PD patients with reduced levels of DA - a hallmark of the condition - and decreases in serotonin, noradrenaline, and GABA (Bernheimer, Birkmayer et al. 1973; Rinne and Sonninen 1973; Riederer, Birkmayer et al. 1977; Scatton, Javoy-Agid et al. 1983; Gerlach, Gsell et al. 1996) and glutamate has also been linked with the pathogenesis of the disease (Blandini, Porter et al. 1996). Neurotransmitter levels were therefore measured in the caudate putamen and forebrain of study animals by LC-MS/MS post mortem.

DA or HVA levels were not quantified due to limitations in the assay; however the DA metabolite DOPAC was measured. No significant decrease in DOPAC levels were observed in the forebrain following all treatments and in the caudate putamen following TCE, chloral or MPTP exposure; however a significant decrease in TaClo treated animals was detected ($P<0.05$, Dunnett's post-test) (Fig. 5.6 A).

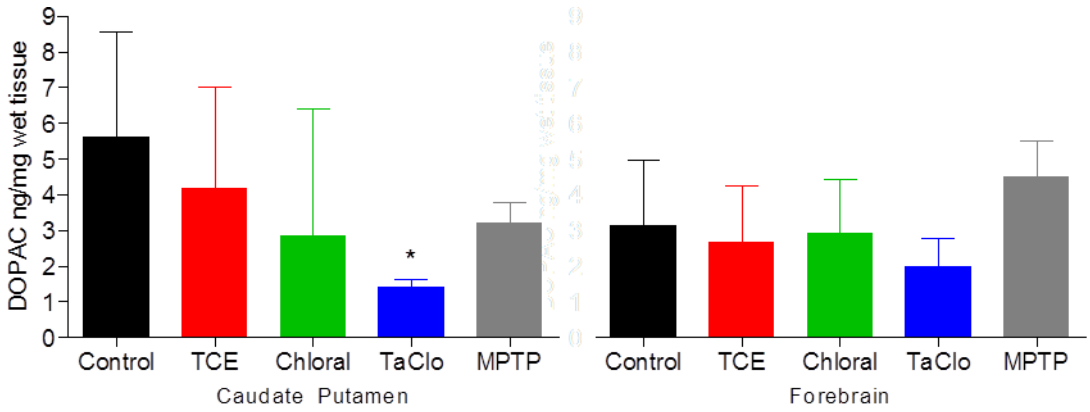

Fig. 5.6 Effect of TCE, Chloral, TaClo & MPTP on caudate putamen & forebrain DOPAC metabolite levels in C57BL/6 mice Levels of DOPAC in Caudate Putamen & Forebrain of TCE (500mg/kg), Chloral (100mg/kg), TaClo (1mg/kg), MPTP (10mg/kg) & vehicle (0.9% NaCl) treated C57BL/6 mice when assessed by LC-MS/MS. Data presented as mean ng/mg wet tissue from duplicate samples ± SD (n=3-6). (A-Caudate & Forebrain) No significant difference between groups, One-way ANOVA. *P<0.05 when compared to vehicle, Dunnett's post-test.

As with DA, 5-HT levels could not be measured in the brain samples due to assay limitations but 5-HT metabolite 5-Hydroxyindoleacetic acid (5-HIAA) was quantified. TCE and chloral did not have any significant effect on 5-HIAA levels in either the caudate putamen or forebrain, but TaClo and MPTP treated groups showed a large and significant increase in 5-HIAA in both brain regions (caudate TaClo & MPTP and forebrain MPTP, P<0.01; forebrain TaClo, P<0.001, all Dunnett's post-test) (Fig. 5.7).

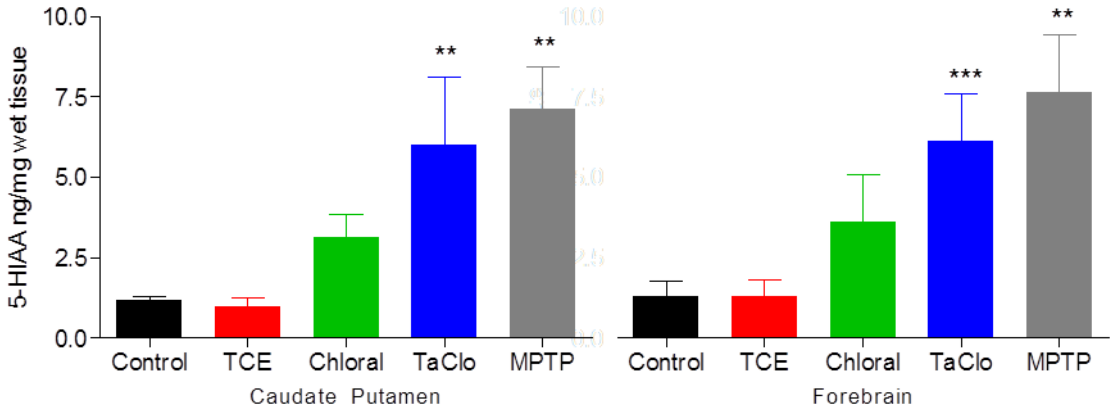

Fig. 5.7 Effect of TCE, Chloral, TaClo & MPTP on caudate putamen & forebrain 5-HIAA levels in C57BL/6 mice Levels of 5-HIAA in Caudate Putamen & Forebrain of TCE (500mg/kg), Chloral (100mg/kg), TaClo (1mg/kg), MPTP (10mg/kg) & vehicle (0.9% NaCl) treated C57BL/6 mice when assessed by LC-MS/MS. Data presented as mean ng/mg wet tissue from duplicate samples ± SD (n=5-6). (Caudate & Forebrain) Significant difference between groups (both P<0.001), One-way ANOVA. ***P<0.001, **P<0.01 when compared to vehicle, Dunnett's post-test.

Levels of GABA, the major inhibitory neurotransmitter in the CNS, were unchanged in the forebrain in all treatment groups, and in the caudate putamen following TCE and MPTP treatment, but were significantly reduced by ~40% in chloral and TaClo exposed animals in the caudate (both P<0.01, Dunnett's post-test) (Fig. 5.8 A). Glutamate, the most common excitatory neurotransmitter in the CNS, was not significantly altered in TCE treated animals in either the caudate putamen or the forebrain, but reduced by about a third in TaClo & MPTP exposed groups and almost completely in chloral dosed animals in both brain regions (caudate TaClo and forebrain TaClo & MPTP, P<0.05; caudate MPTP, P<0.01: cauduate & forebrain chloral, P<0.001, all Dunnett's post-test) (Fig. 5.8 B).

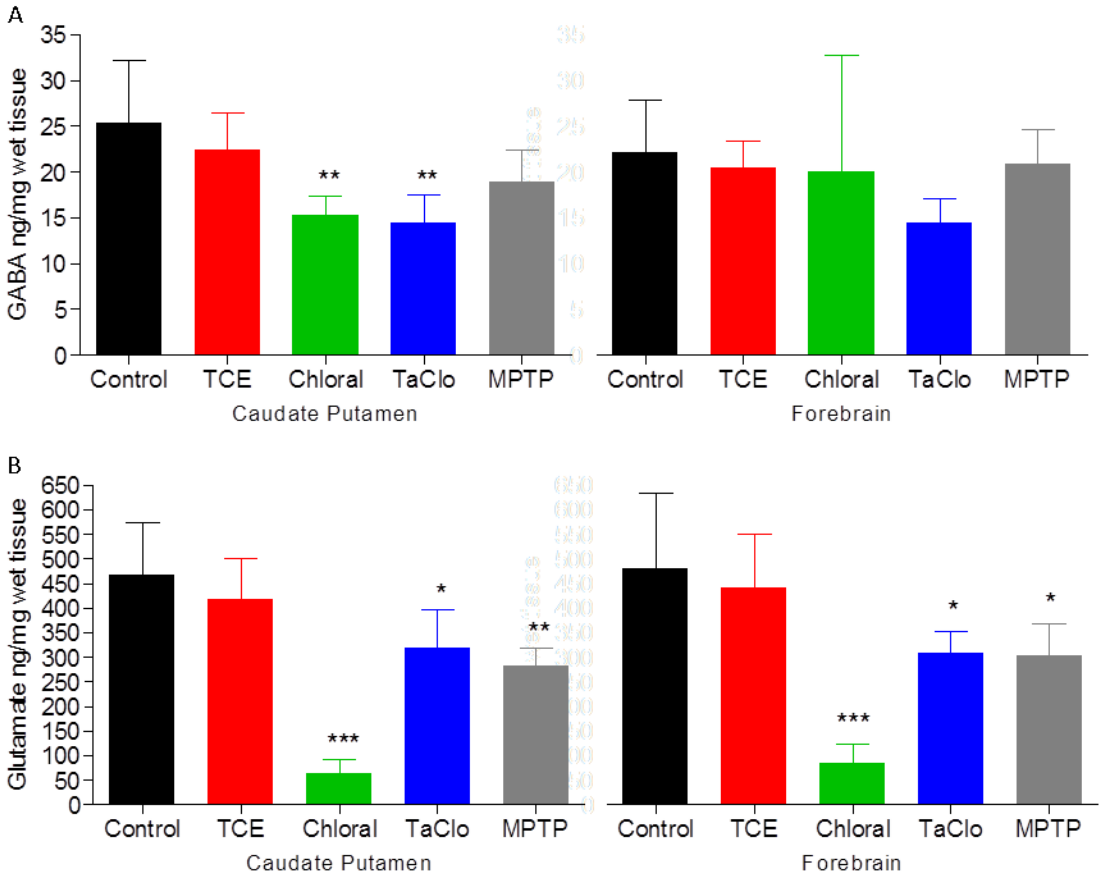

Fig. 5.8 Effect of TCE, Chloral, TaClo & MPTP on caudate putamen & forebrain GABA & Glutamate levels in C57BL/6 mice Levels of (A) GABA & (B) Glutamate in Caudate Putamen & Forebrain of TCE (500mg/kg), Chloral (100mg/kg), TaClo (1mg/kg), MPTP (10mg/kg) & vehicle (0.9% NaCl) treated C57BL/6 mice when assessed by LC-MS/MS. Data presented as mean ng/mg wet tissue from duplicate samples ± SD (n=5-6). (A-Forebrain) No significant difference between groups, (A-Caudate & B-Caudate & Forebrain) significant difference between groups (A-Caudate, P<0.01, B-both, P<0.001), One-way ANOVA. ***P<0.001, **P<0.01, *P<0.05 when compared to vehicle, Dunnett's post-test.

5.3.2 Wistar Rats

5.3.2.1 General Tolerance

1mg/kg TaClo and 100mg/kg Chloral i.p. at 1ml/kg were well tolerated by all animals dosed throughout the study. No obvious signs of discomfort were displayed following dosing and all animals survived until study termination.

500mg/kg TCE i.p. at 1ml/kg was not well tolerated by any rats in this group. All rats showed agitation, vocalisation and signs of pain at injection of the compound. During the study, one rat in this group had to be terminated due to compound related effects (see section 5.3.2.1.1 below for details).

5.3.2.1.1 Clinical Signs

No overt clinical or behavioural abnormalities were observed in the 1mg/ml TaClo or untreated groups over the course of the study.

100mg/kg Chloral treated animals were observed to be drowsy, disorientated and have increased appetite immediately and for 1 hour following dosing but these abnormalities had abated by 4 hours post dose.

500mg/kg TCE treated animals were observed to be agitated, disorientated, guarding/scratching the injected region of the abdomen, have hunched posture and have increased aggression to cage mates immediately and for 1 hour following dosing. These abnormalities were only occasionally observed at 4 hours and were always abated by 24 hours post-dose.

Rat number 20 (500mg/kg TCE) was found to have increased vocalisation when handled throughout the duration of the study.

Rat number 19 (500mg/kg TCE) was found to have diarrhoea on day 45, during a period of decreased weight (see section 5.3.2.1.1 above) and was terminated due to this deterioration in condition. Post mortem revealed distended intestines and a solid blockage in the colon as a possible cause of illness.

All 100mg/kg Chloral and 500mg/kg TCE treated animals were found to have various levels of gut stasis on post mortem, which was likely to have been compound related.

Rat 13 (100mg/kg Chloral) was found to have left lateral and left median liver lobes adhered at post mortem. This was not thought to be compound related due to lack of occurrence in co-treated animals.

5.3.2.1.2 Weight

1mg/kg TaClo and 100mg/kg Chloral treated animals showed similar significant normal increase in weight over the study ($P<0.001$, Two-way, Repeated Measures ANOVA), but 500mg/kg TCE treated rats did not show any significant weight gain over the study (Fig. 5.13). There was a significant effect of treatment over time ($P<0.001$, Two-way Repeated Measures ANOVA), with TCE treated rats not showing the increase seen in chloral and TaClo treated animals (Fig. 5.13). No significant difference between treatment group weights (Two-way, Repeated Measures, ANOVA) or between groups at specific time points (Bonferroni post-test) were seen (Fig. 5.13). The lack of weight gain in the TCE treated rats was considered clinically relevant and related to TCE exposure.

Rat 19 was observed to have significant weight loss (-10-15%) from day 42 to day 45 and as such was terminated on day 45 due to deteriorating condition and as such was excluded from statistical analysis. No other animals had any significant (>10%) weight loss over the course of the study.

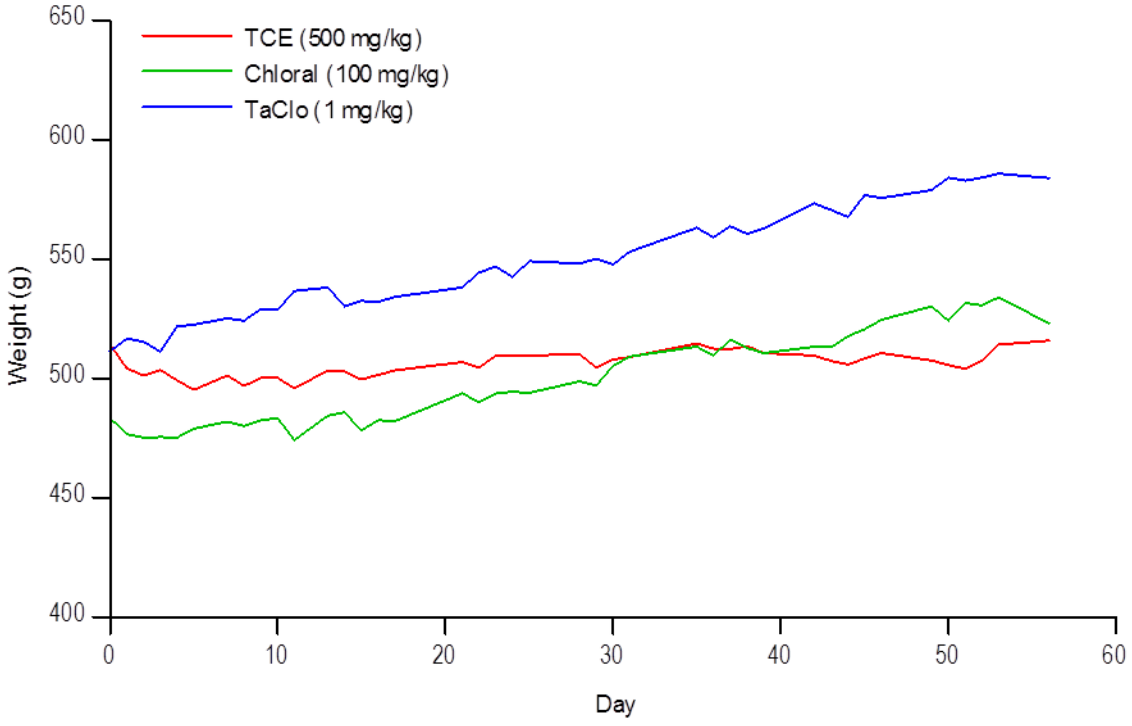

Fig. 5.9 Effect of TCE, Chloral & TaClo on Wistar rat weight Weight (g) of TCE (500mg/kg), Chloral (100mg/kg), TaClo (1mg/kg) treated Wistar rats. Data presented as mean (n=3/4). Significant difference over time ($P<0.001$), and of treatment over time ($P<0.001$) but no significant difference between treatment groups, Two-way Repeated Measures ANOVA.

5.3.2.2 Behavioural Testing

The accelerating rotarod test has also been used in rats so it was used in this study to assess motor function. Rats 1 (Control), 10 (1mg/kg TaClo), 13, 14 (both 100mg/kg chloral) 19 and 20 (both 500mg/kg TCE) were excluded from the analysis due to aversion to performing the task (jumping off apparatus, climbing over lanes, not attempting to walk on rod) from week 2 (Rats 19 & 20), week 6 (Rats 1 & 10) and week 8 (Rats 13 & 14). The reluctance of Rats 19 & 20 may have been treatment-related due to the clinical signs associated with TCE dosing (see section 5.2.3.1.1). A significant decrease in fall latency was observed over the study ($P<0.001$, Two-way, Repeated Measures, ANOVA), which was not treatment-related and there was no significant difference between treatment groups overall (Two-way, Repeated Measures ANOVA) or when compared to the control group at individual time points (Bonferroni post-test) (Fig 5.14 A). This suggests that TCE, chloral & TaClo treatment had no effect on motor function at the doses used in this study.

The grip strength test was also used in this study to complement the data gained from the rotarod. Rat 19 (500mg/kg TCE) was excluded from the analysis due to aversion to performing the task (jumping off apparatus) in week 8; this averseness may have been treatment-related due to the clinical signs associated with TCE dosing (see section 5.2.3.1.1). There were no significant differences observed in grip strength between treatment groups, between the different trials and no significant effect of treatment over time (Two-way, Repeated Measures ANOVA) (Fig 5.14 B). There were also no significant differences between control and compound-treated animals at any time point (Bonferroni post-test), with all treatment groups appearing to stay relatively stable throughout the study apart from a possible trend towards a decrease in grip strength in the 1mg/ml TaClo treated rats (Fig. 5.14 B). This data suggests that TaClo may lead to a decrease in grip strength when dosed twice weekly at 1mg/kg, but TCE and chloral appear to have no effect on rat grip strength at the doses given in this study.

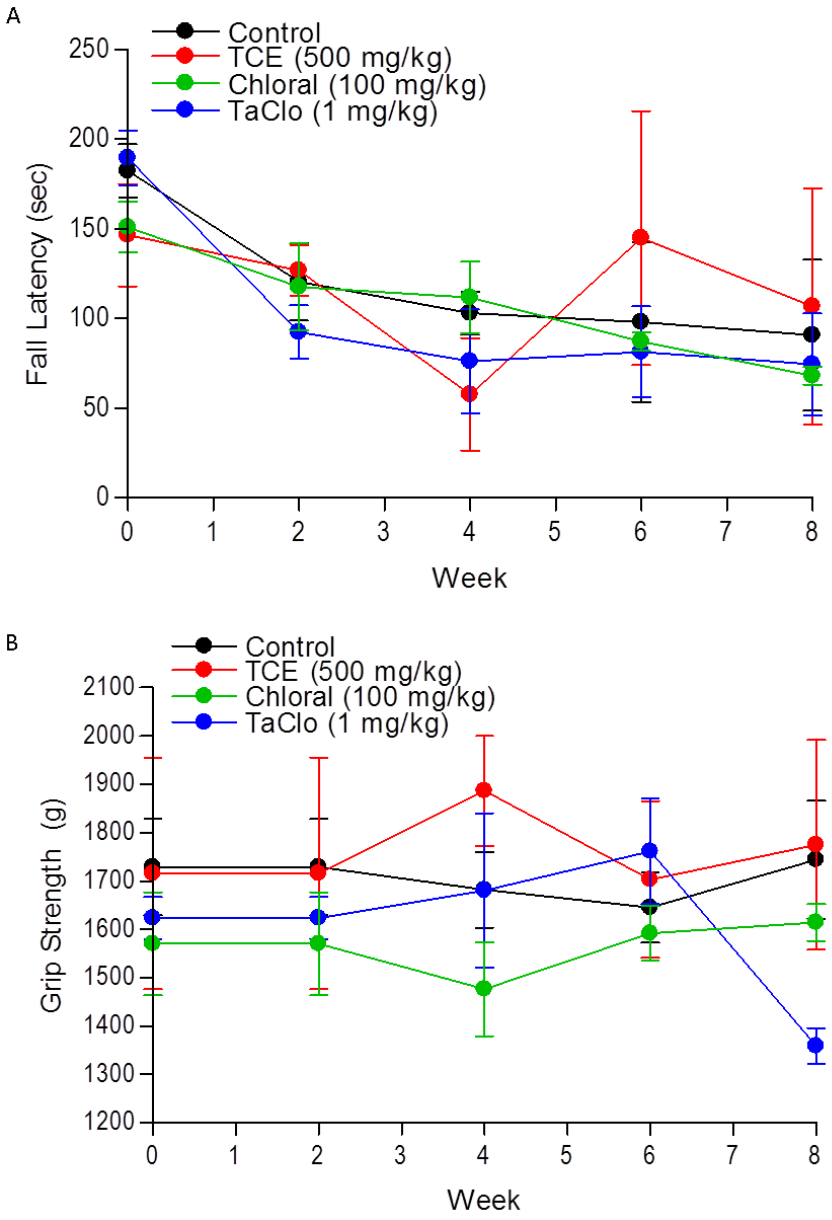

Fig. 5.10 Effect of TCE, Chloral, TaClo & MPTP on Wistar rat motor function and grip strength
Average % control (A) rotarod fall latency & (B) grip strength of TCE (500mg/kg), Chloral (100mg/kg), TaClo (1mg/kg) treated or untreated Wistar rats over time. Data presented as mean % control of triplicate trials ±SEM (n=2-4). Significant difference over time (A, $P<0.001$), No significant difference over time (B), between treatment groups or of treatment over time (A & B), Two-way Repeated Measures ANOVA.

5.3.2.3 Neurotransmitter Levels

Neurotransmitter levels were measured in the caudate putamen and forebrain of study animals by LC-MS/MS post mortem to assess the effect of TCE and metabolite exposure in rats.

In the rats, DA and DOPAC levels were not measured due to limitations in the assay; however in rat brains, 5-HT levels were quantifiable. TCE, chloral & TaClo treatment had no significant effect on HVA (Fig. 5.11 A), 5-HT & 5-HIAA (Fig. 5.12) or GABA & glutamate levels in either the caudate putamen or forebrain of the animals studied (all One-way ANOVA). This suggests the possibility of a species difference in the effect of the chemicals on the neurotransmitter levels when compared with the results seen in the mice.

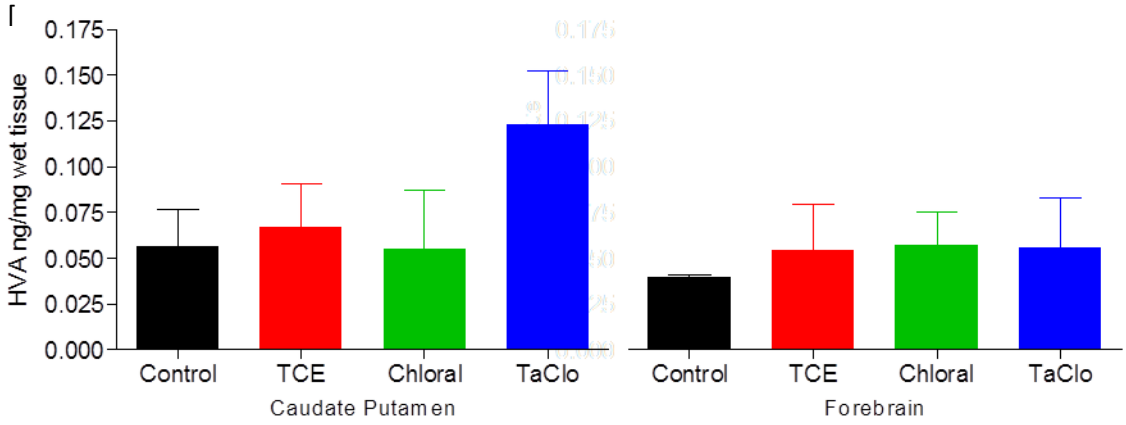

Fig. 5.11 Effect of TCE, Chloral & TaClo on caudate putamen & forebrain HVA levels in Wistar rats Levels of HVA in Caudate Putamen & Forebrain of TCE (500mg/kg), Chloral (100mg/kg) & TaClo (1mg/kg) treated and untreated control Wistar rats when assessed by LC-MS/MS. Data presented as mean ng/mg wet tissue from duplicate samples ± SD (n=2-4). No significant difference between groups, One-way ANOVA.

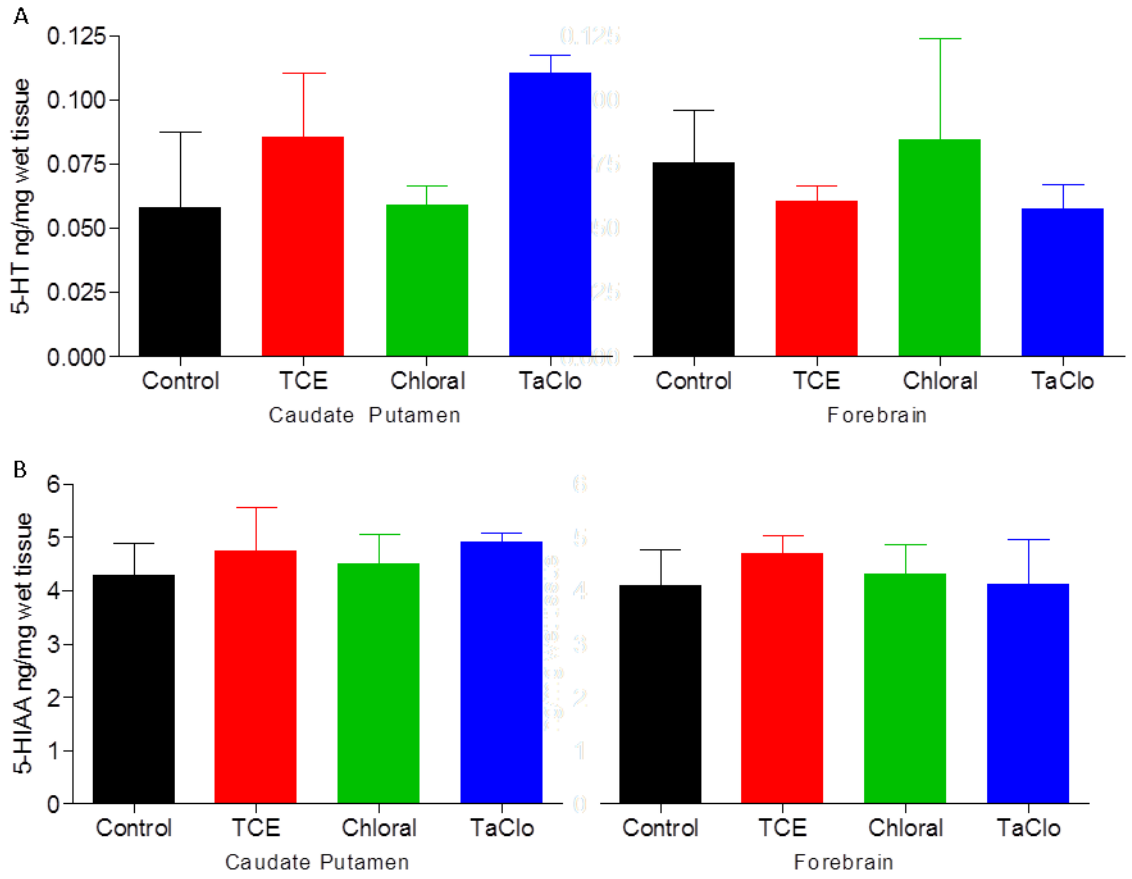

Fig. 5.12 Effect of TCE, Chloral & TaClo on caudate putamen & forebrain 5-HT & 5-HIAA levels in Wistar rats Levels of 5-HT & 5-HIAA in (A) Caudate Putamen & (B) Forebrain of TCE (500mg/kg), Chloral (100mg/kg) & TaClo (1mg/kg) treated and untreated control Wistar rats when assessed by LC-MS/MS. Data presented as mean ng/mg wet tissue from duplicate samples ± SD (n=2-4). No significant difference between groups, One-way ANOVA

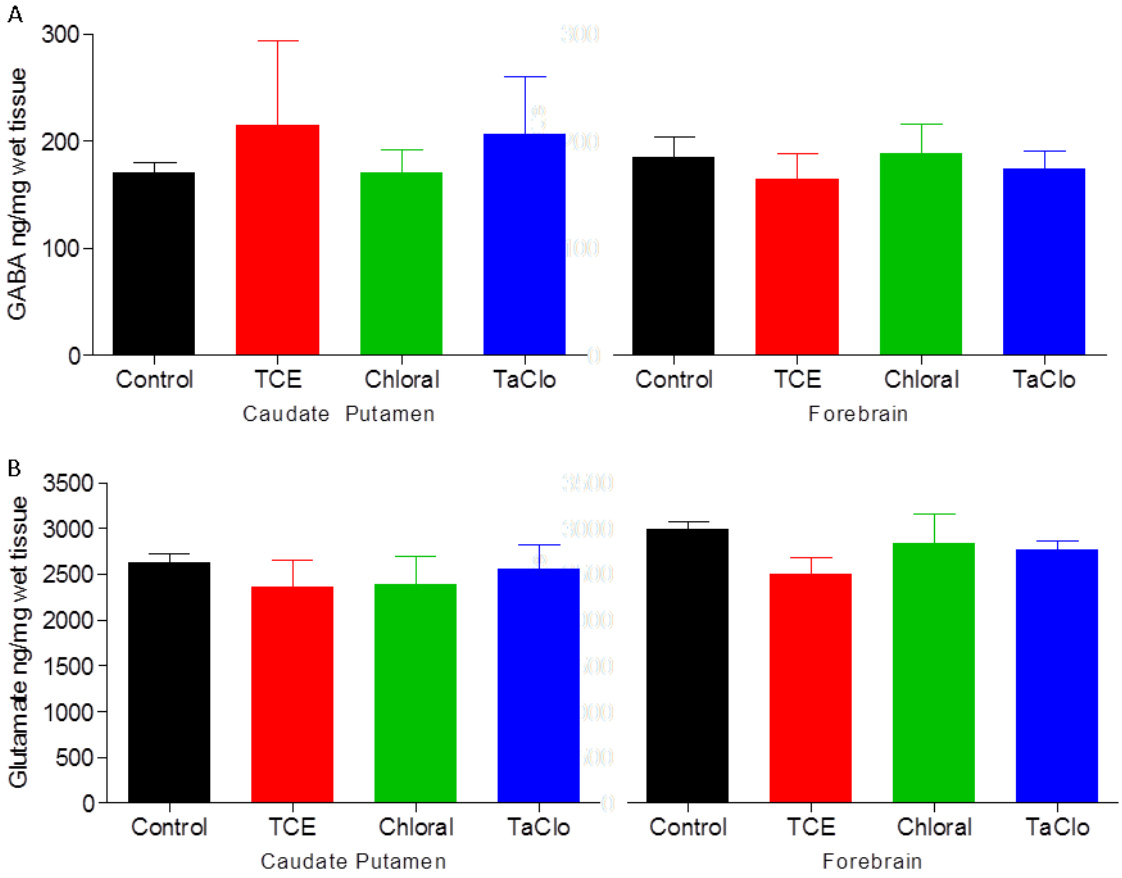

Fig. 5.13 Effect of TCE, Chloral & TaClo on caudate putamen & forebrain GABA & Glutamate levels in Wistar rats Levels of GABA & Glutamate in (A) Caudate Putamen & (B) Forebrain of TCE (500mg/kg), Chloral (100mg/kg) & TaClo (1mg/kg) treated and untreated control Wistar rats when assessed by LC-MS/MS. Data presented as mean ng/mg wet tissue from duplicate samples ± SD (n=4). No significant difference between groups.

5.4 Discussion

5.4.1 Are Chronic TCE, Chloral and TaClo Well Tolerated in C57BL/6 Mice and Wistar Rats?

This study showed TCE, chloral, TaClo and MPTP to be well tolerated by C57BL/6 mice at the doses and regimen used, with no overt toxicity, clinical signs or lack of weight gain apparent (Fig. 5.1). Chloral treated mice were significantly lower in weight than vehicle periodically throughout the study (Fig 5.1) but this group was smaller at study start and gained weight at the same rate as all other groups suggesting that this is not clinically relevant nor related to the treatment.

As in the mice, TaClo was well-tolerated by Wistar rats as dosed in this study, with normal weight gain and no clinical signs or overt toxicity observed throughout the study period (Fig 5.13). However, TCE and chloral were less well-tolerated in this study. Despite being given the same total doses as the mice, chloral induced drowsiness, disorientation and increased appetite and TCE caused abdominal pain on administration, agitation, disorientation, hunched posture and increased aggression as well as a lack of characteristic weight gain in rats. Post mortem investigations found varying levels of gut stasis in all chloral and TCE treated rats. The occurrence of these symptoms in the rats, despite the tolerance of the mice to the same doses, may be due to the fact that the rats were administered the compounds at a ten-fold higher concentration, albeit in a ten-fold lower volume.

The sedative effect seen with chloral is not surprising as the compound is a well-known and widely used anaesthetic agent (Silverman and Muir Iii 1993) and the gut stasis observed in the chloral treated rats correlates with reports of adynamic ileus in anaesthetised rats caused by the irritant property of the compound in the visceral peritoneum (Fleischman, McCracken et al. 1977). Although the reported cases were following higher doses of chloral, our repeated lower administration could be expected to yield the same effects. Chloral treated rats also showed an acute effect on feeding behaviour as seen by constant eating of food pellets placed in the cage directly following dosing; however, as there was no significant weight gain, a persistent increase in appetite does not seem to be the cause of this behaviour. The observed feeding could be possibly due to chloral exposure causing a feeling of emesis in the animals, as it is similar to a phenomenon known as pica, which is illness response behaviour in rats whereby they eat non-nutritive substances due to a lack of ability to vomit (Takeda, Hasegawa et al. 1993), although this does not agree with reports of general reduced food intake in rats administered emetic agents (Takeda, Hasegawa et al. 1993; De Jonghe, Lawler et al. 2009).

While these observations are easily explained, they present problems in the use this of regimen and species as a chronic model to study any possible involvement of chloral in PD.

I.p. administration of TCE induced obvious signs of pain in all rats on administration and continuing for up to 4 hours post dosing. The vocalisation, guarding of injection site and aggression seen in the rats immediately following dosing suggests that TCE was causing acute pain. This may have been due to a number of known solvent effects, such as decreasing local temperature in the injection site, affecting membrane permeability, or an, as yet, uncharacterised effect on local pain receptors or neurons. Further investigation is needed to confirm the cause of this apparent acute pain. The more chronic pain indicated by guarding behaviour and hunched posture may be due to the observation reported that TCE can enhance production of histamine and inflammatory mediators in rat peritoneal mast cells (Seo, Ikeda et al. 2008). TCE treated animals also showed signs of disorientation consistent with reports of dizziness in a large scale investigation in to 188 workers exposed to TCE (Barret, Faure et al. 1984), with symptoms reported in a patient who suffered seizures and slurred speech, disorientation, dissociative amnesia, and bizarre behaviour following inhalation abuse of TCE (Miller, Mycyk et al. 2002) and in a case of industrial TCE exposure where weakness and dizziness were reported (Bond 1996). Post mortem examinations revealed gut stasis in all TCE treated animals and animal 19 had diarrhoea, which is consistent with effects reported in a human population exposed to TCE in drinking water in which 52% of exposed individuals suffered gastrointestinal dysfunction (Byers, Levin et al. 1988). Another possible explanation for the problems observed in the gut could possibly be due to TCE, or chloral formed from TCE, causing irritation in the peritoneum leading to the effects described above. The lack of normal weight gain seen in TCE treated rats (Fig 5.13) may have been due to the stress and pain of the injections, or possibly due to the gastrointestinal problems seen in this group, although the same effects were seen in chloral treated animals which did not show any problems in gaining weight. The lack of weight gain is likely due to the effects of the compound in the peritoneum as reports show normal weight gain in animals administered with TCE at doses up to 1000mg/kg/day in acute and chronic studies when given by oral gavage (Maltoni C, Lefemine G et al. 1986; Goldsworthy and Popp 1987) suggesting there is no direct effect of TCE on appetite.

5.4.2 Do Chronic TCE, Chloral, TaClo and MPTP Treatment Affect Motor Function?

No consistent significant decrease in motor function was observed in TCE, chloral, TaClo or MPTP C57BL/6 mice when assessed by rotarod (Fig. 5.2), Pole (Fig. 5.3), Sticker (Fig. 5.4) or Grip Strength (Fig. 5.5) tests. Generally, all groups' performance in the tests decreased over time; this was believed to be due to habituation to the tests, with animals possibly learning that reduced participation resulted in early cessation of the test and return to the home cage, rather than an actual decrease in motor function, but there were no differences between treatment groups.

The rotarod test has been previously used to show a decrease in motor function following acute exposure to PD toxins MPTP and rotenone (Pan-Montojo, Anichtchik et al. 2010; Chagniel, Robitaille et al. 2012), and Colotla *et al.* showed that rotarod performance was affected by relatively high (9 x 30mg/kg), but not lower (9 x 10 or 20mg/kg) doses of MPTP (Colotla, Flores et al. 1990). All mice in this study showed a change in performance over time; however this was not found to be significantly related to treatment over the course of the study (Fig. 5.2). This is not consistent with results seen in rats exposed to 1000mg/kg TCE five times per week for 6 weeks p.o. which developed a small but significant reduction in rotarod performance (Liu, Choi et al. 2010), although this could be explained by the higher and more acute dosing regimen and species difference. An apparent increase in motor function to ~150% when compared to vehicle treated animals was seen in chloral and TaClo treated mice 8 weeks following first dosing (Fig 5.2). This effect has previously been reported in MPTP treated mice which showed increased activity despite reduced SNpc DA levels (Rousselet, Joubert et al. 2003). There have also been reports of temperature affecting DA levels in mice treated with PD-linked toxins, with increased DA seen following administration of a single dose of rotenone at 21^{o}C, but decreased levels seen at 28^{o}C (Crutchfield and Dluzen 2006). However, as this effect is not seen in any of the other behavioural paradigms, these results are thought to be artefact.

Fine motor control has been shown to be inhibited in MPTP treated mice in the pole test following a relatively high and acute dosing regimen, with mice administered 30mg/kg twice a day for 4 or 5 days (Ogawa, Hirose et al. 1985; Abe, Taguchi et al. 2001). Behavioural analysis of mice in this study by the pole test showed a general increase in the time taken to turn and descend the pole over the duration of the study; however there were no overall differences between the treated and vehicle groups (Fig 5.3). A possible increase in time to descend was seen in TCE, chloral & MPTP at 6 weeks; however this was not significant and had returned to a

similar level to vehicle treated mice by 8 weeks (Fig 5.3 C), suggesting the result is an artefact. When looking at number of falls per three trial session, it is interesting to note that no mouse from the vehicle treated group fell throughout the duration of the study but all other groups had an increase in number of falls, generally from 4 weeks treatment onwards, with chloral treated animals showing significantly more falls at 6 weeks than vehicle (Fig 5.3 D). There was no statistical significance in the effect of treatment on the increase in falls, but at these doses for this exposure there does seem to be a trend towards a decrease in motor function. While previous studies mentioned have reported decreased performance in the pole test following MPTP treatment, this effect was with higher, more acute doses and there are reports of acute lower total doses of 30mg/kg MPTP twice in one day, or 10mg/kg/day for 5 days showing no decrease in motor function as assessed by the test (Rommelfanger, Edwards et al. 2007; Antzoulatos, Jakowec et al. 2010). These reports suggest that our dosing regimen may not be exposing the mice to high enough levels of the toxins. It has also been reported that this decreased performance in the pole test recovers to control levels by 3 days post dosing in C57BL/6 mice administered 4 x 15mg/kg doses of MPTP in one day (Sedelis, Hofele et al. 2000). As our behavioural testing was carried out 3 days post previous dose, this report suggests another possible reason no significant effects were observed. A final observation of caution when analysing the results seen in the pole test lie in the fact that this test is generally widely used to assess endpoint motor function, whereas here it has been used to assess fine motor control throughout the study on a number of occasions. This may mean that habituation and learning or memory may also have an effect on performance and mean more variables are included in the test that may affect its reliability seen in reported use.

The label test has been previously used to show a decrease in motor function in a 6-OHDA PD rat model (Schallert, Fleming et al. 2000) and an α-synuclein overexpressing mutant mouse model of the disease (Fleming, Salcedo et al. 2004). When assessing motor response to aversive stimuli using the label test, all animals showed an increased latency to remove the label over time, with a distinct increase from 4 week trial onward (Fig. 5.4), but this effect was not dependent on treatment. As in the pole test, the label test is generally used as an endpoint motor function assessment, and, as we used repeated tests to determine fine motor control throughout the study, this could be the reason for the decreased performance in the test. As this test relies on the aversive nature of the label on the forehead of the animal, repeated occurrences could lead to habituation and a decrease in the aversive stimuli so reducing the drive to remove the label.

There was a slight decrease in grip strength in all groups when tested in week 8 but no difference between toxin and vehicle-treated animals (Fig 5.5). Grip strength is not thought to be a sensitive marker for motor dysfunction in PD as it has been reported that mice that show a decreased motor function - as assessed by rotarod - have no significant change in grip strength (Sedelis, Hofele et al. 2000).

In TCE, chloral & TaClo treated rats, no reduction in motor function when compared to control animals, or generally over time, was seen when assessed by grip strength (Fig. 5.14 B), while there was a decrease in the performance of all groups on the rotarod from baseline which was not treatment-related and levelled out to a similar level for all post dose tests (Fig. 5.14 A). In both tests a number of animals had to be excluded due to a lack of compliance in the test protocol. This could possibly be explained by the size of the rats which were relatively large (500-600g) and so easily able to escape from the apparatus, or possibly due to habituation to the equipment allowing rats to learn ways to avoid task performance and, in the case of the TCE treated animals, this may have been related to the discomfort and anxiety related with dosing of the compound. Due to the low number of animals included in the analysis of these tests, the clinical effects seen in some groups and the lack of compliance in the tests, the behavioural results reported are not thought to be robust enough from which to draw reliable conclusions.

While there is a report of reduced rotarod performance in TCE exposed rats (Liu, Choi et al. 2010), this study used a far higher and more acute dosing regimen that that used here, possibly explaining the lack of consistency with the results following TCE exposure here. No studies into the effect of chloral on motor function have been found in the literature, and while there have been reports of late-onset reduced spontaneous nocturnal activity and altered responses in apomorphine challenge in rats exposed to TaClo (Sontag, Heim et al. 1995; Heim and Sontag 1997; Sontag, Lange et al. 2009), no comparable tests to those used here have been reported to confirm or challenge the findings of this study with regards to the effects of peripheral TaClo on motor function.

This lack of a significant behavioural effect in our model does not necessarily mean that TCE and its metabolites do not show any PD linked toxicity as although the motor behaviour is a widely used marker of PD progression, motor deficits only manifest later in disease progression, with >70-80% neuronal death in the SNpc is needed before symptoms are detected (Hirsch, Graybiel et al. 1988; Fearnley and Lees 1991; Tillerson, Caudle et al. 2002; Chaudhuri, Healy et al. 2006). Investigation of neurotransmitter levels and DA neuron

numbers in the SNpc need assessment to fully elucidate disease progression, and there are many reports of a decrease in DA levels and DA neuron numbers in the SNpc of toxin treated or genetically modified rodent models of PD without any apparent behavioural effect (Petroske, Meredith et al. 2001; Przedborski, Jackson-Lewis et al. 2001; Jackson-Lewis and Przedborski 2007; Hutter-Saunders, Gendelman et al. 2012).

Taken together, our behavioural battery shows some possible trends towards motor dysfunction in the treated mice but no conclusive evidence. This may be due to a lack of toxicity of the compounds to SNpc DA neurons, insufficient exposure of the toxins achieved in the target brain regions, variability in the tests or inadequate SNpc DA cell death reached to give a phenotypic deficit. Due to lack of compliance in the rats, the behavioural studies were not considered relevant.

5.4.3 Do Chronic TCE, Chloral, TaClo and MPTP Treatment Affect Neurotransmitter Levels?

A LC-MS/MS method was developed to measure neurotransmitter levels in rodent brain homogenates as part of this study. However, the method has not been fully characterised and it is not as sensitive or repeatable as needed. One of the major flaws with the assay is a lack of ability to detect any DA, HVA, 5-HT or noradrenaline (NA) in the mouse, or DA, DOPAC or NA in the rat samples. This could possibly be due to a problem with the solid phase extraction (SPE) not capturing these particular neurotransmitters efficiently or a problem with the stability of the compounds with them potentially degrading through the process. In a study into its stability in aqueous solutions, DA was found to be rapidly oxidised in neutral or basic solutions (Shen and Ye 1994). As we would expect DA to be present in the basic elute of SPE, this oxidation could explain the lack of ability of the assay to detect the DA, with similar effects possibly being seen for 5-HT and NA. As oxidation of these compounds seems a possible cause of the lack of detection of the catecholamines in this assay, future studies could use an antioxidant mixture in the homogenates to increase stability, such as the method described in a study which showed the use of an antioxidant mixture of acetic acid, disodium edetate, l-cysteine and ascorbic acid significantly improved the stability of DA, 5-HT and NA in rat brain homogenates (Thorré, Pravda et al. 1997). In addition, further optimisation of the SPE method should be carried out to confirm or improve its efficacy.

Although DA levels have not been quantified, DA metabolites DOPAC and HVA are relevant indicators of DA level and turnover in the brain. In the mouse study, DOPAC levels were significantly reduced in TaClo treated animals and there were also trends towards reduced

levels in chloral and MPTP treated groups; however these were not significant possibly due to the variability in the assay. The significant reduction in DOPAC following TaClo administration is concurrent with a report of decreased DA and DOPAC metabolism, measured by *in vivo* voltammetry with carbon fibre electrodes, in the striatum of rats intranigrally administered with TaClo (Grote, Clement et al. 1995). A study reports decreased DOPAC and HVA, although interestingly not DA, levels in rats treated with oral TCE at doses of 1000mg/kg/day for 6 weeks (Liu, Choi et al. 2010), which does not correlate with our finding that TCE has no significant effect on DOPAC levels. However, with our chronic i.p. dosing regimen, animals are not exposed to the same level of TCE as in this study. If the hypothesis that the DA neurotoxicity of TCE is mediated by TaClo, the reduction in DOPAC following TaClo exposure we report here may correlate with the work of Liu *et al.*, with the dose of TCE they administered converting to TaClo and reducing DOPAC levels. A study that also administered 10mg/kg MPTP i.p., although in a more acute regimen, found a similar decrease in HPLC measured DOPAC levels in the striatum of exposed mice (Araki, Mikami et al. 2000), and a recent investigation to the effects of MPTP in retinal neurons found that DOPAC and HVA levels were reduced at even relatively low doses of acute MPTP (10mg/kg total) (Hamilton, Trickler et al. 2012). These findings support the possible reduction in DOPAC seen in MPTP exposed animals in this study, and suggest that TaClo, and possibly MPTP, reduce levels of DA metabolites DOPAC in the brains of C57BL/6 mice and may lead to the development of PD.

We found that 5-HT metabolite 5-HIAA was significantly increased in TaClo and MPTP exposed animals, and the chloral groups showed a possible, but not significant trend towards an increased level of 5-HIAA. This increase in 5-HIAA could signify an increase in 5-HT turnover in agreement with a report of increased 5-HT levels following TaClo administration in a mouse model (Gerlach, Xiao et al. 1998). The increase in 5-HIAA seen in the MPTP group correlates, to an extent, with a reports of increased 5-HIAA levels in the striatum, but not cortex, of MPTP dosed mice (Fukuda, Hara et al. 1988) and the striatum and hypothalamus of monkeys exposed to MPTP (Di Paolo, Bedard et al. 1986) and a study in C57BL/6 mice which found dose related increases in 5-HIAA, which correlated with increased motor activity (Chia, Ni et al. 1996). However, this is complicated by studies that found 5-HIAA is decreased in serotonergic neurons (Song and Ehrich 1998) and in *in* vivo brain microdialysate in a rat MPTP model (Ozaki, Nakahara et al. 1987). As depression is a common symptom of PD, the increase in 5-HIAA and decrease in DOPAC seen in this study may be a relevant finding when compared with reports that 5-HIAA is increased and DOPAC and HVA decreased in the cerebro-spinal fluid (CSF) of depressed patients (Mitani, Shirayama et al. 2006), raising the possibility that the animals in this study may develop depression as a sign of PD caused by TaClo or MPTP exposure.

However, more investigations need to be carried out with regards to this, as previous studies have found a decrease in 5-HIAA levels in the CSF of PD patients suffering from depression (Kostić, Djuričić et al. 1987; Mayeux, Stern et al. 1988), and other studies reporting no change in CSF 5-HIAA levels in PD patients at all (Chia, Cheng et al. 1993). A study in rats also found increased 5-HIAA levels in the brains of animals subjected to acute stress (De La Garza II and Mahoney III 2004), the increased 5-HIAA seen in our study could also possibly be due to an increase in stress levels due to any neurotoxic effects resulting from TaClo or MPTP exposure. Changes in serotonin release and turnover, and the clinical effects of these changes, in PD and following exposure to neurotoxins, are complicated as evidenced by the contradictory reports found in the literature on the subject. More investigation is therefore needed into the changes reported in this study to elucidate their significance.

GABA was significantly reduced in the caudate of animals exposed to chloral and TaClo but not those given TCE or MPTP or any group in the forebrain. This is contrary to a report that GABA levels are increased following TaClo administration in rats, however, GABA levels were measured immediately following one acute administration by microdialysis (Gerlach, Xiao et al. 1998), rather than in brain tissue following 8 weeks chronic administration used in this study, which may explain the difference seen. Investigations into the effects of anaesthetics on GABA neurotransmission found that in chloral hydrate anaesthetised rats, GABA firing rates were significantly decreased in the ventral tegmental area (Lee, Steffensen et al. 2001) and SNpc (Windels and Kiyatkin 2006), perhaps offering an explanation into the reduction in GABA seen with chloral exposure here; however, these studies were carried out while the animals were anaesthetised rather than chronically treated with chloral. Studies into chronic low level TCE exposure in gerbils and rats on GABA levels found no significant effect in the hippocampus or cerebellum (gerbils)(Briving, Jacobson et al. 1986), or midbrain (rats) (Honma, Hasegawa et al. 1980), consistent with the results seen here. As GABA levels have been shown to be reduced in the post mortem brains of PD patients (Gerlach, Gsell et al. 1996), and GABA spiny neurons are thought to be part of the mechanism by which striatal DA depletion in PD leads to motor dysfunction, this reduction of GABA in chloral and TaClo exposed mice supports the hypothesis that TCE metabolites lead to development of PD. However, in this study and other reports, TCE did not significantly reduce GABA levels, questioning the hypothesis.

Glutamate was found to be moderately decreased in TaClo and MPTP treated mice and severely depleted in chloral exposed animals in both the caudate putamen and forebrain, but TCE treatment did not affect glutamate levels in either brain region. As mentioned above with regards to GABA, a study found an immediate increase in glutamate levels in rats following

TaClo exposure (Gerlach, Xiao et al. 1998), in contrast to our results; however this may be explained by the difference in experimental protocol. C57BL/6 mice treated with MPTP subchronically, although in a slightly more acute model than used in this study, showed a significant reduction in striatal glutamate, but acutely dosed animals showed increased levels (Robinson, Freeman et al. 2003; Holmer, Keyghobadi et al. 2005). This is in agreement with our findings following MPTP exposure here and also offers a possible explanation for the previously mentioned discrepancy between the decreased glutamate seen in this chronic TaClo exposure model and reports of increased glutamate immediately following acute TaClo treatment, as both TaClo and MPTP are thought to enact their toxic mechanism by inhibition of mitochondrial OXPHOS Complex I. Following chronic TCE exposure, glutamate levels were found to be unchanged in hippocampus, and slightly increased in cerebellum (Briving, Jacobson et al. 1986), but significantly decreased in the midbrain (Honma, Hasegawa et al. 1980), suggesting regionally specific effects of the compound. No direct reports on the effect of chloral on glutamate levels were found; however the effect of chloral on glutamate levels may be due to its general anaesthetic properties, as volatile general anaesthetics have been reported to inhibit glutamate release (Bianchi, Battistin et al. 1991; Schlame and Hemmings Jr 1995; Westphalen and Hemmings Jr 2003).

In the rat study, no treatment groups showed any significant effect on any neurotransmitter levels in either brain region examined. A possible reason behind the lack of effect seen in the rat model may be due to the lack of specificity and accuracy of the LC-MS/MS model and the small number of animals with reportable results (as low as two individuals in some groups) leading to increased error in the assay. Future development of a more acceptable neurotransmitter detection method may allow further investigation of this and propose a reason, if any, behind the lack of effect of TCE, chloral & TaClo on neurotransmitter levels in this study.

5.4.4 Conclusions

TCE, chloral, TaClo and MPTP were extremely well tolerated in C57BL/6 mice in this study at the doses and route of administration used with no overt signs of toxicity reported. TaClo was also well tolerated in Wistar rats, but chloral, and, to a greater extent TCE, were less well tolerated and if any future studies are to be carried out in these compounds in rats a different route of exposure must be developed.

TCE and metabolites induced no significant effect on motor function as assessed by any of the behavioural paradigms used in this study in rats or mice, suggesting substantial degeneration of nigral DA neurons (>70% degeneration) has not occurred.

TCE had no significant effect on neurotransmitter levels in either the caudate putamen or forebrain of exposed animals. However, TaClo and TCE showed some effect on DA and 5-HT metabolite levels in mice, consistent with some reports of PD. TaClo and chloral also showed decreases in GABA, and TaClo, MPTP, and particularly chloral, showed decreases in glutamate levels in mice. The rat model showed no significant changes in any neurotransmitter in either brain region in any treatment group. However, these results need to be regarded with caution, as the LC-MS/MS method developed to measure these levels did not show a consistent level of performance across the study, and could not detect certain neurotransmitters at all.

In conclusion, this pilot study suggests C57BL/6 as a more appropriate model for investigation of TCE neurotoxicity, but behavioural assessment of motor function requires higher dosing or a longer assessment period and neurotransmitter LC-MS/MS needs more development to confirm results seen.

Chapter 6
Chronic Effects of TCE & TaClo on Motor Function, SNpc Neurons and Neurotransmitter Levels of Wild Type and Mutant α-synuclein Overexpressing C57BL/6 Mice

6.1 Introduction

α-synuclein is a small protein found in nerve terminals that is a major constituent of Lewy bodies in PD (Spillantini, Schmidt et al. 1997; Spillantini, Crowther et al. 1998) and has been shown to be integrally important in the development of PD in MPTP treated animals (Dauer, Kholodilov et al. 2002). Mutations in the gene encoding α-synuclein have also been linked with development of PD (Polymeropoulos, Lavedan et al. 1997; Zarranz, Alegre et al. 2004). One such mutation is the replacement of an alanine with a proline at position 30 in the protein (A30P), which was discovered in a German family (Kruger, Kuhn et al. 1998). This mutation has been shown to protect α-synuclein against degradation by the autophagy and the proteasome (Cuervo, Stafanis et al. 2004; Song, Patel et al. 2009), which could increase levels in the cell, and has been shown to increase oligomerisation and fibrillation into toxic aggregates (Conway, Harper et al. 1998; Conway, Lee et al. 2000) which in combination would promote SNpc neuron degradation and aid PD progression. A transgenic strain of C57BL/6 mice expressing human A30P α-synuclein has been developed in the laboratory of Prof. Philipp Kahle at the University of Tubingen using a pan-neuronal Thy1 promoter (Kahle, Neumann et al. 2000). This mouse develops a condition that mimics the development of PD with abnormal age-dependent α-synuclein accumulation in the brainstem and an overexpression of tau phosphorylation seen (Kahle, Neumann et al. 2000; Frasier, Walzer et al. 2005). Spontaneous locomotor activity - as assessed by distance travelled, no of rears and stereotypy counts - significantly increased by 12 months and motor co-ordination - as assessed by accelerating rotarod - significantly decreased by 17.5 months (Freichel, Neumann et al. 2007). Although there are no reports of decreased DA levels or DA neuron number in this model, a related model from the same laboratory which expressed A30P specifically in the olfactory neurons under a different promoter showed a significant decrease in DA in this region and a decrease in DA neuron number, that was not quite significant (P=0.08) (Nuber, Petrasch-Parwez et al. 2011).

In addition to the motor deficits seen in PD, disruption to many other systems may occur, sometimes well before motor symptom development. Some of the major non-motor symptoms of PD include dementia, depression, sleep disturbance, gastrointestinal and autonomic dysfunction and fatigue (for review see (Chaudhuri, Healy et al. 2006)). Dementia and other cognitive deficits are a major area of non-motor PD research, with many studies showing associations between the diseases (Cooper, Sagar et al. 1991; Dubois and Pillon 1997; Emre 2003; Riedel, Klotsche et al. 2008) and Dementia with Lewy Bodies (DLB) providing a condition that shows hallmarks of both diseases (McKeith, Mintzer et al. 2004). The human A30P overexpressing mouse model previously discussed has been shown to induce cognitive

decline when assessed by Morris water maze, and to have α-synuclein pathology in the nucleus of the amygdala (Freichel, Neumann et al. 2007).

While there is evidence for both genetic and environmental risk factors in development of PD, it has been suggested that it is likely that for most cases that there is a complex interplay between these influences in the causation of the disease (Warner, Schapira et al. 2003). This has been supported by studies showing that drosophila expressing mutant DJ-1 are more susceptible to developing PD when exposed to environmental toxins such as paraquat and rotenone (Meulener, Whitworth et al. 2005) and that Parkin null mice are more susceptible to rotenone (Casarejos, Menéndez et al. 2006). However, no increase in sensitivity to MPTP was seen in the human A30P overexpressing mice mentioned above (Rathke-Hartlieb, Kahle et al. 2001), suggesting limitations to this theory.

A reduction in DA neuron number in the SNpc of PD patients is characteristic in disease pathology (Bernheimer, Birkmayer et al. 1973). Methods of counting DA neurons in the SNpc are therefore widely used as a marker of disease progression in toxin driven animal models of the disease (Javoy, Sotelo et al. 1976; Betarbet, Sherer et al. 2000; Khaindrava, Ershov et al. 2010).

In a previous study by Sontag *et al.*, rats treated with 0.2mg/kg TaClo daily for 7 weeks showed no change in apomorphine induced locomotor activity 4 to 9 days following end of treatment, but showed a significant increase 12 weeks later (Sontag, Heim et al. 1995), suggesting that behavioural effects may take time to develop following TaClo treatment and suggesting that testing should extend beyond the dosing period when looking for motor deficits in TCE & TaClo treated animals.

6.1.1 Aims

This study aims to continue to assess the general tolerability of TCE and TaClo in both male and female and wild type and A30P mutant α-synuclein over expressing C57BL/6 mice and to explore any changes in motor or cognitive function, neurotransmitter level or SNpc neuron number in treated animals and to compare susceptibility between mutant and wild type. To achieve this, the dosing paradigm developed in Chapter 5 will be used. More extensive longitudinal motor behaviour will be performed in conjunction with a measure of spatial learning and memory, assessment of neuron numbers by stereology post mortem and previously developed methods to measure neurotransmitter levels by LC-MS/MS.

6.2 Methods

For detailed methods see Material and Methods (Section 2).

A 2-sided power calculation was used to estimate the sample size needed for this study based on the Rotarod data generated in the pilot study in the TCE treated animals, the per cent decrease in latency (25%) needed to achieve statistical significance in TCE exposed rats in the study published by Liu *et al.* (Liu, Choi et al. 2010), a significance level of 0.05 and a power of 0.8. This analysis gave a recommended sample size of 8 animals per group, so we decided to use a group size of 10, 5 male and 5 female, to give significant power to this study across all the various measurements to be used.

Due to the lack of any toxicity or behavioural effects seen in C57BL/6 in the pilot study (Chapter 5), the doses of TCE and TaClo to be used in this study were increased 2-fold with animals administered 1000mg/kg TCE and 2mg/kg TaClo.

Animals were dosed twice weekly for 8 weeks. Motor behaviour assessed every 4 weeks for 40 weeks (32 weeks after dosing completed) cognitive behaviour assessed in week 41 (32 weeks after dosing completed) and brains taken for stereological analysis and neurotransmitter assay on week 42 (34 weeks after dosing completed).

6.2.1 Statistical Analysis

For information on statistical methods see General Statistics (Sections 2.8 & 2.8.2)

No significant difference between male and female groups were found in any test in any treatment at any time point so male and female results were combined to give n=10 in further analysis of results for simplification.

6.3 Results

6.3.1 Genotyping

Human A30P α-synuclein overexpressing mice were bred in house from a trio sourced from the laboratory of Kahle at the University of Tubingen, Germany (Kahle, Neumann et al. 2000). To confirm offspring used in the study had the mutation present, DNA extracted from ear punches from all mice, as well as one of the trio as a positive control and a wild type C57BL/6 negative control, was probed for the presence of the mutation by PCR using primers specific for the A30P mutant gene. All A30P mice on study and the positive control had clearly defined bands present at 247 kbp, whereas the negative control had no band (Fig. 6.1) confirming the presence of the A30P mutation in the bred mice.

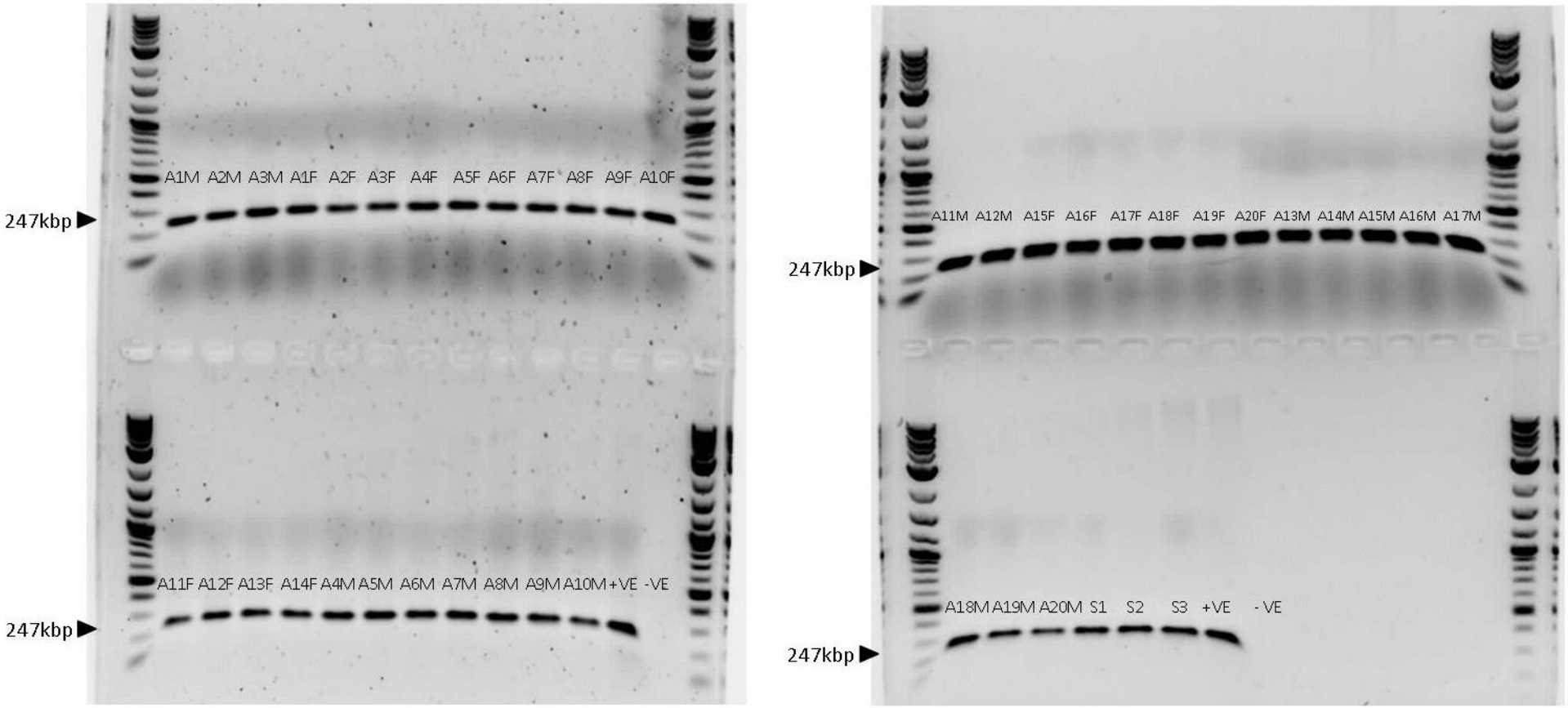

Fig. 6.1 Confirmation of A30P mutant α-synuclein mutation presence DNA was isolated from ear punches taken form all mice to be used on study and the mutation amplified by PCR using primers specific for the insert. Inverted images show PCR product run on a 1% agarose gel alongside molecular size marker with all study animals (A1M-A20M & A1F-A20F), spare animals (S1-3) and a positive control original breeder (+ve) showing a distinct band at 247 kbp that is not present for the negative control wild type (-ve).

6.3.2 General Tolerance

Olive oil, 1000mg/kg TCE and 2mg/kg TaClo i.p. at 10ml/kg were well tolerated-following dosing by all animals throughout the study. No obvious signs of discomfort were displayed following dosing. A proportion of animals had to be terminated due to various clinical abnormalities, none of which were thought to be test-compound related (see section 6.3.2.1 below for details).

6.3.2.1 Clinical Signs

A number of clinical and behavioural abnormalities were observed in all of the treatment groups over the course of the study, some of which led to early termination or required antibiotic treatment, and are described below:

Clinical signs that resulted in early termination of animals are described in Table 6.1. Terminal abnormalities occurred in both A30P and wild type C57BL/6 animals and in olive oil and TCE treated groups but there were no clinical signs resulting in early terminations in any TaClo treated animals.

Post mortem observations resulting from animals with no obvious clinical signs are described in Table 6.2. Lesion found post mortem at study termination in one olive oil treated A30P animal, all other animals no observations post mortem.

Clinical signs that did not result in early termination of animals are described in Table 6.3. Abnormalities occurred in both A30P and wild type C57BL/6 animals and in olive oil and TaClo treated groups but there were no clinical signs in TCE treated animals that did not result in early study termination.

The fighting and wounds on animals A6M, A10M, W2M, & W12-15F (all treatment groups) occurred during a period of building work taking place directly above the animal holding room and are thought to be caused by the stress induced by excess noise caused by this work rather than related to treatment as were spread over all three treatment groups and both A30P mutant and wild type animals.

Animal	Strain	Treatment	Study Day	Clinical Sign	Weight loss	Post Mortem
A13M	A30P	10ml/kg olive oil	178	Weight loss observed, weight maintained until day 192 when found dead	10%	No obvious lesions
W1F	Wild Type	10ml/kg olive oil	17	$2cm^2$ abscess found on abdomen, terminated by anaesthesia and decapitation	No significant	White puss filled growth in abdomen
W5F	Wild type	10ml/kg olive oil	7	Severe weight loss, terminated by cervical dislocation	>20%	No obvious lesions
A6M & A10M	A30P	1000mg/kg TCE	140	Wound to groin area, penis not visible and bladder appeared distended	No significant	Distended bladder
W6M	Wild type	1000mg/kg TCE	140	Subdued, pale extremities, terminated by cervical dislocation	>15%	No obvious lesions

Table 6.1 Terminal clinical signs

Animal	Strain	Treatment	Study Day	Clinical Sign	Weight loss	Post Mortem
A9M	A30P	10ml/kg olive oil	Study termination	No obvious sign	No significant	2cm diameter, white fluid filled cyst found on right kidney

Table 6.2 Post mortem clinical signs

Animal	Strain	Treatment	Study Day	Clinical Sign	Weight loss
W2M	Wild type	1ml/kg olive oil	129	Wounds on back. Treated with Dermasol™* t.d. for 8 days. Wounds closed by end of treatment and completely healed by study day 171.	No significant
A15M	A30P	2mg/kg TaClo	199	Scabs on back and open wound in groin/anal area. Treated with Baytril®** 16 UI, diluted 1 in 10 in saline, s.c. for 9 days. All wounds appeared healed and animal in good condition at end of treatment.	No significant
W13M	Wild type	2mg/kg TaClo	241	$1cm^2$ abscess found on groin (possibly preputial gland). Treated with Baytril®**, 15 UI, diluted 1 in 10 in saline, s.c. for 5 days. Abscess appeared reduced in size over treatment period and healed with animal in good condition at end of treatment.	No significant
W15M	Wild type	2mg/kg TaClo	205	Scab on both flanks. Wounds not considered severe, animal recovered without treatment.	No significant
W11F	Wild type	2mg/kg TaClo	220	Tip of tail severed. Cause unknown, possibly caught in cage lid during bedding change, no clinical relevance.	No significant
W12F W13F W14F W 15F	Wild type	2mg/kg TaClo	73	Various levels of hair loss/barbering on head, back & forearms, continued until the end of the study. Skin was not broken in any cases so not considered detrimental to animals. Thought to be due to stress or dominance behaviour.	No significant

* Dermasol™ -0.05% Clobetasol Propionate BP (International Veterinary, Huntigton Beach, California, USA)
**Baytril® -active ingredient: enrofloxacin (Bayer Animal Health, Newbury, UK)

Table 6.3 Non-terminal clinical signs

6.3.2.2 Weight

Animals in all treatment groups for both A30P mutant and wild type mice showed similar significant normal increase in weight over time (P<0.001, Two-way Repeated Measures ANOVA) with minor fluctuations over the study (Fig 6.2). There was no significant difference in weight between treatment groups or significant effect of treatment over time (Two-way Repeated Measures ANOVA) and no treated animals showed any significantly lower weight at specific time points when compared to the vehicle group (Bonferroni post-test) (Fig. 6.2). This data shows that TCE and TaClo at the exposure levels used in this study have no significant effect on either wild type or A30P mutant mouse body weight.

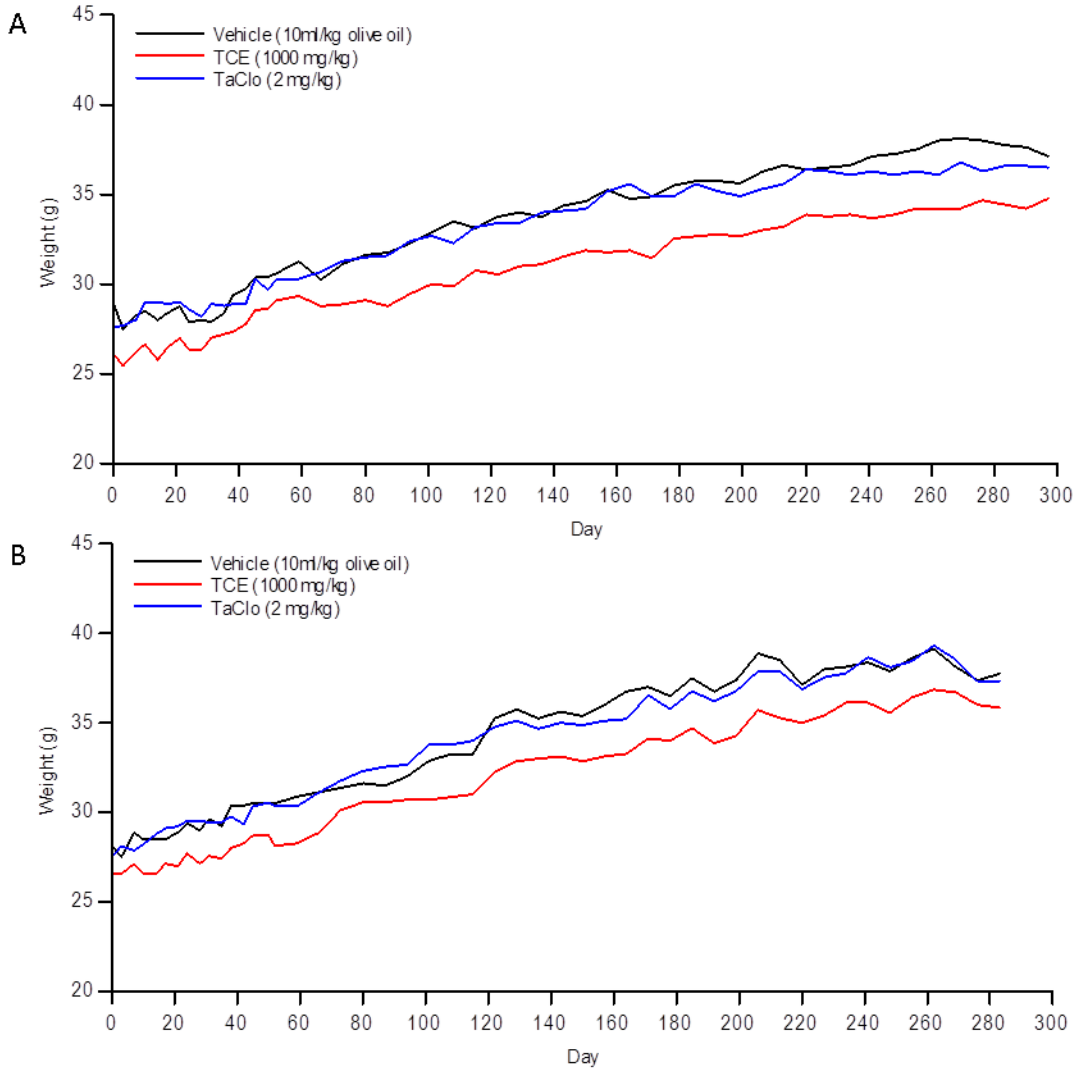

Fig. 6.2 Effect of TCE &TaClo & MPTP on A30P α-synuclein overexpressing & wt C57BL/6 mouse weight Weight (g) of TCE (1000mg/kg), TaClo (2mg/kg) or control (10ml/kg Olive Oil) treated (A) wild-type or (B) A30P C57BL/6 mice over time. Data presented as mean (n=8-10). (A & B) Significant difference over time (P<0.001), No significant difference between treatment groups or of treatment over time, Two-Way Repeated Measures ANOVA

6.3.3 Behavioural Testing

6.3.3.1 Rotarod

To assess motor function in this study, the accelerating rotarod, a well characterised behavioural paradigm used in rodent models (Jones and Roberts 1968), was used prior to and every 4 weeks until 40 weeks after the first dose. Animals were placed on a steadily accelerating rotating rod and time to fall off was recorded. No significant differences between treatment groups and no significant effect of treatment over time were found in either A30P mutant or wild type mice, but there was a significant difference in performance over time across all groups in both A30P and wild type ($P<0.001$, $P<0.05$, respectively, Two-way, Repeated Measures ANOVA) (Fig 6.3). No significant difference was seen at any time point for any treatment when compared to vehicle (Bonferroni post-test). This data suggests that TCE & TaClo have no effect on longitudinal motor function in animals treated at the doses used in this study for 8 weeks and assessed for 40 weeks, but overexpression of A30P mutant α-synuclein may decrease motor function as assessed by the accelerating rotarod test.

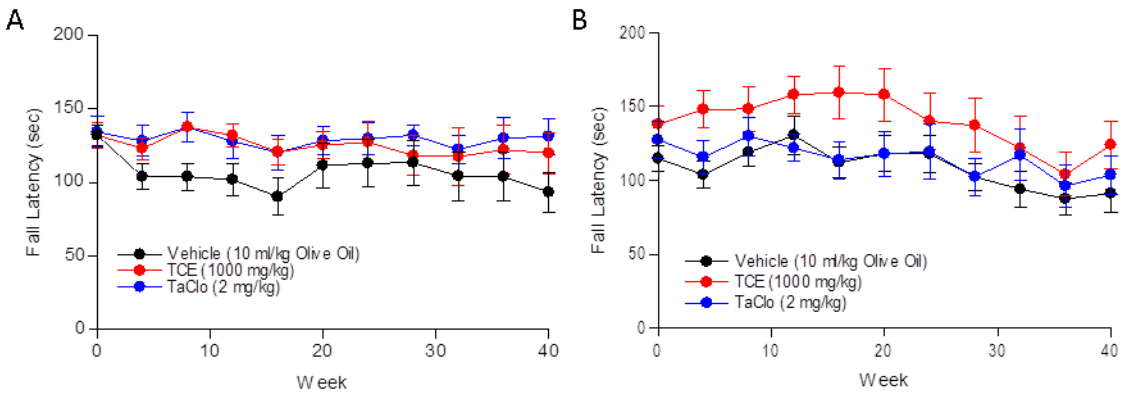

Fig. 6.3 Effect of TCE & TaClo on A30P α-synuclein overexpressing & wt C57BL/6 mouse motor function as assessed by the Rotarod test Average fall latency (sec) of vehicle (10ml/kg olive oil), TCE (100mg/kg) or TaClo (2mg/kg), treated (A) wild-type or (B) A30P C57BL/6 mice over time, triplicate trials. Data presented as mean ± SEM (n=8-10). (A & B) Significant difference over time ($P<0.05$, $P<0.001$ respectively), No significant difference between treatment groups or of treatment over time, Two-Way Repeated Measures ANOVA

6.3.3.2 Pole Test

The pole test, which has been developed to test more fine motor control than the accelerating rotarod in mice (Matsuura, Kabuto et al. 1997), was used in this study to further assess any effects of the treatments on the motor skills of the animals at the same time points as the rotarod test. Animals were placed face up on a pole and total time to complete trial, time to turn on pole, time to descend pole and number of falls per three trials recorded for all animals.

There were no significant differences observed in total trial time between treatment groups or effect of treatment over time, but there was a significant increase in total time over the test period in both A30P overexpressing and wild type mice ($P<0.001$, $P<0.01$ respectively, Two-way, Repeated Measures ANOVA) (Fig 6.4 & 5 A). There were also no significant differences between vehicle and compound-treated animals at any time point (Bonferroni post-test), but there did seem to be a possible trend towards a consistently increased, but not statistically significant, time taken to complete the trial in TCE and TaClo treated mice in the A30P group from ~16 weeks post first dosing maintained until the end of the testing period (Fig 6.5 A).

Similar results were seen when looking at time to turn and time to descend the pole, with no significant differences detected in turn or descent time between treatment groups and no significant effect of treatment over time, but a significant difference in performance was seen over time in A30P and wild type animals in both turning ($P<0.001$, Two-way, Repeated Measures ANOVA) (Fig 6.4 & 5 B) and descent latency ($P<0.001$, $P<0.05$ respectively, Two-way, Repeated Measures ANOVA) (Fig 6.4 & 5 C). Again, no significant differences between vehicle and compound treated animals at any time point were seen, apart from a probably anomalous significant decrease in time to turn on the pole seen at week 28 in wild type TCE treated animals ($P<0.05$, Bonferroni post-test). As in total time, there did seem to be a possible trend towards a consistently increased, but not statistically significant, time taken to descend in TCE and TaClo treated mice when looked at separately in the A30P group from ~16 weeks post first dosing maintained until the end of the testing period (Fig 6.5 C). When looking at turn time, this possible decrease in time between treated and control groups is far less marked (Fig 6.5 C), suggesting that the major effect seen in the difference in the time taken to complete the trial comes from time to descend the pole, rather than turn.

No significant differences in number of falls were seen between treatment groups and no significant effect of treatment over time, but a significant increase was observed in both A30P and wild type mice over time ($P<0.001$, Two-way, Repeated Measures ANOVA) (Fig 6.4 & 5 D). No significant difference in the number of falls was detected between control and TCE & TaClo

treated groups at any time point tested throughout the study (Bonferroni post-test). As seen with total time and descent time, there did seem to be a possible trend towards a consistently increased, but not statistically significant, time taken to descend in TCE and TaClo treated mice when looked at separately in the A30P group from ~16 weeks post first dosing maintained until the end of the testing period with TCE treated animals falling almost twice as often as controls and TaClo treated falling over 1.5 times more often (Fig 6.5 D).

This data suggests that TCE & TaClo may lead to a slight but not significant decrease in longitudinal fine motor control in animals that overexpressed human A30P mutant α-synuclein treated at the doses used in this study for 8 weeks.

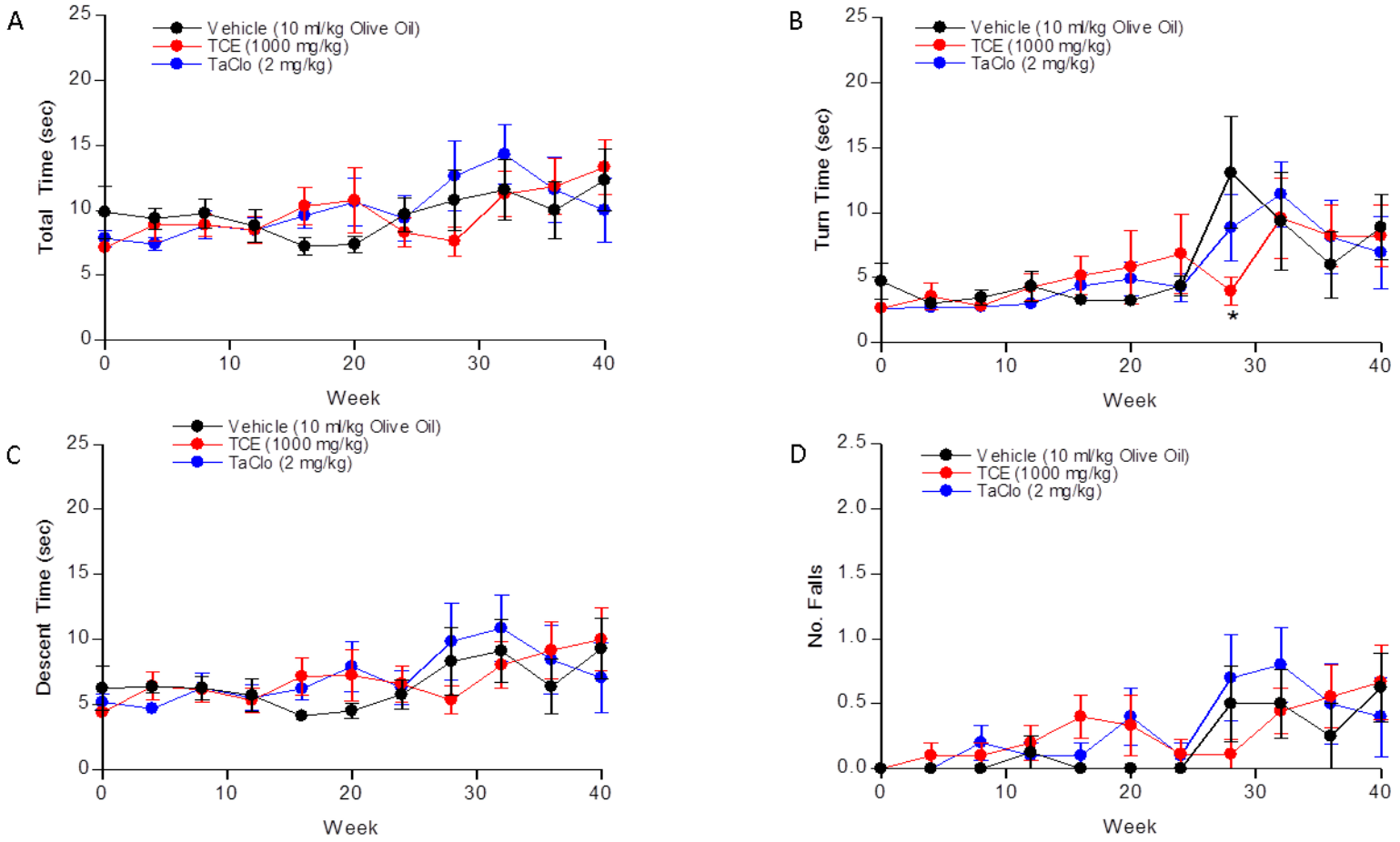

Fig. 6.4 Effect of TCE & TaClo on wild-type C57BL/6 mouse motor function as assessed by the Pole test Average (A) total time, (B) turn time (C) descent time (all sec) & (D) Number of falls per trial of vehicle (10ml/kg olive oil), TCE (100mg/kg) or TaClo (2mg/kg), treated wild-type C57BL/6 mice over time, triplicate trials. Data presented as mean ± SEM (n=8-10). (A-D) Significant difference over time ($P<0.01$, $P<0.001$, $P<0.05$, $P<0.001$, respectively), No significant difference between treatment groups or of treatment over time, Two-Way Repeated Measures ANOVA. *$P<0.05$ when compared to vehicle at relevant time point, Bonferroni post-test

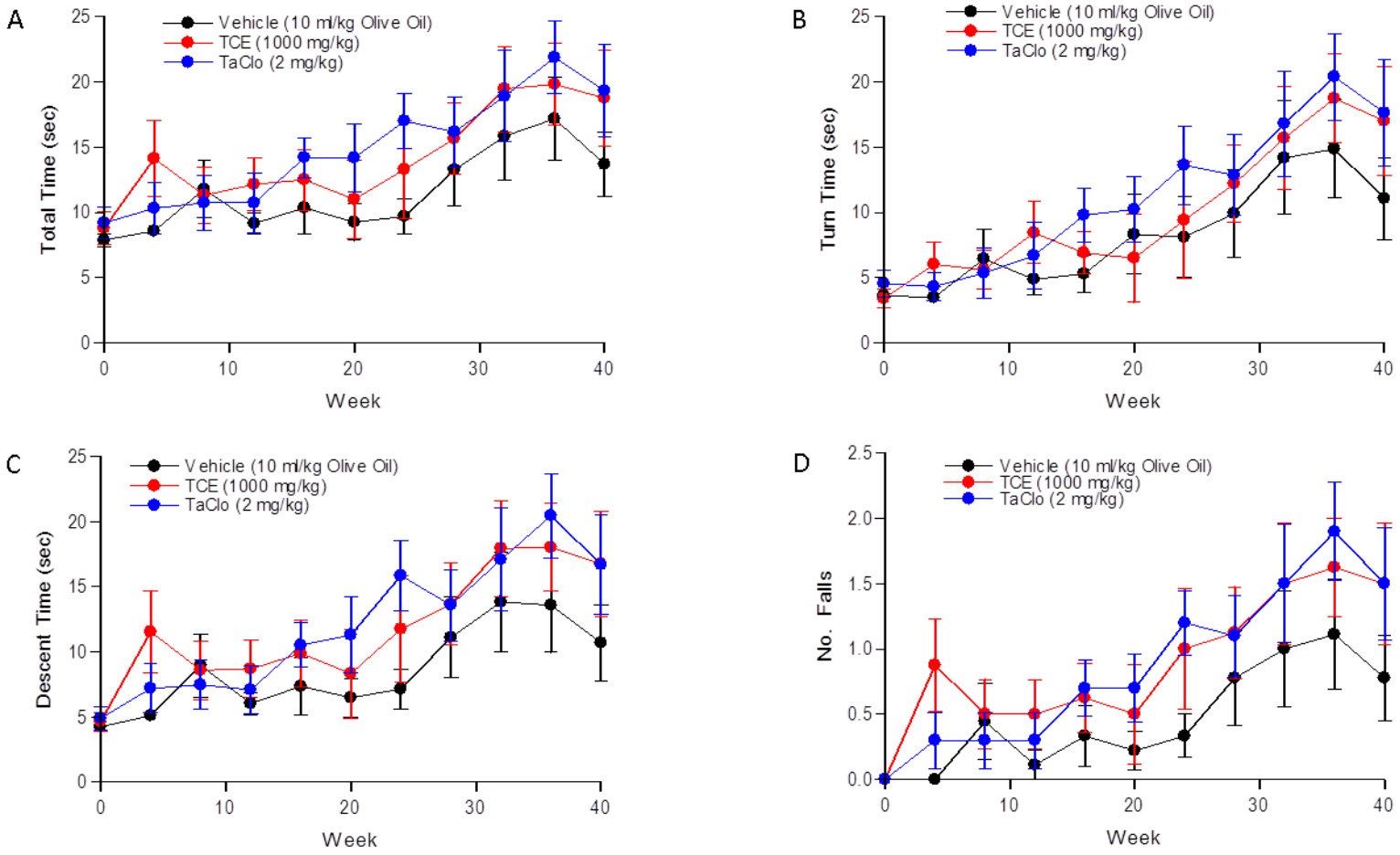

Fig. 6.5 Effect of TCE & TaClo on A30P α-synuclein overexpressing C57BL/6 mouse motor function as assessed by the Pole test Average (A) total time, (B) turn time (C) descent time (all sec) & (D) Number of falls per trial of vehicle (10ml/kg olive oil), TCE (100mg/kg) or TaClo (2mg/kg), treated A30P α-synuclein overexpressing C57BL/6 mice over time, triplicate trials. Data presented as mean ± SEM (n=8-10). (A-D) Significant difference over time (P<0.001), No significant difference between treatment groups or of treatment over time, Two-Way Repeated Measures ANOVA

6.3.3.3 Gait Analysis

Differences in gait and stride length have been reported in animal models of PD (Tillerson, Caudle et al. 2002; Amende, Kale et al. 2005) and have been shown to be a relevant marker of decreased motor function in transgenic mice (Crawley 1999), so animal gait was analysed from post dose weeks 28 to 40 by painting animals' hind paws and running them down a corridor to the home cage allowing measurement of stride length. There were no significant differences observed in average stride length between treatment groups or effect of treatment over time in either A30P or wild type mice, and no significant change between trials in the A30P animals but there was a significant increase in total time over the test period in the wild type groups ($P<0.001$, Two-way, Repeated Measures ANOVA) (Fig 6.6 A). There were also no significant differences between vehicle and compound treated animals at any timepoint apart from in the TCE treated animals at week 32 where a significant increase in TCE treated animals was seen when compared to control ($P<0.01$, Bonferroni post-test); however this change was not maintained with stride length returning to control levels by the next test in week 36, suggesting this potential effect is not relevant. These results suggest that neither TCE nor TaClo treatment mice has any significant effect on stride length in wild type or A30P overexpressing mice.

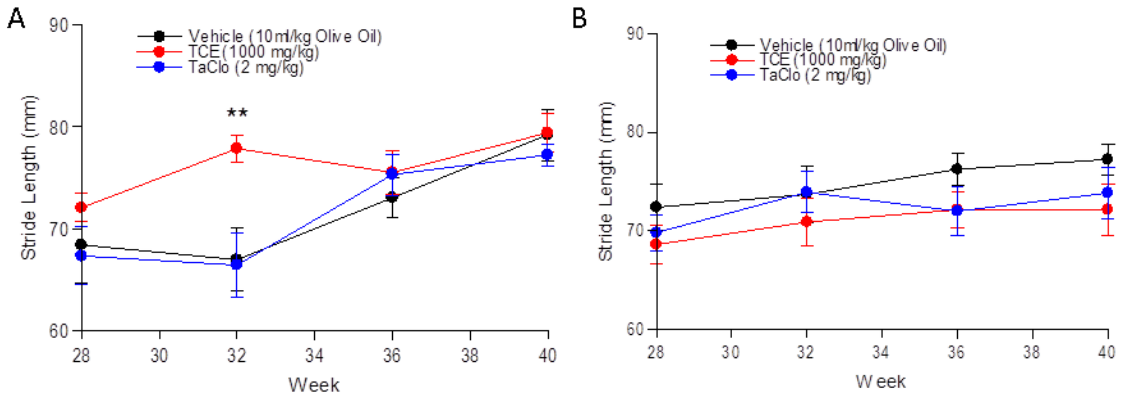

Fig. 6.6 Effect of TCE & TaClo on A30P α-synuclein overexpressing & wt C57BL/6 mouse motor function as assessed by gait analysis Average stride length (mm) of vehicle (10ml/kg olive oil), TCE (100mg/kg) or TaClo (2mg/kg), treated (A) wild-type or (B) A30P C57BL/6 mice over time, triplicate trials. Data presented as mean ± SEM (n=8-10). (A) Significant difference over time ($P<0.001$), (B) No significant difference over time, (A & B) No significant difference between treatment groups or of treatment over time, Two-Way Repeated Measures ANOVA. **$P<0.01$ when compared to vehicle at relevant timepoint, Bonferroni post-test

6.3.3.4 Grip Strength

As abnormalities in grip strength have been reported in mouse models of PD (Colotla, Flores et al. 1990) and spinal pathology has been reported in A30P overexpressing mice (Neumann, Kahle et al. 2002), a test of grip strength using a strain gage was used in this study (Cabe, Tilson et al. 1978). There were no significant differences observed in grip strength between treatment groups and no significant effect of treatment over time in either A30P or wild type mice; however there was a significant difference over time in both groups ($P<0.05$, $P<0.001$ respectively, Two-way, Repeated Measures ANOVA) (Fig 6.7). There were also no significant differences between vehicle and compound treated animals at any timepoint in either A30P or wild type mice (Bonferroni post-test), with all treatment groups appearing to stay relatively stable throughout the study. This data suggests that TCE and TaClo have no effect on mouse grip strength at the doses given in this study.

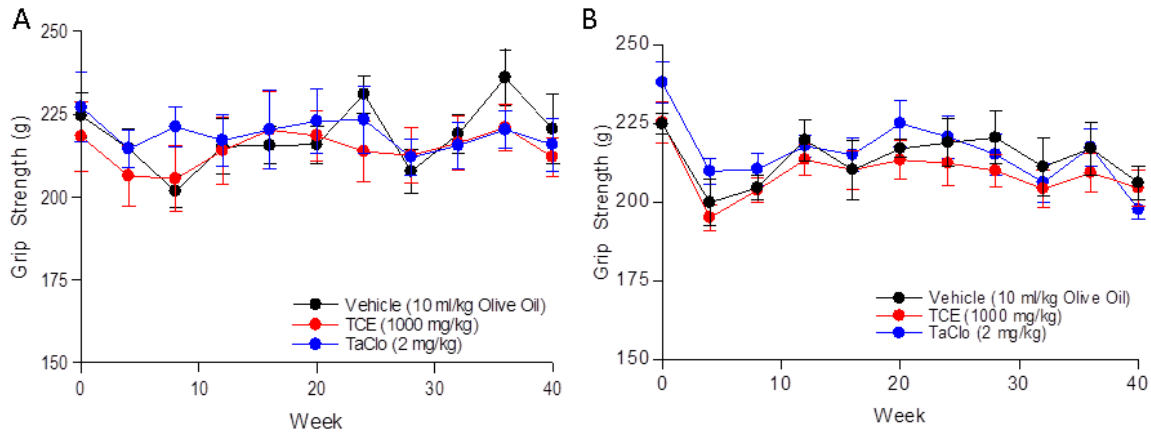

Fig. 6.7 Effect of TCE & TaClo onA30P α-synuclein overexpressing & wt C57BL/6 mouse grip strength Average grip strength (g) of vehicle (10ml/kg olive oil), TCE (100mg/kg) or TaClo (2mg/kg), treated (A) wild-type or (B) A30P C57BL/6 mice over time, triplicate trials. Data presented as mean ± SEM (n=8-10). (A & B) Significant difference over time ($P<0.001$, $P<0.05$ respectively), No significant difference between treatment groups or of treatment over time, Two-Way Repeated Measures ANOVA

6.3.3.5 Barnes Maze

As the A30P overexpressing mouse model used in this study have been shown to have cognitive deficits (Freichel, Neumann et al. 2007), learning and memory were assessed in this study. The Barnes maze is a test used to assess spatial and learning and both short and long term memory using the mouse's ability to find and remember the location of an escape box located under one of 20 equally spaced holes around the edge of a circular maze using visual cues as landmarks (Barnes 1979; Patil, Sunyer et al. 2009).

Learning is assessed using the time to find the escape hole (primary latency), time to enter escape box (total latency), number of errors before finding escape hole (primary errors) and total number of errors before entering escape box (total errors) over four trials for each of 4 consecutive days.

For all four measurements of learning, for all treatment groups and in both A30P and wild type mice, there were no significant differences between treatment groups or of treatment over time but all animals significantly improved at finding and entering the escape box over the days of the study ($P<0.001$, Two-way Repeated Measures ANOVA) (Figs. 6.8 & 9). There is a possible trend towards a decrease in primary latency & errors in the TaClo treated wild type mice on Day 1 (Fig. 6.8 A & C) and an increase in total errors in the TCE treated wild type mice on day 3 (Fig. 6.8 D), although these are not significant (Bonferroni post-test) and on the following Day are back to being the same as control levels, suggesting an anomaly. There also appears to be a slight but non-significant ($P=0.099$, Bonferroni post-test) increase in primary errors in TaClo treated A30P mice when compared to vehicle treated animals on Day 4 (Fig. 6.9 C). This suggests TaClo may lead to a slight decrease in learning ability when combined with overexpression of A30P mutant human α-synuclein in C57BL/6 mice.

Taken together this data suggests that TCE & TaClo, at the exposure levels used in this study, do not lead to significant spatial learning deficits in wild type or A30P mice; however there may be a suggestion that TaClo in combination with overexpressed A30P mutant human α-synuclein may have a small effect on learning as seen by the slight increase in number of errors seen before the escape box was found in A30P mice exposed to TaClo on Day 4 of the learning phase of the Barnes maze.

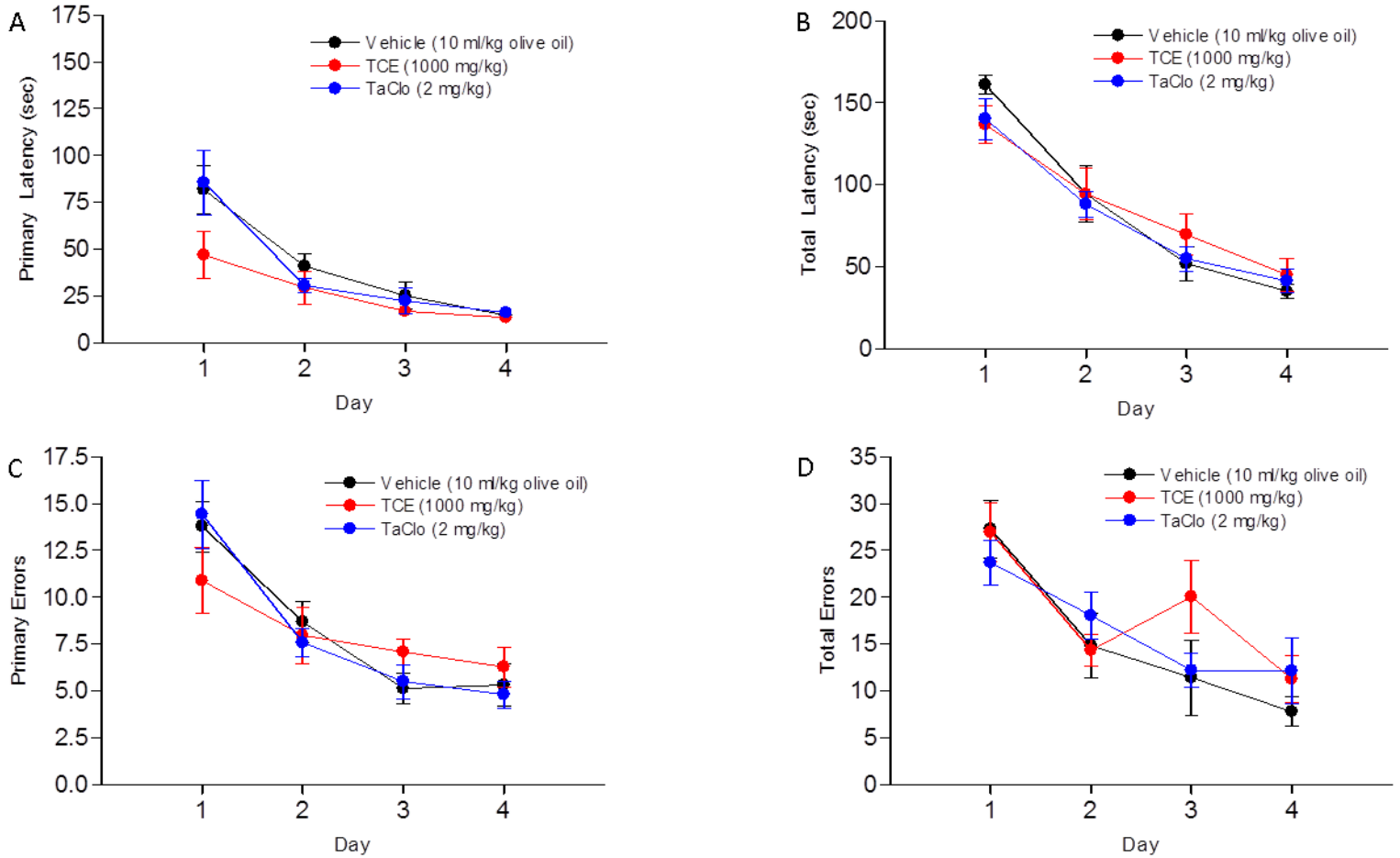

Fig. 6.8 Effect of TCE & TaClo on wt C57BL/6 mouse spatial learning as assessed by the Barnes maze Average (A) primary latency, (B) total latency (both sec), (C) primary errors & (D) total errors to find target of vehicle (10ml/kg olive oil), TCE (100mg/kg) or TaClo (2mg/kg), treated wild-type or C57BL/6 mice over time, quadruplicate trials. Data presented as mean ± SEM (n=8-10). (A-D) Significant difference over time ($P<0.001$), No significant difference between treatment groups or of treatment over time, Two-Way Repeated Measures ANOVA

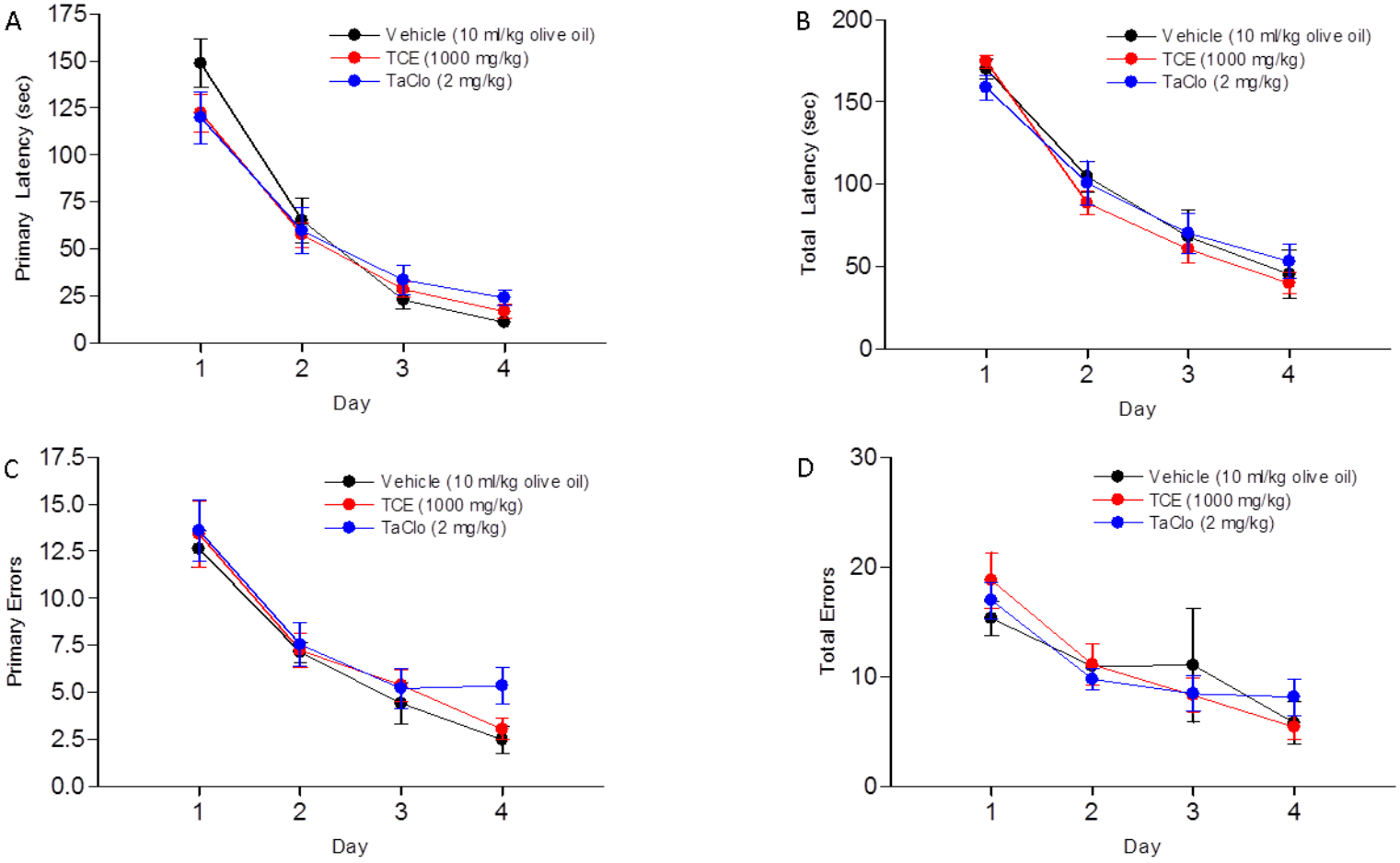

Fig. 6.9 Effect of TCE & TaClo on A30P α-synuclein overexpressing C57BL/6 mouse spatial learning as assessed by the Barnes maze Average (A) primary latency, (B) total latency (both sec), (C) primary errors & (D) total errors to find target of vehicle (10ml/kg olive oil), TCE (100mg/kg) or TaClo (2mg/kg), treated wild-type or C57BL/6 mice over time, quadruplicate trials. Data presented as mean ± SEM (n=8-10). (A-D) Significant difference over time ($P<0.001$), No significant difference between treatment groups or of treatment over time, Two-Way Repeated Measures ANOVA

Memory is assessed in the probe phase of the Barnes maze, where on Day 5 (short term memory) and Day 12 (long term memory) a single trial is carried out with no escape box and primary latency (time to find hole where box should be), number of holes visited, first hole visited and number of nose pokes in each hole of the maze are recorded. A score is also generated by assigning each hole a numerical value based on how far it is from the target hole and calculating the sum of nose pokes in each hole based on these values (e.g 3 pokes in a hole 4 away from target gives a score of 12, 2 pokes in a hole 9 away from target a score of 18 etc.) to give a numerical value to performance in the test.

No significant differences between treatment groups were observed in primary latency in either A30P or wild type animals in either short or long term tests (One-way ANOVA) (Fig 6.10). However in the long term memory test in theA30P animals, there was a trend towards an increase in primary latency with TCE and TaClo treated animals taking 24.38 & 24.20 seconds respectively to find the target hole as compared to 13.50 seconds taken by vehicle treated mice (Fig. 6.10 B(ii)) and in the short term test, vehicle treated wild type animals showed a trend towards an increase in primary latency in vehicle treated animals (Fig. 6.10 A(i)). All other values were similar across treatment groups and between A30P and wild type animals.

There were also no significant differences between treatment groups observed in number of holes visited in either A30P or wild type animals in either short or long term tests (One-way ANOVA) (Fig 6.11). In the long term memory test in theA30P animals, there was a trend towards an increase in primary latency with TCE and TaClo treated animals visiting over 5 holes as compared to below 3 in the vehicle treated group, although this was not significant (Fig. 6.11 B(ii)). All other values were similar across treatment groups and between A30P and wild type animals.

When looking at the primary hole animals visited in the trials, no significant difference in the median hole visited between any of the groups was observed in either short or long term memory probes in either the A30P mutant or wild type mice (Kruskal Wallis test) (Fig. 6.12). In the A30P mutant short term memory test, the TaClo animals showed a trend towards primarily visiting a hole further from the target with an upper quartile of 4.5 as compared to 3 & 2 for vehicle and TCE respectively (Fig. 6.12 B(i)), a finding which was more pronounced in the long term memory test with more TCE and particularly TaClo (upper quartiles of 4 & 6.5 respectively) treated animals showing a preference towards a first move further from the target hole than vehicle (2.5) (Fig. 6.12 B(ii)). In the wild type mice short term memory probe, similar results were seen but with more TCE treated mice (upper quartile of 7) seeming to

show a slight increase in distance from target of first hole visited than vehicle or TaClo (4.5 & 5 respectively) (Fig. 6.12 A(i)), and this trend increased in the long term memory test with less vehicle animals (upper quartile 3) primarily exploring farther from the target than TCE and TaClo (8 & 5.5 respectively) (Fig. 6.12 A(ii)).

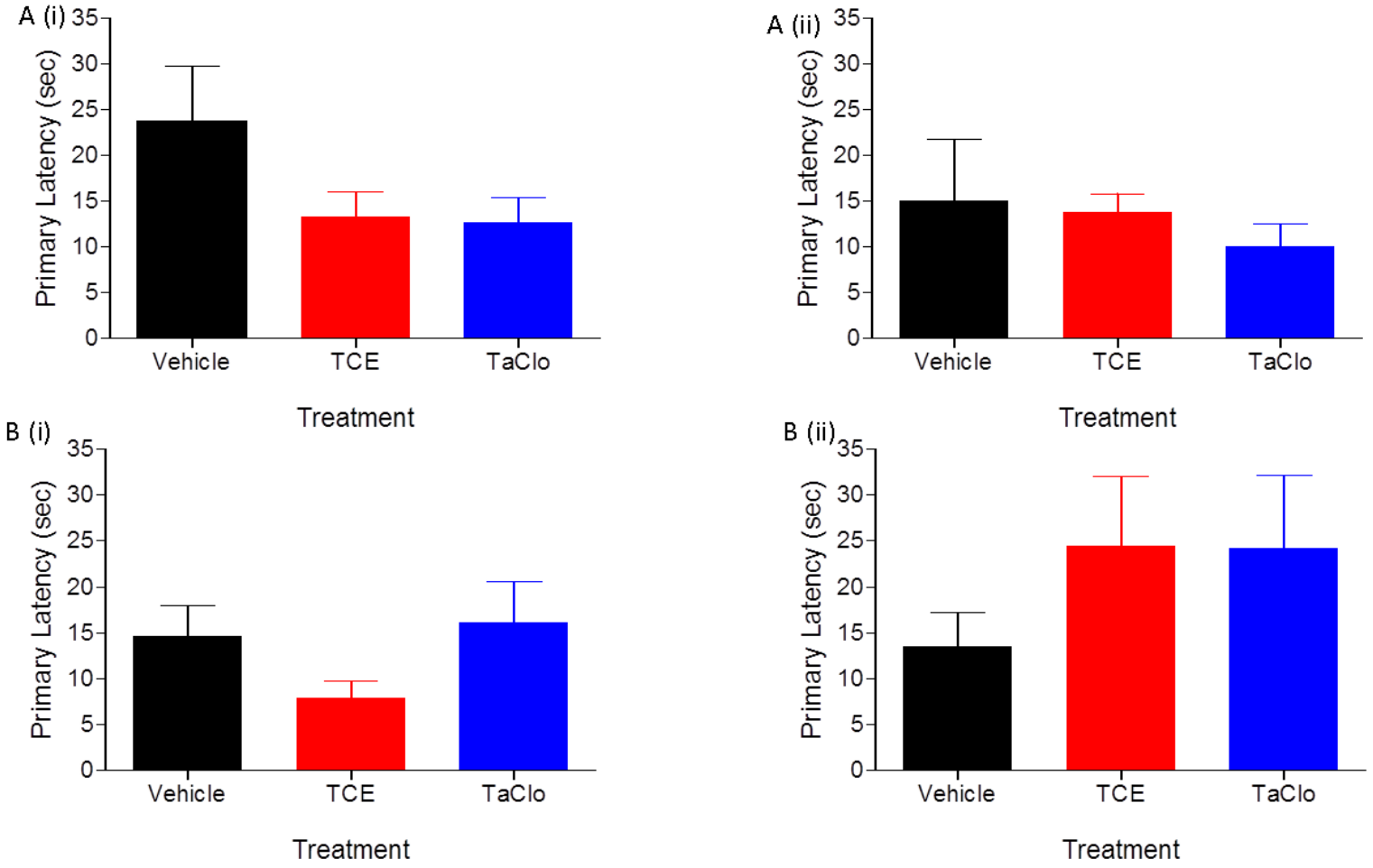

Fig. 6.10 Effect of TCE & TaClo on A30P α-synuclein overexpressing & wt C57BL/6 mouse spatial memory as assessed by the Barnes maze primary latency
Average primary latency (sec) to find target hole during (i) short term (Day 5) or (ii) long term (Day 12) probe test of vehicle (10ml/kg olive oil),TCE (100mg/kg) or TaClo (2mg/kg), treated (A) wild-type or (B) A30P C57BL/6 mice. Data presented as mean ± SEM (n=8-10). No significant difference between treatment groups, One-Way ANOVA.

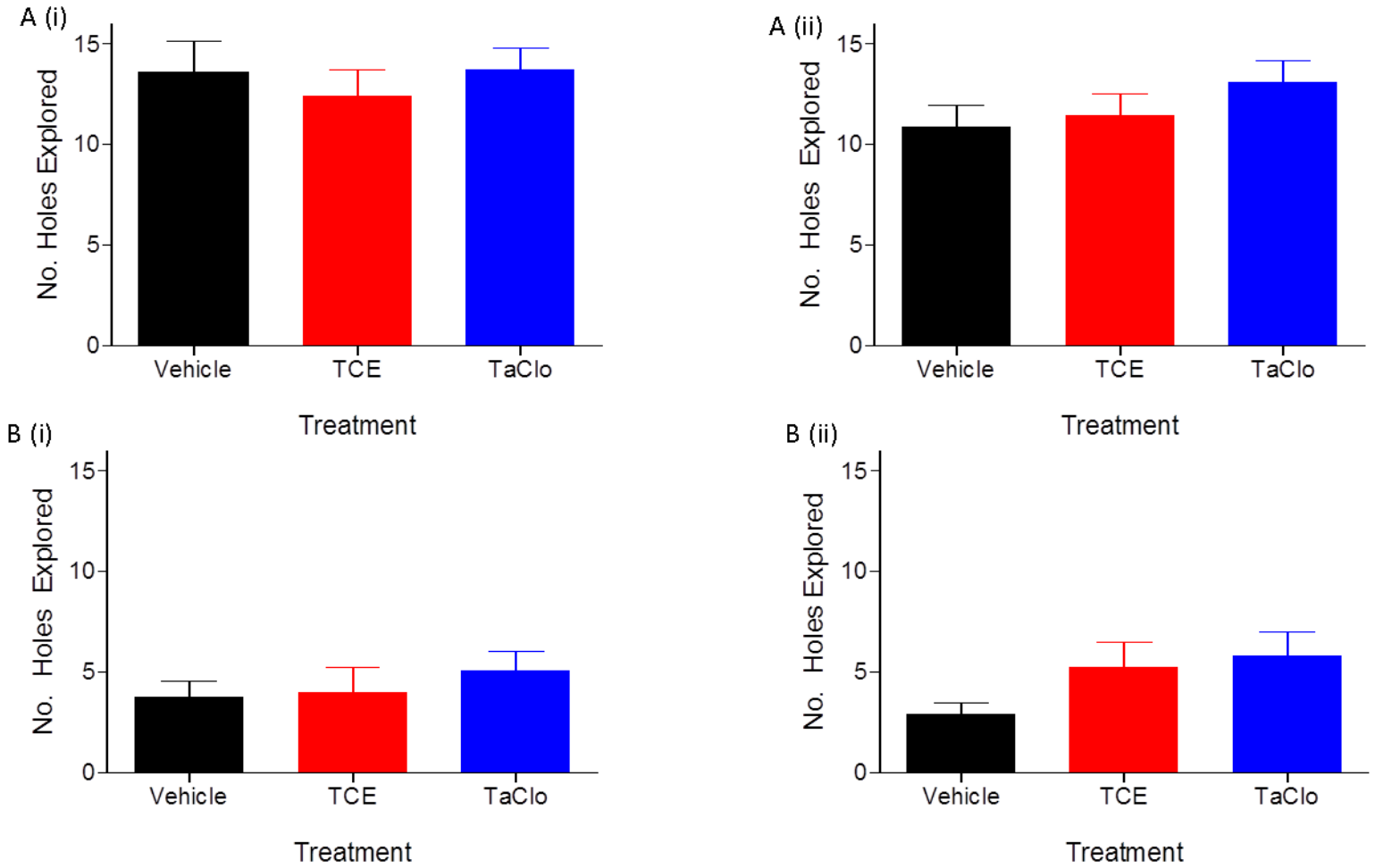

Fig. 6.11 Effect of TCE & TaClo on A30P α-synuclein overexpressing & wt C57BL/6 mouse spatial memory as assessed by the Barnes maze number of holes explored Average no. of holes explored hole during (i) short term (Day 5) or (ii) long term (Day 12) probe test of vehicle (10ml/kg olive oil),TCE (100mg/kg) or TaClo (2mg/kg), treated (A) wild-type or (B) A30P C57BL/6 mice. Data presented as mean ± SEM (n=8-10). No significant difference between treatment groups, One-Way ANOVA.

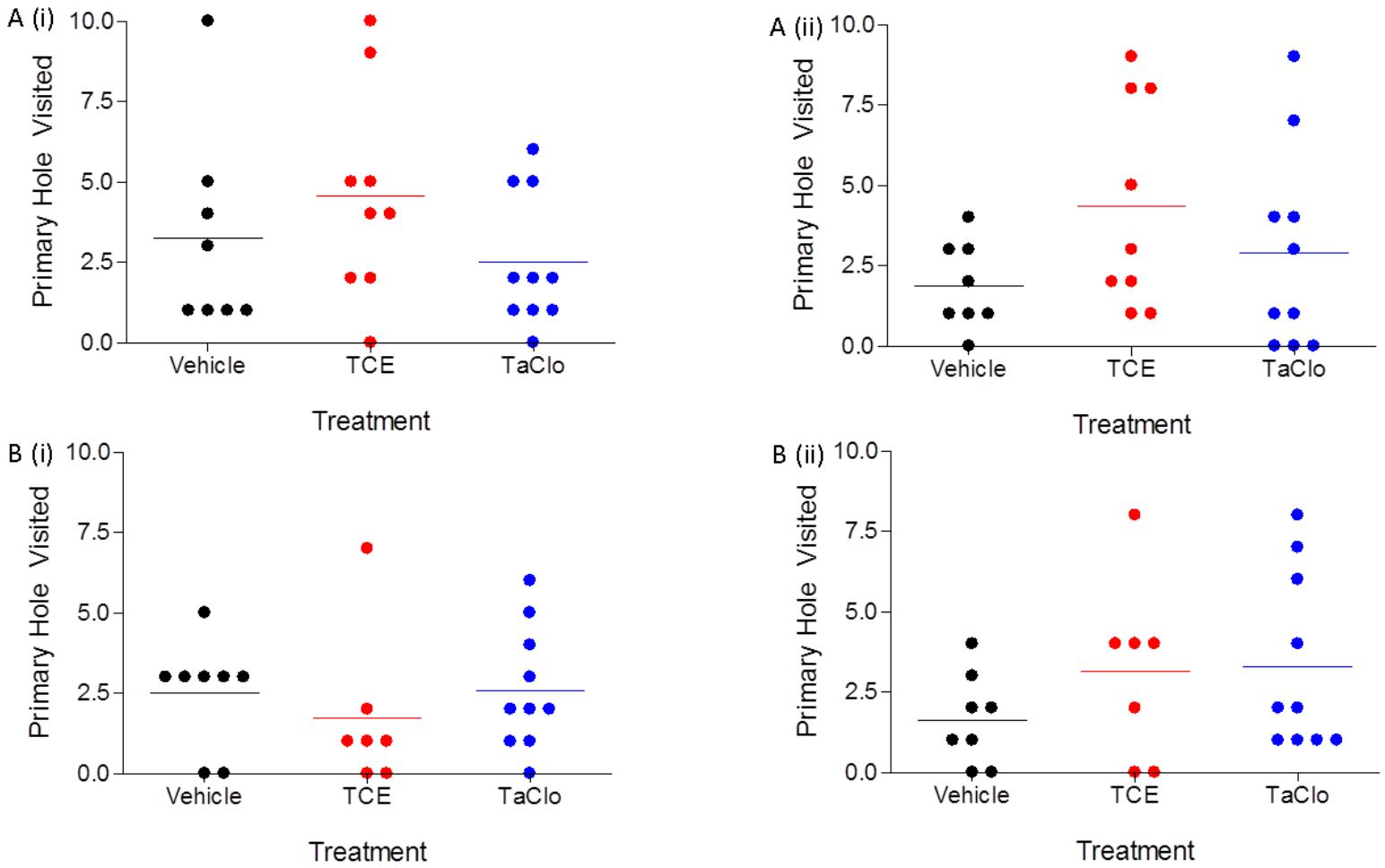

Fig. 6.12 Effect of TCE & TaClo on A30P α-synuclein overexpressing & wt C57BL/6 mouse spatial memory as assessed by the Barnes maze primary hole visited
Primary hole visited during (i) short term (Day 5) or (ii) long term (Day 12) probe test of vehicle (10ml/kg olive oil),TCE (100mg/kg) or TaClo (2mg/kg), treated (A) wild-type or (B) A30P C57BL/6 mice. Data presented as median ± quartiles (n=8-10). No significant difference between treatment groups, Kruskal Wallis test.

In general there were no consistent significant differences between the times TCE or TaClo treated animals poked any holes throughout the maze when compared to vehicle in either strain in short or long term probe tests (unpaired t-test) (Fig 6.13). There were a few holes where a significant difference is seen; wild-type short term probe, hole +5 significantly increased pokes in TCE group; A30P short term probe, hole -3 significantly decreased pokes in TCE group; A30P long term probe, hole +1 significantly increased pokes in TaClo group (all $P<0.05$, unpaired t-test) (Fig. 6.13). However, these results were not consistent across groups and probes and were not considered relevant. When comparing the spread of holes poked away from the target hole, in the A30P mice short term memory probe, the spread is relatively even with the vehicle mice exploring as far as seven holes from target, TCE as far as eight and TaClo exploring as far as the opposite hole to the target (Fig. 6.13 B(i)). In the long term memory probe, there is a more significant difference in exploratory behaviour, with the vehicle treated group exploring no further than three holes away from the target and both the TCE and TaClo treated groups visiting as far as the hole opposite the target (Fig. 6.13 B(ii)). In comparison, the wild type mice of all treatment groups show significantly more nose pokes suggesting more exploratory behaviour and all explore the entire maze in both the long and short term probes, with animals exploring as far as the opposite hole to the target (Fig. 6.13 A).

When using the quantifiable score for each animal, similar results can be seen. In the A30P short term probe there are no significant difference in the median scores between the groups (Kruskal Wallis test); however, the TaClo group shows a far greater upper quartile (62 compared to 18 & 11 in vehicle and TCE respectively), suggesting some animals are exploring more and gaining a higher score following TaClo treatment (Fig 6.14 B (i)), correlating with the greater spread in holes explored seen previously. In the A30P long term memory probe, TCE and TaClo treated groups show a slight, but not significant increase in median score when compared to vehicle (Kruskal Wallis test); however there are quite substantial increases in the upper quartile from 7.5 in the vehicle to 47 in the TCE treated, and 98 in TaClo treated groups (Fig. 6.14 B (ii)) supporting the increase in spread of nose pokes to holes a greater distance from the target in compound treated animals. In wild type animals, no significant differences in median scores or quartile values were seen in either short or long term memory tests (Kruskal Wallis test) but both median and quartile values were higher in wild type groups when compared to A30P animals supporting the increased general exploratory behaviours in the test (Fig 6.14 A).

In summary, there were no statistically differences between treatment groups in either strain in any measure of the probe test. There is a suggestion that TCE & TaClo treated A30P animals

may have some deficit in long term memory with the increased exploration away from the target hole but this cannot be confirmed with this study. There is also a difference between wild-type and A30P animals with wild-type showing far more exploratory behaviour in both short and long term memory probes.

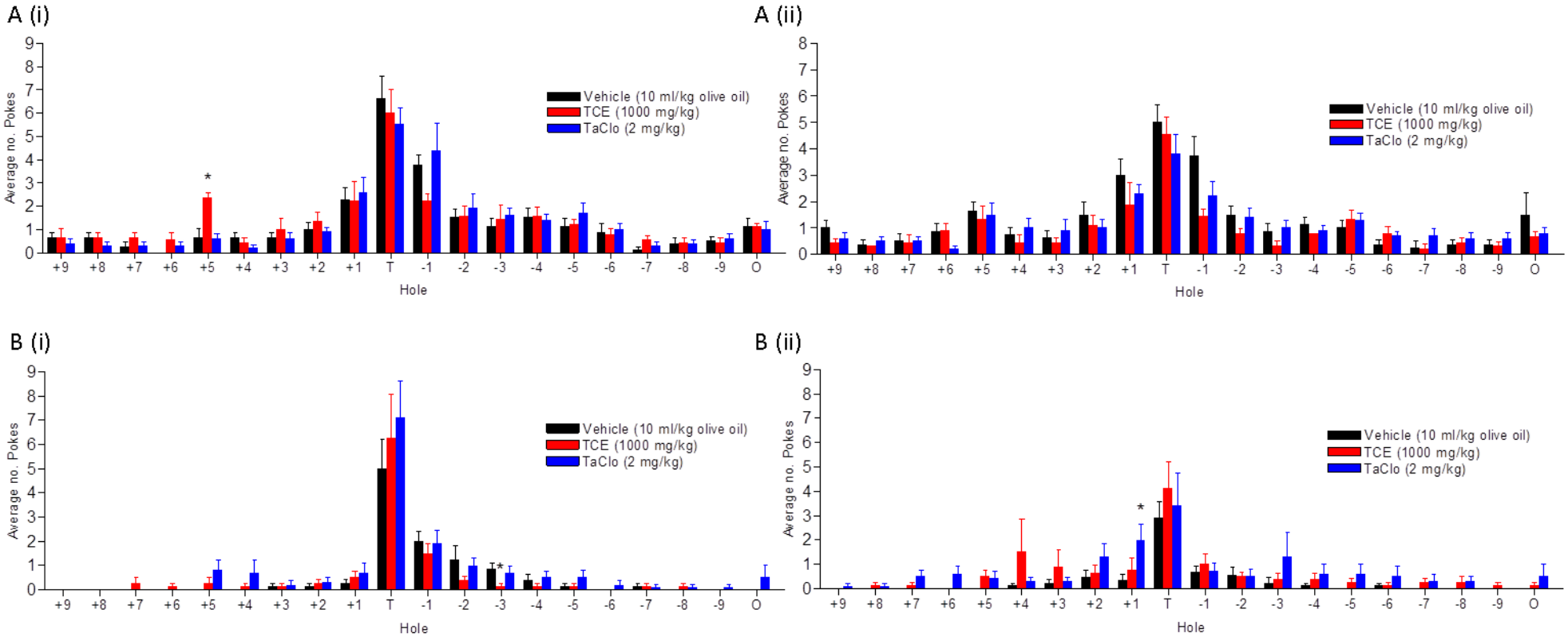

Fig. 6.13 Effect of TCE & TaClo on A30P α-synuclein overexpressing & wt C57BL/6 mouse spatial memory as assessed by the Barnes maze nose pokes Average nose pokes in each hole during (i) short term (Day 5) or (ii) long term (Day 12) probe test of vehicle (10ml/kg olive oil),TCE (100mg/kg) or TaClo (2mg/kg), treated (A) wild-type or (B) A30P C57BL/6 mice. Data presented as mean ± SEM (n=8-10). *P<0.05 when compared to vehicle (unpaired t-test)

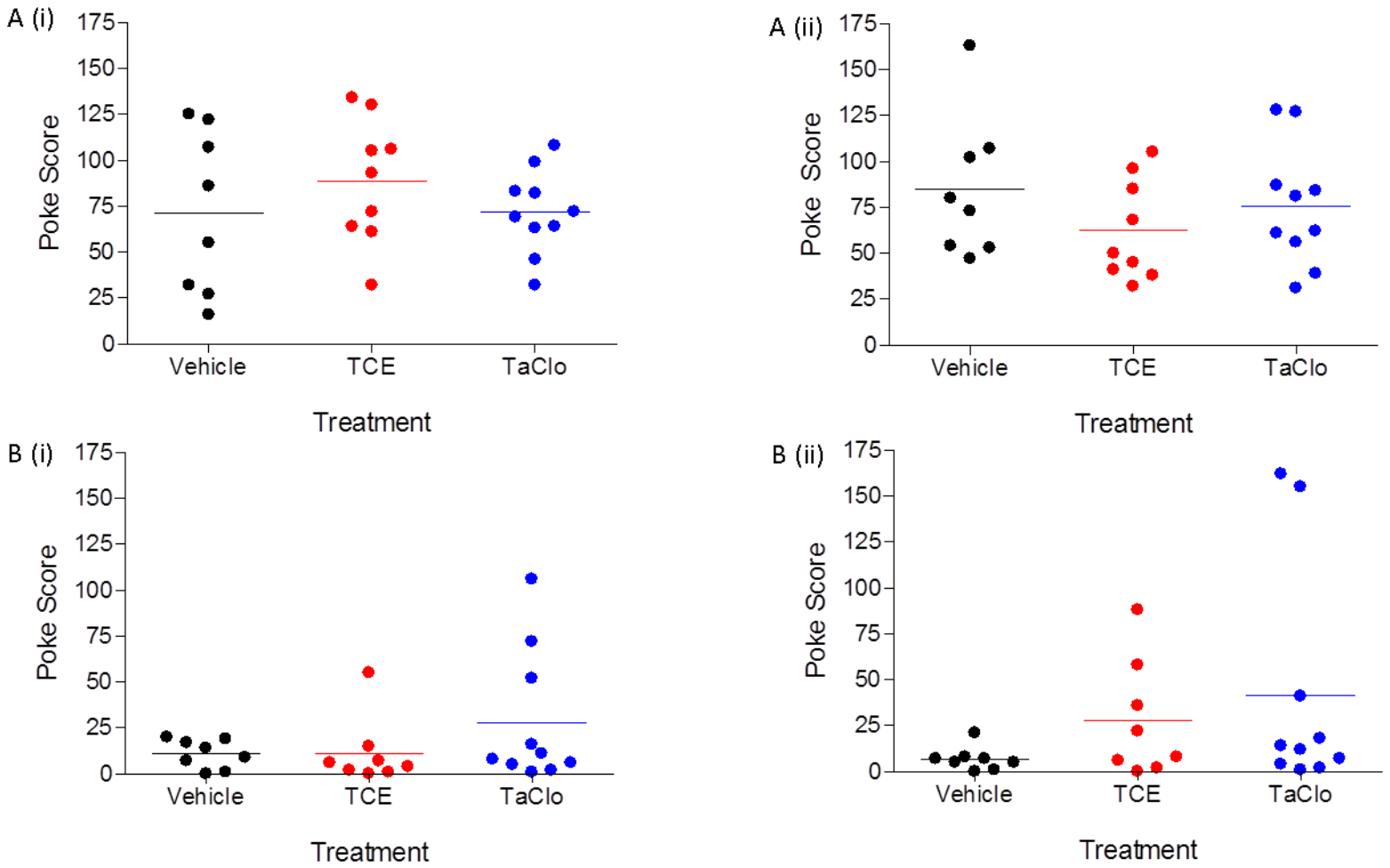

Fig. 6.14 Effect of TCE & TaClo on A30P α-synuclein overexpressing & wt C57BL/6 mouse spatial memory as assessed by the Barnes maze poke score Poke score during (i) short term (Day 5) or (ii) long term (Day 12) probe test of vehicle (10ml/kg olive oil),TCE (100mg/kg) or TaClo (2mg/kg), treated (A) wild-type or (B) A30P C57BL/6 mice. Data presented as median ± quartiles (n=8-10). No significant difference between treatment groups, Kruskal Wallis test

6.3.4 Neurotransmitter Levels

An alteration in neurotransmitter levels has been reported in the brains of PD patients with reduced levels of DA a hallmark of the condition and decreases in serotonin, noradrenaline, and GABA (Bernheimer, Birkmayer et al. 1973; Rinne and Sonninen 1973; Riederer, Birkmayer et al. 1977; Scatton, Javoy-Agid et al. 1983; Gerlach, Gsell et al. 1996) with glutamate also linked with the pathogenesis of the disease (Blandini, Porter et al. 1996). Neurotransmitter levels were therefore measured in the caudate putamen and forebrain of study animals by LC-MS/MS post mortem.

DA levels were not quantified due to limitations in the assay and neither was DOPAC in A30P animals; however DOPAC and HVA were measurable in wild-type animals and HVA in A30P. No significant changes in DOPAC or HVA levels were observed in the either brain region following TCE or TaClo treatment in either strain of mice (One-way ANOVA) (Fig. 6.15). There were also no significant differences seen in HVA levels between wild-type and A30P animals (see Appendix A).

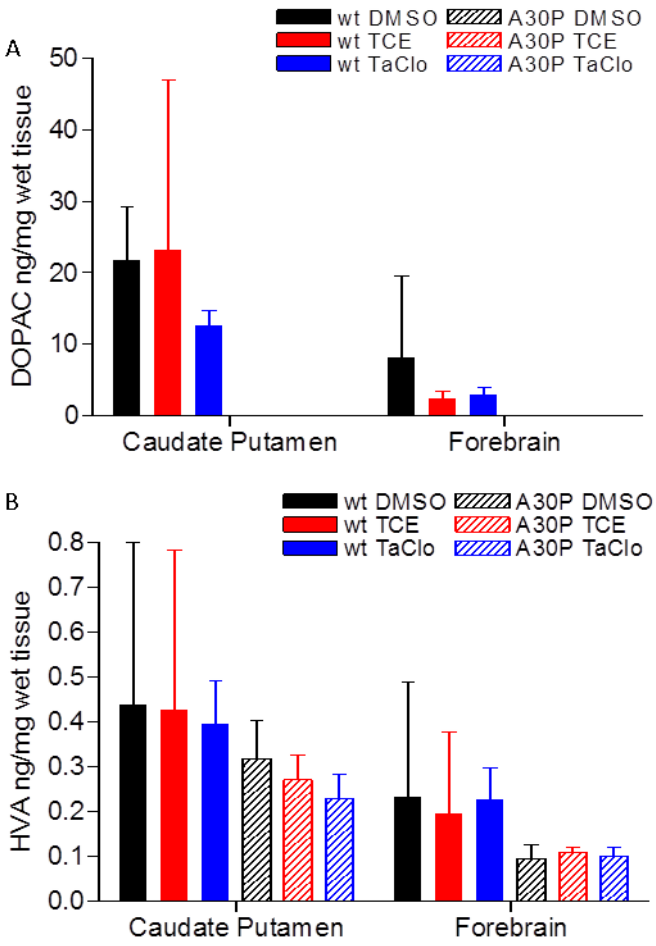

Fig. 6.15 Effect of TCE & TaClo on caudate putamen & forebrain DA metabolite levels in A30P α-synuclein overexpressing & wt C57BL/6 mice Levels of (A) DOPAC & (B) HVA in Caudate Putamen & Forebrain of TCE (1000mg/kg), TaClo (2mg/kg) treated and vehicle (10ml/kg olive oil) in wt & A30P α-synuclein overexpressing C57BL/6 mouse when assessed by LC-MS/MS. Data presented as mean ng/mg wet tissue from duplicate samples ± SD (n=4-10). (A & B, Caudate & Putamen, wt & A30P) No significant difference between groups, One-way ANOVA. NB. All data obtained for A30P mice for DOPAC was below limits of quantification.

5-HT levels could not be measured in the A30P brain samples due to assay limitations but 5-HT in the caudate of wild-type animals and both regions in A30P mice as well as metabolite 5-HIAA in both brain regions of both strains were quantified. TCE or TaClo exposure had no significant effect on 5-HT levels in either the caudate putamen or forebrain of wild type animals, or 5-HIAA levels in brain region of wild-type or A30P overexpressing mice (One-way ANOVA) (Fig. 6.16). However, the levels 5-HT detected in the wild-type mice were extremely low (0.02-0.05ng/mg wet tissue) so may not be reliable due to assay performance. There was a significant reduction in 5-HIAA seen in the A30P overexpressing mice when compared to wild-type (see Appendix A).

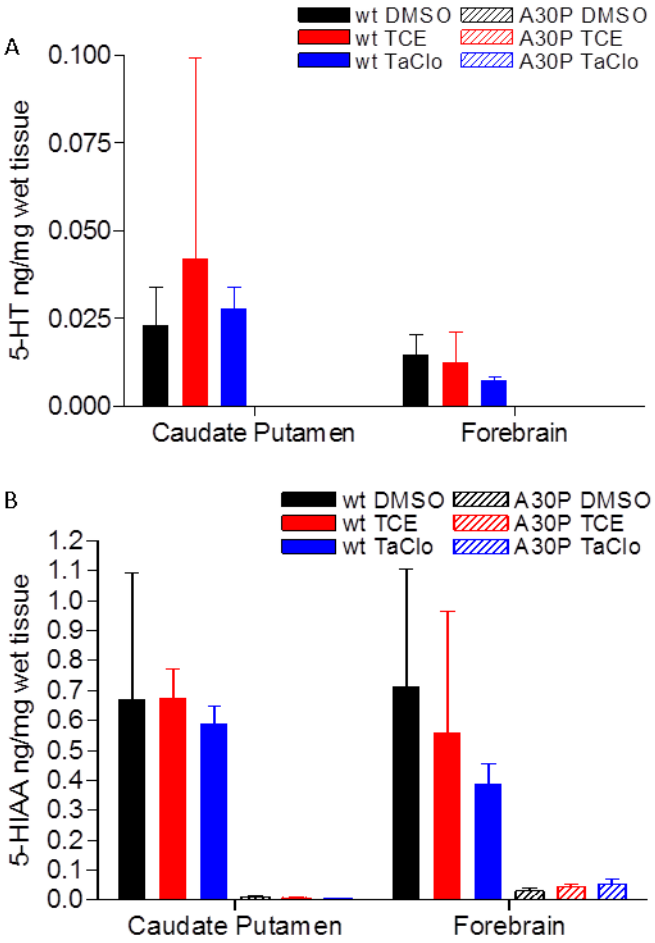

Fig. 6.16 Effect of TCE & TaClo on caudate putamen & forebrain 5-HT levels in A30P α-synuclein overexpressing & wt C57BL/6 mice Levels of (A) 5-HT & (B) 5-HIAA in Caudate Putamen & Forebrain of TCE (1000mg/kg), TaClo (2mg/kg) treated and vehicle (10ml/kg olive oil) in wt & A30P α-synuclein overexpressing C57BL/6 mouse when assessed by LC-MS/MS. Data presented as ng/mg wet tissue from duplicate samples ± SD (n=4-8). (A & B, Caudate & Putamen, wt & A30P) No significant difference between groups, One-way ANOVA.
NB. All data obtained for A30P mice for 5-HT was below limits of quantification.

Levels of GABA were unchanged in the forebrain and caudate putamen following TCE and TaClo treatment in either mouse strain (One-way ANOVA) (Fig. 6.17 A), but were significantly reduced in A30P mice in comparison to wild type animals in both brain regions (see Appendix A). Due to problems with the assay, glutamate could not be measured in A30P animal forebrain and was not significantly altered in TCE or TaClo exposed animals in either the caudate putamen of both strains or the forebrain of wild-type animals (One-way ANOVA) (Fig. 6.17 B). Glutamate levels were also unchanged between both strains in the caudate putamen (see Appendix A).

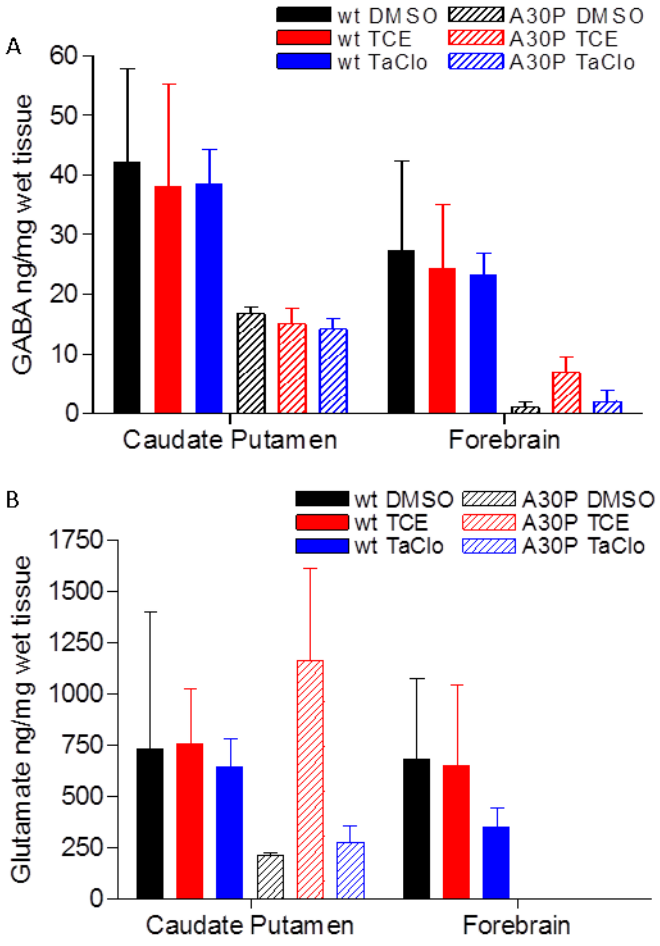

Fig. 6.17 Effect of TCE & TaClo on caudate putamen & forebrain GABA & Glutamate levels in A30P α-synuclein overexpressing & wt C57BL/6 mice Levels of GABA and Glutamate in (A) Caudate Putamen & (B) Forebrain of TCE (1000mg/kg), TaClo (2mg/kg) treated and vehicle (10ml/kg olive oil) in wt & A30P α-synuclein overexpressing C57BL/6 mouse when assessed by LC-MS/MS. Data presented as ng/mg wet tissue from duplicate samples ± SD (n=6-10). (A & B, Caudate & Putamen, wt & A30P) No significant difference between groups, One-way ANOVA.
NB. All data obtained for A30P mice forebrain for glutamate bas below limits of quantification.

6.3.5 SNpc DA Neuron Number

As deterioration of the DA neurons of the SNpc has been shown to be characteristic in PD (Bernheimer, Birkmayer et al. 1973), DA neuron number and size were assessed in this study using stereology. Stereology is a method of estimating geometrical quantities that can be used to estimate the number and size of cells in a defined 3D region from a series of sections. Design based stereological analysis, such as that used in this study, has been shown to accurately estimate DA neuron number in the SNpc of C57BL/6 mice when compared to counts obtained through serial reconstruction (Baquet, Williams et al. 2009). Stereological analysis has previously shown a decrease in DA neuron number in the SNpc of 6-OHDA and MPP+ induced animal models of PD (Sonsalla, Zeevalk et al. 2008; Healy-Stoffel, Ahmad et al. 2012). In this study stereology was used to estimate the number and volume of TH-positively stained DA neurons in the SNpc of fixed and processed brains taken from a proportion of the animals used to assess behaviour.

In both wild-type and A30P overexpressing animals, a significant decrease in TH-positive cells in the SNpc was seen in both TCE (wt: $P<0.001$, A30P: $P<0.05$, unpaired t-test) and TaClo (wt: $P<0.001$, A30P $P<0.01$, unpaired t-test) exposed groups, with number of cells reduced to ~50% vehicle in wild-type and ~70% vehicle in A30P animals (Fig. 6.18 A & 6.20). When comparing TH-positive cell number between mutant and wild-type mice, A30P overexpressing animals showed a significant decrease in cell number to ~70% wild-type in the vehicle and ~80% in the TaClo treated group (both $P<0.05$, unpaired t-test), but there was no significant decrease in the TCE treated animals ($P=0.30$, unpaired t-test) (Fig. 6.18 A & 6.20).

When looking at DA cell density in the SNpc, wild-type animals showed similar results to cell number, with a 50% decrease in density seen in both TCE and TaClo treated animals when compared to vehicle (both $P<0.001$, unpaired t-test) (Fig. 6.17 B & 6.19). A30P overexpressing mice showed a significant difference in density between vehicle TaClo ($P<0.05$, unpaired t-test), but not TCE treated groups ($P=0.18$, unpaired t-test) (Fig. 6.18 B & 6.20). Looking at the effect of A30P overexpression, a significant decrease in TH-positive cell density to 50% of wild type values was seen in the vehicle treated animals ($P<0.001$, unpaired t-test), but no significant effect of the mutation was seen in either TCE or TaClo treated animals ($P=0.30$, 0.06 respectively, unpaired t-test) (Fig. 6.18 B & 6.20).

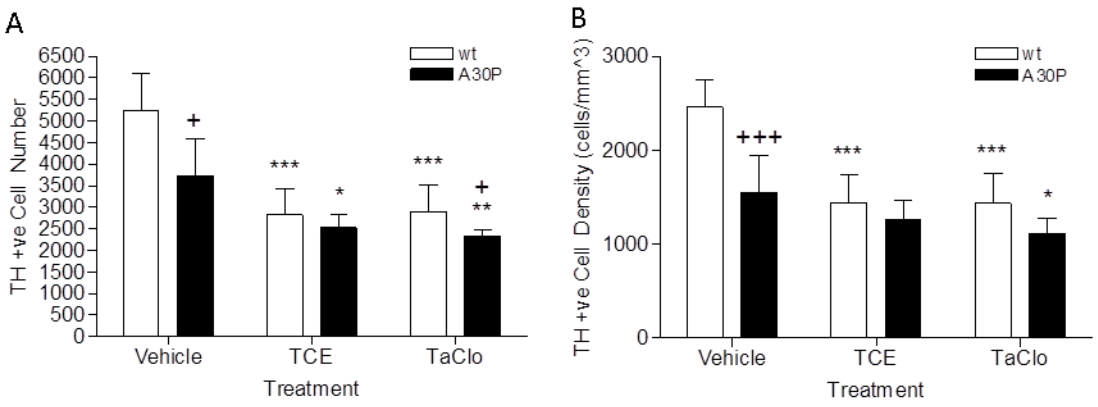

Fig. 6.18 Effect of TCE & TaClo on SNpc DA neuron number and density in A30P α-synuclein overexpressing & wt C57BL/6 mice Total (A) number and (B) density of TH-positive cells in the SNpc of TCE (1000mg/kg), TaClo (2mg/kg) & vehicle (olive oil) treated wt & A30P overexpressing C57BL/6 mice assessed by stereological analysis. Data presented as mean ± SD (n=5/6). ***P<0.001, **P<0.01, *P<0.05 when compared to strain vehicle, +++P<0.001, +P<0.05 when compared to same treatment wt group, both unpaired t-test

TCE or TaClo treatment did not cause any significant change in the volume of TH-positive cells in the SNpc of exposed wild-type or A30P overexpressing mice when compared to vehicle groups (wt: P=0.38, 0.49, A30P: P=0.59, 0.57 respectively, unpaired t-test) (Fig 6.19). A30P overexpressing animals appear to show an increase in DA cell volume when compared to wild-type; however this effect is not significant in vehicle or TCE treated groups (P=0.11, 0.19, respectively, unpaired t-test) but is in the TaClo treated mice with A30P mutant DA cells reduced to 70% of wild-type (P<0.05, unpaired t-test) (Fig. 6.19).

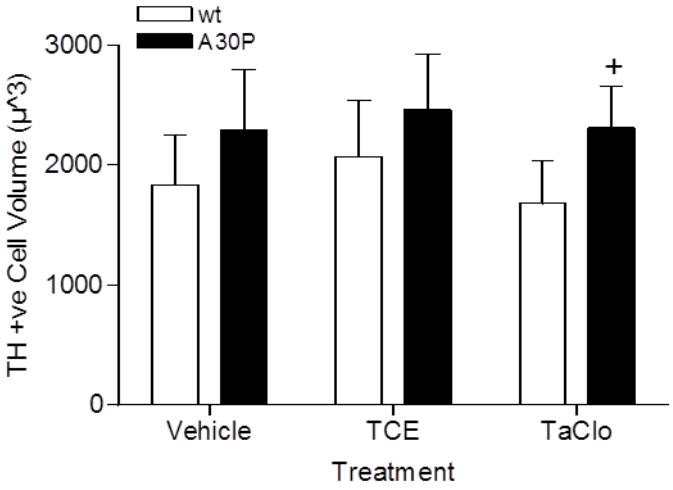

Fig. 6.19 Effect of TCE & TaClo on SNpc DA neuron volume in A30P α-synuclein overexpressing & wt C57BL/6 mice Cell body volume of TH-positive cells in the SNpc of TCE (1000mg/kg), TaClo (2mg/kg) & vehicle (olive oil) treated wt & A30P overexpressing C57BL/6 mice assessed by stereological analysis. Data presented as mean ± SD (n=5/6). +P<0.05 when compared to same treatment wt group, unpaired t-test.

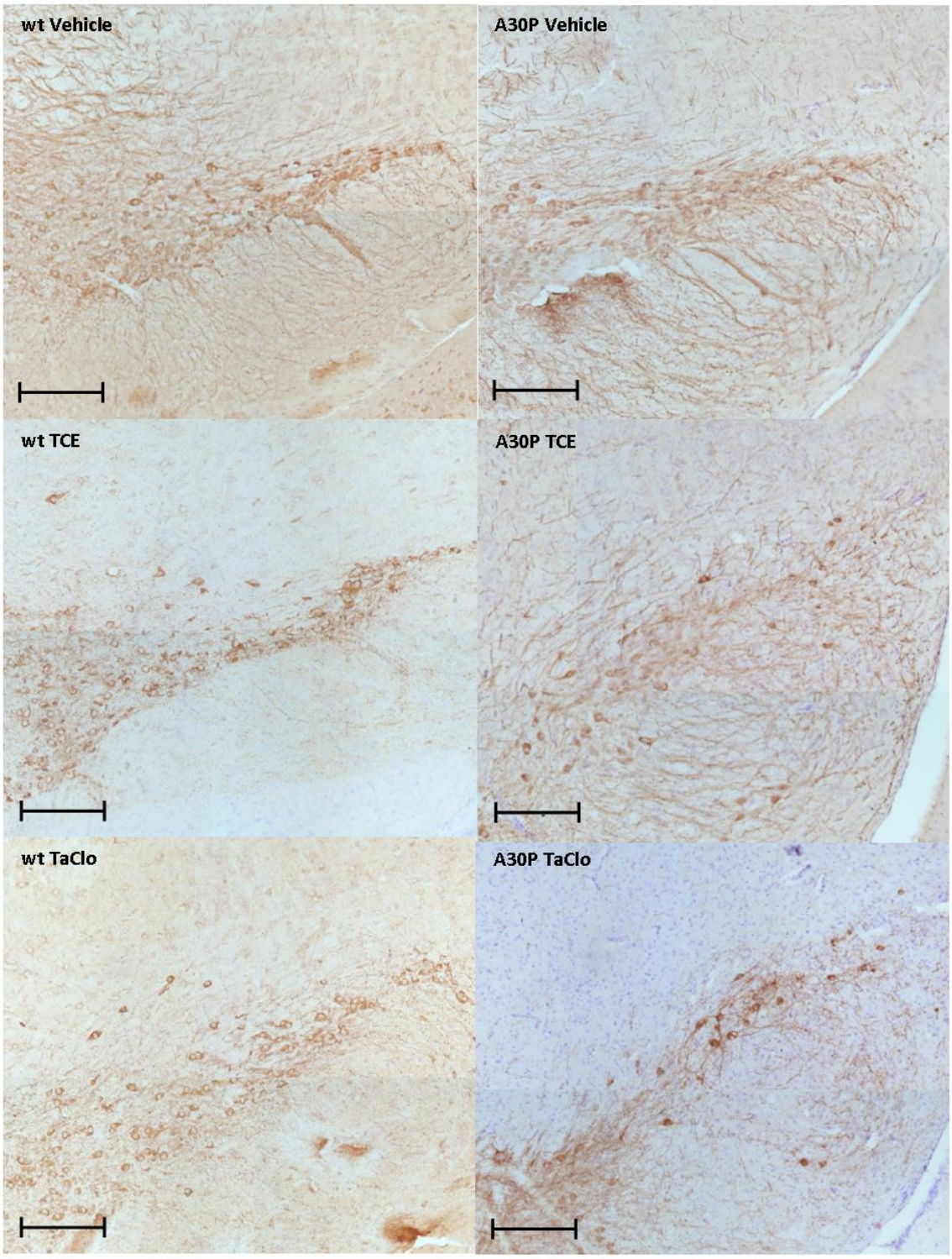

Fig. 6.20 TH positive staining in TCE & TaClo treated A30P α-synuclein overexpressing & wt C57BL/6 mice Representative images of TH positive staining in the SNpc in Control, 500mg/kg TCE & 2mg/kg TaClo in or wt or A30P α-synuclein overexpressing C57BL/6 (x40 magnification, scale bars represent 200µm).

6.4 Discussion

6.4.1 Is Chronic TCE and TaClo Exposure Well Tolerated in Wild Type and A30P Mutant Human α-synuclein Overexpressing C57BL/6 Mice?

During this study, wild-type and A30P mutant overexpressing C57BL/6 mice from all groups generally showed normal weight gain throughout the duration of the study with no significant differences apparent between treatment groups (Fig. 6.2), and no problems were associated with any i.p. dosing injections, suggesting that TCE and TaClo were relatively well tolerated at the doses and regimens used.

However, despite this relatively good tolerance at dosing, a number of clinical and behavioural abnormalities were observed in all of the treatment groups over the course of the study, some of which led to early termination. The most severe abnormalities that resulted in early termination of affected individuals - three animals with severe weight loss, one with an abscess in the abdomen and two with severe fighting injuries - occurred in the vehicle and TCE treated animals in both wild-type and A30P mutant animals, but not in any TaClo dosed mice (Table 6.1). As vehicle and TCE both involved injection of olive oil, whereas TaClo was dosed in 0.9% NaCl due to solubility properties, this suggests that these severe clinical abnormalities observed were likely due to the olive oil rather than test-compound related. It has been reported that olive oil injection to the peritoneum of Sprague Dawley rats can lead to the formation of lipogranulomas, nodules of necrotic, fatty tissue associated with granulomatous inflammation around a deposit of an oily substance (Ramot, Ben-Eliahu et al. 2009), and, separately, that lipogranulomas induced in the abdomen of inbred mice can lead to systemic lupus erythematosus, a systemic autoimmune syndrome resulting in inflammation and tissue damage (Shaheen, Satoh et al. 1999). Ingestion of olive oil has also been shown to lead to diarrhoea (Carper 1989), which could also have occurred if olive oil was injected into the intestines rather than intra-peritoneal cavity during dosing. These suggest possible olive oil related explanations behind the weight loss and abscesses that led to early termination of animals in this study.

A number of clinical signs that were not considered severe enough to need early termination of affected animals (Table 6.3). One wild-type male animal in the TaClo treated group showed a swelling in the abdominal region, which reduced in size and healed with antibiotic treatment. The animal did not show any significant weight loss and appeared in good health following treatment and was therefore considered acceptable to continue on the study. One animal was found with a lost tail tip, which was thought to be due to the tail getting caught in the cage lid

when bedding was changed. One cage of TaClo treated female wild-type animals showed severe barbering behaviour/hair loss to back, forearms and head in four out of five animals. Due to the position of the hair loss and the fact that one animal was not affected; this was thought to be dominance behaviour by the unaffected individual rather than self-inflicted stress behaviour. As no skin was broken and affected animals did not appear subdued, all animals were retained on study; however as this only occurred in one treatment group, this behaviour may have been a sign of increased stress or aggression due to TaClo administration. All other non-terminal signs observed were skin wounds thought to be due to fighting and some needed antibiotic treatment; however no wounds were considered severe enough to warrant study discontinuation. These signs may could indicate increased aggressive or stress behaviour, but no aggression or stress behaviours were tested in this study and as they occurred across all groups and strains were not thought to be treatment related. During the period when the majority of the fighting leading to wounds occurred, construction work was occurring on the floor directly above the animal holding room, with heavy machinery used throughout the light cycle. The noise generated by this work may have caused increased stress in the animals and led to the increase in aggression observed.

6.4.2 Does Chronic TCE and TaClo Exposure Affect Longitudinal Motor Function in Wild Type and A30P Mutant Human α-synuclein Overexpressing C57BL/6 Mice?

As described in Section 5.4.2, the accelerating rotarod test has been used to show a decrease in motor function following exposure to PD-linked neurotoxins, including TCE. No significant decrease in motor function was observed in TCE or TaClo or when compared to vehicle treated groups in wild-type or A30P mutant α-synuclein overexpressing C57BL/6 mice when assessed by rotarod (Fig. 6.3). However, all groups show a slight but significant decrease in rotarod performance over time in both strains of mice, with A30P overexpressing animals appearing to markedly decrease from 20 to 24 weeks in all treatment groups (Fig. 6.3). However, this apparent decrease in motor function as assessed by rotarod in the later stages of the study may be due to habituation to repeated testing incidences, or a weight-related decrease in performance that occurs at animal weights of over 40g (see Appendix B for details) rather than loss of DA neurons. There were no significant differences seen between wild-type and A30P mutant animals in the study (see appendix A), which is consistent with reported lack of discrimination of motor dysfunction assessed by the rotarod in the same strain of A30P mice used in our study until 17months (Freichel, Neumann et al. 2007), with our study terminating at 13 months, and a lack of any effect in a separately generated A30P mutant α-synuclein mouse (Plaas, Karis et al. 2008). Any possible effects on motor function that could have been

seen using this test may have been masked due to problems in consistent performance of the test with individual animals showing an apparent lack of drive in the test, turning around and walking backwards on the treadmill, or attempting to climb dividers between lanes all occurring during testing periods and leading to a decrease in fall latency and leading to increased variability of results.

The pole test has previously been used to show a decline in fine motor performance following exposure to neurotoxins linked to development of PD (see Section 5.4.2). In this study no overall difference was seen in fine motor control as assessed by any examined parameter in the pole test between vehicle and TCE or TaClo treated groups in either wild-type or A30P overexpressing animals; however in all measures of ability to complete the pole task in the A30P mice, the vehicle treated group show consistently slightly higher performance levels from week 20 onwards than both TCE and TaClo treated animals suggesting a possible trend towards an effect (Figs. 6.4 & 6.5). In the wild-type animals at week 28 of the study, the TCE treated group showed a significantly lower time to turn on the test when compared to the vehicle group (Fig. 6.4 B); however, this was the only time in the study any treatment groups showed a significant difference from control and when taken in the context of previous and following measurements is thought to be anomalous. All treatment groups of both strains showed a general increase in the time taken to turn and descend the pole and to complete the task, as well as in the number of falls recorded over the duration of the study (Figs. 6.4 & 5). This decrease in fine motor control seen over time may be due to habituation of the animals to the task as it occurred across all treatment groups and the vast majority of previous published uses of the pole test have not used it repeatedly, with the only published report of repeated use of the pole test found only repeatedly used for 3 weeks (Balkaya, Kröber et al. 2013) as opposed to over 40 weeks in this study. Another possible explanation could be due to a similar weight-related decrease in performance to that seen in the rotarod test occurring at weights of over 40g (see Appendix B). The decrease in performance of all measurements observed appeared far more pronounced in the A30P overexpressing animals when compared to the wild-type; however this was not statistically significant when vehicle treated animals from the two strains were compared (see Appendix A), but suggests a possible trend towards overexpression of A30P mutant α-synuclein leading to a decrease in fine motor control in C57BL/6 mice. Performance in this test showed large inter- and intra-subject variability, due in part to the fact that any mouse falling from the pole was assigned the maximum time of 30 seconds, whereas instances where the task was completed reported average values of 2 to 4 seconds to turn, 3 to 5 seconds to descent and 5 to 8 seconds in total. This led to large

variability in the final data and may have masked any possible effects that TCE or TaClo exposure or A30P overexpression may have caused.

Stride length has been reportedly decreased in MPTP treated C57BL/6 mice (Tillerson, Caudle et al. 2002; Amende, Kale et al. 2005) suggesting it as a relevant marker of motor dysfunction in PD and the strain of A30P mice used have been shown to develop an unsteady gait over time (Neumann, Kahle et al. 2002). No significant differences between vehicle and TCE or TaClo treated groups of either wild-type or A30P overexpressing mice were observed (Fig. 6.6). However, in wild type animals, TCE exposed mice showed significantly longer stride length than vehicle in week 32 only; however, this was thought to be anomalous, as preceding and subsequent data points are closely matched with vehicle data. Interestingly, wild-type mouse stride-length increased significantly over the course of the study, whereas A30P animals did not (Fig. 6.6). A possible explanation for this could be that the wild-type animals got used to the test more rapidly than the mutant due to either differences in learning or anxiety and the later stride length was more representative, although if this was the case it would suggest not enough habituation and training was carried out prior to test start. More exploration into this effect would be needed to ascertain any significance. While the wild-type animals stride length increased and the A30P mutant did not, there were no significant differences between the strains (see Appendix A). This is in contrast to findings by Plaas et al., who found decreased stride length in mouse with an A30P point mutation introduced into the α-synuclein gene at 13 months of age when compared to wild-type (Plaas, Karis et al. 2008). However, they introduced the mutation into the mouse α-synuclein gene rather than introducing mutated human α-synuclein and effects were only seen in forepaw stride length whereas this study measured hind paw stride length.

The data observed in this study suggests that TCE & TaClo, at the dosage used in this study, do not result in sufficient SNpc DA neuron degeneration to cause a significant decrease in motor function as assessed by the accelerating rotarod, pole test or gait analysis in either wild-type or A30P overexpressing C57BL/6 mice. However, some levels of DA cell death may have occurred in the SNpc of treated animals without significant motor dysfunction occurring, as it has been shown that >70-80% cell death is required before behavioural deficits are seen (Hirsch, Graybiel et al. 1988; Fearnley and Lees 1991; Tillerson, Caudle et al. 2002; Chaudhuri, Healy et al. 2006).

There was a significant decrease in grip strength over time in all treatment groups of both strains observed, which manifested as a sharp decrease from pre-dose to 4 weeks which then

levels off across the rest of the study period (Fig. 6.7). No significant difference between TCE or TaClo exposed animals and vehicle was seen in either wild-type or A30P mutant animals (Fig. 6.7) and no significant difference was seen between wild-type or mutant animals (see Appendix A). As previously mentioned in Section 5.4.2, grip strength is not thought to be a sensitive marker for motor dysfunction in PD, however the strain of A30P mutant α-synuclein overexpressing mice used have been reported to show spinal pathology, as the Thy1 promoter expresses the insert in the brainstem and spinal cord and a weakening of extremities (Neumann, Kahle et al. 2002).

As spinal cord pathology has been reported to manifest as a reduction in grip strength and gait abnormalities (Guo, Qiu et al. 2013), and has been implicated in the development of motor dysfunction in the A30P mice used in this study (Neumann, Kahle et al. 2002), these symptoms would have been expected to be have been picked up by our grip strength and gait analysis tests. However, no differences in grip strength or gait were seen between wild-type and A30P mutant animals in this study (Appendix A). Although Neumann *et al.* describe these motor behavioural deficits, they do not specify the age of the mice when the symptoms manifest, suggesting this may only occur at ages above those reached in our study.

6.4.3 Does Chronic TCE and TaClo Exposure Affect Cognitive Function in Wild Type and A30P Mutant Human α-synuclein Overexpressing C57BL/6 Mice?

PD has been widely associated with cognitive decline (Taylor, Saint-Cyr et al. 1986; Cooper, Sagar et al. 1991; Owen, James et al. 1992) and MPTP has been shown to lead to disruption of cognitive behaviour in both exposed human patients (Stern, Tetrud et al. 1990) and animal models (Tanila, Björklund et al. 1998; Yang, He et al. 2004) . In addition, Freichel *et al.* reported a slight decrease in cognition in A30P mutant α-synuclein overexpressing mice, as well as α-synucleinopathy in the central nucleus of the amygdala, an area involved in cognitive behaviour in mice (Freichel, Neumann et al. 2007). Therefore, cognitive function was assessed in this study as spatial learning and memory by means of the Barnes maze.

Spatial learning was assessed by measuring the time and amount of errors prior to the mice finding and entering the target hole (Figs. 6.8 & 9). No significant differences were found between TCE or TaClo treated groups when compared to control in either wild-type or A30P mutant animals in any parameter analysed suggesting that they have no effect on spatial learning. However, when comparing wild-type and A30P mutant animals, A30P mutant animals took significantly longer to find the target hole on the first day of the trial. This

suggests that the A30P mice took longer to realise where the hole was, or remember from the previous trial, suggesting a possible learning deficit when compared to wild type C57BL/6 (see Appendix A for details). No differences were seen in time to enter target or errors before finding target, but, in contrast to the finding that A30P took longer to find the target than wild-type animals, wild-type animals made significantly more errors prior to entering the target box (see Appendix A for details). As this difference is not seen in primary errors, it suggests either a lack of recognition of the box when found, or a lack of drive to escape the maze in wild type animals when compared to A30P mutants, as more searching - and therefore errors - occurs between animals finding and entering the escape box.

Spatial memory was assessed by measuring the time to find the target hole and the distribution of errors away from the target hole, on the day immediately following the end of training (short-term memory) and a week later (long-term memory) (Figs. 6.10-12). No significant differences were seen between TCE or TaClo treated and vehicle groups in short term memory as in either strain. However, a possible trend towards a decrease in time to find target hole in wild-type TCE and TaClo exposed animals compared to vehicle was observed suggesting improved short term memory. However, this finding is not supported by other measures in the test and is thought to be an artefact.

When looking at long term memory, there were no significant differences between treatment groups in either strain (Figs. 6.10-12) suggesting that TCE or TaClo exposure do not lead to long term special memory deficits. There was however a trend towards an increase in time taken to find the first hole and number of holes visited in A30P mutant animals exposed to both TCE and TaClo (Fig. 6.10 & 11 B(ii)). This is supported by the finding that TCE and TaClo exposed A30P mutant animals investigated a far wider range of holes from the target in the long term probe test, with both TCE and TaClo groups containing individuals that explored ten holes away from the target whereas vehicle animals explored no more than three holes from the target (Fig. 6.12). The poke score calculated should reflect this, however the spread of score results suggests that it is a minority animals in each of the TaClo and TCE groups that contributed to the majority of the exploratory behaviour away from the target hole with three individuals in each group scoring over 50 as compared to none in the vehicle group (Fig. 6.13). This could be explained by differences in inter-individual susceptibility, and could still signify an effect of TCE and TaClo in the A30P mutant animals with a higher proportion of individuals showing a decrease in long term spatial memory performance in the test.

This lack of effect of TCE and TaClo on spatial learning and memory in the C57BL/6 mice correlates with a study carried out by Sontag et al., who reported no effect on learning and memory in rats dosed 0.2mg/kg TaClo daily for 7 week, when assessed on the COGITAT hole board (Sontag, Lange et al. 2007). When combined with our results this suggests that TCE/TaClo do not contribute to the cognitive deficits sometimes seen in PD in rodent models. However, other known PD-linked neurotoxins MPTP, 6-OHDA and rotenone have been shown to lead to working and spatial memory impairment in a variety of behavioural tests (Da Cunha, Gevaerd et al. 2001; Miyoshi, Wietzikoski et al. 2002; Ferro, Bellissimo et al. 2005; Moreira, Barbiero et al. 2012), however, no reports of deficits in Barnes maze performance have been found. The effect of A30P mutant α-synuclein expression on cognition has previously been looked at in a drosophila model, which found that overexpression did lead to learning and memory impairment; however, not to the extent than was seen following rotenone exposure (Yy, Jiang et al. 2011). This could support the possible trend towards long term memory problems in A30P overexpressing mice exposed to the potential PD-neurotoxin TaClo observed.

There seems to be a marked difference in performance in both the short and long term probe test between the wild-type and A30P mutant α-synuclein overexpressing mice, with the wild-type animals seeming to have far more exploratory behaviour and therefore more errors than the A30P mutants (see Appendix A for details). This could possibly be due to a reduction in activity levels between the strains, as although this was not seen in the tests of locomotor activity, the tests measured forced locomotor and no measures of spontaneous activity were examined in this study. Another possible explanation could be due to a decreased drive to enter the target box in wild-type animals when compared to A30P overexpressing mice, possibly due to reduced anxiety, is supported by the finding that they made significantly more errors before entering the box during the training phase.

6.4.4 Does Chronic TCE and TaClo Exposure Affect Neurotransmitter Levels in Wild Type and A30P Mutant Human α-synuclein Overexpressing C57BL/6 Mice?

As mentioned previously in section 5.4.3, the LC-MS/MS method developed to measure neurotransmitter levels was not found to give accurate or repeatable results during this study. The results in this investigation in wild-type and A30P overexpressing mice were less reliable than those seen in the pilot study. This was possibly due to the use of perchloric rather than formic acid in the extraction process which was an attempt at a better extraction method but

may have resulted in oxidation of the neurotransmitters before detection, with no or extremely low levels of DA, 5-HT & NA detected and a 10-fold drop in levels of 5-HIAA and HVA in A30P mice when compared to wild-type levels. Levels of DOPAC, glutamate and GABA were relatively similar to those seen in pilot mice, with all three slightly higher than pilot C57BL/6 animals.

No significant changes were found in any neurotransmitter levels in any brain region in either wild-type or A30P overexpressing animals, but this is thought to be related to the poor performance of the LC-MS/MS or SPE as previously mentioned. If the assay is accurate, the fact that there were no significant differences in DA metabolite level in either strain of mice in this study following TaClo exposure, when treatment with half the concentration of TaClo significantly reduced DOPAC levels in C57BL/6 mice in the pilot study may be due to the differing lengths of time between dosing and brain sampling. There have been reports that surviving DA neurons in neurotoxin induced rodent models of SNpc degeneration enter a state of hyperactivity and increase production and release of DA from terminals (Agid, Javoy et al. 1973; Zigmond, Acheson et al. 1984) and decreased DA uptake from the synapse (Garris, Walker et al. 1997) compensate for the loss of DA release from damaged neurons and maintain pathway integrity. As this compensatory process takes time to develop, it may not have yet increased DA levels in the pilot animals as they were culled almost immediately post final dose, whereas the brains of the mice in this study were not sampled until 34 weeks following the final dose giving the animals time to compensate for the loss of DA neurons in the SNpc by increasing DA production.

The significant increase in 5-HIAA levels seen in the TaClo treated pilot study mice is not repeated in this study, with no change seen in the caudate of either strain, with a possible decrease in 5-HIAA in the wild-type, and possible increase in A30P animals not significant. However, these results are not thought to be reliable with levels of 5-HIAA detected of a magnitude smaller than those seen in the pilot animals and the range of the results of individual animals suggesting that the assay was not accurate enough to draw any conclusions from the data generated.

A moderate but significant decrease in GABA and glutamate levels were seen in pilot mice exposed to TaClo. This is not replicated in this study; however, a small reduction in the levels of both neurotransmitters are seen in all wild type animals in both brain regions, and these changes are not significant, possible due to variability of the assay. The A30P overexpressing

results are more fluctuating and seem less reliable making it difficult to draw conclusions from the data.

Almost all neurotransmitters appeared to be present in higher amounts in the wild-type animals in comparison to the A30P overexpressing animals, although only significantly so in GABA and, particularly 5-HIAA (see Appendix A). In the case of 5-HIAA this is almost certainly an assay related decrease as the levels seen in the A30P are >10 times lower than those in the wild-type animals and >100 times lower than those seen in the pilot study mice, an effect that would almost certainly have a major physiological effect.

6.4.5 Does Chronic TCE and TaClo Exposure Affect SNpc DA Neurons in Wild Type and A30P Mutant Human α-synuclein Overexpressing C57BL/6 Mice?

Loss of SNpc DA neurons is a hallmark of the pathology of PD (Bernheimer, Birkmayer et al. 1973; Dickson, Braak et al. 2009; Lees, Hardy et al. 2009). DA neuron numbers were estimated in the SNpc of a proportion of the animals dosed in this study by stereology and a significant decrease was observed in both wild-type and A30P mutant α-synuclein overexpressing mice exposed to TCE and TaClo when compared to those treated with olive oil vehicle (Fig. 6.18 A). This finding is supported by studies that found a similar decrease in DA neuron number of the SNpc of rats more acutely exposed to TCE (Liu, Choi et al. 2010) and animals treated with known PD neurotoxins MPTP and 6-OHDA (Javoy, Sotelo et al. 1976; Seniuk, Tatton et al. 1990).

A30P overexpression led to a significant drop in the SNpc DA neuron numbers in the vehicle and TaClo treated groups, with the effect more pronounced in the vehicle group (Fig. 6.18 A). Although a slight decrease in DA neuron number in the SNpc of TCE and TaClo treated A30P animals was seen when compared to wild-type, no major additive effect was present. This is consistent with reports that sensitivity to MPTP is not increased in the same PD-associated Thy1 promoted A30P mutant α-synuclein transgenic mice used in this study (Rathke-Hartlieb, Kahle et al. 2001) nor in wild-type human α-synuclein overexpressing mice exposed to paraquat (Fernagut, Hutson et al. 2007). Density of DA neurons in the SNpc is relatively consistent with number of neurons in all groups (Fig. 6.18 B), which is to be expected as there is no significant difference in SNpc volume between treatment groups or strain, as calculated during stereology (Fig. 2.9).

Individual DA neuronal volume was measured and although there no effect of treatment was seen in cell volume in either strain, A30P mutant α-synuclein overexpressing animals showed a

trend towards larger cell volumes than wild-type in vehicle and TCE groups and were significantly larger in TaClo treated mice (Fig. 6.19). This correlates with a report of enlarged brainstem and spinal cord neurons in similar mice, overexpressing human A53T mutant α-synuclein (Martin, Pan et al. 2006) and possibly suggests that the cells are under stress as cell swelling is a morphological hallmark of necrosis (Van Cruchten and Van den Broeck 2002), conversely, a post mortem study on the brains of PD patients showed no increase in SNpc cell volume in cells containing Lewy bodies (Gertz, Siegers et al. 1994). The fact that no increase in neuron volume is observed in TCE or TaClo exposed animals of either strain, despite the fact that a reduction in cell number is seen seems to disagree with the hypothesis that increased volume is apparent in cells under stress. This could possibly be explained as there was a long delay (32 weeks) between final chemical exposure and post mortem SNpc DA neuron number assessment and the apparent DA neuron death seen in TCE and TaClo treated mice could have occurred in affected cells in the weeks following dosing with remaining cells unaffected by chemicals that had been cleared from the system by the time the brains were sampled. Another possible explanation for the increase in cell volume in the A30P mice could be that while the mutant animals were generated from the same base strain as the wild-type animals used in the study, C57BL/6, the animals would have been developing down separate lines for a number of generations and spontaneous changes in physiology may have occurred leading to the development of slightly different sized neurons. More investigation is needed into this possible increase in DA neuron size in A30P mice to determine the cause and relevance of the finding.

6.4.6 Conclusions

During this study the olive oil vehicle may have led to some early study terminations due to abdominal problems, and noise from construction work in close proximity to the animal holding rooms may have led to increased stress behaviours. However, these signs were not thought to be TCE or TaClo related, suggesting both to be well tolerated in both wild-type and A30P overexpressing mutant strains, with no severe clinical signs thought to be related to exposure to either chemical.

No effect of TCE or TaClo on motor or cognitive function was seen in either wild-type or A30P mutant α-synuclein overexpressing C57BL/6 mice in this study. However, differences in performance in the Barnes maze between wild-type and mutant animals suggest possible effects of the mutation on spontaneous activity or anxiety levels.

The LC-MS/MS method used to measure neurotransmitter levels in this study gave fluctuating and varied results and did not appear repeatable or accurate, making it difficult to draw any conclusions from the data generated. No significant changes in any neurotransmitter examined were found, and although differences in the levels of 5-HIAA and glutamate were significantly reduced in A30P overexpressing mice in comparison to wild-type, the results were not thought to be physiologically feasible.

TCE and TaClo exposure led to significant DA neuronal loss on the SNpc of animals in both wild-type and A30P mutant α-synuclein overexpressing C57BL/6 mice. Cell numbers were slightly lower in A30P animals than wild-type; however, no additive effect of chemical exposure and A30P overexpression was found. In addition, DA neurons in A30P mutant mice appeared to have a trend towards slightly increased cell volume when compared to wild-type, possibly suggesting A30P mutant α-synuclein mediates some kind of stress response in the cells.

In conclusion, while TCE and TaClo did not appear to lead to any major motor or cognitive deficits in either wild-type or A30P mutant α-synuclein overexpressing C57BL/6 mice, exposure to both chemicals did lead to decreased DA neuronal number in the SNpc suggesting TCE exposure as a possible causative factor in development of PD.

Chapter 7
General Discussion

7.1 Introduction

The principal aim of this thesis was to investigate whether TCE exposure could lead to SNpc DA neurodegeneration and the development of PD and, if so, to investigate possible mechanisms that led to this. Although difficulties were encountered developing an exposure paradigm for TCE in *in vitro* studies, investigations into the administration of known metabolites of TCE report DA neuronal cell death, and a hypothesis of a possible mechanism behind this toxicity has been proposed based on the results observed. This was supported by observations of DA cell death in the SNpc in *in vivo* models of TCE and metabolite exposure.

7.2 TCE Mediated Cell Death *in vitro*

Although TCE did not show any toxicity in either SH-SY5Y or midbrain neurons in the open system models used, high levels of toxicity were observed when SH-SY5Y were exposed to a high TCE atmosphere in a closed system, in agreement with similar work carried out in a previous thesis (Jiang 2008). An accurate closed delivery system needs to be developed to investigate the toxicity of TCE more fully.

TCE mediated neurotoxicity has been hypothesised to be due to the actions of its metabolite TaClo, formed via the intermediate compound chloral (Bringmann, Bruckner et al. 2000; Riederer, Foley et al. 2002; Jiang, Mutch et al. 2007). Chloral and TaClo were both found to be neurotoxic to SH-SY5Y, with TaClo being ten times more potent, supporting this theory. Both compounds were also found to be toxic to stem cell derived midbrain neuron cultures and TaClo was found to be preferentially toxic to DA neurons, implicating it in the DA specific pathology seen in PD. However, chloral did not show this specificity, suggesting it may be cytotoxic by a separate, TaClo independent, mechanism, possibly due to the induction of membrane permeability through its general anaesthetic property.

7.3 Proposed Mechanism of TCE Mediated Cell Death *in vitro*

Investigations into the involvement of programmed cell death mechanisms in TaClo neurotoxicity suggest that necroptosis, and not apoptosis is the major cell death pathway activated by TaClo as the necroptosis inhibitor Nec-1 blocks TaClo cytotoxicity but the pan caspase inhibitor zVAD.fmk does not. This is contrary to reports that apoptosis is the major form of cell death in DA neurons in PD (Anglade 1997; Tatton, Chalmers-Redman et al. 2003; Nagatsu and Sawada 2006). As necroptosis is a relatively recently characterised process, many previously published studies would not have investigated its involvement in PD. It could be suggested that the programmed necrotic death seen in this study could be a cell-specific mechanism; that SH-SY5Y preferentially die by necroptosis, possibly due to the fact they are a

neuroblastoma cell line which will inherently have altered cell death control. However, flow cytometric investigation into cell death showed a distinct difference in phenotype between TaClo and a known apoptosis-inducing agent, staurosporine, with TaClo treated SH-SY5Y showing membrane permeability typical of necrosis and staurosporine dosed cells showing chromatin condensation characteristic of apoptosis.

There is a possible link between necroptosis, PD toxin mediated cell death and the TaClo induced death in this study in the involvement of PARP activation. It has been reported that PARP activation, downstream of RIP1 and upstream of AIF, was essential for necroptosis (Xu, Chua et al. 2010), and also that PARP activation and subsequent NAD+ and ATP depletion is integrally involved in MPTP toxicity in mouse brain and isolated DA neurons (Cosi and Marien 1998; Mandir, Przedborski et al. 1999). With the hypothesis that MPTP is thought to exert its effects via Complex I inhibition and ROS generation, this is interesting with regards to the TaClo mediated cell death reported here, as TaClo also inhibits Complex I and generates ROS (Chapter 4), and, in addition, is thought to depend on the over-activation of PARP, as seen in the effects of a PARP inhibitor on TaClo toxicity in SH-SY5Y (Fig. 3.28). This suggests a possibly integral role for PARP activation due to ROS mediated DNA damage in necroptosis activation and cell death following TaClo exposure.

A recent paper has revealed that nec-1 has the same structure as the kynurenine pathway enzyme IDO inhibitor methyl-thiohydantoin-tryptophan (Vandenabeele, Grootjans et al. 2013). This introduces doubt into the conclusions formed that TaClo leads to cell death through inhibition of RIP1 kinase activity and necroptosis, as the IDO inhibiting effect of nec-1 may contribute to the protection against TaClo seen in this study. However, the supporting evidence demonstrated in this thesis - that an IDO inhibitor does not rescue cells from TaClo toxicity, Nec-1 does not have any effect on TaClo toxicity in RIP1 knockout MEF cells, RIP1 knockout protects against TaClo exposure, levels of cleaved RIP1 are altered in TaClo treated cells, and FACS analysis shows TaClo treated cells present a necrotic phenotype - suggest that RIP1 kinase activity and programmed necrosis is involved in TaClo cytotoxicity.

Although the evidence proposed so far suggests RIP1 mediated necrosis as the death mechanism involved in TaClo neurotoxicity, the fact that RIP1 knockout cells still show significant death suggests that other factors may contribute. Significant death only happens at relatively high exposure levels, at TaClo concentrations that induce almost total inhibition of mitochondrial Complex I, which may induce cell death due to damage caused by excessive ROS production and reduced ATP synthesis.

This study found that oxidative stress is integrally involved in the toxic mechanism of TaClo, as evidenced by the almost complete reversal of TaClo neurotoxicity by the antioxidant NAC and increased levels of superoxide in the mitochondria following TaClo exposure. A possible source for the ROS implicated was suggested by the finding that TaClo was found to be an inhibitor of mitochondrial OXPHOS chain Complex I, an effect that is known to generate superoxide (Lambert and Brand 2004), and that has been widely implicated in PD (Mizuno, Ohta et al. 1989; Schapira, Cooper et al. 1990). This inhibition of Complex I is consistent with the effects of known PD-linked toxins rotenone and MPP+, with studies suggesting a Complex I IC_{50} for rotenone of 0.1-100nM and of 4mM for MPP+, depending on the method and system used (McNaught, Thull et al. 1995; Choi, Kruse et al. 2008). The results of this thesis suggest that TaClo is not as potent as rotenone but more potent than MPP+, with an IC_{50} of approximately 50µM, but the dose and level of TaClo inhibition of Complex I and those that induce SH-SY5Y cell death strongly correlate in the study, suggesting it is a major contributory factor to the demonstrated TaClo neurotoxicity. If TCE does mediate toxicity via metabolism to TaClo and subsequent inhibition of Complex I and oxidative damage, this may explain the SNpc DA neuron specific cell death and development of PD as it has been reported that MPTP derived oxidative stress shows higher toxicity in SN rather than mesolimbic DA neurons, suggesting CI inhibition is preferentially damaging to SN DA neurons (Hung and Lee 1998).

This study also looked at the effect of TaClo exposure on other markers of cell damage. An increase in lysosome number suggest that the activity of autophagic machinery is increased in cells following TaClo treatment, which may be due to an increase in protein damage by the ROS generated in the mitochondria via inhibition of Complex I by TaClo. A subsequent increase in aggresomes (protein aggregates such as LBs) indicates that the autophagic system may have been overwhelmed and unable to deal with the increase in damaged cellular contents. Interestingly, induction of autophagy by rapamycin increased TaClo mediated cell death in this model, suggesting autophagic induction may have a harmful rather than protective effect. This is supported by a report that activation of mTOR, by the neuroprotective protein Oxi-α, and subsequent repression of autophagy in DA neurons protects against ROS mediated death (Choi, Kim et al. 2010). This proposes a possible mechanism by which TaClo inhibits Complex I and increases ROS production, resulting in a harmful activation of autophagy and cell death.

DNA damage would be expected to occur following an increase in cellular ROS levels, and a suggestion of this was seen in the response pattern exhibited following PARP inhibition and TaClo exposure. At low levels of cellular stress, PARP promotes cell survival by mediating DNA

repair, but at higher stress levels, over activation of this pathway depletes NAD levels and negatively affects metabolism leading to a toxic effect of PARP. An increased level of histone H2AX phosphorylation, a direct marker of DNA damage, particularly double strand breaks, was observed following 24 hour TaClo treatment. DNA damage and histone H2AX phosphorylation have been reported in both cellular and *drosophila* models following oxidative stress(Zhao, Traganos et al. 2008; Park, Lee et al. 2012) , suggesting a link between ROS generated by TaClo via mitochondrial Complex I inhibition and DNA damage in the cell possibly contributing to the activation of cell death.

Looking at the relative times that the various events linked with TaClo mediated cell death occurred in this study may give insight into the possible toxic mechanism; a relative timeline of events is summarised in fig. 7.1. Inhibition of mitochondrial Complex I occurs almost immediately as TaClo comes into contact with the enzyme, indicating it as a primary event in the neurotoxic activity of TaClo. However, exactly when this occurs following exposure of the cells to TaClo containing growth media is not immediately obvious as the time for TaClo to enter the cell has not been studied in this project. A previous thesis found that 3 hours following TaClo administration, >90% of the compound was present in the cells as opposed to the media (Jiang 2008), suggesting that TaClo enters the cell rapidly and preferentially and that Complex I would likely be exposed to the compound relatively early following dosing. The next events to occur at 4 hours post dose, with approximately 25% cell death, are an increase in the autophagic marker LC-3, suggesting up regulation of autophagy, and a decrease in the proportion of cleaved RIP1 present, suggesting possible blockade of caspases which may correlate with the activation of necroptosis. 8 hours following first exposure approximately a third of cells are dead and a significant increase in mitochondrially located superoxide and expression of the mitochondrially located oxidative stress sensor molecule DJ-1 are seen, indicating that the mitochondria are under increased oxidative stress. Also at 8 hours post dose, an increase in lysosome number is seen, suggesting that induction of autophagy has occurred, and a significant proportion of the cells are showing a necrotic phenotype characterised by increased membrane permeability. By 12 hours almost half the original cells have died and the antioxidant defence molecule GSH has increased 3-fold and significant numbers of LB-like protein aggregates have developed, suggesting a high level of ROS induced cellular damage. Finally, 24 hours after first being exposed to TaClo, over 80% of cells are dead and caspase-3 has been activated leading to PARP cleavage and calpain-1 has been activated suggesting Ca^{2+} handling has been disrupted. These features suggest the cell is under extreme stress and is suffering terminal breakdown.

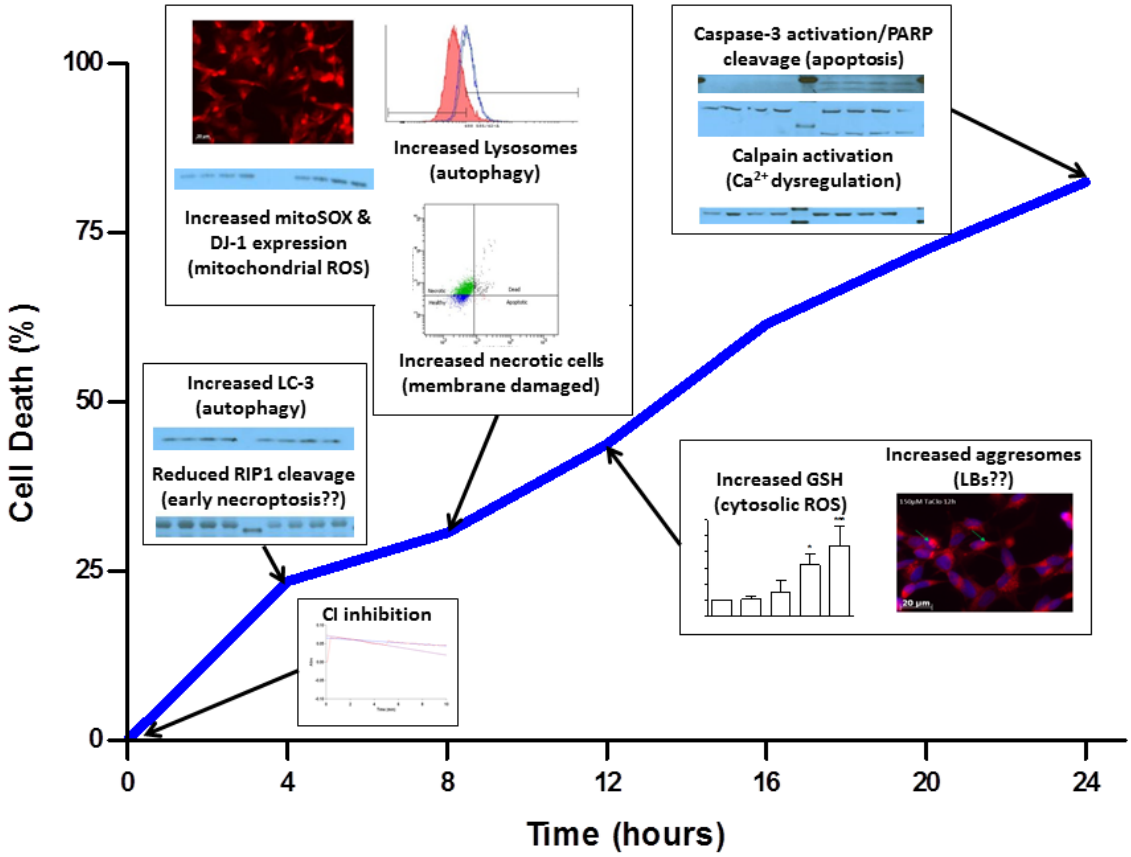

Fig. 7.1. Proposed time course of SH-SY5Y cell death mediated by TaClo Possible time course of events leading to SH-SY5Y death following TaClo exposure and corresponding levels of cell death. CI inhibition happens almost immediately following exposure of TaClo to the Complex, followed at 4 hours by an increase in autophagic induction markers and reduced cleavage of RIP1, which may be an early sign of necroptosis initiation. By 8 hours, significant numbers of cells are showing membrane damage, mitochondrial ROS levels are increased and expression of the mitochondrial ROS defence molecule DJ-1 are up-regulated and an increase in lysosome numbers are seen. At 12 hours exposure, levels of the cytosolic anti-oxidant defence molecule GSH have increased and a substantial number of LB-like aggresomes have been formed. By 24 hours, almost all cells are dead and general cell disintegration as seen by the presence of caspase-3 and calpain activation and PARP cleavage

A hypothesis generated from this evidence can suggest that TaClo enters the cell and mitochondria where it inhibits Complex I leading to increased ROS production which damages cellular contents leading to protein aggregation, increased autophagy, DNA damage and, ultimately, necroptotic cell death.

The original hypothesis of this thesis was that TCE toxicity is mediated by metabolism to TaClo through chloral, a theory that was supported by the finding that both TaClo and chloral are toxic to SH-SY5Y, with TaClo being 10 times more potent. However, further investigations found distinct differences in the effects of chloral and TaClo on cells, suggesting that while chloral is converted to TaClo, it may also contribute to TCE toxicity in its own right. The first difference noted was that while TaClo showed specificity towards DA neurons in inducing

death in midbrain cultures, chloral did not have this effect. Also, Nec-1 and NAC protected against TaClo neurotoxicity but had no significant effect on chloral induced cell death, signifying that necroptosis and oxidative stress are not integrally involved in chloral toxicity. Finally, when looking at inhibition of mitochondrial OXPHOS complexes, chloral was found to have a noticeably different profile to TaClo. TaClo significantly inhibited Complex I at relatively low levels and inhibited Complexes III and IV at higher levels but had no effect on Complex II at all. Chloral, in contrast, severely inhibited Complexes I and II at similar levels, and only had a mild effect on Complex IV. Possibly the most interesting effect was noted when trying to measure Complex III (coenzyme Q;cytochrome c-oxidoreductase). The assay was not able to be carried out as it was found that chloral inhibited the reduction of cytochrome c, at relatively low doses. This could propose a mechanism of chloral toxicity whereby it blocks the reduction of cytochrome c on OXPHOS, increasing ROS and decreasing ATP levels in the cell; however more investigation would be needed to substantiate this theory. Any possible toxic effect of chloral may not be significant in TCE mediated DA cell death, as the concentrations that were needed to elicit any toxicity were relatively high, and *in vivo*, chloral is readily converted to TaClo which has toxic effects at doses far lower than those needed by chloral.

7.4 Effects of TCE Exposure in Animal Models

TCE, its metabolites chloral and TaClo and a positive control, MPTP, did not have any significant effect on motor function as assessed by a behavioural battery in either mouse or rat model following 8 weeks treatment. A possible trend towards decreased fine motor control in the pole test was seen in mice, with all treatment groups having animals that fell from the pole from 4 weeks, whereas no control animals fell at any point in the study; however, this effect was not significant. Although DA or HVA could not be measured directly, a reduction in DA metabolite DOPAC was seen in TaClo exposed mice when measured by LC-MS/MS, but no changes in rat brains. All compounds were well tolerated in mice but TCE and chloral treated rats experienced a range of side effects, so the mouse model was considered preferential for further study.

Wild-type and A30P mutant α-synuclein overexpressing mice were treated with TCE and TaClo to further assess toxic effects of the compounds and to investigate whether they have any synergistic effects with the effects of mutated α-synuclein. As in the pilot study, no significant effects on motor function were seen in exposed animals assessed throughout 8 week dosing period and for the next 32 weeks. There were possible trends towards a motor deficit in A30P overexpressing animals exposed to both TCE and TaClo but this potential effect was not significant, possibly due to inherent variability in the tests. Cognitive function was also

assessed and TCE and TaClo were found to have no significant effect on spatial learning or memory, although a possible small effect on long term memory may have been seen in the extent of exploration away from the target hole seen in TCE and TaClo treated A30P overexpressing mice. However, this result could not be statistically confirmed and would need more exploration to provide more conclusive answers.

Despite the lack of any motor dysfunction, TCE and TaClo were both found to induce approximately 50% DA cell death in the SNpc in wild-type and A30P overexpressing mice to a similar degree. These findings concur with reports that motor dysfunction does not manifest in PD until 70-80% of DA neurodegeneration is seen in the SNpc (Hirsch, Graybiel et al. 1988; Fearnley and Lees 1991; Tillerson, Caudle et al. 2002; Chaudhuri, Healy et al. 2006) and the lack of any conformed motor dysfunction in the test battery used in this study.

The LC-MS/MS method developed to measure neurotransmitter levels in rodent brain homogenates did not prove to have been fully characterised and was not as sensitive or repeatable as needed. The assay showed a lack of ability to detect DA or NA in any of the samples or 5-HT in any of the mouse samples leading to a lack of characterisation of the major neurotransmitters linked with PD development. Possible reasons for the lack of consistency in results from the assay have been discussed in detail in Chapters 5 & 6, and this lack of relaibility has made it difficult to draw any conclusions from the data generated. The most robust data generated appeared to be that for the pilot mice, with relative consistency in presence and levels of DOPAC, HVA, 5-HIAA, glutamate and GABA seen. The results in these neurotransmitters were in general agreement with those reported in toxin generated PD models in the literature with reductions in DOPAC, as well as glutamate and GABA and an a increase in 5-HIAA found in TaClo treated animals. The lack of consistently similar results in TCE and chloral treated animals may be due to a lack of high enough exposure reaching the brain, with TCE in particular known to be an extremely volatile chemical, a large proportion of doses of which are exhaled by exposed animals (Williams-Johnson, Eisenmann et al. 1997). The later study using wild-type and A30P overexpressing mice of the same strain, found similar levels of DA neurodegeneration in the SNpc of both TCE and TaClo dosed animals, although both at double the dose of the pilot, suggesting that this lack of any effect on neurotransmitter levels may be down to assay error and throwing doubt on the significant results seen with TaClo.

When comparing neurotransmitter levels between pilot animals - which were culled almost immediately following the final dosing - and A30P study animals - which were kept for 34 weeks following dosing before brains were taken for analysis - the lack of apparent accuracy of

the assay, especially in the wild-type animals from the A30P study, needs to be taken into account. This is especially manifest in the seeming 100 fold decrease in 5-HIAA levels between pilot A30P animals, which, even taking differences in age into consideration, appears to be physiologically impossible. Any conclusions drawn from attempting to assess this data for possible recovery effects therefore need to be viewed with extreme caution.

Taken together, these results suggest that TCE and TaClo induce cell death in SNpc DA neurons, with TaClo an order of magnitude more potent, but dose regimen and time course examined so far have not led to an extent of cell death to reveal any motor dysfunction. This agrees with the hypothesis that TCE exposure induces PD through metabolism to the DA neurotoxin TaClo.

7.5 Study Limitations

The major limitation of this study is a lack of a successful method of delivery of TCE into the cellular models used, so the majority of studies were carried out using TCE metabolites chloral and TaClo. Due to the volatile nature of TCE, when cells were dosed with TCE directly in growth media, the TCE evaporated from the flask/plate and if the system was closed to keep the levels of TCE constant, cells died due to lack of oxygen. A closed system was developed that allowed a consistent atmosphere of TCE to occur in a container that contained enough oxygen to maintain the cells; however, this model did not allow delivery of specific accurate doses and was impractical. As chloral has been shown to be formed *in vivo* following TCE exposure and TaClo can be formed from chloral in man, suggesting that TaClo may be formed from TCE in theory, the study still has significance and value but a valid TCE delivery system needs to be developed to allow assessment of the effects of the solvent itself in *in vitro* models.

Another limitation of the study is that it was a relatively broad investigation into the neurotoxicity of TCE and its metabolites and the involvement of several pathological mechanisms in this. The study went into relative detail to explore the involvement of oxidative stress and mitochondrial OXPHOS inhibition, however further investigation into mitochondrial membrane potential, mitophagy, ATP turnover and cellular metabolic rate and oxidative defence may have been useful. In addition, although some evidence was found for increased autophagy and DNA damage in TaClo mediated cell death, more in-depth investigation of these areas to confirm their involvement and assess the extent of the contribution they make to the toxicity observed would be useful; however, due to time constraints this was not possible.

The *in vivo* work carried out for this thesis suffered due to the limited time and extent of dosing that was allowed under the UK Animals (Scientific procedures) Act of 1986. Animals could only be dosed twice weekly for 8 weeks, and in the main study in wild-type and A30P mutant α-synuclein overexpressing C57BL/6 mice, animals were not sacrificed for *ex vivo* assessment until 36 weeks later to allow time for possible development of motor dysfunction. This dosing paradigm is semi-chronic and temporary and therefore does not allow the constant low level exposure over time which best models human exposure. It also does not allow examination of the development of pathology, i.e. whether cell death occurs rapidly following dosing or gradually over time, whether any level of recovery occurs or assessment of the persistence of TCE and metabolites. This could have been assessed to some level by examination of the pilot study animal brains, which were sacrificed immediately following dosing; however time constraints did not allow this.

Other limitations of this thesis include the investigations into RIP1 involvement in TaClo mediated cell death using MEFs rather than SH-SY5Y when looking at toxicity in RIP1 knockout cells. A RIP1 knockdown SH-SY5Y cell line was generated using siRNA; however this only reduced RIP1 by ~50% and a stable RIP1 knockout SH-SY5Y line was not available, so MEFs were sourced instead. In addition to this, in many studies investigating necroptosis, RIP3 knockout cells are used to confirm the presence of the death pathway; however, only relatively low levels of RIP3 knockdown were achieved in this study and a knockout line was not sourced. GSH levels were assessed in the study as a sign of increased oxidative stress. The assay researched measured both total GSH and oxidised GSH, with the oxidised form of the protein proportional to the level of oxidative stress. The part of the assay measuring oxidised GSH was not successful in this study so levels of total GSH were used to measure changes in expression and represent an anti-oxidative response. Oxidised GSH can be measured by LC-MS/MS; however, time constraints meant this was not possible in this study. Finally, the behavioural tests used to assess motor function in this project were used repeatedly every 4 weeks for 40 weeks. These tests were designed, and are generally used, for pre and post treatment assessment of function immediately following training in relatively young animals, rather than the repeated use with relatively long gaps in aging individuals used here. This may have contributed to the large variability in results seen with some animals learning how to get around carrying out the tasks, differences in recollection of how to carry out the task between animals, and size, weight and condition of animals affecting performance in the tests as the study progressed. Development of motor function tests that assess the animal in more natural

behaviours that require less/no training would be better used in long term studies requiring repeated assessment.

7.6 Future Directions

The findings of this thesis have opened up various pathways of future research, both *in vitro* and *in vivo*:

7.6.1 Further *in vitro* Investigations

- A method of accurate delivery of TCE that takes into account the volatility of the compound, such as the one described by McDermott *et al*. (McDermott, Allshire et al. 2007), is required to better explore the effects of the solvent itself rather than its metabolites on cellular models.

- Although the toxicity studies carried out in DA model SH-SY5Y in this thesis have been reproduced in stem cell derived midbrain neurons, it would be useful to repeat the mechanistic studies carried out in SH-SY5Y in midbrain cultures as a more representative model for the human SNpc.

- Basic studies were carried out in to the mechanism of chloral mediated cell death in this study; however, it would be interesting to repeat the more in-depth investigations carried out with regards to TaClo toxicity for this compound to see if the hypothesis that TCE neurotoxicity is mediated by TaClo via metabolism through chloral. Further to this, it would be interesting to measure TaClo levels by LC-MS/MS in cells exposed to chloral to examine whether this metabolism takes place in the models used and at what levels TaClo is formed. This would give insight into the involvement, directly or through TaClo formation, that chloral may have in TCE induced neurotoxicity.

- The involvement of autophagy and DNA damage has been suggested in the toxic mechanism of TaClo in SH-SY5Y. More in-depth investigation of these mechanisms would be useful to elucidate the importance and extent of these processes in TaClo neurotoxicity and whether they are causal or secondary mediators of the death seen.

- The involvement of PD-linked mutated proteins such as α-synuclein, PINK1, Parkin and LRRK2 could be analysed to try and develop a more direct link with the disease through measurement of the levels of these proteins in toxin-treated cells or the development of transgenic cell lines with the proteins knocked-out or over-expressing mutant forms.

7.6.2 Further *in/ex vivo* Investigations

- Due to animal licensing limitations, the *in vivo* studies carried out in this thesis were only able to expose animals twice weekly for 8 weeks. A more chronic and long term low level exposure paradigm would be more representative of human TCE exposure and give a more accurate model. A possible alternative would be oral dosing; however, long term oral dosing has a relatively high rate of attrition, especially in mice, due to the comparative ease of accidental lung dosing. Another possible route of exposure would be that used by Blossom *et al*., where animals are exposed to TCE at levels up to 0.1mg/ml in drinking water and housed in enclosed, ventilated caging racks to limit TCE air contamination (Blossom, Doss et al. 2008).

- No significant differences were found in motor function in this thesis, despite up to 50% loss of DA neurons in the SNpc. In future studies it may be useful to examine non-motor symptoms that manifest prior to motor dysfunction in PD, such as GI transit, as markers for the development of the condition. In addition, future studies should use a more robust and consistent positive control, as reports detailing the effects of MPTP exposure are varied. A model that combines chronic MPTP exposure and co-treatment of probenecid could be a more viable and reliable control (Petroske, Meredith et al. 2001).

- Animals from the pilot study carried out in this thesis could have pathology assessed by stereology to examine possible differences between animals sacrificed immediately on cessation and those allowed to develop for more time in the main study, as well as to explore effects in rats and determine whether they are consistent with those seen in mice. In addition, main study and pilot brains could be assessed for the presence of PD markers, such as phosphorylated α-synuclein, by histopathology and regions involved in learning and memory assessed for any possible toxicity in these areas.

- Investigations into the mechanism of TCE mediated neurotoxicity *in vivo* could be used to try and translate the *in vitro* findings of this thesis. Co-treatment of Nec-1 or NAC with TCE and TaClo could be used to examine the involvement of necroptotic cell death and oxidative stress in animal models and *ex vivo* measurement of mitochondrial OXPHOS Complexes in mitochondria isolated from the SNpc of exposed and control animals could explore the extent, if any, of Complex inhibition.

- Pharmacokinetics of TCE could be explored in the animal models developed alongside behavioural and pathological investigations, including the formation, distribution and persistence of TCE and its various metabolites.

7.7 Final Conclusions

In conclusion, the main results of this thesis suggest that TCE does lead to DA neurodegeneration in the SNpc of exposed individuals, probably through metabolism to the neurotoxic compound TaClo. The neurotoxic properties of TaClo are DA specific and relatively potent with death seen at µM concentrations in acute models. The mechanism of neurotoxicity is hypothesised to be through inhibition of mitochondrial Complex I, inducing increased ROS production and damage of intracellular organelles, DNA and proteins, which in turn leads to the activation of autophagy and PARP activation. This intracellular stress instigates RIP1 mediated necroptosis and death of the cells. The hypothesis proposed is summarised in Fig 7.2.

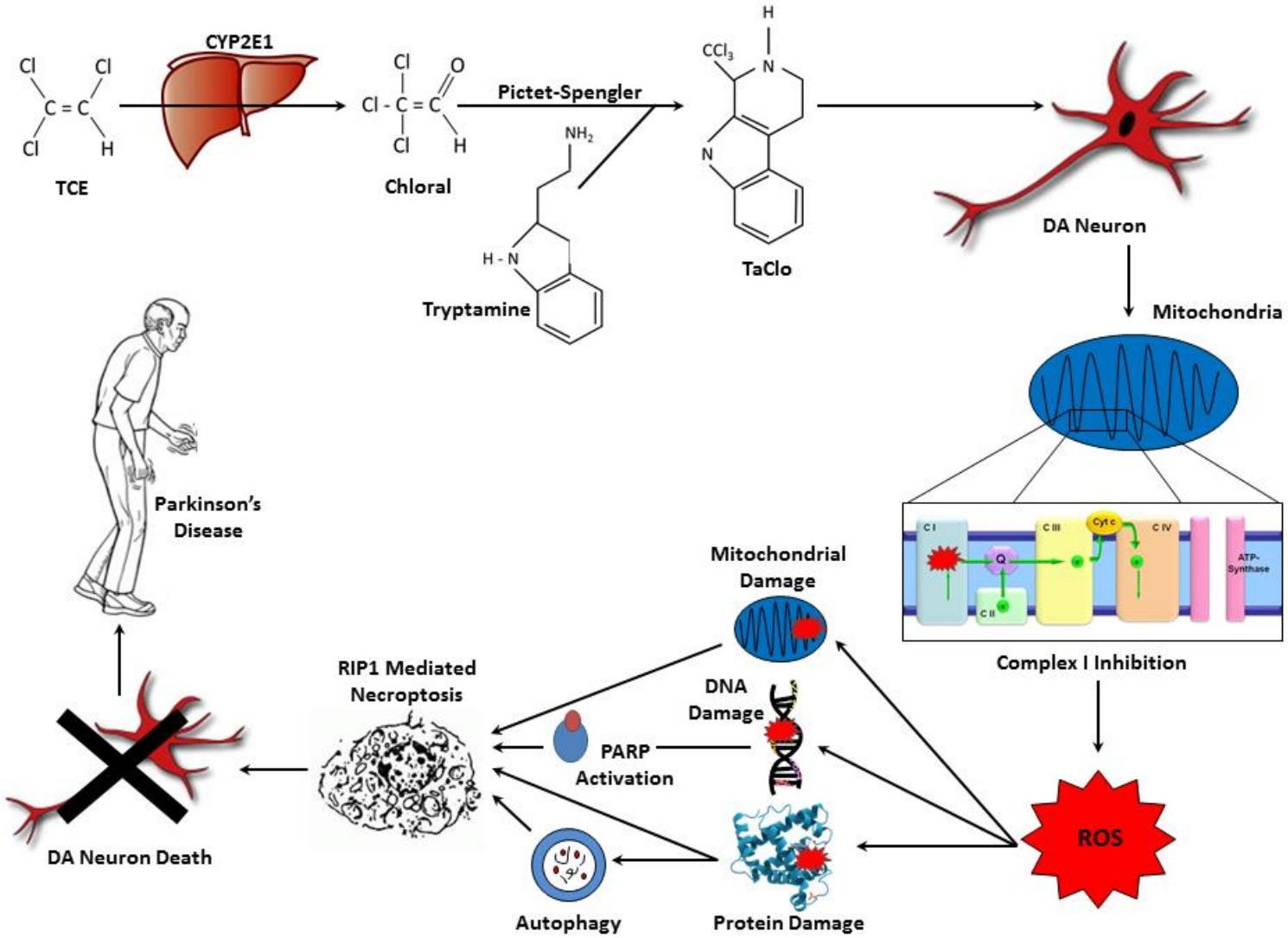

Fig. 7.2. Proposed mechanism of DA cell death and development of PD due to TCE exposure TCE enters the bloodstream of exposed individuals and is metabolised in the liver by CYP2E1 to chloral, which in turn combines with endogenous tryptamine to form TaClo. TaClo can cross the membrane of DA neurons where it inhibits Complex I of the mitochondrial OXPHOS chain generating ROS. The ROS produced then causes further impairment to mitochondria as well as damaging protein, and activating autophagy, and DNA, leading to PARP over activation and ATP depletion. These insults cause the cell to activate RIP1 mediated programmed necrosis (necroptosis) leading to loss of the DA neurons of the SNpc and development of PD

Appendix A
Investigation into the Effects of A30P Mutant α-synuclein Overexpression on the Motor & Cognitive Function, SNpc Neuron Numbers and DA Levels in C57BL/6 Mice

A.1 Introduction

Mutations in the gene encoding α-synuclein have been linked with development of PD (Polymeropoulos, Lavedan et al. 1997; Zarranz, Alegre et al. 2004). One such mutation is the replacement of an alanine with a proline at position 30 in the protein (A30P), which was discovered in a German family (Kruger, Kuhn et al. 1998). This mutation has been shown to protect α-synuclein against degradation by autophagy and the proteasome (Cuervo, Stafanis et al. 2004; Song, Patel et al. 2009), which could increase levels in the cell, and has been shown to increase oligomerisation and fibrillation into toxic aggregates (Conway, Harper et al. 1998; Conway, Lee et al. 2000) which in combination would promote SNpc neuron degradation and aid PD progression.

A transgenic strain of C57BL/6 mice expressing human A30P mutant α-synuclein has been developed in the laboratory of Prof. Philipp Kahle at the University of Tubingen using a pan-neuronal Thy1 promoter (Kahle, Neumann et al. 2000). This mouse develops a condition that mimics the development of PD with abnormal age-dependent α-synuclein accumulation in the brainstem and an overexpression of tau phosphorylation seen (Kahle, Neumann et al. 2000; Frasier, Walzer et al. 2005). Spontaneous locomotor activity, as assessed by distance travelled, number of rears and stereotypy counts, significantly increased by 12 months and motor co-ordination, as assessed by accelerating rotarod, significantly decreased by 17.5 months (Freichel, Neumann et al. 2007). Although there are no reports of decreased DA levels or DA neuron number in this model, a related model from the same laboratory which expressed A30P specifically in the olfactory neurons under a different promoter showed a significant decrease in DA in this region and a decrease in DA neuron number, that was not quite significant (P=0.08) (Nuber, Petrasch-Parwez et al. 2011). This mouse model has also been shown to induce cognitive decline when assessed by Morris water maze, and to have α-synuclein pathology in the nucleus of the amygdala (Freichel, Neumann et al. 2007) suggesting possible cognitive decline in addition to motor symptoms.

A.1.1 Aims

This study aims to assess the effect of A30P mutant α-synuclein over-expression in C57BL/6 mice and to explore any changes in motor or cognitive function, neurotransmitter level or SNpc neuron number in mutant animals. Extensive longitudinal motor behaviour will be performed in conjunction with a measure of spatial learning and memory and previously developed methods to measure neurotransmitter levels by LC-MS/MS and neuron numbers by stereology post mortem.

A.2 Methods

For detailed methods see Material and Methods (Section 2).

The analysis carried out in this study uses the vehicle (10ml/kg olive oil) treated groups of wild type and A30P overexpressing animals from the study described in Chapter 6 (n=8, 5 male & 3 female wild type and 3 male & 5 female A30P due to early terminations in the study).

A.2.1 Statistical Analysis

For information on statistical methods see General Statistics (Sections 2.8 & 2.8.2).

A.3 Results

A.3.1 Behavioural Testing

A.3.1.1 Rotarod

To assess motor function in this study, the accelerating rotarod, a well characterised behavioural paradigm used in rodent models (Jones and Roberts 1968), was used prior to and every 4 weeks until 40 weeks after the first dose. Animals were placed on a steadily accelerating rotating rod and time to fall off was recorded. There was no significant difference between mutant and wild type animals, but were significant differences in performance over time and effect of the mutation over time ($P<0.01$, $P<0.05$, respectively, Two-way Repeated Measures ANOVA). However, the relevance of this difference between groups over time is unclear with both groups of animals fluctuating over the course of the study but the decrease in performance of wild-type animals from week 24, suggesting a possible motor deficit (Fig A.1). No significant difference was seen at any time point for any treatment when compared to vehicle (Bonferroni post-test).

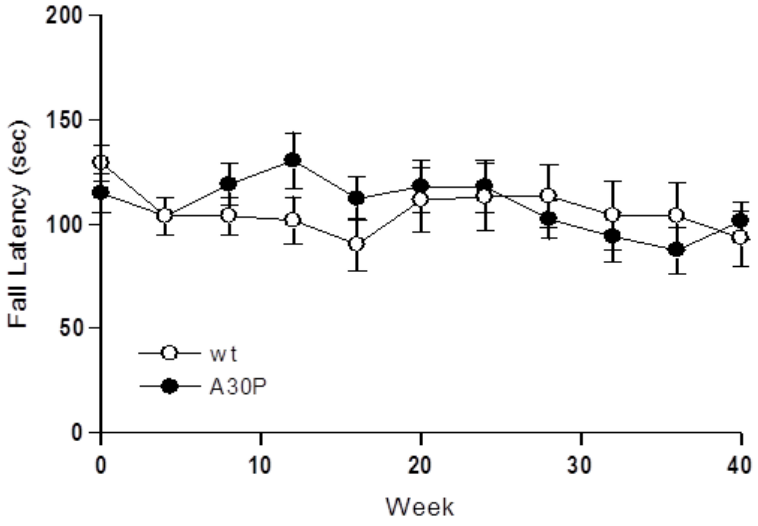

Fig. A.1 Effect of A30P α-synuclein overexpression on C57BL/6 mouse motor function as assessed by the Rotarod test Average fall latency (sec) of wild type and A30P α-synuclein overexpressing C57BL/6 mice over time, triplicate trials. Data presented as mean ± SEM (n=8). Significant difference over time ($P<0.01$) and effect of mutation over time ($P<0.05$), No significant difference between groups, Two-Way Repeated Measures ANOVA

A.3.1.2 Pole Test

The pole test, which has been developed to test more fine motor control than the accelerating rotarod in mice (Matsuura, Kabuto et al. 1997), was used in this study to further assess any effects of the treatments on the motor skills of the animals at the same time points as the rotarod test. Animals were placed face up on a pole and the total time to complete trial, the time to turn on pole, the time to descend pole and number of falls per three trials recorded for all animals.

There was no significant difference between mutant and wild type animals or effect of mutation over time in total time, time to turn, time to descend or number of falls in the pole test, but were significant differences over time for all parameters ($P<0.001$ for time to turn, $P<0.01$ for total time, descent time and number of falls, Two-way Repeated Measures ANOVA). Despite the lack of significant effects, A30P overexpressing mice appeared to take consistently longer to perform the task and to fall more often from approximately 16 weeks until the end of the study period (Fig. A.2). An exception to this trend was observed at week 28 where wild type animal performance level dropped for one trial before returning to normal (Fig. A.2), this result is considered an anomaly.

Taken together this data does not provide any significant evidence of a decrease in fine motor control in A30P overexpressing C57BL/6 animals but does suggest a possible trend towards decreased motor function with the consistently decreased performance of mutant animals compared to wild-type in the later stages of the study.

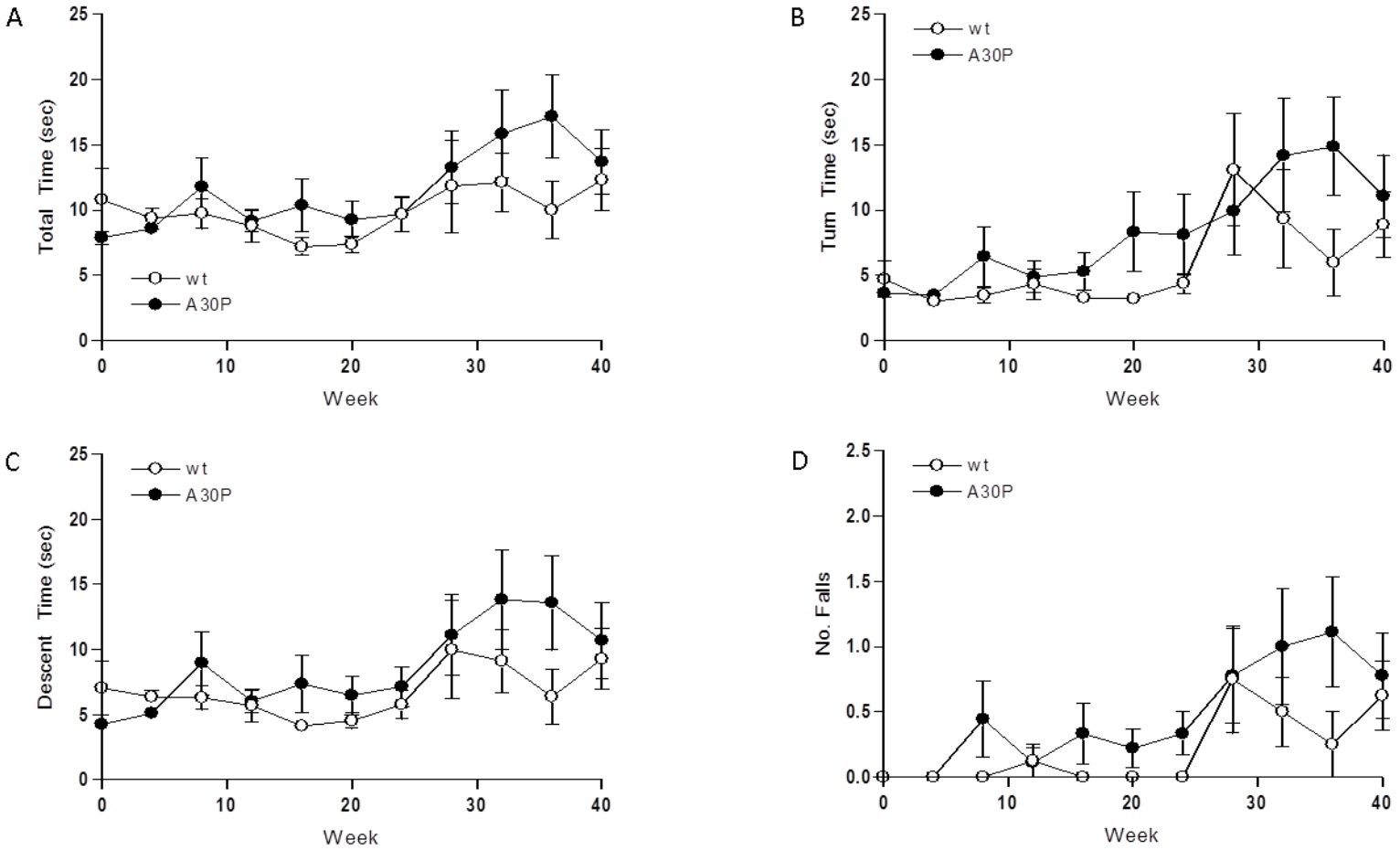

Fig. A.2 Effect of A30P α-synuclein overexpression on C57BL/6 mouse motor function as assessed by the Pole test Average (A) total, (B) turn, (C) descent time (sec) & (D) number of falls of wild type and A30P α-synuclein overexpressing C57BL/6 mice over time, triplicate trials. Data presented as mean ± SEM (n=8). (A-D) Significant difference over time (B, $P<0.001$, A, C, D, $P<0.01$). (A-D) No significant difference between groups or effect of mutation over time, Two-Way Repeated Measures ANOVA.

A.3.1.3 Gait Analysis

Differences in gait and stride length have been reported in animal models of PD (Tillerson, Caudle et al. 2002; Amende, Kale et al. 2005), so animal gait was analysed from post dose weeks 28 to 40 by painting animals' hind paws and running them down a corridor to the home cage allowing measurement of stride length. There were no significant differences observed in average stride length between groups or effect of overexpression of A30P mutant α-synuclein over time, and no significant change between trials in the A30P animals but there was a significant change in stride length over the test period ($P<0.01$, Two-way, Repeated Measures ANOVA) (Fig A.3). There were, in addition, also no significant differences between vehicle and compound-treated animals at any time point (Bonferroni post-test). While the performance of the A30P overexpressing mice remained relatively constant throughout the testing period, the performance of the wild type mice appears to increase from 32 weeks post first dose (Fig A.3). These results suggest that A30P overexpression in C57BL/6 mice has no significant effect on stride length.

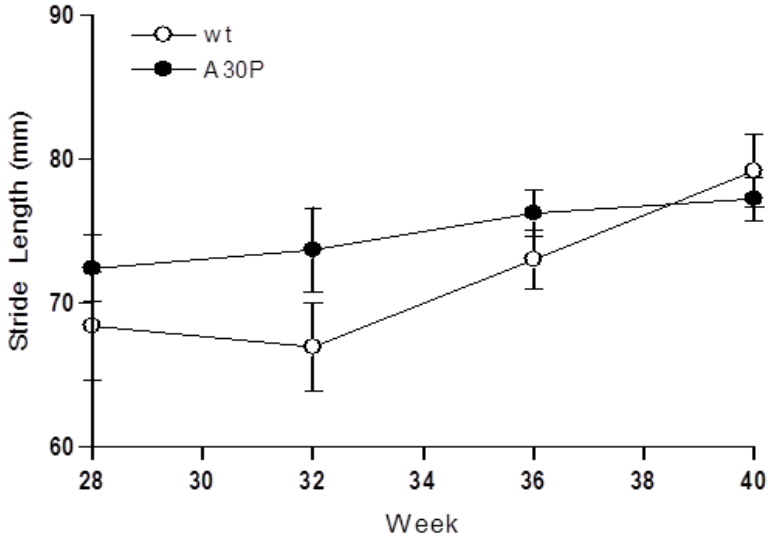

Fig. A.3 Effect of A30P α-synuclein overexpression on C57BL/6 mouse motor function as assessed by gait analysis Average stride length (mm) of wild type and A30P α-synuclein overexpressing C57BL/6 mice over time, triplicate trials. Data presented as mean ± SEM (n=8). Significant difference over time ($P<0.01$), no significant difference between groups, or of mutation over time, Two-Way Repeated Measures ANOVA

A.3.1.4 Grip Strength

As abnormalities in grip strength have been reported in mouse models of PD (Colotla, Flores et al. 1990) and spinal pathology has been reported in A30P overexpressing mice (Neumann, Kahle et al. 2002), a test of grip strength using a strain gage was used in this study (Cabe, Tilson et al. 1978). There were no significant differences observed in grip strength between wild type mice and A30P overexpressing animals and no significant effect of the mutation over time; however there was a significant difference over time in both groups ($P<0.001$, Two-way, Repeated Measures ANOVA) (Fig A.4). There were also no significant differences between groups at any time point (Bonferroni post-test). This data suggests that overexpression of A30P mutant human α-synuclein in C57BL/6 mice does not affect grip strength.

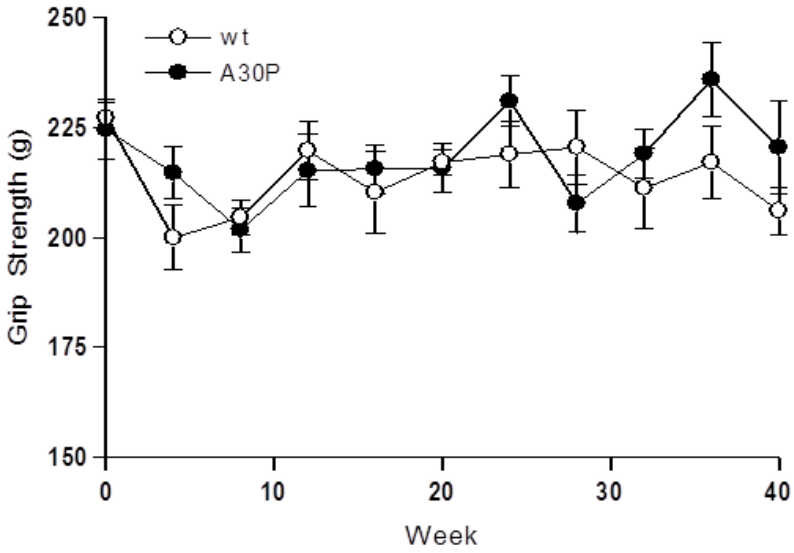

Fig. A.4 Effect of A30P α-synuclein overexpression on C57BL/6 mouse grip strength Average grip strength (g) of wild type and A30P α-synuclein overexpressing C57BL/6 mice over time, triplicate trials. Data presented as mean ± SEM (n=8). Significant difference over time ($P<0.001$), no significant difference between treatment groups, or effect of treatment and mutation over time, Two-Way Repeated Measures ANOVA

A.3.1.5 Barnes Maze

As the A30P overexpressing mouse model used in this study have been shown to have cognitive deficits (Freichel, Neumann et al. 2007), learning and memory were assessed in this study. The Barnes maze is a test used to assess spatial and learning and both short and long term memory using the mouse's ability to find and remember the location of an escape box located under one of 20 equally spaced holes around the edge of a circular maze using visual cues as landmarks (Barnes 1979; Patil, Sunyer et al. 2009).

Learning is assessed using the time to find the escape hole (primary latency), time to enter escape box (total latency), number of errors before finding escape hole (primary errors) and total number of errors before entering escape box (total errors) over four trials for each of four consecutive days.

When comparing A30P and wild type mice, primary latency was significantly higher in A30P mice on Day 1 before reaching a similar level by Day 3 (Fig. 6.10 A & B). This finding is not replicated when looking at total latency (Fig. 6.11 A & B) or primary errors (Fig. 6.12 A & B). However, when looking at the total errors, this finding is reversed, with more errors being made by the wild type than A30P mice before box entry.

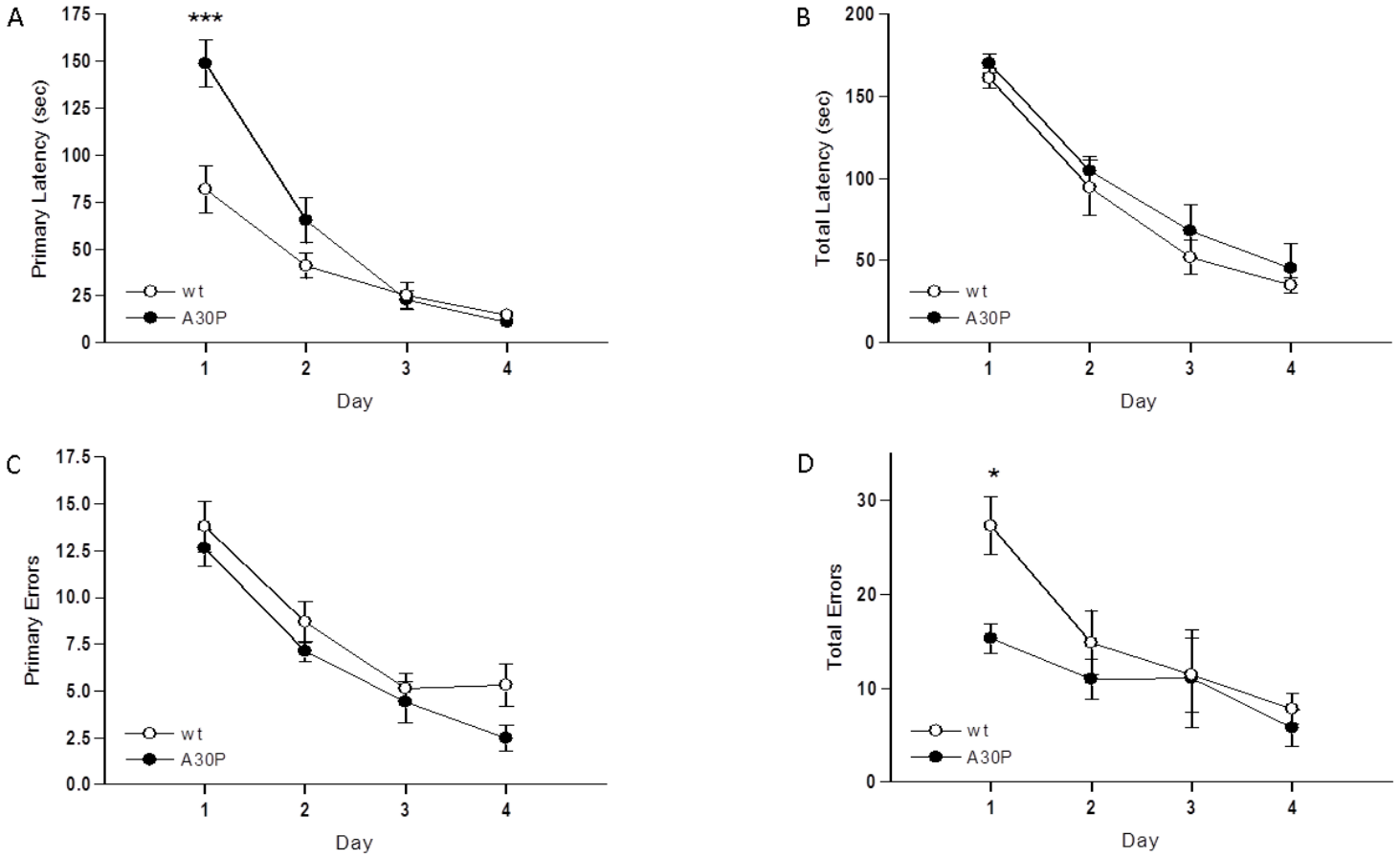

Fig. A.5 Effect of A30P α-synuclein overexpression on wt C57BL/6 mouse spatial learning as assessed by the Barnes maze primary & total latency & errors
Average (A) primary & (B) total latency (sec) and (C) primary & (D) errors to find target of wild type and A30P α-synuclein overexpressing C57BL/6 mice over time, quadruplicate trials. Data presented as mean ± SEM (n=8). (A-D) Significant difference over time (P<0.001), (A) Significant difference between groups (P<0.05) and effect of mutation over time (P<0.001), (B) no significant difference between groups or effect of mutation over time, (C) significant difference between groups (P<0.05), no significant effect of mutation over time. (D) Significant effect of mutation over time (P<0.05), no significant difference between groups, Two-Way Repeated Measures ANOVA. ***P<0.001, *P<0.05 when compared to wild type relevant time point, Bonferroni post-test

Memory is assessed in the probe phase of the Barnes maze, where on Day 5 (short term memory) and Day 12 (long term memory) a single trial is carried out with no escape box and primary latency (time to find hole where box should be), first hole visited and number of nose pokes in each hole of the maze are recorded. A score is also generated by assigning each hole a numerical value based on how far it is from the target hole and calculating the sum of nose pokes in each hole based on these values (e.g 3 pokes in a hole 4 away from target gives a score of 12, 2 pokes in a hole 9 away from target gives a score of 18 etc.) to give a numerical value to performance in the test.

Investigations showed no significant difference between wild-type or A230p overexpressing mice in latency to find the target in either short or long term probes (unpaired t-test); however, wild-type mice did show a trend towards a longer time to find the target in the short (P=0.20) but not long term tests (Fig. A.6)

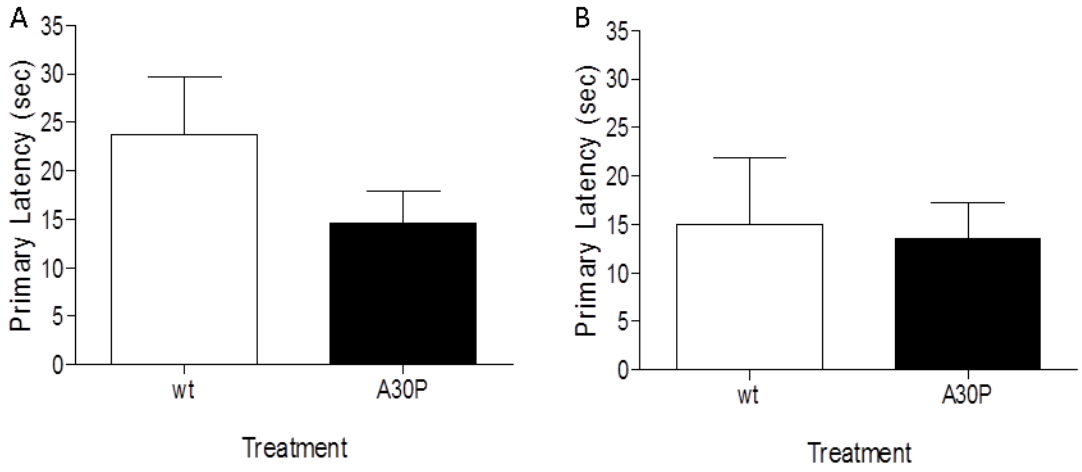

Fig. A.6 Effect of A30P α-synuclein overexpression on C57BL/6 mouse spatial memory as assessed by the Barnes maze primary latency Average primary latency (sec) to find target hole during (A) short term (Day 5) or (B) long term (Day 12) probe test of wild type and A30P α-synuclein overexpressing C57BL/6 mice. Data presented as mean ± SEM (n=8). (A & B) No significant difference between groups, unpaired t-test.

When comparing the first hole visited in both probe tests between A30P mutant and wild-type animals, the results reflected the time taken to find the first hole with no significant difference between groups in either long or short term tests (un-paired t-test) with all mice in both groups first visiting a hole in the correct half of the maze apart from one individual in the wild-type group short term probe which first visiting the opposite hole to the target (Fig. A.7). This may offer a possible explanation for the trend towards higher primary latency observed in the wild-type short term test.

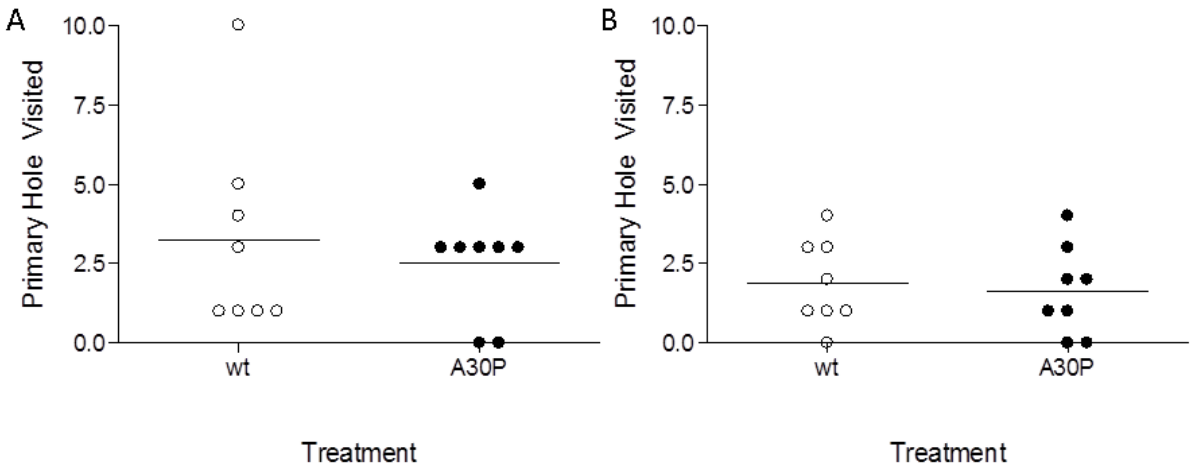

Fig. A.7 Effect of A30P α-synuclein overexpression on C57BL/6 mouse spatial memory as assessed by the Barnes maze primary hole visited Primary hole visited during (A) short term (Day 5) or (B) long term (Day 12) probe test of wild type and A30P α-synuclein overexpressing C57BL/6 mice. Data presented as median ± scatter (n=8). (A & B) No significant difference between groups, unpaired t-test.

There were significant differences between the number of times A30P animals poked their nose in a variety of the holes in the probe test when compared to wild-type mice in both short and long term probes (short, P<0.001, -1, P<0.01, T, P<0.05, +1, +8, +9, -4, -5, -9, O; long, P<0.01, +5, +9, -1, -5, P<0.05, T, +4, +6, -2, -4; all unpaired t-test) (Fig A.8). When comparing the spread of holes poked away from the target hole, the A30P overexpressing animals appear to show a less exploratory behaviour than the wild-type animals with A30P animals only rarely exploring further than four holes from the target and never more than seven and the wild type mice showing significantly more nose pokes throughout the maze suggesting more exploratory behaviour and exploring the entire maze in both the long and short term probes, with animals visiting the opposite hole to the target (Fig. A.8).

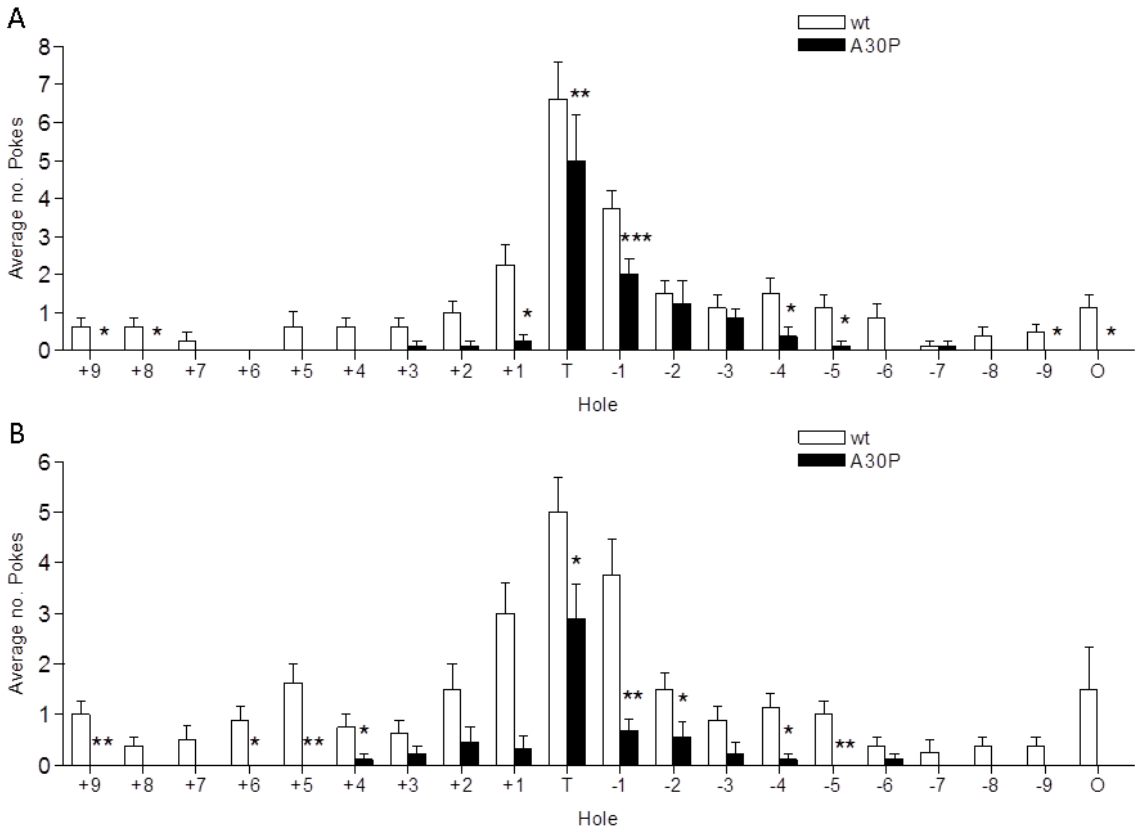

Fig. A.8 Effect of A30P α-synuclein overexpression on C57BL/6 mouse spatial memory as assessed by the Barnes maze nose pokes Average nose pokes in each hole during (A) short term (Day 5) or (B) long term (Day 12) probe test of wild type and A30P α-synuclein overexpressing C57BL/6 mice. Data presented as mean ± SEM (n=8). (A & B) ***P<0.001, **P<0.01, *P<0.05 when compared to wild-type, unpaired t-test.

When using the quantifiable score for each animal, similar results can be seen. Wild type animals have significantly higher scores in both short and long term probes ($P<0.01$ & $P<0.001$ respectively, unpaired t-test). This finding is more pronounced in the long term probe with the lowest scoring wild type animal scoring over double the highest scoring A30P mouse. This would seem to suggest a decrease in spatial memory in the wild-type mice when compared to A30P overexpressing animals but care is needed in analysing the results as the effect may be due to the decreased exploratory behaviour seen in the A30P animals.

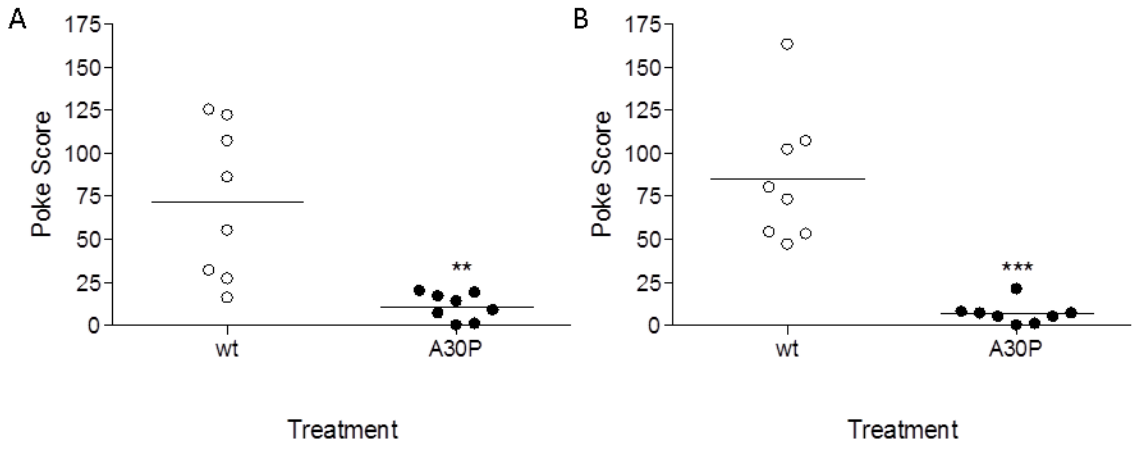

Fig. A.9 Effect of A30P α-synuclein overexpression on C57BL/6 mouse spatial memory as assessed by the Barnes maze poke score Poke Score during (A) short term (Day 5) or (B) long term (Day 12) probe test of wild type and A30P α-synuclein overexpressing C57BL/6 mice. Data presented as median ± scatter (n=8). ***P<0.001, **P<0.01, when compared with wild type, unpaired t-test.

A.3.2 Neurotransmitter Levels

Although there are no reports of decreased DA levels in this model, a related model from the same laboratory which expressed A30P specifically in the olfactory neurons under a different promoter showed a significant decrease in DA in this region (Nuber, Petrasch-Parwez et al. 2011). Neurotransmitter levels were therefore measured in the caudate putamen and forebrain of study animals by LC-MS/MS post mortem.

DA levels were not quantified due to limitations in the assay and neither was DOPAC in A30P animals; however DOPAC and HVA were measurable in wild-type animals and HVA in wild-type. No significant changes in DOPAC or HVA levels were observed in the either brain region between mouse strains in HVA (unpaired t-test) (Fig. A.10).

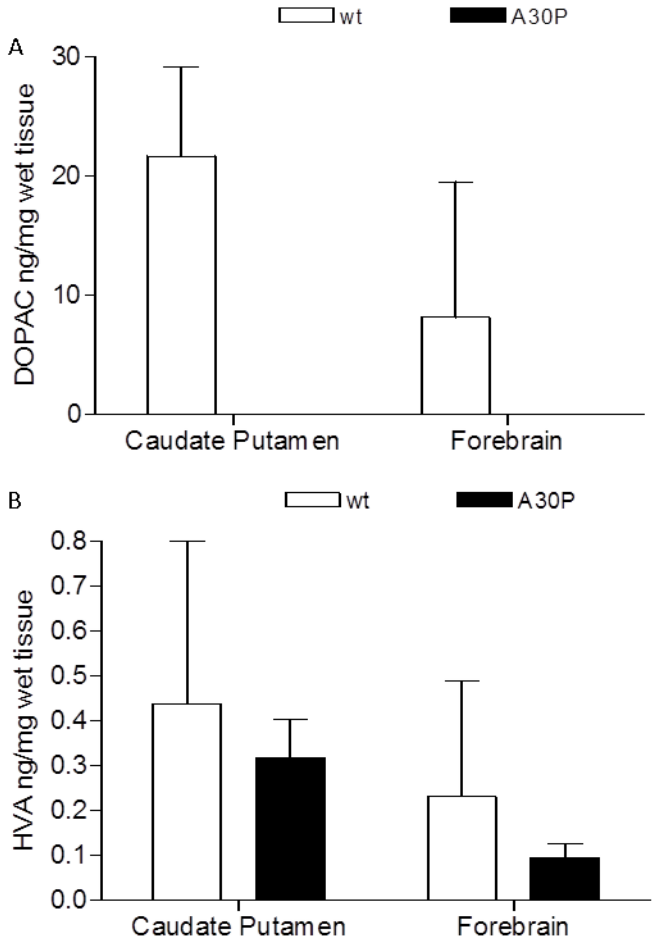

Fig. A.10 Effect of A30P α-synuclein overexpression on caudate putamen & forebrain DA metabolite levels in C57BL/6 mice Levels of (A) DOPAC & (B) HVA in Caudate Putamen & Forebrain wt & A30P overexpressing C57BL/6 mice when assessed by LC-MS/MS. Data presented as mean ng/mg wet tissue from duplicate samples ± SD (n=4-10). (A & B) No significant difference between groups, unpaired t-test.

5-HT levels could not be measured in the A30P brain samples due to assay limitations but 5-HT in the caudate of wild-type animals and both regions in A30P mice as well as metabolite 5-HIAA in both brain regions of both strains were quantified. A30P overexpression significantly reduced 5-HIAA levels in both the caudate putamen and forebrain of mice in this study (caudate, $P<0.05$; forebrain, $P<0.01$; both unpaired t-test) (Fig. A.11)

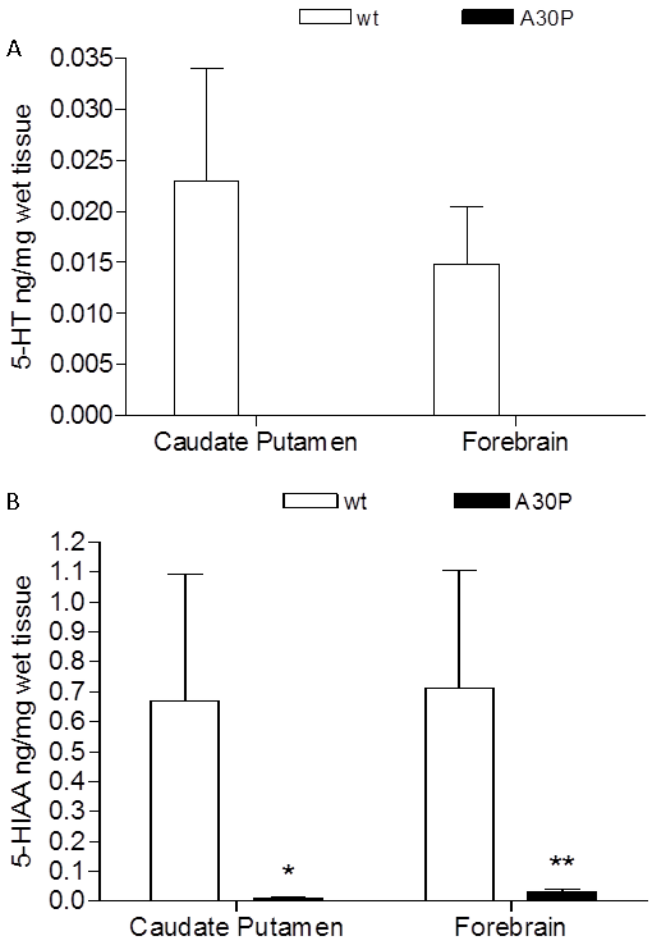

Fig. A.11 Effect of A30P α-synuclein overexpression on caudate putamen & forebrain 5-HT levels in C57BL/6 mice Levels of (A) 5-HT & (B) 5-HIAA in Caudate Putamen & Forebrain wt & A30P overexpressing C57BL/6 mice when assessed by LC-MS/MS. Data presented as mean ng/mg wet tissue from duplicate samples ± SD (n=4-10). (A) No significant difference between groups, (B) significantly different from wt, *P<0.05, **P<0.01, all unpaired t-test.

Levels of GABA were significantly reduced in A30P mice in comparison to wild type animals in both brain regions (both P<0.01, unpaired t-test) (Fig. A.12 A). Due to problems with the assay, glutamate could not be measured in A30P animal forebrain and was not significantly altered between strains in the caudate putamen (unpaired t-test) (Fig. A.11 B).

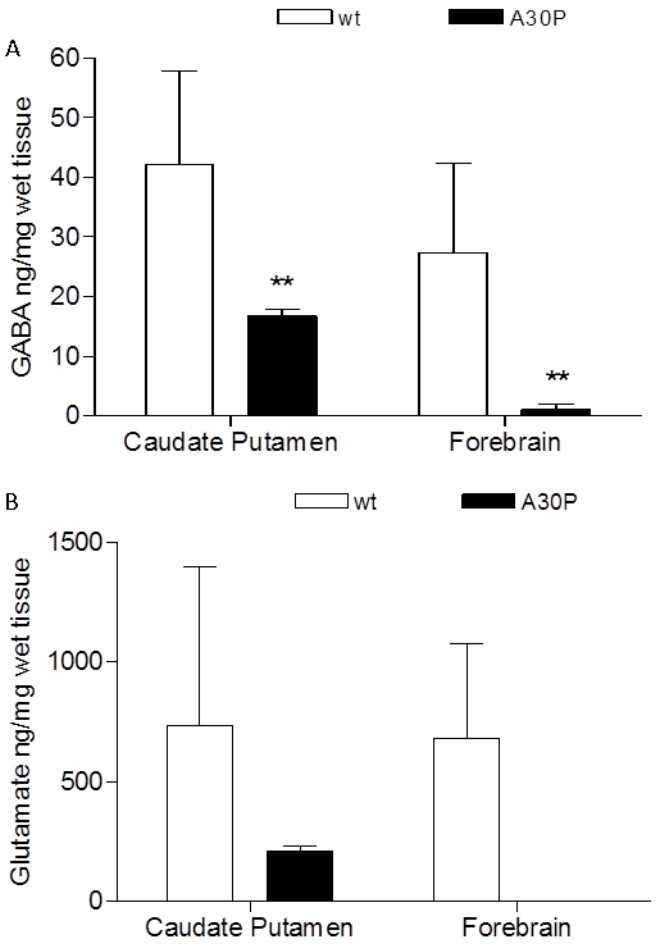

Fig. A.12 Effect of A30P α-synuclein overexpression on caudate putamen & forebrain GABA & Glutamate levels in C57BL/6 mice Levels of (A) GABA & (B) Glutamate in Caudate Putamen & Forebrain wt & A30P overexpressing C57BL/6 mice when assessed by LC-MS/MS. Data presented as mean ng/mg wet tissue from duplicate samples ± SD (n=6-8). (A) Significantly different from wt, (B) no significant difference between groups, **P<0.01, all unpaired t-test.

A.3.3 SNpc DA Neuron Number

As deterioration of the DA neurons of the SNpc has been shown to be characteristic in PD (Bernheimer, Birkmayer et al. 1973), DA neuron number and size were assessed in this study using stereology. Stereology is a method of estimating geometrical quantities that can be used to estimate the number and size of cells in a defined 3D region from a series of sections. Design based stereological analysis, such as that used in this study, has been shown to accurately estimate DA neuron number in the SNpc of C57BL/6 mice when compared to counts obtained through serial reconstruction (Baquet, Williams et al. 2009).In this study, stereology was used to estimate the number and volume of TH-positively stained DA neurons in the SNpc of fixed and processed brains taken from a proportion of the animals used to assess behaviour.

A30P overexpressing animals appear to show an increase in DA cell volume when compared to wild-type; however this effect is not quite significant (P=0.11, unpaired t-test) (Fig. A.13). However, A30P overexpressing animals did show a significant decrease in cell number to 71% wild-type number (P<0.05, unpaired t-test) (Fig. A.13 A), and a significant decrease in TH-positive cell density to 56% of wild type values (P<0.001, unpaired t-test) (Fig. A.13 B).

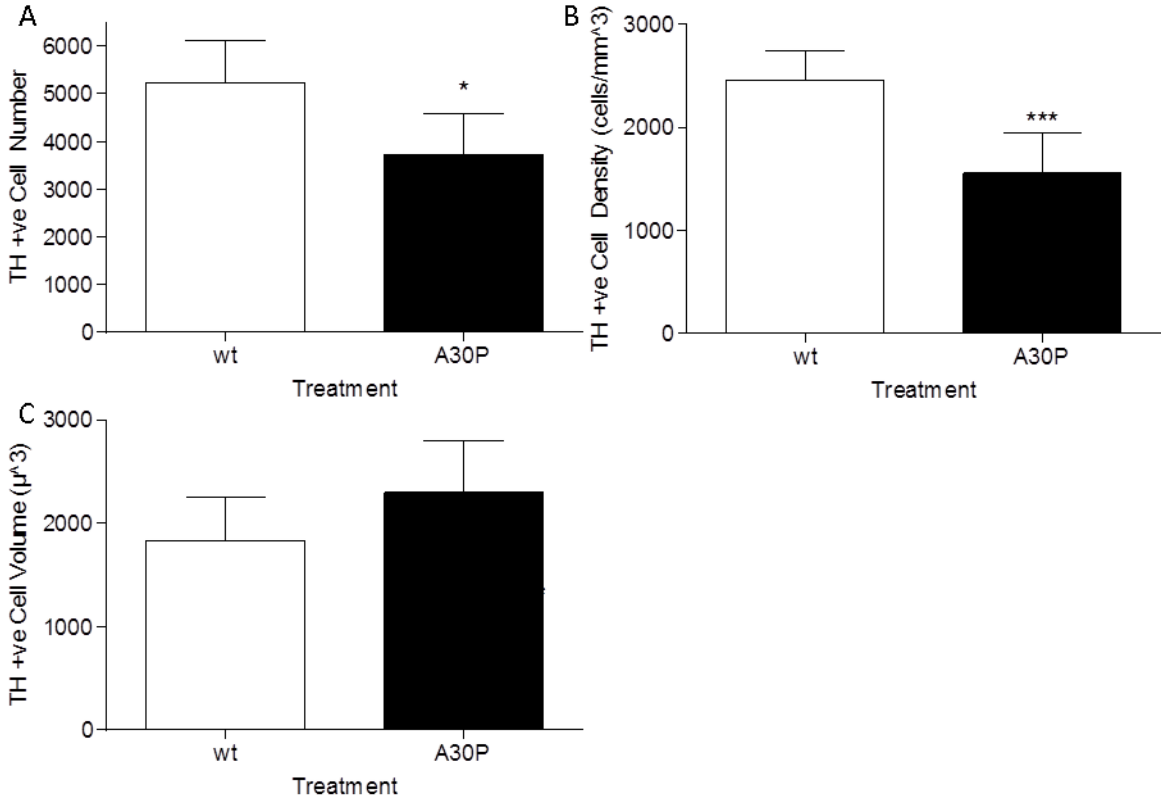

Fig. A.13 Effect A30P α-synuclein overexpression on SNpc DA Neuron number, density & volume in C57BL/6 mice Total (A) number, (B) density & (C) cell body volume of TH-positive cells in the SNpc of wt & A30P overexpressing C57BL/6 mice assessed by stereology. Data presented as mean ± SD (n=6). ***P<0.001, *P<0.05 when compared to wt, unpaired t-test

A.4 Discussion

As described in Section 5.4.2, the accelerating rotarod test has been used to show a decrease in motor function following exposure to PD-linked neurotoxins. Both wild-type and A30P overexpressing mice show a slight but significant decrease in rotarod performance, with A30P overexpressing animals appearing to markedly decrease from 24 weeks until week 40 where it slightly rises again (Fig. A.1). However, this apparent decrease in motor function as assessed by rotarod in the later stages of the study may be due to habituation to repeated testing incidences, or a weight-related decrease in performance that occurs at animal weights of over 40g (see Appendix B for details) rather than loss of DA neurons. There were no significant differences seen between wild-type and A30P mutant animals in the study but, a significant effect of the mutation over time was seen with A30P animals showing a greater decrease in performance over time, suggesting an overexpression of A30P mutant α-synuclein in mice may lead to decreased motor performance. This is not consistent with reported lack of discrimination of motor dysfunction assessed by the rotarod in the same strain of A30P mice used in our study until 17months (Freichel, Neumann et al. 2007), with our study terminating at 13 months, and a lack of any effect in a separately generated A30P mutant α-synuclein mouse (Plaas, Karis et al. 2008), and may be a statistical artefact as the difference in performance over time is not consistent or marked at any point. The ability to discriminate effects on motor function using this test may have been masked due to problems in consistent performance of the test with individual animals showing an apparent lack of drive in the test, turning around and walking backwards on the treadmill, or attempting to climb dividers between lanes, all occurring during testing periods and leading to a decrease in fall latency and leading to increased variability of results.

The pole test has previously been used to show a decline in fine motor performance following exposure to neurotoxins linked to development of PD (see Section 5.4.2). In this study, all parameters of the pole test showed a significant decrease in performance over time, but no overall difference was seen in fine motor control for wild-type and A30P overexpressing groups of animals nor any significant effect of the mutation over time (Fig. A.2). All treatment groups of both strains showed a general increase in the time taken to turn and descend the pole and to complete the task, as well as in the number of falls recorded over the duration of the study (Fig. A.2). This decrease in fine motor control seen over time may be due to habituation of the animals to the task as it occurred across all treatment groups and the vast majority of previous published uses of the pole test have not used it repeatedly, with the only published report of repeated use of the pole test found only repeatedly used for 3 weeks (Balkaya, Kröber et al. 2013) as opposed to over 40 weeks in this study. Another possible

explanation could be due to a similar weight-related decrease in performance to that seen in the rotarod test occurring at weights of over 40g (see Appendix B). Although there were no significant differences in performance of the test between wild-type and mutant animals, A30P overexpressing mice showed consistently lower performance across all measured parameters, suggesting a possible trend towards overexpression of A30P mutant α-synuclein leading to a decrease in fine motor control in C57BL/6 mice. Performance in this test showed large inter- and intra-subject variability, due in part to the fact that any mouse falling from the pole was assigned the maximum time of 30 seconds, whereas instances where the task was completed reported average values of 2 to 4 seconds to turn, 3 to 5 seconds to descent and 5 to 8 seconds in total. This led to large variability in the final data and may have masked any possible effects that A30P overexpression may have caused.

The strain of A30P mice used in this study have been shown to develop an unsteady gait over time (Neumann, Kahle et al. 2002), suggesting a possible effect of the mutation on gait and stride length. We observed no significant differences between wild-type and A30P overexpressing mice or effect of the mutation on stride length, but did see a significant difference in performance over time (Fig. A.3). Interestingly, wild-type mouse stride length appeared to increase substantially over the course of the study, whereas A30P animals did not to the same extent (Fig. A.3). A possible explanation for this could be that the wild-type animals got used to the test more rapidly than the mutant due to either differences in learning or anxiety and the later stride length was more representative, or due to the fact that A30P animal stride length was decreased relative to the normal increase in repeated tests seen with wild-type animals. If this was the case it would suggest not enough habituation and training was carried out prior to test start and definitive conclusions cannot be drawn from the results seen, with and more exploration into this effect needed to ascertain any significance. Findings by Plaas et al. showed significantly decreased stride length in mouse with an A30P point mutation introduced into the α-synuclein gene at 13 months of age when compared to wild-type (Plaas, Karis et al. 2008). However, they introduced the mutation into the mouse α-synuclein gene rather than introducing mutated human α-synuclein and effects were only seen in forepaw stride length whereas this study measured hind paw stride length.

The data observed in this study suggests that overexpression of A30P mutant α-synuclein in C57BL/6 does not result in sufficient SNpc DA neuron degeneration to cause a significant decrease in motor function as assessed by the accelerating rotarod, pole test or gait analysis. However, some levels of DA cell death may have occurred in the SNpc of mutant animals without significant motor dysfunction occurring, as it has been shown that >70-80% cell death

is required before behavioural deficits are seen (Hirsch, Graybiel et al. 1988; Fearnley and Lees 1991; Tillerson, Caudle et al. 2002; Chaudhuri, Healy et al. 2006).

There was a significant variation in grip strength over time in both strains observed, which manifested as a sharp decrease from pre-dose to 4 weeks which then generally levels off across the rest of the study period with periodic fluctuations occurring. However, no significant difference was seen between wild-type or mutant animals nor an effect of mutation over time observed (Fig. A.4). As previously mentioned in Section 5.4.2, grip strength is not thought to be a sensitive marker for motor dysfunction in PD; however the strain of A30P mutant α-synuclein overexpressing mice used have been reported to show spinal pathology, as the Thy1 promoter expresses the insert in the brainstem and spinal cord and causes a weakening of extremities (Neumann, Kahle et al. 2002). As spinal cord pathology has been reported to manifest as a reduction in grip strength and gait abnormalities (Guo, Qiu et al. 2013), and has been implicated in the development of motor dysfunction in the A30P mice used in this study (Neumann, Kahle et al. 2002), these symptoms would have been expected to be have been picked up by our grip strength and gait analysis tests. However, no differences in grip strength or gait were seen between wild-type and A30P mutant animals in this study Although Neumann *et al.* describe these motor behavioural deficits, they do not specify the age of the mice when the symptoms manifest, suggesting this may only occur at ages above those reached in our study.

PD has been widely associated with cognitive decline (Taylor, Saint-Cyr et al. 1986; Cooper, Sagar et al. 1991; Owen, James et al. 1992) and there have been reports of a slight decrease in cognition in A30P mutant α-synuclein overexpressing mice, as well as α-synucleinopathy in the central nucleus of the amygdala, an area involved in cognitive behaviour in mice (Freichel, Neumann et al. 2007). Therefore, cognitive function was assessed in this study as special learning and memory by means of the Barnes maze.

Spatial learning was assessed by measuring the time and number of errors prior to the mice finding and entering the target hole (Fig. A.5). When comparing wild-type and A30P mutant animals, A30P mutant animals took significantly longer to find the target hole on the first day of the test, and there was a significant effect of the mutation over time. This suggests that the A30P mice took longer to realise where the hole was, or remember from the previous trial, suggesting a possible learning deficit when compared to wild type C57BL/6. No differences were seen in time to enter target or errors before finding target, but, in contrast to the finding that A30P took longer to find the target than wild-type animals, wild-type animals made

significantly more errors prior to entering the target box, and the mutation had a significant effect over time. As this difference is not seen in primary errors, it suggests either a lack of recognition of the box when found, or a lack of drive to escape the maze in wild type animals when compared to A30P mutants, as more searching, and therefore errors, occurs between animals finding and entering the escape box.

Spatial memory was assessed by measuring the time to find the target hole and the distribution of errors away from the target hole, on the day immediately following the end of training (short-term memory) and a week later (long-term memory) (Figs. A.6-9). The effect of A30P mutant α-synuclein expression on cognition has previously been looked at in a drosophila model, which found that overexpression did lead to learning and memory impairment, but, not to the extent that was seen following exposure to the PD linked neurotoxin rotenone (Yy, Jiang et al. 2011). When looking at primary latency and primary hole visited, there are no apparent differences in the long term probe, and while there may appear to be a trend towards increased primary latency in wild-type animals short-term probe, this effect is not significant and, excluding one outlier, there are no apparent differences in first hole visited (Fig. A.6 & 7). There seems to be a marked difference in performance in both the short and long term probe test between the wild-type and A30P mutant α-synuclein overexpressing mice, with the wild-type animals seeming to have far more exploratory behaviour and therefore significantly more errors at a number of holes than the A30P mutants. As the significant increase in errors is spread across the whole maze with wild-type animals showing similarly significantly more pokes at holes near the target as well as opposite the target, this is not thought to be due to an effect on memory, but more an effect on general activity. This is also manifested by a far greater spread of average pokes from the target hole in wild-type animals and corresponding significantly increased poke score (Fig. A.8 & 9). This could possibly be due to a difference in activity levels between the strains. Although this was not seen in the tests of locomotor activity, the tests measured forced locomotor and no measures of spontaneous activity were examined in this study. Another possible explanation could be due to a decreased drive to enter the target box in wild-type animals when compared to A30P overexpressing mice, possibly due to reduced anxiety, which is supported by the finding that they made significantly more errors before entering the box during the training phase. One possible explanation for this could be that there have been reports of hyperactivity in DA leisioned animals (Pycock, Kerwin et al. 1980), possibly due to compensatory increased DA production in remaining DA neurons (Agid, Javoy et al. 1973; Zigmond, Acheson et al. 1984).

The LC-MS/MS method developed to measure neurotransmitter levels was not found to give accurate or repeatable results during this study. The results in this investigation in wild-type and A30P overexpressing mice were less reliable than those seen in the pilot study (Chapter 5). This was possibly due to the use of perchloric rather than formic acid in the extraction process which was an attempt at a better extraction method but may have resulted in oxidation of the neurotransmitters before detection, with no or extremely low levels of DA, 5-HT & NA detected and a 10-fold drop in levels of 5-HIAA and HVA when compared to wild-type levels. Levels of DOPAC, glutamate and GABA were relatively similar to those seen in pilot mice study, with all three slightly higher than pilot C57BL/6 animals. Almost all neurotransmitters appeared to be present in higher amounts in the wild-type animals in comparison to the A30P overexpressing animals, although only significantly so in GABA and, particularly 5-HIAA (see Appendix A). In the case of 5-HIAA this is almost certainly an assay related decrease as the levels seen in the A30P are >10 times lower than those in the wild-type animals and >100 times lower than those seen in the pilot study mice, an effect that would almost certainly have a major physiological effect.

Loss of SNpc DA neurons is a hallmark of the pathology of PD (Bernheimer, Birkmayer et al. 1973; Dickson, Braak et al. 2009; Lees, Hardy et al. 2009). DA neuron numbers were estimated in the SNpc of a proportion of the animals in this study by stereology and A30P overexpression led a significant drop in the SNpc DA neuron numbers and density when compared to vehicle (Fig. A.14 A&B), suggesting that overexpression of A30P mutant α-synuclein in mouse brain leads to toxicity in DA neurons and possibly contributes to PD. The fact that no motor function was observed despite loss of approximately 30% SNpc DA neurons is consistent with the widespread report that behavioural deficits are only seen when 70-80% DA neuronal loss occurs in the SNpc (Hirsch, Graybiel et al. 1988; Fearnley and Lees 1991; Tillerson, Caudle et al. 2002; Chaudhuri, Healy et al. 2006).

Individual DA neuronal volume was measured and A30P mutant α-synuclein overexpressing animals showed a trend towards larger cell volumes than wild-type, although this effect is not quite significant (Fig. A.13 C). This correlates with a report of enlarged brainstem and spinal cord neurons in similar mice, overexpressing human A53T mutant α-synuclein (Martin, Pan et al. 2006) and possibly suggests that the cells are under stress as cell swelling is a morphological hallmark of necrosis (Van Cruchten and Van den Broeck 2002); conversely, a post mortem study on the brains of PD patients showed no increase in SNpc cell volume in cells containing Lewy bodies (Gertz, Siegers et al. 1994). Another possible explanation for the increase in cell volume in the A30P mice could be that while the mutant animals were generated from the

same base strain as the wild-type animals used in the study, C57BL/6, the animals would have been developing down separate lines for a number of generations and spontaneous changes in physiology may have occurred leading to the development of slightly different sized neurons. More investigation is needed into this possible increase in DA neuron size in A30P mice to determine the cause and relevance of the finding.

In conclusion, although there were no significant differences in motor behaviour in the motor function tests, or consistent changes in neurotransmitter levels, mutant human A30P α-synuclein did lead to a 30% decrease in SNpc DA neuronal number. This suggests that if the animals survived for longer, functional and biochemical changes may occur at ages greater than the 14 months in this study. In addition to this, while there were not thought to be significant changes in learning or memory in the Barnes maze, A30P overexpressing animals did appear to show a significant decrease in exploratory behaviour in the test, a finding which may merit more investigation.

Appendix B
Investigation into the Effects of Weight on Performance in Motor Function Tests in A30P Mutant a-synuclein Overexpressing C57BL/6 Mice

B.1 Introduction

Motor function is an important behavioural marker used to assess development of PD. The rotarod test and pole test are two widely used paradigms designed to measure motor function in rodent models of the disease (Jones and Roberts 1968; Matsuura, Kabuto et al. 1997). While performing these tests over a long period in the study described in Chapter 6, it was noticed that as some animals grew larger, their ability to perform in the rotarod and pole tests decreased. If this effect is found to be significant, it could impair the ability of the tests to detect motor dysfunction in the study.

A.1.1 Aims

This study aims to assess the effect of weight on performance in motor function tests in A30P mutant α-synuclein over-expressing C57BL/6 mice. Motor behaviour will be assessed by the rotarod and pole tests.

B.2 Methods

For detailed methods see Material and Methods (Section 2).

The analysis carried out in this study uses the A30P overexpressing animals from the study described in Chapter 6 (n=27, 12 male & 15 female due to early terminations in the study) and the data from the final behavioural assessment carried out on week 40 of the study with the animals in the age range 53-56 weeks and with weights ranging from 29-54g at this point.

B.2.1 Statistical Analysis

Statistical significance was analysed using SPSS Statistics 17.0 (2008) and bivariate correlation assessed by Pearson's r test for correlations. Statistical significance was considered when *P<0.05, **P<0.01 or ***P<0.001.

B.3 Results

B.3.1 Rotarod

The accelerating rotarod is a well characterised behavioural paradigm used to detect motor dysfunction in rodent models (Jones and Roberts 1968). Animals are placed on a steadily accelerating rotating rod and time to fall off recorded. The test had been carried out every 4 weeks for 40 weeks in this study. The results from the final testing period (Week 40) and the weights of the animals recorded in the same week were used to assess whether the weight of the animals has any effect on performance in the test.

A Pearson product-moment correlation coefficient was computed to assess the relationship between animal bodyweight and fall latency on the accelerating rotarod. There was a significant negative correlation between the two variables ($r = -0.616$, $P<0.001$), which can be seen in the scatter plot in Fig. B.1. These results suggest that there is a relatively strong correlation between increased body weight and decreased performance on the rotarod.

Looking at the data, it appears that the major decrease in performance occurs when the mice reach 40g in body weight; therefore it was decided to split the mice into two groups, those weighing more than 40g and those weighing less than 40g. The Pearson product-moment correlation coefficient was again used to assess the relationship between animal bodyweight and fall latency on the rotarod in the two separate groups and found no significant correlation in the animals which weighed 40g or below ($r=0.098$, $P=0.700$), but there was a significant negative correlation between weight and rotarod performance in the animals weighing 40g and above ($r= -0.821$, $P<0.01$) (Fig. B.2 A). This correlation is stronger than that seen in the whole group of animals and suggests that animals weighing over 40g struggle to stay on the accelerating rotarod.

To see how this correlation relates to performance, average fall latency of animals weighing 40g or below was compared with those weighing more than 40g. Animals weighing over 40g had a significantly lower fall latency than those weighing 40g or below ($P<0.01$, unpaired t-test) (Fig. B.2 B), supporting the proposal that when animals reach 40g body weight, performance in the accelerating rotarod test decreases as weight increases.

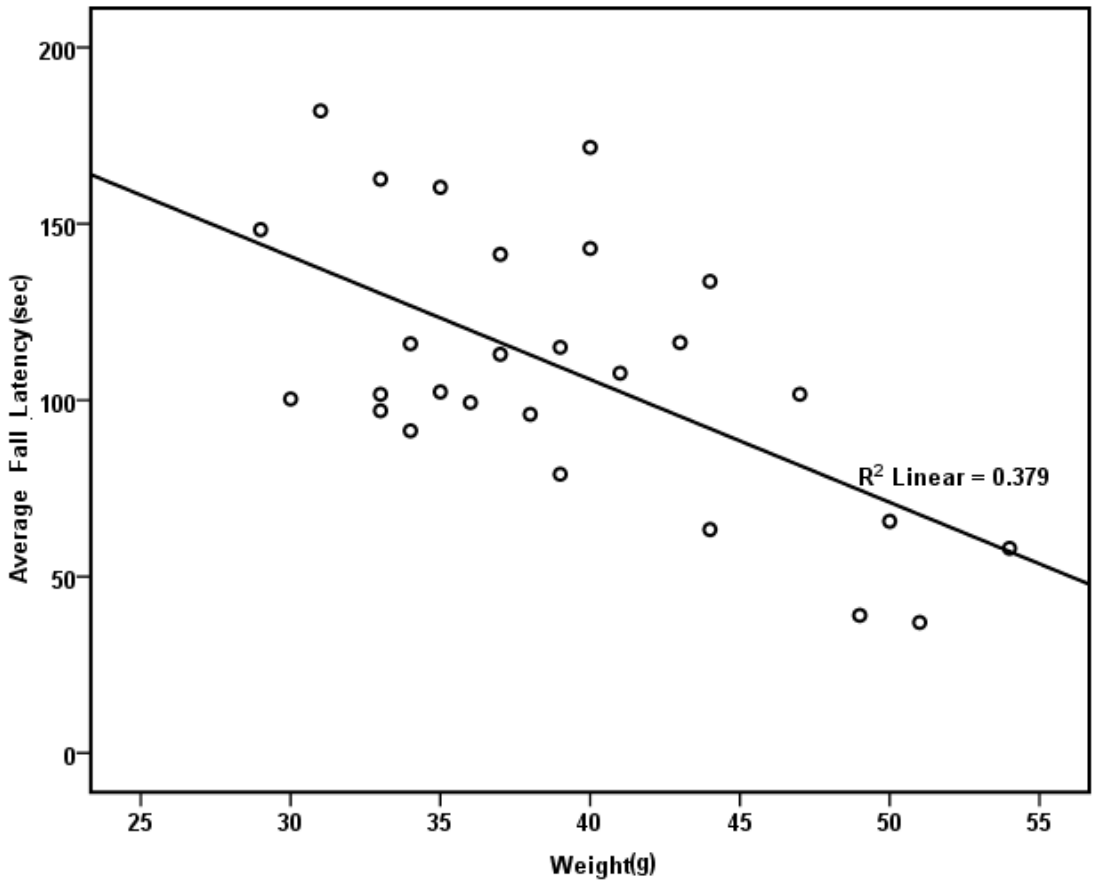

Fig. B.1 Effect of weight on performance in the Rotarod test in A30P α-synuclein overexpressing C57BL/6 mice Average fall latency (sec) in rotarod test and weight (g) of A30P α-synuclein overexpressing C57BL/6 mice in week 40 of testing. Data presented as mean fall latency from triplicate trials and weight measured in the same week (n=27) with linear fit line (R^2 = 0.379). Significant negative correlation between weight and average fall latency (r= -0.616, P<0.001) Pearson's r test for correlations.

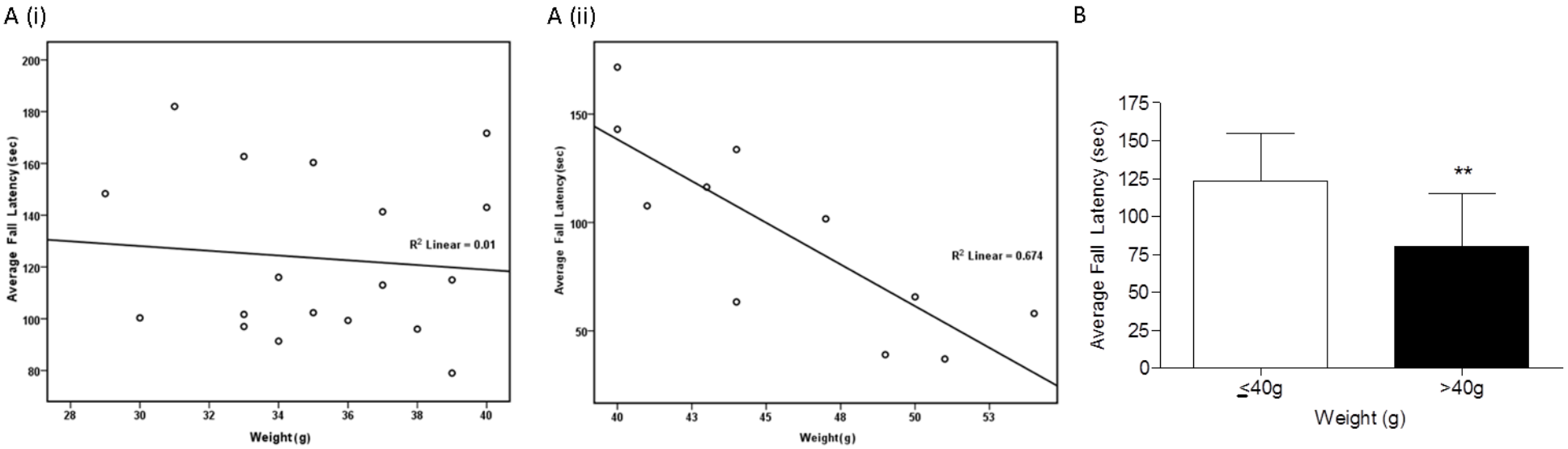

Fig. B.2 Difference in performance between A30P α-synuclein overexpressing C57BL/6 mice weighing above and below 40g in the Rotarod test (A) Average fall latency (sec) in rotarod test and weight (g) of (i) ≤40g or (ii) ≥40g A30P α-synuclein overexpressing C57BL/6 mice in week 40 of testing. Data presented as mean fall latency from triplicate trials and weight measured in the same week (n=27) with linear fit line (i, R^2 = 0.01, ii, R^2 = 0.674). (i) No significant correlation between weight and average fall latency (r= -0.098, P=0.700). (ii) Significant negative correlation between weight and average fall latency (r= -0.821, P<0.01) Pearson's r test for correlations. (B) Average fall latency in rotarod test of A30P α-synuclein overexpressing C57BL/6 mice weighing ≤40g (n=18) or >40g (n=9) in week 40 of testing. Data presented as mean ± SD of triplicate trials. **P<0.01 when compared to ≤40g, unpaired t-test

B.3.2 Pole Test

The pole test has been developed to test more fine motor control than the accelerating rotarod in mice (Matsuura, Kabuto et al. 1997). Animals are placed face up on a pole and the total time to complete trial, time to turn on the pole, the time to descend the pole and the number of falls per three trials recorded. As with the rotarod, the test had been carried out every 4 weeks for 40 weeks in this study and the results from the final testing period (Week 40) and the weights of the animals recorded in the same week were used to assess whether the weight of the animals has any effect on performance in the test.

A Pearson product-moment correlation coefficient was again used to assess the relationship between animal bodyweight and performance on the pole test. There was a significant positive correlation between the two variables when looking at total time to perform the test ($r=0.704$, $P<0.001$) (Fig. B.3), time to turn on the pole ($r=0.718$, $P<0.001$) (Fig. B.4), time to descend the pole ($r=0.684$, $P<0.001$) (Fig. B.5) and number of times an animal fell from the pole per three trials ($r=0.685$, $P<0.001$) (Fig. B.6). These results suggest that there is a relatively strong correlation between increased body weight and increased time taken to complete the pole test or number of falls while taking part in the test.

When the animals were separated into those weighing at most 40g and those weighing above 40g, there was no significant correlation between weight and performance in any of the measures looked at in the pole test (data not shown). However, when individual performance was assessed, animals weighing over 40g showed a reduction in ability to perform the test, with significantly increased total, turn and descent latency and number of falls seen (all $P<0.01$, unpaired t-test) (Fig. B.7). These results suggest that increased body weight does have an effect on performance in the pole test; however, this seems to occur across the range of weights observed in this study as opposed to only above a certain weight as seen in the rotarod test.

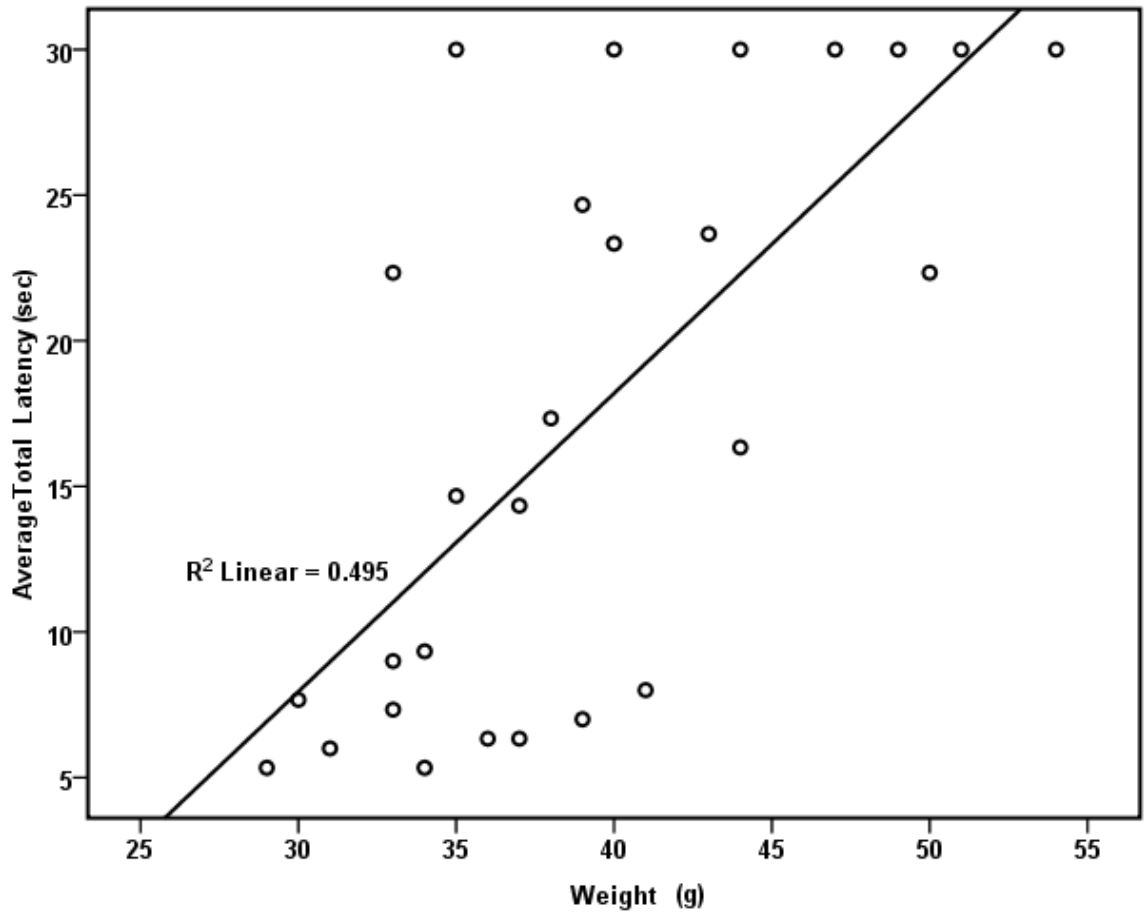

Fig. B.3 Effect of weight on total latency in the Pole test in A30P α-synuclein overexpressing C57BL/6 mice Average total latency (sec) on the pole test and weight (g) of A30P α-synuclein overexpressing C57BL/6 mice in week 40 of testing. Data presented as mean fall latency from triplicate trials and weight measured in the same week (n=27) with linear fit line (R^2 = 0.495). Significant positive correlation between weight and average total latency (r=0.704, P<0.001), Pearson's r test for correlations.

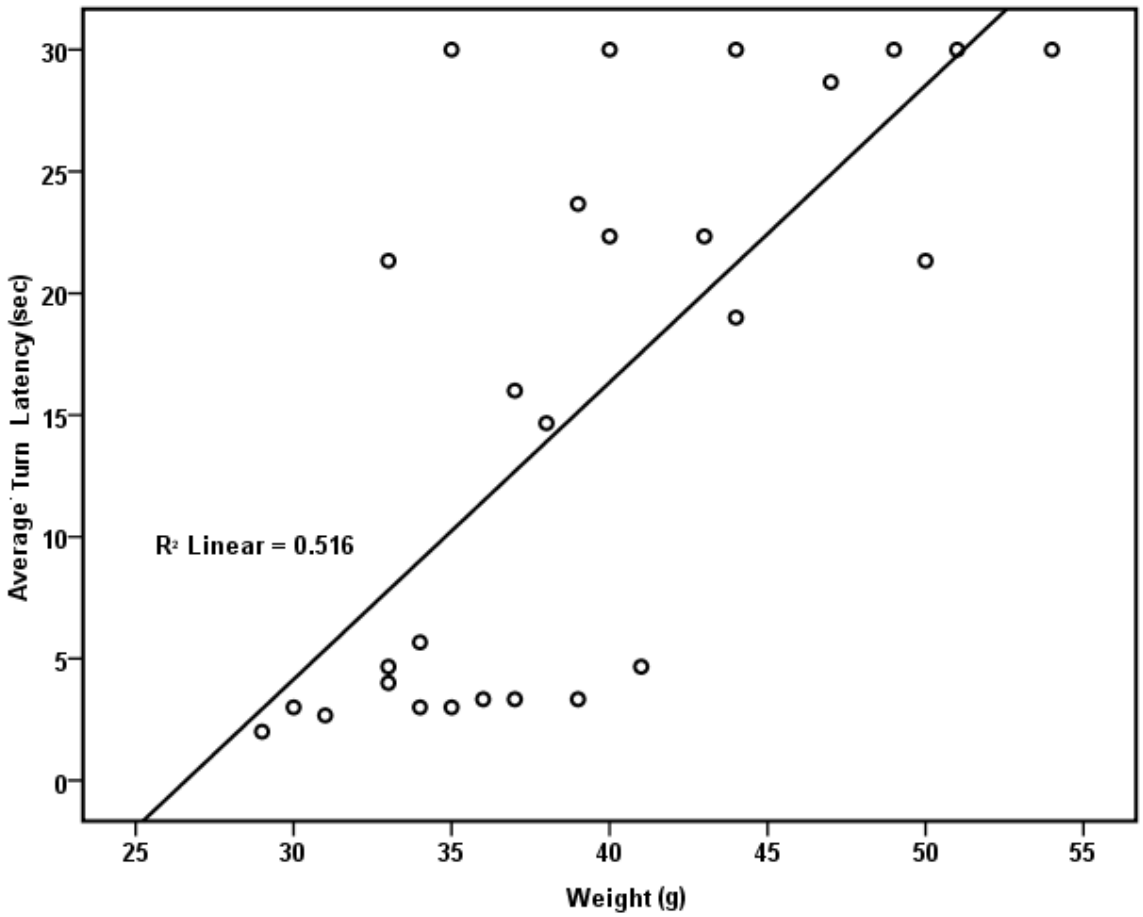

Fig. B.4 Effect of weight on turn latency in the Pole test in A30P α-synuclein overexpressing C57BL/6 mice Average turn latency (sec) on the pole test and weight (g) of A30P α-synuclein overexpressing C57BL/6 mice in week 40 of testing. Data presented as mean turn latency from triplicate trials and weight measured in the same week (n=27) with linear fit line (R^2 = 0.516). Significant positive correlation between weight and average turn latency (r=0.718, P<0.001), Pearson's r test for correlations.

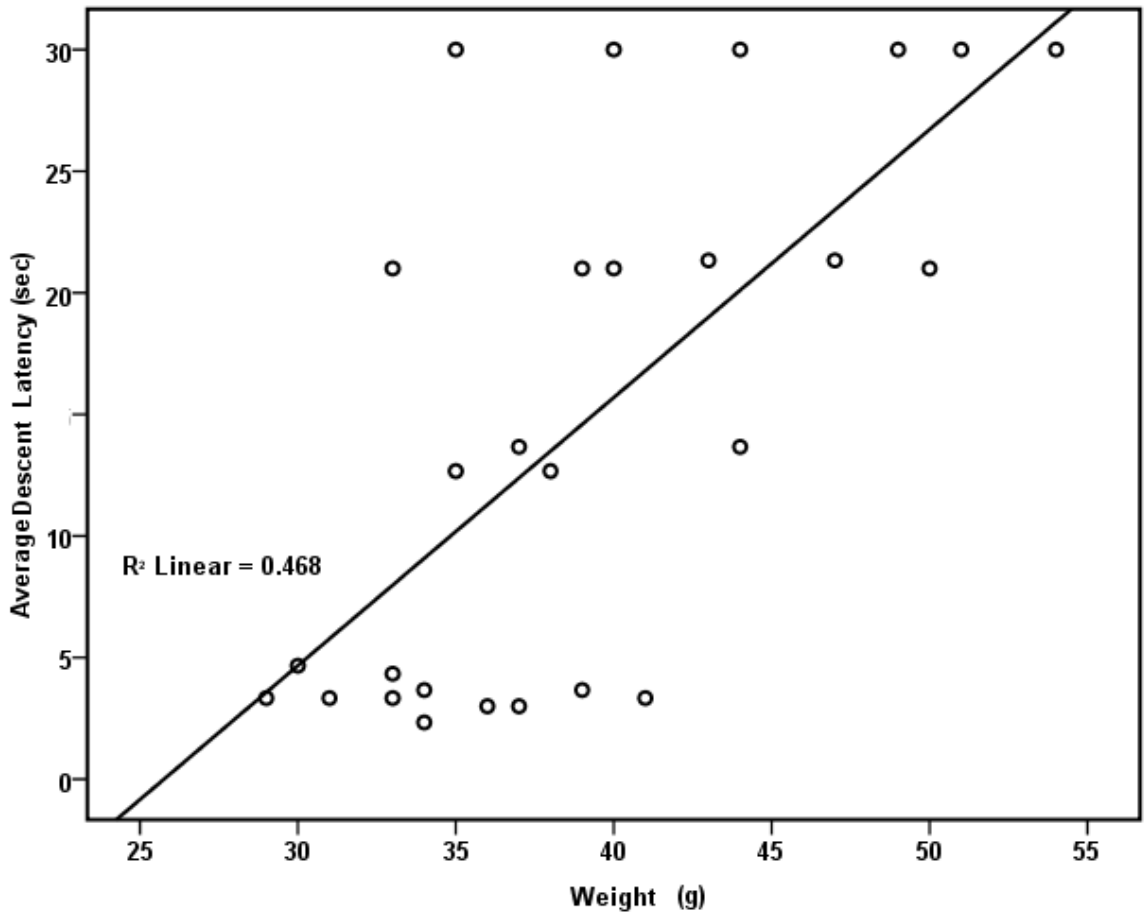

Fig. B.5 Effect of weight on descent latency in the Pole test in A30P α-synuclein overexpressing C57BL/6 mice Average descent latency (sec) on the pole test and weight (g) of A30P α-synuclein overexpressing C57BL/6 mice in week 40 of testing. Data presented as mean total latency from triplicate trials and weight measured in the same week (n=27) with linear fit line (R^2 = 0.468). Significant positive correlation between weight and average descent latency (r=0.684, P<0.001), Pearson's r test for correlations.

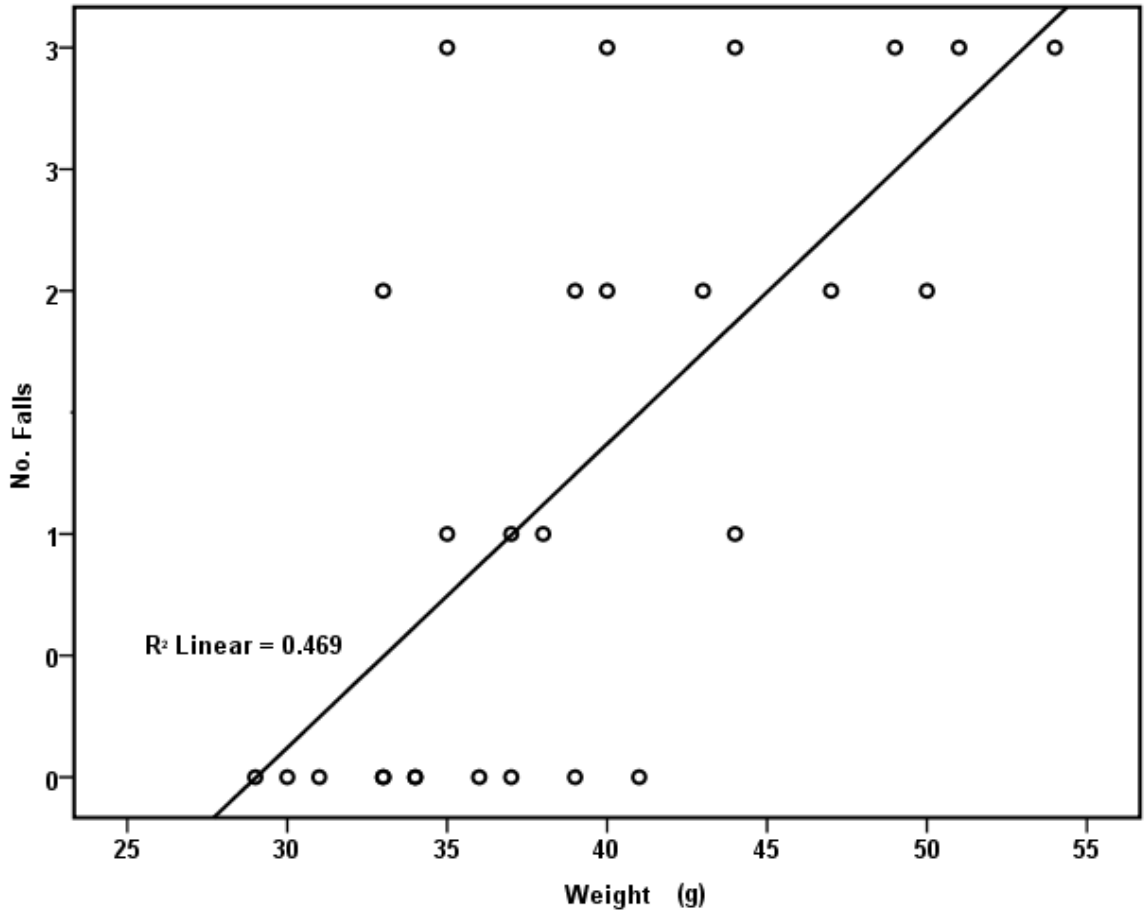

Fig. B.6 Effect of weight on number of falls in the Pole test in A30P α-synuclein overexpressing C57BL/6 mice Average number of falls on the pole test and weight (g) of A30P α-synuclein overexpressing C57BL/6 mice in week 40 of testing. Data presented as mean number of falls from triplicate trials and weight measured in the same week (n=27) with linear fit line (R^2 = 0.469). Significant positive correlation between weight and average number of falls (r=0.685, P<0.001), Pearson's r test for correlations

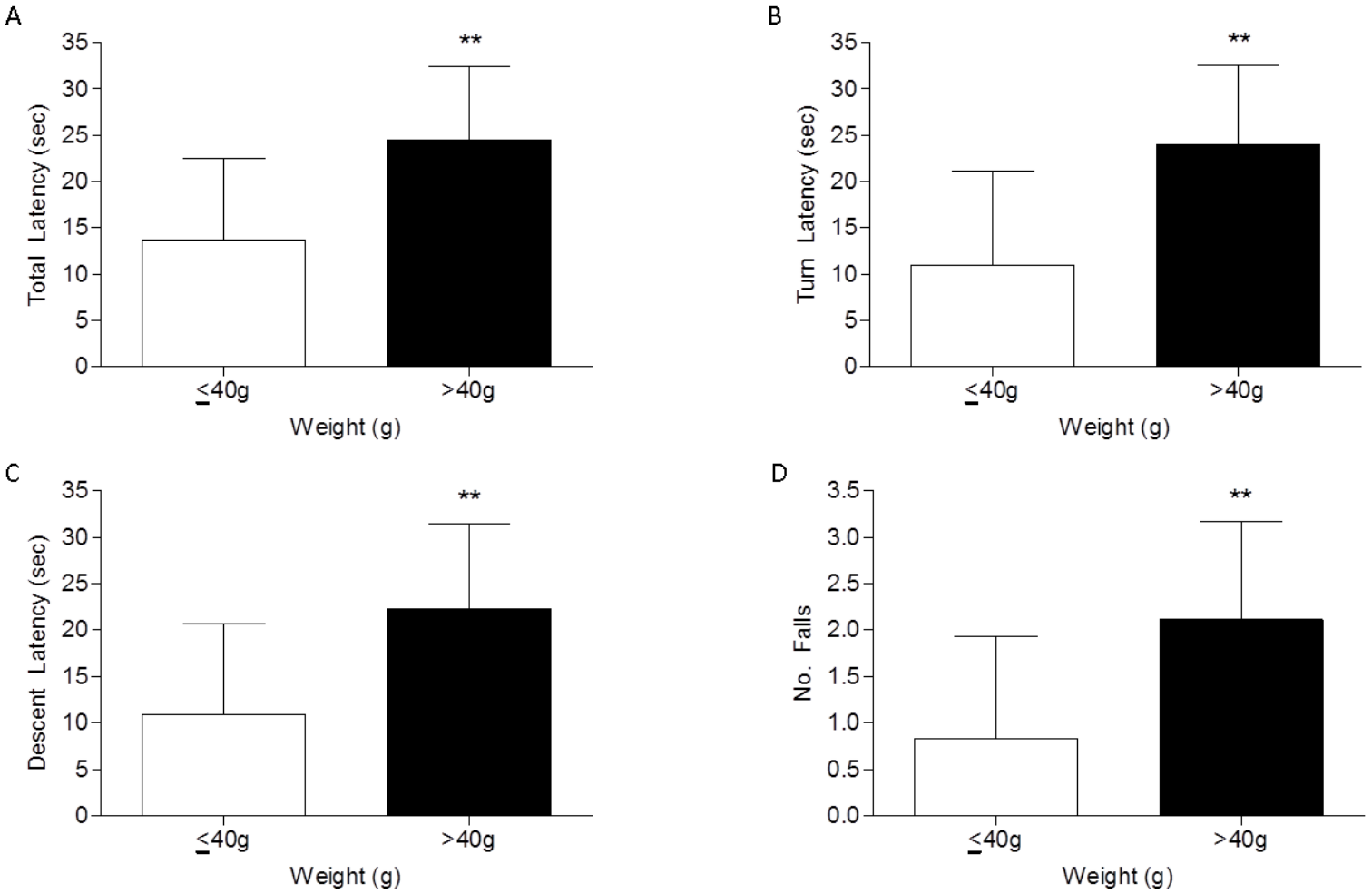

Fig. B.7 Difference in Performance between A30P α-synuclein overexpressing C57BL/6 mice weighing above and below 40g in the Pole test Average (A) total, (B) turn & (C) descent latency and (D) number of falls in pole test of A30P α-synuclein overexpressing C57BL/6 mice weighing ≤40g (n=18) or >40g (n=9) in week 40 of testing. Data presented as mean ± SD of triplicate trials. **P<0.01 when compared to ≤40g, unpaired t-test

B.4 Discussion

This study shows a relatively strong correlation between increased weight and decreased performance in motor function assessed by the accelerating rotarod. This effect seems to occur only when the mice weigh 40g and performance decreases relative to weight gain from this point as weight gets higher. Possible reasons for this could be due to an increase in abdomen size occurring due to the extra body weight obstructing the ability of the animal to stay on the rotating drum, more effort required to keep a heavier body stable and moving throughout the test, or the weight gain could be a sign of a general reduction in athletic condition of the animal reducing ability in the test rather than the extra weight itself reducing performance.

In the pole test, there is also a general correlation between increased weight and decreased performance in the test across all measures (turn time, descent time, total time and number of falls), suggesting that weight negatively affects pole test performance. This result was seen across the entire weight range of animals in the study (29-54g), unlike the results seen in the rotarod where the effect on performance only occurred at 40g and above. This may mean that the pole test is more susceptible to be effected by weight gain, possibly due to the fact that it is a more difficult task requiring more fine motor control that the rotarod, or may just be due to the fact that errors on the pole test are given a maximum score, punishing errors more strictly than in the rotarod and greatly increasing the variability in the test. These effects in the pole test may be due to the increased strength needed to support the weight of larger animals as they manoeuvre on the pole or, as in the rotarod, awkwardness in performing the test due to greater body/abdomen size.

A major limitation with these findings is that they were only examined in human A30P mutant α-synuclein overexpressing animals as these animals were the ones that experienced the large increases in weight that were shown to affect performance. Whether this weight gain correlates with decreased motor function due to the α-synuclein overexpression or some other effect of the mutation may be the cause of the results seen and the study would need repeating in a more controlled manner using wild-type mice to confirm.

Despite these limitations, these findings are useful to know with regards future studies investigating motor function, especially longitudinal studies or those where treatments or

mutations may increase body mass, as this study has shown that animals weight may affect results and would need to be controlled for.

Appendix C
Sample Statistical Analyses

C.1 One-way ANOVA (TaClo Toxicity Curve, Fig. 3.9)
Analysed using SPSS, output:

Treatment

Case Processing Summary

		Cases					
		Valid		Missing		Total	
	Treatment	N	Percent	N	Percent	N	Percent
Viability	0.2% DMSO	3	100.0%	0	.0%	3	100.0%
	1000uM TaClo	3	100.0%	0	.0%	3	100.0%
	500uM TaClo	3	100.0%	0	.0%	3	100.0%
	200uM TaClo	3	100.0%	0	.0%	3	100.0%
	100uM TaClo	3	100.0%	0	.0%	3	100.0%
	50uM TaClo	3	100.0%	0	.0%	3	100.0%
	20uM TaClo	3	100.0%	0	.0%	3	100.0%
	10uM TaClo	3	100.0%	0	.0%	3	100.0%
	5uM TaClo	3	100.0%	0	.0%	3	100.0%
	1uM TaClo	3	100.0%	0	.0%	3	100.0%

Tests of Normality[b]

		Kolmogorov-Smirnov[a]			Shapiro-Wilk		
	Treatment	Statistic	df	Sig.	Statistic	df	Sig.
Viability	1000uM TaClo	.297	3	.	.917	3	.443
	500uM TaClo	.269	3	.	.950	3	.567
	200uM TaClo	.218	3	.	.988	3	.787
	100uM TaClo	.359	3	.	.811	3	.140
	50uM TaClo	.362	3	.	.804	3	.125
	20uM TaClo	.278	3	.	.940	3	.528
	10uM TaClo	.324	3	.	.877	3	.317
	5uM TaClo	.190	3	.	.998	3	.904
	1uM TaClo	.287	3	.	.929	3	.486

a. Lilliefors Significance Correction

b. Viability is constant when Treatment = 0.2% DMSO. It has been omitted.

Oneway

[DataSet0] H:\PCK\SY5Y Toxicity Assays\TaClo\Final TaClo Data.sav

Test of Homogeneity of Variances

Viability

Levene Statistic	df1	df2	Sig.
2.368	9	20	.052

ANOVA

Viability

	Sum of Squares	df	Mean Square	F	Sig.
Between Groups	33366.024	9	3707.336	27.287	.000
Within Groups	2717.253	20	135.863		
Total	36083.278	29			

Post Hoc Tests

Multiple Comparisons

Viability

Dunnett t (2-sided)[a]

(I) Treatment	(J) Treatment	Mean Difference (I-J)	Std. Error	Sig.	95% Confidence Interval	
					Lower Bound	Upper Bound
1000uM TaClo	0.2% DMSO	-90.74912*	9.51710	.000	-118.7893	-62.7090
500uM TaClo	0.2% DMSO	-92.81401*	9.51710	.000	-120.8542	-64.7738
200uM TaClo	0.2% DMSO	-83.22956*	9.51710	.000	-111.2697	-55.1894
100uM TaClo	0.2% DMSO	-53.19971*	9.51710	.000	-81.2399	-25.1595
50uM TaClo	0.2% DMSO	-28.22190*	9.51710	.048	-56.2621	-.1817
20uM TaClo	0.2% DMSO	-22.56426	9.51710	.154	-50.6044	5.4759
10uM TaClo	0.2% DMSO	-20.02346	9.51710	.246	-48.0636	8.0167
5uM TaClo	0.2% DMSO	-18.25837	9.51710	.331	-46.2985	9.7818
1uM TaClo	0.2% DMSO	-11.01708	9.51710	.816	-39.0572	17.0231

a. Dunnett t-tests treat one group as a control, and compare all other groups against it.

*. The mean difference is significant at the 0.05 level.

C.2 Two-way ANOVA (TaClo & N-acetylcysteine, Fig 4.4B)
Analysed using SPSS, output:

Combined

Case Processing Summary

		Cases					
		Valid		Missing		Total	
	Combined	N	Percent	N	Percent	N	Percent
Viability	0.2% DMSO	3	100.0%	0	.0%	3	100.0%
	5mM NAC	3	100.0%	0	.0%	3	100.0%
	2.5mM NAC	3	100.0%	0	.0%	3	100.0%
	150uM TaClo	3	100.0%	0	.0%	3	100.0%
	150uM TaClo & 5mM NAC	3	100.0%	0	.0%	3	100.0%
	150uM TaClo & 2.5mM NAC	3	100.0%	0	.0%	3	100.0%
	100uM TaClo	3	100.0%	0	.0%	3	100.0%
	100uM TaClo & 5mM NAC	3	100.0%	0	.0%	3	100.0%
	100uM TaClo & 2.5mM NAC	3	100.0%	0	.0%	3	100.0%

Tests of Normality[b]

	Combined	Kolmogorov-Smirnov[a]			Shapiro-Wilk		
		Statistic	df	Sig.	Statistic	df	Sig.
Viability	5mM NAC	.345	3	.	.838	3	.210
	2.5mM NAC	.272	3	.	.946	3	.552
	150uM TaClo	.313	3	.	.894	3	.368
	150uM TaClo & 5mM NAC	.319	3	.	.885	3	.340
	150uM TaClo & 2.5mM NAC	.283	3	.	.935	3	.507
	100uM TaClo	.214	3	.	.990	3	.804
	100uM TaClo & 5mM NAC	.253	3	.	.965	3	.639
	100uM TaClo & 2.5mM NAC	.177	3	.	1.000	3	.967

a. Lilliefors Significance Correction

b. Viability is constant when Combined = 0.2% DMSO. It has been omitted.

Univariate Analysis of Variance

Between-Subjects Factors

		Value Label	N
Toxin	.00	0.2% DMSO	9
	1.00	150uuM TaClo	9
	2.00	100uM TaClo	9
Inhibitor	.00	0.2% DMSO	9
	1.00	5mM NAC	9
	2.00	2.5mM NAC	9

Tests of Between-Subjects Effects

Dependent Variable:Viability

Source	Type III Sum of Squares	df	Mean Square	F	Sig.
Corrected Model	15074.636[a]	8	1884.330	216.262	.000
Intercept	169806.995	1	169806.995	19488.483	.000
Toxin	7993.360	2	3996.680	458.693	.000
Inhibitor	4807.239	2	2403.619	275.860	.000
Toxin * Inhibitor	2274.038	4	568.509	65.247	.000
Error	156.838	18	8.713		
Total	185038.468	27			
Corrected Total	15231.474	26			

a. R Squared = .990 (Adjusted R Squared = .985)

Post Hoc Tests

Toxin

Multiple Comparisons

Viability

Dunnett t (2-sided)[a]

(I) Toxin	(J) Toxin	Mean Difference (I-J)	Std. Error	Sig.	95% Confidence Interval	
					Lower Bound	Upper Bound
150uuM TaClo	0.2% DMSO	-41.9791*	1.39150	.000	-45.3167	-38.6415
100uM TaClo	0.2% DMSO	-24.2367*	1.39150	.000	-27.5743	-20.8991

Based on observed means.

The error term is Mean Square(Error) = 8.713.

a. Dunnett t-tests treat one group as a control, and compare all other groups against it.

*. The mean difference is significant at the 0.05 level.

Homogeneous Subsets

Inhibitor

Multiple Comparisons

Viability

Dunnett t (2-sided)[a]

(I) Inhibitor	(J) Inhibitor	Mean Difference (I-J)	Std. Error	Sig.	95% Confidence Interval	
					Lower Bound	Upper Bound
5mM NAC	0.2% DMSO	31.2259*	1.39150	.000	27.8883	34.5635
2.5mM NAC	0.2% DMSO	23.9745*	1.39150	.000	20.6369	27.3121

Based on observed means.

The error term is Mean Square(Error) = 8.713.

a. Dunnett t-tests treat one group as a control, and compare all other groups against it.

*. The mean difference is significant at the 0.05 level.

Univariate Analysis of Variance

Between-Subjects Factors

		Value Label	N
Combined	.00	0.2% DMSO	3
	1.00	5mM NAC	3
	2.00	2.5mM NAC	3
	3.00	150uM TaClo	3
	4.00	150uM TaClo & 5mM NAC	3
	5.00	150uM TaClo & 2.5mM NAC	3
	6.00	100uM TaClo	3
	7.00	100uM TaClo & 5mM NAC	3
	8.00	100uM TaClo & 2.5mM NAC	3

Tests of Between-Subjects Effects

Dependent Variable:Viability

Source	Type III Sum of Squares	df	Mean Square	F	Sig.
Corrected Model	15074.636[a]	8	1884.330	216.262	.000
Intercept	169806.995	1	169806.995	19488.483	.000
Combined	15074.636	8	1884.330	216.262	.000
Error	156.838	18	8.713		
Total	185038.468	27			
Corrected Total	15231.474	26			

a. R Squared = .990 (Adjusted R Squared = .985)

Post Hoc Tests

Combined

Multiple Comparisons

Viability

Bonferroni

(I) Combined	(J) Combined	Mean Difference (I-J)	Std. Error	Sig.	95% Confidence Interval	
					Lower Bound	Upper Bound
0.2% DMSO	5mM NAC	-4.3034	2.41014	1.000	-13.3999	4.7930
	2.5mM NAC	.1752	2.41014	1.000	-8.9212	9.2717
	150uM TaClo	73.0382*	2.41014	.000	63.9418	82.1347
	150uM TaClo & 5mM NAC	18.5966*	2.41014	.000	9.5002	27.6931
	150uM TaClo & 2.5mM NAC	30.1742*	2.41014	.000	21.0778	39.2707
	100uM TaClo	44.2497*	2.41014	.000	35.1532	53.3461
	100uM TaClo & 5mM NAC	9.3171*	2.41014	.041	.2207	18.4136
	100uM TaClo & 2.5mM NAC	15.0150*	2.41014	.000	5.9186	24.1115
5mM NAC	0.2% DMSO	4.3034	2.41014	1.000	-4.7930	13.3999
	2.5mM NAC	4.4787	2.41014	1.000	-4.6178	13.5751
	150uM TaClo	77.3417*	2.41014	.000	68.2452	86.4381
	150uM TaClo & 5mM NAC	22.9001*	2.41014	.000	13.8036	31.9965

	150uM TaClo & 2.5mM NAC	34.4776*	2.41014	.000	25.3812	43.5741
	100uM TaClo	48.5531*	2.41014	.000	39.4567	57.6496
	100uM TaClo & 5mM NAC	13.6205*	2.41014	.001	4.5241	22.7170
	100uM TaClo & 2.5mM NAC	19.3185*	2.41014	.000	10.2220	28.4149
2.5mM NAC	0.2% DMSO	-.1752	2.41014	1.000	-9.2717	8.9212
	5mM NAC	-4.4787	2.41014	1.000	-13.5751	4.6178
	150uM TaClo	72.8630*	2.41014	.000	63.7665	81.9594
	150uM TaClo & 5mM NAC	18.4214*	2.41014	.000	9.3249	27.5178
	150uM TaClo & 2.5mM NAC	29.9990*	2.41014	.000	20.9025	39.0954
	100uM TaClo	44.0744*	2.41014	.000	34.9780	53.1709
	100uM TaClo & 5mM NAC	9.1419*	2.41014	.048	.0454	18.2383
	100uM TaClo & 2.5mM NAC	14.8398*	2.41014	.000	5.7433	23.9362
150uM TaClo	0.2% DMSO	-73.0382*	2.41014	.000	-82.1347	-63.9418
	5mM NAC	-77.3417*	2.41014	.000	-86.4381	-68.2452
	2.5mM NAC	-72.8630*	2.41014	.000	-81.9594	-63.7665
	150uM TaClo & 5mM NAC	-54.4416*	2.41014	.000	-63.5381	-45.3452
	150uM TaClo & 2.5mM NAC	-42.8640*	2.41014	.000	-51.9605	-33.7676
	100uM TaClo	-28.7886*	2.41014	.000	-37.8850	-19.6921
	100uM TaClo & 5mM NAC	-63.7211*	2.41014	.000	-72.8176	-54.6247
	100uM TaClo & 2.5mM NAC	-58.0232*	2.41014	.000	-67.1197	-48.9268

150uM TaClo & 5mM NAC	0.2% DMSO	-18.5966*	2.41014	.000	-27.6931	-9.5002
	5mM NAC	-22.9001*	2.41014	.000	-31.9965	-13.8036
	2.5mM NAC	-18.4214*	2.41014	.000	-27.5178	-9.3249
	150uM TaClo	54.4416*	2.41014	.000	45.3452	63.5381
	150uM TaClo & 2.5mM NAC	11.5776*	2.41014	.005	2.4811	20.6740
	100uM TaClo	25.6530*	2.41014	.000	16.5566	34.7495
	100uM TaClo & 5mM NAC	-9.2795*	2.41014	.042	-18.3760	-.1831
	100uM TaClo & 2.5mM NAC	-3.5816	2.41014	1.000	-12.6780	5.5149
150uM TaClo & 2.5mM NAC	0.2% DMSO	-30.1742*	2.41014	.000	-39.2707	-21.0778
	5mM NAC	-34.4776*	2.41014	.000	-43.5741	-25.3812
	2.5mM NAC	-29.9990*	2.41014	.000	-39.0954	-20.9025
	150uM TaClo	42.8640*	2.41014	.000	33.7676	51.9605
	150uM TaClo & 5mM NAC	-11.5776*	2.41014	.005	-20.6740	-2.4811
	100uM TaClo	14.0755*	2.41014	.001	4.9790	23.1719
	100uM TaClo & 5mM NAC	-20.8571*	2.41014	.000	-29.9535	-11.7606
	100uM TaClo & 2.5mM NAC	-15.1592*	2.41014	.000	-24.2556	-6.0627
100uM TaClo	0.2% DMSO	-44.2497*	2.41014	.000	-53.3461	-35.1532
	5mM NAC	-48.5531*	2.41014	.000	-57.6496	-39.4567
	2.5mM NAC	-44.0744*	2.41014	.000	-53.1709	-34.9780
	150uM TaClo	28.7886*	2.41014	.000	19.6921	37.8850

	150uM TaClo & 5mM NAC	-25.6530*	2.41014	.000	-34.7495	-16.5566
	150uM TaClo & 2.5mM NAC	-14.0755*	2.41014	.001	-23.1719	-4.9790
	100uM TaClo & 5mM NAC	-34.9326*	2.41014	.000	-44.0290	-25.8361
	100uM TaClo & 2.5mM NAC	-29.2346*	2.41014	.000	-38.3311	-20.1382
100uM TaClo & 5mM NAC	0.2% DMSO	-9.3171*	2.41014	.041	-18.4136	-.2207
	5mM NAC	-13.6205*	2.41014	.001	-22.7170	-4.5241
	2.5mM NAC	-9.1419*	2.41014	.048	-18.2383	-.0454
	150uM TaClo	63.7211*	2.41014	.000	54.6247	72.8176
	150uM TaClo & 5mM NAC	9.2795*	2.41014	.042	.1831	18.3760
	150uM TaClo & 2.5mM NAC	20.8571*	2.41014	.000	11.7606	29.9535
	100uM TaClo	34.9326*	2.41014	.000	25.8361	44.0290
	100uM TaClo & 2.5mM NAC	5.6979	2.41014	1.000	-3.3985	14.7944
100uM TaClo & 2.5mM NAC	0.2% DMSO	-15.0150*	2.41014	.000	-24.1115	-5.9186
	5mM NAC	-19.3185*	2.41014	.000	-28.4149	-10.2220
	2.5mM NAC	-14.8398*	2.41014	.000	-23.9362	-5.7433
	150uM TaClo	58.0232*	2.41014	.000	48.9268	67.1197
	150uM TaClo & 5mM NAC	3.5816	2.41014	1.000	-5.5149	12.6780
	150uM TaClo & 2.5mM NAC	15.1592*	2.41014	.000	6.0627	24.2556
	100uM TaClo	29.2346*	2.41014	.000	20.1382	38.3311
	100uM TaClo & 5mM NAC	-5.6979	2.41014	1.000	-14.7944	3.3985

Based on observed means.

The error term is Mean Square(Error) = 8.713.

*. The mean difference is significant at the 0.05 level.

C.3 Two-way Repeated Measures ANOVA (A30P Pole Test total time, Fig 6.4 A)
Analysed using GraphPad Prism, output:

Table Analyzed	Data 1			
Two-way RM ANOVA	Matching by cols			
Source of Variation	% of total variation	P value		
Interaction	2.09	0.9629		
Time	17.32	P<0.0001		
Treatment	3.26	0.2601		
Subjects (matching)	27.4714	P<0.0001		
Source of Variation	P value summary	Significant?		
Interaction	ns	No		
Time	***	Yes		
Treatment	ns	No		
Subjects (matching)	***	Yes		
Source of Variation	Df	Sum-of-squares	Mean square	F
Interaction	20	397.3	19.87	0.5058
Time	10	3296	329.6	8.393
Treatment	2	620.8	310.4	1.425
Subjects (matching)	24	5228	217.8	5.546
Residual	240	9425	39.27	
Number of missing values	0			

Bonferroni posttests				

Vehicle (10 ml/kg Olive Oil) vs. TCE (1000 mg/kg)				
Treatment	Vehicle (10 ml/kg Olive Oil)	TCE (1000 mg/kg)	Difference	95% CI of diff.
0	7.889	8.792	0.9028	-10.25 to 12.06
4	8.593	14.13	5.532	-5.625 to 16.69
8	11.78	11.33	-0.4444	-11.60 to 10.71
12	9.148	12.17	3.019	-8.139 to 14.18
16	10.37	12.5	2.13	-9.028 to 13.29
20	9.259	11	1.741	-9.417 to 12.90
24	9.704	13.29	3.588	-7.570 to 14.75
28	13.26	15.67	2.407	-8.750 to 13.56
32	15.85	19.46	3.606	-7.551 to 14.76
36	17.19	19.83	2.648	-8.509 to 13.81
40	13.7	18.75	5.046	-6.111 to 16.20

Treatment	Difference	t	P value	Summary
0	0.9028	0.2494	P > 0.05	ns
4	5.532	1.528	P > 0.05	ns
8	-0.4444	0.1228	P > 0.05	ns
12	3.019	0.8338	P > 0.05	ns
16	2.13	0.5883	P > 0.05	ns
20	1.741	0.4809	P > 0.05	ns
24	3.588	0.9911	P > 0.05	ns
28	2.407	0.665	P > 0.05	ns
32	3.606	0.9962	P > 0.05	ns
36	2.648	0.7315	P > 0.05	ns
40	5.046	1.394	P > 0.05	ns

Vehicle (10 ml/kg Olive Oil) vs.				

TaClo (2 mg/kg)				
Treatment	Vehicle (10 ml/kg Olive Oil)	TaClo (2 mg/kg)	Difference	95% CI of diff.
0	7.889	9.2	1.311	-9.239 to 11.86
4	8.593	10.33	1.741	-8.810 to 12.29
8	11.78	10.73	-1.044	-11.59 to 9.506
12	9.148	10.73	1.585	-8.965 to 12.14
16	10.37	14.2	3.83	-6.721 to 14.38
20	9.259	14.2	4.941	-5.610 to 15.49
24	9.704	17	7.296	-3.254 to 17.85
28	13.26	16.17	2.907	-7.643 to 13.46
32	15.85	18.9	3.048	-7.502 to 13.60
36	17.19	21.87	4.681	-5.869 to 15.23
40	13.7	19.33	5.63	-4.921 to 16.18
Treatment	Difference	t	P value	Summary
0	1.311	0.383	P > 0.05	ns
4	1.741	0.5085	P > 0.05	ns
8	-1.044	0.3051	P > 0.05	ns
12	1.585	0.4631	P > 0.05	ns
16	3.83	1.119	P > 0.05	ns
20	4.941	1.443	P > 0.05	ns
24	7.296	2.131	P > 0.05	ns
28	2.907	0.8494	P > 0.05	ns
32	3.048	0.8905	P > 0.05	ns
36	4.681	1.368	P > 0.05	ns
40	5.63	1.645	P > 0.05	ns

References

References

Abbott, R. D., H. Petrovitch, et al. (2001). "Frequency of bowel movements and the future risk of Parkinson's disease." Neurology **57**(3): 456-462.

Abdelkarim, G. E., K. Gertz, et al. (2001). "Protective effects of PJ34, a novel, potent inhibitor of poly(ADP-ribose) polymerase (PARP) in in vitro and in vivo models of stroke." International journal of molecular medicine **7**(3): 255-260.

Abe, K., K. Taguchi, et al. (2001). "Biochemical and pathological study of endogenous 1-benzyl-1,2,3,4-tetrahydroisoquinoline-induced parkinsonism in the mouse." Brain Research **907**(1–2): 134-138.

Abeliovich, A., Y. Schmitz, et al. (2000). "Mice lacking α-synuclein display functional deficits in the nigrostriatal dopamine system." Neuron **25**(1): 239-252.

Acín-Pérez, R., M. P. Bayona-Bafaluy, et al. (2004). "Respiratory complex III is required to maintain complex I in mammalian mitochondria." Molecular Cell **13**(6): 805-815.

Adler, C. H., K. D. Sethi, et al. (1997). "Ropinirole for the treatment of early Parkinson's disease." Neurology **49**(2): 393-399.

Agid, Y., F. Javoy, et al. (1973). "Hyperactivity of remaining dopaminergic neurones after partial destruction of the nigro striatal dopaminergic system in the rat." NATURE NEW BIOL. **245**(144): 150-151.

Akundi, R. S., M. Hüll, et al. (2003). 1-Trichloromethyl-1,2,3,4-tetrahydro-β-carboline (TaClo) Induces Apoptosis in Human Neuroblastoma Cell Lines. **1010:** 304-306.

Akundi, R. S., A. Macho, et al. (2004). "1-Trichloromethyl-1,2,3,4-tetrahydro-β-carboline-induced apoptosis in the human neuroblastoma cell line SK-N-SH." Journal of Neurochemistry **91**(2): 263-273.

Al-Chalabi, A., A. Dürr, et al. (2009). "Genetic variants of the α-synuclein gene SNCA are associated with multiple system atrophy." PLoS ONE **4**(9).

Alam, Z. I., A. Jenner, et al. (1997). "Oxidative DNA damage in the Parkinsonian brain: An apparent selective increase in 8-hydroxyguanine levels in substantia nigra." Journal of Neurochemistry **69**(3): 1196-1203.

Alberts, B., A. Johnson, et al. (1994). Molecular Biology of the Cell

5: 113a Abstract #653.

Albin, R. L. and J. T. Greenamyre (1992). "Alternative excitotoxic hypotheses." Neurology **42**(4 II): 733-738.

Albin, R. L., A. B. Young, et al. (1989). "The functional anatomy of basal ganglia disorders." Trends in Neurosciences **12**(10): 366-375.

Alegre-Abarrategui, J., H. Christian, et al. (2009). "LRRK2 regulates autophagic activity and localizes to specific membrane microdomains in a novel human genomic reporter cellular model." Human Molecular Genetics **18**(21): 4022-4034.

Alexander, G. E., M. R. Delong, et al. (1986). "Parallel Organization of Functionally Segregated Circuits Linking Basal Ganglia and Cortex." Annual Review of Neuroscience **9**: 357-381.

Alnemri, E. S., D. J. Livingston, et al. (1996). "Human ICE/CED-3 Protease Nomenclature." Cell **87**(2): 171.

Altmann, L., P. Welge, et al. (2002). "Chronic exposure to trichloroethylene affects neuronal plasticity in rat hippocampal slices." Environmental Toxicology and Pharmacology **12**(3): 157-167.

Alvarez, V., A. I. Corao, et al. (2008). "Mitochondrial transcription factor A (TFAM) gene variation in Parkinson's disease." Neuroscience Letters **432**(1): 79-82.

Amende, I., A. Kale, et al. (2005). "Gait dynamics in mouse models of Parkinson's disease and Huntington's disease." Journal of NeuroEngineering and Rehabilitation **2**.

Amijee, H., J. Madine, et al. (2009). "Inhibitors of protein aggregation and toxicity." Biochemical Society Transactions **37**(4): 692-696.

Anglade, P. (1997). "Apoptosis and autophagy in nigral neurons of patients with Parkinson's disease." Histology and Histopathology **12**(1): 25-31.

Anichtchik, O. V., J. Kaslin, et al. (2004). "Neurochemical and behavioural changes in zebrafish Danio rerio after systemic administration of 6-hydroxydopamine and 1-methyl-4-phenyl-1,2,3,6-tetrahydropyridine." Journal of Neurochemistry **88**(2): 443-453.

Antzoulatos, E., M. W. Jakowec, et al. (2010). "Sex differences in motor behavior in the MPTP mouse model of Parkinson's disease." Pharmacology Biochemistry and Behavior **95**(4): 466-472.

Araki, T., T. Mikami, et al. (2000). "Biochemical and immunohistological changes in the brain of 1-methyl-4-phenyl-1,2,3,6-tetrahydropyridine (MPTP)-treated mouse." European Journal of Pharmaceutical Sciences **12**(3): 231-238.

Armstrong, D. A. and J. D. Buchanan (1978). "Reactions of O-.2, H2O2 and other oxidants with sulfhydryl enzymes." Photochemistry and Photobiology **28**(4-5): 743-755.

Armstrong, R. A., P. L. Lantos, et al. (2007). "Progressive supranuclear palsy (PSP): a quantitative study of the pathological changes in cortical and subcortical regions of eight cases." Journal of Neural Transmission **114**(12): 1569-1577.

Aslan, R., M. Tütüncü, et al. (2000). "Acute Phase Effect of Trichloroethylene Ingestion on Some Biological Markers in Dogs." Turkish Journal of Veterinary and Animal Sciences **24**(2): 109-112.

Augustine, J. J., K. A. Bodziak, et al. (2007). "Use of sirolimus in solid organ transplantation." Drugs **67**(3): 369-391.

Bader, M., S. Benjamin, et al. (2011). "A conserved F box regulatory complex controls proteasome activity in Drosophila." Cell **145**(3): 371-382.

Bader, V., X. R. Zhu, et al. (2005). "Expression of DJ-1 in the adult mouse CNS." Brain Research **1041**(1): 102-111.

Baik, J. H., R. Picetti, et al. (1995). "Parkinsonian-like locomotor impairment in mice lacking dopamine D2 receptors." Nature **377**(6548): 424-428.

Baker, M., I. Litvan, et al. (1999). "Association of an extended haplotype in the tau gene with progressive supranuclear palsy." Human Molecular Genetics **8**(4): 711-715.

Balkaya, M., J. Kröber, et al. (2013). "Characterization of long-term functional outcome in a murine model of mild brain ischemia." Journal of Neuroscience Methods **213**(2): 179-187.

Banerjee, R., M. F. Beal, et al. (2010). "Autophagy in neurodegenerative disorders: Pathogenic roles and therapeutic implications." Trends in Neurosciences **33**(12): 541-549.

Baquet, Z. C., D. Williams, et al. (2009). "A comparison of model-based (2D) and design-based (3D) stereological methods for estimating cell number in the substantia nigra pars compacta (SNpc) of the C57BL/6J mouse." Neuroscience **161**(4): 1082-1090.

Barclay, C. L. and A. E. Lang (1997). "Dystonia in progressive supranuclear palsy." Journal of Neurology Neurosurgery and Psychiatry **62**(4): 352-356.

Bargmann, C. I. (1998). "Neurobiology of the Caenorhabditis elegans genome." Science **282**(5396): 2028-2033.

Barnes, C. A. (1979). "Memory deficits associated with senescence: A neurophysiological and behavioral study in the rat." Journal of Comparative and Physiological Psychology **93**(1): 74-104.

Barret, L., J. Faure, et al. (1984). "Trichloroethylene occupational exposure: elements for better prevention." International Archives of Occupational and Environmental Health **53**(4): 283-289.

Bartels, A. L. and K. L. Leenders (2007). "Neuroinflammation in the pathophysiology of Parkinson's disease: Evidence from animal models to human in vivo studies with [11C]-PK11195 PET." Movement Disorders **22**(13): 1852-1856.

Bashkatova, V., M. Alam, et al. (2004). "Chronic administration of rotenone increases levels of nitric oxide and lipid peroxidation products in rat brain." Experimental Neurology **186**(2): 235-241.

Bass, D. A., J. W. Parce, et al. (1983). "Flow cytometric studies of oxidative product formation by neutrophils: A graded response to membrane stimulation." Journal of Immunology **130**(4): 1910-1917.

Beal, M. F. (2001). "Experimental models of Parkinson's disease." Nature Reviews Neuroscience **2**(5): 325-332.

Beal, M. F., R. T. Matthews, et al. (1998). "Coenzyme Q10 attenuates the 1-methyl-4-phenyl-1,2,3,6- tetrahydropyridine (MPTP) induced loss of striatal dopamine and dopaminergic axons in aged mice." Brain Research **783**(1): 109-114.

Bedford, L., D. Hay, et al. (2008). "Depletion of 26S proteasomes in mouse brain neurons causes neurodegeneration and lewy-like inclusions resembling human pale bodies." Journal of Neuroscience **28**(33): 8189-8198.

Belin, A. C., B. F. Björk, et al. (2007). "Association study of two genetic variants in mitochondrial transcription factor A (TFAM) in Alzheimer's and Parkinson's disease." Neuroscience Letters **420**(3): 257-262.

Belloc, F., P. Dumain, et al. (1994). "A flow cytometric method using Hoechst 33342 and propidium iodide for simultaneous cell cycle analysis and apoptosis determination in unfixed cells." Cytometry **17**(1): 59-65.

Belluzzi, E., M. Bisaglia, et al. (2012). "Human SOD2 modification by dopamine quinones affects enzymatic activity by promoting its aggregation: Possible implications for Parkinson's disease." PLoS ONE **7**(6).

Bender, A., K. J. Krishnan, et al. (2006). "High levels of mitochondrial DNA deletions in substantia nigra neurons in aging and Parkinson disease." Nature Genetics **38**(5): 515-517.

Benson, R. (2000). Concise International Chemical Assessment Document 25 - Chloral Hydrate. W. H. Organisation.

Berman, S. B. and T. G. Hastings (1999). "Dopamine oxidation alters mitochondrial respiration and induces permeability transition in brain mitochondria: Implications for Parkinson's disease." Journal of Neurochemistry **73**(3): 1127-1137.

Bernheimer, H., W. Birkmayer, et al. (1973). "Brain dopamine and the syndromes of Parkinson and Huntington Clinical, morphological and neurochemical correlations." Journal of the Neurological Sciences **20**(4): 415-455.

Bernheimer, H., W. Birkmayer, et al. (1973). "Brain dopamine and the syndromes of Parkinson and Huntington. Clinical, morphological and neurochemical correlations." Journal of the Neurological Sciences **20**(4): 415-455.

Betarbet, R., R. M. Canet-Aviles, et al. (2006). "Intersecting pathways to neurodegeneration in Parkinson's disease: Effects of the pesticide rotenone on DJ-1, α-synuclein, and the ubiquitin-proteasome system." Neurobiology of Disease **22**(2): 404-420.

Betarbet, R., T. B. Sherer, et al. (2000). "Chronic systemic pesticide exposure reproduces features of Parkinson's disease." Nature Neuroscience **3**(12): 1301-1306.

Betarbet, R., T. B. Sherer, et al. (2002). "Animal models of Parkinson's disease." BioEssays **24**(4): 308-318.

Beyer, R. E. (1992). "An analysis of the role of coenzyme Q in free radical generation and as an antioxidant." Biochemistry and cell biology = Biochimie et biologie cellulaire **70**(6): 390-403.

Bezard, E., I. Gerlach, et al. (2006). "5-HT1A receptor agonist-mediated protection from MPTP toxicity in mouse and macaque models of Parkinson's disease." Neurobiology of Disease **23**(1): 77-86.

Bezard, E., C. E. Gross, et al. (1999). "Absence of MPTP-induced neuronal death in mice lacking the dopamine transporter." Experimental Neurology **155**(2): 268-273.

Bhat, H. K., M. F. Kanz, et al. (1991). "Ninety day toxicity study of chloroacetic acids in rats." Fundamental and Applied Toxicology **17**(2): 240-253.

Bhidayasiri, R., D. E. Riley, et al. (2001). "Pathophysiology of slow vertical saccades in progressive supranuclear palsy." Neurology **57**(11): 2070-2077.

Bhushan Shrivastav, B., T. Narahashi, et al. (1976). "Mode of action of trichloroethylene on squid axon membranes." Journal of Pharmacology and Experimental Therapeutics **199**(1): 179-188.

Bianchi, M., T. Battistin, et al. (1991). "2,6-Diisopropylphenol, a general anesthetic, inhibits glutamate action on rat synaptosomes." Neurochemical Research **16**(4): 443-446.

Bijsterbosch, M. K., A. M. Duursma, et al. (1981). "The plasma volume of the Wistar rat in relation to the body weight." Experientia **37**(4): 381-382.

Bindoff, L. A., M. A. Birch-Machin, et al. (1991). "Respiratory chain abnormalities in skeletal muscle from patients with Parkinson's disease." Journal of the Neurological Sciences **104**(2): 203-208.

Birdi, S., A. H. Rajput, et al. (2002). "Progressive supranuclear palsy diagnosis and confounding features: Report on 16 autopsied cases." Movement Disorders **17**(6): 1255-1264.

Biskup, S., D. J. Moore, et al. (2006). "Localization of LRRK2 to membranous and vesicular structures in mammalian brain." Annals of Neurology **60**(5): 557-569.

Blandini, F., R. H. P. Porter, et al. (1996). "Glutamate and Parkinson's disease." Molecular Neurobiology **12**(1): 73-94.

Blommaart, E. F. C., J. J. F. P. Luiken, et al. (1995). "Phosphorylation of ribosomal protein S6 is inhibitory for autophagy in isolated rat hepatocytes." Journal of Biological Chemistry **270**(5): 2320-2326.

Blossom, S. J., J. C. Doss, et al. (2008). "Developmental exposure to trichloroethylene promotes CD4+ T cell differentiation and hyperactivity in association with oxidative stress and neurobehavioral deficits in MRL+/+ mice." Toxicology and Applied Pharmacology **231**(3): 344-353.

Blossom, S. J., S. Melnyk, et al. (2012). "Postnatal exposure to trichloroethylene alters glutathione redox homeostasis, methylation potential, and neurotrophin expression in the mouse hippocampus." NeuroToxicology **33**(6): 1518-1527.

Bohgaki, T., J. Mozo, et al. (2011). "Caspase-8 inactivation in T cells increases necroptosis and suppresses autoimmunity in Bim -/- mice." Journal of Cell Biology **195**(2): 277-291.

Boix, J., N. Llecha, et al. (1997). "Characterization of the cell death process induced by staurosporine in human neuroblastoma cell lines." Neuropharmacology **36**(6): 811-821.

Boller, F., T. Mizutani, et al. (1980). "Parkinson disease, dementia, and Alzheimer disease: Clinicopathological correlations." Annals of Neurology **7**(4): 329-335.

Bonapace, L., B. C. Bornhauser, et al. (2010). "Induction of autophagy-dependent necroptosis is required for childhood acute lymphoblastic leukemia cells to overcome glucocorticoid resistance." Journal of Clinical Investigation **120**(4): 1310-1323.

Bond, G. R. (1996). "Hepatitis, rash and eosinophilia following trichloroethylene exposure: A case report and speculation on mechanistic similarity to halothane induced hepatitis." Journal of Toxicology - Clinical Toxicology **34**(4): 461-466.

Bonifati, V., P. Rizzu, et al. (2003). "Mutations in the DJ-1 gene associated with autosomal recessive early-onset parkinsonism." Science **299**(5604): 256-259.

Bonifati, V., P. Rizzu, et al. (2003). "Mutations in the DJ-1 gene associated with autosomal recessive early-onset parkinsonism." Science **299**(5604): 256-259.

Bouchard, V. J., M. Rouleau, et al. (2003). "PARP-1, a determinant of cell survival in response to DNA damage." Experimental Hematology **31**(6): 446-454.

Boujrad, H., O. Gubkina, et al. (2007). "AIF-mediated programmed necrosis: A highly regulated way to die." Cell Cycle **6**(21): 2612-2619.

Boulares, A. H., A. G. Yakovlev, et al. (1999). "Role of poly(ADP-ribose) polymerase (PARP) cleavage in apoptosis. Caspase 3-resistant PARP mutant increases rates of apoptosis in transfected cells." Journal of Biological Chemistry **274**(33): 22932-22940.

Boulton, S. J., P. C. Keane, et al. (2012). "Real-time monitoring of superoxide generation and cytotoxicity in neuroblastoma mitochondria induced by 1-trichloromethyl- 1,2,3,4-tetrahydro-beta-carboline." Redox Report **17**(3): 108-114.

Braak, H., K. Del Tredici, et al. (2003). "Staging of brain pathology related to sporadic Parkinson's disease." Neurobiol Aging **24**(2): 197-211.

Braak, H., K. Del Tredici, et al. (2003). "Staging of brain pathology related to sporadic Parkinson's disease." Neurobiology of Aging **24**(2): 197-211.

Braak, H., E. Ghebremedhin, et al. (2004). "Stages in the development of Parkinson's disease-related pathology." Cell and Tissue Research **318**(1): 121-134.

Braak, H., M. Sastre, et al. (2007). "Development of α-synuclein immunoreactive astrocytes in the forebrain parallels stages of intraneuronal pathology in sporadic Parkinson's disease." Acta Neuropathologica **114**(3): 231-241.

Bras, J., J. Simán-Sánchez, et al. (2009). "Lack of replication of association between GIGYF2 variants and Parkinson disease." Human Molecular Genetics **18**(2): 341-346.

Breckenridge, C. B., N. C. Sturgess, et al. (2013). "Pharmacokinetic, neurochemical, stereological and neuropathological studies on the potential effects of paraquat in the substantia nigra pars compacta and striatum of male C57BL/6J mice." NeuroToxicology **37**(0): 1-14.

Brenner-Lavie, H., E. Klein, et al. (2009). "Mitochondrial complex I as a novel target for intraneuronal DA: Modulation of respiration in intact cells." Biochemical Pharmacology **78**(1): 85-95.

Bretaud, S., C. Allen, et al. (2007). "p53-dependent neuronal cell death in a DJ-1-deficient zebrafish model of Parkinson's disease." Journal of Neurochemistry **100**(6): 1626-1635.

Bringmann, G., R. Bruckner, et al. (2000). "Effect of 1-trichloromethyl-1,2,3,4-tetrahydro-β-carboline (TaClo) on human serotonergic cells." Neurochemical Research **25**(6): 837-843.

Bringmann, G., D. Feineis, et al. (2000). "Bromal-derived tetrahydro-β-carbolines as neurotoxic agents: Chemistry, impairment of the dopamine metabolism, and inhibitory effects on mitochondrial respiration." Bioorganic and Medicinal Chemistry **8**(6): 1467-1478.

Bringmann, G., R. God, et al. (1999). "Identification of the dopaminergic neurotoxin 1-trichloromethyl-1,2,3,4- tetrahydro-β-carboline in human blood after intake of the hypnotic chloral hydrate." Analytical Biochemistry **270**(1): 167-175.

Bringmann, G., R. God, et al. (1995). "TaClo as a neurotoxic lead: Improved synthesis, stereochemical analysis, and inhibition of the mitochondrial respiratory chain." Journal of Neural Transmission, Supplement(46): 245-254.

Bringmann, G., R. God, et al. (1995). "The TaClo concept: 1-trichloromethyl-1,2,3,4-tetrahydro-β-carboline (Taclo), a new toxin for dopaminergic neurons." Journal of Neural Transmission, Supplement(46): 235-244.

Bringmann, G., M. Münchbach, et al. (2001). "Studies on single-strand scissions to cell-free plasmid DNA by the dopaminergic neurotoxin 'TaClo' (1-trichloromethyl-1,2,3,4-tetrahydro-β-carboline)." Neuroscience Letters **304**(1-2): 41-44.

Briving, C., I. Jacobson, et al. (1986). "Chronic effects of perchloroethylene and trichloroethylene on the gerbil brain amino acids and glutathione." NeuroToxicology **7**(1): 101-108.

Brooks, D. J. (2002). "Diagnosis and management of atypical Parkinsonian syndromes." Neurology in Practice **72**(1): i10-i16.

Brooks, W. J., M. F. Jarvis, et al. (1989). "Astrocytes as a primary locus for the conversion MPTP into MPP+." Journal of Neural Transmission **76**(1): 1-12.

Burkhardt, C. R., C. M. Filley, et al. (1988). "Diffuse Lewy body disease and progressive dementia." Neurology **38**(10): 1520-1528.

Burns, R. S., C. C. Chiueh, et al. (1983). "A primate model of parkinsonism: Selective destruction of dopaminergic neurons in the pars compacta of the substantia nigra by N-methyl-4-phenyl-1,2,3,6-tetrahydropyridine." Proceedings of the National Academy of Sciences of the United States of America **80**(14 I): 4546-4550.

Byers, V. S., A. S. Levin, et al. (1988). "Association between clinical symptoms and lymphocyte abnormalities in a population with chronic domestic exposure to industrial solvent-contaminated domestic water supply and a high incidence of leukaemia." Cancer Immunology Immunotherapy **27**(1): 77-81.

Byrne, K. G., R. Pfeiffer, et al. (1994). "Gastrointestinal dysfunction in Parkinson's disease. A report of clinical experience at a single center." J Clin Gastroenterol **19**(1): 11-16.

Cabe, P. A., H. A. Tilson, et al. (1978). "A simple recording grip strength device." Pharmacology Biochemistry and Behavior **8**(1): 101-102.

Cabin, D. E., K. Shimazu, et al. (2002). "Synaptic vesicle depletion correlates with attenuated synaptic responses to prolonged repetitive stimulation in mice lacking α-synuclein." Journal of Neuroscience **22**(20): 8797-8807.

Cadenas, E. and K. J. A. Davies (2000). "Mitochondrial free radical generation, oxidative stress, and aging." Free Radical Biology and Medicine **29**(3-4): 222-230.

Cady, S. G. and M. Sono (1991). "1-methyl-dl-tryptophan, β-(3-benzofuranyl)-dl-alanine (the oxygen analog of tryptophan), and β-[3-benzo(b)thienyl]-dl-alanine (the sulfur analog of tryptophan) are competitive inhibitors for indoleamine 2,3-dioxygenase." Archives of Biochemistry and Biophysics **291**(2): 326-333.

Candy, J. M., R. H. Perry, et al. (1983). "Pathological changes in the nucleus of meynert in Alzheimer's and Parkinson's diseases." Journal of the Neurological Sciences **59**(2): 277-289.

Canet-Aviles, R. M., M. A. Wilson, et al. (2004). "The Parkinson's disease DJ-1 is neuroprotective due to cysteine-sulfinic acid-driven mitochondrial localization." Proceedings of the National Academy of Sciences of the United States of America **101**(24): 9103-9108.

Carper, J. (1989). The Food Pharmacy New York, NY, Bantam Books.

Carter, R. J., L. A. Lione, et al. (1999). "Characterization of progressive motor deficits in mice transgenic for the human Huntington's disease mutation." Journal of Neuroscience **19**(8): 3248-3257.

Casarejos, M. J., J. Menéndez, et al. (2006). "Susceptibility to rotenone is increased in neurons from parkin null mice and is reduced by minocycline." Journal of Neurochemistry **97**(4): 934-946.

Castello, P. R., D. A. Drechsel, et al. (2007). "Mitochondria are a major source of paraquat-induced reactive oxygen species production in the brain." Journal of Biological Chemistry **282**(19): 14186-14193.

Cattano D., Straiko M.M.W., et al. (2008). "Chloral hydrate induces and lithium prevents neuroapoptosis in the infant mouse brain." Anesthesiology **109**: A315.

Chagniel, L., C. Robitaille, et al. (2012). "Partial dopamine depletion in MPTP-treated mice differentially altered motor skill learning and action control." Behavioural Brain Research **228**(1): 9-15.

Chan, D. C. (2006). "Mitochondria: Dynamic Organelles in Disease, Aging, and Development." Cell **125**(7): 1241-1252.

Chang, Y. F., C. M. Cheng, et al. (2006). "The F-box protein Fbxo7 interacts with human inhibitor of apoptosis protein cIAP1 and promotes cIAP1 ubiquitination." Biochemical and Biophysical Research Communications **342**(4): 1022-1026.

Chaudhuri, K. R., D. G. Healy, et al. (2006). "Non-motor symptoms of Parkinson's disease: Diagnosis and management." Lancet Neurology **5**(3): 235-245.

Chaudhuri, K. R., D. G. Healy, et al. (2006). "Non-motor symptoms of Parkinson's disease: diagnosis and management." The Lancet Neurology **5**(3): 235-245.

Chen, L., M. J. Thiruchelvam, et al. (2006). "Proteasome dysfunction in aged human α-synuclein transgenic mice." Neurobiology of Disease **23**(1): 120-126.

Chen, S. Y., L. Y. Chiu, et al. (2011). "zVAD-induced autophagic cell death requires c-Src-dependent ERK and JNK activation and reactive oxygen species generation." Autophagy **7**(2): 217-228.

Chen, T. Y., K. H. Chi, et al. (2009). "Reactive oxygen species are involved in FasL-induced caspase-independent cell death and inflammatory responses." Free Radical Biology and Medicine **46**(5): 643-655.

Cheng, C. H., H. R. Chang, et al. (2008). "Possible Mechanism by Which Rapamycin Increases Cyclosporine Nephrotoxicity." Transplantation Proceedings **40**(7): 2373-2375.

Cheung, Z. H. and N. Y. Ip (2009). "The emerging role of autophagy in Parkinson's disease." Molecular Brain **2**(1).

Chia, L. G., F. C. Cheng, et al. (1993). "Monoamines and their metabolites in plasma and lumbar cerebrospinal fluid of Chinese patients with Parkinson's disease." Journal of the Neurological Sciences **116**(2): 125-134.

Chia, L. G., D. R. Ni, et al. (1996). "Effects of 1-methyl-4-phenyl-1,2,3,6-tetrahydropyridine and 5,7-dihydroxytryptamine on the locomotor activity and striatal amines in C57BL/6 mice." Neuroscience Letters **218**(1): 67-71.

Cho, Y., S. Challa, et al. (2009). "Phosphorylation-Driven Assembly of the RIP1-RIP3 Complex Regulates Programmed Necrosis and Virus-Induced Inflammation." Cell **137**(6): 1112-1123.

Choi, J., A. I. Levey, et al. (2004). "Oxidative Modifications and Down-regulation of Ubiquitin Carboxyl-terminal Hydrolase L1 Associated with Idiopathic Parkinson's and Alzheimer's Diseases." Journal of Biological Chemistry **279**(13): 13256-13264.

Choi, K.-C., S.-H. Kim, et al. (2010). "A novel mTOR activating protein protects dopamine neurons against oxidative stress by repressing autophagy related cell death." Journal of Neurochemistry **112**(2): 366-376.

Choi, W. S., S. E. Kruse, et al. (2008). "Mitochondrial complex I inhibition is not required for dopaminergic neuron death induced by rotenone, MPP+, or paraquat." Proceedings of the National Academy of Sciences of the United States of America **105**(39): 15136-15141.

Christofferson, D. E. and J. Yuan (2010). "Necroptosis as an alternative form of programmed cell death." Current Opinion in Cell Biology **22**(2): 263-268.

Chu, C. T. (2010). "A pivotal role for PINK1 and autophagy in mitochondrial quality control: implications for Parkinson disease." Hum Mol Genet **19**(R1): R28-37.

Chung, K. K. K., Y. Zhang, et al. (2001). "Parkin ubiquitinates the alpha-synuclein-interacting protein, synphilin-1: implications for Lewy-body formation in Parkinson disease." Nature Medicine **7**(10): 1144-1150.

Cicmanec, J. L., L. W. Condie, et al. (1991). "90-day toxicity study of dichloroacetate in dogs." Fundamental and Applied Toxicology **17**(2): 376-389.

Ciechanover, A. and P. Brundin (2003). "The ubiquitin proteasome system in neurodegenerative diseases: sometimes the chicken, sometimes the egg." Neuron **40**(2): 427-446.

Clark, J., E. L. Clore, et al. (2010). "Oral N-Acetyl-cysteine attenuates loss of dopaminergic terminals in α-synuclein overexpressing mice." PLoS ONE **5**(8): 10.1371/journal.pone.0012333.

Cleeter, M. W. J., J. M. Cooper, et al. (1992). "Irreversible inhibition of mitochondrial complex I by 1-methyl-4-phenylpyridinium: Evidence for free radical involvement." Journal of Neurochemistry **58**(2): 786-789.

Clejan, L. and S. I. Cederbaum (1989). "Synergistic interactions between NADPH-cytochrome P-450 reductase, paraquat, and iron in the generation of active oxygen radicals." Biochemical Pharmacology **38**(11): 1779-1786.

Cochemé, H. M. and M. P. Murphy (2008). "Complex I is the major site of mitochondrial superoxide production by paraquat." Journal of Biological Chemistry **283**(4): 1786-1798.

Cohen, G., R. Farooqui, et al. (1997). "Parkinson disease: A new link between monoamine oxidase and mitochondrial electron flow." Proceedings of the National Academy of Sciences of the United States of America **94**(10): 4890-4894.

Cohen, G. M. (1997). "Caspases: The executioners of apoptosis." Biochemical Journal **326**(1): 1-16.

Colapinto, M., S. Mila, et al. (2006). "α-Synuclein protects SH-SY5Y cells from dopamine toxicity." Biochemical and Biophysical Research Communications **349**(4): 1294-1300.

Colotla, V. A., E. Flores, et al. (1990). "Effects of MPTP on locomotor activity in mice." Neurotoxicology and Teratology **12**(4): 405-407.

Committee on Human Health Risks of Trichloroethylene, N. R. C. (2006). Assessing the Human Health Risks of Trichloroethylene: Key Scientific Issues The National Academies Press.

Conrad, C., A. Andreadis, et al. (1997). "Genetic evidence for the involvement of τ in progressive supranuclear palsy." Annals of Neurology **41**(2): 277-281.

Conway, K. A., J. D. Harper, et al. (1998). "Accelerated in vitro fibril formation by a mutant α-synuclein linked to early-onset Parkinson disease." Nature Medicine **4**(11): 1318-1320.

Conway, K. A., S. J. Lee, et al. (2000). "Acceleration of oligomerization, not fibrillization, is a shared property of both α-synuclein mutations linked to early-onset Parkinson's disease: Implications for pathogenesis and therapy." Proceedings of the National Academy of Sciences of the United States of America **97**(2): 571-576.

Conway, K. A., J. C. Rochet, et al. (2001). "Kinetic stabilization of the α-synuclein protofibril by a dopamine-α-synuclein adduct." Science **294**(5545): 1346-1349.

Cooke, M. S., M. D. Evans, et al. (2003). "Oxidative DNA damage: Mechanisms, mutation, and disease." FASEB Journal **17**(10): 1195-1214.

Cookson, M. R. (2003). "Pathways to parkinsonism." Neuron **37**(1): 7-10.

Cookson, M. R. (2010). "DJ-1, PINK1, and their effects on mitochondrial pathways." Mov Disord **25 Suppl 1**: S44-48.

Cooper, J. A., H. J. Sagar, et al. (1991). "Cognitive impairment in early, untreated Parkinson's disease and its relationship to motor disability." Brain **114**(5): 2095-2122.

Cosi, C. and M. Marien (1998). "Decreases in mouse brain NAD+ and ATP induced by 1-methyl-4-phenyl- 1,2,3,6-tetrahydropyridine (MPTP): Prevention by the poly(ADP-ribose) polymerase inhibitor, benzamide." Brain Research **809**(1): 58-67.

Cotzias, G. C., M. H. Van Woert, et al. (1967). "Aromatic amino acids and modification of parkinsonism." New England Journal of Medicine **276**(7): 374-379.

Coulom, H. and S. Birman (2004). "Chronic exposure to rotenone models sporadic Parkinson's disease in Drosophila melanogaster." Journal of Neuroscience **24**(48): 10993-10998.

Crawley, J. N. (1999). "Behavioral phenotyping of transgenic and knockout mice: experimental design and evaluation of general health, sensory functions, motor abilities, and specific behavioral tests." Brain Research **835**(1): 18-26.

Crocker, S. J., P. D. Smith, et al. (2003). "Inhibition of calpains prevents neuronal and behavioral deficits in an MPTP mouse model of Parkinson's disease." Journal of Neuroscience **23**(10): 4081-4091.

Crosby, N., K. H. Deane, et al. (2003). "Amantadine in Parkinson's disease." Cochrane database of systematic reviews (Online)(1).

Crosby, N. J., K. H. Deane, et al. (2003). "Amantadine for dyskinesia in Parkinson's disease." Cochrane database of systematic reviews (Online)(2).

Crutchfield, K. C. and D. E. Dluzen (2006). "Rotenone produces opposite effects upon mouse striatal dopamine function as a result of environmental temperature." Neurotoxicity Research **9**(1): 15-21.

Cuervo, A. M. and J. F. Dice (2000). "Age-related decline in chaperone-mediated autophagy." Journal of Biological Chemistry **275**(40): 31505-31513.

Cuervo, A. M., L. Stafanis, et al. (2004). "Impaired degradation of mutant α-synuclein by chaperone-mediated autophagy." Science **305**(5688): 1292-1295.

Cummings, J. L. (1988). "Intellectual impairment in Parkinson's disease: Clinical, pathologic, and biochemical correlates." Journal of Geriatric Psychiatry and Neurology **1**(1): 24-36.

Da Costa, C. A., K. Ancolio, et al. (2000). "Wild-type but not Parkinson's disease-related Ala-53 → Thr mutant α-Synuclein protects neuronal cells from apoptotic stimuli." Journal of Biological Chemistry **275**(31): 24065-24069.

Da Cunha, C., M. S. Gevaerd, et al. (2001). "Memory disruption in rats with nigral lesions induced by MPTP: A model for early Parkinson's disease amnesia." Behavioural Brain Research **124**(1): 9-18.

Dagda, R. K., S. J. Cherra, 3rd, et al. (2009). "Loss of PINK1 function promotes mitophagy through effects on oxidative stress and mitochondrial fission." J Biol Chem **284**(20): 13843-13855.

Dale, G. E., A. Probst, et al. (1992). "Relationships between Lewy bodies and pale bodies in Parkinson's disease." Acta Neuropathol **83**(5): 525-529.

Damier, P., E. C. Hirsch, et al. (1993). "Glutathione peroxidase, glial cells and Parkinson's disease." Neuroscience **52**(1): 1-6.

Dantzer, F., V. Schreiber, et al. (1999). "Involvement of poly(ADP-ribose) polymerase in base excision repair." Biochimie **81**(1-2): 69-75.

Dauer, W., N. Kholodilov, et al. (2002). "Resistance of α-synuclein null mice to the parkinsonian neurotoxin MPTP." Proceedings of the National Academy of Sciences of the United States of America **99**(22): 14524-14529.

Davidson, I. W. F. and R. P. Beliles (1991). "Consideration of the target organ toxicity of trichloroethylene in terms of metabolite toxicity and pharmacokinetics." Drug Metabolism Reviews **23**(5-6): 493-599.

Davidzon, G., P. Greene, et al. (2006). "Early-onset familial parkinsonism due to POLG mutations." Annals of Neurology **59**(5): 859-862.

Davis, C. W., B. J. Hawkins, et al. (2010). "Nitration of the mitochondrial complex I subunit NDUFB8 elicits RIP1- and RIP3-mediated necrosis." Free Radical Biology and Medicine **48**(2): 306-317.

Davis, G. C., A. C. Williams, et al. (1979). "Chronic parkinsonism secondary to intravenous injection of meperidine analogues." Psychiatry Research **1**(3): 249-254.

Dawson, V. L. and T. M. Dawson (1996). "Nitric oxide neurotoxicity." Journal of Chemical Neuroanatomy **10**(3-4): 179-190.

Day, R. M., Y. J. Suzuki, et al. (2003). "Regulation of glutathione by oxidative stress in bovine pulmonary artery endothelial cells." Antioxid Redox Signal **5**(6): 699-704.

de Flora, S., C. Bennicelli, et al. (1985). "In vivo effects of N-acetylcysteine on glutathione metabolism and on the biotransformation of carcinogenic and/or mutagenic compounds." Carcinogenesis **6**(12): 1735-1745.

de Jong, P. J., J. P. Lakke, et al. (1984). "CSF GABA levels in Parkinson's disease." Advances in neurology **40**: 427-430.

De Jonghe, B. C., M. P. Lawler, et al. (2009). "Pica as an adaptive response: Kaolin consumption helps rats recover from chemotherapy-induced illness." Physiology and Behavior **97**(1): 87-90.

De La Garza II, R. and J. J. Mahoney III (2004). "A distinct neurochemical profile in WKY rats at baseline and in response to acute stress: Implications for animal models of anxiety and depression." Brain Research **1021**(2): 209-218.

Declercq, W., T. Vanden Berghe, et al. (2009). "RIP Kinases at the Crossroads of Cell Death and Survival." Cell **138**(2): 229-232.

Degterev, A., J. Hitomi, et al. (2008). "Identification of RIP1 kinase as a specific cellular target of necrostatins." Nature Chemical Biology **4**(5): 313-321.

Degterev, A., Z. Huang, et al. (2005). "Chemical inhibitor of nonapoptotic cell death with therapeutic potential for ischemic brain injury." Nature chemical biology **1**(2): 112-119.

DeLong, M. R. (1990). "Primate models of movement disorders of basal ganglia origin." Trends in Neurosciences **13**(7): 281-285.

Dereli, E. E. and A. Yaliman (2010). "Comparison of the effects of a physiotherapist-supervised exercise programme and a self-supervised exercise programme on quality of life in patients with Parkinson's disease." Clinical Rehabilitation **24**(4): 352-362.

Desole, M. S., M. Miele, et al. (1995). "Neuronal antioxidant system and MPTP-induced oxidative stress in the striatum and brain stem of the rat." Pharmacology Biochemistry and Behavior **51**(4): 581-592.

Devi, L., V. Raghavendran, et al. (2008). "Mitochondrial import and accumulation of α-synuclein impair complex I in human dopaminergic neuronal cultures and Parkinson disease brain." Journal of Biological Chemistry **283**(14): 9089-9100.

Dexter, D., C. Carter, et al. (1986). "Lipid peroxidation as cause of nigral cell death in Parkinson's disease." Lancet **2**(8507): 639-640.

Dexter, D. T., C. J. Carter, et al. (1989). "Basal lipid peroxidation in substantia nigra is increased in Parkinson's disease." Journal of Neurochemistry **52**(2): 381-389.

Di Fonzo, A., H. F. Chien, et al. (2007). "ATP13A2 missense mutations in juvenile parkinsonism and young onset Parkinson disease." Neurology **68**(19): 1557-1562.

Di Fonzo, A., E. Fabrizio, et al. (2009). "GIGYF2 mutations are not a frequent cause of familial Parkinson's disease." Parkinsonism and Related Disorders **15**(9): 703-705.

Di Maria, E., M. Tabaton, et al. (2000). "Corticobasal degeneration shares a common genetic background with progressive supranuclear palsy." Annals of Neurology **47**(3): 374-377.

Di Paolo, T., P. Bedard, et al. (1986). "Long-term effects of MPTP on central and peripheral catecholamine and indoleamine concentrations in monkeys." Brain Research **379**(2): 286-293.

Diaz-Corrales, F. J., M. Asanuma, et al. (2005). "Rotenone induces aggregation of γ-tubulin protein and subsequent disorganization of the centrosome: Relevance to formation of inclusion bodies and neurodegeneration." Neuroscience **133**(1): 117-135.

Dickson, D. W., H. Braak, et al. (2009). "Neuropathological assessment of Parkinson's disease: refining the diagnostic criteria." The Lancet Neurology **8**(12): 1150-1157.

Dickson, D. W., H. Braak, et al. (2009). "Neuropathological assessment of Parkinson's disease: refining the diagnostic criteria." Lancet Neurol **8**(12): 1150-1157.

Dixon, M. and J. H. Quastel (1923). "CCCXLVIII. - A new type of reduction-oxidation system. Part I. Cysteine and glutathione." Journal of the Chemical Society, Transactions **123**: 2943-2953.

Dlasková, A., L. Hlavatá, et al. (2008). "Oxidative stress caused by blocking of mitochondrial Complex I H+ pumping as a link in aging/disease vicious cycle." The International Journal of Biochemistry & Cell Biology **40**(9): 1792-1805.

Donaldson, J., D. McGregor, et al. (1982). "Manganese neurotoxicity: A model for free radical mediated neurodegeneration." Canadian Journal of Physiology and Pharmacology **60**(11): 1398-1405.

Double, K. L., M. Maywald, et al. (1998). "In vitro studies of ferritin iron release and neurotoxicity." Journal of Neurochemistry **70**(6): 2492-2499.

Du, C., M. Fang, et al. (2000). "Smac, a mitochondrial protein that promotes cytochrome c-dependent caspase activation by eliminating IAP inhibition." Cell **102**(1): 33-42.

Dubois, B. and B. Pillon (1997). "Cognitive deficits in Parkinson's disease." Journal of Neurology **244**(1): 2-8.

Dupont, E., J. M. Burgunder, et al. (1997). "Tolcapone added to Levodopa in stable Parkinsonian patients: A double-blind placebo-controlled study." Movement Disorders **12**(6): 928-934.

Duprez, L., E. Wirawan, et al. (2009). "Major cell death pathways at a glance." Microbes and Infection **11**(13): 1050-1062.

Dykens, J. A. (1994). "Isolated cerebral and cerebellar mitochondria produce free radicals when exposed to elevated Ca2+ and Na+: Implications for neurodegeneration." Journal of Neurochemistry **63**(2): 584-591.

Ekstrand, M. I., M. Terzioglu, et al. (2007). "Progressive parkinsonism in mice with respiratory-chain-deficient dopamine neurons." Proceedings of the National Academy of Sciences of the United States of America **104**(4): 1325-1330.

El-Agnaf, O. M. A., R. Jakes, et al. (1998). "Aggregates from mutant and wild-type α-synuclein proteins and NAC peptide induce apoptotic cell death in human neuroblastoma cells by formation of β-sheet and amyloid-like filaments." FEBS Letters **440**(1-2): 71-75.

Ellwart, J. W. and P. Dormer (1990). "Vitality measurement using spectrum shift in Hoechst 33342 stained cells." Cytometry **11**(2): 239-243.

Emre, M. (2003). "Dementia associated with Parkinson's disease." Lancet Neurology **2**(4): 229-237.

Enari, M., H. Sakahira, et al. (1998). "A caspase-activated DNase that degrades DNA during apoptosis, and its inhibitor ICAD." Nature **391**(6662): 43-50.

Esrefoglu, M. (2009). "Cell injury and death: Oxidative stress and antioxidant defense system: Review." Turkiye Klinikleri Journal of Medical Sciences **29**(6): 1660-1676.

Esteves, A. R., D. M. Arduíno, et al. (2010). "Dysfunctional mitochondria uphold calpain activation: Contribution to Parkinson's disease pathology." Neurobiology of Disease **37**(3): 723-730.

Exner, N., B. Treske, et al. (2007). "Loss-of-function of human PINK1 results in mitochondrial pathology and can be rescued by parkin." Journal of Neuroscience **27**(45): 12413-12418.

Faucheux, B. A., J. J. Hauw, et al. (1997). "The density of [125I]-transferrin binding sites on perikarya of melanized neurons of the substantia nigra is decreased in Parkinson's disease." Brain Research **749**(1): 170-174.

Feany, M. B. and W. W. Bender (2000). "A Drosophila model of Parkinson's disease." Nature **404**(6776): 394-398.

Fearnley, J. M. and A. J. Lees (1991). "Ageing and Parkinson's disease: Substantia nigra regional selectivity." Brain **114**(5): 2283-2301.

Felitsyn, N., P. W. Stacpoole, et al. (2007). "Dichloroacetate causes reversible demyelination in vitro: Potential mechanism for its neuropathic effect." Journal of Neurochemistry **100**(2): 429-436.

Fernagut, P. O., C. B. Hutson, et al. (2007). "Behavioral and histopathological consequences of paraquat intoxication in mice: Effects of α-synuclein over-expression." Synapse **61**(12): 991-1001.

Fernandes, V. S., J. R. Santos, et al. (2012). "Repeated treatment with a low dose of reserpine as a progressive model of Parkinson's disease." Behavioural Brain Research **231**(1): 154-163.

Fernandez, Y., I. Subirade, et al. (1995). "Microsomal membrane peroxidation by an Fe3+/paraquat system: Consequences of phenobarbital induction." Biological Trace Element Research **47**(1-3): 9-16.

Ferrante, R. J., J. B. Schulz, et al. (1997). "Systemic administration of rotenone produces selective damage in the striatum and globus pallidus, but not in the substantia nigra." Brain Research **753**(1): 157-162.

Ferrer, I., E. Perez, et al. (2007). "Abnormal levels of prohibitin and ATP synthase in the substantia nigra and frontal cortex in Parkinson's disease." Neuroscience Letters **415**(3): 205-209.

Ferro, M. M., M. I. Bellissimo, et al. (2005). "Comparison of bilaterally 6-OHDA- and MPTP-lesioned rats as models of the early phase of Parkinson's disease: Histological, neurochemical, motor and memory alterations." Journal of Neuroscience Methods **148**(1): 78-87.

Fett, M. E., A. Pilsl, et al. (2010). "Parkin is protective against proteotoxic stress in a transgenic zebrafish model." PLoS One **5**(7): e11783.

Fett, M. E., A. Pilsl, et al. (2010). "Parkin is protective against proteotoxic stress in a transgenic zebrafish model." PLoS ONE **5**(7).

Filosto, M., P. Tonin, et al. (2009). "Definite multiple system atrophy in a german family." Journal of Neurology, Neurosurgery and Psychiatry **80**(4): 449-450.

Finsterer, J. (2006). "Central nervous system manifestations of mitochondrial disorders." Acta Neurol Scand **114**: 217-238.

Fleischman, R. W., D. McCracken, et al. (1977). "Adynamic ileus in the rat induced by chloral hydrate." Laboratory Animal Science **27**(2): 238-243.

Fleming, S. M., J. Salcedo, et al. (2004). "Early and progressive sensorimotor anomalies in mice overexpressing wild-type human α-synuclein." Journal of Neuroscience **24**(42): 9434-9440.

Floor, E. and M. G. Wetzel (1998). "Increased protein oxidation in human substantia nigra pars compacta in comparison with basal ganglia and prefrontal cortex measured with an improved dinitrophenylhydrazine assay." Journal of Neurochemistry **70**(1): 268-275.

Fong, C. S., R. M. Wu, et al. (2007). "Pesticide exposure on southwestern Taiwanese with MnSOD and NQO1 polymorphisms is associated with increased risk of Parkinson's disease." Clinica Chimica Acta **378**(1-2): 136-141.

Fonzo, A. D., M. C. J. Dekker, et al. (2009). "FBXO7 mutations cause autosomal recessive, early-onset parkinsonian- pyramidal syndrome." Neurology **72**(3): 240-245.

Forkert, P. G. and D. W. Birch (1989). "Pulmonary toxicity of trichloroethylene in mice. Covalent binding and morphological manifestations." Drug Metabolism and Disposition **17**(1): 106-113.

Forno, L. S., L. E. DeLanney, et al. (1993). "Similarities and differences between MPTP-induced parkinsonsim and Parkinson's disease. Neuropathologic considerations." Advances in neurology **60**: 600-608.

Forno, L. S., J. W. Langston, et al. (1986). "Locus ceruleus lesions and eosinophilic inclusions in MPTP-treated monkeys." Annals of Neurology **20**(4): 449-455.

Frasier, M., M. Walzer, et al. (2005). "Tau phosphorylation increases in symptomatic mice overexpressing A30P α-synuclein." Experimental Neurology **192**(2): 274-287.

Freichel, C., M. Neumann, et al. (2007). "Age-dependent cognitive decline and amygdala pathology in α-synuclein transgenic mice." Neurobiology of Aging **28**(9): 1421-1435.

Friedman, D. I., J. Jankovic, et al. (1992). "Neuro-ophthalmic findings in progressive supranuclear palsy." Journal of Clinical Neuro-Ophthalmology **12**(2): 104-109.

Fuentes-Prior, P. and G. S. Salvesen (2004). "The protein structures that shape caspase activity, specificity, activation and inhibition." Biochemical Journal **384**(2): 201-232.

Fukuda, H., K. Hara, et al. (1988). "1-Methyl-4-phenyl-1,2,3,6-tetrahydropyridine (MPTP) enhances tryptophan hydroxylase activity in mouse striatum, but not in the frontal cortex." Brain Research **449**(1-2): 399-402.

Fukushima, T., T. Tawara, et al. (1995). "Radical formation site of cerebral complex I and Parkinson's disease." Journal of Neuroscience Research **42**(3): 385-390.

Gai, W. P., H. X. Yuan, et al. (2000). "In situ and in vitro study of colocalization and segregation of Î±-synuclein, ubiquitin, and lipids in Lewy bodies." Experimental Neurology **166**(2): 324-333.

Gaiter, D., M. Westerlund, et al. (2006). "LRRK2 expression linked to dopamine-innervated areas." Annals of Neurology **59**(4): 714-719.

Galloway, P. G., P. Mulvihill, et al. (1992). "Filaments of Lewy bodies contain insoluble cytoskeletal elements." Am J Pathol **140**(4): 809-822.

Galter, D., K. Pernold, et al. (2010). "MitoPark mice mirror the slow progression of key symptoms and L-DOPA response in Parkinson's disease." Genes, Brain and Behavior **9**(2): 173-181.

Gandhi, S., A. Wood-Kaczmar, et al. (2009). "PINK1-associated Parkinson's disease is caused by neuronal vulnerability to calcium-induced cell death." Mol Cell **33**(5): 627-638.

Gao, H., W. Yang, et al. (2012). "DJ-1 protects dopaminergic neurons against rotenone-induced apoptosis by enhancing ERK-dependent mitophagy." Journal of Molecular Biology **423**(2): 232-248.

Garris, P. A., Q. D. Walker, et al. (1997). "Dopamine release and uptake rates both decrease in the partially denervated striatum in proportion to the loss of dopamine terminals." Brain Research **753**(2): 225-234.

Garside, H. J., M. P. Burnham, et al. (2012). "Implementation of screening and mechanistic assays for the detection of mitochondrial toxicity via inhibition of the electron transfer chain " Society of Toxicology General Meeting, San Francisco: Poster #459.

Gash, D. M., K. Rutland, et al. (2008). "Trichloroethylene: Parkinsonism and complex 1 mitochondrial neurotoxicity." Annals of Neurology **63**(2): 184-192.

Gaweda-Walerych, K., K. Safranow, et al. (2010). "Mitochondrial transcription factor A variants and the risk of Parkinson's disease." Neuroscience Letters **469**(1): 24-29.

Gegg, M. E., J. M. Cooper, et al. (2009). "Silencing of PINK1 expression affects mitochondrial DNA and oxidative phosphorylation in dopaminergic cells." PLoS ONE **4**(3): 10.1371/journal.pone.0004756.

Geisler, S., K. M. Holmstrom, et al. (2010). "PINK1/Parkin-mediated mitophagy is dependent on VDAC1 and p62/SQSTM1." Nat Cell Biol **12**(2): 119-131.

Gerlach, M., D. Ben-Shachar, et al. (1994). "Altered brain metabolism of iron as a cause of neurodegenerative diseases." J. Neurochem. **63**: 793-807.

Gerlach, M., K. Double, et al. (1997). "Iron in the Parkisonian substantia nigra." Mov. Disord. **12**: 258-260.

Gerlach, M., M. Gotz, et al. (1996). "Acute MPTP treatment produces no changes in mitochondrial complex activities and indices of oxidative damage in the common marmoset ex vivo one week after exposure to the toxin." Neurochemistry International **28**(1): 41-49.

Gerlach, M., W. Gsell, et al. (1996). "A post mortem study on neurochemical markers of dopaminergic, GABA-ergic and glutamatergic neurons in basal ganglia-thalamocortical circuits in Parkinson syndrome." Brain Research **741**(1-2): 142-152.

Gerlach, M., A. Y. Xiao, et al. (1998). "1-Trichloromethyl-1,2,3,4-tetrahydro-β-carboline increases extracellular serotonin and stimulates hydroxyl radical production in rats." Neuroscience Letters **257**(1): 17-20.

Gertz, H. J., A. Siegers, et al. (1994). "Stability of cell size and nucleolar size in Lewy body containing neurons of substantia nigra in Parkinson's disease." Brain Research **637**(1-2): 339-341.

Ghorayeb, I., P. O. Fernagut, et al. (2002). "Dystonia is predictive of subsequent altered dopaminergic responsiveness in a chronic 1-methyl-4-phenyl-1,2,3,6-tetrahydropyridine + 3-nitropropionic acid model of striatonigral degeneration in monkeys." Neuroscience Letters **335**(1): 34-38.

Gibb, W. R. G. and A. J. Lees (1988). "The relevance of the Lewy body to the pathogenesis of idiopathic Parkinson's disease." Journal of Neurology Neurosurgery and Psychiatry **51**(6): 745-752.

Gibb, W. R. G., P. J. Luthert, et al. (1989). "Corticobasal degeneration." Brain **112**(5): 1171-1192.

Gilman, S., P. A. Low, et al. (1999). "Consensus statement on the diagnosis of multiple system atrophy." Journal of the Neurological Sciences **163**(1): 94-98.

Gilman, S., G. K. Wenning, et al. (2008). "Second consensus statement on the diagnosis of multiple system atrophy." Neurology **71**(9): 670-676.

Gispert, S., F. Ricciardi, et al. (2009). "Parkinson phenotype in aged PINK1-deficient mice is accompanied by progressive mitochondrial dysfunction in absence of neurodegeneration." PLoS One **4**(6): e5777.

Gitler, A. D., A. Chesi, et al. (2009). "α-Synuclein is part of a diverse and highly conserved interaction network that includes PARK9 and manganese toxicity." Nature Genetics **41**(3): 308-315.

Glass, C. K., K. Saijo, et al. (2010). "Mechanisms Underlying Inflammation in Neurodegeneration." Cell **140**(6): 918-934.

Glass, J. D., D. G. Culver, et al. (2002). "Very early activation of m-calpain in peripheral nerve during Wallerian degeneration." Journal of the Neurological Sciences **196**(1-2): 9-20.

Gluck, M. R. and G. D. Zeevalk (2004). "Inhibition of brain mitochondrial respiration by dopamine and its metabolites: Implications for Parkinson's disease and catecholamine-associated diseases." Journal of Neurochemistry **91**(4): 788-795.

Goldman, S. M., P. J. Quinlan, et al. (2011). "Solvent exposures and parkinson disease risk in twins." Annals of Neurology: n/a-n/a.

Goldman, S. M., P. J. Quinlan, et al. (2012). "Solvent exposures and Parkinson disease risk in twins." Annals of Neurology **71**(6): 776-784.

Goldsworthy, T. L. and J. A. Popp (1987). "Chlorinated hydrocarbon-induced peroxisomal enzyme activity in relation to species and organ carcinogenicity." Toxicology and Applied Pharmacology **88**(2): 225-233.

González-Polo, R. A., M. Niso-Santano, et al. (2007). "Inhibition of paraquat-induced autophagy accelerates the apoptotic cell death in neuroblastoma SH-SY5Y cells." Toxicological Sciences **97**(2): 448-458.

Good, C. H., A. F. Hoffman, et al. (2011). "Impaired nigrostriatal function precedes behavioral deficits in a genetic mitochondrial model of parkinson's disease." FASEB Journal **25**(4): 1333-1344.

Good, P. F., A. Hsu, et al. (1998). "Protein nitration in Parkinson's disease." Journal of Neuropathology and Experimental Neurology **57**(4): 338-342.

Goodwin, V. A., S. H. Richards, et al. (2008). "The effectiveness of exercise interventions for people with Parkinson's disease: A systematic review and meta-analysis." Movement Disorders **23**(5): 631-640.

Goossens, V., G. Stangé, et al. (1999). "Regulation of Tumor Necrosis Factor-Induced, Mitochondria- and Reactive Oxygen Species-Dependent Cell Death by the Electron Flux through the Electron Transport Chain Complex I." Antioxidants and Redox Signaling **1**(3): 285-295.

Gottwald, M. D., J. L. Bainbridge, et al. (1997). "New pharmacotherapy for Parkinson's disease." Annals of Pharmacotherapy **31**(10): 1205-1217.

Grace, A. A. and B. S. Bunney (1983). "Intracellular and extracellular electrophysiology of nigral dopaminergic neurons. 2. Action potential generating mechanisms and morphologic correlates." Neuroscience **10**(2): 317-331.

Grasbon-Frodl, E. M., S. Kösel, et al. (1999). "Analysis of mitochondrial targeting sequence and coding region polymorphisms of the manganese superoxide dismutase gene in German Parkinson disease patients." Biochemical and Biophysical Research Communications **255**(3): 749-752.

Green, T. (1997). "Trichloroethylene induced cancer in animals and its relevance to humans." Journal of Occupational Health **39**(4): 261-273.

Green, T. (2000). "Pulmonary toxicity and carcinogenicity of trichloroethylene: Species differences and modes of action." Environmental Health Perspectives **108**(SUPPL. 2): 261-264.

Greenamyre, J. T., G. MacKenzie, et al. (1999). Mitochondrial dysfunction in Parkinson's disease. Biochemical Society Symposium. **66:** 85-97.

Greene, J. G. and J. T. Greenamyre (1996). "Bioenergetics and glutamate excitotoxicity." Progress in Neurobiology **48**(6): 613-634.

Greggio, E., S. Jain, et al. (2006). "Kinase activity is required for the toxic effects of mutant LRRK2/dardarin." Neurobiology of Disease **23**(2): 329-341.

Griffin, D. C. and M. Landon (1981). "Additional components of bovine heart cytochrome c oxidase demonstrated by high-resolution polyacrylamide-gel electrophoresis in the presence of chloral hydrate." Biochemical Journal **197**(2): 333-344.

Griffith, H. R., O. C. Okonkwo, et al. (2008). "Reduced brain glutamate in patients with Parkinson's disease." NMR in Biomedicine **21**(4): 381-387.

Griffith, O. W. (1982). "Mechanism of action, metabolism, and toxicity of buthionine sulfoximine and its higher homologs, potent inhibitors of glutathione synthesis." Journal of Biological Chemistry **257**(22): 13704-13712.

Grote, C., H. W. Clement, et al. (1995). "Biochemical lesions of the nigrostriatal system by TaClo (1-trichloromethyl-1,2,3,4-tetrahydro-β-carboline) and derivatives." Journal of Neural Transmission, Supplement(46): 275-281.

Guehl, D., E. Bezard, et al. (1999). "Trichloroethylene and parkinsonism: A human and experimental observation." European Journal of Neurology **6**(5): 609-611.

Guella, I., A. Pistocchi, et al. (2011). "Mutational screening and zebrafish functional analysis of GIGYF2 as a Parkinson-disease gene." Neurobiology of Aging **32**(11): 1994-2005.

Gundersen, H. J. and E. B. Jensen (1987). "The efficiency of systematic sampling in stereology and its prediction." Journal of Microscopy **147**: Pt 3/.

Gundersen, H. J. G., P. Bagger, et al. (1988). "The new stereological tools: Disector, fractionator, mucleator and point sampled intercepts and their use in pathological research and diagnosis." APMIS **96**(10): 857-881.

Gunderson, H. J. G. (1988). "The nucleator." Journal of Microscopy **151**(1): 3-21.

Gunter, T. E., L. Buntinas, et al. (2000). "Mitochondrial calcium transport: Mechanisms and functions." Cell Calcium **28**(5-6): 285-296.

Guo, J., W. Qiu, et al. (2013). "Motor neuron degeneration in a mouse model of seipinopathy." Cell Death and Disease **4**(3).

Guo, Y., J. Jankovic, et al. (2009). "GIGYF2 Asn56Ser and Asn457Thr mutations in Parkinson disease patients." Neuroscience Letters **454**(3): 209-211.

Haas, R. H., F. Nasirian, et al. (1995). "Low platelet mitochondrial complex I and complex II/III activity in early untreated parkinson's disease." Annals of Neurology **37**(6): 714-722.

Hamilton, W. R., W. J. Trickler, et al. (2012). "Effects of 1-methyl-4-phenyl-1,2,3,6-tetrahydropyridine (MPTP) on retinal dopaminergic system in mice." Neuroscience Letters **515**(2): 107-110.

Hantraye, P., M. Varastet, et al. (1993). "Stable parkinsonian syndrome and uneven loss of striatal dopamine fibres following chronic MPTP administration in baboons." Neuroscience **53**(1): 169-178.

Hao, L. Y., B. I. Giasson, et al. (2010). "DJ-1 is critical for mitochondrial function and rescues PINK1 loss of function." Proceedings of the National Academy of Sciences of the United States of America **107**(21): 9747-9752.

Hara, K., Y. Momose, et al. (2007). "Multiplex families with multiple system atrophy." Archives of Neurology **64**(4): 545-551.

Hartai, Z., P. Klivenyi, et al. (2005). "Kynurenine metabolism in plasma and in red blood cells in Parkinson's disease." Journal of the Neurological Sciences **239**(1): 31-35.

Hashimoto, M., L. J. Hsu, et al. (1999). "Oxidative stress induces amyloid-like aggregate formation of NACP/α- synuclein in vitro." NeuroReport **10**(4): 717-721.

Hastings, T. G. (1995). "Enzymatic oxidation of dopamine: The role of prostaglandin H synthase." Journal of Neurochemistry **64**(2): 919-924.

He, S., L. Wang, et al. (2009). "Receptor Interacting Protein Kinase-3 Determines Cellular Necrotic Response to TNF-α." Cell **137**(6): 1100-1111.

Healy-Stoffel, M., S. O. Ahmad, et al. (2012). "A novel use of combined tyrosine hydroxylase and silver nucleolar staining to determine the effects of a unilateral intrastriatal 6-hydroxydopamine lesion in the substantia nigra: A stereological study." Journal of Neuroscience Methods **210**(2): 187-187.

Heim, C. and K. H. Sontag (1997). "The halogenated tetrahydro-β-carboline 'TaClo': A progressively-acting neurotoxin." Journal of Neural Transmission, Supplement(50): 107-111.

Hely, M. A., J. G. L. Morris, et al. (2005). "Sydney Multicenter Study of Parkinson's disease: Non-L-dopa-responsive problems dominate at 15 years." Movement Disorders **20**(2): 190-199.

Higashi, S., E. Iseki, et al. (2010). "GIGYF2 is present in endosomal compartments in the mammalian brains and enhances IGF-1-induced ERK1/2 activation." Journal of Neurochemistry **115**(2): 423-437.

Hirsch, E., A. M. Graybiel, et al. (1988). "Melanized dopaminergic neurons are differentially susceptible to degeneration in Parkinson's disease." Nature **334**(6180): 345-348.

Hitomi, J., D. E. Christofferson, et al. (2008). "Identification of a Molecular Signaling Network that Regulates a Cellular Necrotic Cell Death Pathway." Cell **135**(7): 1311-1323.

Hoffer, E., Y. Baum, et al. (1996). "N-acetylcysteine increases the glutathione content and protects rat alveolar type II cells against paraquat-induced cytotoxicity." Toxicology Letters **84**(1): 7-12.

Holler, N., R. Zaru, et al. (2000). "Fas triggers an alternative, caspase-8-independent cell death pathway using the kinase RIP as effector molecule." Nature Immunology **1**(6): 489-495.

Holloway, R., I. Shoulson, et al. (2000). "Pramipexole vs Levodopa as initial treatment for Parkinson disease: A randomized controlled trial." Journal of the American Medical Association **284**(15): 1931-1938.

Holmer, H. K., M. Keyghobadi, et al. (2005). "Dietary restriction affects striatal glutamate in the MPTP-induced mouse model of nigrostriatal degeneration." Synapse **57**(2): 100-112.

Honma, T., H. Hasegawa, et al. (1980). "Changes of free amino acid content in rat brain after exposure to trichloroethylene and tetrachloroethylene." Industrial Health **18**(1): 1-7.

Hoppel, C. L., D. Greenblatt, et al. (1987). "Inhibition of mitochondrial respiration by analogs of 4-phenylpyridine and 1-methyl-4-phenylpyridinium cation (MPP+), the neurotoxic metabolite of MPTP." Biochemical and Biophysical Research Communications **148**(2): 684-693.

Hoppins, S., L. Lackner, et al. (2007). "The machines that divide and fuse mitochondria." Annu Rev Biochem **76**: 751-780.

Hossain Khan, F., T. Sen, et al. (2005). "Inhibition of rat brain mitochondrial electron transport chain activity by dopamine oxidation products during extended in vitro incubation: Implications for Parkinson's disease." Biochimica et Biophysica Acta (BBA) - Molecular Basis of Disease **1741**(1-2): 65-74.

Houlden, H., M. Baker, et al. (2001). "Corticobasal degeneration and progressive supranuclear palsy share a common tau haplotype." Neurology **56**(12): 1702-1706.

Hsu, H. L., J. N. Huang, et al. (1996). "TNF-Dependent recruitment of the protein kinase RIP to the TNF receptor-1 signaling complex." Immunity **4**(4): 387-396.

Hsu, H. L., J. Xiong, et al. (1995). "The TNF receptor 1-associated protien TRADD signals cell-death and NF-kappa-B activation." Cell **81**(4): 495-504.

Hsu, L. J., Y. Sagara, et al. (2000). "α-synuclein promotes mitochondrial deficit and oxidative stress." American Journal of Pathology **157**(2): 401-410.

Hung, H. C. and E. H. Y. Lee (1998). "MPTP produces differential oxidative stress and antioxidative responses in the nigrostriatal and mesolimbic dopaminergic pathways." Free Radical Biology and Medicine **24**(1): 76-84.

Hur, G. M., J. Lewis, et al. (2003). "The death domain kinase RIP has an essential role in DNA damage-induced NF-κB activation." Genes and Development **17**(7): 873-882.

Hutter-Saunders, J. A. L., H. E. Gendelman, et al. (2012). "Murine motor and behavior functional evaluations for acute 1-methyl-4-phenyl-1,2,3,6-tetrahydropyridine (MPTP) intoxication." Journal of Neuroimmune Pharmacology **7**(1): 279-288.

Iancu, R., P. Mohapel, et al. (2005). "Behavioral characterization of a unilateral 6-OHDA-lesion model of Parkinson's disease in mice." Behavioural Brain Research **162**(1): 1-10.

Ikeda, K. (1997). "Basic pathology of corticobasal degeneration." Neuropathology **17**(2): 127-133.

Irrcher, I., H. Aleyasin, et al. (2010). "Loss of the Parkinson's disease-linked gene DJ-1 perturbs mitochondrial dynamics." Hum Mol Genet **19**(19): 3734-3746.

Issels, R. D., A. Nagele, et al. (1988). "Promotion of cystine uptake and its utilization for glutathione biosynthesis induced by cysteamine and n-acetylcysteine." Biochemical Pharmacology **37**(5): 881-888.

Iwashita, A., S. Yamazaki, et al. (2004). "Neuroprotective effects of a novel poly(ADP-ribose) polymerase-1 inhibitor, 2-{3-[4-(4-chlorophenyl)-1-piperazinyl] propyl}-4(3H)-quinazolinone (FR255595), in an in vitro model of cell death and in mouse 1-methyl-4-phenyl-1,2,3,6-tetrahydropyridine model of Parkinson's disease." Journal of Pharmacology and Experimental Therapeutics **309**(3): 1067-1078.

Jackson-Lewis, V. and S. Przedborski (2007). "Protocol for the MPTP mouse model of Parkinson's disease." Nature Protocols **2**(1): 141-151.

Jana, S., A. K. Maiti, et al. (2007). "Dopamine but not 3,4-dihydroxy phenylacetic acid (DOPAC) inhibits brain respiratory chain activity by autoxidation and mitochondria catalyzed oxidation to quinone products: Implications in Parkinson's disease." Brain Research **1139**(1): 195-200.

Janetzky, B., G. Gille, et al. (1999). "Effect of highly halogenated β-carbolines on dopaminergic cells in culture and on mitochondrial respiration." Drug Development Research **46**(1): 51-56.

Janetzky, B., R. God, et al. (1995). "1-Trichloromethyl-1,2,3,4-tetrahydro-β-carboline, a new inhibitor of complex I." Journal of Neural Transmission, Supplement(46): 265-273.

Javoy, F., C. Sotelo, et al. (1976). "Specificity of dopaminergic neuronal degeneration induced by intracerebral injection of 6 hydroxydopamine in the nigrostriatal dopamine system." Brain Research **102**(2): 201-215.

Jellinger, K. A. (1997). "Morphological substrates of dementia in parkinsonism. A critical update." Journal of Neural Transmission, Supplement(51): 57-82.

Jellinger, K. A., K. Seppi, et al. (2002). "Impact of coexistent Alzheimer pathology on the natural history of Parkinson's disease." Journal of Neural Transmission **109**(3): 329-339.

Jenner, P. (1993). "Altered mitochondrial function, iron metabolism and glutathione levels in Parkinson's disease." Acta Neurologica Scandinavica, Supplement **87**(146): 6-13.

Jenner, P., D. T. Dexter, et al. (1992). "Oxidative stress as a cause of nigral cell death in Parkinson's disease and incidental Lewy body disease." Annals of Neurology **32**(SUPPL.): S82-S87.

Jha, N., O. Jurma, et al. (2000). "Glutathione depletion in PC12 results in selective inhibition of mitochondrial complex I activity: Implications for Parkinson's disease." Journal of Biological Chemistry **275**(34): 26096-26101.

Jiang, X. and X. Wang (2004). "Cytochrome C-mediated apoptosis." Annu Rev Biochem **73**: 87-106.

Jiang, Z. (2008). An investigation of the neurotoxicity of trichloroethylene and its metabolite TaClo. PhD, Newcastle University.

Jiang, Z., E. Mutch, et al. (2007). "A Possible Mechanism for the Neurotoxicity of Trichloroethylene to Man." Toxicology Abstracts **240**: 164-192.

Jin, J., G. E. Meredith, et al. (2005). "Quantitative proteomic analysis of mitochondrial proteins: relevance to Lewy body formation and Parkinson's disease." Brain Res Mol Brain Res **134**(1): 119-138.

Jones, B. J. and D. J. Roberts (1968). "The quantiative measurement of motor inco-ordination in naive mice using an acelerating rotarod." Journal of Pharmacy and Pharmacology **20**(4): 302-304.

Jones, J. M., P. Datta, et al. (2003). "Loss of Omi mitochondrial protease activity causes the neuromuscular disorder of mnd2 mutant mice." Nature **425**(6959): 721-727.

Jones, J. M., P. Datta, et al. (2003). "Loss of Omi mitochondrial protease activity causes the neuromuscular disorder of mnd2 mutant mice." Nature **425**(6959): 721-727.

Junn, E., W. H. Jang, et al. (2009). "Mitochondrial localization of DJ-1 leads to enhanced neuroprotection." Journal of Neuroscience Research **87**(1): 123-129.

Kabeya, Y., N. Mizushima, et al. (2000). "LC3, a mammalian homologue of yeast Apg8p, is localized in autophagosome membranes after processing." EMBO Journal **19**(21): 5720-5728.

Kahle, P. J., M. Neumann, et al. (2000). "Subcellular localization of wild-type and Parkinson's disease-associated mutant α-synuclein in human and transgenic mouse brain." Journal of Neuroscience **20**(17): 6365-6373.

Kanazawa, T., T. Uchihara, et al. (2008). "Three-layered structure shared between Lewy bodies and lewy neurites-three-dimensional reconstruction of triple-labeled sections." Brain Pathol **18**(3): 415-422.

Kao, S. Y. (2009). "DNA damage induces nuclear translocation of parkin." Journal of Biomedical Science **16**(1).

Karl, P. I. and P. A. Friedman (1983). "Competition between paraquat and putrescine for accumulation by rat lung slices." Toxicology **26**(3-4): 317-323.

Kaufmann, P., K. Engelstad, et al. (2006). "Dichloroacetate causes toxic neuropathy in MELAS: A randomized, controlled clinical trial." Neurology **66**(3): 324-330.

Kaufmann, S. H., S. Desnoyers, et al. (1993). "Specific proteolytic cleavage of poly(ADP-ribose) polymerase: An early marker of chemotherapy-induced apoptosis." Cancer Research **53**(17): 3976-3985.

Kawamoto, Y., Y. Kobayashi, et al. (2008). "Accumulation of HtrA2/Omi in neuronal and glial inclusions in brains with α-synucleinopathies." Journal of Neuropathology and Experimental Neurology **67**(10): 984-993.

Keane, P. C., M. Kurzawa, et al. (2011). "Mitochondrial dysfunction in Parkinson's disease." Parkinson's Disease: 10.4061/2011/716871.

Keeney, P. M., J. Xie, et al. (2006). "Parkinson's Disease Brain Mitochondrial Complex I Has Oxidatively Damaged Subunits and Is Functionally Impaired and Misassembled." The Journal of Neuroscience **26**(19): 5256-5264.

Kerr, J. F., A. H. Wyllie, et al. (1972). "Apoptosis: a basic biological phenomenon with wide-ranging implications in tissue kinetics." British Journal of Cancer **26**(4): 239-257.

Khaindrava, V. G., P. V. Ershov, et al. (2010). "Optimization of counting process of dopaminergic neurons in substantia nigra of parkinsonian mice." Tsitologiya **52**(6): 423-430.

Khan, M. M., A. Ahmad, et al. (2010). "Resveratrol attenuates 6-hydroxydopamine-induced oxidative damage and dopamine depletion in rat model of Parkinson's disease." Brain Research **1328**: 139-151.

Khan, S., S. Priyamvada, et al. (2009). "Effect of trichloroethylene (TCE) toxicity on the enzymes of carbohydrate metabolism, brush border membrane and oxidative stress in kidney and other rat tissues." Food and Chemical Toxicology **47**(7): 1562-1568.

Khateeb, S., H. Flusser, et al. (2006). "PLA2G6 mutation underlies infantile neuroaxonal dystrophy." American Journal of Human Genetics **79**(5): 942-948.

Kim, R. H., P. D. Smith, et al. (2005). "Hypersensitivity of DJ-1-deficient mice to 1-methyl-4-phenyl-1,2,3,6- tetrahydropyrindine (MPTP) and oxidative stress." Proceedings of the National Academy of Sciences of the United States of America **102**(14): 5215-5220.

Kim, S., L. Dayani, et al. "RIP1 kinase mediates arachidonic acid-induced oxidative death of oligodendrocyte precursors." International Journal of Physiology, Pathophysiology and Pharmacology **2**(2): 137-147.

Kim, S. J., J. Y. Sung, et al. (2003). "Parkin Cleaves Intracellular α-Synuclein Inclusions via the Activation of Calpain." Journal of Biological Chemistry **278**(43): 41890-41899.

Kim, Y. S., M. J. Morgan, et al. (2007). "TNF-Induced Activation of the Nox1 NADPH Oxidase and Its Role in the Induction of Necrotic Cell Death." Molecular Cell **26**(5): 675-687.

Kirby, D. M., D. R. Thorburn, et al. (2007). "Biochemical Assays of Respiratory Chain Complex Activity." Methods in Cell Biology **80**: 93-119.

Kirches, E. (2009). "Do mtDNA mutations participate in the pathogenesis of sporadic Parkinson's disease?" Current Genomics **10**(8): 585-593.

Kirk, R., H. Laman, et al. (2008). "Structure of a conserved dimerization domain within the F-box protein Fbxo7 and the PI31 proteasome inhibitor." Journal of Biological Chemistry **283**(32): 22325-22335.

Kish, S. J., J. Tong, et al. (2008). "Preferential loss of serotonin markers in caudate versus putamen in Parkinson's disease." Brain **131**(1): 120-131.

Kitada, T., S. Asakawa, et al. (1998). "Mutations in the parkin gene cause autosomal recessive juvenile parkinsonism." Nature **392**(6676): 605-608.

Kitada, T., Y. Tong, et al. (2009). "Absence of nigral degeneration in aged parkin/DJ-1/PINK1 triple knockout mice." Journal of Neurochemistry **111**(3): 696-702.

Klegeris, A., S. Pelech, et al. (2008). "α-Synuclein activates stress signaling protein kinases in THP-1 cells and microglia." Neurobiology of Aging **29**(5): 739-752.

Klionsky, D. J. (2007). "Autophagy: From phenomenology to molecular understanding in less than a decade." Nature Reviews Molecular Cell Biology **8**(11): 931-937.

Klivenyi, P., D. St. Clair, et al. (1998). "Manganese superoxide dismutase overexpression attenuates MPTP toxicity." Neurobiology of Disease **5**(4): 253-258.

Kluin, K. J., N. L. Foster, et al. (1993). "Perceptual analysis of speech disorders in progressive supranuclear palsy." Neurology **43**(3 I): 563-566.

Knyihár-Csillik, E., B. Csillik, et al. (2004). "Decreased expression of kynurenine aminotransferase-I (KAT-I) in the substantia nigra of mice after 1-methyl-4-phenyl-1,2,3,6-tetrahydropyridine (MPTP) treatment." Neuroscience **126**(4): 899-914.

Kochen, W., D. Kohlmüller, et al. (2003). "The endogeneous formation of highly chlorinated tetrahydro-β- carbolines as a possible causative mechanism in idiopathic Parkinson's disease." **527**: 253-263.

Korner, A. and J. Pawelek (1982). "Mammalian tyrosinase catalyzes three reactions in the biosynthesis of melanin." Science **217**(4565): 1163-1165.

Korsmeyer, S. J., M. C. Wei, et al. (2000). "Pro-apoptotic cascade activates BID, which oligomerizes BAK or BAX into pores that result in the release of cytochrome c." Cell Death and Differentiation **7**(12): 1166-1173.

Kostić, V. S., B. M. Djuričić, et al. (1987). "Depression and parkinson's disease: possible role of serotonergic mechanisms." Journal of Neurology **234**(2): 94-96.

Kraytsberg, Y., E. Kudryavtseva, et al. (2006). "Mitochondrial DNA deletions are abundant and cause functional impairment in aged human substantia nigra neurons." Nature Genetics **38**(5): 518-520.

Krebiehl, G., S. Ruckerbauer, et al. (2010). "Reduced basal autophagy and impaired mitochondrial dynamics due to loss of Parkinson's disease-associated protein DJ-1." PLoS One **5**(2): e9367.

Kroemer, G., L. Galluzzi, et al. (2009). "Classification of cell death: Recommendations of the Nomenclature Committee on Cell Death 2009." Cell Death and Differentiation **16**(1): 3-11.

Kroemer, G. and B. Levine (2008). "Autophagic cell death: the story of a misnomer." Nat Rev Mol Cell Biol **9**(12): 1004-1010.

Krueger, M. J., A. K. Tan, et al. (1993). "Is complex II involved in the inhibition of mitochondrial respiration by N-methyl-4-phenylpyridinium cation (MMP+) and N-methyl-β-carbolines?" Biochemical Journal **291**(3): 673-676.

Kruger, R., W. Kuhn, et al. (1998). "Ala30Pro mutation in the gene encoding α-synuclein in Parkinson's disease." Nature Genetics **18**(2): 106-108.

Kruger, R., M. Sharma, et al. (2009). "A large-scale genetic association study to evaluate the contribution of Omi/HtrA2 (PARK13) to Parkinson's disease." Neurobiol Aging.

Kuhn, D. M., R. E. Arthur Jr, et al. (1999). "Tyrosine hydroxylase is inactivated by catechol-quinones and converted to a redox-cycling quinoprotein: Possible relevance to Parkinson's disease." Journal of Neurochemistry **73**(3): 1309-1317.

Kuhn, D. M., D. M. Francescutti-Verbeem, et al. (2006). Dopamine quinones activate microglia and induce a neurotoxic gene expression profile: Relationship to methamphetamine-induced nerve ending damage. **1074:** 31-41.

Kurlemann, G., I. Paetzke, et al. (1995). "Therapy of complex I deficiency: Peripheral neuropathy during dichloroacetate therapy." European Journal of Pediatrics **154**(11): 928-932.

Kuwahara, T., A. Koyama, et al. (2006). "Familial Parkinson mutant α-synuclein causes dopamine neuron dysfunction in transgenic Caenorhabditis elegans." Journal of Biological Chemistry **281**(1): 334-340.

Kuzuhara, S., H. Mori, et al. (1988). "Lewy bodies are ubiquitinated. A light and electron microscopic immunocytochemical study." Acta Neuropathol **75**(4): 345-353.

Laitinen, L. V., A. T. Bergenheim, et al. (1992). "LEKSELLS POSTEROVENTRAL PALLIDOTOMY IN THE TREATMENT OF PARKINSONS-DISEASE." Journal of Neurosurgery **76**(1): 53-61.

Lakso, M., S. Vartiainen, et al. (2003). "Dopaminergic neuronal loss and motor deficits in Caenorhabditis elegans overexpressing human α-synuclein." Journal of Neurochemistry **86**(1): 165-172.

Laman, H., J. M. Funes, et al. (2005). "Transforming activity of Fbxo7 is mediated specifically through regulation of cyclin D/cdk6." EMBO Journal **24**(17): 3104-3116.

Lambert, A. J. and M. D. Brand (2004). "Inhibitors of the quinone-binding site allow rapid superoxide production from mitochondrial NADH:ubiquinone oxidoreductase (complex I)." Journal of Biological Chemistry **279**(38): 39414-39420.

Langston, J. W., P. Ballard, et al. (1983). "Chronic parkinsonism in humans due to a product of meperidine-analog synthesis." Science **219**(4587): 979-980.

Lashuel, H. A., D. Hartley, et al. (2002). "Neurodegenerative disease: amyloid pores from pathogenic mutations." Nature **418**(6895): 291.

Lashuel, H. A., B. M. Petre, et al. (2002). "Alpha-synuclein, especially the Parkinson's disease-associated mutants, forms pore-like annular and tubular protofibrils." J Mol Biol **322**(5): 1089-1102.

Lass, A., S. Agarwal, et al. (1997). "Mitochondrial ubiquinone homologues, superoxide radical generation, and longevity in different mammalian species." Journal of Biological Chemistry **272**(31): 19199-19204.

Lautier, C., S. Goldwurm, et al. (2008). "Mutations in the GIGYF2 (TNRC15) Gene at the PARK11 Locus in Familial Parkinson Disease." American Journal of Human Genetics **82**(4): 822-833.

Lee, B. D., J. H. Shin, et al. (2010). "Inhibitors of leucine-rich repeat kinase-2 protect against models of Parkinson's disease." Nature Medicine **16**(9): 998-1000.

Lee, R. S., S. C. Steffensen, et al. (2001). "Discharge profiles of ventral tegmental area GABA neurons during movement, anesthesia, and the sleep-wake cycle." Journal of Neuroscience **21**(5): 1757-1766.

Lees, A. J., J. Hardy, et al. (2009). "Parkinson's disease." Lancet **373**(9680): 2055-2066.

Lees, A. J., J. Hardy, et al. (2009). "Parkinson's disease." The Lancet **373**(9680): 2055-2066.

Lein, E. S., M. J. Hawrylycz, et al. (2007). "Genome-wide atlas of gene expression in the adult mouse brain." Nature **445**(7124): 168-176.

Lemaire, C., K. Andréau, et al. (1998). "Inhibition of caspase activity induces a switch from apoptosis to necrosis." FEBS Letters **425**(2): 266-270.

Leng, Y. and D. M. Chuang (2006). "Endogenous α-synuclein is induced by valproic acid through histone deacetylase inhibition and participates in neuroprotection against glutamate-induced excitotoxicity." Journal of Neuroscience **26**(28): 7502-7512.

Leroy, E., R. Boyer, et al. (1998). "The ubiquitin pathway in Parkinson's disease [6]." Nature **395**(6701): 451-452.

Levine, B. and G. Kroemer (2008). "Autophagy in the Pathogenesis of Disease." Cell **132**(1): 27-42.

Lhermitte J, K., W.M., and McAlpine, D. (1924). "On the occurrence of abnormal deposits of iron in the brain in parkinsonism with special reference to its localisation." J. Neurol. Psychopathol. **5**: 195-208.

Li, H., H. Zhu, et al. (1998). "Cleavage of BID by caspase 8 mediates the mitochondrial damage in the Fas pathway of apoptosis." Cell **94**(4): 491-501.

Li, N., Y. He, et al. (2011). "D -galactose induces necroptotic cell death in neuroblastoma cell lines." Journal of Cellular Biochemistry **112**(12): 3834-3844.

Li, N., K. Ragheb, et al. (2003). "Mitochondrial complex I inhibitor rotenone induces apoptosis through enhancing mitochondrial reactive oxygen species production." Journal of Biological Chemistry **278**(10): 8516-8525.

Li, P., D. Nijhawan, et al. (1997). "Cytochrome c and dATP-dependent formation of Apaf-1/caspase-9 complex initiates an apoptotic protease cascade." Cell **91**(4): 479-489.

Li, X., J. C. Patel, et al. (2010). "Enhanced striatal dopamine transmission and motor performance with LRRK2 overexpression in mice is eliminated by familial Parkinson's disease mutation G2019S." Journal of Neuroscience **30**(5): 1788-1797.

Liang, X. H., S. Jackson, et al. (1999). "Induction of autophagy and inhibition of tumorigenesis by beclin 1." Nature **402**(6762): 672-676.

Licker, V., E. Kövari, et al. (2009). "Proteomics in human Parkinson's disease research." Journal of Proteomics **73**(1): 10-29.

Lill, R., R. Dutkiewicz, et al. (2006). "Mechanisms of iron-sulfur protein maturation in mitochondria, cytosol and nucleus of eukaryotes." Biochim Biophys Acta **1763**(7): 652-667.

Lin, M. T. and M. F. Beal (2006). "Mitochondrial dysfunction and oxidative stress in neurodegenerative diseases." Nature **443**: 778-795.

Lin, Y., A. Devin, et al. (1999). "Cleavage of the death domain kinase RIP by Caspase-8 prompts TNF-induced apoptosis." Genes and Development **13**(19): 2514-2526.

Lindersson, E., R. Beedholm, et al. (2004). "Proteasomal Inhibition by α-Synuclein Filaments and Oligomers." Journal of Biological Chemistry **279**(13): 12924-12934.

Lindersson, E. K., P. Højrup, et al. (2004). "α-synuclein filaments bind the transcriptional regulator HMGB-1." NeuroReport **15**(18): 2735-2739.

Liou, H. H., M. C. Tsai, et al. (1997). "Environmental risk factors and Parkinson's disease: A case-control study in Taiwan." Neurology **48**(6): 1583-1588.

Litvan, I., G. Campbell, et al. (1997). "Which clinical features differentiate progressive supranuclear palsy (Steele-Richardson-Olszewski syndrome) from related disorders? A clinicopathological study." Brain **120**(1): 65-74.

Liu, D., R. Gharavi, et al. (2009). "Nicotinamide prevents NAD + depletion and protects neurons against excitotoxicity and cerebral Ischemia: NAD + consumption by sirt1 may endanger energetically compromised neurons." NeuroMolecular Medicine **11**(1): 28-42.

Liu, M., D. Y. Choi, et al. (2010). "Trichloroethylene induces dopaminergic neurodegeneration in Fisher 344 rats." Journal of Neurochemistry **112**(3): 773-783.

Liu, W., C. Vives-Bauza, et al. (2009). "PINK1 Defect Causes Mitochondrial Dysfunction, Proteasomal Deficit and α-Synuclein Aggregation in Cell Culture Models of Parkinson's Disease." PLoS ONE **4**(2).

Liu, Y., L. Fallon, et al. (2002). "The UCH-L1 gene encodes two opposing enzymatic activities that affect α-synuclein degradation and Parkinson's disease susceptibility." Cell **111**(2): 209-218.

Liu, Z., X. Wang, et al. (2008). "A Drosophila model for LRRK2-linked parkinsonism." Proceedings of the National Academy of Sciences of the United States of America **105**(7): 2693-2698.

Lock, E. A. and C. J. Reed (2006). "Trichloroethylene: Mechanisms of renal toxicity and renal cancer and relevance to risk assessment." Toxicological Sciences **91**(2): 313-331.

Lotharius, J. and K. L. O'Malley (2000). "The Parkinsonism-inducing drug 1-methyl-4-phenylpyridinium triggers intracellular dopamine oxidation: A novel mechanism of toxicity." Journal of Biological Chemistry **275**(49): 38581-38588.

Lozano, A. M., A. E. Lang, et al. (1995). "Effect of GPI Pallidotomy on Motor Function in Parkinson's Disease." Lancet **346**(8987): 1383-1387.

Lu, K. T., M. C. Ko, et al. (2008). "Neuroprotective effects of resveratrol on MPTP-induced neuron loss mediated by free radical scavenging." Journal of Agricultural and Food Chemistry **56**(16): 6910-6913.

Lundvig, D., E. Lindersson, et al. (2005). "Pathogenic effects of α-synuclein aggregation." Molecular Brain Research **134**(1): 3-17.

Luo, X., I. Budihardjo, et al. (1998). "Bid, a Bcl2 interacting protein, mediates cytochrome c release from mitochondria in response to activation of cell surface death receptors." Cell **94**(4): 481-490.

Luoma, P., A. Melberg, et al. (2004). "Parkinsonism, premature menopause, and mitochondrial DNA polymerase γ mutations: Clinical and molecular genetic study." Lancet **364**(9437): 875-882.

Mackenzie, I. R. A., MD, FRCPC. (2001). "The pathology of Parkinson's disease." BCMJ **43**(3): 142-147 - Articles.

Mahoney, D. J., H. H. Cheung, et al. (2008). "Both cIAP1 and cIAP2 regulate TNFα-mediated NF-κB activation." Proceedings of the National Academy of Sciences of the United States of America **105**(33): 11778-11783.

Malagelada, C., Z. H. Jin, et al. (2010). "Rapamycin protects against neuron death in in vitro and in vivo models of Parkinson's disease." Journal of Neuroscience **30**(3): 1166-1175.

Maltoni C, Lefemine G, et al. (1986). Experimental research on trichloroethylene carcinogenesis. Archives of research on industrial carcinogenesis series, Princeton, NJ: Princeton Scientific Publishing Co. Inc. **V**.

Mandir, A. S., S. Przedborski, et al. (1999). "Poly(ADP-ribose) polymerase activation mediates 1-methyl-4-phenyl- 1,2,3,6-tetrahydropyridine (MPTP)-induced Parkinsonism." Proceedings of the National Academy of Sciences of the United States of America **96**(10): 5774-5779.

Mann, D. M. A. and D. Jones (1990). "Deposition of amyloid (A4) protein within the brains of persons with dementing disorders other than Alzheimer's disease and Down's syndrome." Neuroscience Letters **109**(1-2): 68-75.

Manning-Bog, A. B., A. L. McCormack, et al. (2002). "The herbicide paraquat causes up-regulation and aggregation of α-synuclein in mice: Paraquat and α-synuclein." Journal of Biological Chemistry **277**(3): 1641-1644.

Marella, M., B. B. Seo, et al. (2008). "Protection by the NDI1 gene against neurodegeneration in a rotenone rat model of Parkinson's disease." PLoS ONE **3**(1).

Margolis, E. B., A. R. Coker, et al. (2010). "Reliability in the identification of midbrain dopamine neurons." PLoS ONE **5**(12).

Marini, A. M., R. H. Lipsky, et al. (1992). "Accumulation of 1-methyl-4-phenyl-1,2,3,6-tetrahydropyridine in cultured cerebellar astrocytes." Journal of Neurochemistry **58**(4): 1250-1258.

Martin, L. J., Y. Pan, et al. (2006). "Parkinson's disease α-synuclein transgenic mice develop neuronal mitochondrial degeneration and cell death." Journal of Neuroscience **26**(1): 41-50.

Martínez Banaclocha, M. (2000). "N-Acetylcysteine elicited increase in complex I activity in synaptic mitochondria from aged mice: implications for treatment of Parkinson's disease." Brain Research **859**(1): 173-175.

Martínez, M., N. Martínez, et al. (1999). "Hypothesis: Can N-acetylcysteine be beneficial in Parkinson's disease?" Life Sciences **64**(15): 1253-1257.

Martins, L. M., A. Morrison, et al. (2004). "Neuroprotective role of the reaper-related serine protease HtrA2/Omi revealed by targeted deletion in mice." Molecular and Cellular Biology **24**(22): 9848-9862.

Mash, D. C., J. Pablo, et al. (1990). "Characterization and distribution of transferrin receptors in the rat brain." Journal of Neurochemistry **55**(6): 1972-1979.

Masliah, E., E. Rockenstein, et al. (2000). "Dopaminergic loss and inclusion body formation in α-synuclein mice: Implications for neurodegenerative disorders." Science **287**(5456): 1265-1269.

Mastroberardino, P. G., E. K. Hoffman, et al. (2009). "A novel transferrin/TfR2-mediated mitochondrial iron transport system is disrupted in Parkinson's disease." Neurobiology of Disease **34**(3): 417-431.

Matsubara, K., M. A. Collins, et al. (1993). "Potential bioactivated neurotoxicants, N-methylated-β-carbolinium ions, are present in human brain." Brain Research **610**(1): 90-96.

Matsuoka, Y., M. Vila, et al. (2001). "Lack of nigral pathology in transgenic mice expressing human α-synuclein driven by the tyrosine hydroxylase promoter." Neurobiology of Disease **8**(3): 535-539.

Matsuura, K., H. Kabuto, et al. (1997). "Pole test is a useful method for evaluating the mouse movement disorder caused by striatal dopamine depletion." Journal of Neuroscience Methods **73**(1): 45-48.

Mattila, P. M., J. O. Rinne, et al. (2000). "Alpha-synuclein-immunoreactive cortical Lewy bodies are associated with cognitive impairment in Parkinson's disease." Acta Neuropathologica **100**(3): 285-290.

Maull, E. A. and L. H. Lash (1998). "Trichloroethylene: A current review of metabolism, mode of action, and regulatory considerations." Toxic Substance Mechanisms **17**(2): 153-169.

Mayeaux, R., Y. Stern, et al. (1984). "Altered serotonin metabolism in depressed patients with Parkinson's disease." Neurology **34**(5): 642-646.

Mayeux, R., Y. Stern, et al. (1988). "The relationship of serotonin to depression in Parkinson's disease." Movement disorders : official journal of the Movement Disorder Society **3**(3): 237-244.

McCord, J. M., B. B. Keele Jr, et al. (1971). "An enzyme-based theory of obligate anaerobiosis: the physiological function of superoxide dismutase." Proceedings of the National Academy of Sciences of the United States of America **68**(5): 1024-1027.

McCormack, A. L. and D. A. Di Monte (2003). "Effects of L-dopa and other amino acids against paraquat-induced nigrostriatal degeneration." Journal of Neurochemistry **85**(1): 82-86.

McDermott, C., A. Allshire, et al. (2007). "Validation of a method for acute and subchronic exposure of cells in vitro to volatile organic solvents." Toxicology in Vitro **21**(1): 116-124.

McKeith, I., J. Mintzer, et al. (2004). "Dementia with Lewy bodies." Lancet Neurology **3**(1): 19-28.

McKeith, I. G., D. Galasko, et al. (1996). "Consensus guidelines for the clinical and pathologic diagnosis of dementia with Lewy bodies (DLB): report of the consortium on DLB international workshop." Neurology **47**(5): 1113-1124.

McNaught, K. S., P. Shashidharan, et al. (2002). "Aggresome-related biogenesis of Lewy bodies." Eur J Neurosci **16**(11): 2136-2148.

McNaught, K. S. P., R. Belizaire, et al. (2003). "Altered proteasomal function in sporadic Parkinson's disease." Experimental Neurology **179**(1): 38-46.

McNaught, K. S. P., R. Belizaire, et al. (2002). "Selective loss of 20S proteasome alpha-subunits in the substantia nigra pars compacta in Parkinson's disease." Neuroscience Letters **326**(3): 155-158.

McNaught, K. S. P. and P. Jenner (2001). "Proteasomal function is impaired in substantia nigra in Parkinson's disease." Neuroscience Letters **297**(3): 191-194.

McNaught, K. S. P., C. Mytilineou, et al. (2002). "Impairment of the ubiquitin-proteasome system causes dopaminergic cell death and inclusion body formation in ventral mesencephalic cultures." Journal of Neurochemistry **81**(2): 301-306.

McNaught, K. S. P., C. W. Olanow, et al. (2003). "Proteolytic stress: A unifying concept for the etiopathogenesis of Parkinson's disease." Annals of Neurology **53**(SUPPL. 3): S73-S86.

McNaught, K. S. P., U. Thull, et al. (1995). "Inhibition of complex I by isoquinoline derivatives structurally related to 1-methyl-4-phenyl-1,2,3,6-tetrahydropyridine (MPTP)." Biochemical Pharmacology **50**(11): 1903-1911.

Meredith, G. E., S. Totterdell, et al. (2009). "Impaired glutamate homeostasis and programmed cell death in a chronic MPTP mouse model of Parkinson's disease." Experimental Neurology **219**(1): 334-340.

Merims, D., R. Galili-Mosberg, et al. (2000). "Apomorphine: An underutilized therapy for Parkinson's disease." Movement Disorders **15**(5): 789-794.

Meulener, M., A. J. Whitworth, et al. (2005). "Drosophila DJ-1 mutants are selectively sensitive to environmental toxins associated with Parkinson's disease." Current Biology **15**(17): 1572-1577.

Mi, K. L., J. K. Soon, et al. (2007). "Resveratrol protects SH-SY5Y neuroblastoma cells from apoptosis induced by dopamine." Experimental and Molecular Medicine **39**(3): 376-384.

Micheau, O. and J. Tschopp (2003). "Induction of TNF receptor I-mediated apoptosis via two sequential signaling complexes." Cell **114**(2): 181-190.

Mihm, M. J., B. L. Schanbacher, et al. (2001). "Free 3-nitrotyrosine causes striatal neurodegeneration in vivo." The Journal of neuroscience : the official journal of the Society for Neuroscience **21**(11).

Miller, D. W., R. Ahmad, et al. (2003). "L166P mutant DJ-1, causative for recessive Parkinson's disease, is degraded through the ubiquitin-proteasome system." Journal of Biological Chemistry **278**(38): 36588-36595.

Miller, P. W., M. B. Mycyk, et al. (2002). "An unusual presentation of inhalant abuse with dissociative amnesia." Veterinary and Human Toxicology **44**(1): 17-19.

Mitani, H., Y. Shirayama, et al. (2006). "Plasma levels of homovanillic acid, 5-hydroxyindoleacetic acid and cortisol, and serotonin turnover in depressed patients." Progress in Neuro-Psychopharmacology and Biological Psychiatry **30**(3): 531-534.

Mitsumoto, A. and Y. Nakagawa (2001). "DJ-1 is an indicator for endogenous reactive oxygen species elicited by endotoxin." Free Radical Research **35**(6): 885-893.

Mitsumoto, A., Y. Nakagawa, et al. (2001). "Oxidized forms of peroxiredoxins and DJ-1 on two-dimensional gels increased in response to sublethal levels of paraquat." Free Radical Research **35**(3): 301-310.

Miyoshi, E., S. Wietzikoski, et al. (2002). "Impaired learning in a spatial working memory version and in a cued version of the water maze in rats with MPTP-induced mesencephalic dopaminergic lesions." Brain Research Bulletin **58**(1): 41-47.

Mizuno, Y., S. Ohta, et al. (1989). "Deficiencies in complex I subunits of the respiratory chain in Parkinson's disease." Biochemical and Biophysical Research Communications **163**(3): 1450-1455.

Mogi, M., M. Harada, et al. (1994). "Interleukin-1β, interleukin-6, epidermal growth factor and transforming growth factor-α are elevated in the brain from parkinsonian patients." Neuroscience Letters **180**(2): 147-150.

Mogi, M., M. Harada, et al. (1996). "Interleukin (IL)-1β, IL-2, IL-4, IL-6 and transforming growth factor-α levels are elevated in ventricular cerebrospinal fluid in juvenile parkinsonism and Parkinson's disease." Neuroscience Letters **211**(1): 13-16.

Mogi, M., M. Harada, et al. (1994). "Tumor necrosis factor-α (TNF-α) increases both in the brain and in the cerebrospinal fluid from parkinsonian patients." Neuroscience Letters **165**(1-2): 208-210.

Molina-Jiménez, M. F., M. I. Sánchez-Reus, et al. (2005). "Effect of fraxetin on antioxidant defense and stress proteins in human neuroblastoma cell model of rotenone neurotoxicity. Comparative study with myricetin and N-acetylcysteine." Toxicology and Applied Pharmacology **209**(3): 214-225.

Moreira, C. G., J. K. Barbiero, et al. (2012). "Behavioral, neurochemical and histological alterations promoted by bilateral intranigral rotenone administration: A new approach for an old neurotoxin." Neurotoxicity Research **21**(3): 291-301.

Morgan, M. J., Y. S. Kim, et al. (2008). "TNFα and reactive oxygen species in necrotic cell death." Cell Research **18**(3): 343-349.

Morgan, N. V., S. K. Westaway, et al. (2006). "PLA2G6, encoding a phospholipase A2, is mutated in neurodegenerative disorders with high brain iron." Nature Genetics **38**(7): 752-754.

Mori, H., T. Kondo, et al. (1998). "Pathologic and biochemical studies of juvenile parkinsonism linked to chromosome 6q." Neurology **51**(3): 890-892.

Morris, C. M., J. M. Candy, et al. (1994). "Transferrin receptors in the Parkinsonian midbrain." Neuropathology and Applied Neurobiology **20**(5): 468-472.

Moser, V. C., P. M. Phillips, et al. (1999). "Behavioral evaluation of the neurotoxicity produced by dichloroacetic acid in rats." Neurotoxicology and Teratology **21**(6): 719-731.

Moubarak, R. S., V. J. Yuste, et al. (2007). "Sequential activation of poly(ADP-ribose) polymerase 1, calpains, and bax is essential in apoptosis-inducing factor-mediated programmed necrosis." Molecular and Cellular Biology **27**(13): 4844-4862.

Muftuoglu, M., B. Elibol, et al. (2004). "Mitochondrial complex I and IV activities in leukocytes from patients with parkin mutations." Movement Disorders **19**(5): 544-548.

Muqit, M. M. K., S. M. Davidson, et al. (2004). "Parkin is recruited into aggresomes in a stress-specific manner: Over-expression of parkin reduces aggresome formation but can be dissociated from parkin's effect on neuronal survival." Human Molecular Genetics **13**(1): 117-135.

Murakami, T., M. Shoji, et al. (2004). "Pael-R Is Accumulated in Lewy Bodies of Parkinson's Disease." Annals of Neurology **55**(3): 439-442.

Na, S. J., A. G. DiLella, et al. (2010). "Molecular Profiling of a 6-Hydroxydopamine Model of Parkinson's Disease." Neurochemical Research: 1-12.

Nagatsu, T. (2002). "Parkinson's disease: Changes in apoptosis-related factors suggesting possible gene therapy." Journal of Neural Transmission **109**(5-6): 731-745.

Nagatsu, T. and M. Sawada (2006). "Cellular and molecular mechanisms of Parkinson's disease: neurotoxins, causative genes, and inflammatory cytokines." Cellular and molecular neurobiology **26**(4-6): 781-802.

Nagley, P., G. C. Higgins, et al. (2010). "Multifaceted deaths orchestrated by mitochondria in neurones." Biochimica et Biophysica Acta - Molecular Basis of Disease **1802**(1): 167-185.

Nakamura, K., V. M. Nemani, et al. (2008). "Optical reporters for the conformation of α-synuclein reveal a specific interaction with mitochondria." Journal of Neuroscience **28**(47): 12305-12317.

Nakatogawa, H., K. Suzuki, et al. (2009). "Dynamics and diversity in autophagy mechanisms: Lessons from yeast." Nature Reviews Molecular Cell Biology **10**(7): 458-467.

Nakayama, G. R., M. C. Caton, et al. (1997). "Assessment of the Alamar Blue assay for cellular growth and viability in vitro." Journal of Immunological Methods **204**(2): 205-208.

Nappi, A. J., E. Vass, et al. (1995). "The effects of hydroxyl radical attack on dopa, dopamine, 6-hydroxydopa, and 6-hydroxydopamine." Pigment cell research / sponsored by the

European Society for Pigment Cell Research and the International Pigment Cell Society **8**(6): 283-293.

Narendra, D., A. Tanaka, et al. (2008). "Parkin is recruited selectively to impaired mitochondria and promotes their autophagy." Journal of Cell Biology **183**(5): 795-803.

Narendra, D. P., S. M. Jin, et al. (2010). "PINK1 is selectively stabilized on impaired mitochondria to activate Parkin." PLoS Biol **8**(1): e1000298.

Narendra, D. P., S. M. Jin, et al. (2010). "PINK1 is selectively stabilized on impaired mitochondria to activate Parkin." PLoS Biology **8**(1).

Nass, R., D. H. Hall, et al. (2002). "Neurotoxin-induced degeneration of dopamine neurons in Caenorhabditis elegans." Proceedings of the National Academy of Sciences of the United States of America **99**(5): 3264-3269.

Nath, U., Y. Ben-Shlomo, et al. (2003). "Clinical features and natural history of progressive supranuclear palsy: A clinical cohort study." Neurology **60**(6): 910-916.

Nath, U., Y. Ben-Shlomo, et al. (2001). "The prevalence of progressive supranuclear palsy (Steele-Richardson-Olszewski syndrome) in the UK." Brain **124**(7): 1438-1449.

Navarro, A., A. Boveris, et al. (2009). "Human brain cortex: mitochondrial oxidative damage and adaptive response in Parkinson disease and in dementia with Lewy bodies." Free Radical Biology and Medicine **46**(12): 1574-1580.

Neumann, M., P. J. Kahle, et al. (2002). "Misfolded proteinase K-resistant hyperphosphorylated α-synuclein in aged transgenic mice with locomotor deterioration and in human α-synucleinopathies." Journal of Clinical Investigation **110**(10): 1429-1439.

Ng, C. H., S. Z. S. Mok, et al. (2009). "Parkin protects against LRRK2 G2019S mutant-induced dopaminergic neurodegeneration in Drosophila." Journal of Neuroscience **29**(36): 11257-11262.

Nicholls, D. G. and S. L. Budd (1998). "Neuronal excitotoxicity: The role of mitochondria." BioFactors **8**(3-4): 287-299.

Nichols, W. C., D. K. Kissell, et al. (2009). "Variation in GIGYF2 is not associated with Parkinson disease." Neurology **72**(22): 1886-1892.

Nicholson, D. W., A. Ali, et al. (1995). "Identification and inhibition of the ICE/CED-3 protease necessary for mammalian apoptosis." Nature **376**(6535): 37-43.

Nicklas, W. J., I. Vyas, et al. (1985). "Inhibition of NADH-linked oxidation in brain mitochondria by 1-methyl-4-phenyl-pyridine, a metabolite of the neurotoxin, 1-methyl-4-phenyl-1,2,5,6-tetrahydropyridine." Life Sciences **36**(26): 2503-2508.

Nicklas, W. J., S. K. Youngster, et al. (1987). "MPTP, MPP+ and mitochondrial function." Life Sciences **40**(8): 721-729.

Nishikawa, K., H. Li, et al. (2003). "Alterations of structure and hydrolase activity of parkinsonism-associated human ubiquitin carboxyl-terminal hydrolase L1 variants." Biochemical and Biophysical Research Communications **304**(1): 176-183.

Nuber, S., E. Petrasch-Parwez, et al. (2011). "Olfactory neuron-specific expression of A30P alpha-synuclein exacerbates dopamine deficiency and hyperactivity in a novel conditional model of early Parkinson's disease stages." Neurobiology of Disease **44**(2): 192-204.

Oakley, A. E., J. F. Collingwood, et al. (2007). "Individual dopaminergic neurons show raised iron levels in Parkinson disease." Neurology **68**(21): 1820-1825.

Ogawa, N., Y. Hirose, et al. (1985). "A simple quantitative bradykinesia test in MPTP-treated mice." Research Communications in Chemical Pathology and Pharmacology **50**(3): 435-441.

Ogawa, T., W. R. Matson, et al. (1992). "Kynurenine pathway abnormalities in Parkinson's disease." Neurology **42**(9): 1702-1706.

Ohta, M., T. Saito, et al. (2001). "Effect of trichloroethylene on spatiotemporal pattern of LTP in mouse hippocampal slices." International Journal of Neuroscience **111**(3-4): 257-271.

Olanow, C. W. (1993). "A rationale for monoamine oxidase inhibition as neuroprotective therapy for Parkinson's disease." Movement Disorders **8**(SUPPL. 1): S1-S7.

Olanow, C. W., D. P. Perl, et al. (2004). "Lewy-body formation is an aggresome-related process: a hypothesis." Lancet Neurol **3**(8): 496-503.

Oldendorf, W. H. and J. Szabo (1976). "Amino acid assignment to one of three blood brain barrier amino acid carriers." American Journal of Physiology **230**(1): 94-98.

Orth, M., S. J. Tabrizi, et al. (2004). "G209A mutant alpha synuclein expression specifically enhances dopamine induced oxidative damage." Neurochemistry International **45**(5): 669-676.

Osaka, H., Y. L. Wang, et al. (2003). "Ubiquitin carboxy-terminal hydrolase L1 binds to and stabilizes monoubiquitin in neuron." Human Molecular Genetics **12**(16): 1945-1958.

Östergren, A., A. Annas, et al. (2004). "Long-term retention of neurotoxic β-carbolines in brain neuromelanin." Journal of Neural Transmission **111**(2): 141-157.

Östergren, A., A. Fredriksson, et al. (2006). "Norharman-induced motoric impairment in mice: Neurodegeneration and glial activation in substantia nigra." Journal of Neural Transmission **113**(3): 313-329.

Outeiro, T. F., E. Kontopoulos, et al. (2007). "Sirtuin 2 inhibitors rescue α-synuclein-mediated toxicity in models of Parkinson's disease." Science **317**(5837): 516-519.

Owen, A. M., M. James, et al. (1992). "Fronto-striatal cognitive deficits at different stages of Parkinson's disease." Brain **115**(6): 1727-1751.

Ozaki, N., D. Nakahara, et al. (1987). "Acute effects of 1-methyl-4-phenylpyridinium ion (MPP+) on dopamine and serotonin metabolism in rat striatum as assayed in vivo by a micro-dialysis technique." Journal of Neural Transmission **70**(3-4): 241-250.

Öztaş, E. and T. Topal (2003). "A cell protective mechanism in a murine model of Parkinson's disease." Turkish Journal of Medical Sciences **33**(5): 295-299.

Palacino, J. J., D. Sagi, et al. (2004). "Mitochondrial Dysfunction and Oxidative Damage in parkin-deficient Mice." Journal of Biological Chemistry **279**(18): 18614-18622.

Pan-Montojo, F., O. Anichtchik, et al. (2010). "Progression of Parkinson's disease pathology is reproduced by intragastric administration of rotenone in mice." PLoS ONE **5**(1).

Pan, T., S. Kondo, et al. (2008). "The role of autophagy-lysosome pathway in neurodegeneration associated with Parkinson's disease." Brain **131**(8): 1969-1978.

Pan, T., P. Rawal, et al. (2009). "Rapamycin protects against rotenone-induced apoptosis through autophagy induction." Neuroscience **164**(2): 541-551.

Pang, Z. and J. W. Geddes (1997). "Mechanisms of cell death induced by the mitochondrial toxin 3- nitropropionic acid: Acute excitotoxic necrosis and delayed apoptosis." Journal of Neuroscience **17**(9): 3064-3073.

Papp, M. I., J. E. Kahn, et al. (1989). "Glial cytoplasmic inclusions in the CNS of patients with multiple system atrophy (striatonigral degeneration, olivopontocerebellar atrophy and Shy-Drager syndrome)." Journal of the Neurological Sciences **94**(1-3): 79-100.

Park, J., S. B. Lee, et al. (2006). "Mitochondrial dysfunction in Drosophila PINK1 mutants is complemented by parkin." Nature **441**(7097): 1157-1161.

Park, J. S., S. H. Lee, et al. (2012). "Age- and oxidative stress-induced DNA damage in Drosophila intestinal stem cells as marked by Gamma-H2AX." Experimental Gerontology **47**(5): 401-405.

Park, J. S., P. Mehta, et al. (2011). "Pathogenic effects of novel mutations in the P-type ATPase ATP13A2 (PARK9) causing Kufor-Rakeb syndrome, a form of early-onset parkinsonism." Human Mutation **32**(8): 956-964.

Parker Jr., W. D., J. K. Parks, et al. (2008). "Complex I deficiency in Parkinson's disease frontal cortex." Brain Research **1189**: 215-218.

Patil, S. S., B. Sunyer, et al. (2009). "Evaluation of spatial memory of C57BL/6J and CD1 mice in the Barnes maze, the Multiple T-maze and in the Morris water maze." Behavioural Brain Research **198**(1): 58-68.

Perez, R. G., J. C. Waymire, et al. (2002). "A role for α-synuclein in the regulation of dopamine biosynthesis." Journal of Neuroscience **22**(8): 3090-3099.

Petit, A., T. Kawarai, et al. (2005). "Wild-type PINK1 prevents basal and induced neuronal apoptosis, a protective effect abrogated by Parkinson disease-related mutations." Journal of Biological Chemistry **280**(40): 34025-34032.

Petroske, E., G. E. Meredith, et al. (2001). "Mouse model of Parkinsonism: a comparison between subacute MPTP and chronic MPTP/probenecid treatment." Neuroscience **106**(3): 589-601.

Pfister, J. A., C. Ma, et al. (2008). "Opposing effects of sirtuins on neuronal survival: SIRT1-mediated neuroprotection is independent of its deacetylase activity." PLoS ONE **3**(12).

Pillon, B., B. Deweer, et al. (1994). "Are explicit memory disorders of progressive supranuclear palsy related to damage to striatofrontal circuits? Comparison with Alzheimer's Parkinson's, and Huntington's diseases." Neurology **44**(7): 1264-1270.

Plaas, M., A. Karis, et al. (2008). "Alpha-synuclein A30P point-mutation generates age-dependent nigrostriatal deficiency in mice." Journal of Physiology and Pharmacology **59**(2): 205-216.

Plowey, E. D., S. J. Cherra Iii, et al. (2008). "Role of autophagy in G2019S-LRRK2-associated neurite shortening in differentiated SH-SY5Y cells." Journal of Neurochemistry **105**(3): 1048-1056.

Plun-Favreau, H., K. Klupsch, et al. (2007). "The mitochondrial protease HtrA2 is regulated by Parkinson's disease-associated kinase PINK1." Nature Cell Biology **9**(11): 1243-1252.

Pollock, N. J., S. S. Mirra, et al. (1986). "Filamentous aggregates in Pick's disease, progressive supranuclear palsy, and Alzheimer's disease share antigenic determinants with microtubule-associated protein, tau." Lancet **2**(8517): 1211.

Polymeropoulos, M. H., C. Lavedan, et al. (1997). "Mutation in the α-synuclein gene identified in families with Parkinson's disease." Science **276**(5321): 2045-2047.

Ponsen, M. M., D. Stoffers, et al. (2004). "Idiopathic hyposmia as a preclinical sign of Parkinson's disease." Annals of Neurology **56**(2): 173-181.

Posadas, I., P. Santos, et al. (2012). "Acetaminophen Induces Human Neuroblastoma Cell Death through NFKB Activation." PLoS ONE **7**(11).

Prasad, K. N., W. C. Cole, et al. (1999). "Multiple antioxidants in the prevention and treatment of Parkinson's disease." Journal of the American College of Nutrition **18**(5): 413-423.

Presgraves, S. P., T. Ahmed, et al. (2003). "Terminally differentiated SH-SY5Y cells provide a model system for studying neuroprotective effects of dopamine agonists." Neurotoxicity Research **5**(8): 579-598.

Przedborski, S., Q. Chen, et al. (2001). "Oxidative post-translational modifications of α-synuclein in the 1-methyl-4-phenyl- 1,2,3,6-tetrahydropyridine (MPTP) mouse model of Parkinson's disease." Journal of Neurochemistry **76**(2): 637-640.

Przedborski, S., V. Jackson-Lewis, et al. (2000). "The parkinsonian toxin MPTP: Action and mechanism." Restorative Neurology and Neuroscience **16**(2): 135-142.

Przedborski, S., V. Jackson-Lewis, et al. (2001). "The parkinsonian toxin 1-methyl-4-phenyl-1,2,3,6-tetrahydropyridine (MPTP): A technical review of its utility and safety." Journal of Neurochemistry **76**(5): 1265-1274.

Przedborski, S., K. Tieu, et al. (2004). "MPTP as a mitochondrial neurotoxic model of Parkinson's disease." Journal of Bioenergetics and Biomembranes **36**(4 SPEC.ISS.): 375-379.

Przedborski, S. and M. Vila (2001). "MPTP: A review of its mechanisms of neurotoxicity." Clinical Neuroscience Research **1**(6): 407-418.

Przuntek, H., B. Conrad, et al. (1999). "SELEDO: A 5-year long-term trial on the effect of selegiline in early parkinsonian patients treated with levodopa." European Journal of Neurology **6**(2): 141-150.

Puthalakath, H., L. A. O'Reilly, et al. (2007). "ER Stress Triggers Apoptosis by Activating BH3-Only Protein Bim." Cell **129**(7): 1337-1349.

Pycock, C. J., R. W. Kerwin, et al. (1980). "Effect of lesion of cortical dopamine terminals on subcortical dopamine receptors in rats." Nature **286**(5768): 74-77.

Rabey, J. M., I. Sagi, et al. (2000). "Rasagiline Mesylate, a New Mao-B Inhibitor for the Treatment of Parkinson's Disease: A Double-Blind Study as Adjunctive Therapy to Levodopa." Clinical Neuropharmacology **23**(6): 324-330.

Radi, R., J. S. Beckman, et al. (1991). "Peroxynitrite oxidation of sulfhydryls: The cytotoxic potential of superoxide and nitric oxide." Journal of Biological Chemistry **266**(7): 4244-4250.

Ramana, C. V., P. Patel, et al. (2010). "A combined experimental and density functional theory study on the Pd-mediated cycloisomerization of o-alkynylnitrobenzenes - Synthesis of isatogens and their evaluation as modulators of ROS-mediated cell death." European Journal of Organic Chemistry(31): 5955-5966.

Rami, A. (2003). "Ischemic neuronal death in the rat hippocampus: The calpain-calpastatin-caspase hypothesis." Neurobiology of Disease **13**(2): 75-88.

Ramirez, A., A. Heimbach, et al. (2006). "Hereditary parkinsonism with dementia is caused by mutations in ATP13A2, encoding a lysosomal type 5 P-type ATPase." Nature Genetics **38**(10): 1184-1191.

Ramonet, D., J. P. L. Daher, et al. (2011). "Dopaminergic Neuronal loss, Reduced Neurite Complexity and Autophagic Abnormalities in Transgenic Mice Expressing G2019S Mutant LRRK2." PLoS ONE **6**(4).

Ramot, Y., S. Ben-Eliahu, et al. (2009). "Subcutaneous and intraperitoneal lipogranulomas following subcutaneous injection of olive oil in Sprague-Dawley rats." Toxicologic Pathology **37**(7): 882-886.

Rana, M., I. De Coo, et al. (2000). "An out-of-frame cytochrome b gene deletion from a patient with parkinsonism is associated with impaired complex III assembly and an increase in free radical production." Annals of Neurology **48**(5): 774-781.

Rappold, P. M., M. Cui, et al. (2011). "Paraquat neurotoxicity is mediated by the dopamine transporter and organic cation transporter-3." Proceedings of the National Academy of Sciences of the United States of America **108**(51): 20766-20771.

Rathke-Hartlieb, S., P. J. Kahle, et al. (2001). "Sensitivity to MPTP is not increased in Parkinson's disease-associated mutant α-synuclein transgenic mice." Journal of Neurochemistry **77**(4): 1181-1184.

Rausch, W. D., M. Abdel-Mohsen, et al. (1995). "Studies of the potentially endogenous toxin TaClo (1-trichloromethyl-1,2,3,4-tetrahydro-β-carboline) in neuronal and glial cell cultures." Journal of Neural Transmission, Supplement(46): 255-263.

Reif, J. S., J. B. Burch, et al. (2003). "Neurobehavioral effects of exposure to trichloroethylene through a municipal water supply." Environmental Research **93**(3): 248-258.

Reiter, C. D., R.-J. Teng, et al. (2000). "Superoxide Reacts with Nitric Oxide to Nitrate Tyrosine at Physiological pH via Peroxynitrite." Journal of Biological Chemistry **275**: 32460-23466.

Richardson, J. R., Y. Quan, et al. (2005). "Paraquat neurotoxicity is distinct from that of MPTP and rotenone." Toxicological Sciences **88**(1): 193-201.

Riedel, O., J. Klotsche, et al. (2008). "Cognitive impairment in 873 patients with idiopathic Parkinson's disease: Results from the German Study on Epidemiology of Parkinson's Disease with Dementia (GEPAD)." Journal of Neurology **255**(2): 255-264.

Riederer, P., W. Birkmayer, et al. (1977). "Brain-noradrenaline and 3-methoxy-4-hydroxyphenylglycol in Parkinson's syndrome." Journal of Neural Transmission - General Section **41**(4): 241-251.

Riederer, P., P. Foley, et al. (2002). "Biochemical and pharmacological characterization of 1-trichloromethyl-1,2,3,4-tetrahydro-β-carboline: A biologically relevant neurotoxin?" European Journal of Pharmacology **442**(1-2): 1-16.

Rink, E. and M. F. Wullimann (2002). "Connections of the ventral telencephalon and tyrosine hydroxylase distribution in the zebrafish brain (Danio rerio) lead to identification of an ascending dopaminergic system in a teleost." Brain Research Bulletin **57**(3-4): 385-387.

Rinne, J. O., M. S. Lee, et al. (1994). "Corticobasal degeneration: A clinical study of 36 cases." Brain **117**(5): 1183-1196.

Rinne, U. K. and V. Sonninen (1973). "Brain catecholamines and their metabolites in Parkinsonian patients. Treatment with levodopa alone or combined with a decarboxylase inhibitor." Archives of Neurology **28**(2): 107-110.

Robinson, S., P. Freeman, et al. (2003). "Acute and subchronic MPTP administration differentially affects striatal glutamate synaptic function." Experimental Neurology **180**(1): 73-86.

Rogakou, E. P., D. R. Pilch, et al. (1998). "DNA Double-stranded Breaks Induce Histone H2AX Phosphorylation on Serine 139." Journal of Biological Chemistry **273**(10): 5858-5868.

Rojo, A., R. S. Pernaute, et al. (1999). "Clinical genetics of familial progressive supranuclear palsy." Brain **122**: 1233-1245.

Rommelfanger, K. S., G. L. Edwards, et al. (2007). "Norepinephrine loss produces more profound motor deficits than MPTP treatment in mice." Proceedings of the National Academy of Sciences of the United States of America **104**(34): 13804-13809.

Ross, C. A. and M. A. Poirier (2004). "Protein aggregation and neurodegenerative disease." Nature Medicine **10**(SUPPL.): S10-S17.

Ross, G. W., H. Petrovitch, et al. (2008). "Association of olfactory dysfunction with risk for future Parkinson's disease." Annals of Neurology **63**(2): 167-173.

Ross, O. A., C. Vilariño-Güell, et al. (2010). "Reply to: SNCA variants are associated with increased risk of multiple system atrophy." Annals of Neurology **67**(3): 414-415.

Ross, R. A., B. A. Spengler, et al. (1983). "Coordinate morphological and biochemical interconversion of human neuroblastoma cells." Journal of the National Cancer Institute **71**(4): 741-747.

Rossignol, R., R. Gilkerson, et al. (2004). "Energy Substrate Modulates Mitochondrial Structure and Oxidative Capacity in Cancer Cells." Cancer Research **64**(3): 985-993.

Rousselet, E., C. Joubert, et al. (2003). "Behavioral changes are not directly related to striatal monoamine levels, number of nigral neurons, or dose of parkinsonian toxin MPTP in mice." Neurobiology of Disease **14**(2): 218-228.

Saftig, P., W. Beertsen, et al. (2008). "LAMP-2: A control step fot phagosome and autophagosome maturation." Autophagy **4**(4): 510-512.

Saggu, H., J. Cooksey, et al. (1989). "A selective increase in particulate superoxide dismutase activity in parkinsonian substantia nigra." Journal of Neurochemistry **53**(3): 692-697.

Sallinen, V., J. Kolehmainen, et al. (2010). "Dopaminergic cell damage and vulnerability to MPTP in Pink1 knockdown zebrafish." Neurobiology of Disease **40**(1): 93-101.

Sanders L.H., Mastroberardino P. G., et al. (2010). "DNA damage precedes cell death in rotenone rat model of Parkinson's disease." Neuroscience **Poster 252**.

Sas, K., H. Robotka, et al. (2007). "Mitochondria, metabolic disturbances, oxidative stress and the kynurenine system, with focus on neurodegenerative disorders." Journal of the Neurological Sciences **257**(1–2): 221-239.

Sauerbeck, A., R. Hunter, et al. (2012). "Traumatic brain injury and trichloroethylene exposure interact and produce functional, histological, and mitochondrial deficits." Experimental Neurology **234**(1): 85-94.

Scatton, B., F. Javoy-Agid, et al. (1983). "Reduction of cortical dopamine, noradrenaline, serotonin and their metabolites in Parkinson's disease." Brain Research **275**(2): 321-328.

Schallert, T., S. M. Fleming, et al. (2000). "CNS plasticity and assessment of forelimb sensorimotor outcome in unilateral rat models of stroke, cortical ablation, parkinsonism and spinal cord injury." Neuropharmacology **39**(5): 777-787.

Schapira, A. H. V., J. M. Cooper, et al. (1990). "Mitochondrial Complex I deficiency in Parkinson's disease." Journal of Neurochemistry **54**(3): 823-827.

Schapira, A. H. V., V. M. Mann, et al. (1990). "Anatomic and disease specificity of NADH CoQ1 reductase (complex I) deficiency in Parkinson's disease." Journal of Neurochemistry **55**(6): 2142-2145.

Scherfler, C., Z. Puschban, et al. (2000). "Complex motor disturbances in a sequential double lesion rat model of striatonigral degeneration (multiple system atrophy)." Neuroscience **99**(1): 43-54.

Schlame, M. and H. C. Hemmings Jr (1995). "Inhibition by volatile anesthetics of endogenous glutamate release from synaptosomes by a presynaptic mechanism." Anesthesiology **82**(6): 1406-1416.

Schlossmacher, M. G., M. P. Frosch, et al. (2002). "Parkin localizes to the Lewy bodies of Parkinson disease and dementia with Lewy bodies." American Journal of Pathology **160**(5): 1655-1667.

Schmidt, C. J., C. K. Black, et al. (1990). "Chloral hydrate anesthesia antagonizes the neurotoxicity of 3,4-methylenedioxymethamphetamine." European Journal of Pharmacology **191**(2): 213-216.

Schmidt, M. L., J. Murray, et al. (1991). "Epitope map of neurofilament protein domains in cortical and peripheral nervous system Lewy bodies." Am J Pathol **139**(1): 53-65.

Schmidt, S. K., S. Siepmann, et al. (2012). "Influence of Tryptophan Contained in 1-Methyl-Tryptophan on Antimicrobial and Immunoregulatory Functions of Indoleamine 2,3-Dioxygenase." PLoS ONE **7**(9): e44797.

Schneider, S. A., C. Paisan-Ruiz, et al. (2010). "ATP13A2 mutations (PARK9) cause neurodegeneration with brain iron accumulation." Movement Disorders **25**(8): 979-984.

Scholz, S. W., H. Houlden, et al. (2009). "SNCA variants are associated with increased risk for multiple system atrophy." Annals of Neurology **65**(5): 610-614.

Schrag, A., Y. Ben-Shlomo, et al. (2000). "Cross sectional prevalence survey of idiopathic Parkinson's disease and parkinsonism in London." British Medical Journal **321**(7252): 21-22.

Schrag, A., G. K. Wenning, et al. (2008). "Survival in multiple system atrophy." Movement Disorders **23**(2): 294-296.

Schulze-Osthoff, K., A. C. Bakker, et al. (1992). "Cytotoxic activity of tumor necrosis factor is mediated by early damage of mitochondrial functions. Evidence for the involvement of mitochondrial radical generation." Journal of Biological Chemistry **267**(8): 5317-5323.

Sechi, G. P., V. Agnetti, et al. (1992). "Acute and persistent parkinsonism after use of diquat." Neurology **42**(1): 261-263.

Sedelis, M., K. Hofele, et al. (2000). "MPTP susceptibility in the mouse: Behavioral, neurochemical, and histological analysis of gender and strain differences." Behavior Genetics **30**(3): 171-182.

Sedelis, M., R. K. W. Schwarting, et al. (2001). "Behavioral phenotyping of the MPTP mouse model of Parkinson's disease." Behavioural Brain Research **125**(1–2): 109-125.

Seleznev, K., C. Zhao, et al. (2006). "Calcium-independent phospholipase A2 localizes in and protects mitochondria during apoptotic induction by staurosporine." Journal of Biological Chemistry **281**(31): 22275-22288.

Seniuk, N. A., W. G. Tatton, et al. (1990). "Dose-dependent destruction of the coeruleus-cortical and nigral-striatal projections by MPTP." Brain Research **527**(1): 7-20.

Seo, M., K. Ikeda, et al. (2008). "Enhancing effect of chlorinated organic solvents on histamine release and inflammatory mediator production." Toxicology **243**(1-2): 75-83.

Setsuie, R., Y. L. Wang, et al. (2007). "Dopaminergic neuronal loss in transgenic mice expressing the Parkinson's disease-associated UCH-L1 I93M mutant." Neurochemistry International **50**(1): 119-129.

Shaheen, V. M., M. Satoh, et al. (1999). "Immunopathogenesis of environmentally induced lupus in mice." Environmental Health Perspectives **107**(SUPPL. 5): 723-727.

Shaik, I. H. and R. Mehvar (2006). "Rapid determination of reduced and oxidized glutathione levels using a new thiol-masking reagent and the enzymatic recycling method:

Application to the rat liver and bile samples." Analytical and Bioanalytical Chemistry **385**(1): 105-113.

Shannon, K. M., J. P. Bennett Jr, et al. (1997). "Efficacy of pramipexole, a novel dopamine agonist, as monotherapy in mild to moderate Parkinson's disease." Neurology **49**(3): 724-728.

Sharma, A., P. Kaur, et al. (2007). "Attenuation of 1-methyl-4-phenyl-1, 2,3,6-tetrahydropyridine induced nigrostriatal toxicity in mice by N-acetyl cysteine." Cellular and Molecular Biology **53**(1): 48-55.

Sheehan, J. P., R. H. Swerdlow, et al. (1997). "Altered calcium homeostasis in cells transformed by mitochondria from individuals with Parkinson's disease." Journal of Neurochemistry **68**(3): 1221-1233.

Shen, Y. and M. Y. Ye (1994). "Determination of the stability of dopamine in aqueous solutions by high performance liquid chromatography." Journal of Liquid Chromatography **17**(7): 1557-1565.

Sherer, T. B., R. Betarbet, et al. (2002). "Environment, mitochondria, and Parkinson's disease." Neuroscientist **8**(3): 192-197.

Sherer, T. B., R. Betarbet, et al. (2002). "An in vitro model of Parkinson's disease: Linking mitochondrial impairment to altered α-synuclein metabolism and oxidative damage." Journal of Neuroscience **22**(16): 7006-7015.

Sherer, T. B., R. Betarbet, et al. (2003). "Mechanism of Toxicity in Rotenone Models of Parkinson's Disease." Journal of Neuroscience **23**(34): 10756-10764.

Sherer, T. B., P. A. Trimmer, et al. (2001). "Chronic reduction in complex I function alters calcium signaling in SH-SY5Y neuroblastoma cells." Brain Research **891**(1-2): 94-105.

Shimoda-Matsubayashi, S., H. Matsumine, et al. (1996). "Structural dimorphism in the mitochondrial targeting sequence in the human manganese superoxide dismutase gene. A predictive evidence for conformational change to influence mitochondrial transport and a study of allelic association in Parkinson's disease." Biochemical and Biophysical Research Communications **226**(2): 561-565.

Shimura, H., N. Hattori, et al. (2000). "Familial Parkinson disease gene product, parkin, is a ubiquitin-protein ligase." Nature Genetics **25**(3): 302-305.

Shimura, H., M. G. Schlossmacher, et al. (2001). "Ubiquitination of a new form of α-synuclein by parkin from human brain: Implications for Parkinson's disease." Science **293**(5528): 263-269.

Shinde, S. and K. Pasupathy (2006). "Respiratory-chain enzyme activities in isolated mitochondria of lymphocytes from patients with Parkinson's disease: Preliminary study." Neurology India **54**(4): 390-393.

Shu, H. D., M. Takeuchi, et al. (1996). "The tumor necrosis factor receptor 2 signal transducers TRAF2 and c-IAP1 are components of the tumor necrosis factor receptor 1 signaling complex." Proceedings of the National Academy of Sciences of the United States of America **93**(24): 13973-13978.

Shults, C. W., R. H. Haas, et al. (1997). "Coenzyme Q10 levels correlate with the activities of complexes I and II/III in mitochondria from Parkinsonian and nonparkinsonian subjects." Annals of Neurology **42**(2): 261-264.

Sian, J., D. T. Dexter, et al. (1994). "Alterations in glutathione levels in Parkinson's disease and other neurodegenerative disorders affecting basal ganglia." Annals of Neurology **36**(3): 348-355.

Silverman, J. and W. W. Muir Iii (1993). "A review of laboratory animal anesthesia with chloral hydrate and chloralose." Laboratory Animal Science **43**(3): 210-216.

Silvestri, L., V. Caputo, et al. (2005). "Mitochondrial import and enzymatic activity of PINK1 mutants associated to recessive parkinsonism." Human Molecular Genetics **14**(22): 3477-3492.

Singaram, C., E. A. Gaumnitz, et al. (1995). "Dopaminergic defect of enteric nervous system in Parkinson's disease patients with chronic constipation." The Lancet **346**(8979): 861-864.

Slee, E. A., C. Adrain, et al. (2001). "Executioner Caspase-3, -6, and -7 Perform Distinct, Non-redundant Roles during the Demolition Phase of Apoptosis." Journal of Biological Chemistry **276**(10): 7320-7326.

Slee, E. A., H. Zhu, et al. (1996). "Benzyloxycarbonyl-Val-Ala-Asp (OMe) fluoromethylketone (Z-VAD.FMK) inhibits apoptosis by blocking the processing of CPP32." Biochemical Journal **315**(1): 21-24.

Smith, L. A., M. J. Jackson, et al. (2005). "Multiple small doses of levodopa plus entacapone produce continuous dopaminergic stimulation and reduce dyskinesia induction in MPTP-treated drug-naïve primates." Movement Disorders **20**(3): 306-314.

Smith, W. W., Z. Pei, et al. (2006). "Kinase activity of mutant LRRK2 mediates neuronal toxicity." Nature Neuroscience **9**(10): 1231-1233.

Snyder, H., K. Mensah, et al. (2003). "Aggregated and monomeric α-synuclein bind to the S6' proteasomal protein and inhibit proteasomal function." Journal of Biological Chemistry **278**(14): 11753-11759.

Sofic, E., K. W. Lange, et al. (1992). "Reduced and oxidized glutathione in the substantia nigra of patients with Parkinson's disease." Neuroscience Letters **142**(2): 128-130.

Sofic, E., P. Riederer, et al. (1988). "Increased iron (III) and total iron content in post mortem substantia nigra of parkinsonian brain." J. Neural. Transm **74**: 199-205.

Soma, H., I. Yabe, et al. (2006). "Heredity in multiple system atrophy." Journal of the Neurological Sciences **240**(1-2): 107-110.

Song, W., A. Patel, et al. (2009). "The Parkinson disease-associated A30P mutation stabilizes α-synuclein against proteasomal degradation triggered by heme oxygenase-1 over-expression in human neuroblastoma cells." Journal of Neurochemistry **110**(2): 719-733.

Song, X. and M. Ehrich (1998). "MPTP-induced modulation of neurotransmitters in SH-SY5Y human neuroblastoma cells." International Journal of Toxicology **17**(6): 677-701.

Sonsalla, P. K., G. D. Zeevalk, et al. (2008). "Chronic intraventricular administration of 1-methyl-4-phenylpyridinium as a progressive model of Parkinson's disease." Parkinsonism and Related Disorders **14**(SUPPL.2): S116-S118.

Sontag, K. H., C. Heim, et al. (1995). "Long-term behavioural effects of TaClo (1-trichloromethyl-1,2,3,4-tetrahydro-β-carboline) after subchronic treatment in rats." Journal of Neural Transmission, Supplement(46): 283-289.

Sontag, T. A., K. W. Lange, et al. (2007). The long-term effects of the neurotoxin l-trichloromethyl-1,2,3,4- tetrahydro-β-carboline (TaClo) on cognitive performance in rats**:** 149-154.

Sontag, T. A., K. W. Lange, et al. (2009). "Alterations of nocturnal activity in rats following subchronic oral administration of the neurotoxin 1-trichloromethyl-1,2,3,4-tetrahydro-β- carboline." Journal of Neural Transmission **116**(10): 1267-1271.

Sontag, T. A., K. W. Lange, et al. (2009). "Alterations of nocturnal activity in rats following subchronic oral administration of the neurotoxin 1-trichloromethyl-1,2,3,4-tetrahydro-β-carboline." Journal of Neural Transmission **116**(10): 1267-1271.

Spillantini, M. G., R. A. Crowther, et al. (1998). "alpha-Synuclein in filamentous inclusions of Lewy bodies from Parkinson's disease and dementia with lewy bodies." Proc Natl Acad Sci U S A **95**(11): 6469-6473.

Spillantini, M. G., R. A. Crowther, et al. (1998). "α-Synuclein in filamentous inclusions of Lewy bodies from Parkinson's disease and dementia with Lewy bodies." Proceedings of the National Academy of Sciences of the United States of America **95**(11): 6469-6473.

Spillantini, M. G., M. L. Schmidt, et al. (1997). "Alpha-synuclein in Lewy bodies." Nature **388**(6645): 839-840.

Spillantini, M. G., M. L. Schmidt, et al. (1997). "α-synuclein in Lewy bodies." Nature **388**(6645): 839-840.

Steckley, D., M. Karajgikar, et al. (2007). "Puma is a dominant regulator of oxidative stress induced bax activation and neuronal apoptosis." Journal of Neuroscience **27**(47): 12989-12999.

Steele, J. C., J. C. Richardson, et al. (1964). "Progressive Supranuclear Palsy. A Heterogeneous Degeneration Involving the Brain Stem, Basal Ganglia and Cerebellum with Vertical Gaze and Pseudobulbar Palsy, Nuchal Dystonia and Dementia." Archives of Neurology **10**: 333-359.

Stennicke, H. R., J. M. Jürgensmeier, et al. (1998). "Pro-caspase-3 is a major physiologic target of caspase-8." Journal of Biological Chemistry **273**(42): 27084-27090.

Stern, Y., J. W. Tetrud, et al. (1990). "Cognitive change following MPTP exposure." Neurology **40**(2): 261-264.

Storch, A., Y. I. Hwang, et al. (2006). "Cytotoxicity of chloral-derived β-carbolines is not specific towards neuronal nor dopaminergic cells." Journal of Neural Transmission **113**(12): 1895-1901.

Strauss, K. M., L. M. Martins, et al. (2005). "Loss of function mutations in the gene encoding Omi/HtrA2 in Parkinson's disease." Human Molecular Genetics **14**(15): 2099-2111.

Striessnig, J., A. Koschak, et al. (2006). "Role of voltage-gated L-type Ca2+ channel isoforms for brain function." Biochemical Society Transactions **34**(5): 903-909.

Su, X., H. J. Federoff, et al. (2009). "Mutant α-synuclein overexpression mediates early proinflammatory activity." Neurotoxicity Research **16**(3): 238-254.

Sun, L., H. Wang, et al. (2012). "Mixed lineage kinase domain-like protein mediates necrosis signaling downstream of RIP3 kinase." Cell **148**(1-2): 213-227.

Sun, X. M., M. MacFarlane, et al. (1999). "Distinct caspase cascades are initiated in receptor-mediated and chemical-induced apoptosis." Journal of Biological Chemistry **274**(8): 5053-5060.

Sun, Z. and A. D. Gitler (2008). "Discovery and characterization of three novel synuclein genes in zebrafish." Developmental Dynamics **237**(9): 2490-2495.

Sunyer, B., S. Patil, et al. (2007). "Barnes maze, a useful task to assess spatial reference memory in the mice." Nature Protocol Exchange.

Surmeier, D. J., J. N. Guzman, et al. (2010). "Calcium, cellular aging, and selective neuronal vulnerability in Parkinson's disease." Cell Calcium **47**(2): 175-182.

Swerdlow, R. H., L. I. Golbe, et al. (2000). "Mitochondrial dysfunction in cybrid lines expressing mitochondrial genes from patients with progressive supranuclear palsy." Journal of Neurochemistry **75**(4): 1681-1684.

Szabadkai, G. and M. R. Duchen (2008). "Mitochondria: the hub of cellular Ca2+ signaling." Physiology (Bethesda) **23**: 84-94.

Szabo, C., B. Zingarelli, et al. (1996). "DNA strand breakage, activation of poly(ADP-ribose) synthetase, and cellular energy depletion are involved in the cytotoxicity in macrophages and smooth muscle cells exposed to peroxynitrite." Proceedings of the National Academy of Sciences of the United States of America **93**(5): 1753-1758.

Tain, L. S., R. B. Chowdhury, et al. (2009). "Drosophila HtrA2 is dispensable for apoptosis but acts downstream of PINK1 independently from Parkin." Cell Death and Differentiation **16**(8): 1118-1125.

Taira, T., Y. Saito, et al. (2004). "DJ-1 has a role in antioxidative stress to prevent cell death." EMBO Reports **5**(2): 213-218.

Tait, S. W. G. and D. R. Green (2008). "Caspase-independent cell death: Leaving the set without the final cut." Oncogene **27**(50): 6452-6461.

Takahashi, T., N. Amano, et al. (1996). "Corticobasal degeneration: Widespread argentophilic threads and glia in addition to neurofibrillary tangles. Similarities of cytoskeletal abnormalities in corticobasal degeneration and progressive supranuclear palsy." Journal of the Neurological Sciences **138**(1-2): 66-77.

Takeda, N., S. Hasegawa, et al. (1993). "Pica in rats is analogous to emesis: An animal model in emesis research." Pharmacology Biochemistry and Behavior **45**(4): 817-821.

Takeshige, K. and S. Minakami (1979). "NADH- and NADPH-dependent formation of superoxide anions by bovine heart submitochondrial particles and NADH-ubiquinone reductase preparation." Biochemical Journal **180**(1): 129-135.

Tan, E. K., P. Ho, et al. (2010). "PLA2G6 mutations and Parkinson's disease." Annals of Neurology **67**(1): 148.

Tan, J., T. Zhang, et al. (2011). "Regulation of intracellular manganese homeostasis by Kufor-Rakeb syndrome-associated ATP13A2 protein." Journal of Biological Chemistry **286**(34): 29654-29662.

Tan, L. and J. T. Yu (2012). "The kynurenine pathway in neurodegenerative diseases: Mechanistic and therapeutic considerations." Journal of the Neurological Sciences **323**(1-2): 1-8.

Tanaka, Y., G. Guhde, et al. (2000). "Accumulation of autophagic vacuoles and cardiomyopathy LAMP-2-deficient mice." Nature **406**(6798): 902-906.

Tanila, H., M. Björklund, et al. (1998). "Cognitive changes in mice following moderate MPTP exposure." Brain Research Bulletin **45**(6): 577-582.

Tas, J. and G. Westerneng (1981). "Fundamental aspects of the interaction of propidium diiodide with nucleic acids studied in a model system of polyacrylamide films." Journal of Histochemistry and Cytochemistry **29**(8): 929-936.

Tatton, W. G., R. Chalmers-Redman, et al. (2003). "Apoptosis in Parkinson's disease: Signals for neuronal degradation." Annals of Neurology **53**(SUPPL. 3): S61-S72.

Taylor, A. E., J. A. Saint-Cyr, et al. (1986). "Frontal lobe dysfunction in Parkinson's disease." Brain **109**(5): 845-883.

Temkin, V., Q. Huang, et al. (2006). "Inhibition of ADP/ATP exchange in receptor-interacting protein-mediated necrosis." Molecular and Cellular Biology **26**(6): 2215-2225.

Terman, A. (1995). "The effect of age on formation and elimination of autophagic vacuoles in mouse hepatocytes." Gerontology **41**(SUPPL. 2): 319-326.

Testa, C. M., T. B. Sherer, et al. (2005). "Rotenone induces oxidative stress and dopaminergic neuron damage in organotypic substantia nigra cultures." Molecular Brain Research **134**(1): 109-118.

Thapa, R. J., S. H. Basagoudanavar, et al. (2011). "NF-κB protects cells from gamma interferon-induced RIP1-dependent necroptosis." Molecular and Cellular Biology **31**(14): 2934-2946.

Thiffault, C., J. W. Langston, et al. (2000). "Increased striatal dopamine turnover following acute administration of rotenone to mice." Brain Research **885**(2): 283-288.

Thoenen, H. and J. P. Tranzer (1968). "Chemical sympathectomy by selective destruction of adrenergic nerve endings with 6-hydroxydopamine." Naunyn-Schmiedebergs Archiv für Pharmakologie und Experimentelle Pathologie **261**(3): 271-288.

Thorré, K., M. Pravda, et al. (1997). "New antioxidant mixture for long term stability of serotonin, dopamine and their metabolites in automated microbore liquid chromatography with dual electrochemical detection." Journal of Chromatography B: Biomedical Sciences and Applications **694**(2): 297-303.

Tiangyou, W., G. Hudson, et al. (2006). "POLG1 in idiopathic Parkinson disease." Neurology **67**(9): 1698-1700.

Tillerson, J. L., W. M. Caudle, et al. (2002). "Detection of behavioral impairments correlated to neurochemical deficits in mice treated with moderate doses of 1-methyl-4-phenyl-1,2,3,6-tetrahydropyridine." Experimental Neurology **178**(1): 80-90.

Tinsley, R. B., C. R. Bye, et al. (2009). "Dopamine D2 receptor knockout mice develop features of Parkinson disease." Annals of Neurology **66**(4): 472-484.

Tison, F., F. Yekhlef, et al. (2000). "Prevalence of multiple system atrophy." Lancet **355**(9202): 495-496.

Tong, Y., E. Giaime, et al. (2012). "Loss of leucine-rich repeat kinase 2 causes age-dependent bi-phasic alterations of the autophagy pathway." Molecular Neurodegeneration: 2.

Trojanowski, J. Q., M. Goedert, et al. (1998). "Fatal attractions: abnormal protein aggregation and neuron death in Parkinson's disease and Lewy body dementia." Cell Death Differ **5**(10): 832-837.

Trulson, M. E., M. S. Cannon, et al. (1985). "Effects of chronic methamphetamine on the nigral-striatal dopamine system in rat brain: Tyrosine hydroxylase immunochemistry and quantitative light microscopic studies." Brain Research Bulletin **15**(6): 569-577.

U.S. Department of Health, E. a. W. (1976). "Carcinogenesis bioassay of trichloroethylene." VET.TOXICOL. **18**(3): 166.

Ungerstedt, U. (1968). "6-hydroxy-dopamine induced degeneration of central monoamine neurons." European Journal of Pharmacology **5**(1): 107-110.

Valente, E. M., P. M. Abou-Sleiman, et al. (2004). "Hereditary early-onset Parkinson's disease caused by mutations in PINK1." Science **304**(5674): 1158-1160.

Valente, E. M., P. M. Abou-Sleiman, et al. (2004). "Hereditary early-onset Parkinson's disease caused by mutations in PINK1." Science **304**(5674): 1158-1160.

Van Cruchten, S. and W. Van den Broeck (2002). "Morphological and biochemical aspects of apoptosis, oncosis and necrosis." Anatomia, Histologia, Embryologia **31**(4): 214-223.

Van Duijn, C. M., M. C. J. Dekker, et al. (2001). "PARK7, a novel locus for autosomal recessive early-onset parkinsonism, on chromosome 1p36." American Journal of Human Genetics **69**(3): 629-634.

Van Ham, T. J., K. L. Thijssen, et al. (2008). "C. elegans model identifies genetic modifiers of α-synuclein inclusion formation during aging." PLoS Genetics **4**(3).

Van Raam, B. J., D. E. Ehrnhoefer, et al. (2013). "Intrinsic cleavage of receptor-interacting protein kinase-1 by caspase-6." Cell Death and Differentiation **20**(1): 86-96.

Vandenabeele, P., S. Grootjans, et al. (2013). "Necrostatin-1 blocks both RIPK1 and IDO: consequences for the study of cell death in experimental disease models." Cell Death Differ **20**(2): 185-187.

Ved, R., S. Saha, et al. (2005). "Similar patterns of mitochondrial vulnerability and rescue induced by genetic modification of α-synuclein, parkin, and DJ-1 in Caenorhabditis elegans." Journal of Biological Chemistry **280**(52): 42655-42668.

Vercammen, D., R. Beyaert, et al. (1998). "Inhibition of caspases increases the sensitivity of L929 cells to necrosis mediated by tumor necrosis factor." Journal of Experimental Medicine **187**(9): 1477-1485.

Vilariño-Güell, C., O. A. Ross, et al. (2009). "Reported mutations in GIGYF2 are not a common cause of Parkinson's disease." Movement Disorders **24**(4): 619-620.

Vilariño-Güell, C., A. I. Soto-Ortolaza, et al. (2011). "MAPT H1 haplotype is a risk factor for essential tremor and multiple system atrophy." Neurology **76**(7): 670-672.

Volles, M. J. and P. T. Lansbury Jr (2002). "Vesicle permeabilization by protofibrillar α-synuclein is sensitive to Parkinson's disease-linked mutations and occurs by a pore-like mechanism." Biochemistry **41**(14): 4595-4602.

Volles, M. J., S. J. Lee, et al. (2001). "Vesicle permeabilization by protofibrillar α-synuclein: Implications for the pathogenesis and treatment of Parkinson's disease." Biochemistry **40**(26): 7812-7819.

Wabnitz, G. H., C. Goursot, et al. (2010). "Mitochondrial translocation of oxidized cofilin induces caspase-independent necrotic-like programmed cell death of T cells." Cell Death and Disease **1**(7): 10.1038/cddis.2010.1036.

Wakabayashi, K., K. Tanji, et al. (2007). "The Lewy body in Parkinson's disease: molecules implicated in the formation and degradation of alpha-synuclein aggregates." Neuropathology **27**(5): 494-506.

Wakabayashi, K., Y. Toyoshima, et al. (1999). "Restricted occurrence of Lewy bodies in the dorsal vagal nucleus in a patient with late-onset parkinsonism." J Neurol Sci **165**(2): 188-191.

Wakabayashi, K., M. Yoshimoto, et al. (1998). "α-synuclein immunoreactivity in glial cytoplasmic inclusions in multiple system atrophy." Neuroscience Letters **249**(2-3): 180-182.

Waldner, R., Z. Puschban, et al. (2001). "No functional effects of embryonic neuronal grafts on motor deficits in a 3-nitropropionic acid rat model of advanced striatonigral degeneration (multiple system atrophy)." Neuroscience **102**(3): 581-592.

Wang, C., R. Lu, et al. (2007). "Drosophila overexpressing parkin R275W mutant exhibits dopaminergic neuron degeneration and mitochondrial abnormalities." Journal of Neuroscience **27**(32): 8563-8570.

Wang, F., M. Nguyen, et al. (2007). "SIRT2 deacetylates FOXO3a in response to oxidative stress and caloric restriction." Aging Cell **6**(4): 505-514.

Wang, H.-L., A.-H. Chou, et al. (2011). "PARK6 PINK1 mutants are defective in maintaining mitochondrial membrane potential and inhibiting ROS formation of substantia nigra dopaminergic neurons." Biochimica et Biophysica Acta (BBA) - Molecular Basis of Disease **1812**(6): 674-684.

Wang, V., S.-Y. Chen, et al. (2010). "Val-9Ala and Ile + 58Thr polymorphism of MnSOD in Parkinson's disease." Clinical Biochemistry **43**(12): 979-982.

Wang, Y., V. L. Dawson, et al. (2009). "Poly(ADP-ribose) signals to mitochondrial AIF: A key event in parthanatos." Experimental Neurology **218**(2): 193-202.

Wang, Z., H. Jiang, et al. (2012). "The mitochondrial phosphatase PGAM5 functions at the convergence point of multiple necrotic death pathways." Cell **148**(1-2): 228-243.

Warner, T. T., A. H. V. Schapira, et al. (2003). "Genetic and environmental factors in the cause of Parkinson's disease." Annals of Neurology **53**(SUPPL. 3): S16-S25.

Watmough, N. J., M. A. Birch-Machin, et al. (1989). "Tissue specific defect of complex I of the mitochondrial respiratory chain." Biochemical and Biophysical Research Communications **160**(2): 623-627.

Weaver, F. M., K. Follett, et al. (2009). "Bilateral deep brain stimulation vs best medical therapy for patients with advanced parkinson disease: A randomized controlled trial." JAMA - Journal of the American Medical Association **301**(1): 63-73.

Webb, J. L., B. Ravikumar, et al. (2003). "α-synuclein Is Degraded by Both Autophagy and the Proteasome." Journal of Biological Chemistry **278**(27): 25009-25013.

Webb, J. L., B. Ravikumar, et al. (2004). "Microtubule disruption inhibits autophagosome-lysosome fusion: Implications for studying the roles of aggresomes in polyglutamine diseases." International Journal of Biochemistry and Cell Biology **36**(12): 2541-2550.

Weisiger, R. A. and I. Fridovich (1973). "Superoxide dismutase. Organelle specificity." Journal of Biological Chemistry **248**(10): 3582-3592.

Wen, L., W. Wei, et al. (2008). "Visualization of monoaminergic neurons and neurotoxicity of MPTP in live transgenic zebrafish." Developmental Biology **314**(1): 84-92.

West, A. B., D. J. Moore, et al. (2005). "Parkinson's disease-associated mutations in leucine-rich repeat kinase 2 augment kinase activity." Proceedings of the National Academy of Sciences of the United States of America **102**(46): 16842-16847.

West, M. J., L. Slomianka, et al. (1991). "Unbiased stereological estimation of the total number of neurons in the subdivisions of the rat hippocampus using the optical fractionator." Anatomical Record **231**(4): 482-497.

Westphalen, R. I. and H. C. Hemmings Jr (2003). "Selective depression by general anesthetics of glutamate versus GABA release from isolated cortical nerve terminals." Journal of Pharmacology and Experimental Therapeutics **304**(3): 1188-1196.

Whitehouse, P. J., J. C. Hedreen, et al. (1983). "Basal forebrain neurons in the dementia of Parkinson disease." Annals of Neurology **13**(3): 243-248.

Whitworth, A. J., J. R. Lee, et al. (2008). "Rhomboid-7 and HtrA2/Omi act in a common pathway with the Parkinson's disease factors Pink1 and Parkin." DMM Disease Models and Mechanisms **1**(2-3): 168-174.

Wilkinson, K. D., K. Lee, et al. (1989). "The neuron-specific protein PGP 9.5 is a ubiquitin carboxyl-terminal hydrolase." Science **246**(4930): 670-673.

Williams-Johnson, M., C. J. Eisenmann, et al. (1997). Toxicological Profile for Trichloroethylene. U. S. D. f. H. a. H. Services.

Willis, S. N., J. I. Fletcher, et al. (2007). "Apoptosis initiated when BH3 ligands engage multiple Bcl-2 homologs, not Bax or Bak." Science **315**(5813): 856-859.

Windels, F. and E. A. Kiyatkin (2006). "General anesthesia as a factor affecting impulse activity and neuronal responses to putative neurotransmitters." Brain Research **1086**(1): 104-116.

World Health Organization, United Nations Environment Programme, et al. (1985). Environmental Health Criteria 50: Trichloroethylene. International Programme on Chemical Safety.

Wright Willis, A., B. A. Evanoff, et al. (2010). "Geographic and ethnic variation in Parkinson disease: A population-based study of us medicare beneficiaries." Neuroepidemiology **34**(3): 143-151.

Wu, C. and J. Schaum (2000). "Exposure assessment of trichloroethylene." Environmental Health Perspectives **108**(SUPPL. 2): 359-363.

Wüllner, U., P. A. Löschmann, et al. (1996). "Glutathione depletion potentiates MPTP and MPP+ toxicity in nigral dopaminergic neurones." NeuroReport **7**(4): 921-923.

Xie, H. R., L. S. Hu, et al. (2010). "SH-SY5Y human neuroblastoma cell line: In vitro cell model of dopaminergic neurons in Parkinson's disease." Chinese Medical Journal **123**(8): 1086-1092.

Xie, Z. and D. J. Klionsky (2007). "Autophagosome formation: Core machinery and adaptations." Nature Cell Biology **9**(10): 1102-1109.

Xiong, N., Jia, M., Xiong, J., Huang, J., Wang, T. (2012). "Implication of autophagy in Parkinson's disease: Rotenone-based models." Movement Disorders **27 Suppl 1**: 1521.

Xu, X., C. C. Chua, et al. (2010). "The role of PARP activation in glutamate-induced necroptosis in HT-22 cells." Brain Research **1343**: 206-212.

Xu, Y., S. Huang, et al. (2006). "Poly(ADP-ribose) polymerase-1 signaling to mitochondria in necrotic cell death requires RIP1/TRAF2-mediated JNK1 activation." Journal of Biological Chemistry **281**(13): 8788-8795.

Yan, Y., D. Yang, et al. (2005). "Directed differentiation of dopaminergic neuronal subtypes from human embryonic stem cells." Stem Cells **23**(6): 781-790.

Yang, D., Z. J. Zhang, et al. (2008). "Human embryonic stem cell-derived dopaminergic neurons reverse functional deficit in Parkinsonian rats." Stem Cells **26**(1): 55-63.

Yang, J., L. He, et al. (2004). "Early administration of nicotinamide prevents learning and memory impairment in mice induced by 1-methyl-4-phenyl-1, 2, 3, 6-tetrahydropyridine." Pharmacology Biochemistry and Behavior **78**(1): 179-183.

Yang, L. and M. F. Beal (2011). Determination of neurotransmitter levels in models of parkinson's disease by HPLC-ECD. **793:** 401-415.

Yang, Y., S. Gehrke, et al. (2005). "Inactivation of Drosophila DJ-1 leads to impairments of oxidative stress response and phosphatidylinositol 3-kinase/Akt signaling." Proceedings of the National Academy of Sciences of the United States of America **102**(38): 13670-13675.

Yang, Y., Y. Ouyang, et al. (2008). "Pink1 regulates mitochondrial dynamics through interaction with the fission/fusion machinery." Proc Natl Acad Sci U S A **105**(19): 7070-7075.

Ye, Y.-C., H.-J. Wang, et al. (2012). "RIP1-mediated mitochondrial dysfunction and ROS production contributed to tumor necrosis factor alpha-induced L929 cell necroptosis and autophagy." International Immunopharmacology **14**(4): 674-682.

Yokota, T., K. Sugawara, et al. (2003). "Down regulation of DJ-1 enhances cell death by oxidative stress, ER stress, and proteasome inhibition." Biochemical and Biophysical Research Communications **312**(4): 1342-1348.

Yokoyama, H., H. Kuroiwa, et al. (2010). "Poly(ADP-ribose)polymerase inhibitor can attenuate the neuronal death after 1-methyl-4-phenyl-1,2,3,6-tetrahydropyridine-induced neurotoxicity in mice." Journal of Neuroscience Research **88**(7): 1522-1536.

Yoritaka, A., N. Hattori, et al. (1997). "An immunohistochemical study on manganese superoxide dismutase in Parkinson's disease." Journal of the Neurological Sciences **148**(2): 181-186.

Yoshida, E., K. Mokuno, et al. (1994). "Cerebrospinal fluid levels of superoxide dismutases in neurological diseases detected by sensitive enzyme immunoassays." Journal of the Neurological Sciences **124**(1): 25-31.

Yoshimori, T., A. Yamamoto, et al. (1991). "Bafilomycin A1, a specific inhibitor of vacuolar-type H+-ATPase, inhibits acidification and protein degradation in lysosomes of cultured cells." Journal of Biological Chemistry **266**(26): 17707-17712.

Yoshino, H., H. Tomiyama, et al. (2010). "Phenotypic spectrum of patients with PLA2G6 mutation and PARK14-linked parkinsonism." Neurology **75**(15): 1356-1361.

Youle, R. J. and A. Strasser (2008). "The BCL-2 protein family: Opposing activities that mediate cell death." Nature Reviews Molecular Cell Biology **9**(1): 47-59.

Yount, E. A., S. Y. Felten, et al. (1981). "2-Chloropropionate and dichloroacetate: Metabolic effects and toxicity to nerve and testis in rats." Federation Proceedings **40**(6): 485.

Yu, S. W., H. Wang, et al. (2002). "Mediation of poty(ADP-ribose) polymerase-1 - Dependent cell death by apoptosis-inducing factor." Science **297**(5579): 259-263.

Yuan, J., R. Adamski, et al. (2010). "Focus on histone variant H2AX: To be or not to be." FEBS Letters **584**(17): 3717-3724.

Yumino, K., I. Kawakami, et al. (2002). "Paraquat- and diquat-induced oxygen radical generation and lipid peroxidation in rat brain microsomes." Journal of Biochemistry **131**(4): 565-570.

Yy, S., M. Jiang, et al. (2011). "Rotenone induces more serious learning and memory impairment than α-synuclein A30P does in Drosophila." Journal of Shanghai University **15**(3): 229-234.

Zahid, M., M. Saeed, et al. (2011). "Formation of dopamine quinone-DNA adducts and their potential role in the etiology of Parkinson's disease." IUBMB Life **63**(12): 1087-1093.

Zarranz, J. J., J. Alegre, et al. (2004). "The New Mutation, E46K, of α-Synuclein Causes Parkinson and Lewy Body Dementia." Annals of Neurology **55**(2): 164-173.

Zhang, D. W., J. Shao, et al. (2009). "RIP3, an energy metabolism regulator that switches TNF-induced cell death from apoptosis to necrosis." Science **325**(5938): 332-336.

Zhang, H., C. Zhong, et al. (2009). "Granulysin induces cathepsin B release from lysosomes of target tumor cells to attack mitochondria through processing of bid leading to Necroptosis." Journal of immunology (Baltimore, Md. : 1950) **182**(11): 6993-7000.

Zhang, J., N. Hattori, et al. (2000). "Association between a polymorphism of ubiquitin carboxy-terminal hydrolase L1 (UCH-L1) gene and sporadic Parkinson's disease." Parkinsonism and Related Disorders **6**(4): 195-197.

Zhang, J., G. Perry, et al. (1999). "Parkinson's disease is associated with oxidative damage to cytoplasmic DNA and RNA in substantia nigra neurons." American Journal of Pathology **154**(5): 1423-1429.

Zhang, W., T. Wang, et al. (2005). "Aggregated α-synuclein activates microglia: A process leading to disease progression in Parkinson's disease." FASEB Journal **19**(6): 533-542.

Zhao, H., F. Traganos, et al. (2008). "Oxidative stress induces cell cycle-dependent Mre11 recruitment, ATM and Chk2 activation and histone H2AX phosphorylation." Cell Cycle **7**(10): 1490-1495.

Zhao, Z., X. Zhang, et al. (2010). "Protection of pancreatic β-cells by group VIA phospholipase A 2-mediated repair of mitochondrial membrane peroxidation." Endocrinology **151**(7): 3038-3048.

Zhou, H., J. Chen, et al. (2012). "Melatonin protects against rotenone-induced cell injury via inhibition of Omi and Bax-mediated autophagy in Hela cells." Journal of Pineal Research **52**(1): 120-127.

Zhu, M., Z. J. Qin, et al. (2006). "α-synuclein can function as an antioxidant preventing oxidation of unsaturated lipid in vesicles." Biochemistry **45**(26): 8135-8142.

Ziering, A., L. Berger, et al. (1947). "Piperidine derivatives; 4-arylpiperidines." Journal of Organic Chemistry **12**(6): 894-903.

Zigmond, M. J., A. L. Acheson, et al. (1984). "Neurochemical compensation after nigrostriatal bundle injury in an animal model of preclinical Parkinsonism." Archives of Neurology **41**(8): 856-861.

Zimprich, A., S. Biskup, et al. (2004). "Mutations in LRRK2 cause autosomal-dominant parkinsonism with pleomorphic pathology." Neuron **44**(4): 601-607.

Zimprich, A., C. Schulte, et al. (2009). "PARK11 gene (GIGYF2) variants Asn56Ser and Asn457Thr are not pathogenic for Parkinson's disease." Parkinsonism and Related Disorders **15**(7): 532-534.

Zong, W. X., D. Ditsworth, et al. (2004). "Alkylating DNA damage stimulates a regulated form of necrotic cell death." Genes and Development **18**(11): 1272-1282.